

# Investigation into the fate and transport in groundwater of agriculturally derived phosphorus compounds.

UMI Number: U585418

All rights reserved

INFORMATION TO ALL USERS

The quality of this reproduction is dependent upon the quality of the copy submitted.

In the unlikely event that the author did not send a complete manuscript and there are missing pages, these will be noted. Also, if material had to be removed, a note will indicate the deletion.



UMI U585418

Published by ProQuest LLC 2013. Copyright in the Dissertation held by the Author.  
Microform Edition © ProQuest LLC.

All rights reserved. This work is protected against  
unauthorized copying under Title 17, United States Code.



ProQuest LLC  
789 East Eisenhower Parkway  
P.O. Box 1346  
Ann Arbor, MI 48106-1346

## DECLARATION

This work has not previously been accepted in substance for any degree and is not concurrently submitted in candidature for any degree.

Signed Andrew Gray (candidate) Date 03 March 2011

## STATEMENT 1

This thesis is being submitted in partial fulfillment of the requirements for the degree of PhD

Signed Andrew Gray (candidate) Date 03 March 2011

## STATEMENT 2

This thesis is the result of my own independent work/investigation, except where otherwise stated. Other sources are acknowledged by explicit references.

Signed Andrew Gray (candidate) Date ...03 March 2011

## STATEMENT 3

I hereby give consent for my thesis, if accepted, to be available for photocopying and for inter-library loan, and for the title and summary to be made available to outside organisations.

Signed Andrew Gray (candidate) Date ...03 March 2011

## STATEMENT 4: PREVIOUSLY APPROVED BAR ON ACCESS

I hereby give consent for my thesis, if accepted, to be available for photocopying and for inter-library loans **after expiry of a bar on access previously approved by the Graduate Development Committee.**

Signed ..... (candidate) Date ...03 March 2011

# **Investigation into the fate and transport in groundwater of agriculturally derived phosphorus compounds.**

**By**

**Andrew Gray  
BSc (Hons), MSc, FGS**

**School of Earth and Ocean Sciences  
Cardiff University  
Wales**

**This thesis is being submitted in partial fulfilment of the requirement for the degree of PhD.**

## **Abstract**

### **Investigation into the fate and transport in groundwater of agriculturally derived phosphorus compounds**

Phosphates are ubiquitous in the environment, where they are essential for life; however at excessive levels they can cause significant environmental damage. This project investigates the spatial and temporal occurrence of phosphorus in groundwater, and phosphorus transport through the vadose zone. Concentrating on agriculturally-derived phosphates, the research elucidates the geochemical relationships between phosphorus species and geology. The project has two study locations. A section of the Lower Usk Valley in Monmouthshire was the principal site; the Eden Valley in Cumbria was used as a comparison case study.

With highly heterogeneous distributions, phosphorus often showed significant concentrations in both soil and groundwater. In groundwater Soluble Reactive Phosphorus (SRP) ranged from  $1.07 \text{ mg l}^{-1}$  to undetectable. Maximum soil leachable SRP was measured at  $55 \text{ mg kg}^{-1}$  and soil Total Phosphorus (TP)  $113 \text{ mg kg}^{-1}$  while in an adjacent borehole groundwater SRP was undetectable. Phosphorus was found at intermediate concentrations beneath potential hotspots created by large manure piles; effluent  $85 \text{ mg l}^{-1}$ . Analysis by X-ray diffraction and analytical scanning electron microscopy did not identify soil phosphate minerals at these and other sites; this suggests that precipitation reactions are not a dominant source or sink of agricultural phosphorus in local soils. The results of the geochemical investigations indicates that iron and manganese oxides are providing sorption sites for phosphates, influencing their mobility and observed concentration in groundwater.

Data obtained from in-situ borehole loggers were used to characterise the aquifer zone of the study area and understand the groundwater response to external drivers such as fertilizer application and rainfall. Groundwater and species transport modelling of the Usk area indicates that local parameter heterogeneity is critically important. The groundwater modelling, supported by a statistical analysis of the data, has increased and refined our conceptual understanding of the fate and transport of phosphorus in groundwater.

## Contents

<b>Chapter 1</b>	<b>Introduction</b>	<b>1</b>
1.1	Background	1
1.2	Aims and objectives	2
1.3	Thesis outline	4
<b>Chapter 2</b>	<b>Literature review</b>	<b>5</b>
2.1	Introduction	5
2.1.1	Background	5
2.1.2	Environmental pathways	7
2.2	Phosphorus chemistry	10
2.2.1	Phosphate geochemistry	10
2.2.2	Phosphate geochemistry relationships	12
2.2.3	Phosphate hierarchy	14
2.3	Phosphorus in groundwater	19
2.4	Past & present methods of phosphorus analysis and quantification	21
2.4.1	Operational fractions	21
2.4.2	Nomenclature	21
2.4.3	Sample preparation	24
2.4.4	Analysis methods	26
2.5	Environmental quality standards	31
2.6	Summary	33
<b>Chapter 3</b>	<b>Methods</b>	<b>34</b>
3.1	Introduction	34
3.1.1	Sampling protocols	34
3.2	Water: fieldwork and laboratory analysis	35
3.2.1	Containers	35
3.2.2	Sampling	35
3.2.3	Field measurements	37
3.2.4	CTD divers	37
3.2.5	Analysis methods	38
3.3	Soil fieldwork and laboratory analysis	42
3.3.1	Method	43

3.4	External data	49
3.4.1	Mapping	49
3.5	Statistical analysis	52
3.5.1	Methods	52
3.6	Modelling	56
3.6.1	2D modelling: FlowNet	57
3.6.2	3D modelling: MODFLOW	57
3.6.3	Risk assessment modelling with P20 ver 3.1	58
3.7	Quality Control	59
3.7.1	Analytical limits of detection	59
3.7.2	Other equipment	62
3.8	Quality issues	63
3.8.1	Laboratory practice	63
3.8.2	Statistical analysis: quality assurance	63
3.8.3	Data sources	65
<b>Chapter 4</b>	<b>Usk Valley</b>	<b>67</b>
4.1	Geological setting	67
4.1.1	Description of area	67
4.1.2	Regional structure	70
4.1.3	Lithostratigraphy	71
4.2	Hydrogeology	76
4.2.1	Water sources	76
4.3	Aquifer properties	78
4.3.1	General	78
4.3.2	Raglan Mudstone Formation	78
4.3.3	Conceptual model	85
4.4	Summary	87

<b>Chapter 5</b>	<b>Usk Valley groundwater</b>	<b>88</b>
5.1	Introduction	88
5.1.1	Data quality assurance	89
5.2	Physical hydrology	92
5.2.1	Logger data	92
5.3	Groundwater / surface water interactions	108
5.4	Groundwater geochemistry	115
5.4.1	Eh-pH diagrams	115
5.4.2	Multiprobe parameter statistical analysis	120
5.4.3	Autocorrelation analysis	124
5.4.4	Ion balance analysis	126
5.4.5	Piper diagrams	127
5.4.6	River Usk	131
5.5	Geochemical correlations	132
5.5.1	Occurrence of phosphorus	132
5.5.2	SRP time series	138
5.5.3	Species Associations	141
5.6	Field testing	158
5.6.1	Hydraulic conductivity determinations	158
5.7	Summary	164
<b>Chapter 6</b>	<b>Usk Valley soil</b>	<b>165</b>
6.1	Introduction	165
6.2	Soil Leaching	167
6.2.1	Acid leaching results	167
6.2.2	Dried soil results	170
6.2.3	Estimation of local soil partition coefficient	185
6.2.4	Soluble unreactive phosphorus (SUP)	189
6.2.5	Soil column results and discussion	192
6.3	Geochemistry and mineralogy	203
6.3.1	XRD results and discussion	203
6.3.2	Scanning electron microscope results and discussion	204
6.4	Summary	214

<b>Chapter 7</b>	<b>Lower Usk Valley groundwater modelling</b>	<b>216</b>
7.1	Introduction	216
7.2	Hydrological conceptual model	217
7.2.1	Topography	217
7.2.2	Water table	217
7.2.3	Boundary conditions	223
7.2.4	Hydraulic parameters	224
7.2.5	Conceptual model	225
7.3	2D Flow Model (FlowNet)	227
7.4	3D regional modelling with MODFLOW	232
7.4.1	Regional model	232
7.4.2	Specified head boundary condition	239
7.4.3	No-flow boundary condition	243
7.4.4	Regional modelling Summary	248
7.5	3D local modelling with MODFLOW	249
7.5.1	Local Model	249
7.5.2	Specified head boundary condition	252
7.5.3	No-flow boundary condition	259
7.5.4	Local model summary	262
7.6	Contaminant transport	263
7.6.1	Geochemical conceptual model	263
7.7	Risk assessment modelling with P20 ver 3.1	281
7.8	Modelling summary	284
<b>Chapter 8</b>	<b>Eden Valley case study</b>	<b>286</b>
8.1	Introduction	286
8.1.1	General	286
8.2	Geological setting	288
8.2.1	Regional structure	289
8.2.2	Lithostratigraphy	290
8.2.3	Penrith Sandstone	292
8.2.4	General sequence	298
8.3	Hydrogeology	300
8.3.1	Water sources	300

8.4	Aquifer properties	305
8.4.1	Penrith Sandstone Formation	305
8.4.2	Conceptual hydrogeology Eden Valley	312
8.5	Physical hydrology – Eden Valley	314
8.5.1	Results and discussion	317
8.5.2	Eden Valley physical hydrology conclusion	337
8.6	Groundwater geochemistry	339
8.6.1	Introduction	339
8.6.2	Eh-pH diagram	339
8.6.3	Autocorrelation analyss	340
8.6.4	Ion balance analysis	342
8.6.5	Geochemical correlation	343
8.7	Summary	348
<b>Chapter 9</b>	<b>Conclusions</b>	<b>349</b>
9.1	Synopsis	349
9.1.1	Aquifer mechanics	350
9.1.2	Soil analysis	353
9.1.3	Groundwater analysis	355
9.1.4	Modelling	356
9.1.5	Interpretation	358
9.2	Revised conceptual model	361
9.2.1	Physical drivers	361
9.2.2	Geochemical processes	363
9.3	Conclusion summary	365
9.4	Recommendations	367

## Table of Figures

Figure 1-1	Flow chart of methodology to be adapted during project investigation.	3
Figure 2-1	Manure storage on fractured bedrock, Eden Valley Cumbria.	7
Figure 2-2	Mineral fertiliser bales, Eden Valley.	8
Figure 2-3	Schematic phosphorus cycle.	10
Figure 2-4	Diagram : dominant phosphate species in relation to pH scale.	14
Figure 2-5	Diagram of phosphorus hierarchy.	16
Figure 2-6	Schematic of sorption process.	20
Figure 2-7	Sample preparation and analysis flow chart.	23
Figure 2-8	Phosphomolybdenum Blue.	30
Figure 3-1	Inertial pump tubing at Llandowlais Farm BH.	35
Figure 3-2	Hanna Instrument multimeter and measuring jug at UGDN.	36
Figure 3-3	CTD diver and laptop downloading at Cow House Well.	37
Figure 3-4	Calibration peak analysis (using analytical standard No III).	39
Figure 3-5	Colour development in standards.	40
Figure 3-6	Hach Lange digital titrator and accessories.	41
Figure 3-7	Soil pH probe in hole left by extraction of a soil column from the 'potato field'.	42
Figure 3-8	HDPE sample bottles used as reaction vessels for soil analysis.	44
Figure 3-9	Soil samples after centrifuging, only effective on one sample.	45
Figure 3-10	Soil column experiment apparatus.	46
Figure 3-11	Diffractiongram for Potato Field Bottom soil.	47
Figure 3-12	ESEM-EDX image of precipitate from Crag Nook farm, Eden Valley.	48
Figure 3-13	Auto-correlograms for synthetic rainfall data..	54
Figure 3-14	Cross-correlation analysis of synthetic hydrograph data.	55
Figure 4-1	UK location map of the Usk Valley, Wales.	68
Figure 4-2	Map of Usk project area showing sampling locations by type.	69
Figure 4-3	Cross section Lower Usk Valley.	70
Figure 4-4	Schematic stratigraphic column for Usk Valley project area.	71
Figure 4-5	Bedrock geology and fluvial system in project area.	72

Figure 4-6	Enlargement of Raglan Mudstones at Glen Court Farm.	73
Figure 4-7	Superficial geology overlying bedrock.	75
Figure 4-8	Spring and collection butt at Tump Farm, east flank of valley.	79
Figure 4-9	Soils map showing distinct changes in soil type in project area.	82
Figure 4-10	Aquifer vulnerability map of project area.	84
Figure 4-11	Headworks: open access.	85
Figure 4-12	Conceptual geology, hydrogeology and phosphorus transport.	86
Figure 5-1	Location ID map.	88
Figure 5-2	Borehole dip data and manual dip values.	90
Figure 5-3	Comparison of EC and temperature readings from borehole loggers and Hanna multiprobe.	91
Figure 5-4	Borehole logger data for the Usk Valley area.	93
Figure 5-5	Llantrisant borehole, flooded manhole.	94
Figure 5-6	Autocorrelation plots for monthly water rest levels within the Usk Valley.	97
Figure 5-7	Borehole logger daily temperature data for all locations.	99
Figure 5-8	Polynomial trend analysis of daily temperature data.	100
Figure 5-9	Daily rainfall and temperature for LTRI and LUSK boreholes.	101
Figure 5-10	Electrical conductivity daily data for Usk boreholes.	103
Figure 5-11	Daily EC and rainfall from loggers.	105
Figure 5-12	Cross correlation of daily rainfall and logger EC.	106
Figure 5-13	Monthly rainfall for Usk Valley area.	108
Figure 5-14	Autocorrelation of rainfall for Usk Valley area.	109
Figure 5-15	Cross correlation for Usk Valley borehole and rainfall.	110
Figure 5-16	Cross correlation for Usk Valley borehole and rainfall.	111
Figure 5-17	Cross correlation between borehole locations.	112
Figure 5-18	Cross correlation of River Usk and borehole hydrographs for most proximal locations.	113
Figure 5-19	River Usk and borehole hydrographs.	114
Figure 5-20	Eh-pH plot of sampled waters from the Usk Valley.	116
Figure 5-21	Eh-pH progression and separation of waters on west bank of River Usk.	117
Figure 5-22	Eh-pH of eastern flank waters showing distinct zonation.	118

Figure 5-23	EH-DO scatter plot of Usk Valley waters.	119
Figure 5-24	Box plots of Usk Valley ph and ORP measurements.	121
Figure 5-25	Box plots of Usk Valley multiprobe parameters DO% and TDS.	122
Figure 5-26	Box plots of Usk Valley multiprobe parameters EC and Temperature to investigate spatial distribution patterns.	123
Figure 5-27	Autocorrelation, random signal.	124
Figure 5-28	Autocorrelation analysis of multiprobe data.	125
Figure 5-29	Autocorrelation analysis of multiprobe data.	126
Figure 5-30	Piper diagram of Usk waters.	128
Figure 5-31	Individual locations Usk Valley, showing straight line solution/precipitation relationship with calcium for HFW.	129
Figure 5-32	Individual locations Usk Valley, showing straight line solution/precipitation relationship with calcium for UGDN.	130
Figure 5-33	Box plot of SRP concentration by location.	136
Figure 5-34	Usk Valley total dissolved phosphorus (ICP-MS analysis).	137
Figure 5-35	Autocorrelation plots of SRP at selected locations.	138
Figure 5-36	Concentration time series for SRP.	139
Figure 5-37	SRP time series EA and project data combined.	140
Figure 5-38	Box plot of Usk Valley anion data to show significant difference in concentration for sulphate and chloride.	143
Figure 5-39	Box plot of Usk Valley anion data to show significant difference in concentration for bicarbonate data.	144
Figure 5-40	Correlation of nitrate and SRP at LDOW and LTRI.	145
Figure 5-41	Box plot of Fe data for Usk Valley.	148
Figure 5-42	Autocorrelation of iron by location.	149
Figure 5-43	Sample bottles, LUSK and PENC are darker due to presence of suspended 'rust'.	150
Figure 5-44	Steel bolt sorption experiment.	151
Figure 5-45	Results of steel bolt sorption experiment.	152
Figure 5-46	Eh-pH diagram of Usk Waters with stability field of iron.	153
Figure 5-47	Deposition of iron hydroxide in feeder pipe to storage butt at Oaktree Farm spring.	155
Figure 5-49	SEM image #2 of iron bolt precipitate.	156
Figure 5-50	SUP and SRP average values for Usk ground and surface waters.	157

Figure 5-51	Constant rate pumping test at Llewellyn borehole.	158
Figure 5-52	Pumping test results and analysis for test at Cow House BH	160
Figure 5-53	Single borehole dilution tracer test for Usk boreholes.	162
Figure 5-54	Cow house well; CTD diver and table salt prior to tracer test.	163
Figure 6-1	Map of soil sample locations for Usk Valley superimposed on imagery photo showing cultivation features.	166
Figure 6-2	Total phosphorus for selected locations.	167
Figure 6-3	Locations for MANU, POTA and SCRUB.	168
Figure 6-4	Acid leaching results at LUSK and LTRI.	169
Figure 6-5	Box plots for SRP and TDP (mg/kg) for all locations and epochs.	171
Figure 6-6	Box plots for selected anions all locations and epochs.	173
Figure 6-7	Box plots for selected anions all locations and epochs.	174
Figure 6-8	Box plots for selected cations: Fe and K all locations and epochs.	175
Figure 6-9	Box plots for selected cations: Ca and Na all locations and epochs.	176
Figure 6-10	Phosphorus fraction for potato field location.	177
Figure 6-11	Phosphorus fractions and anions for the Scrub field and manure pile.	178
Figure 6-12	Phosphorus fractions and anions for BH locations.	179
Figure 6-13	Cation analysis for POTA, SCRUB and MANU.	181
Figure 6-14	Cation analysis for remaining soil sample locations.	183
Figure 6-15	Comparison for all locations potassium, iron and SRP.	184
Figure 6-16	Soil remedial targets for comparison with analysed soil total phosphorus concentration.	188
Figure 6-17	Comparison of SUP and SRP for Usk Valley Soils.	190
Figure 6-18	Possible movement of phosphorus fraction through the soil zone showing the conceptual relative sizes of the data in Table 6-2.	191
Figure 6-19	Collection of soil column 2 Jan 09.	192
Figure 6-20	Anion data for soil column experiment.	193
Figure 6-21	Cation data for soil column leaching experiment.	194
Figure 6-22	Spiked column results for all experiments.	195
Figure 6-23	Ty-Coch Farm Potato Field (POTA), standing water and desiccation cracks.	196
Figure 6-24	Anion leachate results for 2 <sup>nd</sup> soil column experiment.	197

Figure 6-25	Cations leached from soil column.	198
Figure 6-26	Results of spiked sample passed through soil column.	199
Figure 6-27	Soil column 2 experimental setup and falling head measurements.	201
Figure 6-28	Diffractiongram for Potato Field Bottom.	203
Figure 6-29	SEM image of dihydrogen potassium phosphate used as 'control' for soils analysis.	204
Figure 6-30	SEM image of soil from Hill Farm manure pile (SOI1).	206
Figure 6-31	SEM image of soil from Hill Farm manure pile (SOI2).	207
Figure 6-32	SEM image for soil (SOI1) at Llanusk Farm BH (LUSK).	208
Figure 6-33a-c	SEM image of filter residue at LTRI BH;(SOI2).	210
Figure 6-34	SEM image of filter detritus at LUSK BH.	211
Figure 6-35	SEM image of filter detritus from LUSK BH (SOI4).	212
Figure 6-36	SEM image for LUSK filter, spectrum # 2.	213
Figure 6-37	Groundwater sample at Llanusk Farm BH (LUSK).	214
Figure 7-1	DTM of the Usk Valley and environs.	218
Figure 7-2	Schematic realisation of the borehole logs and lithology for the Usk Valley.	220
Figure 7-3	Groundwater contours derived from project borehole measurements.	221
Figure 7-4	Groundwater contours using additional groundwater data.	222
Figure 7-5	Intersection of modelled groundwater table and the topographic surface.	223
Figure 7-6	Ludlow Shales at Woodbury Quarry from Gray (2004).	225
Figure 7-7	Revised conceptual model of the Usk Valley hydrogeology.	226
Figure 7-8	Flownet model HFW to River Usk.	227
Figure 7-9	Head distribution along model row 1 for Figure 7-8.	228
Figure 7-10	East flank model, Glen Court House to the River Usk.	229
Figure 7-11	Head distribution along row 1; for east flank models.	230
Figure 7-12	Geological setting for MODFLOW Regional model domain.	233
Figure 7-13	Conceptual boundary conditions in plan and profile for Regional model.	234
Figure 7-14	Realisation of the rivers and major mapped faults in the area.	236
Figure 7-15	Realisation of the ground to the Regional model surface.	237

Figure 7-16 MODFLOW Layer 3 groundwater direction vectors for whole model domain.	242
Figure 7-17 Sensitivity analysis graph in Raglan Mudstone Formation for no-flow boundary condition.	244
Figure 7-18 MODFLOW Layer 3 groundwater direction vectors for whole no-flow boundary model domain.	246
Figure 7-19 MODFLOW Flowlines for no-flow boundary condition superimposed on DTM.	247
Figure 7-20 MODFLOW realisation of the local area with the Local model domain.	250
Figure 7-21 Conceptual boundary conditions for local model.	251
Figure 7-22 MODFLOW Flowlines for local specified head condition boundary superimposed on DTM.	255
Figure 7-23 MODFLOW particle tracking.	256
Figure 7-24 MODFLOW Flowlines for no-flow boundary head condition boundary superimposed on DTM.	261
Figure 7-25 Refined geochemical conceptual model of the Usk Valley.	264
Figure 7-26 MODFLOW, larger scale model of western locations.	267
Figure 7-27 MODFLOW, recharge species in valley area layer 1.	268
Figure 7-28 MODFLOW, recharge and constant source term species plume profiles.	269
Figure 7-29 MODFLOW, seasonal recharge source term simulations.	271
Figure 7-30 MODFLOW seasonal recharge source term simulation profile views through Pencarreg Farm Borehole.	273
Figure 7-31 MODFLOW, equidistant path lines to Pencarreg Farm Borehole.	274
Figure 7-32 Distance v Time graph for particles released at surface to travel to PENC borehole.	275
Figure 7-33 Pseudo breakthrough curves for non-sorbing conservative species at three different observation Boreholes.	278
Figure 7-34 Autocorrelation of model species concentration output.	280
Figure 7-35 Breakthrough curves for groundwater SRP as a function of areal extent and concentration.	282

Figure 8-1 Eden Valley location maps.	287
Figure 8-2 Geological map, of the Vale of Eden and surrounding stratigraphy.	288
Figure 8-3 Stratigraphic column of main geological units in the study area.	289
Figure 8-4 Schematic cross section based on BGS map sheet 24 Penrith.	290
Figure 8-5 Till over Glacial sands and gravels at Bonniemount Quarry.	291
Figure 8-6 Massive dune bedding at Cowraik Quarry.	293
Figure 8-7 Penrith Sandstone core plugs.	294
Figure 8-8 Major faults and locations of the high fells area north of Penrith.	295
Figure 8-9 Fracture patterns in well-cemented competent Penrith Sandstone at Cowraik Quarry.	296
Figure 8-10 Friable sands below hard bands at Bowman's Quarry.	297
Figure 8-11 General lithological sequence in northern and plateau zones of Penrith Sandstone.	298
Figure 8-12 Blocky weathered zone above more competent hard bands at Bowscar Quarry.	299
Figure 8-13 Surface water features: Major tributaries of the River Eden.	303
Figure 8-14 Surface ponds and bogs.	304
Figure 8-15 Groundwater contours.	306
Figure 8-16 Soils map of Eden Valley.	310
Figure 8-17 Conceptual diagram of Eden Valley Hydrogeology and agricultural inputs.	313
Figure 8-18 EA monitoring borehole location and geology map.	315
Figure 8-19 Type hydrographs as identified by Streetly and Chillingworth.	316
Figure 8-20 C type hydrographs for Eden Valley.	319
Figure 8-21 A and B Type hydrographs.	320
Figure 8-22 Selection of autocorrelation and partial autocorrelation (PACF) plots for the Type hydrographs.	323
Figure 8-23 Selected spectral analysis plots for Type Hydrographs.	327
Figure 8-24 Seasonal conceptual model to illustrate rapid movement of recharge to the water table.	333
Figure 8-25 Schematic of potential cascade effect through the unsaturated zone.	334
Figure 8-26 The effect of fissure density and storativity on a local area.	337
Figure 8-27 Eh-pH data for Eden Valley samples.	339

## **Glossary and abbreviations**

A glossary of terms and acronyms used in this thesis are detailed in table I. A list of phosphorus nomenclature is also at Table 2-1

Table I Glossary of abbreviations

Abbreviation	Meaning	Remarks
ACF	Autocorrelation factor	
BGS	British Geological Survey	
BH	Borehole	Generic to included wells
Br	Brook	
CCF	Cross correlation factor	
CEH	Centre for Ecology and Hydrology	
DEFRA	Department for Environment, Food and Rural Affairs	
df	Degrees of freedom	
ESEM	Environmental scanning electron microscope	
Fm	Formation	Geological unit
GPS	Global positioning system	
GR	National Grid Reference	
IC	Ion Chromatography	
ICP-MS	Induced coupled plasma-mass spectrometry	
Ls	Limestone	
N (n)	Number of analysis pairs	
p<0.05	Estimated probability type I error	95%
PACF	Partial auto correlation factor	
PWS	Public water supply	
R <sup>2</sup> or (r <sup>2</sup> )	Correlation coefficient	
Ss	Sandstone	
USGS	United States Geological Survey	

## Chapter 1 Introduction

### 1.1 Background

Phosphorus is a ubiquitous element in the environment. It does not occur naturally as pure phosphorus, but as organic and inorganic phosphate compounds. In recent years phosphorus has been the subject of increased environmental research. This is perhaps due, in part, to it being associated with its accessory macro nutrient nitrate; with their relationship governed by provenance, use and prevailing environmental conditions. Together these nutrients can cause 'down stream' environmental and drinking water quality issues. Due to its normally low concentrations phosphorus is not considered a drinking water contaminant of concern.

A literature search indicates that phosphorus in groundwater has not been historically well studied, recent review papers deal with surface water environments (Jarvie et al. 2002; Heathwaite et al. 2005b). Past studies were predominantly concerned with agricultural run off to field drains and rivers, surface water bodies and soil retention. Therefore significant gaps exist in our knowledge about the behaviour of phosphorus in the groundwater compartment. This research shortfall is beginning to be addressed, with more studies being conducted both domestically and worldwide. In the United Kingdom the Environment Agency (EA), the Centre for Ecology and Hydrology (CEH), the Department for Environment, Food and Rural Affairs (DEFRA), and other bodies are supporting research. The state of knowledge within the UK can be summed up by the following taken from the executive summary of a government sponsored report and a synopsis from a related data source:

“[The] Literature review suggests that anthropogenic sources which may pose P leaching risks to groundwater include accumulation of soil P levels as a consequence of long-term over-fertilization of arable and grassland; manure heaps & unlined slurry storage facilities; leaking mains water pipes and sewers and septic tank discharges” (SNIFFER 2008).

“Significant uncertainty remains in defining natural background concentrations of phosphorus in groundwater, given the limitations of the available data on groundwater quality, aquifer properties (especially mineralogy) and P sources” (SNIFFER 2008).

“The United Kingdom Technical Advisory Group Groundwater Task Team have identified limitations in knowledge relating to understanding the origin (natural and anthropogenic), fate and transport of phosphorus within the sub-surface and in groundwater, with particular regard to the potential impact on dependent surface waters and terrestrial ecosystems” (Holman et al. 2008).

## **1.2 Aims and objectives**

The aims of the project are to investigate the fate and transport of phosphorus in groundwater. This will be achieved by a systematic investigation of phosphorus in an agricultural setting (Figure 1-1). The project is based in two distinct agricultural regions of the UK. The main study site is part of the Lower Usk Valley Monmouthshire. This is complimented by a case study in the Eden Valley, Cumbria.

The scientific questions that this thesis addresses are:

- Is the amount of phosphorus in the groundwater at a significant level relative to EQS?
- What is its distribution?
- What are the sources of the phosphorus and are they measurable?

The aims of the project are to

- Investigation of the spatial and temporal occurrence of groundwater phosphate in the project areas.
- Investigation of phosphorus in the soil zone, which is the point of contact for local groundwater recharge.

The objectives of the investigation are to:

- Establish the physical relationships between observed parameters within the project area to characterise aquifer transport mechanisms.

- Establish relationships between the geochemical species and identify processes that may link them to the transport mechanisms.
- Model the results to obtain a better conceptual understanding of the geo-physical processes operating within the project areas.
- To address research gaps dealing with phosphorus in groundwater and its significance for environmental receptors.

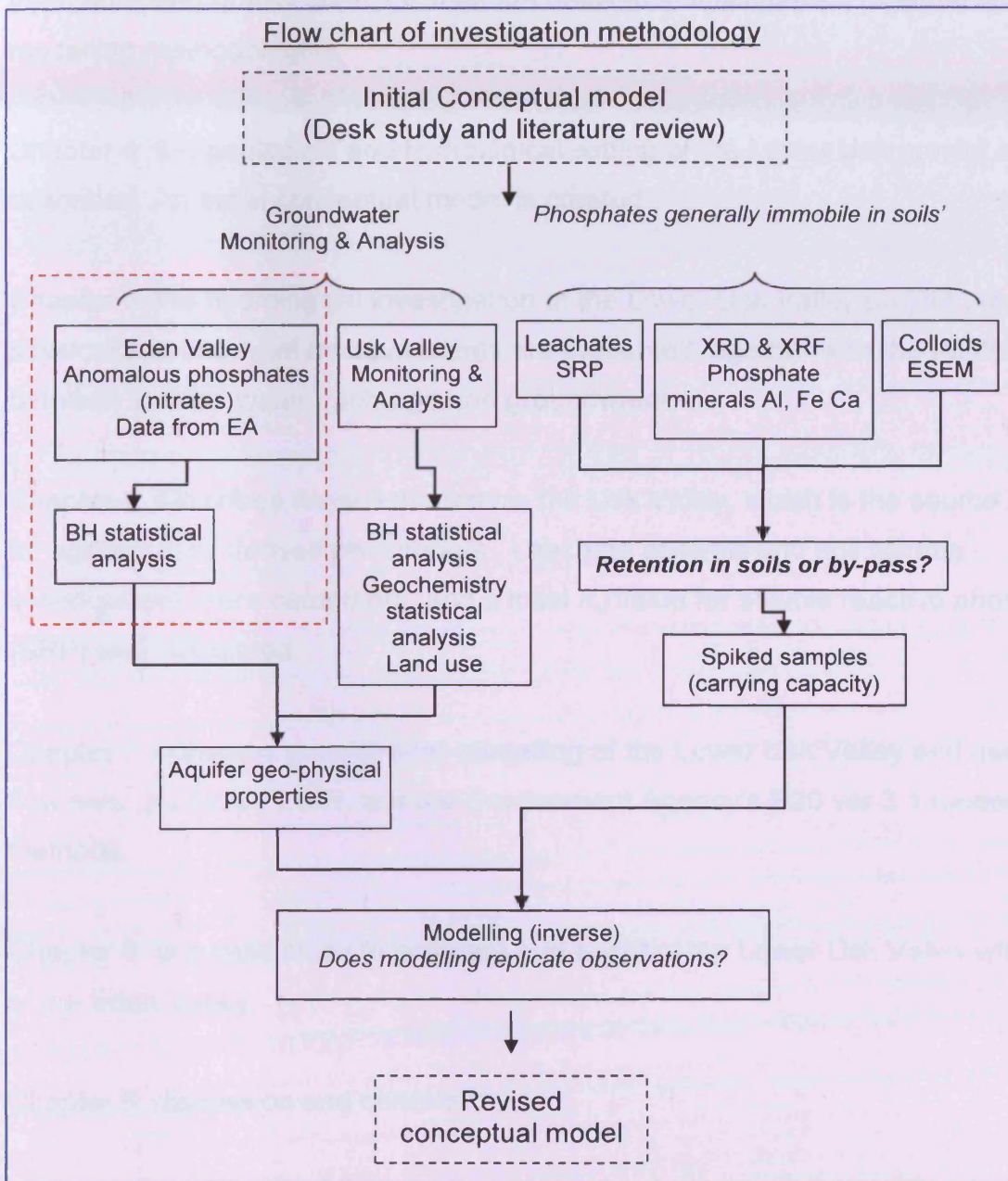


Figure 1-1 Flow chart of methodology to be adapted during project investigation. Note red outlined square indicates re-analysis of existing data.

### **1.3 Thesis outline**

Chapter 2: a literature review dealing with the occurrence of phosphorus, known chemical species relationships, nomenclature and analytical methods.

Chapter 3: the field and laboratory technical methods are described. Analysis of the results and quality control issues are detailed in this chapter, together with the modelling methodologies.

Chapter 4: the geological and hydrological setting of the Lower Usk project area is described. An initial conceptual model is created.

Chapter 5: the hydrological investigation of the Lower Usk Valley project area. The physical and chemical measurements are presented together with the relationships between surface water, recharge and groundwater.

Chapter 6: describes the soil analysis in the Usk Valley, which is the source zone for agriculturally derived phosphorus. Leachate analysis and soil column investigations were carried out, and a local  $K_d$  value for soluble reactive phosphorus (SRP) was calculated.

Chapter 7: concerns groundwater modelling of the Lower Usk Valley and uses 2D flow nets, 3D MODFLOW, and the Environment Agency's P20 ver 3.1 modelling methods.

Chapter 8: is a case study to compare and contrast the Lower Usk Valley with that of the Eden Valley.

Chapter 9: discussion and conclusion.

## Chapter 2 Literature review

### 2.1 Introduction

#### 2.1.1 Background

Phosphorus is a highly reactive non-metal element; it is also a macronutrient essential for healthy growth and vitality. Due to its high reactivity it does not occur in its elemental state, but may be found as the orthophosphate ion  $P_yO_4^{x-}$ ; a phosphorus atom bonded to four oxygen atoms, the exact form dependent upon local environmental chemistry. The most common forms are  $H_2PO_4^-$ ;  $HPO_4^{2-}$  and  $PO_4^{3-}$  with the dominant ion controlled by local pH conditions. It is in these soluble forms that phosphorus is most readily available for plant uptake. Phosphorus is considered to be the limiting nutrient in freshwater aquatic ecosystems and soils, but not in marine systems due to its greater abundance in this compartment (Heathwaite et al. 2005a; Griffioen 2006). Excess phosphorus in a system may lift the capacity of an ecosystem to the next limiting factor, for example. carbon, light or another nutrient (Reynolds and Davies 2001).

Despite being the eleventh most abundant element, phosphorus tends to form localised marine sedimentary deposits of economic importance (Krauskopff and Bird 1995). These geological deposits occur as apatite (a phosphate rock) mainly consisting of an insoluble calcium phosphate mineral  $Ca_3(PO_4)_2 X$ , where X may be OH, F or Cl. The Ca can also be substituted by Mn, Sr and Y. Due to the general insolubility of these apatite minerals they require processing with sulphuric or phosphoric acids to manufacture fertilizers, which incidentally may remove the micro nutrients. Phosphorus can also occur in more acidic conditions as an iron or aluminium phosphate mineral. Current levels of exploitation of phosphate reserves are leading to a shortage that may become critical in two or three generations (Krauskopff and Bird 1995; NHM 1998; Manahan 2005).

Phosphorus is found in both inorganic and organic compounds. Inorganic forms include phosphate minerals, and compounds such as phosphoric acid ( $H_3PO_4$ ). Organic phosphorus compounds are contained within living tissue and also bonded to organic carbon compounds by a carbon-phosphorus bond (C-P).

Manufactured organophosphates have wide applications as veterinary ectoparasiticides, flame retardants, and more insidiously as the nerve gases Sarin and Tabun. The amount of phosphorus in a soil may be relatively high, but in an immobile form. The soil may only release the phosphorus slowly or in insufficient quantity to support rapid (seasonal) high yield plant growth, (Schachtman et al. 1998).

As an essential macronutrient, phosphorus is therefore added to soils as a fertiliser; traditionally through animal and human manures, and with industrialisation by man-made mineral-derived fertilisers. The later also contain, depending upon the fertiliser mix, other nutrients and elements such as N, K, Cl and trace elements. At the time of writing (July 09) the cost of mineral fertilisers is rising and their use is becoming more prohibitive with reliance, where practical, on animal manures (Pers. Comm., N. Bowyer, local farmer).

Excess phosphate applied to agricultural land can become attached to soil particles with subsequent erosion or run-off potential to surface water. Due to its high sorption affinity these erosion losses occur mainly during the winter (DEFRA 2002). Once in a surface water body phosphorus is available to plants and phytoplankton in the dissolved orthophosphate phase, where an excess may contribute towards eutrophication in still water bodies. This tends to be in the form of algal blooms and cyanobacteria that can cause environmental damage, including lowering of dissolved oxygen levels and drinking water quality issues. Phosphorus also costs the water industry millions of pounds in cleaning-up effected water bodies, such as removal of scums and toxins released by cyanobacteria; (WHO 2002). Cell rupture of cyanobacteria can release toxins into the water which have caused deaths to humans in Brazil and severe illness in the UK (Howard 1994).

Phosphates are generally considered to be immobile in soils, this is in part due to low solubility, and they also tend to have good soil sorption capacities. However, "all soils have a critical point where phosphate load exceeds the adsorption capacity" (Heredia and Fernandez Cirelli 2007), and recent research has shown that phosphorus will "move(s) downward under certain conditions" (Shuman 2003).

### 2.1.2 **Environmental pathways**

Owing to its occurrence and uses, phosphate can be found in increasing concentrations above normal environmental background levels. The two main users are agriculture and industry. In 2002 over 40% of phosphates found in English [surface] waters originated from agricultural land (Hansard 2002).

#### Agriculture

Phosphates are added to soils to increase productivity, and excess can be considered as a diffuse pollution source. Within the European Union the Nitrates Directive (96/676/EEC) and Codes of Good Agricultural Practice (DEFRA 2007) stipulate that manures may only be applied at distinct times as a function of crop and soil type. The result is the requirement to store excess manures and slurries in lagoons or mounds (Figure 2-1). These may act as pollution point sources, and if injudiciously situated upon thin soils and fractured bedrock they may provide point sources for migration to the water table as well as overland flow. However Goody (Pers. comm) suggests that the subsurface of soil-based lagoons tend to be clogged due to the waxy nature of the slurry, and thus can impede the vertical movement of contaminants.



*Figure 2-1 Manure storage on fractured bedrock, Eden Valley Cumbria. Photo A Gray*

The application of organophosphate herbicides and insecticides such as Diazinon will also provide a diffuse source potential. Previous incorrect disposal has been known to cause legacy problems (Boxall et al. 2002). Advancements in knowledge and recent legislation have decreased the environmental impacts and potency of these chemicals; however, due mainly to costs, the use of banned compounds in the developed world still persists.

Other point sources may include mineral fertiliser storage areas and spillage (Figure 2-2). After applications of agricultural chemicals the wash-down residue from agricultural machinery may either runoff to surface water or local soak-aways. Desiccation cracks in swelling clays (smectite), worm holes, root channels and drift-free fractured bedrock may all provided preferential pathways to the unsaturated zone, by-passing potentially sorbing soil organic material.



Figure 2-2 Mineral fertiliser bales, Eden Valley. Photo A. Gray.

Due to the presence of phosphorus from diffuse agricultural pollution the current estimates for water treatment costs in the UK is approximately £55 million year<sup>-1</sup>; compared to that of nitrate which is £16 million year<sup>-1</sup> for waters exceeding the drinking water standards of 50mg NO<sub>3</sub><sup>-</sup> (DEFRA 2002).

### Urban waste water

Urban waste water comprises a variety of sources; it may be sewage (black water), domestic waste (grey water), storm drainage or any combination. It is also subject to its own legislation, European Directive 91/271/EEC. One of the Directive's aims, dependent upon sensitivity classification, is to reduce the flux of phosphorus to receiving waters. The waste water can contain amongst other species, organic phosphorus material from sewage and food preparation (mainly industrial), and phosphates from detergents and inappropriate disposal of domestic herbicides and other products.

Historically phosphates have been used in detergents and other industrial uses such as in boilers as a water softener by ion exchange processes (Manahan 2005). Sodium tripolyphosphate ( $\text{Na}_5\text{P}_3\text{O}_{10}$ ) a polyphosphate has amongst others been used in detergents and cleaning products; it is therefore soluble and hydrolysis can lead to the liberation of phosphate ions in receiving waters.

The use of ion exchange zeolites is increasingly being used as an alternative to phosphate. Domestic detergents available from supermarkets contain about 5% phosphonate, which is an organic phosphorus chelating agent. Human urine represents 1% of urban wastewater, but contributes approximately 45% of phosphate loading to wastewater (Lawton 2006).

## 2.2 Phosphorus chemistry

### 2.2.1 Phosphate geochemistry

#### General

Phosphorus is in group 15 of the periodic table. It has an atomic No 15 and mass 30.97g/mol, and is the eleventh most abundant element in the crust. It has an oxidation state of +5 ( $P^{5+}$ ), although in organophosphorus compounds the range -3 to +5 has been observed, the most common being +5, +3 and -3. It forms compounds with many elements, hydrides, chlorides, bromides, oxides, sulphides. A schematic diagram Figure 2-3 shows the basic phosphorus cycle.

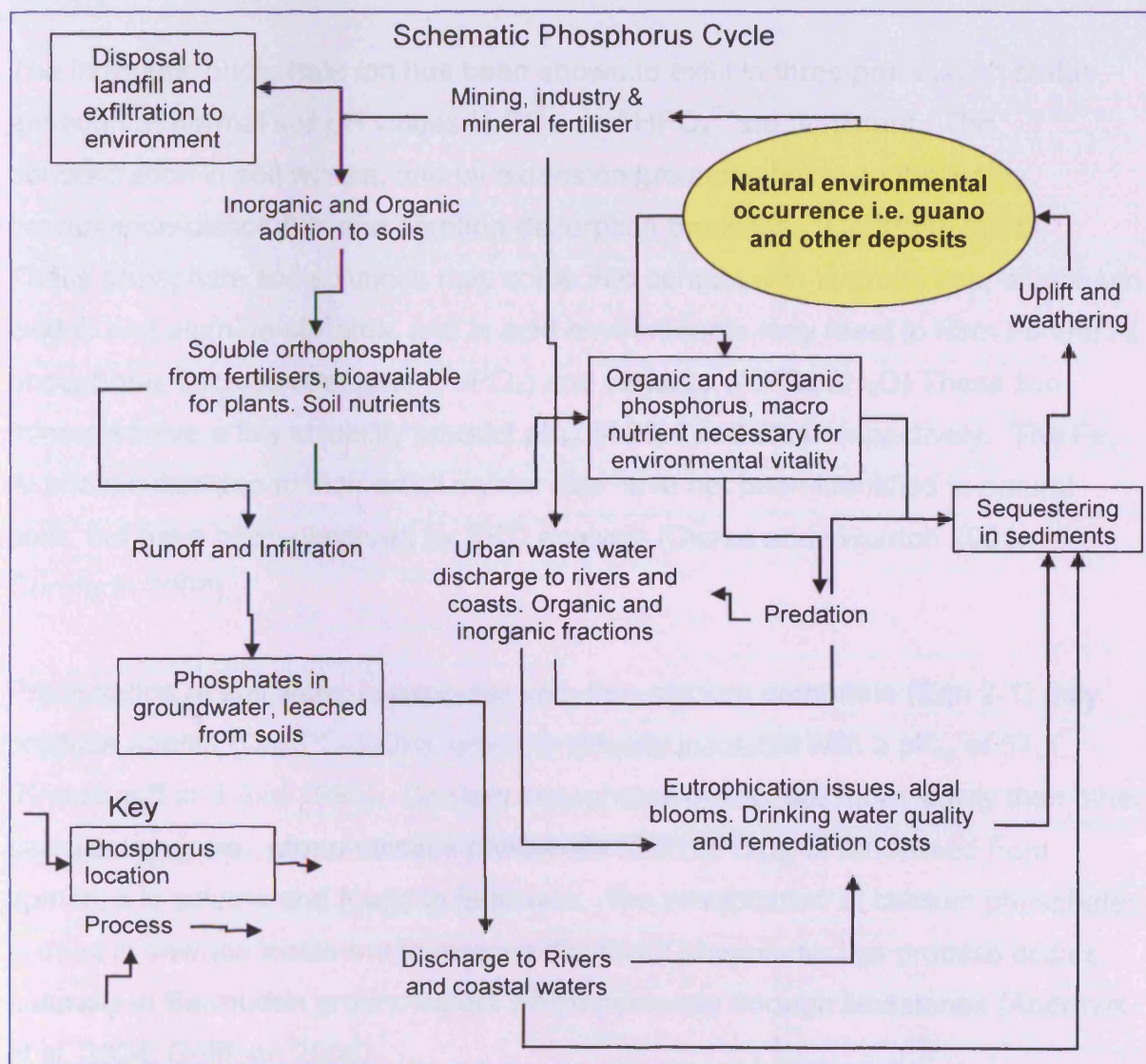


Figure 2-3 Schematic phosphorus cycle. Adapted from (Krauskopff and Bird 1995; Skelton 2003; Manahan 2005).

### Soil phosphorus

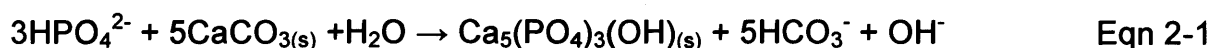
Sedimentary phosphorus consists of the following (Manahan 2005; Weiner 2008):

- Mineral phosphate, apatite or non-apatite
- Non-occluded, where the orthophosphate ion is bound to the surface of another molecule such as SiO<sub>2</sub> or CaCO<sub>3</sub>, and is generally more soluble and available than apatite.
- Occluded, where phosphate ions are absorbed or contained within the matrix of hydrated iron and aluminium oxides and aluminosilicates. This form is not as readily available as the non-occluded phosphorus.
- Detrital organic phosphorus.

The inorganic phosphate ion has been shown to exist in three protonation states, although at normal soil pH values H<sub>2</sub>PO<sub>4</sub><sup>-</sup> and HPO<sub>4</sub><sup>2-</sup> are dominant. The concentration in soil waters, and by extension groundwater, is controlled by precipitation-dissolution and sorption-desorption processes (Cornforth 2008).

These phosphate soil solutions may come into contact with hydrous iron, aluminium oxides and alumino-silicates, and in acid environments may react to form Fe and Al phosphates such as strengite, (FePO<sub>4</sub>) and variscite (AlPO<sub>4</sub> 2H<sub>2</sub>O) These two minerals have a low solubility product pK<sub>sp</sub> of 26.4 and 22.1 respectively. The Fe, Al phosphates due to their small crystal size have not been identified in natural soils, but have been observed by XRD analysis (Clarke and Wharton 2001; Cornforth 2008).

Precipitation of soil water phosphates with free calcium carbonate (Eqn 2-1) may produce apatite (Ca<sub>5</sub>(PO<sub>4</sub>)<sub>3</sub>OH), which is virtually insoluble with a pK<sub>sp</sub> of 57.8 (Krauskopff and Bird 1995). Calcium phosphates precipitate more slowly than other chemical species. Mono-calcium phosphate (Ca(H<sub>2</sub>PO<sub>4</sub>)<sub>2</sub>) is processed from apatite; it is soluble and found in fertilisers. The precipitation of calcium phosphates is used in sewage treatment to remove dissolved phosphate; this process occurs naturally in Bermudan groundwaters which percolate through limestones (Andrews et al. 2004; Griffioen 2006).



Soil lithology also controls the sorption ability of soluble phosphate; work on peaty and high organic matter (OM) soils in Ireland have shown that there was a negative correlation with phosphate sorption compared with mineral soils (Daly et al. 2001). It is believed that organic acids from the high OM soils block sorption sites. In addition there may be less potential Fe and Al hydroxides sorption sites in these peaty soils, allowing greater levels of phosphate mobilisation and a greater potential to migrate to groundwater. Additionally if these peaty soils are drained, this will allow greater mineralisation of organic phosphorus as oxygen enters the soil (Daly et al. 2001).

### Sorption

Sorption is a generic term which encompasses three distinct processes, adsorption, absorption, and surface precipitation (epitaxial overgrowth). The phosphate anion will displace a  $\text{OH}_2$  or  $\text{OH}^-$  from the surface of a metal oxide, form an electrostatic bond with the oxide and be taken up from solution, thus lowering the soil water concentration. These reactions do exhibit a pH, concentration and temperature dependence. Mustafa et al (2003) have shown that sorption of  $\text{H}_2\text{PO}_4^-$  and  $\text{HPO}_4^{2-}$  which replace  $\text{OH}^-$  from iron hydroxide  $\text{Fe}(\text{OH})_3$  increases with temperature and concentration. If the sorbed phosphate anion subsequently diffuses into the metal oxide it is considered to be absorbed. The rate or degree of sorption and desorption is controlled by environmental parameters, these rates can be measured and distinct linear or non-linear isotherms are observed (Stumm and Morgan 1996; Fetter 2004; Appelo and Postma 2005; Hiscock 2005; Cornforth 2008).

## **2.2.2 Phosphate geochemistry relationships**

### Species associations

#### *Dissolved oxygen*

Weak inverse relationships have been shown to exist with soluble reactive phosphorus and dissolved oxygen (DO) levels ( $r^2=0.10$ ,  $p<0.001$ ) (Carlyle and Hill 2001). The authors admit that there may be some sampling issues affecting the results. Zones of denitrification with reduced  $\text{O}_2$  levels may therefore release soluble phosphates.

### *Iron*

Several studies, such as on the River Boyne in Canada have shown that the microbial reduction of ferric iron ( $\text{Fe}^{3+}$ ) to ferrous ( $\text{Fe}^{2+}$ ) is linked with increasing dissolved phosphorus (Carlyle and Hill 2001). A weak positive linear relationship was observed between soluble reactive phosphorus and ferrous (II) iron ( $r^2 = 0.24$ ,  $p < 0.001$ ).

A further caveat to the study spatially fixes the iron reduction zone and increased soluble reactive phosphorus beyond the denitrification zone. Studies of North American lakes indicate that there may be constant relationships between the phosphorus fractions regardless of the alkalinity or trophic status (Carlyle and Hill 2001). This was believed to be due to the presence of iron controlling the sediment phosphorus concentration. Oxidation of ferrous iron was also shown to lower the concentration of soluble reactive phosphorus due to the adsorption of phosphate ions to the ferric oxy-hydroxides. This reaction has been observed in exfiltrating groundwater and is described as a fast reaction, occurring within hours at near neutral pH and when oxygen is not limiting. However, immobilisation of phosphate during aeration of waters cannot be solely attributed to adsorption binding to a ferric oxide phase. High iron content in a sample is reported as having the potential to cause precipitation, subsequent loss and false low measurements of the sample concentration (Carlyle and Hill 2001)

### *Nitrate*

Phosphates are commonly associated with nitrate, which is the major accessory nutrient in fertilisers and species of concern in its own (Butcher et al. 2003). Nitrate is highly soluble and mobile whilst phosphates tend not to be. A study on chalk (Goody et al. 1998) has shown that slurry from a lagoon can rapidly penetrate the unsaturated zone by fissure flow, and indicates that in one borehole total phosphorus (TP) increases with depth while nitrate decreases. The borehole geochemistry of the Eden Valley indicates that the occurrence of high nitrate boreholes does not always correspond with high phosphorus (Gray 2006).

### Dissociation – environmental dominance

In acidic solution environments the principal phosphate ion will be  $\text{H}_2\text{PO}_4^-$  (aq) (dihydrogen phosphate). In neutral conditions at pH 7.2 the  $\text{HPO}_4^{2-}$  (aq) ion is the major ion present, while at pH over 12.4 the unhydrolysed ion  $\text{PO}_4^{3-}$  (aq) dominates (Figure 2-4).

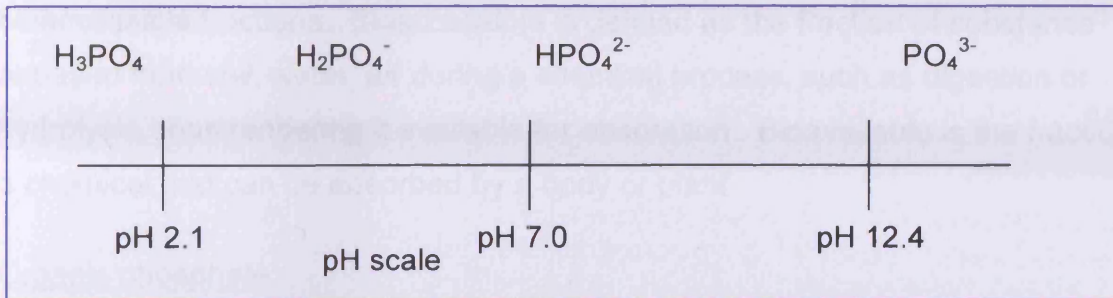


Figure 2-4 Diagram to show dominant phosphate species in relation to pH scale , (Krauskopff and Bird 1995; Andrews et al. 2004).

### 2.2.3 Phosphate hierarchy

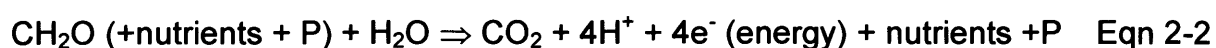
Phosphorus occurs in the environment as either organic or inorganic forms including biomass (Figure 2-5). The inorganic form has two associations based upon environmental pH and mineralogy. It may exist as dissolved or particulate phases and there is a continuum and interaction within the forms which makes measurement of the fractions difficult. The total phosphorus pool (TP) consists of the following various fractions (Haygarth and Jarvis 1997; Jarvie et al. 2002; Heathwaite et al. 2005b):

- Labile phosphorus, which is loosely bound.
- Phosphorus associated with aluminium, iron, and manganese oxides and hydroxides.
- Calcium associated phosphorus.
- Organic phosphorus.
- Residual phosphorus, which is mainly organic phosphorus.

The labile phosphorus, Al, Fe and Mn oxyhydrates are also known as non-apatite inorganic phosphorus (NAIP), while the calcium associated fraction is named apatite phosphorus (AP) with a formula:  $\text{Ca}_3(\text{PO}_4)_2(\text{X})$ . Non-apatite inorganic phosphorus and part of the organic fraction have the greatest potential to release phosphorus to sediments and are thus the most environmentally important bioaccessible fractions. Bioaccessible is defined as the fraction of substance released from soil, water, air during a chemical process, such as digestion or hydrolysis, thus rendering it available for absorption. Bioavailable is the fraction of a chemical that can be absorbed by a body or plant.

### Organic phosphate

This is phosphate that is bound to plant or animal tissue, and is formed by biological processes, such as plant uptake of dissolved phosphate ions and higher life forms eating plant and animal tissue. Organic phosphate is often associated with the non-reactive, non-bioavailable fraction of total phosphorus. Thus a soil may contain organic phosphate in the form of soil biota and humic material as part of its total phosphorus budget. Degradation (hydrolysis) of organic phosphorus, specifically organic matter from wetlands, moors and bogs, will produce bioaccessible inorganic phosphate ions (Eqn 2-2);  $\text{HPO}_4^{2-}(\text{aq})$ ,  $\text{H}_2\text{PO}_4^-(\text{aq})$  and  $\text{PO}_4^{3-}(\text{aq})$  (Krauskopff and Bird 1995; Griffioen 2006).



Organic phosphorus contains C-P, C-O-P and P-O-P bonds, although the C-P bond is less well reported and is very resistant to hydrolysis and oxidation (Worsfold et al. 2005). Two main classes of organic phosphorus appear to predominate in natural waters. These are low and large molecular weight compounds. The low weight is believed to originate from bacterial and algal metabolism. The high weight compounds are believed to be bound in humic complexes or acids which degrade in UV light releasing orthophosphate (Carlson and Simpson 1996).

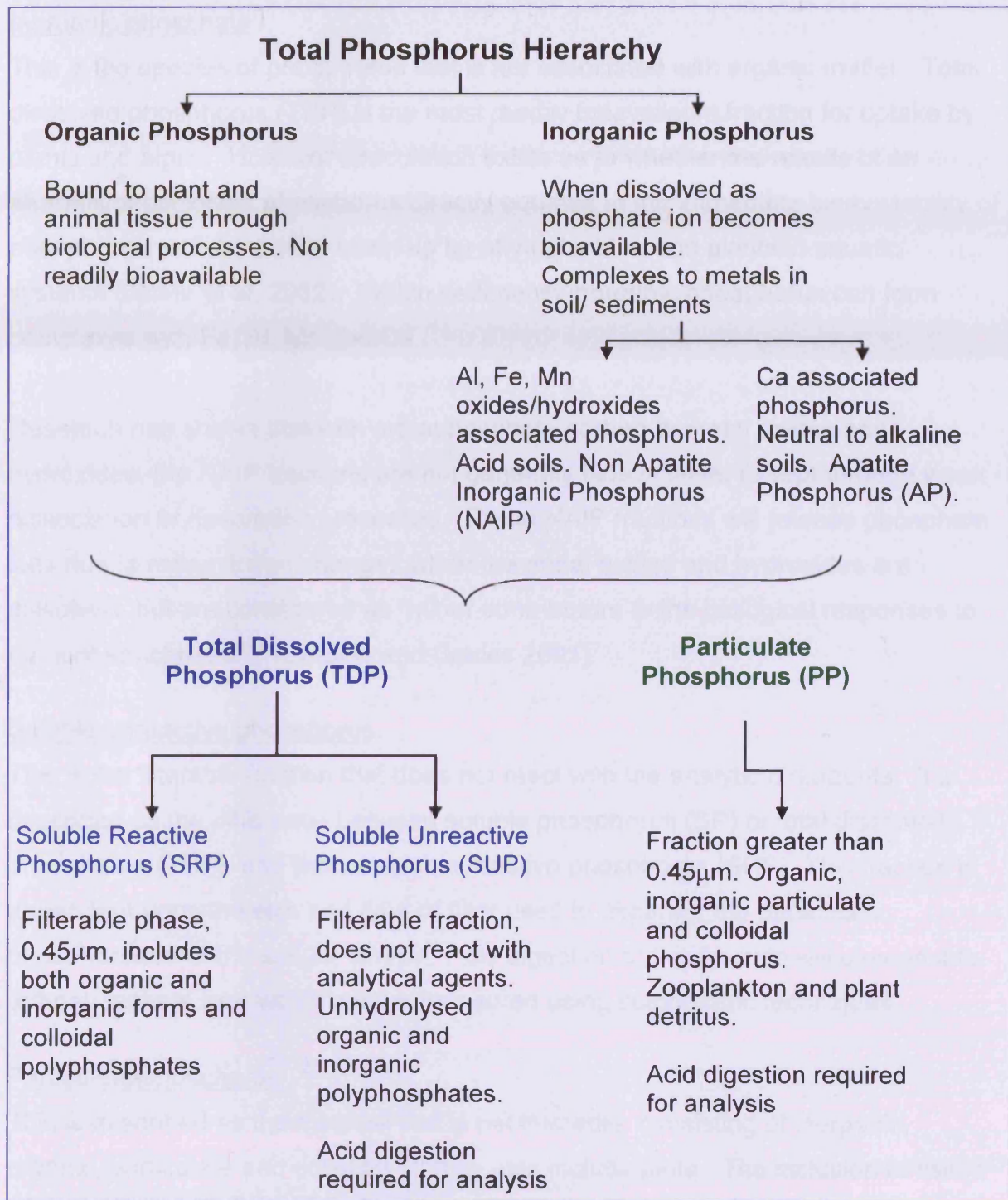


Figure 2-5 Diagram of phosphorus hierarchy, adapted from (Worsfold et al. 2005).

### Inorganic phosphate

This is the species of phosphorus that is not associated with organic matter. Total dissolved phosphorus (TDP) is the most readily bioavailable fraction for uptake by plants and algae. However speculation exists as to whether the results of an analysis of dissolved phosphorus directly equates to the immediate bioavailability of phosphorus, which may be taken up by phytoplankton and plants in aquatic systems (Jarvie et al. 2002). Within sediments inorganic phosphorus can form complexes with Fe, Al, Mn and Ca.

Research has shown that with orthophosphate sorbed to metal oxides and hydroxides, the NAIP fractions are not generally bioavailable, except through weak dissociation or desorption processes. These NAIP fractions will release phosphate ions due to redox driven changes when the metal oxides and hydroxides are dissolved, but are considered as “minor contributors to the biological responses to nutrient enrichment” (Reynolds and Davies 2001).

### Soluble unreactive phosphorus

This is the filterable fraction that does not react with the analytical reagents. It is described as the difference between soluble phosphorus (SP) or total dissolved phosphorus (TDP), and that of soluble reactive phosphorus (SRP). This fraction is dependent upon the size and type of filter used to separate the particulate phosphorus from the soluble phase. Acid digestion of this fraction will change it to orthophosphate ions which can be measured using colorimetric techniques.

### Particulate phosphorus

This is described as the material that is not filterable, consisting of inorganic, organic, particulate and colloidal. It may also include biota. The inclusion of tissue phosphorus in studies is questionable due to sampling problems; however in closed systems this fraction can be recycled. The distinction between dissolved (soluble) and particulate fractions is based on separation through a 0.45µm filter, which is somewhat arbitrary, but is considered convenient and provides reproducible results (Robards et al. 1994). As a general rule the filtered size should be quoted (Jarvie et al. 2002).

### Soluble reactive phosphorus (SRP)

This fraction has previously been called dissolved inorganic phosphorus. The new nomenclature, SRP, is believed to reflect a more realistic description as the filterable phase of this sample was not necessarily dissolved or inorganic (Jarvie et al. 2002). 'Reactive' indicates that this fraction will react directly with analytical reagents, and can include both inorganic and organic forms. This is due to the fact that some organic forms may hydrolyse, and some inorganic polyphosphates do not react with the analytical reagents. Uncertainty exists as to whether the soluble reactive phosphorus represents the ortho-form or is biologically available (Jarvie et al. 2002). The soluble fraction may also contain colloidal phosphorus and any labile and organic phosphate which is hydrolysed during determinations.

The most biological available forms of phosphorus are found in solution as the orthophosphate ion, and coincide well with measurable soluble reactive phosphorus. SRP is also defined as the fraction of a sample that passes through a 0.45 $\mu$ m filter, and which will react with the molybdate blue reagent or molybdate-reactive phosphorus (MRP). SRP is considered 'to define that orthophosphate which is readily available for biological uptake' (Nurnberg 1984; Worsfold et al. 2005). However Jones (1992) in Haygarth et al (1997), indicates that the free [soluble] orthophosphate only represented a fraction of the total determined as MRP.

"The terms dissolved and soluble phosphorus are conventionally used to denote that portion of species that are operationally separated by filtration through a defined pore size (usually 0.45 $\mu$ m or 0.2 $\mu$ m). However it is widely recognised that the filterable fraction also includes high molecular mass colloidal species. Use of the term filterable is therefore preferable to either dissolved or soluble, which imply the presence of pure solution" (McKelvie 2005). "Filtration through a 0.45 $\mu$ m membrane filter separates dissolved from suspended forms of phosphorus. No claim is made that filtration through a 0.45 $\mu$ m filter is a true separation of suspended and dissolved forms of phosphorus; it is merely a convenient and replicable analytical technique designed to make a defined separation (APHA 1999).

### 2.3 Phosphorus in groundwater

Phosphorus containing compounds that are pertinent to water quality include the following (Haygarth et al. 1997; Jarvie et al. 2002):

- Orthophosphates
- Polyphosphates or condensed (dehydrated) phosphates
- Organic phosphate; biodegradation or oxidation releases orthophosphate

The amount of phosphorus in surface and groundwaters will fluctuate with seasonal variation, infiltration or run-off, biological activity, and physical-chemical conditions. For example, within chalk catchments seasonal variations in pH affecting dissolved carbon dioxide ( $\text{DCO}_2$ ) influence the phosphorus concentration. These temporal variations also affect run-off and leaching potential.

#### Anion sorption

In clay minerals anion sorption is constrained to the mineral edge, rather than the surface, thus the anion exchange capacity (AEC) is significantly smaller than the cation exchange capacity (CEC). The sorption of anions is also a function of size and charge (Figure 2-6). Larger anions have a lower hydration which favours sorption; the accepted anion sorption sequence (van der Perk 2006) is:



Thus if phosphate ions are present it is most unlikely that nitrate and chloride will be sorbed, these latter ions are generally accepted to be conservative and non-sorbing in groundwater (Fitts 2002; Fetter 2004; Appelo and Postma 2005). Chloride and nitrate can however be sorbed to positive charged colloidal particles at low pH (Manahan 2005).

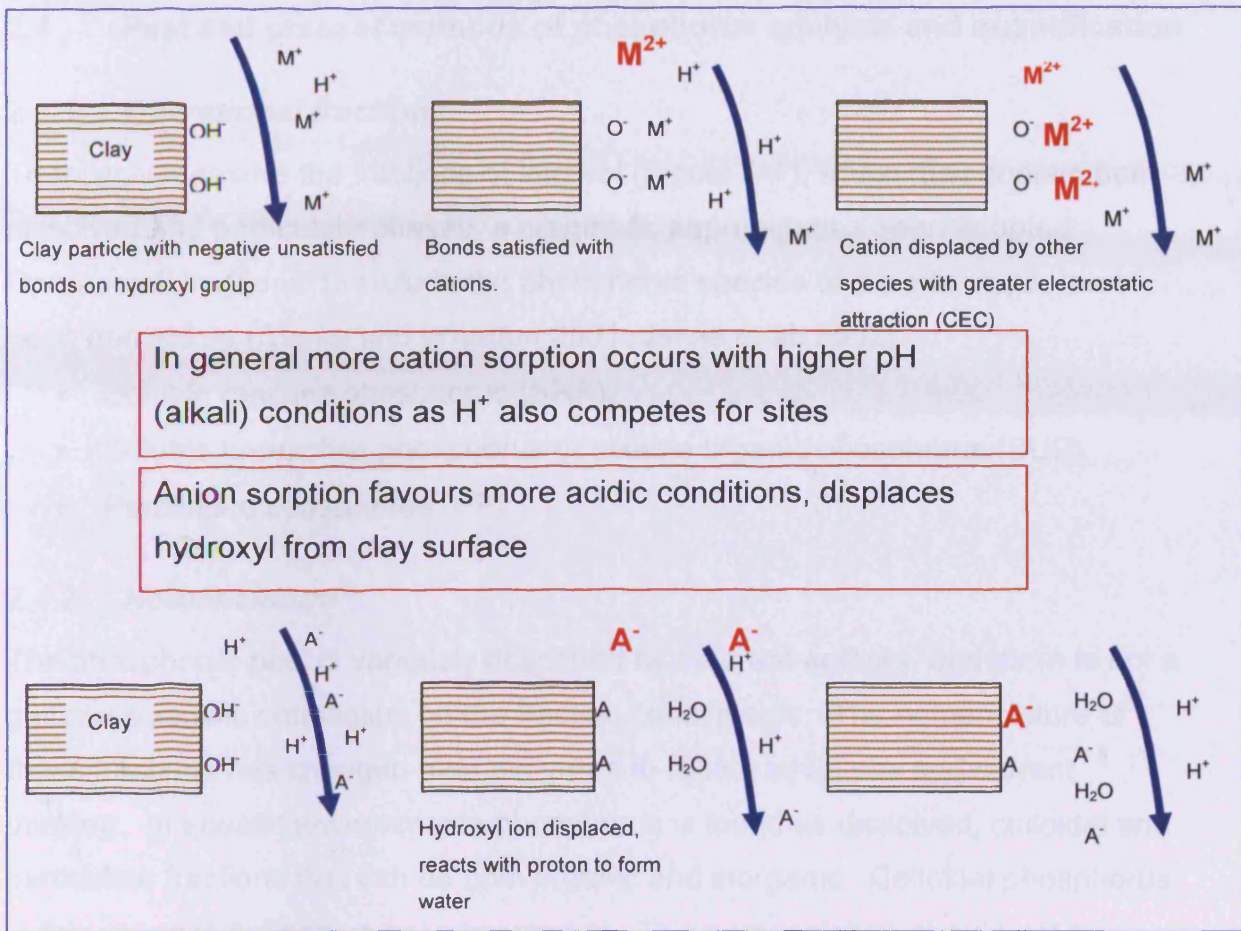


Figure 2-6 Schematic of sorption process. Thus phosphate sorption is more likely to favour acid conditions when surface charges are positive.

## 2.4 Past and present methods of phosphorus analysis and quantification

### 2.4.1 Operational fractions

To reliably measure the fractions of interest (Figure 2-7), which may contain both dissolved and particulate phases, a pragmatic approach has been adopted.

Operational fractions' to include the phosphorus species of a similar type, have been defined as (Clarke and Wharton 2001; Jarvie et al. 2002):

- Soluble reactive phosphorus (SRP).
- Soluble unreactive phosphorus or soluble organic phosphorus (SUP).
- Particulate phosphorus (PP).

### 2.4.2 Nomenclature

The phosphorus pool is variously described by different authors, and there is not a general scientific consensus on the fraction constituents. The nomenclature of these fractions has changed over the years to reflect advances and current thinking. In aquatic environments phosphorus is found as dissolved, colloidal and particulate fractions that can be both organic and inorganic. Colloidal phosphorus in this sense is defined as polyphosphates. This nomenclature should not be confused with colloids: fine particles  $<0.2\mu\text{m}$  which can be both organic and inorganic material such as clays with sorbed phosphorus.

The following acronyms (Table 2-1) are taken from Worsfold et al. (2005) and the Environment Agency data base. The table presents the various nomenclatures to describe the environmental species and fractions of phosphorus, note many acronyms describe the same fraction such as  $\text{DRP}=\text{FRP}=\text{SRP}$ . For consistency operational definition may stipulate that fraction which passes through a standard filter size. A particle size of  $0.45\mu\text{m}$  is usually adopted to distinguish between dissolved and particulate matter (van der Perk 2006).

**Table 2-1 Acronyms used in phosphorus hierarchy, after Worsfold et al. (2005) Note Environment Agency designations and data base species ID.**

Acronym	Meaning	Acronym	Meaning
DAHP	Dissolved acid hydrolysable phosphorus	SRP	Soluble reactive phosphorus
DOP	Dissolved organic phosphorus	SUP	Soluble unreactive phosphorus
DRP	Dissolved reactive phosphorus	TAHP	Total acid hydrolysable phosphorus
FRP	Filterable reactive phosphorus	TDP	Total dissolved phosphorus
MRP	Molybdate reactive phosphorus (SRP)	TOP	Total organic phosphorus
PAHP	Particulate acid hydrolysable phosphorus	TP	Total phosphorus
POP	Particulate organic phosphorus	TPP	Total particulate phosphorus
PRP	Particulate reactive phosphorus	TRP	Total reactive phosphorus
Environment Agency Designation		Meaning?	Data base ID
Orthophosphate as P		SRP	0180
Ortho phosphate dissolved		SUP?	0191
Phosphate		TDP	0192
Phosphorus total as P		TP	0348
Phosphate as P			9449

Jarvie et al (2002) indicate that MRP requires further classification. In filtered samples MRP is equivalent to SRP values, while in unfiltered samples MRP is the equivalent of SRP and a portion of the particulate fraction which is reactive to the phosphomolybdenum blue colorimetric determination. It is further stated that the "MRP determined on unfiltered samples is routinely referred to as orthophosphate as P by the Environment Agency of England and Wales". A sample preparation and analysis flow chart is shown in Figure 2-7.

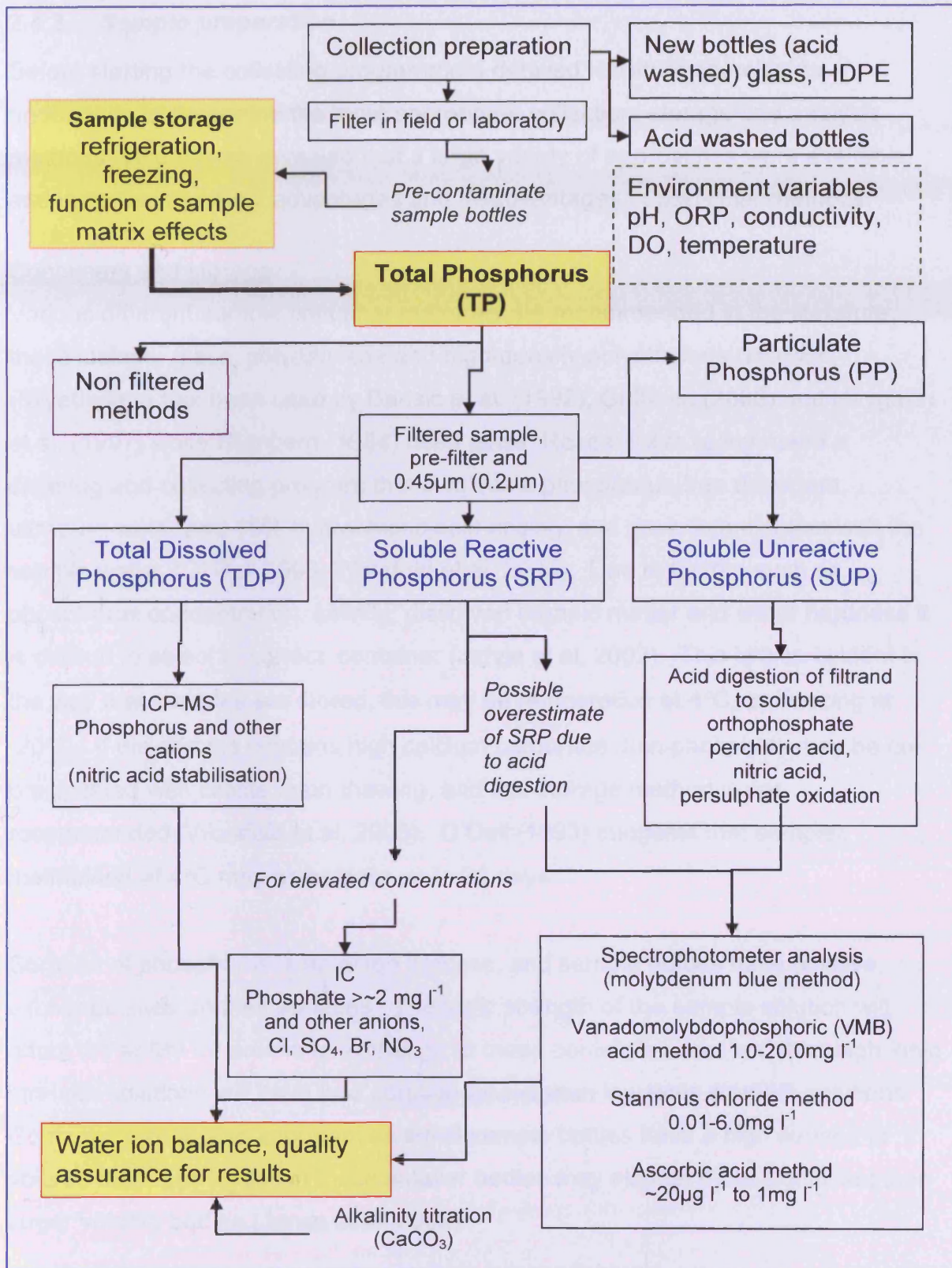


Figure 2-7 Sample preparation and analysis flow chart. After Perzynski (2000).

### 2.4.3 **Sample preparation**

Before starting the collecting programme a detailed literature search was undertaken to determine the most appropriate collection, storage and analysis methods. This search revealed that a large variety of approaches were available, and indicated the likely advantages and disadvantages of particular methods.

#### Containers and storage

Various different sample container materials are recommended in the literature, these include; glass, polyethylene and high-density polyethylene (HDPE). Polyethylene has been used by Barisic et al. (1992); Griffioen (2006) and Haygarth et al. (1997) while Numberg (1984) used glass. Researchers recommend a cleaning and collecting program that involves a phosphorus-free detergent, ultrapure water and 10% hydrochloric acid rinsing, and pre-contamination with the sample water, (O' Dell 1993; Worsfold et al. 2005). Due to factors such as phosphorus concentration, salinity, dissolved organic matter and water hardness it is difficult to select a 'correct' container (Jarvie et al. 2002). This is also evident in the way that samples are stored; this may be refrigeration at 4°C, or freezing at -20°C. If the sample contains high calcium carbonate then phosphate may be co-precipitated with calcite upon thawing, and this storage method is not recommended (Worsfold et al. 2005). O'Dell (1993) suggests that samples maintained at 4°C may be held for up to 28 days.

Sorption of phosphorus is an anion process, and sample bottles have positive exchange sites on their surfaces. The ionic strength of the sample solution will affect the ability for anions to exchange at these container sites, and thus high ionic strength solutions will have less sorption losses than low ionic strength solutions. Container size is also important as small sample bottles have a high surface to volume ratio, and losses in these smaller bottles may also be more significant than larger volume bottles (Jarvie et al. 2002).

For soluble reactive phosphorus samples refrigeration is the preferred choice, and 1% by volume chloroform is added to inhibit bacterial growth (Heredia and Fernandez Cirelli 2007). The use of chloroform addition in samples with high organic matter is to be avoided as this may initiate release of cellular enzymes into the sample. It is also recommended that samples are stored in the dark, to prevent photosynthetic reactions.

The stability of dissolved organic phosphorus, the soluble unreactive phosphorus fraction is not well understood (Carlyle and Hill 2001). It is possible that hydrolysis reactions may continue in the sample. The use of sulphuric acid to preserve the sample may digest some suspended organic material within the sample, this method is used to prevent phosphorus precipitation with iron (O' Dell 1993; Carlyle and Hill 2001). Autoclaving of thawed samples showed no difference with non-autoclaved samples when analysed for dissolved organic phosphorus (Worsfold et al. 2005).

Worsfold et al (2005) provide a table of storage protocols for varying environmental phosphorus fractions and matrices, although groundwater is absent from the list. The best option is to shorten the time between sampling and analysis, which lessens any transformations of the various fractions during storage (Haygarth et al. 1997).

### Filtration

Any samples should be immediately filtered after collection (Carlyle and Hill 2001), as this will prevent [lower] short term changes in phosphorus fractions, such as hydrolysis of suspended organic phosphorus. A 0.2 $\mu$ m filter is suggested by (Worsfold et al. 2005), as this removes a great deal of phytoplankton and bacteria that may pass through a larger filter, and may alter soluble phosphate during storage. They also recommend that excessive filtration pressure is avoided as this may cause algal cell rupture and release of their contents into the sample.

#### 2.4.4 Analysis methods

Analysis of environmental phosphorus needs to account for the various fractions, and their potential to be contained within the three main natural water components; soluble reactive, soluble un-reactive and particulate phosphorus. The standard methods for phosphorus water analysis require the separation of soluble or dissolved fractions from the particulate fraction by 0.45 $\mu$ m or 0.7 $\mu$ m filtration. The soluble fractions then rely on the specific reactions of the phosphate ion, which may be free, bound as a polyphosphate or contained within organic material in the sample with an acidified molybdate reagent (O' Dell 1993; Jarvie et al. 2002; Worsfold et al. 2005). For example, organic phosphorus is converted by oxidative digestion to its constituent phosphate components before analysis.

A distinction is made between acid hydrolysable phosphorus, which is normally found in sewage type samples, with sulphuric acid, and that of persulphate digestion for organic fractions (O' Dell 1993). This is further supported by Robards et al (1994); polyphosphates (condensed phosphates) are considered to be resistant to hydrolysis in natural waters and the mild hydrolytic conditions encountered during molybdate colorimetric determinations. However mild acid hydrolysis at ~100°C will convert this fraction to orthophosphate for subsequent analysis. The hydrolysis of the organic fraction is minimised by judicious selection of hydrolysis time and temperature. However debate exists as to the validity of the selective separation between the organic and condensed fractions, (Robards et al. 1994). The acid hydrolysable fraction can consist of both dissolved and particulate components. A summary of the fractions of main interest in phosphorus analysis is given in Table 2-2.

Measurement of total dissolved phosphorus (TDP) involves the digestion of a filtered sample to convert organic, colloidal and polyphosphates to orthophosphate. This can then be analysed by standard methods such as the molybdenum blue method described by Murphy and Riley (1962) and subsequently refined by (O' Dell 1993; Perzynski 2000).

Total phosphorus (TP) follows the same analytical procedure but on an unfiltered sample. The effectiveness of the standard digestion techniques varies and the values obtained require careful consideration due in part to incomplete digestion of organic phosphorus and matrix effects (Jarvie et al. 2002).

*Table 2-2 Phosphorus samples and their analysis methodology. After Robards et al. (1994) Jarvie et al. (2002); Worsfold et al. (2005).*

<b>Total Phosphorus</b>	
Total dissolved plus particulate phosphorus in a sample	
Total Reactive Phosphorus	Molybdate reactive fraction of unfiltered sample which may include some 'reactive' particulate phosphorus
Total Hydrolysable Phosphorus	Fraction that is acid hydrolysable
Total Organic Phosphorus	Organic fraction, determined using persulphate digestion methods
<b>Total Dissolved Phosphorus</b>	
Digestion of filtered samples to decompose organic, polyphosphates and colloidal P species to the orthophosphate ion which can then be determined by colorimetric techniques. Plus Dissolved Reactive Phosphorus	
Dissolved Reactive Phosphorus (SRP)	Orthophosphate ions in solution, which are measured by direct molybdate reactive analysis
Dissolved Acid Hydrolysable Phosphorus (DAHP)	Filtered fraction that is acid hydrolysable.
Dissolved Organic Phosphorus (DOP)	Filtered organic fraction obtained by persulphate oxidative digestion
<b>Total Particulate Phosphorus</b>	
That fraction which does not pass through the operational filter of determination	

The phosphate ions can be analysed by Ion Chromatography (IC), colorimetric determinations and Inductively Coupled Plasma – Mass Spectrometry (ICP-MS). The latter measures the total dissolved phosphorus (Jarvie et al. 2002), plus any particulate or organic phosphorus that has passed through the 0.45µm pre filter.

The IC method relies on ion-exchange in a resin and industry standard columns are available for particular species such as hydrogen phosphate for 'normal waters'. It is important to note that the ICP-MS reported fraction is total dissolved fraction and not total phosphorus as it is not possible to analyse an un-unfiltered sample.

### Digestion methods

The following methodologies for digestion and colorimetric analysis have been abstracted from Standard Methods for the Examination of Water and Wastewater, 13th Edn.

Digestion methods are used to assess the organic matter fraction (soluble unreactive phosphorus), and any particulate [suspended] phosphorus that may have been filtered. This organic bound phosphorus, with C-P and C-O-P bonds, is oxidised (hydrolysed) orthophosphate. Interferences and detection limits are governed by the colorimetric methodology used, not the digestion method. There are three main methods, which involve two steps:

Steps:

- Conversion of the phosphorus fraction of interest to soluble orthophosphate.
- Colorimetric analysis of this soluble orthophosphate by reaction with ammonium molybdate (molybdenum blue).

Digestion methods:

- Perchloric acid method. This is the most vigorous and time consuming, and is used for 'difficult' samples such as soils and sediments.
- Nitric acid - sulphuric acid method. This is recommended for most samples.
- Persulphate oxidation. This is described as the simplest technique, but the results should be checked against one of the preceding more vigorous digestion techniques.

#### 2.4.5 **Specific project phosphorus analytical requirements:**

##### Ion chromatography

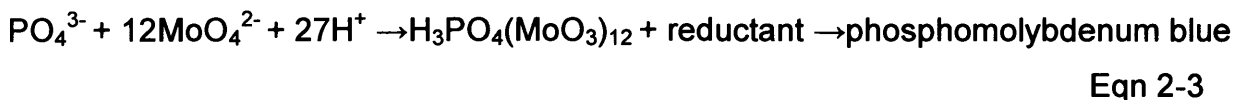
The samples are first filtered using a 0.45µm filter to provide the soluble reactive fraction which may still contain unhydrolysed organic phosphorus material. This is then diluted depending upon the expected concentration of the sample. Additional filtration may also be undertaken at 0.2µm (Jarvie et al. 2002).

##### Inductively coupled plasma-mass spectrometry

Analysis resolution for phosphate is in the region of <1ng/ml (Gill 1997). Stabilisation of water samples requires acidification with 10% Nitric acid (HNO<sub>3</sub>). It is possible that this acid may cause some digestion of filterable organic phosphorus in some samples and thus over determine the amount of soluble phosphorus in the sample (Jarvie et al. 2002)

##### Colorimetric analysis

Analysis of phosphorus can also use the reaction of phosphate with acidified molybdate reagent, which produces phosphomolybdate heteropoly acid (Eqn 2-3). This is then reduced to an intensely blue coloured compound and determined spectrophotometrically, (Worsfold et al. 2005).



The original methodology was described by Murphy and Riley (1962). In practice the methodology requires a two stage process; acid digestion of the sample, followed by spectral analysis. The spectral absorbance of the sample in absorbance units is measured against a blank. The method requires that calibration is undertaken prior to analysis in order to determine an absorbance calibration curve with which to determine the sample concentration. The method selected is based upon a function of the expected concentration range of the dissolved orthophosphate.

The reductant can vary, with ascorbic acid and tin(II) chloride the most commonly used. Using ascorbic acid causes a slow colour development and antimony is used as a catalyst. The rate of colour development (Figure 2-8) necessitates that readings cannot be taken until full colour development is achieved (Jarvie et al. 2002; Worsfold et al. 2005).



Figure 2-8 Phosphomolybdenum Blue. Colour development in calibration samples, 1mg P l<sup>-1</sup> (LHS) to lab blank on RHS. Photo A Gray.

Colorimetric analysis can also be performed on the filterable soluble reactive phosphorus fraction, that which is also analysed in the IC and ICP-MS. This method also determines acid labile phosphorus, which may overestimate the amount of free (bioavailable) phosphate in the fraction. In a similar manner any suspended matter retained in the filter can be analysed, the solid material being digested with acid in the first instance.

#### *Ascorbic acid method*

The minimum detectable concentration is quoted as approximately 10µg P l<sup>-1</sup> (0.01mg P l<sup>-1</sup>) but is a function of the light path used (Perzynski 2000). Interferences are caused by arsenates in concentrations as low as 0.1mg As l<sup>-1</sup>. If present at 1mg l<sup>-1</sup> concentrations hexavalent chromium (Cr(VI)) and nitrite (NO<sub>2</sub><sup>-</sup>) will give phosphorus concentration results that are lower by about 3%. When these are present at concentrations of 10mg l<sup>-1</sup> results may be as low as 10%-15%. Sodium sulphide and silicate do not cause interferences when present in concentrations between 1.0-10mg l<sup>-1</sup>. A spectrophotometer with a wavelength of 880nm is required.

## 2.5 Environmental quality standards

EC Directive 75/440/EEC (1975) quality standards for surface waters intended for the abstraction of drinking water specifies two standards for phosphorus as guideline values;  $0.4\text{mg H}_2\text{PO}_5 \text{ l}^{-1}$  for class A1, and  $0.7\text{mg H}_2\text{PO}_5 \text{ l}^{-1}$  for class A2. There is no indication as to how these values have been derived, although the parameters have been included to satisfy the ecological requirement of certain types of environment (EEC 1975). The amount of phosphate in drinking water is not a determinand in Statutory Instrument 2000 No. 3184; The Water Supply (Water Quality) Regulations 2000. Neither does it occur in WHO guidelines for drinking water quality (3<sup>rd</sup> Edn) (Annex 4, Chemical summary tables) (WHO 2002). A standards reference to phosphorus in drinking water can be found in an Environment Agency publication and states a maximum of  $2200\mu\text{g P l}^{-1}$  (Leeson et al. 2003; SNIFFER 2008). It is not considered a specific threat to human well being in the UK (Pers. comm., Drinking Water Inspectorate).

For the Groundwater Directive 80/68/EEC (1980) and subsequently transposed into the Groundwater Quality Regulations 1998 two lists, I and II were determined depending upon their biotoxicity, accumulation or persistence of contaminants in water. List I contains numerous organophosphates such as Diazinon a veterinary medicine and chloroform (previously used as a sample preservative).

List II contains inorganic compounds or elemental phosphorus (JAGDAG; EU 1980; Sheils 1993; EU 2007) The two lists have been superseded by new legislation The Groundwater Regulations 2009. In this legislation classification is described as hazardous or non-hazardous; organophosphorus remains as a hazardous substance. The new regulations incorporate the Water Framework Directive (WFD) (2000/60/EEC) and the new Groundwater Directive on the Protection of Groundwater Against Pollution and Deterioration (2006/118/EC). Standards for the WFD are tabulated for both rivers and lakes. Groundwater is conspicuous by its absence. The tabulation is based upon a classification system from high to poor quality.

The definition of 'high' standards (annual means) for SRP in rivers is within the range of  $30\mu\text{g l}^{-1}$  to  $50\mu\text{g l}^{-1}$  for three river typologies. This typology is based upon elevation and mean alkalinity. Good status is achieved for values  $50\mu\text{g l}^{-1}$  to  $120\mu\text{g l}^{-1}$  for the same typology. The Habitats Directive also lists environmental quality standards for river systems:

- natural for most river systems is:  $20\text{-}30\mu\text{g l}^{-1}$ .
- guideline (mid / good status) is  $40\text{-}100\mu\text{g l}^{-1}$ .
- threshold is  $60\text{-}200\mu\text{g l}^{-1}$ .

Values vary for headwaters and large rivers, these values are tabulated as Total Reactive Phosphorus (TRP). These values have been deemed to satisfy "Good Ecological Status" as required by the WFD (UKTAG 2006).

Data obtained from the Environment Agency for the Eden Valley, Cumbria, have the groundwater orthophosphate as P (the equivalent of SRP) quality level tabulated as  $0.153\text{mg l}^{-1}$  ( $153\mu\text{g l}^{-1}$ ). This value is based upon the Class A1 and A2 values in 75/440/EEC (1975) (Pers. comm., J Ingram) The Environment Agency indicate that the range of orthophosphate ( $\text{PO}_4$ ) in UK untreated groundwater is  $<0.02$  to  $2706\mu\text{g l}^{-1}$  (EA 2009a). They further classify quality indicators for phosphate in rivers as listed in Table 2-3.

*Table 2-3 Classification of river waters by phosphate content (EA 2009)*

Classification	Description	Limit $\text{mg P l}^{-1}$
1	Very low	0.02
2	Low	0.06
3	Moderate	0.1
4	High	0.2
5	Very high	1.0
6	Excessively high	>1.0

## 2.6 Summary

Phosphorus is an abundant element and important for healthy life and vitality in both the plant and animal kingdoms. It is however not always readily available for plant uptake due mainly to the poor solubility of the compounds it forms under various environmental conditions. This has led to the increased application of both mineral and manure fertilisers to agricultural land to boost crop yields. This increased flux is in part retained within the soil zone; however soluble phosphate does migrate to the water table.

It has been shown that there are associations between phosphorus and other chemical species, notably dissolved oxygen and iron. Phosphate tends to be liberated from sorption sites and be more mobile under reducing conditions.

The measurement of phosphorus is not a simple and straightforward process; this is due to the various forms or fractions that are encountered in the environment. These are soluble or particulate, reactive or unreactive to analytical techniques and organic or inorganic forms.

There currently does not exist an environmental quality standard for phosphorus in groundwater within UK legislation. The surface water values have been adopted by the UK regulatory authority in lieu of such EQS guidance.

## Chapter 3 Methods

### 3.1 Introduction

In order to assess the amount of phosphorus in the groundwater and its ultimate fate it is first necessary to quantify these values, consider pathways and investigate the physical mechanisms or aquifer characteristics that may influence the transport of entrained phosphorus.

Physical measurements of quantities are undertaken by a direct measurement of a sample be this groundwater chemistry or head. These measurements must be considered in both a spatial and temporal context. A single observation is a snapshot; several observations may suggest a trend, whilst multiple observations may indicate a system. The temporal interval must be chosen with an economy of accuracy coupled with an understanding of the process. Too long an interval risks missing important perturbations which can indicate processes (Ling 2007).

Spatial distribution can indicate heterogeneity or homogeneity within a defined zone, however the distribution interval must, in a similar fashion to the temporal scale, be designed so that any interpolation between measurement nodes is meaningful, and represents to some extent the 'ground truth'. This information can then be represented as a model that will aid interpretation of the processes.

#### 3.1.1 *Sampling protocols*

The sampling and analysis protocols for ground, surface water and soil samples were taken from a variety of sources such as BSI (1993, 2007) and Jarvie et al (2002). The protocols consider such things as borehole purging, cross-contamination, storage and preservation, representative sample, analysis capability and sample identification.

## 3.2 Water: fieldwork and laboratory analysis

### 3.2.1 Containers

250 ml Nalgene® high density polyethylene (HDPE) containers were used. During the Eden Valley sampling period a mixture of these and glass bottles were also used as part of the sampling method development.

### 3.2.2 Sampling

The sampling sites such as Figure 3–1 consisted of a mixture of private boreholes or associated taps, shallow wells, surface streams and rivers. For boreholes the recommended practice is to purge 3 borehole volumes before obtaining the sample (BSI 2007) Fortunately the private boreholes were all in use as either domestic or farmyard supplies. It was deemed that this constant use would negate the necessity of purging the borehole. For the shallow wells at Hill Farm Well and Cow House Well it was not practical to purge three volumes.



*Figure 3-1 Inertial pump tubing at Llandowlais Farm BH, note the sample colour in 1l container. Photo A Gray.*

Groundwater samples were obtained by:

- Hand bailer ~1l capacity, inertial pump tubing or tap direct feed. The bailer was pre-contaminated with sample waters which were also used to rinse multimeters and sample containers prior to measurements and sample capture.

- A 5m and 10m x12mm diameter inertial pump tube set was used to obtain samples from private boreholes, this tubing was able to fit through the pump support plate. A sufficient volume (~2.5l and 5l) was pre-pumped in order to thoroughly pre-contaminate the tube before the sample was taken Figure 3-1.
- At farm locations, such as Glen Court Farm, it was possible to obtain samples from yard taps, when access to the borehole was impractical. Unfortunately the residence time of the sample out of the borehole could not be ascertained, however as working locations it is hoped that this would be minimal.

During sampling gloves were worn to prevent cross contamination, sample bottles were marked with a unique location ID and stored in Ziploc bags in a cool box. Samples were always obtained (Figure 3-2) and secured separately before multimeter measurements were obtained.

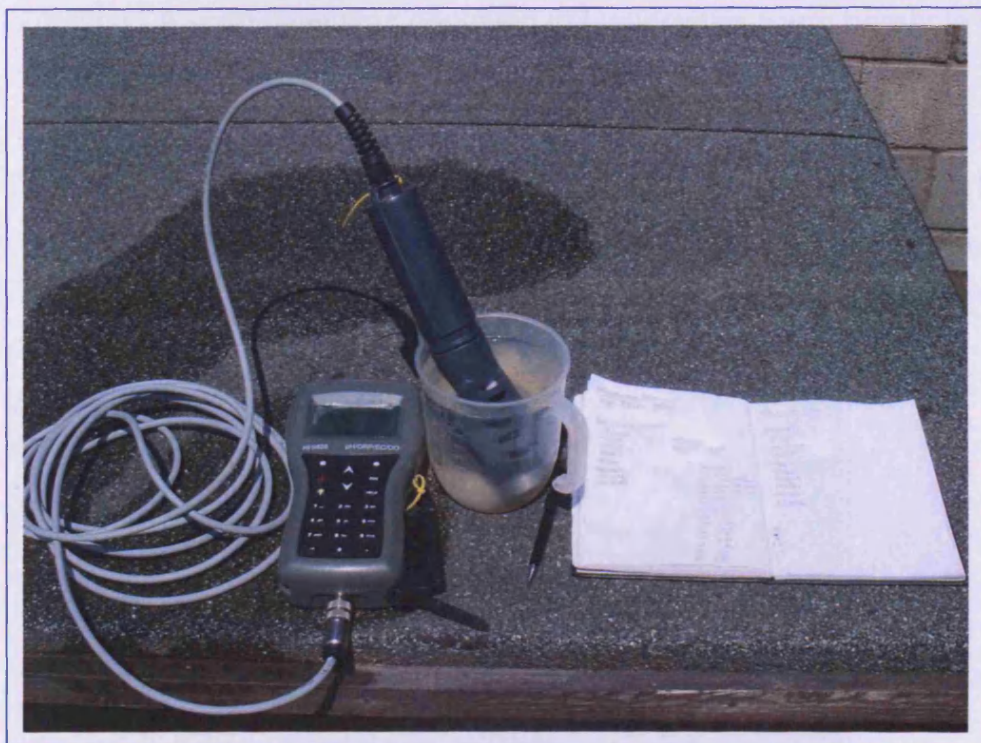


Figure 3-2 Hanna Instrument multimeter and measuring jug at UGDN. Photo A Gray.

### 3.2.3 *Field measurements*

Environmental parameters were measured in the field using a Hanna Instruments HI9828 multimeter. This was calibrated before each use and check measurements undertaken at the end of the sampling. The multimeter measurements consisted of pH, ORP, DO, EC, T and TDS, (Figure 3-2). A series of between 4 to 6 measurements were made and recorded in the internal memory of the multimeter; written values were also recorded.

### 3.2.4 *CTD divers*

These were deployed in 5 boreholes within the Usk project area; Hill Farm Well, Cow House Well and borehole, Llanusk Farm borehole, and Llantrisant borehole. As the majority of the boreholes were in use the logging interval was synchronised and set at 1 hour; it was hoped that this interval would bracket any domestic pumping. A sixth diver was deployed in Llandowlais Farm borehole in early January 2009.

The divers were periodically retrieved, and data was downloaded in the field without disruption to the recording (Figure 3-3). In addition to the diver data, manual dip measurements were made with a standard dip meter tape. Dips were also recorded during the monthly sampling for geochemistry.

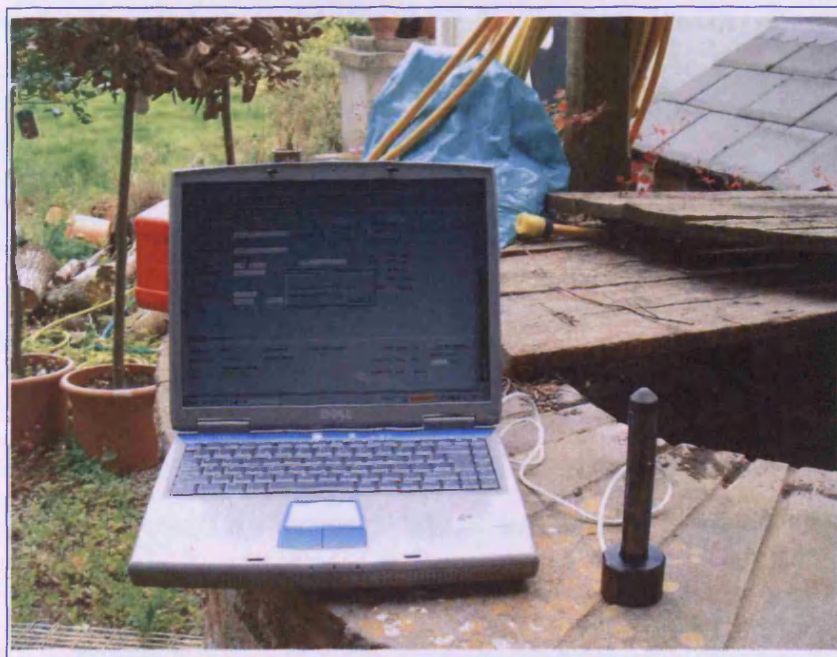


*Figure 3-3 CTD diver and laptop downloading at Cow House Well. Note red fuel container behind laptop on well parapet. Photo A Gray.*

### 3.2.5 Analysis methods

Water sample analysis for seven major anions was undertaken using Ion Chromatography (IC) methods. Inductively Coupled Plasma – Mass Spectrometry (ICPMS) was used for a suite of cations and metalloids. Spectrophotometer determinations were also carried out for SRP (range ~0.01 mg l<sup>-1</sup> to 1 mg l<sup>-1</sup>) as the IC limit of detection was not sensitive enough. Alkalinity was obtained in the field. Prior to analysis, samples were filtered using 0.45µm Millipore filter. Some additional water determinations were done using a 0.22µm filter, and some unfiltered samples were also analysed for SRP. For quality control a number of replicates from each sampling period were analysed, this was normally 25% or above.

#### Ion Chromatography

Analysis was undertaken using a DIONEX DX80. This uses an isocratic methodology where the composition of the eluent, a liquid carrier for the sample (analyte), remains constant throughout the process. The column in use analysed for the following anions, F, Cl, NO<sub>2</sub><sup>-</sup>, Br, NO<sub>3</sub><sup>-</sup>, HPO<sub>4</sub><sup>2-</sup>, and SO<sub>4</sub><sup>2-</sup>; results are expressed in mg l<sup>-1</sup> (ppm). The analysis performs a conductance and time measurement that is converted into a 'chromatogram'. This consists of peaks, with the area under the peak curve equating to the concentration based upon calibration with standard samples (Figure 3-4). The calculation is:

$$\text{Area} = \text{width at } p/2 \times \text{height } p \quad \text{Eqn 3-1}$$

Where  $p$  is the peak height.

For each sample two analyses were made and the mean of the result accepted based upon tolerance criteria (see statistical analysis section).

Where a replicate was also analysed it was possible to undertake standard deviation analysis of the results. The instrument was periodically calibrated by laboratory staff and several 'stock' analyses were also run to test laboratory procedures.

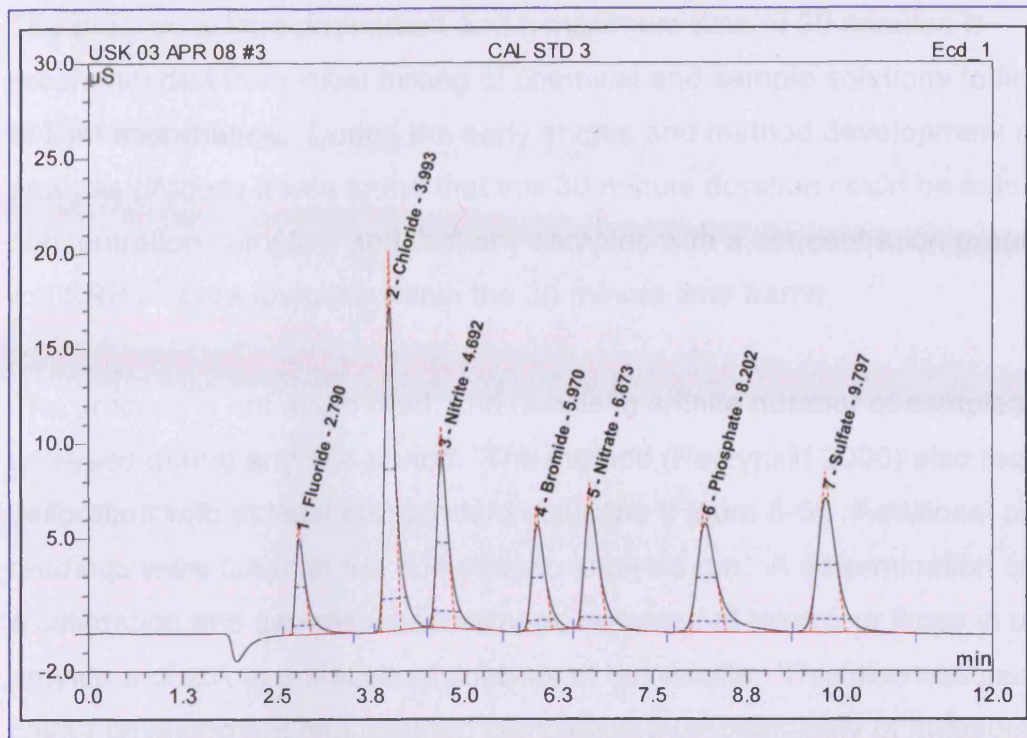


Figure 3-4 Calibration peak analysis (using analytical standard No III).

#### Inductively Coupled Plasma – Mass Spectrometry

Analysis of cations in the water samples was undertaken using a ThermoElemental X-Series with detection limits typically in ppb and a high sensitivity. A 0.45 $\mu$ m filtered sample was prepared with the addition of 10% nitric acid to stabilise the matrix. The samples were analysed for the major cations: Na, Mg, Ca, K, Al, Fe, together with addition trace and minor constituents; 26 in total. In a similar fashion to the IC samples, at least four analyses were undertaken on each sample, and standard deviations produced together with a coefficient of variation, to identify outliers.

#### Spectrophotometry

In order to analyse for SRP at low concentrations ( $\sim 0.01 \text{ mg l}^{-1}$  –  $1.0 \text{ mg l}^{-1}$ ) spectrophotometric determinations were undertaken. A Perkin Elmer Lambda 2 UV-Vis spectrophotometer set at 880nm was used throughout. The process relies on the formation of a deep blue colour due to the reduction of antimony-phosphomolybdate in a sulphuric acid medium. The method used is that of (Perzynski 2000) which is a modified version of Murphy and Riley (1962).

The process is time dependant and a maximum time of 30 minutes is recommended from initial mixing of chemical and sample solutions to final reading of light absorbance. During the early stages and method development of this analysis process it was found that this 30 minute duration could be extended for low concentration samples, and that any samples with a concentration greater than 1.0 mg SRP l<sup>-1</sup> were unstable within the 30 minute time frame.

The process is not automated, and results in a finite number of samples being analysed during any one period. The method (Perzynski 2000) also requires a calibration with at least six standard solutions (Figure 3-5). Additional calibration readings were taken at the end of each analysis run. A determination consisted of a calibration and sample measurement, repeated at least four times in order to provide a check and statistical analysis of the results. This also ensured that full colour development had reached completion by repeatability of measured absorbance values.



Figure 3-5 Colour development in standards. From L-R 1.5, 1.0, 0.75, 0.5, 0.25, 0.1, 0.05, 0.025 mg P l<sup>-1</sup> and deionised water blank. Photo A Gray.

In common with the IC and ICP-MS samples, analysis was undertaken on 0.45µm filtered samples (Jarvie et al. 2002). Some additional analysis was also undertaken on unfiltered and 0.22µm filtered samples (Haygarth et al. 1997). For turbid samples a slight modification to the process is required; however turbid samples were only present on a few occasions when analysing manure leachates and some soils. In general dilution and filtration was sufficient to reduce the turbidity to an acceptable level, and a differencing calculation approach was employed.

### Alkalinity

Alkalinity is described as the analysis process on a filtered sample while acid neutralising capacity (ANC) is the same method undertaken on a whole water sample (Rounds 2006). This was done using the Hach Lange Digital Titrator, a field portable system (Figure 3-6). Samples were initially titrated to an end point of pH 4.5, (Jeffers; Pickering 1980), although this assumes that all the alkalinity within the sample is caused by carbonate species. Later field titrations used the inflection method which may be a more true indication of the stoichiometric carbonate species endpoint. This may vary from pH 5.38 to pH 4.32 varying as a function of temperature and ionic strength, (Pickering 1980; Rounds 2006).

The process was to titrate 100ml of sample with 1.6N sulphuric acid, which gave a ratio of one turn to 1mg l<sup>-1</sup> alkalinity reported as CaCO<sub>3</sub> equivalent.



*Figure 3-6 Hach Lange digital titrator and accessories. Note meter readings (zeros) which indicate the number of turns and pocket pH meter for pH end point values. Note green solution for indicator end-point. . Photo A Gray.*

### 3.3 Soil fieldwork and laboratory analysis

While the project is concerned primarily with the fate and transport of phosphorus in groundwater, fertilisers which are soil amendments, are believed to be the main source of phosphorus in the groundwater. Analysis of soils was undertaken in order to gauge the amount of phosphorus in the soils, investigate the carrying capacity, and to ascertain if a critical load point is reached (Heredia and Fernandez Cirelli 2007). It was also done in order to generate and derive values that could be carried forward into the groundwater modelling. Several methods were employed, including; acid leaching, water leaching and column experiments. All have their advantages and disadvantages. Soil leaching tests are valuable in that they can indicate which constituents are mobile under different conditions. X-ray diffraction and diffusion analysis on bulk soil powders can also reveal bulk mineralogy and elemental analysis.

Soil pH was obtained from the leachates after thorough mixing; a soil pH meter was used from January 2009 (Figure 3-7).



*Figure 3-7 Soil pH probe in hole left by extraction of a soil column from the 'potato field'. Note slight acid value, 6.04, suitable for Fe/Al phosphate minerals and clayey nature of soil. Photo A. Gray.*

### 3.3.1 **Method**

A number of British Standards, (BSI 2006, 2008), exist for the investigation of soils and granular materials. In the geochemistry and hydrogeology laboratories at Cardiff University a standard acid digestion and bulk analysis of contaminated granular material was in practice (BSI 2002). Previous development work in the autumn of 2007 and project requirements led to the development of tests that were deemed suitable and repeatable.

#### Soil preparation

Soil samples were obtained from several sources, including cultivated land, pasture, manure tips and fallow field locations. Samples were transported in plastic bags and refrigerated until required. Where possible, obvious plant material was removed prior to weighing and drying in an oven at 50°C until no weight change was recorded. These values were used to estimate the amount of water content in the sample. Sub-samples of the dried soil were then powdered, again obvious plant detritus was removed, and the fraction that passed through a 63 µm mesh sieve was retained.

#### Soil leachates

The standard Cardiff University laboratory acid leaching test consisted of ~1.0g of the retained dried soil leached in 10ml 2M nitric acid in a 15 ml test tube. This was tumbled for 24hrs, with the tumbling machine set at 7 RPM. After 24 hours 2ml of the leachate was eluted, filtered to 0.45µm, and diluted with 8ml deionised water for analysis by ICP-MS. Anion analysis was not performed in order to protect the IC resin column.

Initially separate deionised water leaching tests for cations, anions and SRP were also undertaken in the 15 ml test tubes. This involved much duplication and processing. A later method involved up-scaling the reacting vessel using HDPE sample bottles (Figure 3-8) and soil sample size; the total eluent required was pre-calculated and the soil to water ration maintained at 1:10 i.e. 1g soil:10 ml water.

The use of these larger soil leachate samples solved any issues with heterogeneity with the various sub-samples that were previously used for the individual analysis methods. In addition it was possible to more easily change the soil:water ratio to investigate the effect of potential desorption of any ions into solution.



*Figure 3-8 HDPE sample bottles used as reaction vessels for soil analysis. Photo A Gray.*

The samples were tumbled for 24 hours in accordance with the British Standards instructions. These indicate that after this period the samples are allowed to stand for 15 minutes and then filtered (BSI 2002, 2008). The samples consisted of a suspension of soil material and it proved impossible to filter at the prescribed time, even with sequence filtration. The use of a centrifuge was also attempted, but again proved ineffective (Figure 3-9).

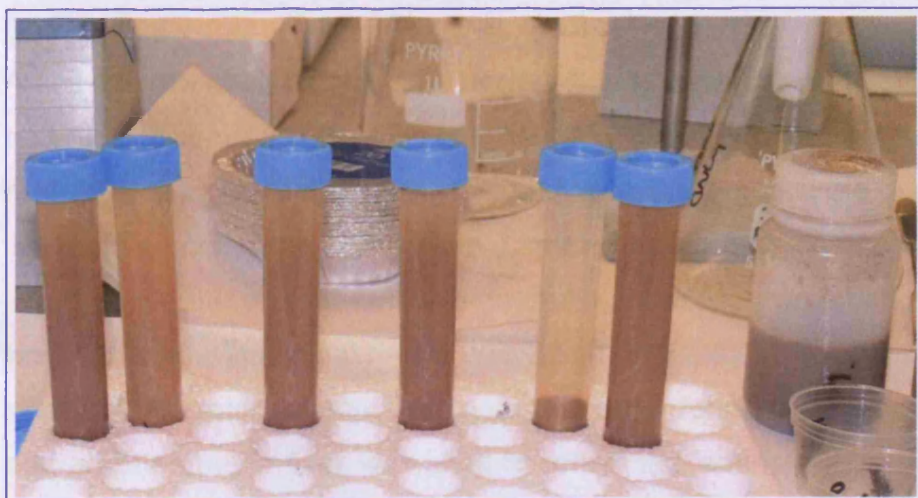


Figure 3-9 Soil samples after centrifuging, only effective on one sample. Note HDPE bottle on right with original soil suspension. Photo A Gray.

The only viable methodology was to allow the samples to gravity settle over the course of several days. Even then filtration to  $0.45\ \mu\text{m}$  proved extremely difficult for the majority of the samples, pre-filtration using  $5\ \mu\text{m}$  filters was again ineffective, indicating that there may be a particular particle size (colloid fraction) that remained in suspension. The problem of filtering samples after the tumbling, especially those from clay-rich soils, is well recognised (T. Jones *pers comm.*), and researchers typically follow the BS protocol, but note the extended time between finishing tumbling and being able to filter the samples. This delay can raise issues of continuing biological activity and sorption de-sorption potential into the bottom sediments, (BSI 2008). Some of the samples associated with the potato and scrub field once filtered retained an organic or 'iron stained' colour, while in others this was removed.

The addition of 10% nitric acid as a matrix stabiliser was believed to initiate precipitation within the sample (Figure 3-12). This precipitation was only observed in soil and farmyard effluent samples for ICP-MS and on occasion the spectrophotometer samples; the ascorbic acid was believed to be the catalyst. The precipitate began to form after several minutes, was suspended within the sample vial, and due to the time interval between preparation and analysis became substantial. This was overcome by careful eluting of a sub-sample for analysis.

### Soil column

A soil column analysis was also undertaken to further investigate the leaching potential of some project area soils. This was done to attempt to replicate more realistic ground recharge pathways and measure any soluble or de-sorbing species. The column consisted of a 6.8 cm diameter x 50 cm perspex pipe. This was inserted into the ground and with careful manipulation an intact soil column profile was obtained. The initial profile was 28 cm in depth. This was then mounted in a series of laboratory clamps with a ceramic filter funnel to prevent column collapse and an Erlenmeyer flask was used to collect the leachate (Figure 3-10 and Figure 3-7).

A series of experiments were run by passing a known amount of deionised water through the column and collecting the leachate. For one experiment the known volume was passed through several times in order to increase contact time with the soil. An amount of by-pass (channelling) flow between the soil and inside of the tube wall was inevitable and observed. As the deionised water was added the transit time of the water was observed to reduce; most probably due to swelling clays. Once the deionised water experiments were finished a spiked sample of dihydrogen potassium phosphate was then passed through the column in order to investigate sorption potential.



*Figure 3-10 Soil column experiment apparatus, note 1l bottle in background that has been allowed to gravity settle before analysis. Photo A Gray.*

### X-Ray Diffraction

A sub-sample of the 63  $\mu\text{m}$  powdered soils was taken and analysed by X-ray diffraction (XRD). A Phillips Automated Powder Diffractometer PW1710 was used to investigate bulk mineralogy. The X-Ray generator is a copper tube anode CuK $\alpha$  at 35kV 40 mA, the scan angle ( $2\theta^\circ$ ) was set from  $2^\circ$  to  $70^\circ$ . Diffractograms were subsequently analysed against the database software PW1876 PC-Identify v 1.0b. Particular care was taken to identify phosphorus minerals, if present (Figure 3-11). A list of d values is available in Jenkins et al (1986) which allow for a search of specific (phosphate) minerals in the soil sample.

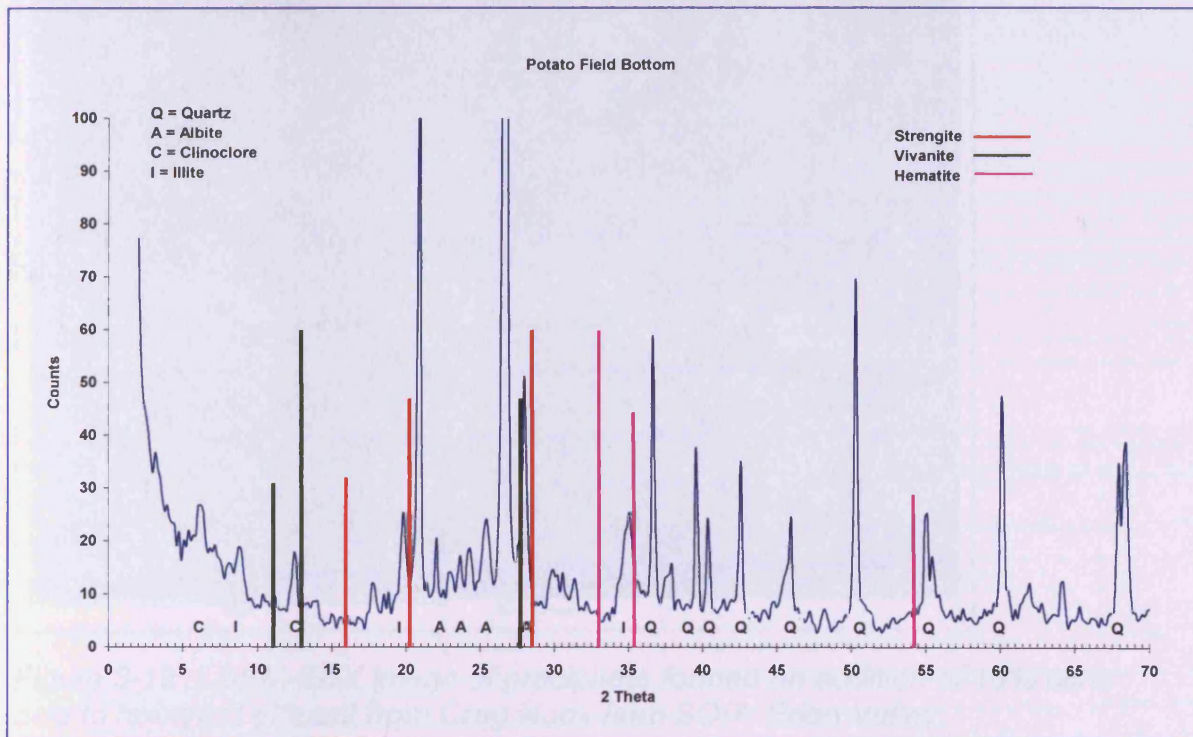


Figure 3-11 Diffractogram for Potato Field Bottom soil. Note vertical scale exaggerated to show detail. Selected mineral peak locations identified and vertical coloured lines represent the position of minerals of interest, size represents location of first three peak positions.

### Analytical Environmental Scanning Electron Microscope (ESEM)

This was undertaken using a Cambridge Instruments (LEO) S360 with a secondary electron detector for surface imaging. The elemental analytical mode employed an Oxford Instruments INCA Energy (EDX) X-ray analysis system. This analysis was carried out on soil powders, filter residues, and precipitates; looking for phosphorus minerals (Figure 3-12). Using the ESEM-EDX it was possible to analyse individual soil grains and perform element mapping (hot spot) within the field of view.

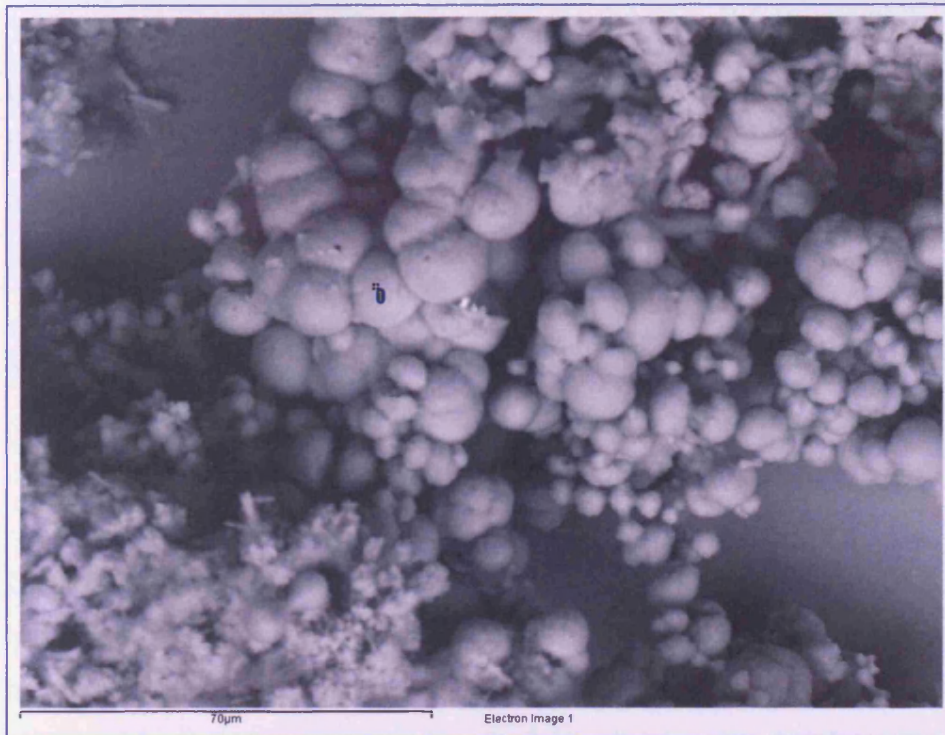


Figure 3-12 ESEM-EDX image of precipitate formed on addition of 10% nitric acid to farmyard effluent from Crag Nook farm SO17, Eden Valley.

Table 3-1 EDX elemental analysis of Figure 3-12.

Element	Weight%	Atomic%	Element	Weight%	Atomic%
C	9.41	15.75	P	0.40	0.26
O	49.24	61.91	Cl	0.79	0.45
Na	1.38	1.21	K	0.70	0.36
Mg	2.18	1.80	Ca	33.65	16.89
Si	1.57	1.12	Fe	0.69	0.25

From the atomic abundance data (Table 3-1), it is possible to interpret the likely mineral. The recommended method is by using the bespoke MINDAT.org website (Ralph and Ralph 2009).

### 3.4 External data

A variety of external data were made available for the project, this included borehole logs and geology information from The British Geological Survey (BGS), groundwater geochemistry and borehole hydrograph data from the Environment Agency (NW region and Wales), rainfall data, and groundwater geochemistry from Welsh Water. A CD of all relevant data is contained as an enclosure to this thesis.

#### 3.4.1 Mapping

Use was made of the Edina Digimap Collection, a service that is available through a licence for University tertiary education (EDINA 2006). This service provided digital mapping for GIS and general applications. Place names where applicable and spellings are taken from the Ordnance Survey mapping.

Mapping used was:

- Usk Valley Sheet 152, and sheet 172 (OS 2005c, 2007)
- Eden Valley Sheet OL19 & OL5, (OS 2005b, a)

Geological mapping, including Aquifer Vulnerability, Soils and Hydrogeological maps were used as the basis for conceptual modelling and initial estimation of hydrogeological properties. Additional geological information for both areas was obtained from the accompanying geological memoirs, (Welch et al. 1961; Squirrell et al. 1969; Arthurton 1981).

- Usk Valley  
Geology: Sheet 249 and 250, Special sheet #9 (BGS 1969, 1971, 1981).  
Aquifer Vulnerability: (SSLRC 1996).  
Soils: (SSLRC 1983c).  
Hydrogeology: Sheet 17 (BGS 1986).
- Eden Valley  
Geology: Sheet 24, 30 and 31 (BGS 1974a, b, 2004).  
Aquifer Vulnerability: Sheet 3, 4 and 7 (SSLRC 1997a, b, c, d).  
Soils: Sheet 1 (SSEW 1977; SSLRC)

This mapping data, together with terrain models, was replicated in digital format and in some instances was available through the Edina service. The Environment Agency (Wales) provided catchment spatial data for the Usk Valley area. Terrain information was re-sampled using the ArcGIS 9.2 Map Manager software. All mapping and GIS data manipulation was undertaken on the National Grid, (UTM, OSGB36), heights above Ordnance Datum, Newlyn.

### Survey

To minimise the potential of spatial error for the Usk Valley data, and to reduce the height of borehole data logger information to the National Grid, a Real Time Kinematic (RT) GPS survey was undertaken on 12 November 2008. Heights obtained for the individual boreholes are estimated to be accurate to +/- 2.5 cm. This survey also generated more accurate 2D position information, deemed to be accurate to +/-1.5 cm. Due to the small extent of the Usk project area; this increased accuracy becomes critical for the more accurate calculation of hydraulic gradients.

Spatial data for the Eden Valley was obtained, where available, from borehole logs. Horizontal positional errors are subsumed within the mapping scale and areal extent of the valley. Height is more critical in groundwater investigations and it is not known how height values were obtained. For the older records this is possibly from map interpolation and for records without this information the only recourse of action. This height is likely to be only accurate to half the contour interval, ~5 m.

### Borehole logs

These were obtained courtesy of the British Geological Survey, from their records office at Wallingford, Oxfordshire. The dates the boreholes were drilled ranges from the 1940's to recent. The data consisted of:

- 17 records for the Usk Valley
- 80 records for the Eden Valley

A further four borehole logs for the Usk area were provided by Apex Drilling, and the Environment Agency provided a log for the Llewellyn monitoring borehole. A synopsis of the logs for all locations is in Enclosure 1 CD.

### Hydrology and hydrogeology

Data for four boreholes within the greater Usk catchment was made available for the project, of these only one location, Llewellyn, was deemed suitable for further use. The Environment Agency (NW) has a series of 19 monitoring boreholes within the immediate Eden Valley area, of these 11 were deemed suitable for further investigation, see Enclosure 1. The data of various times and resolutions, and is a mixture of both manual and automated borehole dips. The data spans 29 years, the most recent data available was 2006.

### *Rainfall*

For the Usk Valley a station, Estavarney Farm 335384 203210, about 3Km to the north of Usk town, and, Sluvad Farm 331800 199300, 5Km to the west was provided. This Usk data covered the period 2006 to end of project. Rainfall data for the Eden Valley was provided by the BGS.

### *Surface water*

River data for the Usk and Olway Brook was available from the CEH (National Rivers Archive) (CEH 2005, 2008).

### Hydrochemistry

Geochemistry data for the Usk and Eden Valleys was obtained from the Environment Agency; this is a combination of their own data and that of water supply companies.

For the Usk Valley the Environment Agency (Wales) provided data for three locations from their groundwater quality monitoring program, two groundwater locations, Llandowlais Farm and Usk Garden Centre were regular sampling points. The third location Llewellyn was used by the University as a training borehole for sampling and pumping tests. The Agency's data has a temporal resolution of about six months and consists of a larger species suite determination. Phosphate data for Wales was also provided by Welsh Water. The data set for the Eden Valley contains a mixture of temporal scale snapshots for 125 locations. However closer inspection shows that for the majority of these locations the sampling interval or sample population is insufficient to undertake meaningful statistical or temporal analysis.

### 3.5 Statistical analysis

Statistical analysis was undertaken using embedded functions within Microsoft® Excel, and SPSS v14 and v16; a statistical software package available through Cardiff University. The default level of significance for SPSS is 95%. Results are represented as bar or box plots with significance lines as appropriate. In statistical analysis, random sampling is a prerequisite in order to eliminate bias and systematic errors. However, due to the nature of the investigation random sampling is not always possible; boreholes are located for access, and sampling intervals are non-random.

#### 3.5.1 *Methods*

##### Regression analysis

In essence the hydrograph is a time variant data set. Long term trends are unlikely to be linear and may comprise of the following (Ferdowsian and Pannell 2009):

- Rising trend. This will reduce over time as levels rise and thus the hydraulic gradient increases as will the discharge rate. This is attributed to local groundwater flow.
- Linear long term trends. Observed in intermediate or regional systems and have higher recharge to discharge ratios, this reduces build-up of higher hydraulic gradients to generate significant flow.
- Rising trends due to compartmentalisation. The trend in a compartment will rise until overtopping into a lower compartment occurs. This lower compartment will then experience a rising trend.

##### Spearman's non parametric correlation analysis

Correlation analysis was undertaken in order to determine if observed parameters were correlated at a level of statistical significance. Spearman's correlation uses the ranks of the observed variables.

### Autocorrelation analysis

Autocorrelation is a self-correlation of a single variable. It can be used to determine if the values in a data set are random or there is an underlying non-random trend. The length, or lag, of this trend is determined by the observation length, such as time or distance units. A sample correlogram (Figure 3-13) generated from synthetic data for random and seasonal data, demonstrates this form of analysis.

### Spectral analysis

Spectral analysis was also performed on time series data in order to determine if there was an underlying frequency or periodicity within the data (Figure 3-13).

Figure 3-13 also contains synthetic rainfall data for a 16 month time series, which is a sub-sample of the 48 month set. Analysis of this using the same SPSS program shows that it is possible to analyse for shorter duration series with reasonable results; although the statistical significance decreases. The spectral plot shows an idealised case with spikes at 0.083 and 0.25. This equates to a period of 1/12 and 1/4 indicating a yearly cycle (a repeat once every twelve months 1/12) with an underlying three monthly seasonality. The denominator value is a function of the measured interval in this case monthly. A data set larger than 16 months is required for meaningful spectral analysis.

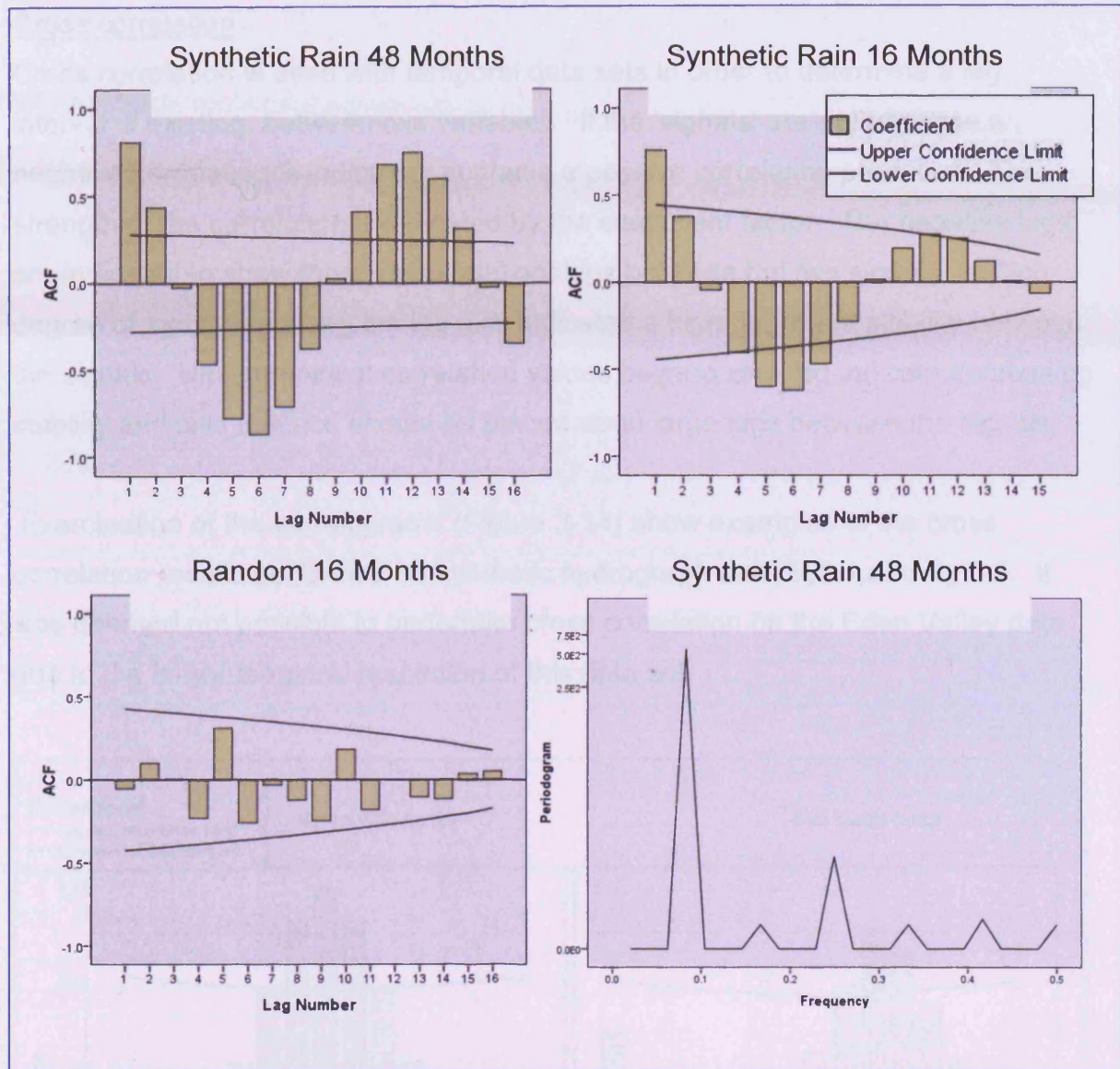


Figure 3-13 Auto-correlograms for synthetic rainfall and a spectral frequency plot of the 48 month seasonal and 16 month random data. Autocorrelation factor (ACF) is a measure of the strength of correlation. Lag number is the measured interval, in this case months. Spectral frequency indicates a return period every 0.083 or 1/12 months thus yearly and 0.25 or 1/4: seasonal every three months.

#### Analysis of variance (ANOVA)

This statistical test was performed in order to confirm differences between the same observed parameters, such as pH, at different boreholes. The results may aid interpretation of homogeneity or heterogeneity within the aquifer. The non-parametric alternative Kruskal-Wallis method was used.

### Cross correlation

Cross correlation is used with temporal data sets in order to determine a lag interval, if existing, between two variables. If the 'signals' are out of phase a negative correlation is indicated; in phase a positive correlation produced. The strength of the correlation is indicated by the coefficient factor. The negative lags are indicated to show the cyclical relationships between the two signals. A high degree of symmetry along the lag axis indicates a high degree of stability between the signals. Unsymmetrical correlation values beyond zero lag indicate decreasing stability and less reliance should be placed upon large lags between the signals.

Examination of the correlograms (Figure 3-14) show examples of the cross correlation results performed on synthetic hydrograph data Sy0.1 and Sy 0.3. It was deemed not possible to undertake cross correlation on the Eden Valley data due to the larger temporal resolution of this data set.

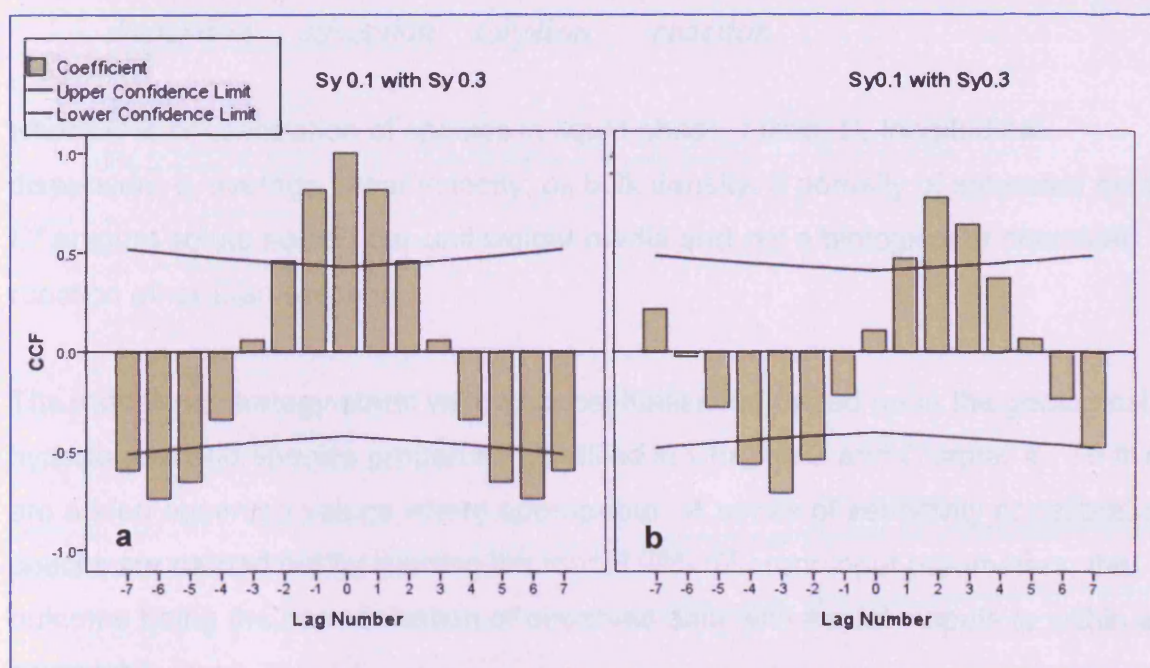


Figure 3-14 Cross-correlation analysis of synthetic hydrograph data. (a), shows the situation represented by a zero lag, main peak in histogram is at lag 0, whilst; (b) shows the synthetic lag of 2 time units. Note symmetry. Cross correlation factor (CCF) is a measure of the strength of correlation.

### 3.6 Modelling

Groundwater modelling was undertaken and designed to combine the physical and chemical analysis of the Usk Valley results. The modelling outputs can provide temporal 3D visualisation of the groundwater flow field. These results are subject to modelling inputs and the scale of observation. Inputs include observed hydrological parameters; or literature values as an initial estimate. The outputs are calibrated on known or observed data, normally head or contaminant concentration values; although it has been suggested that temporal calibration can also be achieved on water samples with an age label.

The aim of the modelling is to investigate the elements in Eqn 3-2, which is shown in 1D form (Fetter 2008):

$$\frac{\partial C}{\partial t} = D_L \frac{\partial^2 C}{\partial x^2} - v_x \frac{\partial C}{\partial x} - \frac{\rho_B}{\theta} \frac{\partial C^*}{\partial t} + \left( \frac{\partial C}{\partial t} \right)_{rxn}$$

*dispersion      advection      sorption      reaction*

Eqn 3-2

where  $C$  is concentration of species in liquid phase;  $t$  time;  $D_L$  longitudinal dispersion;  $v_x$  average linear velocity;  $\rho_B$  bulk density;  $\theta$  porosity of saturated media;  $C^*$  amount solute sorbed per unit weight media and  $rxn$  a biological or chemical reaction other than sorption.

The modelling strategy starts with a conceptualisation based upon the geological, hydrological and species properties identified in Chapter 2 and Chapter 4. To this are added observed values where appropriate. A series of sensitivity or calibration checks are carried out by running the model with different input parameters; the outcome being the harmonisation of observed data with model outputs to within an acceptable level.

A series of models and scenarios were produced in both 2D (FlowNet) (Wang 2005) and 3D (MODFLOW) (MacDonald and Harbaugh 1988). Additional sensitivity analysis to  $K_d$  values and transport times was undertaken using the Environment Agency's Remedial Targets worksheet P20 v3.1 (Carey et al. 2006b).

### 3.6.1 2D modelling: FlowNet

Flownet modelling is a method of representing the distribution of heads, groundwater flow lines and discharges in two-dimensions. It is able to provide a first line indication of conceptual or potential groundwater flow scenarios using realistic parameters. Cardiff University has access to a flow net program which allows more complicated anisotropic systems to be modelled (Wang 2005). The model can be considered to represent 2D cross-section groundwater flow, sources and sinks with stream tube particle tracking time elements.

The Flownet modelling was undertaken to test the hydrogeological conceptual model, the main investigations were:

- Validity and effect of homogeneous geological units.
- To test the calculated Raglan Mudstone Formation parameters and their interaction with literature values for adjacent zones.
- Sensitivity analysis of the groundwater heads to changes in the hydraulic properties of the model.
- Investigate advective flow patterns.
- Investigate advection travel time and groundwater age relationships at a discharge point.
- Investigation of the concept of elevated groundwater heads on the flanks being the drivers for flow.

### 3.6.2 3D modelling: MODFLOW

MODFLOW, an industry approved groundwater program, was used to further investigate the potential groundwater regime. MODFLOW is a finite difference flow model which is designed to solve the governing groundwater flow equation:

$$\frac{\partial}{\partial x} \left[ K_x \frac{\partial h}{\partial x} \right] + \frac{\partial}{\partial y} \left[ K_y \frac{\partial h}{\partial y} \right] + \frac{\partial}{\partial z} \left[ K_z \frac{\partial h}{\partial z} \right] + W = S_s \frac{\partial h}{\partial t}$$

or

$$T_x \frac{\partial^2 h}{\partial x^2} + T_y \frac{\partial^2 h}{\partial y^2} + T_z \frac{\partial^2 h}{\partial z^2} + W = S \frac{\partial h}{\partial t}$$

Eqn 3-3

where  $K_x$  is the hydraulic conductivity in the  $x$  direction;  $W$  is sources and sinks;  $S_s$  is specific storage;  $T$  is transmissivity and  $S$  is storage coefficient (specific yield ( $S_y$ ) in unconfined aquifers),

The program allows the user to assign a number of aquifer properties including; topographic elevations, recharge rates, aquifer layers, and hydraulic conductivity zones via a GUI interface. A calibration package calculates a difference between observed groundwater head at a location (observation borehole) and model calculated values. This function was used extensively to ensure quality control within the simulations and to ground truth.

The aim of the MODFLOW modelling was to:

- Harmonise and confirm in a vigorous manner the derived hydraulic parameters with a calibrated advective 3D flow model.
- To create a robust platform in order to investigate conceptual species spatial and temporal relationships within the model space.
- Test the hydrogeological and hydro chemical conceptual model.

### 3.6.3 ***Risk assessment modelling with P20 ver 3.1***

The Environment Agency's risk assessment worksheet is able to consider long duration transport problems and provides a remedial target concentration for the source term based upon the distance to a receptor or compliance point (Carey et al. 2006b).

The aim of this modelling was to:

- Confirm groundwater advection and contaminant transport times.
- Sensitivity analysis on input parameters and transport times.

### 3.7 Quality Control

Where appropriate user calibration of field instrumentation was undertaken prior to field work, this included pH meters (multi parameter) for both groundwater and alkalinity analysis. Some functions such as temperature are factory calibration only.

#### 3.7.1 Analytical limits of detection

Limit of detection (LOD) can be defined as the lowest quantity of a species which can be detected from a known absence of the species within a stated confidence (Wisconsin 1996; Gill 1997; Schibler et al. 2007; Westgard 2008). The limit of detection for a species will vary due to the analysis method.

Spectrophotometric determination of SRP is quoted as  $10 \mu\text{g l}^{-1}$  and the practical operational upper limit was determined to be  $1.0 \text{ mg l}^{-1}$  (Perzynski 2000). The Dionex DX80 IC has a lower limit of approximately  $1.0 \text{ mg l}^{-1}$  for phosphate.

#### ICP-MS

The limit of detection is calculated as:

$$LOD = \frac{3\sigma_{blanks}}{s} \quad \text{Eqn 3-4}$$

Where  $3\sigma_{blanks}$  is three times the standard deviation of the blank measurements and  $s$  is the sensitivity or gradient of the regression line. Limit of detection values in ppb for phosphorus (Iain MacDonald, *Pers. comm.*) are in Enclosure 1 CD.

#### Ion Chromatography

The Dionex DX80 is calibrated using a system of standard solutions. A seven anion standard II, which is standardised against National Institute of Standards & Technology Standard Reference Material, is provided by the manufacturer together with a certificate of analysis.

Test analysis of a spiked sample was undertaken periodically by the laboratory staff to check that the calibration was maintained. Blanks are run concurrently with samples and also provide a verification of instrument quality control. Minimum levels of detection can be calculated from these blank analysis, (Wisconsin 1996; Schibler et al. 2007; Westgard 2008).

$$LOD = Blank_{mean} + 3\sigma_{blank}$$

$$LOD \approx MDL$$

$$MDL = t \times \sigma$$

Eqn 3-5

The method detection limit (MDL) is defined as the concentration of a substance that can be measured and reported with 99% confidence that the analyte is greater than zero (Wisconsin 1996). If blanks have not been measured, the LOD can be calculated by analysis of standard solutions where:

$$LOD = c + 3\sigma_{analyte}$$

Eqn 3-6

Where  $\sigma$  is the sample standard deviation (n-1), not population standard deviation (n), and  $t$  is the Student's t value for 99% confidence interval,  $c$  is the intercept of the regression line of observed against standard.

The limit of quantification (LOQ) is defined as the level above which quantitative results may be obtained with a specified degree of confidence (99%), (Wisconsin 1996).

$$LOQ = 10\sigma_{analyte}$$

Eqn 3-7

Results of the calibration are in Enclosure 1 (CD).

### Spectrophotometer

The spectrophotometer is calibrated manually. A series of a minimum of six spiked blanks are prepared, within the range of interest, and measurements of absorbance units are recorded for each sample. This data are then plotted as absorbance units against known concentration and a regression line obtained; the gradient becoming the calibration factor. This process is required for every determination that is undertaken, and also serves as a quality control check over the total determinations.

The LOD can be determined by application of the MDL (Eqn 3-5] but not the intercept method (Eqn 3-6] as the definition of a water spike without phosphate would have zero absorbance, and the method requires a background correction to zero units with two water samples.

Values of LOD and LOQ (Table 3-2) show the results for calculations using all calibration factor regression data and two randomly selected determinations. The stated LOD is approximately  $10\mu\text{g l}^{-1}$ , (Perzynski 2000), which conforms to the values obtained by the different calculation methodologies. Average recoveries appear good, however analysis of individual results shows that the lower calibration spikes have a recovery rate as low as 55%. In addition, the signal to noise ratio is lower for the low concentration spikes. The otherwise large values give confidence that the method is measuring the absorbance of the complex, and procedural interferences are low.

*Table 3-2 LOD and LOQ data for spectrophotometric analysis values in  $\text{mg l}^{-1}$  where appropriate.*

	Calibration Factors	02-Dec-08	04-Mar-08
sd	0.007	0.002	0.001
Student's t	2.492	3.143	3.143
n	25	7	7
MDL=tx3sd	0.017	0.006	0.003
LOQ	0.07	0.02	0.03
LOD 3sd/s	0.01	0.01	0.005
Average Recovery %		90	96
Signal/Noise		14 to 780	90 to 600

### 3.7.2 Other equipment

#### Geoprobes

Parameters that require calibration are pH, dissolved oxygen (DO) and electrical conductivity (EC). pH was calibrated using a two point method; pH 4.01 and 7.01, with pH 10.01 also used periodically. Dissolved oxygen was also a two point method; 100% oxygen in the atmosphere and 0% in a solution of sodium thiosulphate, with no dissolved oxygen present. Electrical conductivity is a one point calibration using a standard 1413 $\mu$ S/cm solution. The Hanna 9828 has the following stated accuracies (Table 3-3):

*Table 3-3 Specifications for Hanna 9828 multimeter.*

pH	DO	EC	ORP
$\pm 0.02$ units	$\pm 1.5\%$ of reading or $\pm 1\%$ of reading (whichever is greater)	$\pm 1\%$ of reading or $\pm 1\mu$ S/cm (whichever is greater)	$\pm 1.0$ mV

#### Borehole CTD loggers

Van Essen DI 263 CTD loggers reading conductivity, temperature and depth are calibrated by the manufacturer; the electrical conductivity readings were selected to record specific conductivity (related to 25°C). Depth values are subject to barometric effects, and the raw observations are recalculated to provide a 'true' height of water above the diver. The barometer diver was co-located with the diver at Hill Farm Well. This value is then combined with the suspension string length to calculate a well dip or height above datum value.

## 3.8 Quality issues

### 3.8.1 *Laboratory practice*

Designated plastic and glassware was purchased for the project, and used throughout to avoid cross contamination. This equipment was rinsed in deionised water and then washed in 10% HCl for 24 hours and then double rinsed in deionised water. When general laboratory equipment was used it was also pre-washed in 10% HCl prior to use.

#### Procedural blanks

As part of the sampling protocols and laboratory practice, procedural blanks were made and analysed together with field samples. Deionised water was placed in a similar container and accompanied the field sampling or was subjected to the same procedures as a soil reaction vessel. Procedural blanks were also produced for the calibration standards for the spectrophotometer analysis.

#### Field measurements

To combat hysteresis, an analysis memory effect, in the multimeter, a number of measurements were recorded. Despite this it was noted during observations that the multimeter and smaller pH pocket probe used for alkalinity determinations (Figure 3-6) did exhibit a lag response or variation in reading.

### 3.8.2 *Statistical analysis: quality assurance*

#### Standard deviation

It is possible to undertake statistical analysis of the results of any analysis obtained. The simplest is the mean of all determinations; however this does not provide a 'quality indicator' for each individual observation. This can be done by calculating the standard deviation ( $\sigma$  or  $sd$ ), which is a measure of the precision of each individual observation (Eqn 3-8). The standard error of the mean result, precision of mean, can be calculated from Eqn (3-9).

$$\sigma = \sqrt{\frac{\sum r^2}{n-1}} \Rightarrow \sigma^2 = \frac{\sum r^2}{n-1} \quad \text{Eqn 3-8}$$

$$\bar{\sigma} = \frac{\sigma}{\sqrt{n}} \quad \text{Eqn 3-9}$$

where  $r^2$  is the residual squared.

An observation rejection criterion was based upon any value having a residual greater than  $\pm 2.5\sigma$ . The coefficient of determination and standard deviation was used for the ICP-MS data. Coefficient of variation ( $c_v$ ) (Eqn 3-10) is a useful tool when there are magnitude differences in the data and may suggest that the geometric mean ( $mean_g$ ) may be more appropriate (I McDonald, *Pers. comm.*).

$$c_v = \frac{\sigma}{mean_a} \quad \text{Eqn 3-10}$$

### Tolerance

Tolerance relates to instrumentation characteristics and acceptable, and departure from the desired analysis outcome of equal values. The number of samples, or analyses, required to achieve a required tolerance can be calculated (Eqn 3-11). For example given a working tolerance of  $1\text{mg l}^{-1}$  and a maximum standard deviation of 0.6, the minimum number of observations is two:

$$\begin{aligned} n &= \frac{\text{confidence}^2 \cdot \sigma^2}{\text{Tolerance}^2} \\ n &= \frac{1.96^2 \times 0.6^2}{1^2} \\ n &= 2 \text{ observations (1.4 observations)} \end{aligned} \quad \text{Eqn 3-11}$$

### 3.8.3 **Data sources**

#### General quality statement

The data obtained for this study is a mixture of both project-derived and external data. The external data were obtained from reputable sources and is used in a variety of Agency applications. The external data, unlike the project-derived data, is a mixture of temporal and spatial resolutions produced for other applications; as such data mining must be undertaken to obtain relevant values and facts. Much of the geochemistry is derived from 'working boreholes'. The results apply to the whole capture zone, rather than discrete investigated horizons that may indicate stratification, age and preferential flow paths.

#### *Grid coordinates and elevations*

Unless otherwise stated all coordinates quoted are referenced to the British National Grid, United Kingdom Transverse Mercator. Airy Spheroid, Ordnance Survey of Great Britain, 1936 Datum (OSGB 1936). The one hundred kilometre grid identification squares have been omitted, unless their inclusion was required. Elevations refer to topographic values, while height is a generic term to denote relative positions. Map elevations are in metres (m) above mean sea level, Newlyn Datum (AOD), depths to or from surfaces or a local datum point are in metres unless otherwise stated with the suffix or prefix bgl (below ground level). Where appropriate reduced groundwater elevations are based upon survey values, borehole log records or map contours, which are judged to have an accuracy of 'half the map contour interval' (Military Survey 1988).

#### *Maps*

All maps, unless otherwise stated, are orientated to grid north. They have been produced at scale, and reduced to allow documentation.

#### *Copyright*

The mapping and other digital data used in this project are subject to copyright controls. Permissions have been obtained to reproduce and use copyrighted material.

*BGS*

Reproduced by permission of the British Geological Survey. ©NERC. All rights reserved. IPR/80-06C.

*Ordnance Survey*

Reproduced by permission of Ordnance Survey © Crown Copyright/database right 2006 An Ordnance Survey/EDINA supplied service (data from Edina Digimap).

*Soil Survey*

Reproduced with the permission of Cranfield University National Soil Resources Institute.

*CEH*

Reproduced by permission from the Centre for Ecology and Hydrology, © NERC.

## **Chapter 4 Usk Valley**

### **4.1 Geological setting**

#### **4.1.1 *Description of area***

The project area comprises approximately 25km<sup>2</sup> in the lower Usk Valley, with the town of Usk located in the north-western corner (Figure 4-1 and Figure 4-2). The underlying aquifer is classed as a minor aquifer (SSEW 1977; Jones et al. 2000). The River Usk flows from the northwest around Usk and then southwards in a series of large meanders through the centre of the area. The river forms the lowest feature in a broad, approximately 1.5km wide, flat bottomed valley; within the project area the valley has an approximate north south alignment. The valley sides are moderately steep, rising from about 20m above ordnance datum (AOD) to 148m on the east, and 115m on the west flanks. The A449 a major trunk road runs north to south on the east flank.

There are some small scale industrial units located on the west bank of the town. The remainder of the local area is sheep and cattle farming on the valley flanks and arable crops on the valley floor. The hamlets of Llantrisant and Llangibby form the southern gateway to the project area, and numerous farms and isolated buildings cover the area. The project area falls in the boundary between National Grid Reference 100km identification squares ST and SO. Sample points were selected to give the best possible spatial distribution and were subject to the goodwill of local landowners.

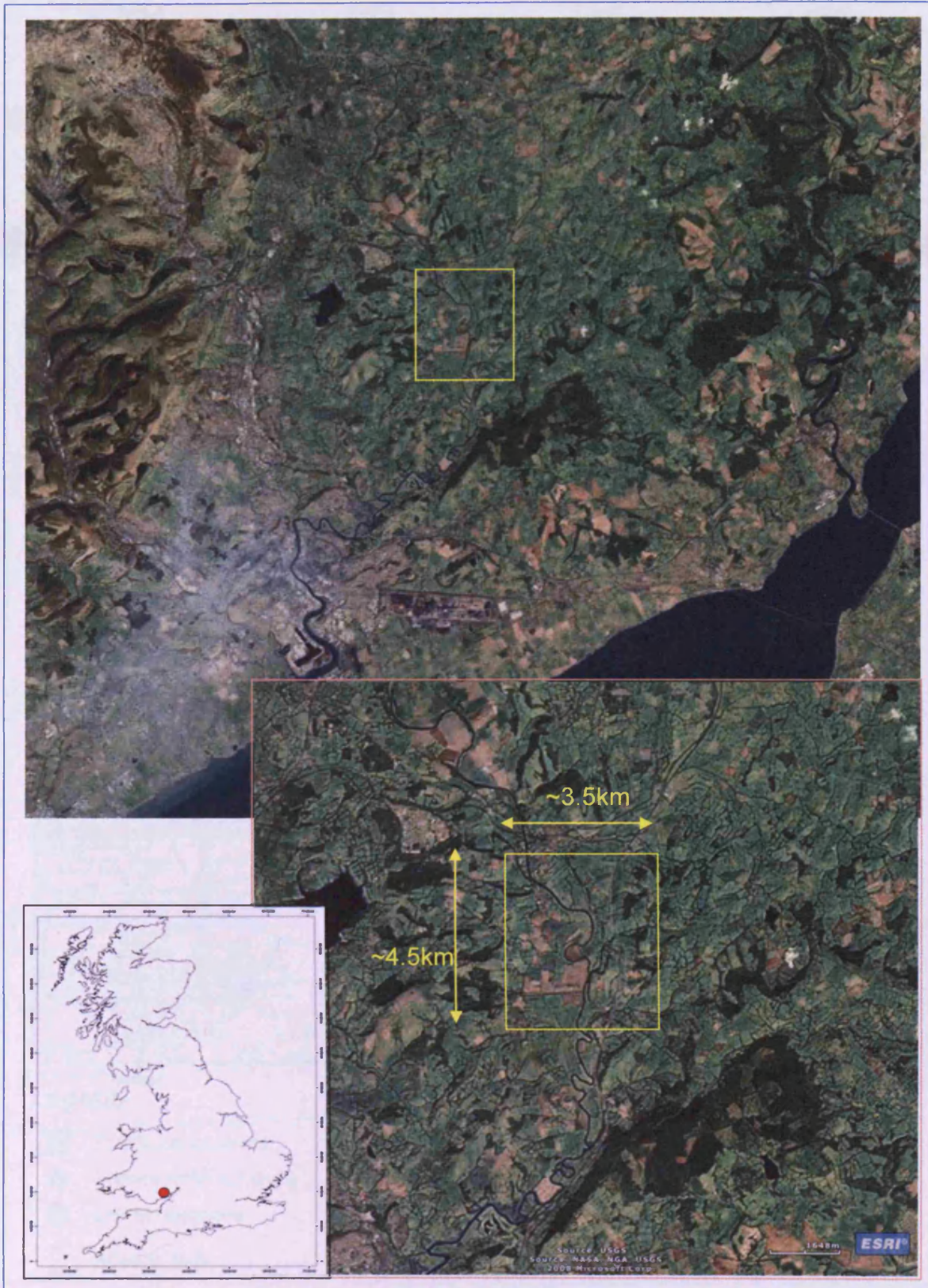


Figure 4-1 UK location map of the Usk Valley, Wales. Images from ESR, project area outlined in yellow.

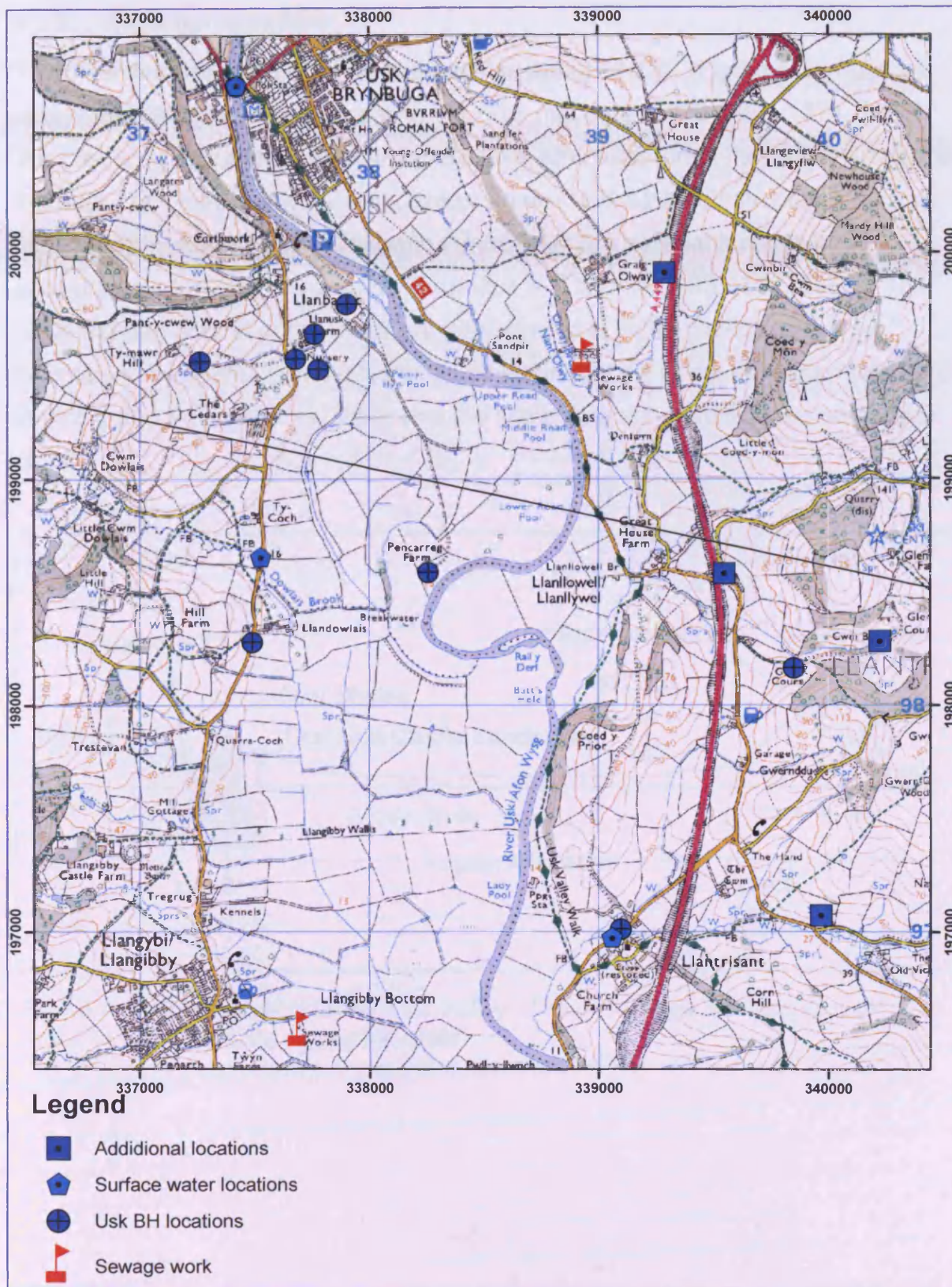


Figure 4-2 Map of Usk project area showing sampling locations by type. National Grid coordinates in metres UKTM. See endpaper maps for location names. Black line is profile section

#### 4.1.2 Regional structure

The general trend of dip is to the southeast at about 10-20° (Figure 4-3), although many local variations are recorded in the BGS mapping (BGS 1969, 1971, 1981). The Usk Anticline, a large north-south trending structure, forms the higher ground to the west. The map section also indicates smaller fault bounded structures such as the Llangibby Anticline and Craigwith Syncline on the east flank of this larger structure; this tends to increase the local dips in this area (BGS 1969, 1971). The north-western portion of the valley and project area is highly faulted, these are aligned sub-parallel or parallel to the dip direction and cross cut the folds. The BGS mapping and Squirrell et al (1969) indicate some conjugate faults to the southwest of Usk.

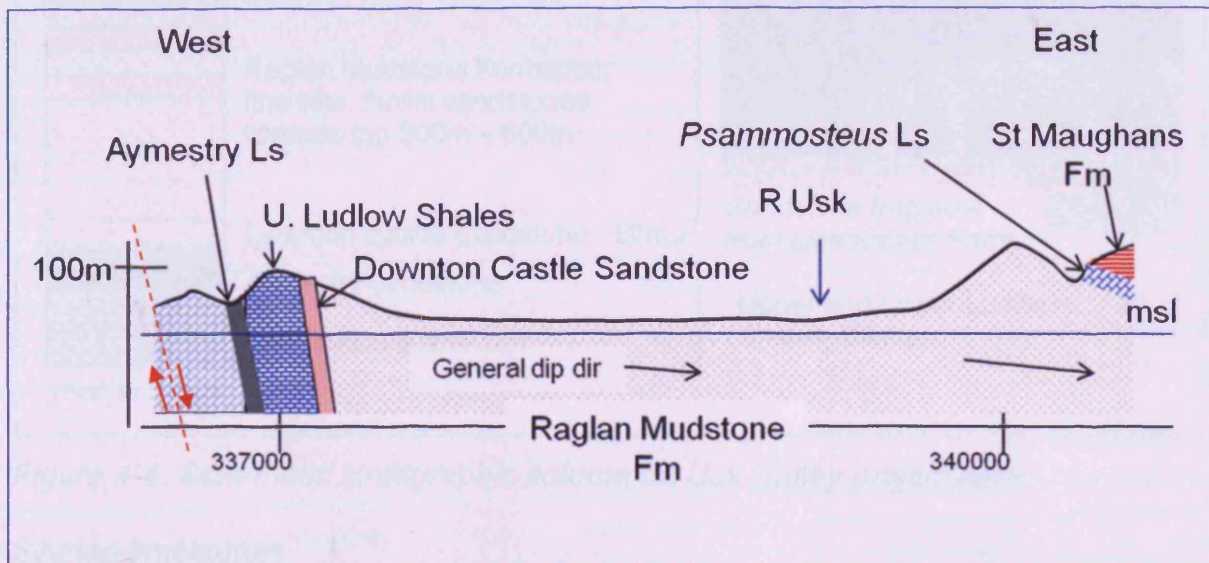


Figure 4-3 Cross section Lower Usk Valley. Drawn to scale and graphically reduced. Note easting values for scale

### 4.1.3 Lithostratigraphy

The geology of the area comprises a mixed lithology of Lower Palaeozoic limestones, sandstones, marls, and Recent terrace gravels and alluviums (Figure 4-4 and Figure 4-5 ).

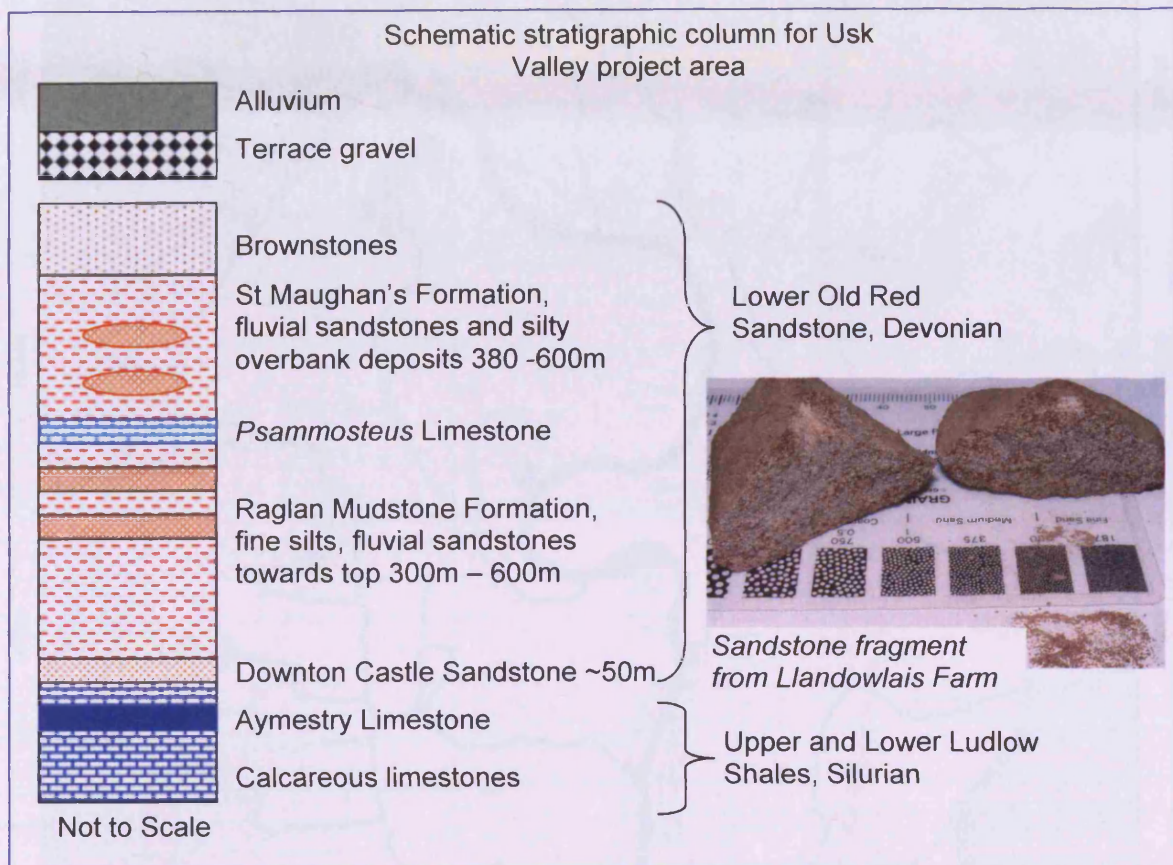


Figure 4-4 Schematic stratigraphic column for Usk Valley project area.

#### Silurian limestones

On the western flank of the valley (Figure 4-5) rocks of Silurian age are present: these consist of the Usk Limestone, an outlier of Wenlock age; Ludlow limestones and mudstones; the Lower Llanbadoc beds and silty mudstones of the Forest Beds. Extensive faulting is also indicated on the BGS mapping (BGS 1969, 1971). The upper Ludlow lithology consist of a succession of “clay and friable calcareous layers” with the “occasional nodular band” (Squirrell et al. 1969). These lithologies are believed to be fractured; the proximity to the anticline axis and observed faulting supporting this observation (Jones et al. 2000; Moreau et al. 2004). Field observations of the same lithologies elsewhere further support this (Gray 2004).

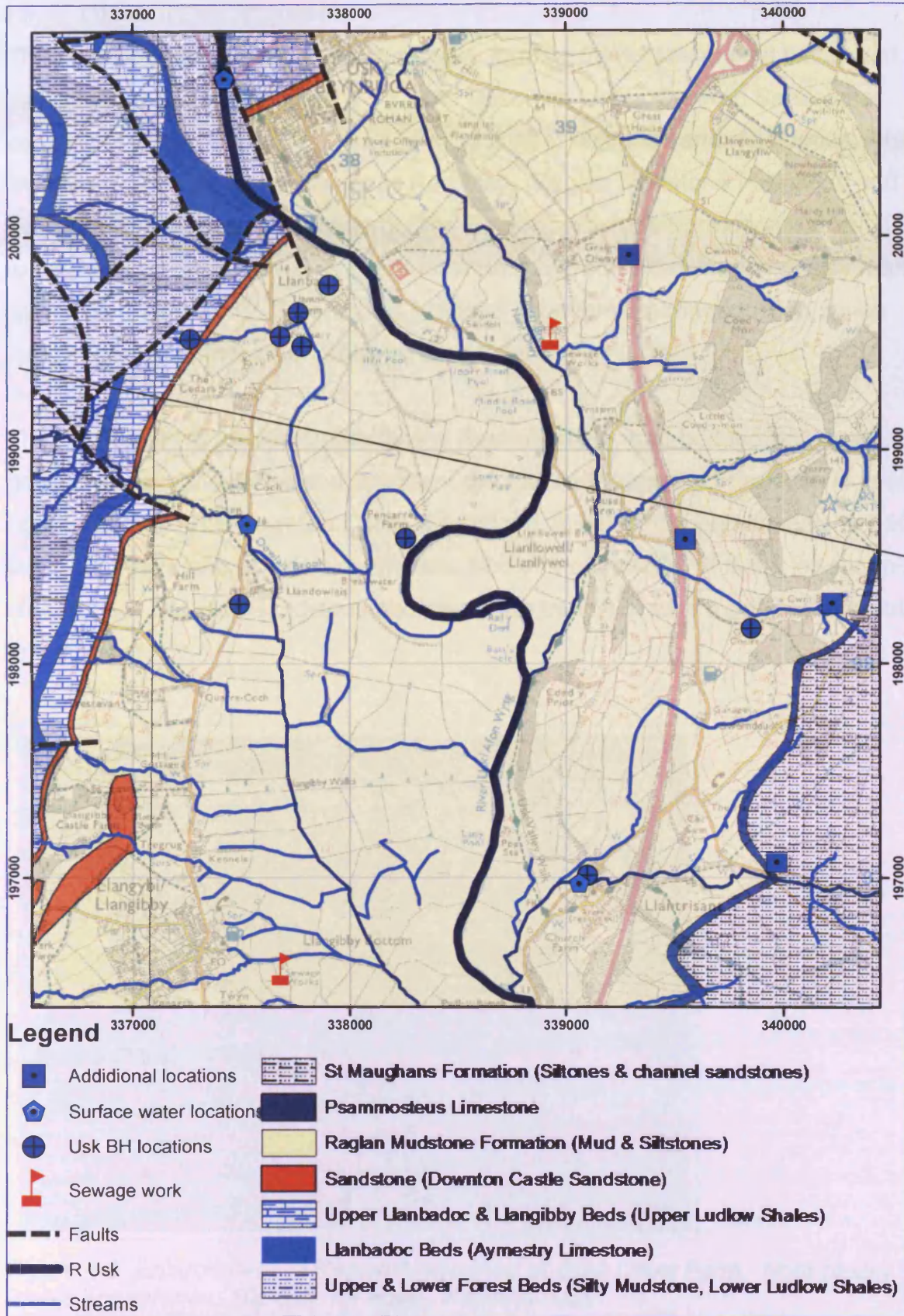


Figure 4-5 Bedrock geology and fluvial system in project area. Black line is line of cross section

### Lower Old Red Sandstones

This Formation dominates the project area, forming the west and east flanks and valley bottom lithology (Figure 4-5 ). The Devonian Lower Old Red Sandstone consists of thinly-bedded fine-grained sandstones, siltstones and mudstones, which weather to produce the argillaceous Red Marl, (Raglan Mudstone Formation and overlying St Maughan's Formation). The Raglan Mudstone Formation is from 305 to 610m thick. This Formation is predominantly a reddish brown marl or silty marl, with mica (Figure 4-6). Green spots believed to be ferrous iron reduction zones were observed in the upper profile at Glen Court Farm.

The upper units of the Raglan Mudstone Formation are inter-bedded with coarser grained fluvial sandstones and abundant calcretes although the Formation is itself poorly bedded. The Downton Castle Sandstone, a well developed sandstone ~50m thick, is present and exposed on the east limb of the anticline. It is the lowest unit of the Lower Old Red Sandstone and marks the transition from marine to terrestrial environments



*Figure 4-6 Enlargement of Raglan Mudstones at Glen Court Farm. Note blocky friable appearance; 10p coin for scale. Photo A Gray.*

The *Psammosteus* Limestone outcrops in the lower southeast and extreme northeast of the area, and is at the top of the Raglan Mudstone Formation (Figures 4-4 and 4-5). This is well-jointed, hard, between 5m to 1m thick and bedding is rarely seen.

The St Maughan's Formation is described as a succession of fluvial channel sandstones with accompanying overbank mud and siltstones (Figures 4-4 and 4-5). Marls are dominant and are lithologically similar to the lower Raglan Mudstone Formation. Calcretes are also present, mainly as reworked clasts; thickness is between 380 to 610m. These lithologies are deeply incised by small streams and form large steep-sided rounded hill features (Squirrell et al. 1969; Jones et al. 2000).

The former described lithologies are overlain by the Brownstone Group, which is not important in the project area.

#### Terrace deposits

Terrace deposits, which overlie the Raglan Mudstone Formation, outcrop along the western flank of the project area (Figure 4-6). This forms an almost continuous section, which is only interdicted by alluvium from larger water courses draining this west flank. These have been identified as the 2<sup>nd</sup> Terrace of the River Usk and are believed to consist of a gravely lithology. They are notably absent or have not been mapped on the lower eastern flanks of the valley side. A higher terrace exists but does not occur in the project area.

#### Alluvial deposits

The alluvium (Figure 4-7) commonly contains gravel and is poorly bedded; however within the wider valley zones this gives way to silt and sand. The thickness is reported as 15m near Newport on the coast, and beds of peat have also been recorded. The alluvium forms as tongues into the Raglan and St Maughan's Mudstone Formation on either side of the valley.

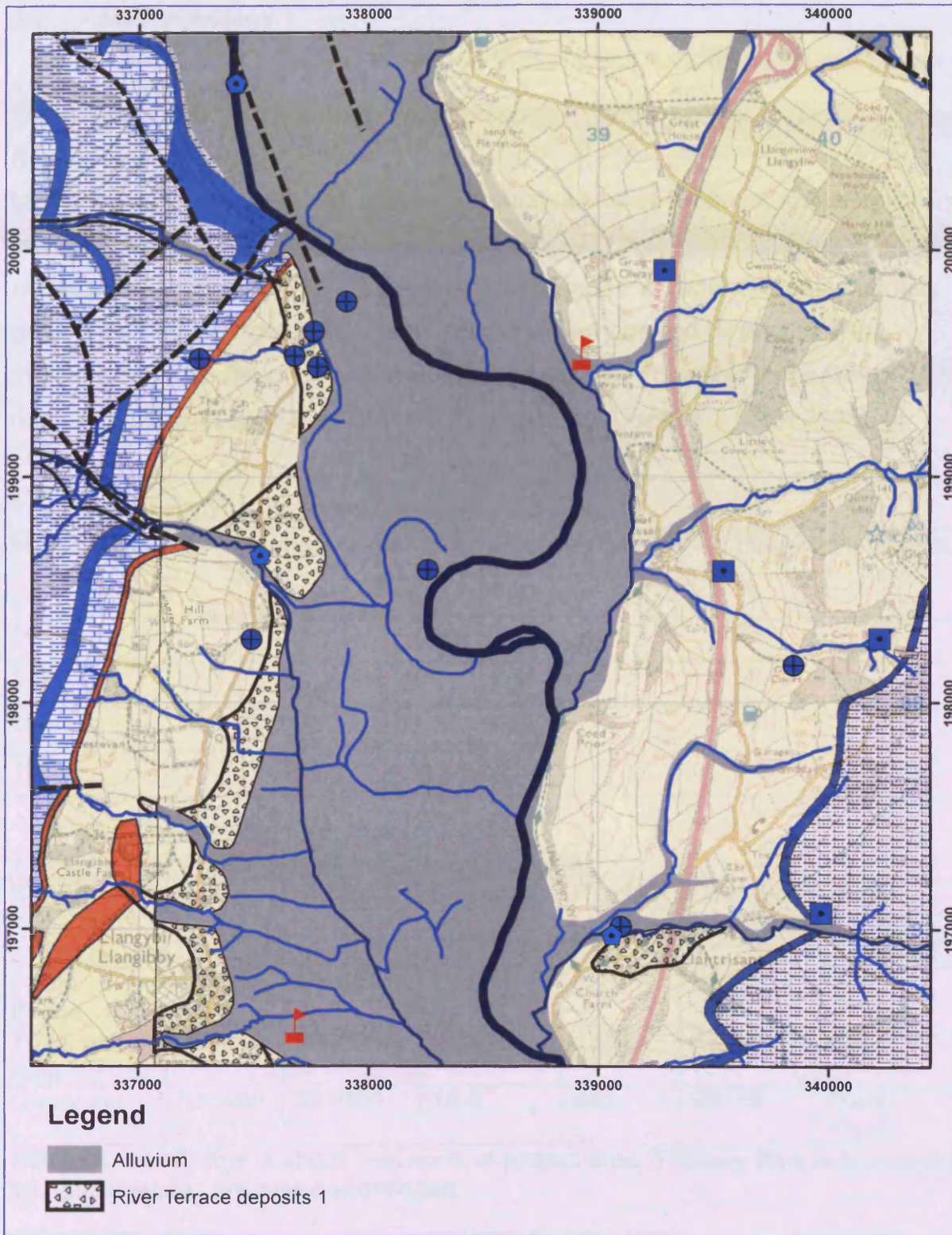


Figure 4-7 Superficial geology overlying bedrock. For bedrock and location legend see Figure 4-5

## 4.2 Hydrogeology

### 4.2.1 Water sources

#### Rainfall and evapotranspiration

MORECS data for square 156 indicates annual rainfall of 1069mm, and effective rainfall of 449mm. The project area is situated within the upper northeast quadrant of the MOREC square. The adjacent data is tabulated in Table 4-1; data courtesy of the Environment Agency (Wales). Rainfall will be affected by proximity to maritime areas and is in the shadow of the South Wales coalfield to the west. CEH rainfall data based upon the 1961-1990 average is in Table 4-2 (CEH 2008).

*Table 4-1 MOREC data for Usk and surrounding areas.*

MOREC Square	Annual rainfall mm	Effective rainfall mm	Evapotranspiration %
146	1281	746	58
147	819	273	33
156	1069	449	42
157	883	304	34

*Table 4-2 CEH River gauging station data for Usk.*

Station	Easting	Northing	Elevation m (AOD)	Rainfall mm	CEH Stn	River
Chain Bridge	334500	205600	22.6	1363	56001	Usk
Trostery Weir	335800	204200	20.4	1358	56010	Usk
Olway Inn	338400	201000	15.0	951	56015	Olway Brook

Notes: Chain Bridge is about 7km north of project area, Trostery Weir is 5km north and observations are now discontinued.

#### Borehole logs

A schematic diagram of the borehole logs and water rest levels provided is in Chapter 7. They are of insufficient quality to produce a 3D stratigraphy model for the area. They indicate confining conditions with the aquifer.

### Surface water

Surface water is dominated by the River Usk and Olway Brook. There are no major lake surface water bodies in the area other than Llandegfedd Reservoir about 5km to the west. At least one house (Cow House) has a large pond, which is lined and the water comes from a newly installed borehole. The Usk at Chain Bridge has a mean flow of 28.17m<sup>3</sup>/sec (NERC 2006). The project area falls entirely within the Usk catchment.

### Drainage

The River Usk dominates the project area, and is tidal to Newbridge, GR 338400 194800. The Olway Brook is a secondary surface water body draining the north-eastern part of the area, with a mean flow of 1.5 m s<sup>-1</sup>. There are several moderate-sized streams that drain the upper slopes, incising quite deeply in places, these flow both east and west to the River Usk. Some artificial field drainage is also known to be present (Pers. comm., N Bowyer a local farmer). Surface runoff during heavy rain events from the steep slopes is high (Pers. observation) and puddle storage on these slopes is low, although animal hoof prints do provide numerous 'mini-ponding' sites in places. The runoff potential from the Winter Rainfall Acceptance Potential (WRAP) map has the designation Class 1 (Boorman et al. 1995).

### Flooding

The valley bottom is prone to flooding. This is reported by local landowners, and this is also shown on the Environment Agency (Wales) map (Bernard and Delay 2008).

### Sewerage and landfill

The town of Usk generates sewerage; a waste water treatment works is located close to the Olway Brook at GR 338900 199600. The numerous small farms on the hill slopes are believed to have septic tanks. The hydrogeological map of South Wales indicates the presence of an old, unlined landfill containing domestic waste, which is believed to have been closed by 1976. The landfill is believed to have been located at GR 338800 199800 adjacent to the Olway Brook and several hundred metres west of Graig Olway (BGS 1986).

### **4.3 Aquifer properties**

#### **4.3.1 General**

The underlying sediments constitute a minor aquifer, and as such are not exploited for public water supply. The number of private boreholes within the region suggests that shallow groundwater is readily available. Investigation of the historic map archive also shows a number of wells and springs in the area, indication that groundwater has played an important role in water supply. The eastern portion of the valley is not connected to the water mains.

#### **4.3.2 Raglan Mudstone Formation**

While there is a large thickness of Raglan and St Maughan's Formation, permeability is limited. The interbedded sandstones have larger permeabilities, but are interbedded between low permeability siltstones, mudstones and marls, and may not be laterally extensive. Cementation and porosity within the Formations is variable. Friable sands exist as a result of carbonate cement leaching, while some may have low primary porosity due to quartz overgrowths. The calcrete horizons may provide zones of higher fracture permeability, although the *Psammosteus* Limestone is often associated with marshy ground and a notable spring horizon (Figure 4-7) suggesting a decrease in permeability (Squirrell et al. 1969; Jones et al. 2000) although Squirrell et al. (1969) suggests that it is 'well-jointed'.

The Red Marls which form over half the thickness of the Raglan and St Maughan's Mudstone Formations are described as essentially impermeable (Squirrell et al. 1969). This lithology is indicative of an anisotropic system, and a multi-layered aquifer system is believed to be operating in the hydraulically isolated sandstones. BGS (1986) further describes the water bearing parts of the Raglan Mudstone Formation as the *Psammosteus* Limestone and the Downton Castle Sandstone, with numerous springs at the base of the sandstone. Yields are described as low, and wells were constructed to increase the size of seepage areas. It also states that the water is very hard in excess of 450 mg l<sup>-1</sup> nearly all due to the presence of carbonates.

At depth compaction and diagenesis has caused hardening and the formation of impermeable bands. Fracture closure at depth is also believed to be important and an effective saturated depth of 40m is taken for most practical purposes (Jones et al. 2000). The presence of springs on both flanks of the valley is recorded on Ordnance Survey mapping (OS 2005c, 2007) and utilised as a source of water Figure 4-8.



*Figure 4-8 Spring and collection butt at Tump Farm, east flank of valley.*

#### Groundwater Flow

Jones et al 2000, report that steep hydraulic gradients of 0.01 to 0.1 have been observed, which may reflect a local topographic influence. The large topographic elevation differences between the flanks and valley bottom are also believed to drive a “strong hydraulic gradient forcing water through the aquifer” and that gradients are topographically controlled (Moreau et al. 2004).

#### Storage (S) and Porosity(n)

A lack of storage values for the Old Red Sandstone is reported by Jones et al (2000). Porosity data are lacking for the project area. Data available are from outside the immediate project area.

### Transmissivity (T)

The main controls on transmissivity are the lateral and vertical anisotropy due to lithological changes (Jones et al. 2000). Pumping test analysis has resulted in transmissivity ranges of 10-100 m<sup>2</sup> day<sup>-1</sup> although in the Raglan Mudstone Formation, four tests recorded values of 4-13 m<sup>2</sup> day<sup>-1</sup>. It is believed that the observed range was caused by:

- Interconnection of bedding plane fractures at a local level. This may provide high transmissivity for short duration pumping tests.
- Data bias, as pumping tests are preferentially carried out on boreholes that are believed to have a better production rate. Only four tests have been carried out within the Raglan Mudstone Formation.
- Burial depth and rebound effects on fracture development caused by the presence of the Welsh ice sheet during the Tertiary glaciations.

Pumping test data (March 2005), for Llewellyn monitoring borehole (ST) 339544 198583 provided by the EA gives a value of 58 m<sup>2</sup> day<sup>-1</sup> (Cooper-Jacob straight line). Recovery data from February 2007 results in a value of 95 m<sup>2</sup> day<sup>-1</sup> for the early data and 40m<sup>2</sup> day<sup>-1</sup> for late data (Cooper-Jacob). The Theis Modified Recovery method produces a value of 95 m<sup>2</sup> day<sup>-1</sup> for the early data.

### Drift cover

Figure 4-7 shows the extent of the drift and modern sediments cover within the project area. The data was obtained from the Edina Digimap service and verified by inspection of BGS mapping (BGS 1969, 1971, 1981).

### Regolith

The project area has only four soils types which may influence the aquifer properties; these are tabulated in Table 4-3 and a map (Figure 4-9). The 541 soil type is further describes as a "typical brown earth, which is non-alluvial with a non-calcareous subsoil without significant clay enrichment". The 561 are "brown alluvial soils and are loamy or clayey soils again with non-calcareous subsurface horizon developed in alluvium," (SSLRC 1983c).

Table 4-3 Soil characteristics of Usk Valley area.

Soil name	Map	Geology	Characteristics	Land use	Catchment location
Milford	541a	Devonian sandstone, siltstone, mudstone & slate	Well drained fine loamy reddish soils over rock. Some steep slopes	Dairying, cereals,	Valley sides
Lugwardine	561d	Reddish river alluvium	Deep stoneless permeable reddish fine silty soils. Similar coarse silty soils locally. Associated with fine silty soils variably affected by groundwater. Flat land and risk of flooding	Stock, cereals	Valley bottom
Cegin	713d	Drift from Palaeozoic slatty mudstones & siltstones	Slowly permeable seasonally waterlogged fine silty & clayey soils. Some fine silty & fine loamy soils with slowly permeable subsoils and slight seasonal waterlogging on slopes		
Fladbury	813d	River alluvium	Stoneless clayey, fine silty & fine loamy soils affected by groundwater. Flat land & risk of flooding	Stock & winter cereals, permanent grassland	Southwest part of area

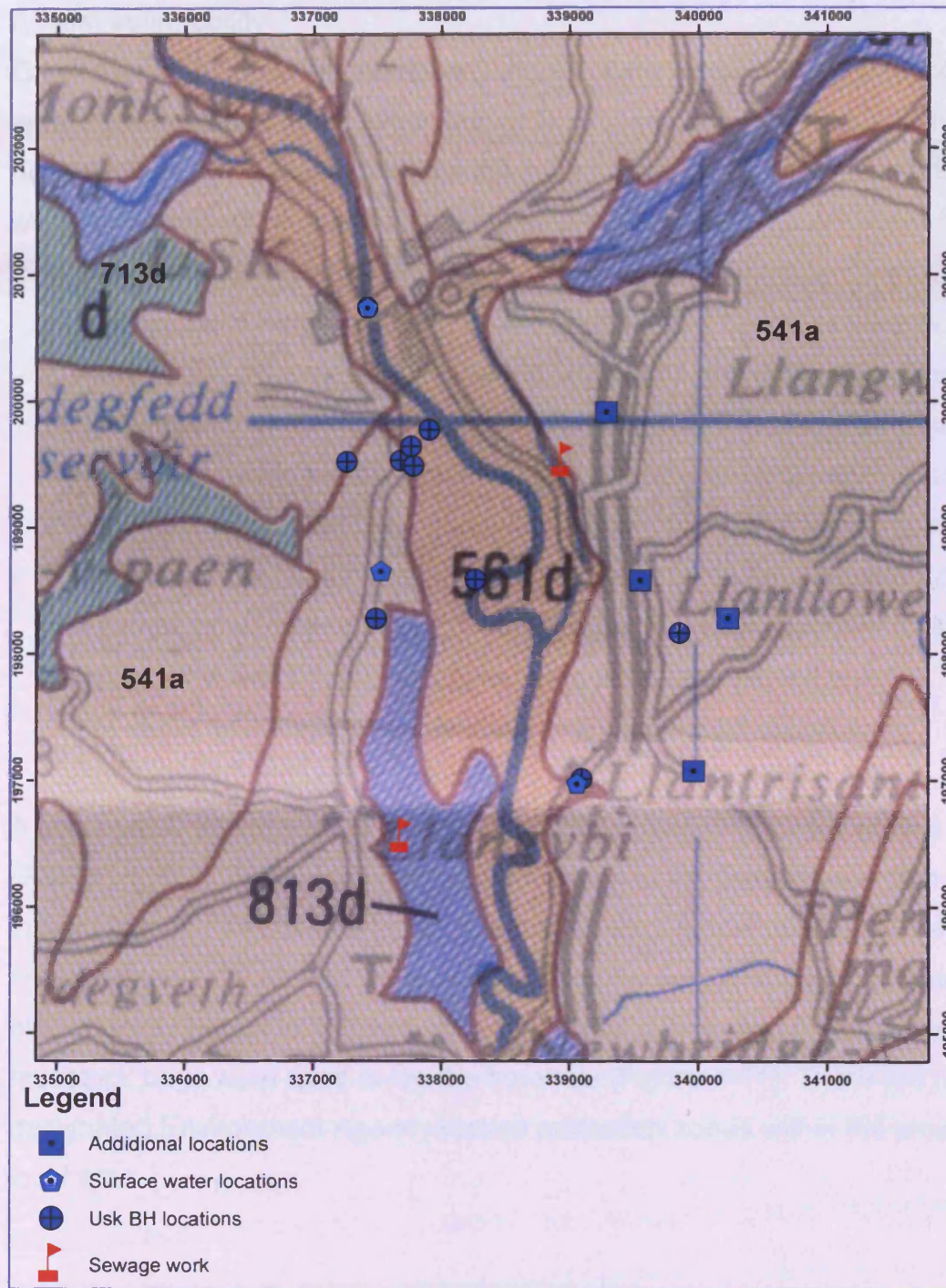


Figure 4-9 Soils map showing distinct changes in soil type in project area (SSLRC 1983c). See Table 4-3 for soils description

### Aquifer vulnerability

Groundwater vulnerability mapping (Figure 4-10) indicates that within the project area the minor aquifer has two vulnerability classes; 'Soils of high leaching potential' and 'Soils of intermediate leaching potential'. Both classes are at level 1 within their respective sub-classes; the following descriptions are taken from the map legend (SSLRC 1996):

- High; "Soils with little ability to attenuate diffuse source pollutants and in which non-adsorbed diffuse source pollutants and liquid discharges have the potential to move rapidly to underlying strata or to shallow groundwater"
- H1 "Soils which readily transmit liquid discharges because they are either shallow, or susceptible to rapid flow directly to rock, gravel or groundwater"
- Intermediate; "Soils which have a moderate ability to attenuate diffuse source pollutants or in which it is possible that non-adsorbed diffuse source pollutants and liquid discharges could penetrate the soil layer"
- I1 "Soils which can possibly transmit a wide range of pollutants".

A non-aquifer designation is given to the high ground west of the project area (SSLRC 1996). The potential for contamination of the groundwater from borehole ingress is high. This is due to the poor condition of some sampled borehole headworks. While several were isolated from the surrounding ground surface, others were only protected by hessian rags and in one case old agricultural feedstock bags were used to lag the borehole (Figure 4-11). There are no designated Environment Agency source protection zones within the project and local area.

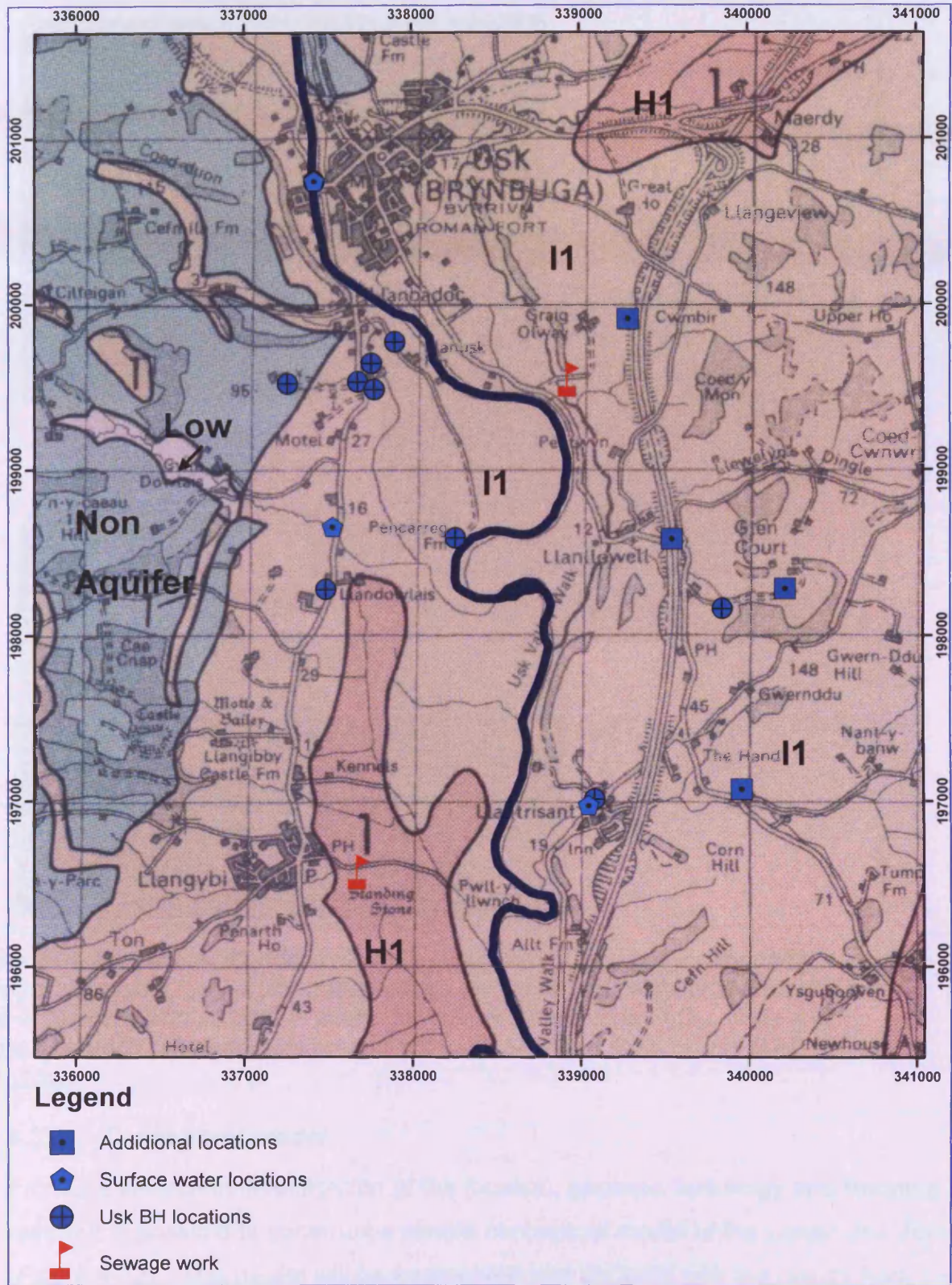


Figure 4-10 Aquifer vulnerability map of project area (SSLRC 1996). River Usk in blue.



*Figure 4-11 Headworks: open access, unprotected and lagged by agricultural bags. The label on the blue plastic bags circled in yellow show they contained NPK fertiliser with soluble in water phosphorus pentoxide  $P_2O_5$ . Note weed killer, oil and fuel containers on well parapet; Location Cow House Well. Photo A Gray.*

### 4.3.3 **Conceptual model**

From the preceding investigation of the location, geology, hydrology and literature review it is possible to construct a simple conceptual model of the Lower Usk Valley (Figure 4-12). This model will be augmented and updated with the results from the succeeding chapters, and will be carried forward into the modelling phase of the investigation.

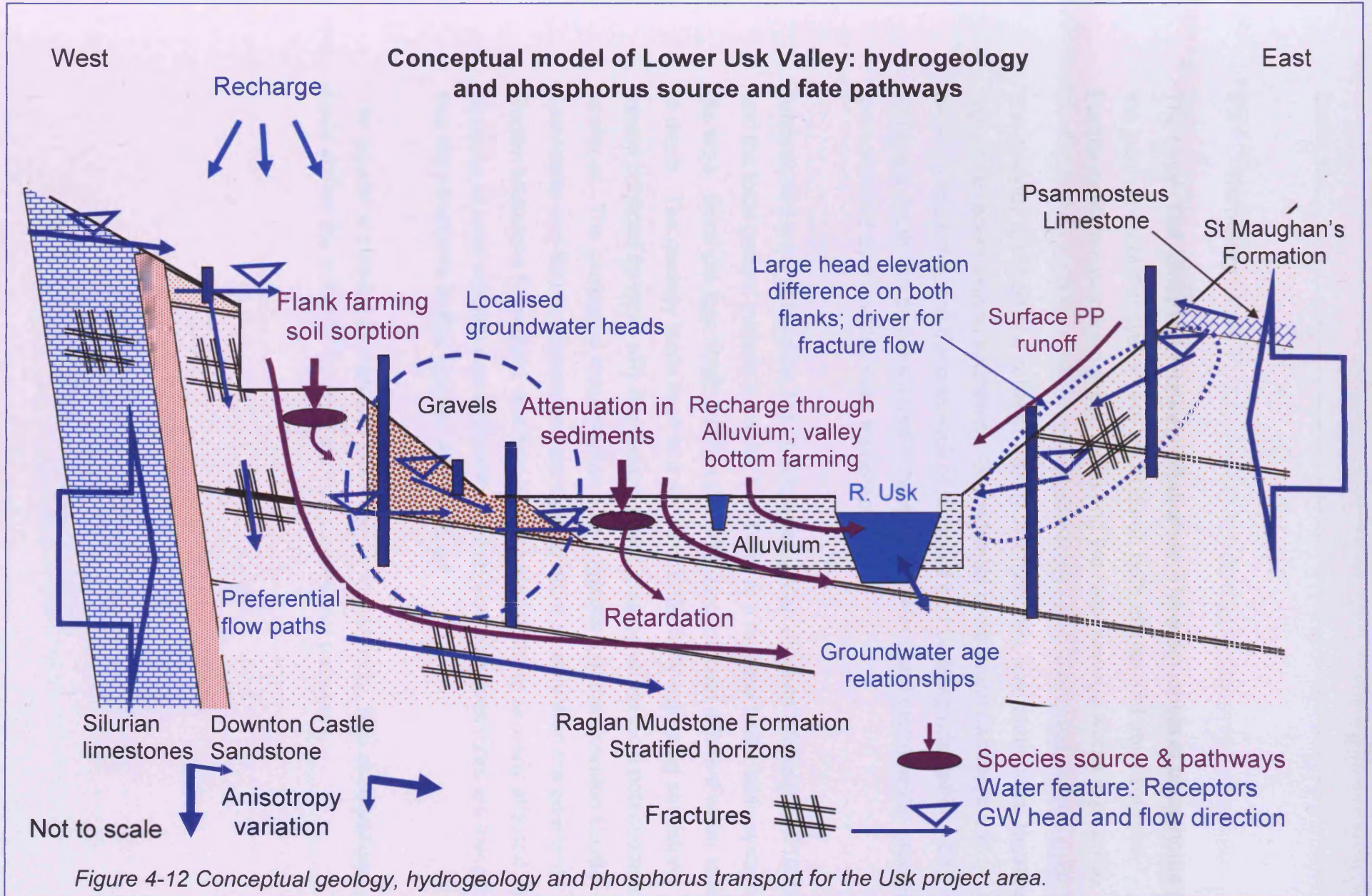


Figure 4-12 Conceptual geology, hydrogeology and phosphorus transport for the Usk project area.

#### 4.4 Summary

The Lower Usk valley is a relatively small area. The main inputs of phosphorus to the local groundwater system are agricultural; both diffuse and point sources. Further contamination from septic tanks and the local sewage works is possible.

The geology is varied and consists mostly of limestones and mudstones, together with more recent alluvial sediments. Groundwater preferential pathways are believed to exist due to the presence of fractures and bedding orientation. The saturated depth can be considered to be shallow ~40m, and groundwater gradients are controlled by the valley flank topography.

Analysis of the borehole dips, the Hydrogeology Map of south Wales (BGS 1986), and the local ground surface indicates that there is a multiple water table system in the area. Borehole logs obtained from the BGS also indicate different water strikes at depth. The geology lends itself to a series of potentially saturated sandstone lenses confined by more silty clay layers, which may generate local potentiometric surfaces. The geological cross section also suggests that the Downton Castle Sandstone and Silurian limestones are dipping more steeply than the adjacent Raglan Mudstone Formation, and that bedding anisotropy is similarly affected. The absence of local artesian flow also indicates that confining pressures are low and that the sandstone lenses may be very localised

The aquifer is classed as high and intermediate vulnerability; field observations have shown the potential for point source contaminant pathways.

## Chapter 5 Usk Valley groundwater

### 5.1 Introduction

Observations were made at thirteen groundwater and surface water locations within the lower Usk Valley. The observations were made in order to characterise the physical aquifer, and establish the spatial and temporal extent and concentration of phosphorus. A map with location ID codes is provided (Figure 5-1).

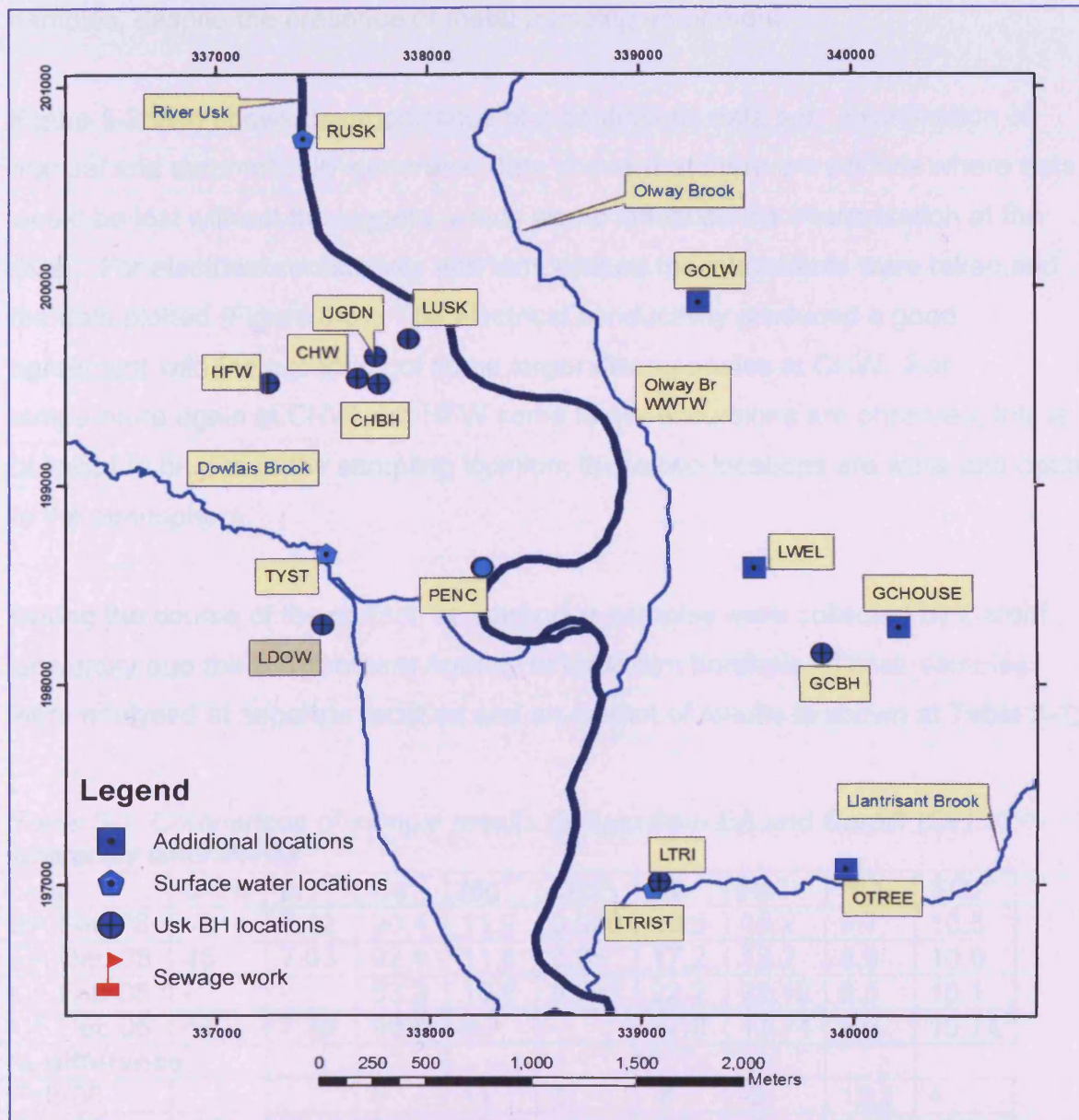


Figure 5-1 Location ID map, base map removed to assist clarity. River Usk shown winding through central project area.

### 5.1.1 Data quality assurance

Before the data were analysed, checks for quality assurance were undertaken; this involved comparison with equivalent or derived measurements and statistical analysis. The general reconciliation of manual dip and calculated logger depth to water were acceptable; some large excursions were noted but are believed to be a whole decimetre misreading (Figure 5-2). String was used to suspend the loggers in preference to steel wire rope so as to avoid the possibility of contamination in the samples, despite the presence of metal pumping equipment.

Figure 5-2 also shows the importance of a continuous data set. Examination of manual and automatically-generated data shows that there are periods where data would be lost without the loggers, which would influence the interpretation of the data. For electrical conductivity and temperature measurements were taken and the data plotted (Figure 5-3). The electrical conductivity produced a good agreement with the exception of some larger discrepancies at CHW. For temperature again at CHW and HFW some larger excursions are observed; this is believed to be due to the sampling location; these two locations are wells and open to the atmosphere.

During the course of the project, synchronous samples were collected by Cardiff University and the Environment Agency at Llewellyn borehole. These samples were analysed at separate facilities and an extract of results is shown at Table 5-1:

*Table 5-1 Comparison of sample results derived from EA and Cardiff (CF) University laboratories.*

Date	DO%	pH	Ca <sup>2+</sup>	Mg <sup>2+</sup>	SRP	Cl <sup>-</sup>	Na <sup>+</sup>	NO <sub>3</sub> <sup>-</sup>	SO <sub>4</sub> <sup>2-</sup>
EA Feb-08	-	7.12	90.4	11.9	0.059	20.5	16.2	9.7	10.5
EA Dec-08	46	7.03	92.8	11.8	0.05	17.2	13.2	8.5	10.0
CF Feb-08	-	-	83.3	10.6	0.057	22.2	22.12	8.5	10.1
CF Dec-08	54	7.36	90.6	8.7	-	17.8	13.74	8.5	10.74
<b>% difference</b>									
Feb-08			8	11	3	-8	-3	12.3	4
Dec-08	-17	-5	2	26		-3	-4	0	-7.4

Values in mg l<sup>-1</sup> or appropriate units

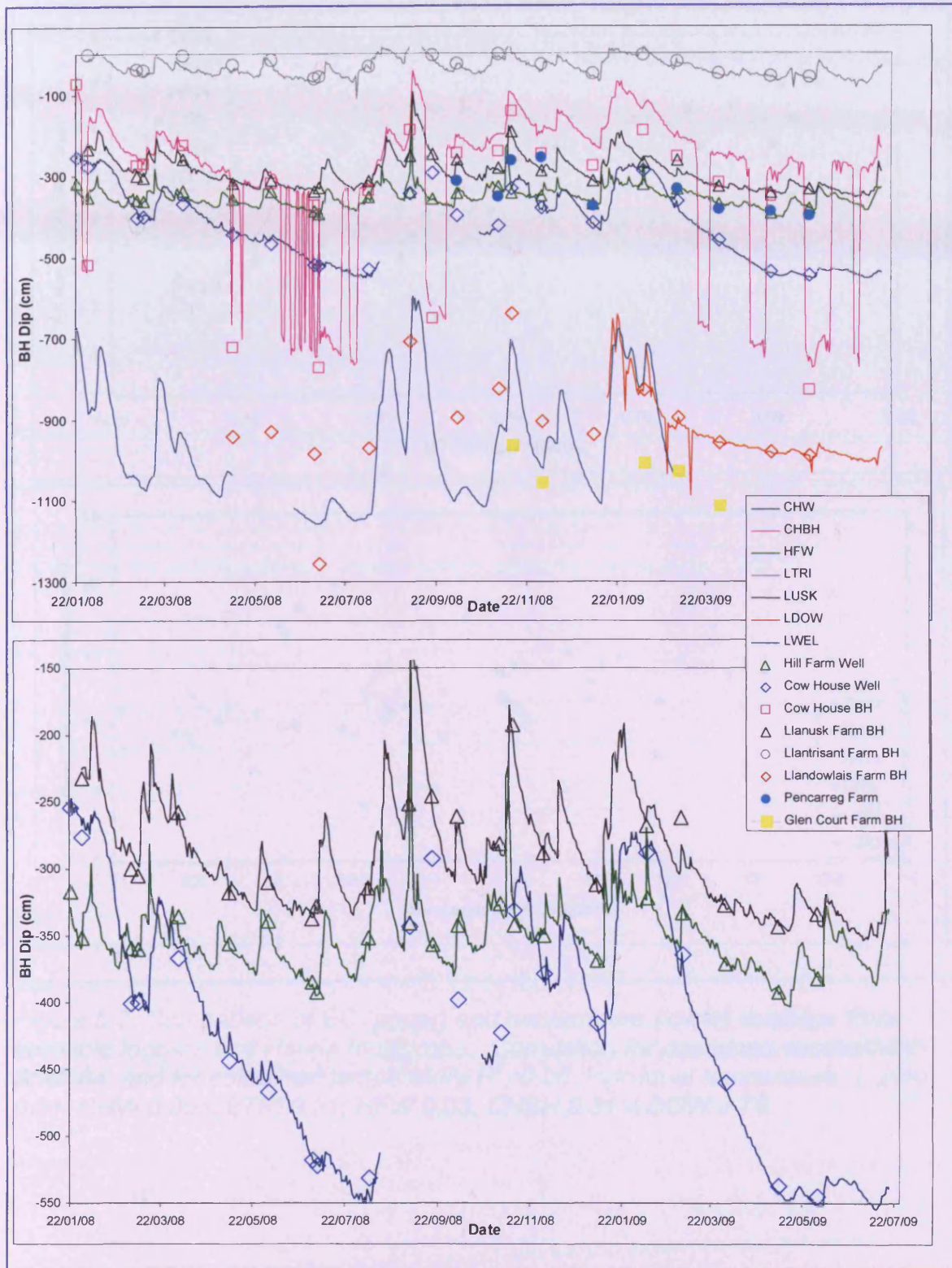


Figure 5-2 Borehole dip data and manual dip values. Lower hydrograph to show correlation of selected Boreholes (some data locations omitted). Manual dips as points and full location name, logger data continuous lines.

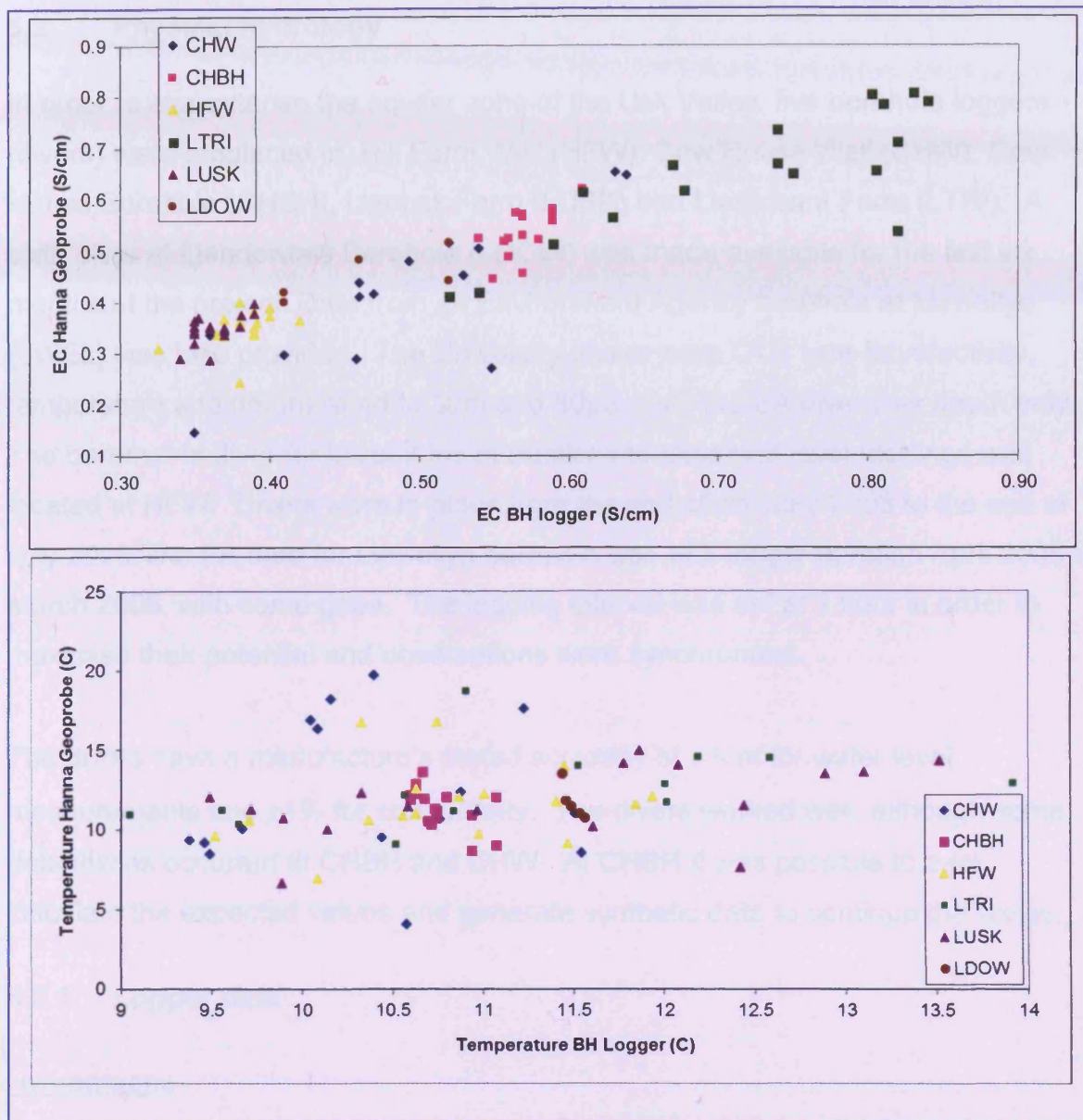


Figure 5-3 Comparison of EC (upper) and temperature (lower) readings from borehole loggers and Hanna multiprobe. Correlation for combined conductivity  $R^2=0.84$ , and for combined temperature  $R^2=0.06$  Individual temperature: LUSK 0.21; CHW 0.004; LTRI 0.21; HFW 0.03; CHBH 0.31; LDOW 0.76.

## 5.2 Physical hydrology

In order to characterise the aquifer zone of the Usk Valley, five borehole loggers (divers) were emplaced in, Hill Farm Well (HFW), Cow House Well (CHW), Cow House Borehole (CHBH), Llanusk Farm (LUSK) and Llantrisant Farm (LTRI). A sixth diver at Llandowlais Borehole (LDOW) was made available for the last six months of the project. Data from an Environment Agency borehole at Llewellyn (LWEL) was also provided. The University divers were CTD type (conductivity, temperature and depth) rated to 30m and  $80\mu\text{S cm}^{-1}$ ; the EA diver was depth only. The barometric diver for barometric corrections to observed level readings was located at HFW. Divers were in-place from the end of January 2008 to the end of July 2009. The EA data for Llewellyn borehole was of a longer duration April 2005 to March 2009, with some gaps. The logging interval was set at 1 hour in order to maximise their potential and observations were synchronous.

The divers have a manufacture's stated accuracy of  $\pm 3\text{cm}$  for water level measurements and  $\pm 1\%$  for conductivity. The divers worked well, although some data losses occurred at CHBH and CHW. At CHBH it was possible to back calculate the expected values and generate synthetic data to continue the series.

### 5.2.1 *Logger data*

#### Hydrographs

The hydrograph data are presented as well dip rather than height above Ordnance Datum as this reduces the vertical scale interval. Two graphs are shown; all available data and the common project period (Figure 5-4).

The data gaps in the series are apparent, and the rapid drawdowns in the CHBH data are caused by prolonged pumping (by the owners). It is also noted that the values in LTRI becomes positive on some occasions; this is due to flooding of the manhole and choice of a local datum (top of casing flange plate). The location is not artesian, but the water table does rise very close to the ground surface.

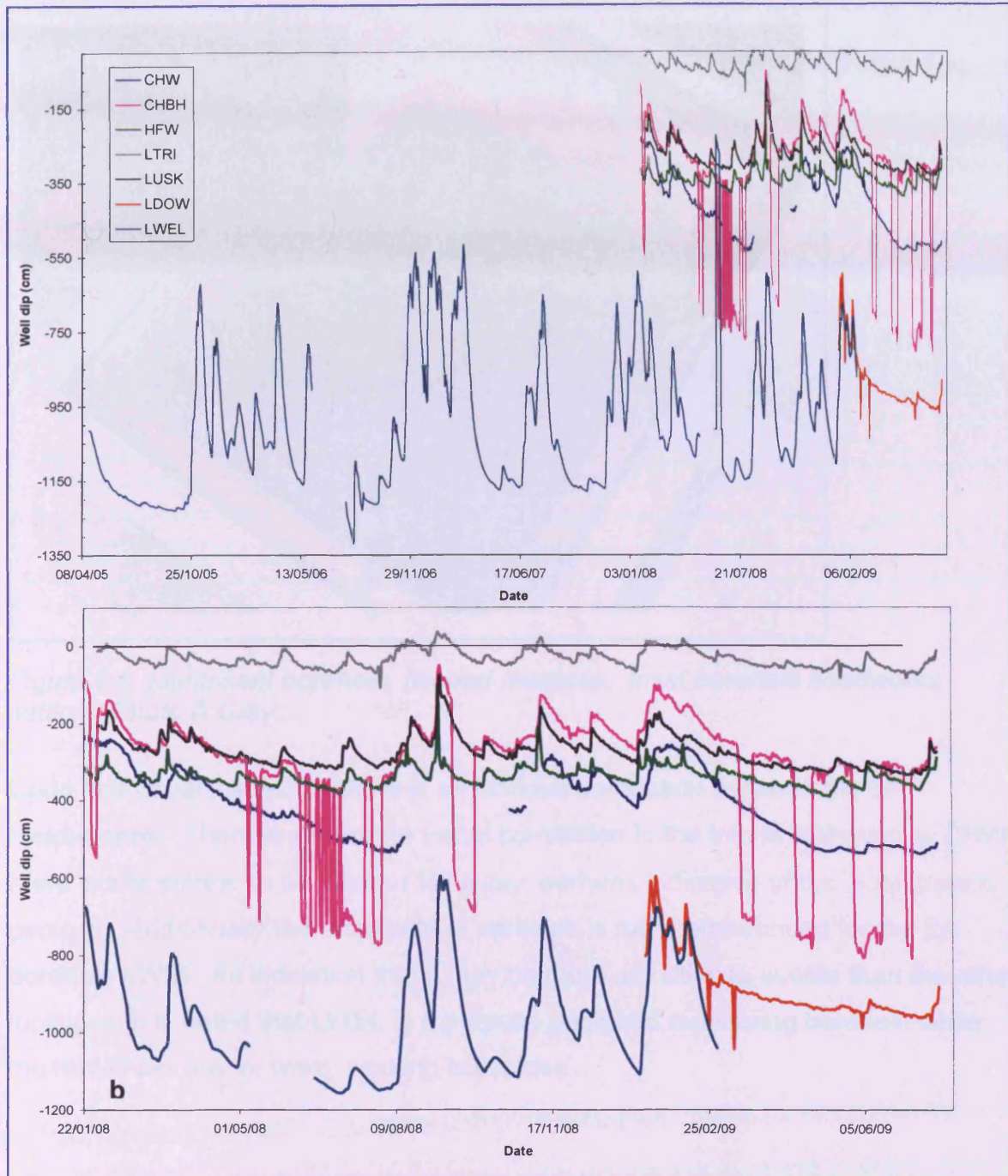


Figure 5-4 Borehole logger data for the Usk Valley area. (a), all data. (b), project timeline data. Note difference in date interval for lower hydrograph.



*Figure 5-5 Llantrisant borehole, flooded manhole. Inset borehole headworks setting. Photo A Gray.*

Upon first visual inspection there is an obvious correlation between the BH hydrographs. There is also some visual correlation in the trends, although at CHW there would appear to be a larger fall away, perhaps indicative of the local gravels geology. Additionally the amplitude of variation is more pronounced for the EA borehole LWEL, an indication that it may be more sensitive to events than the other locations. It is noted that LWEL is a purpose designed monitoring borehole while the remainder are, or were, working boreholes.

Hydrograph correlation

A correlation analysis of the borehole data was undertaken to test the apparent visual correlation of the water rest levels. The hourly data was reduced to daily readings at 2300hrs; this time was chosen as it was believed that any major domestic use would be finished. The results of this analysis are in Table 5-2.

*Table 5-2 Spearman's correlation: daily (2300hrs) water rest levels.*

		CHW	CHBH	HFW	LTRI	LUSK	LDOW	LWEL
CHW	Correlation t	1	.835**	.606**	.730**	.862**	.917**	.900**
	Sig.	.	0	0	0	0	0	0
	N	469	469	469	461	461	188	286
CHBH	Correlation		1	.698**	.746**	.827**	.751**	.859**
	Sig.		.	0	0	0	0	0
	N			542	534	534	188	359
HFW	Correlation t			1	.869**	.769**	.705**	.729**
	Sig.			.	0	0	0	0
	N				539	539	188	364
LTRI	Correlation				1	.874**	.862**	.882**
	Sig.				.	0	0	0
	N					539	188	356
LUSK	Correlation					1	.874**	.892**
	Sig.					.	0	0
	N						188	356
LDOW	Correlation t						1	.909**
	Sig.						.	0
	N							46
LWEL	Correlation							1
	Sig.							.
	N							

\*\*Correlation is significant at the 0.01 level (2-tailed).

In addition to the logger data the manual dips have also been correlated (Table 5-3), which provides information on the boreholes that did not have loggers. The results show strong positive correlation with PENC and GCFM, indicating a degree of homogeneity in the aquifer. It also suggests that the difference between the manual dips and logger dips are comparable.

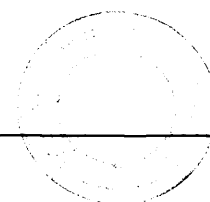


Table 5-3 Spearman's correlation: manual dip correlations.

		HFW	CHW	CHBH	LUSK	LTRI	LDOW	PENC	GCFM
HFW	Correlation	1	.579**	.740**	.676**	.807**	.829**	0.661	.857*
	Sig.		0.003	0	0.001	0	0	0.053	0.014
	N		24	24	22	22	18	9	7
CHW	Correlation			.647**	.854**	.696**	.849**	.900**	.964**
	Sig.			0.001	0	0	0	0.001	0
	N			24	22	22	18	9	7
CHBH	Correlation				.599**	.596**	.955**	.833**	.964**
	Sig.				0.003	0.003	0	0.005	0
	N				22	22	18	9	7
LUSK	Correlation					.893**	.941**	.817**	.929**
	Sig.					0	0	0.007	0.003
	N					22	17	9	7
LTRI	Correlation						.933**	.762*	1.000**
	Sig.						0	0.017	
	N						17	9	7
LDOW	Correlation							.767*	1.000**
	Sig.							0.016	
	N							9	7
PENC	Correlation								.829*
	Sig.								0.042
	N								6
GCFM	Correlation								
	Sig.								
	N								

\*\*Correlation is significant at the 0.01 level (2-tailed).

\*Correlation is significant at the 0.05 level (2-tailed).

### Autocorrelation

The Usk hydrograph data was also statistically analysed by autocorrelation techniques. While it is recommended that the data length be about three times the length of the period of interest (Nielson and Wendroth 2003; Hill and Lewicki 2007) this was not possible with the Usk data. However as seasonality is being examined, the values at the chosen lag interval should indicate the presence or absence of a serial dependency.

The auto correlation plots (Figure 5-6) are based upon a 30 day reduction of hourly data. The lag interval is therefore a monthly equivalent. Interpretation of the correlograms indicates that there is a seasonal signature in CHW and CHBH; this is apparent in the negative anti-correlation after lag 4. Due to a short data set, the significance of the lags is at the statistical limit, the seasonal pattern is however dominant and confidence is imparted to the analysis.

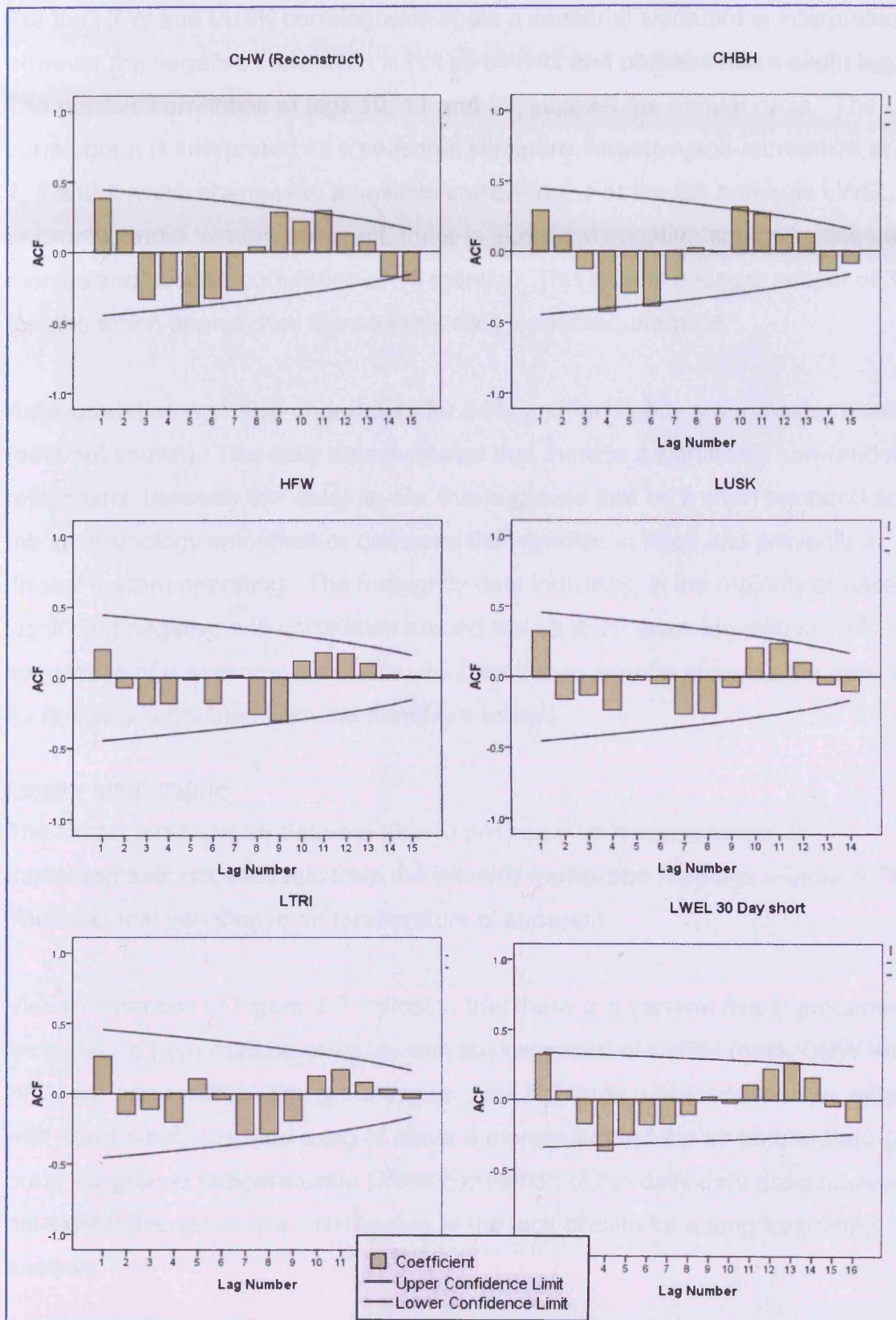


Figure 5-6 Autocorrelation plots for monthly water rest levels within the Usk Valley.

For the HFW and LUSK correlograms again a seasonal signature is interpreted, however the negative correlation is not as distinct and perhaps has a slight lag. The positive correlation at lags 10, 11 and 12, suggest the annual cycle. The LTRI correlogram is interpreted as a seasonal signature, negative anti-correlation at lag 7, 8 and 9 which changes to a positive correlation. For the EA borehole LWEL the seasonal nature is more apparent; there is statistical negative anti-correlation at 4 months and positive correlation at 13 months. This data is a longer subset of 32 months which approaches the analysis data length requirement.

Autocorrelation was also undertaken for daily and fortnightly groundwater levels (data not shown). The daily data indicates that there is a significant non-random relationship between the water levels, this suggests that on a short temporal scale the local lithology smoothes or dampens the variation in head and prevents a 'flashy' system operating. The fortnightly data indicates, in the majority of cases, a significant negative anti-correlation around the 18 to 22 week lag interval; this is suggestive of a seasonal pattern to which credence may be given as the data set for analysis is doubled from the monthly intervals.

#### Logger temperature

The logger temperature data are able to provide a continuous series of measurements not available from the monthly multiprobe readings (Figure 5-7). The seasonal variation in air temperature is apparent.

Visual inspection of Figure 5-7 indicates that there is a general rise in groundwater temperature from April 08 onwards with the exception of CHBH (note, CHW and HFW are open wells). The groundwater data indicates a seasonal nature, albeit with lower amplitude, and a lag of about 3 months behind the air temperature (a proxy for ground temperature). Cross correlation of the daily data does however not exhibit this value; this may be due to the lack of data for a long frequency analysis.

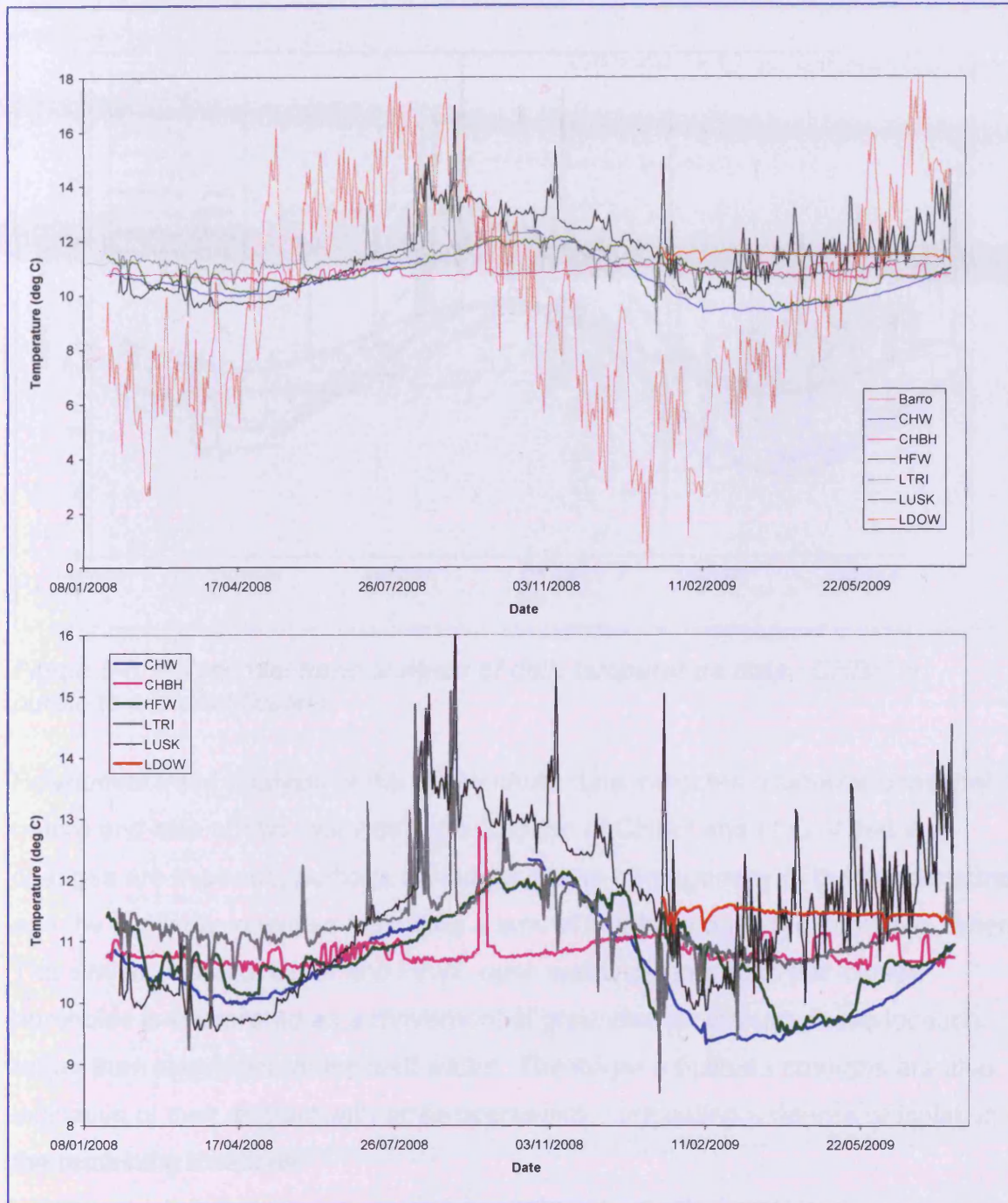


Figure 5-7 Borehole logger daily temperature data for all locations. Upper diagram includes air temperature from barometric logger (Barro). Lower diagram groundwater temperature only.

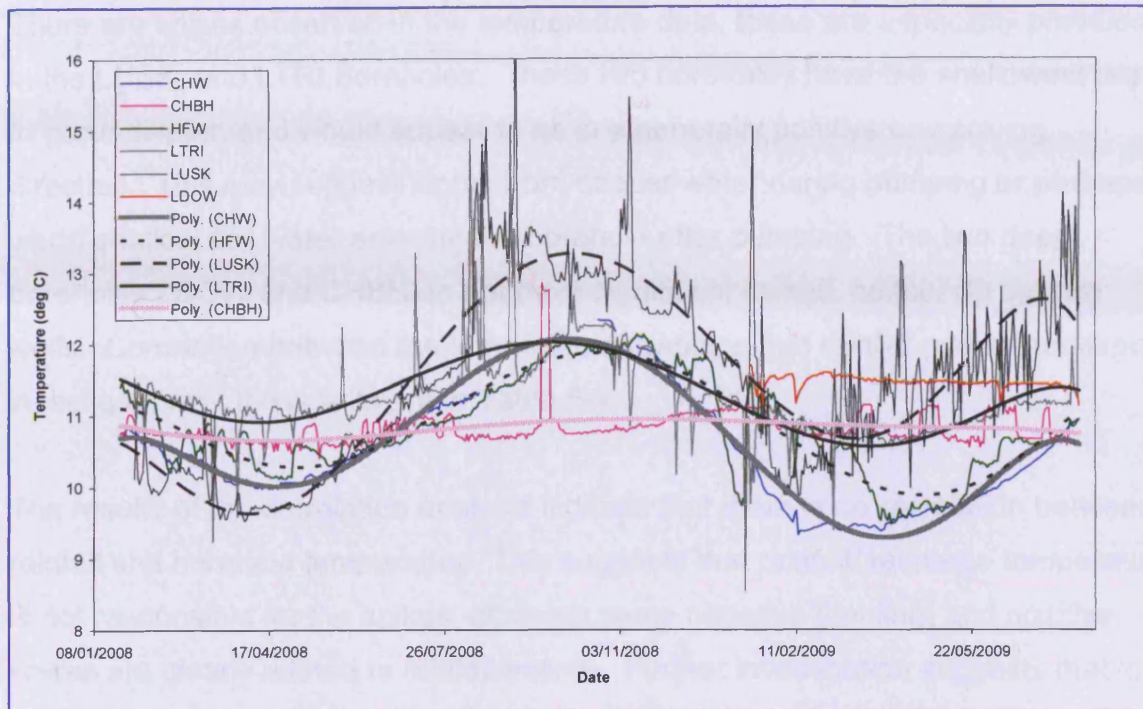


Figure 5-8 Polynomial trend analysis of daily temperature data. CHBH in purple to aid identification.

Polynomial trend analysis of the temperature data indicates a sinuous seasonal nature and also shows that with the exception of CHBH and LDOW that the changes are in phase, perhaps an indication the homogeneity of the aquifer zone, and the similarity in values indicating a lack of stratification in the sampling zones. The similar phase of CHW and HFW, open wells, compared to the 'closed' boreholes is interpreted as a movement of groundwater through these location rather than stagnation of the well water. The larger amplitude changes are also indicative of their contact with air temperatures, suggesting a degree of isolation for the remaining locations.

The largest amplitude at LUSK is believed to be caused by its location on the valley floor (less shading) where preferential warming of the soil may impart a signature to the interstitial groundwater/ recharge. This suggests that the water sampled is from a relatively shallower horizon. This should be compared with the CHBH trend which is more linear in appearance, which may indicate that the sampled waters (the logger was at about 11m bgl) were more isolated from any seasonal warming effect. Or different horizons have been recorded.

There are spikes observed in the temperature data, these are especially prevalent in the LUSK, and LTRI Boreholes. These two boreholes have the shallowest depth to groundwater, and would appear to be in a generally positive or warming direction. This may suggest inputs from deeper water during pumping or perhaps warm shallow soil water entering the borehole after pumping. The two deep boreholes LDOW and CHBH do not have significant spikes, neither do the two wells. Correlation between the temperature readings and rainfall was undertaken to investigate this; the results are in Table 5-4:

The results of the correlation analysis indicate that there is no correlation between rainfall and borehole temperature. This suggests that rainfall/ recharge temperature is not responsible for the spikes, although some negative (cooling) and positive spikes are clearly related to rainfall events. Further investigation suggests that in fact the relationship may be more complicated; cooling spikes appear in the winter months, while warming spikes appearing the summer months (Figure 5-9).

Seasonal ground temperatures may also augment the cooling or warming effect on recharge. This suggests that the temperature perturbations are a result of recharge rather than pumping.

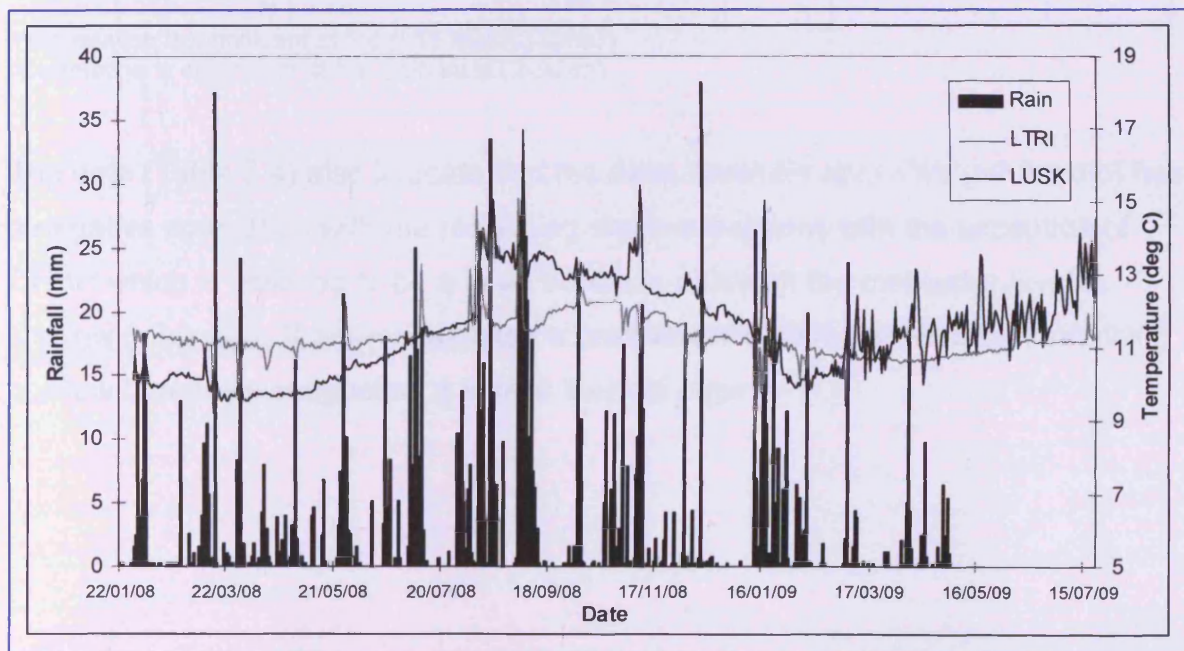


Figure 5-9 Daily rainfall and temperature for LTRI and LUSK boreholes which are shallowest in project area. Note occurrence of positive and negative spikes with rainfall events.

Table 5-4 Spearman's correlation: Daily rainfall and borehole temperature.

		Rain	Barro	CHW	CHBH	HFW	LTRI	LUSK	LDOW
Rain	Correlation	1.000	.098*	.052	-.084	.032	.031	.042	-.040
	Sig.		.034	.312	.071	.486	.514	.367	.682
	N		465	387	465	465	457	457	106
Barro	Correlation		1.000	.198**	-.202**	.081	.329**	.362**	-.566**
	Sig.			.000	.000	.057	.000	.000	.000
	N			469	547	547	539	539	188
CHW	Correlation			1.000	.212**	.708**	.844**	.416**	-.614**
	Sig.				.000	.000	.000	.000	.000
	N				469	469	461	461	188
CHBH	Correlation				1.000	.284**	.135**	.258**	.180*
	Sig.					.000	.002	.000	.013
	N					547	539	539	188
HFW	Correlation					1.000	.735**	.515**	-.123
	Sig.						.000	.000	.092
	N						539	539	188
LTRI	Correlation						1.000	.501**	-.616**
	Sig.							.000	.000
	N							539	188
LUSK	Correlation							1.000	-.518**
	Sig.								.000
	N								188
LDOW	Correlation								1.000
	Sig.								
	N			188					

\*\*Correlation is significant at the 0.01 level (2-tailed).

\*Correlation is significant at the 0.05 level (2-tailed).

The data (Table 5-4) also indicate that the deep borehole at LDOW (~9.5m dip) has a negative correlation with the remaining shallow locations with the exception of CHBH which is believed to be a deep borehole although the rest water level is shallow (~3m dip). It further indicates a positive correlation between the remaining shallow boreholes suggesting a similar thermal regime.

### Logger electrical conductivity (EC)

Electrical conductivity measurements were also obtained from the borehole loggers. Conductivity has been used as an indication of contamination by ionic species (Ling 2007) and an excursion from 'background' may indicate anthropogenic or natural influences on the groundwater. The data are plotted in Figure 5-10 and shows in the most part a steady state situation (neutral trend) with some potential correlations between boreholes. Notable perturbations are observed, some of which are project tracer test experiments with NaCl.

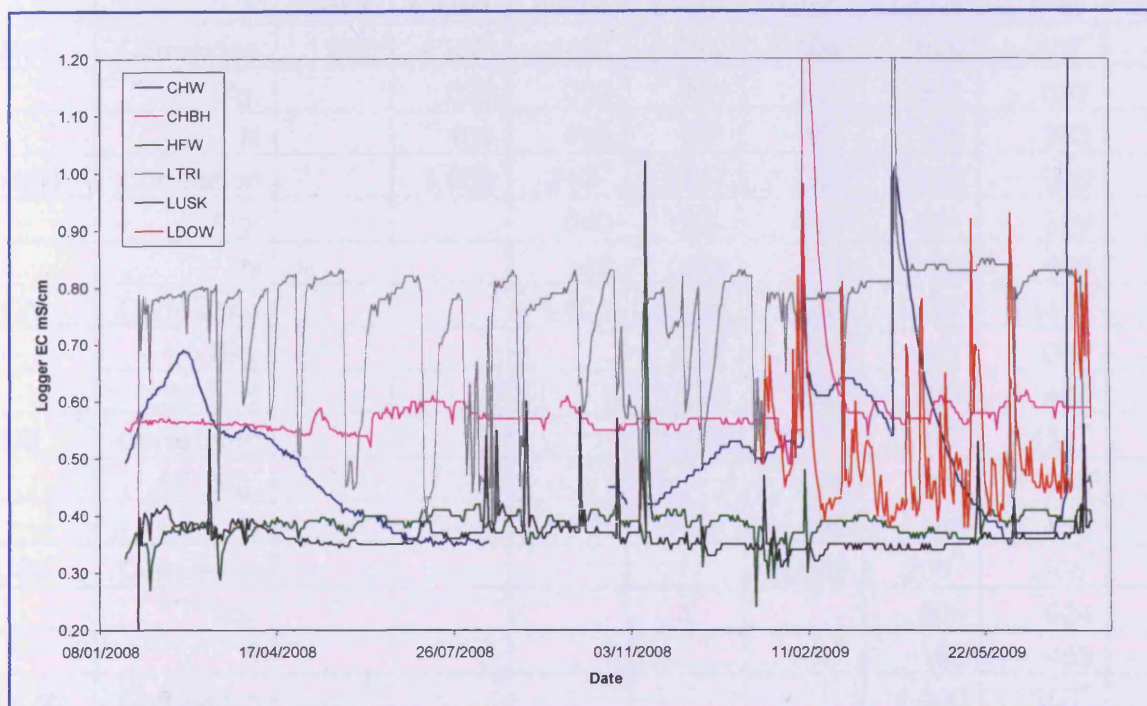


Figure 5-10 Electrical conductivity daily data for Usk boreholes.

The steady state or neutral trend is exhibited in all but CHW, which has the appearance of a seasonal signature. A similar pattern is not seen in HFW, the other well location. This difference may be a lithological change, recharge, or perhaps road salt inputs in the winter months as the location is within 30m of a major road, as is LDOW. However this is a deeper borehole and winter run-off may be bypassing the borehole capture zone as LDOW is only 4m from the same road. Chloride is higher in the winter months at CHW. LTRI is also within 15m of another road which could be expected to receive winter grit.

The EC data (Table 5-5) indicates both negative and positive correlations between the boreholes. In order to understand the causes of the results in Table 5-5 the data was plotted with daily rainfall (Figure 5-11). The rainfall and LTRI data indicates a good visual (negative) correlation which is interpreted as a dilution effect, whereas at LDOW and LUSK the rainfall would appear to be flushing and causing a perturbation increase in EC, (correlation is positive).

*Table 5-5 Spearman's correlation of Logger EC data between boreholes and rainfall.*

		CHW	CHBH	HFW	LTRI	LUSK	LDOW	E' rney	Sulvad
CHW	Correlation	1.000	-.103*	-.443**	.095*	-.105*	.029	-.107*	-.271**
	Sig.		.026	.000	.041	.024	.692	.037	.000
	N		469	469	461	461	188	383	201
CHBH	Correlation		1.000	.213**	.193**	-.006	-.047	-.030	.079
	Sig.			.000	.000	.882	.521	.529	.219
	N			542	534	534	188	456	241
HFW	Correlation			1.000	-.046	.063	-.097	-.141**	.090
	Sig.				.290	.143	.187	.002	.166
	N				539	539	188	461	241
LTRI	Correlation				1.000	-.213**	-.365**	-.125**	-.133*
	Sig.					.000	.000	.008	.043
	N					539	188	453	233
LUSK	Correlation					1.000	.205**	.106*	-.097
	Sig.						.005	.024	.138
	N						188	453	233
LDOW	Correlation						1.000	.355**	.478**
	Sig.							.000	.001
	N							106	46
*E' rney	Correlation							1.000	.915**
	Sig.								.000
	N								241
Sulvad	Correlation								1.000
	Sig.								
	N								

\*Correlation is significant at the 0.05 level (2-tailed).

\*\*Correlation is significant at the 0.01 level (2-tailed).

\*E' rney = Estavarney Farm

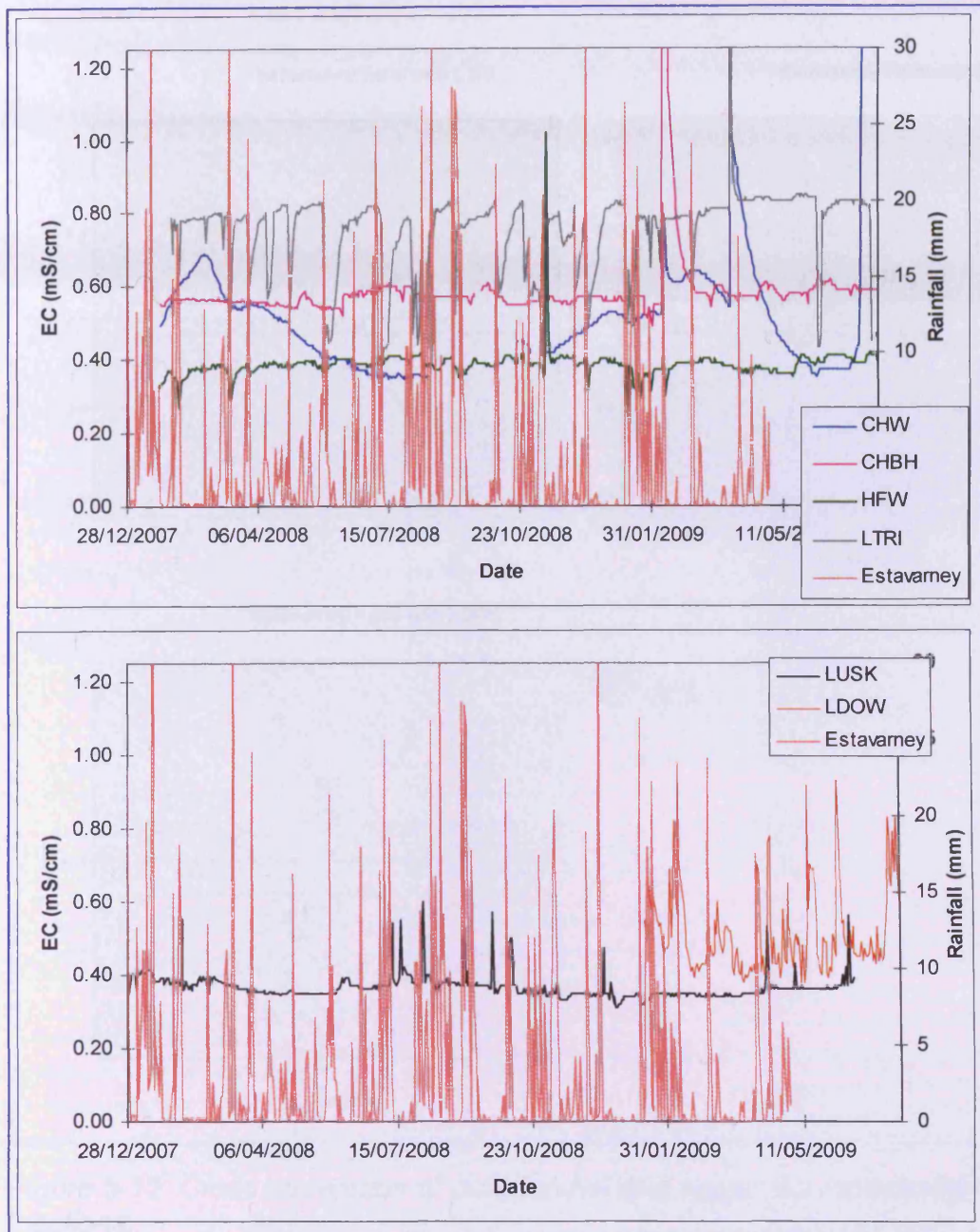


Figure 5-11 Daily EC and rainfall from loggers.

Cross correlation of the EC data with rainfall could therefore be expected to produce significant results. Figure 5-12 shows the negative zero lag at LTRI although it is only just at acceptable statistical significance, due to the unexplained wide perturbations. At LUSK there is evidence of a similar negative zero lag followed by a strong lag at day 1 indicating perhaps a minimal delay in flow characteristics. At LDOW the lag is zero and positive suggesting a good connection within the aquifer.

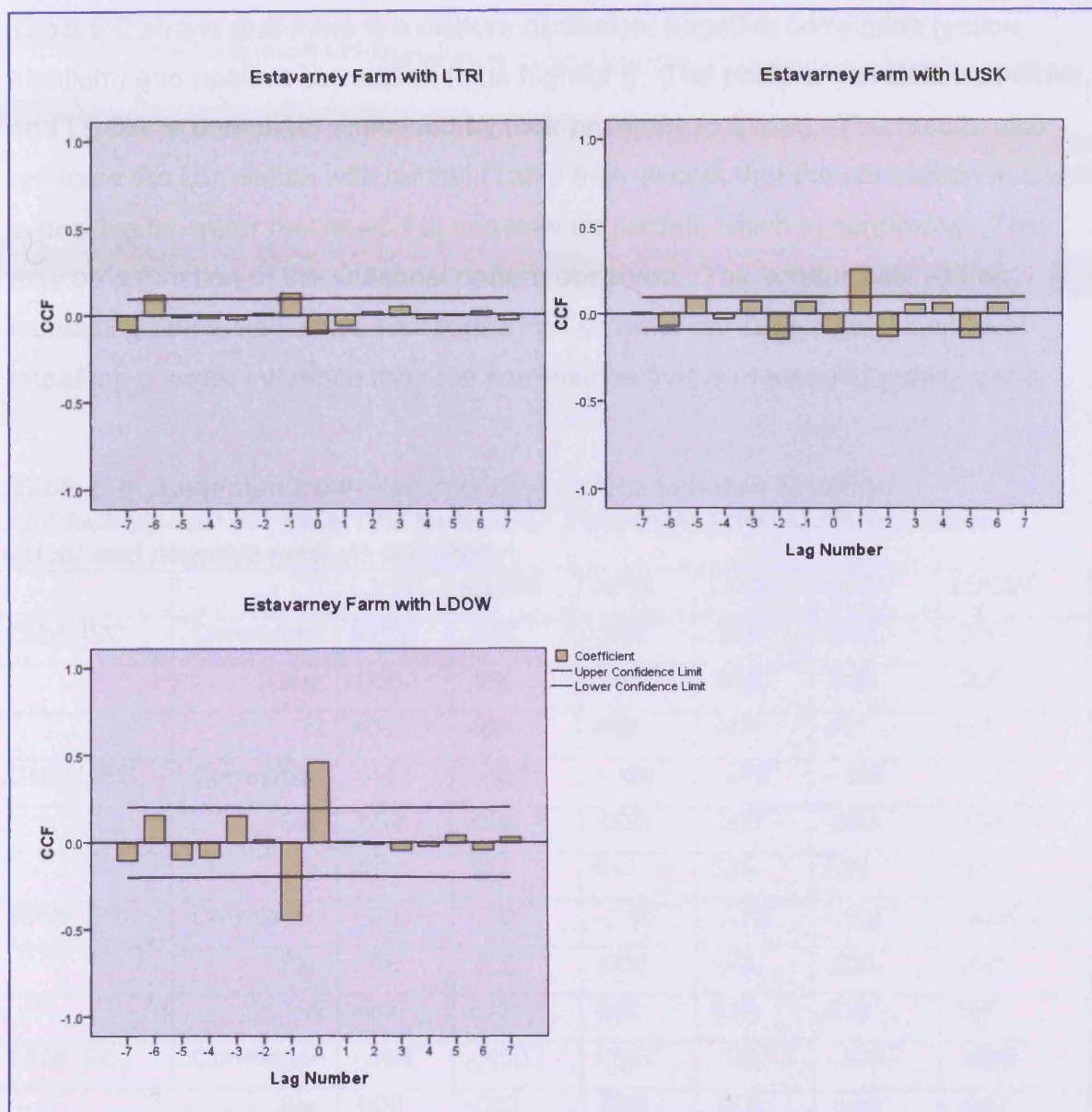


Figure 5-12 Cross correlation of daily rainfall and logger EC for selected locations.

The final EC analysis that can be undertaken is that of correlation with water rest level. If EC can be used as a proxy for contamination (Ling 2007) then correlation with rises or falls (corrected values AOD) in water level could suggest flushing or dilution processes within the borehole capture zone. Correlation results of the daily values are in Table 5-6. As the correlation is with head values AOD (to avoid confusion with dip values) a positive correlation is a rise in both water level (recharge event) and a rise in EC.

Table 5-6 shows that there is a mixture of dilution, negative correlation (yellow highlight) and positive correlation (blue highlight). The positive correlation at CHW, and LDOW is potentially explained by their proximity to a road. The results also reinforce the correlation with rainfall (Table 5-5), except that the correlation at CHW is positive for water rest level, but negative for rainfall, which is perplexing. This may be a function of the seasonal pattern observed. The conductivity values increasing and falling with a winter rise and summer fall in well water rest level imparting a larger influence than the correlations that is measuring a daily trend.

*Table 5-6 Spearman's correlation of daily values between Electrical conductivity and BH water rest level AOD. Data highlighted to show positive (blue) and negative (yellow) correlation.*

		CHW	CHBH	HFW	LTRI	LUSK	LDOW
CHW_EC	Correlation	.497**	.488**	.202**	.288**	.314**	.366**
	Sig.	.000	.000	.000	.000	.000	.000
	N	469	469	469	461	461	188
CHBH_EC	Correlation	-.417**	-.404**	-.198**	-.218**	-.336**	-.155*
	Sig.	.000	.000	.000	.000	.000	.033
	N	469	542	547	539	539	188
HFW_EC	Correlation	-.397**	-.385**	-.166**	-.283**	-.307**	-.438**
	Sig.	.000	.000	.000	.000	.000	.000
	N	469	542	547	539	539	188
LTRI_EC	Correlation	-.394**	-.400**	-.657**	-.631**	-.575**	-.629**
	Sig.	.000	.000	.000	.000	.000	.000
	N	461	534	539	539	539	188
LUSK_EC	Correlation	-.108*	.124**	.154**	.190**	.286**	-.642**
	Sig.	.021	.004	.000	.000	.000	.000
	N	461	534	539	539	539	188
LDOW_EC	Correlation	.063	.203**	.386**	.373**	.254**	.134
	Sig.	.389	.005	.000	.000	.000	.067
	N	188	188	188	188	188	188

### 5.3 Groundwater / surface water interactions

#### Rainfall

The hydrograph correlograms are an expression of the geology, flow-path and antecedent rainfall (Figure 5-13). Autocorrelation analysis of the rainfall data (Figure 5-14) indicates that for the more local station Estavarney Farm, there is a seasonal signature. It is not a strong signature; this is believed to be due to the unseasonable rainfall patterns in the preceding three years (flooding in 2007 and 2008). If autocorrelation is performed on long term data from an external station then a seasonal pattern is exhibited. Analysis of these data with the local stations also produces a strong positive correlation despite the spatial separation and thus it is possible to surmise that the local stations also have a long term seasonal nature. Correlation coefficients between Estavarney Farm and Sulvad are in Table 5-5.

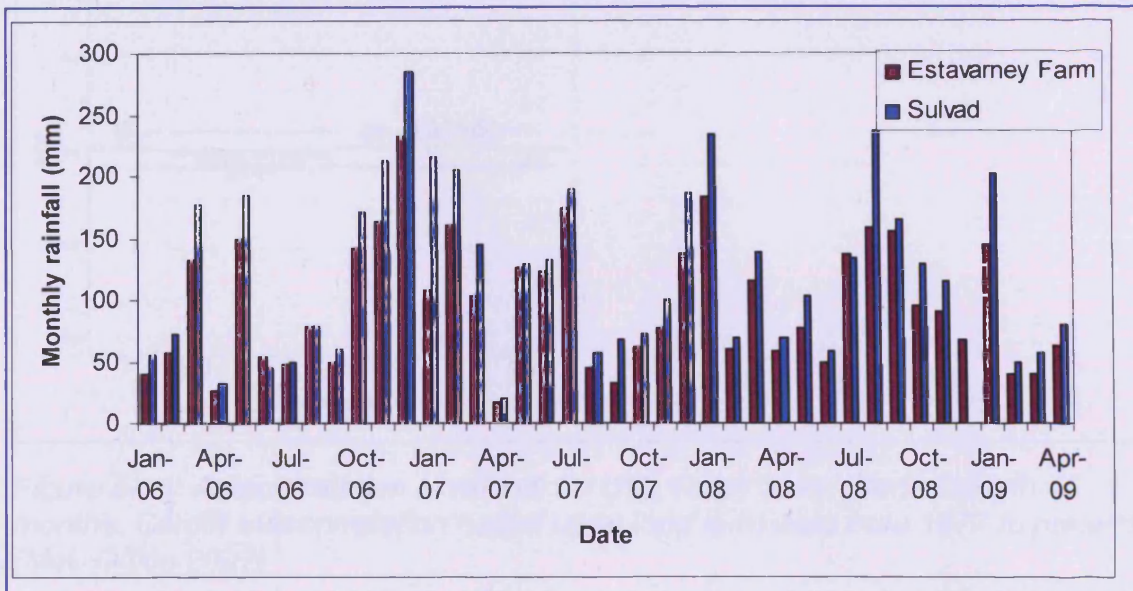


Figure 5-13 Monthly rainfall for Usk Valley area. Data from EA.

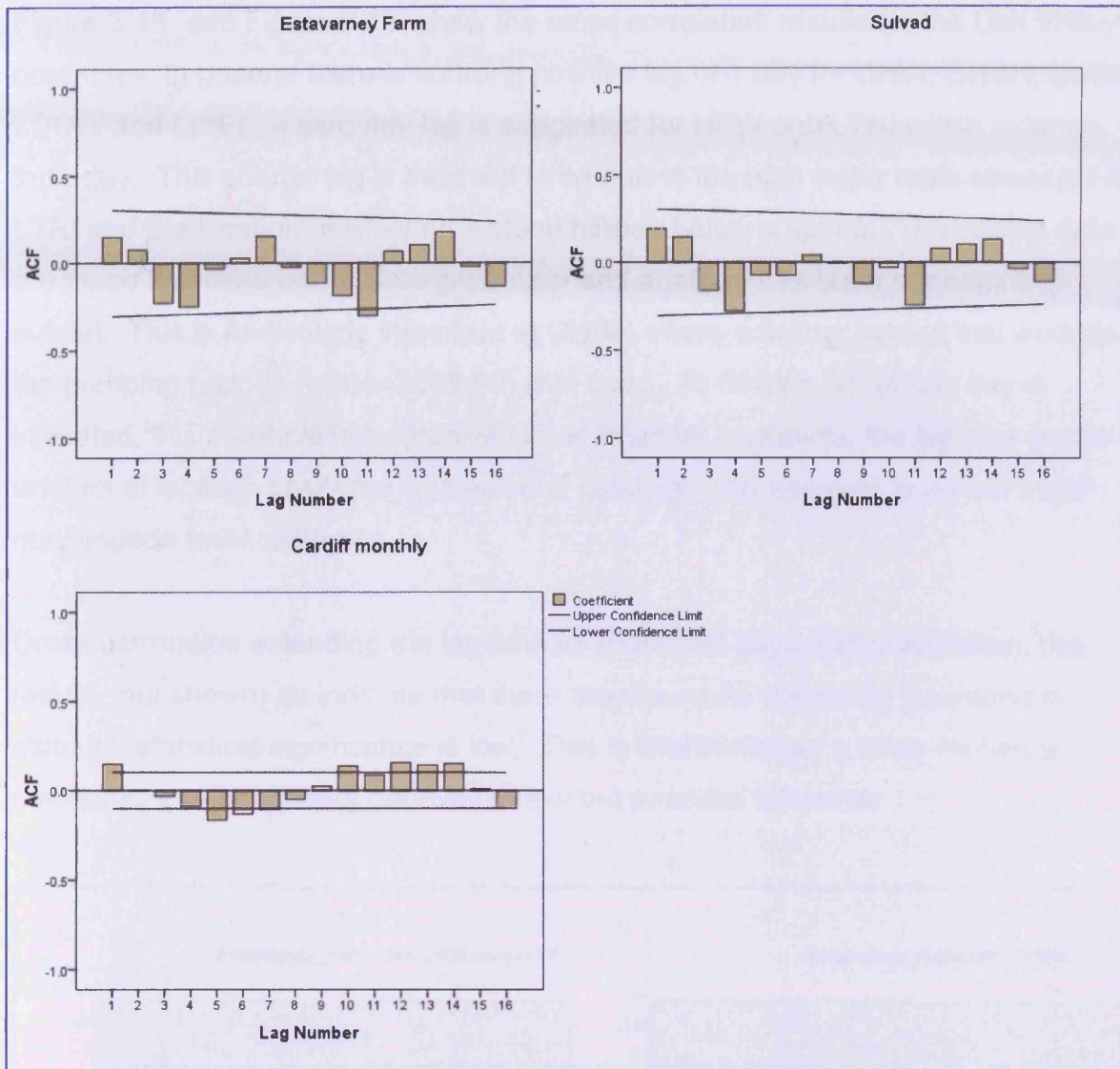


Figure 5-14 Autocorrelation of rainfall for Usk Valley area. Series length 40 months. Cardiff autocorrelation based upon long term data from 1977 to present (Met. Office 2007)

Cross correlation

Cross correlation analysis was undertaken to investigate the presence of a potential lag in groundwater response to rainfall (recharge) events. Fortuitously as lag (in this analysis) is measured in days there was sufficient daily groundwater and rainfall data.

Figure 5-16 and Figure 5-15 show the cross correlation results for the Usk Valley boreholes. In general there is a strong positive lag of 1 day for CHW, CHBH, LUSK, LDOW and LWEL, a zero day lag is suggested for HFW and LTRI which extends for 1 day. This shorter lag is believed to be due to the high water table observed at LTRI and the location of HFW on a steep hillside below a spring. The subset data are those locations where data gaps exist and analysis has been done on the subset. This is particularly important at CHBH where a further subset that excluded the pumping periods (winter 2008-09) was used. At CHW a lag of one day is indicated, this borehole is located within or adjacent to gravels; the lag may be an artefact of location sheltered by trees and buildings and adjacent to a road which may impede local infiltration.

Cross correlation extending the lag time to 30 and 60 days was undertaken, the results (not shown) do indicate that there may be some additional lag intervals although statistical significance is low. This is interpreted as a delay recharge mechanism, or secondary pathway of low but potential influence.

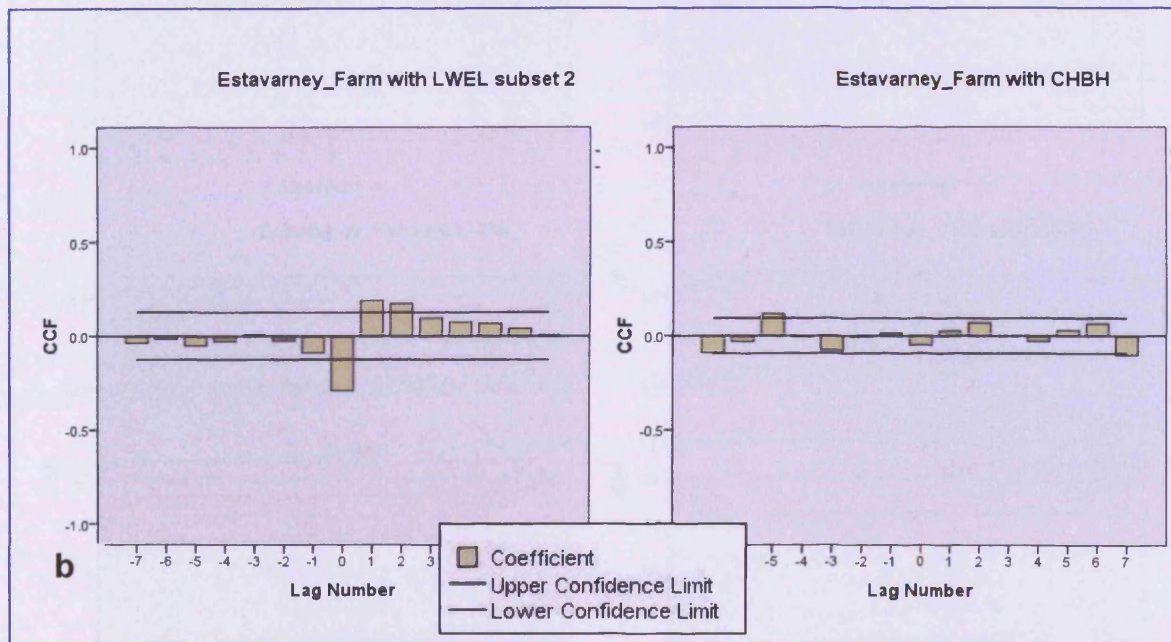


Figure 5-15 Cross correlation for Usk Valley borehole and rainfall. Lag interval in days.

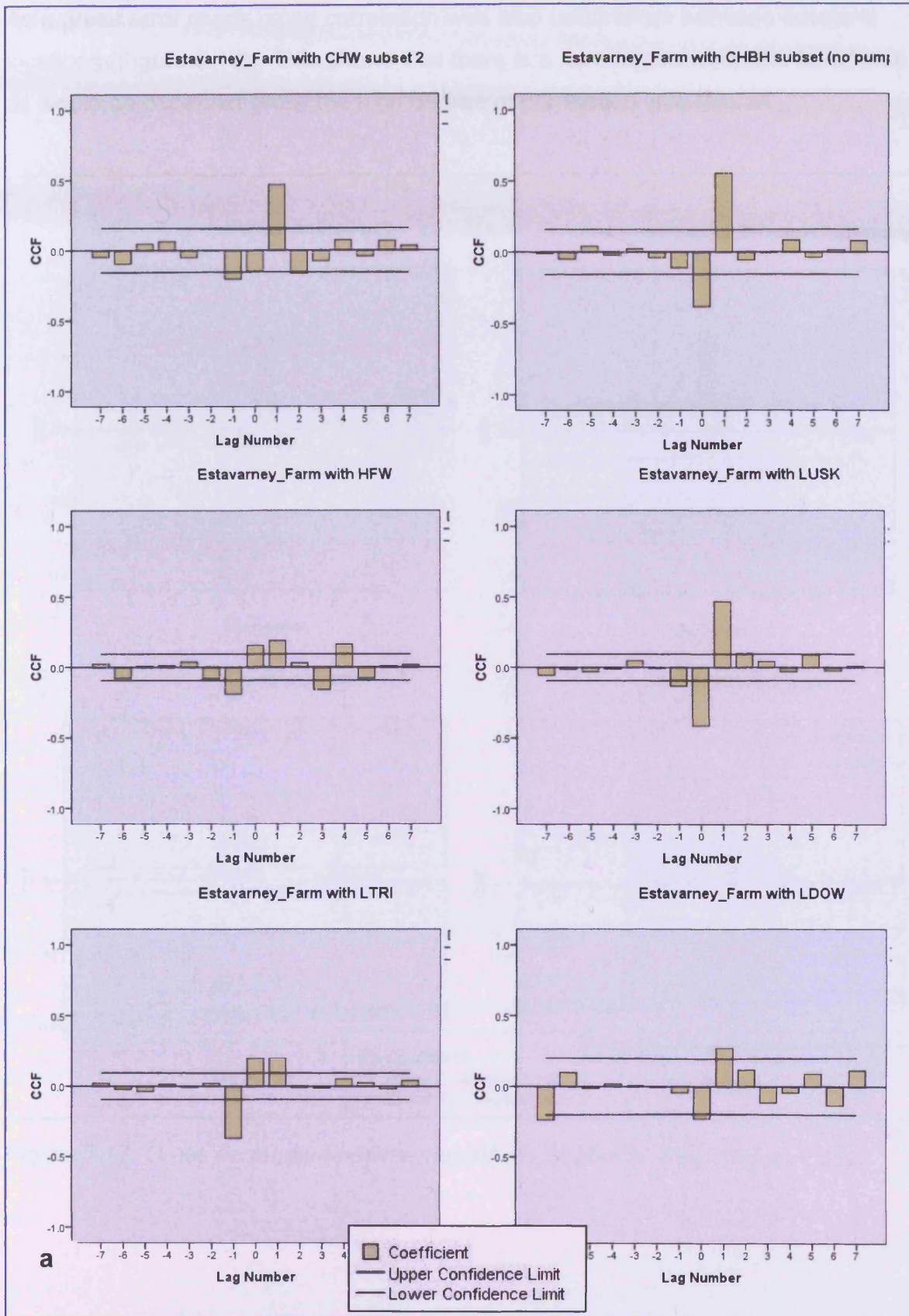


Figure 5-16 Cross correlation for Usk Valley borehole and rainfall. Lag interval in days.

As a gross error check cross correlation was also undertaken between borehole locations (Figure 5-17). This shows that there is a zero lag between the boreholes as would be expected given the high degree of correlation with rainfall.

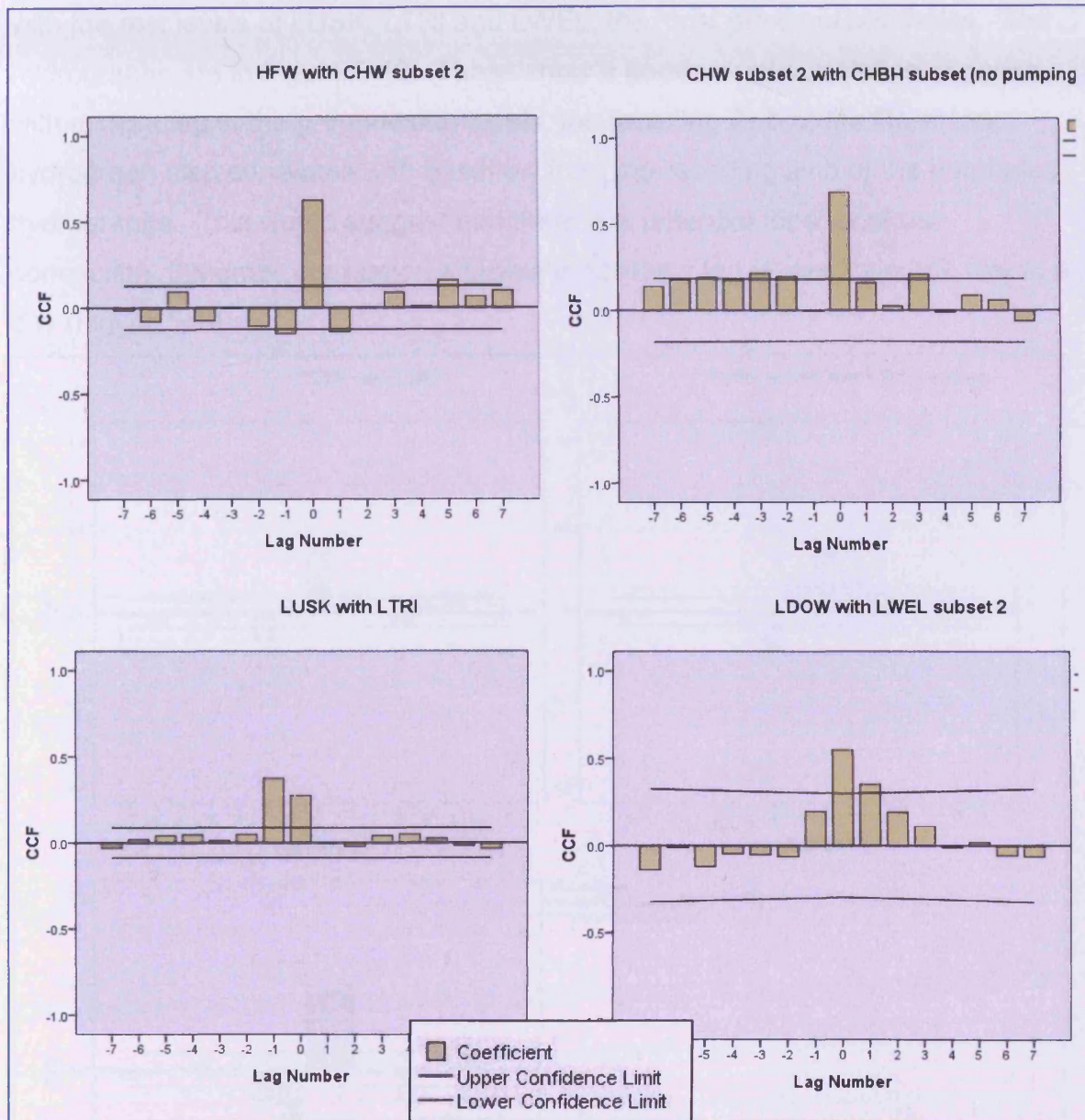


Figure 5-17 Cross correlation between borehole locations. Lag interval 1 day.

Connection to the River Usk

Hydrograph data for the River Usk was obtained from the Hydrometry team at the Environment Agency (Wales). This data is for Chain Bridge which is approximately 8 Km upriver from the centre of the project area. The data was analysed together with the rest levels of LUSK, LTRI and LWEL, the most proximal boreholes. The hydrographs are in Figure 5-19. These show a good visual correlation of peaks, with a slight lag in the groundwater levels, the receding limb of the River Usk hydrograph also correlates with baseflow from the receding limb of the boreholes hydrographs. This would suggest that there is a potential for a localised connection, the cross correlation analysis indicates a lag of less than one day to a day (Figure 5-18).

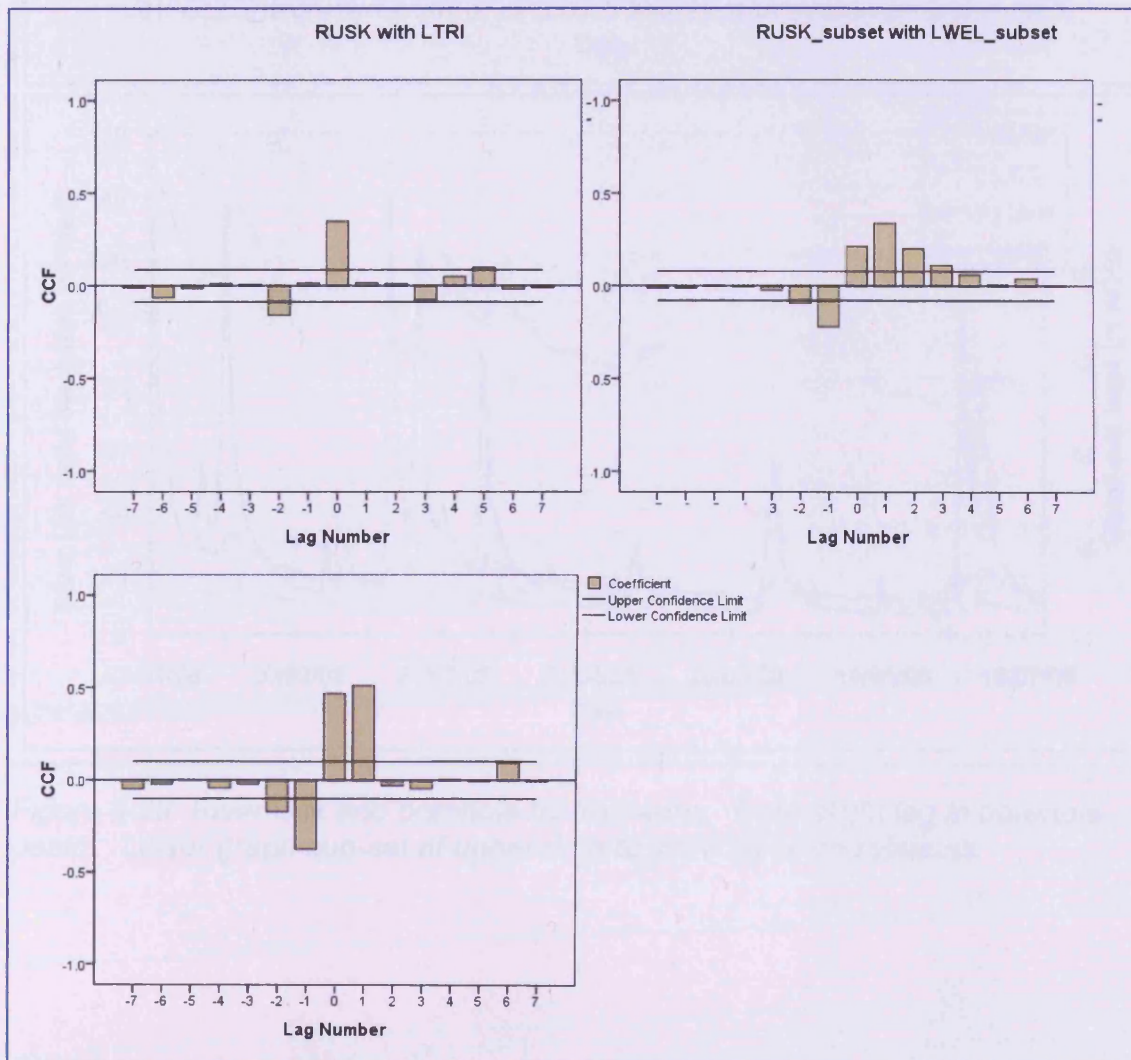


Figure 5-18 Cross correlation of River Usk and borehole hydrographs for most proximal locations.

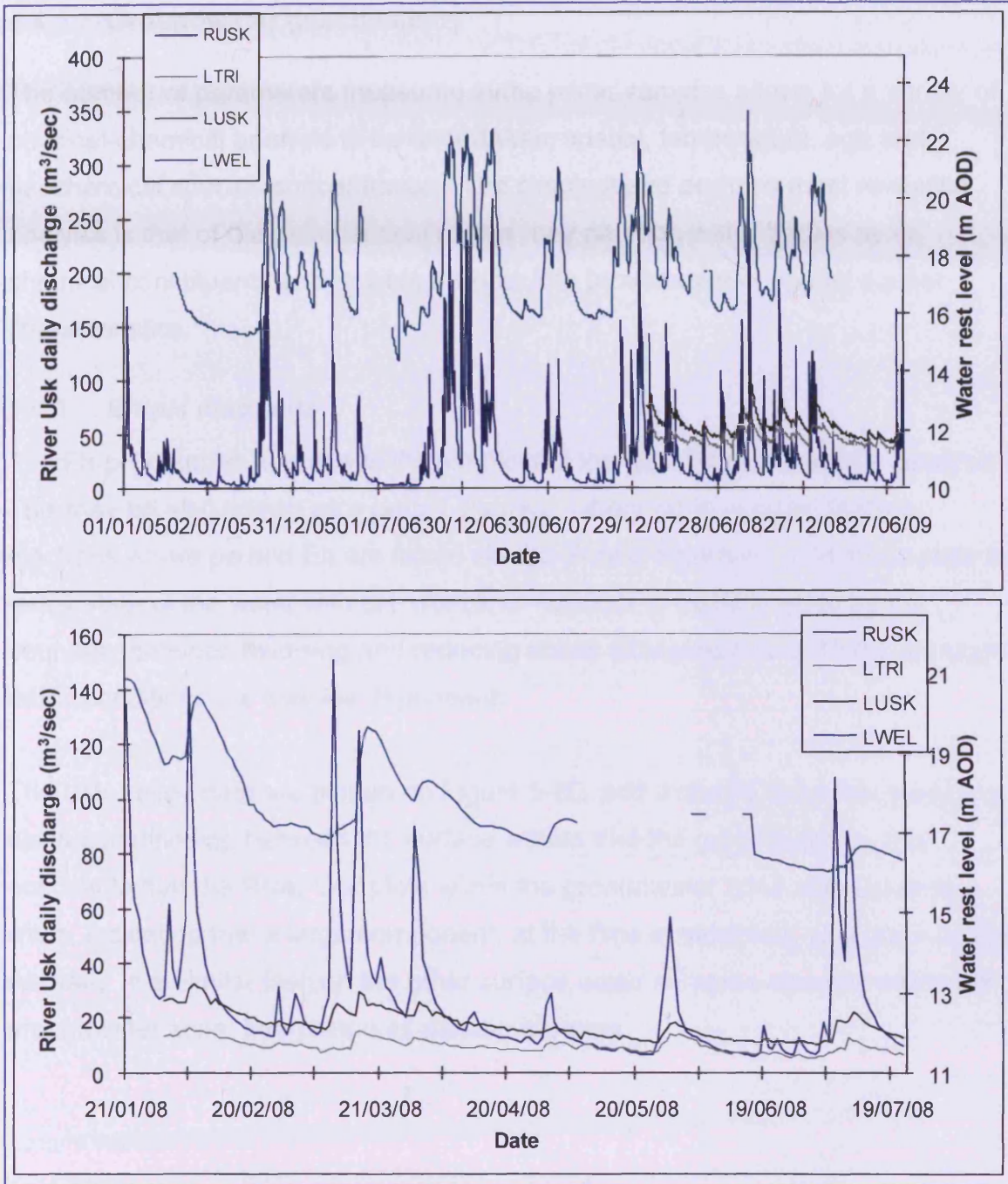


Figure 5-19 River Usk and borehole hydrographs. Note slight lag in borehole peaks. Lower graph sub-set of upper data to show peak correlations.

## 5.4 Groundwater geochemistry

The number of parameters measured in the water samples allows for a variety of physical-chemical analysis to be undertaken; spatial, temperature, age and geochemical species concentration. The simplest and perhaps most revealing analysis is that of the geochemical as this may partition water bodies by its chemical constituents and provide insights into provenance or spatial aquifer characteristics.

### 5.4.1 *Eh-pH diagrams*

The Eh-pH diagram is perhaps the simplest of the geochemical partition analysis. This may be also known as a *pe*-pH diagram, where *pe* is  $-\text{Log}a_e^-$  (activity electrons where *pe* and Eh are linked via the Nernst equation). It in effect plots the redox state of the water with pH. An Eh of <200mV is considered to be the boundary between oxidising and reducing zones (Robertson et al 1998), although redox conditions are species dependent.

The Usk Valley data are plotted on Figure 5-20, and it can be seen that there is a distinct partitioning between the surface waters and the groundwaters. It is noticeable that the River Usk plots within the groundwater zone of the stability limits, indicating that a large component, at the time of sampling, was groundwater derived. In a similar fashion the other surface water samples also plot within the groundwater zone, interpreted as gaining systems.

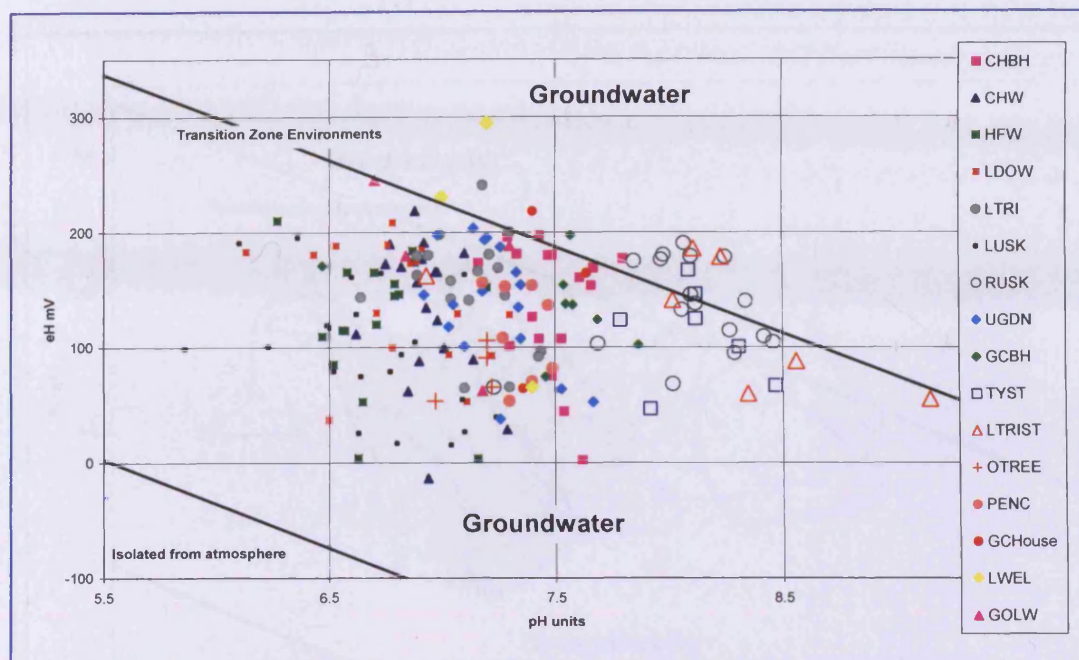


Figure 5-20 Eh-pH plot of sampled waters from the Usk Valley. Historic data included. Surface waters plotted as open symbols. Black lines indicate the isolated from atmosphere and transition zone boundaries.

The Eh-pH diagram is perhaps easiest interpreted as zones. Figure 5-21 shows zones of overlap and more importantly delineation between waters. Some large excursions are believed to be due to use of historical data, obtained with less accurate equipment. An initial division of the samples is considered. Examination of Figure 5-21 and Figure 5-1, shows that despite their close proximity CHW and CHBH are different. There would appear to be a progression (increase in pH) from HFW towards the UGDN and CHBH. This pattern is also matched with the two boreholes further down-valley LDOW towards PENC. The obvious exception is LUSK, this however may be due to the steel casing within the borehole, but there is a similar construction to Pencarreg Farm borehole.

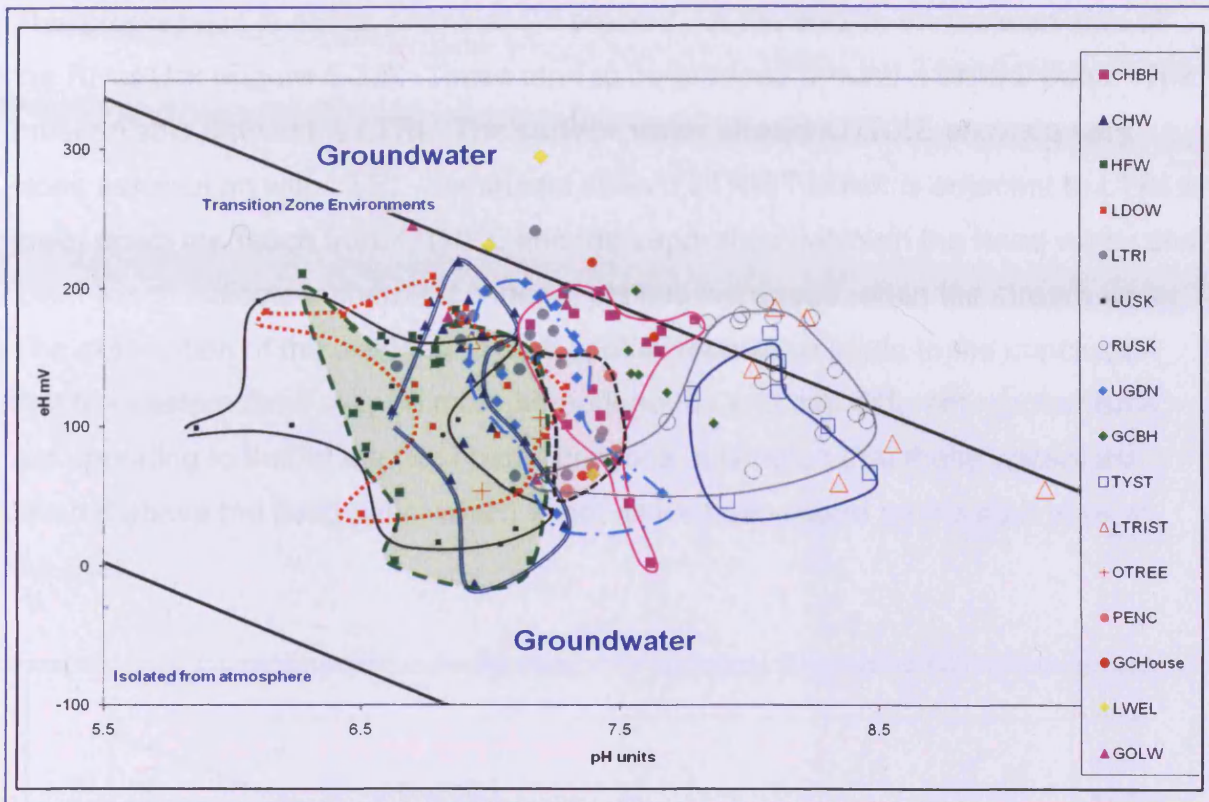


Figure 5-21 Eh-pH progression and separation of waters on west bank of River Usk. Green highlight to aid identification, location data 'footprint' highlighted by solid or dashed lines.

This progression is not as prominent, if present, for the waters on the east side of the River Usk (Figure 5-22). These tend to be grouped around a central point. The most reliable data set is LTRI. The surface water stream OTREE shows a very close association with LTRI. Llantrisant stream LTRIST which is adjacent to LTRI is lower down the reach from OTREE and the separation between the head water and lower reach indicate a chemical change; pH has increased within the stream water. The association of the waters and their spatial separation leads to the conclusion that the eastern flank may be more homogeneous and that different mechanisms are operating to that of the west bank locations. It is noted that these waters are located above the flood plain, which is not as well developed on the east bank of the river.

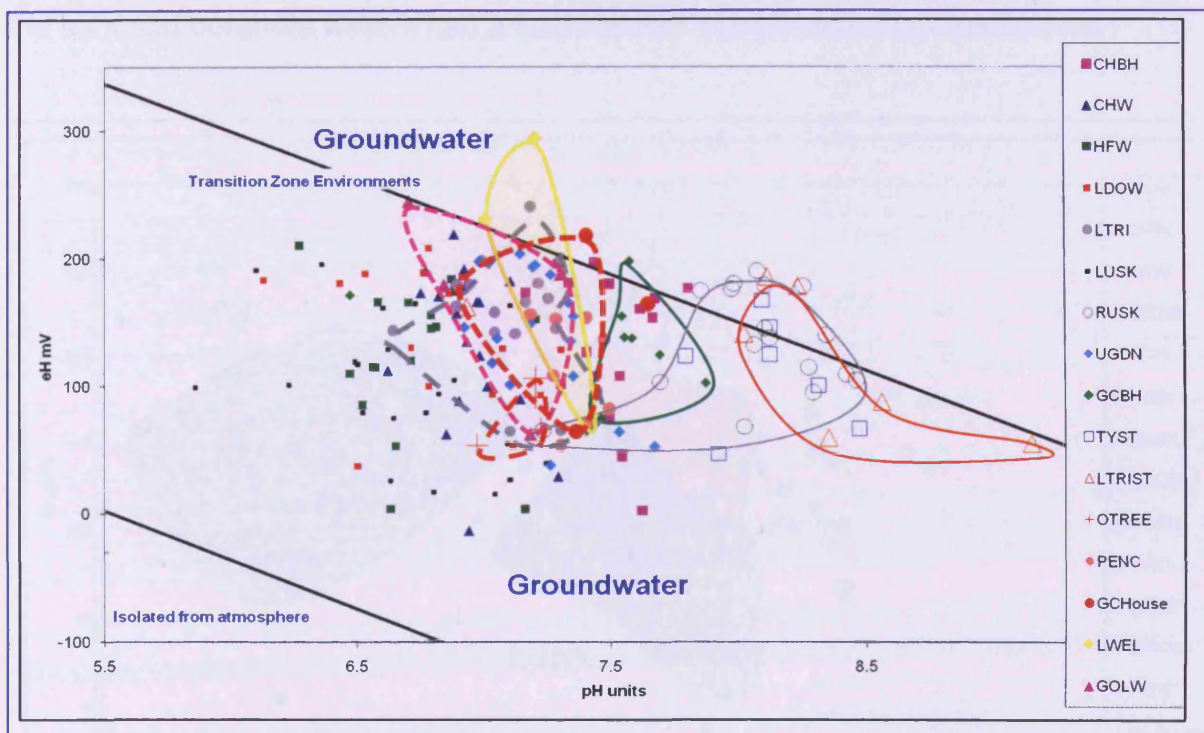


Figure 5-22 Eh-pH of eastern flank waters showing distinct zonation (footprint) in some samples. West bank location data is not enclosed by lines. Surface water locations are open symbols.



#### 5.4.2 **Multiprobe parameter statistical analysis**

The Eh-pH results together with the multiprobe data were also investigated by the Kruskal-Wallis non-parametric ANOVA equivalent, and are best represented as box plots (Figure 5-24 , Figure 5-25 and Figure 5-26). The box results indicate that for the Usk area pH changes are a dominant characteristic that may be attributable to local geology/ regolith variations.

The most obvious differences are in locations RUSK, TYST and LTRIST (red ellipse), which are surface waters with higher pH, Spatial examination of the groups [CHBH, UGDN, PENC & GCBH] and [CHW, HFW, LDOW, LTRI & LUSK] indicate that the first group are deeper and believed to penetrate to the Raglan Mudstone, while the latter are shallower. LDOW is located on the gravels; however the dip values indicate that the rest water level is ~12m AOD about the elevation of the valley floor. The two wells CHW & HFW sample gravels and calcareous limestones whereas LTRI and LUSK may preferentially sample from the alluvium. The difference between PENC and LUSK is perplexing as they are believed to be of similar design and lithological sampling.

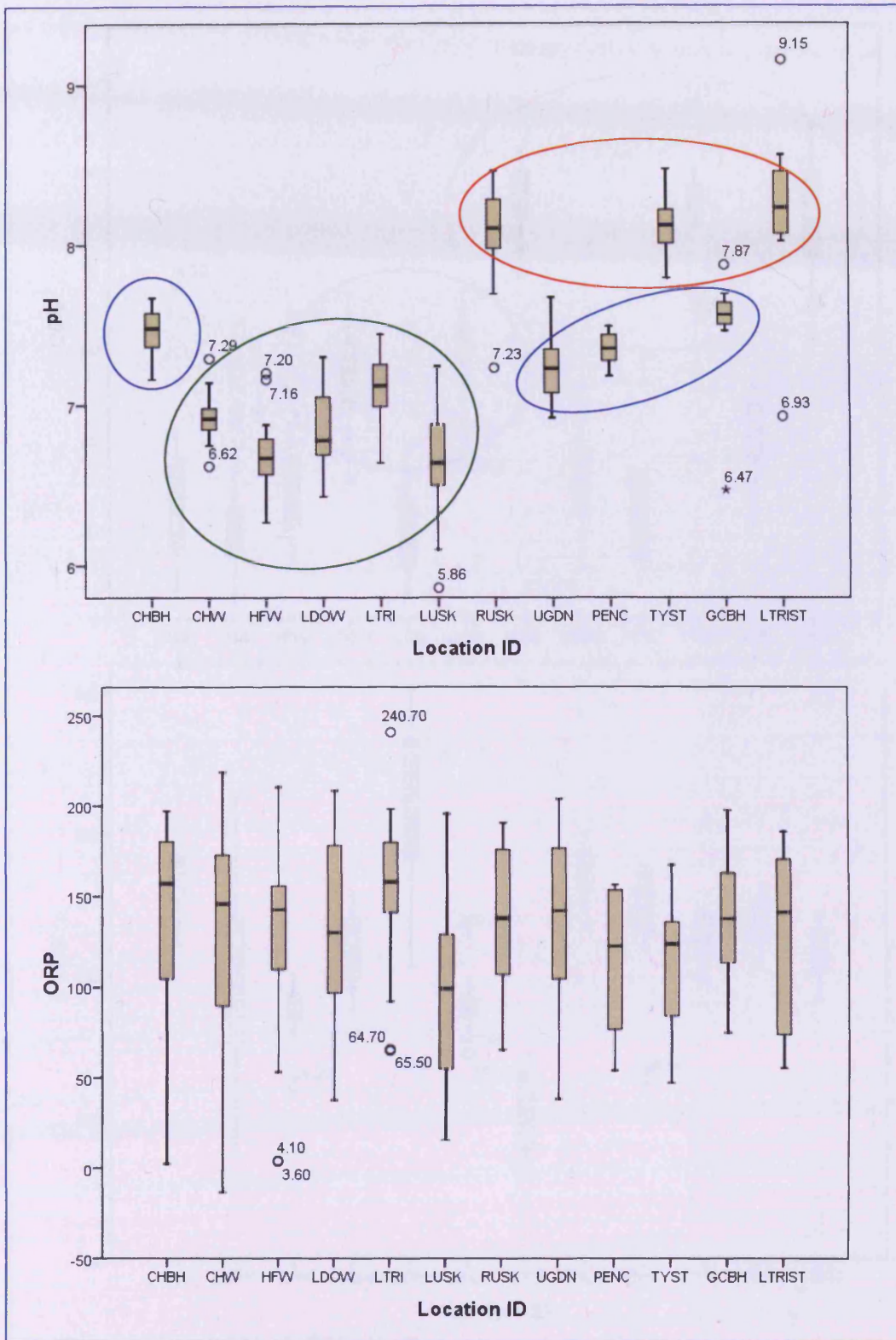


Figure 5-24 Box plots of Usk Valley ph and ORP measurements. The solid black line is the median value. Significant similar data groupings are enclosed by colour ellipse. Outlier values in pH plot are circled; representing 'outlier data' beyond 1.5 box lengths.

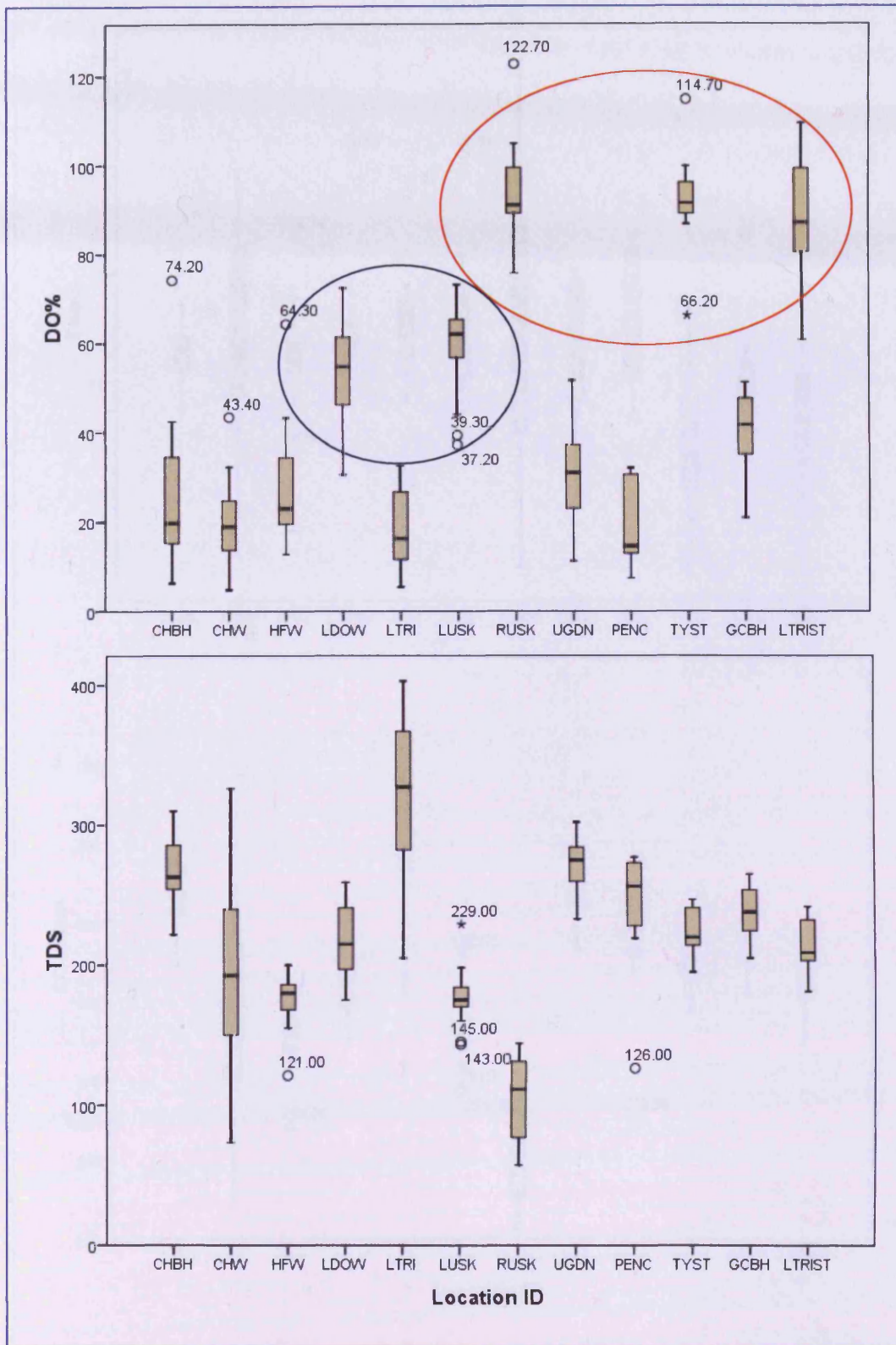


Figure 5-25 Box plots of Usk Valley multiprobe parameters DO% and TDS to investigate spatial distribution patterns. Note higher surface water DO% values red ellipse, and LDOW and LUSK vales blue ellipse c,f, Figure 5-23.

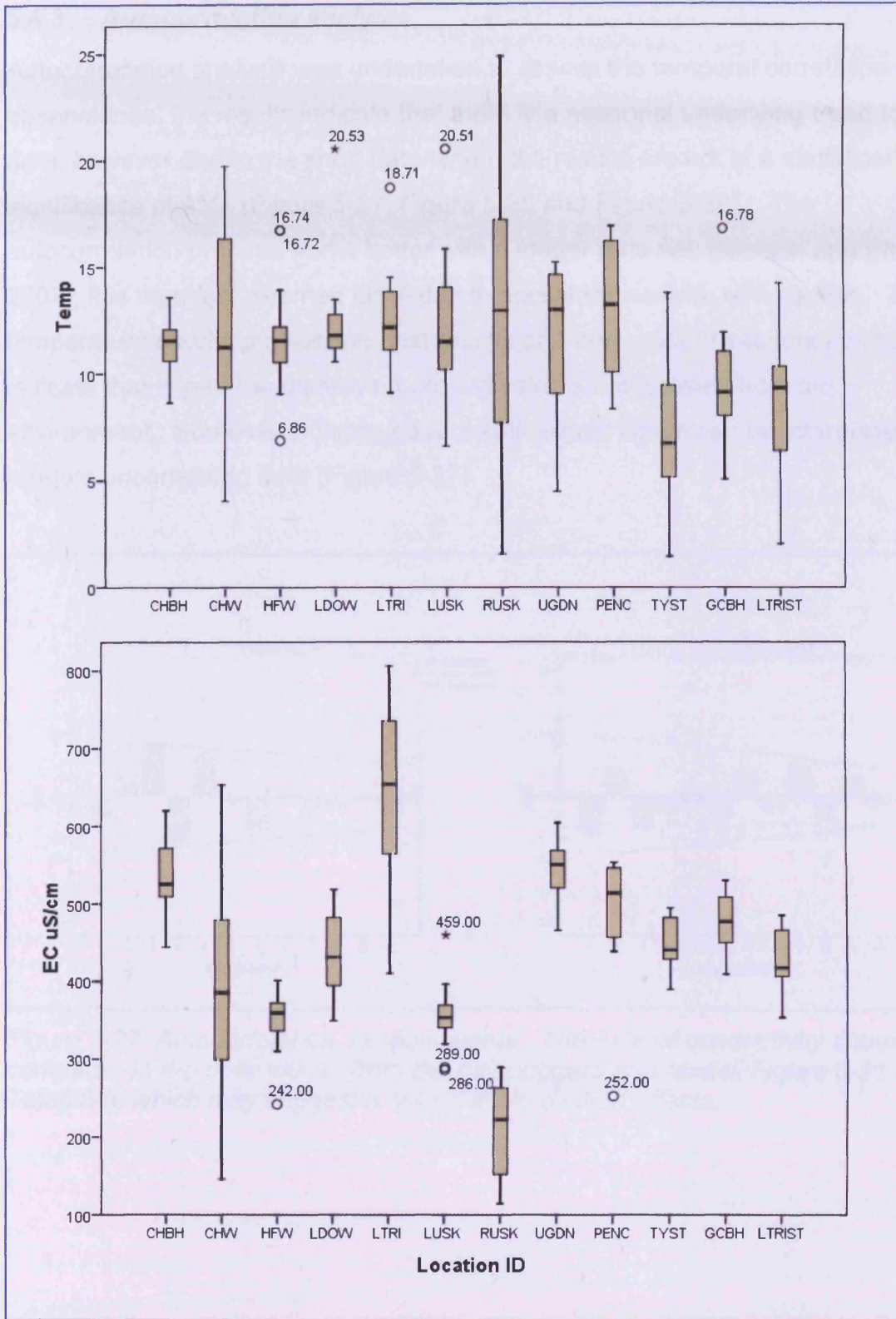


Figure 5-26 Box plots of Usk Valley multiprobe parameters EC and Temperature to investigate spatial distribution patterns.

### 5.4.3 Autocorrelation analysis

Autocorrelation analysis was undertaken to assess the temporal correlation of the observations, the results indicate that there is a seasonal underlying trend to the data, however due to the short data length the results are not at a statistical significance of 95% (Figure 5-27, Figure 5-28 and Figure 5-29). The autocorrelation process works better with a longer data set, (Nielson and Wendroth 2003), it is therefore deemed justifiable to accept the results, with caution. The temperature results provide the best results of a non random seasonal pattern and indicate that in part the underlying groundwater is not isolated from the environment. Some data displayed a chaotic signal which can be interpreted as random uncorrelated data (Figure 5-27).

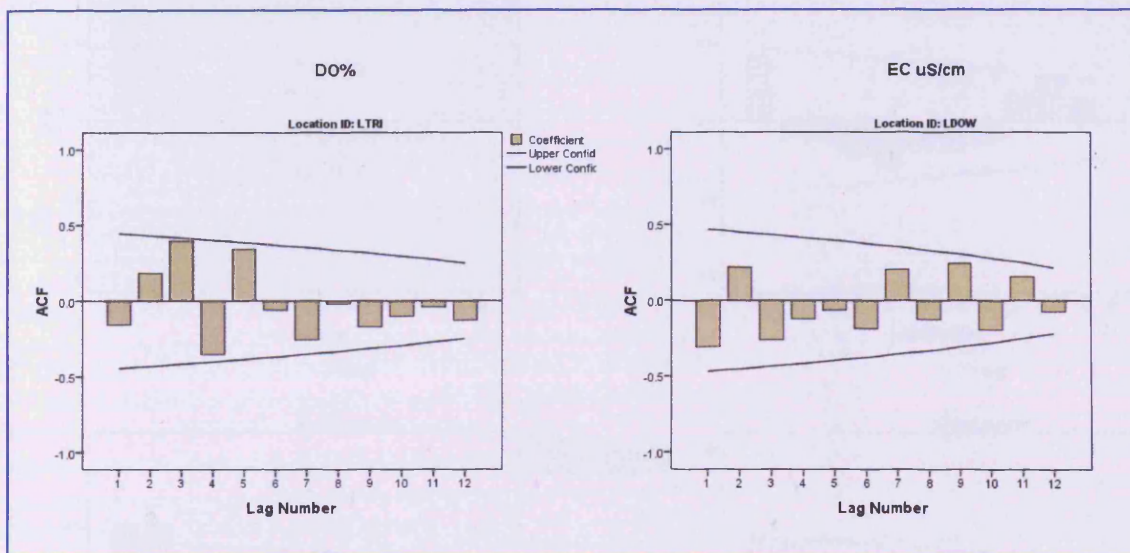


Figure 5-27 Autocorrelation, random signal. The ACF of conductivity should be compared to the daily values from the data loggers and rainfall Figure 5-11 and Table 5-5, which may suggest a sensitivity to dilution effects.

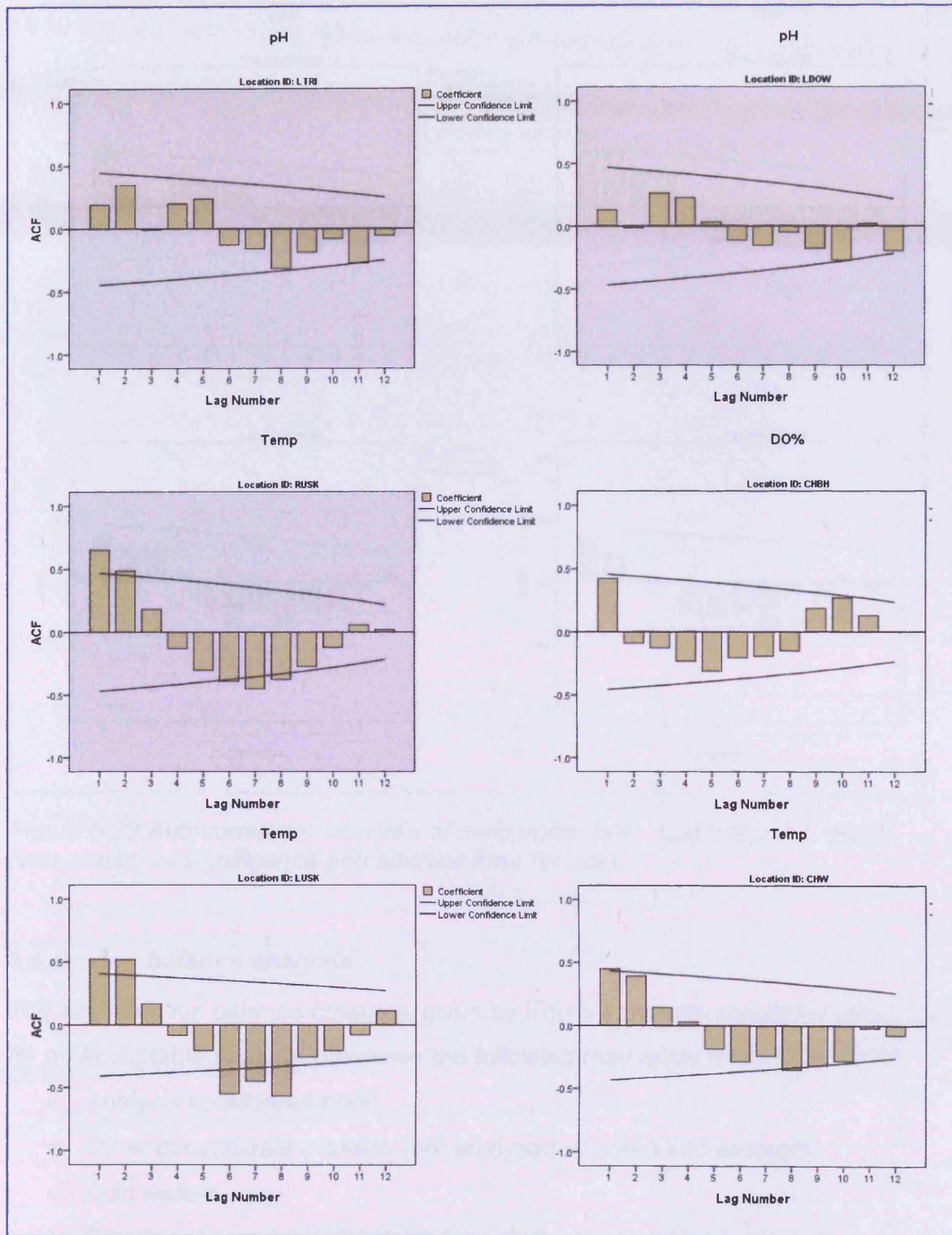


Figure 5-28 Autocorrelation analysis of multiprobe data. Lag interval 1 month. Note statistical significance for temperature and sinuous form for DO% and pH with a lag interval of ~6 months for negative autocorrelation.

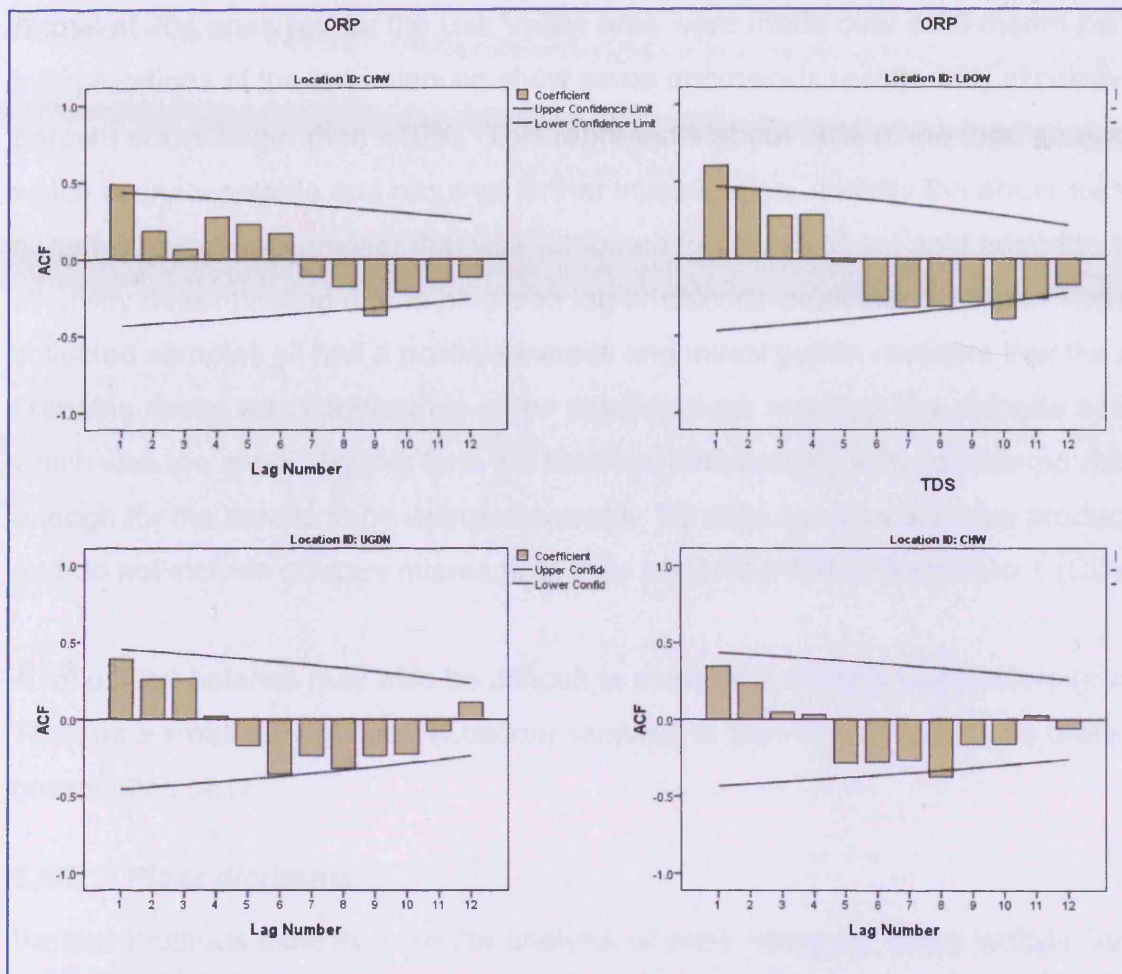


Figure 5-29 Autocorrelation analysis of multiprobe data. Lag interval 1 month. Note statistical significance and sinuous form for data.

#### 5.4.4 Ion balance analysis

The accepted ion balance criteria is given by Eqn 5-1, results should be within  $\pm 5\%$  for an acceptable analysis otherwise the following may apply (Hounslow 1995):

- Analysis considered poor.
- Other constituents present, (not analysed or taken into account).
- Acid waters.
- Significant presence of organic ions (indicated by coloured water).

$$\text{Ion balance}\% = \frac{\sum \text{cations} - \sum \text{anions}}{\sum \text{cations} + \sum \text{anions}} \times 100$$

Eqn 5-1

A total of 204 analyses for the Usk Valley area were made over a 16 month period. Interpretations of the ion balances show some anomalous results with excessive percent errors larger than  $\pm 10\%$ . This represents about 30% of the total analysis, which is unacceptable and requires further investigation. Initially the errors were negative (excessive anions) that was attributed to excess titrant acid added to the alkalinity determination due to pH probe lag or chloride peak interference. The final collected samples all had a positive excess and investigation revealed that the most probable cause was interference of the chloride peak resulting in a chloride assay which was too small. By this time the titration methodology was considered robust enough for the results to be deemed correct. Titration curves were also produced and do not include obvious misreading, they are presented in Enclosure 1 (CD).

A robust ion balance may also be difficult to achieve in dilute groundwaters (low TDS) as a small denominator ( $\Sigma \text{cations} + \text{anions}$ ) in Eqn 5-1 will result in a more pronounced error.

#### 5.4.5 *Piper diagrams*

Various methods exist to show the analysis of water samples; these include Stiff diagrams and pie charts. A common representation method is the Piper diagram, which plots the concentration of the major cations and anions;  $\text{Ca}^{2+}$ ,  $\text{Mg}^{2+}$ ,  $\text{Na}^+$ ,  $\text{K}^+$ ,  $\text{HCO}_3^-$ ,  $\text{CO}_3^{2-}$ ,  $\text{SO}_4^{2-}$  and  $\text{Cl}^-$ . The Piper diagram may also be used to make a tentative determination of the groundwater origin (Hounslow 1995).

An analysis of the Usk waters (Figure 5-30) gives the classification of having a temporary hardness, or calcium-magnesium bicarbonate waters. This interpretation is supported by ion analysis of hardness using calcium and magnesium concentrations.

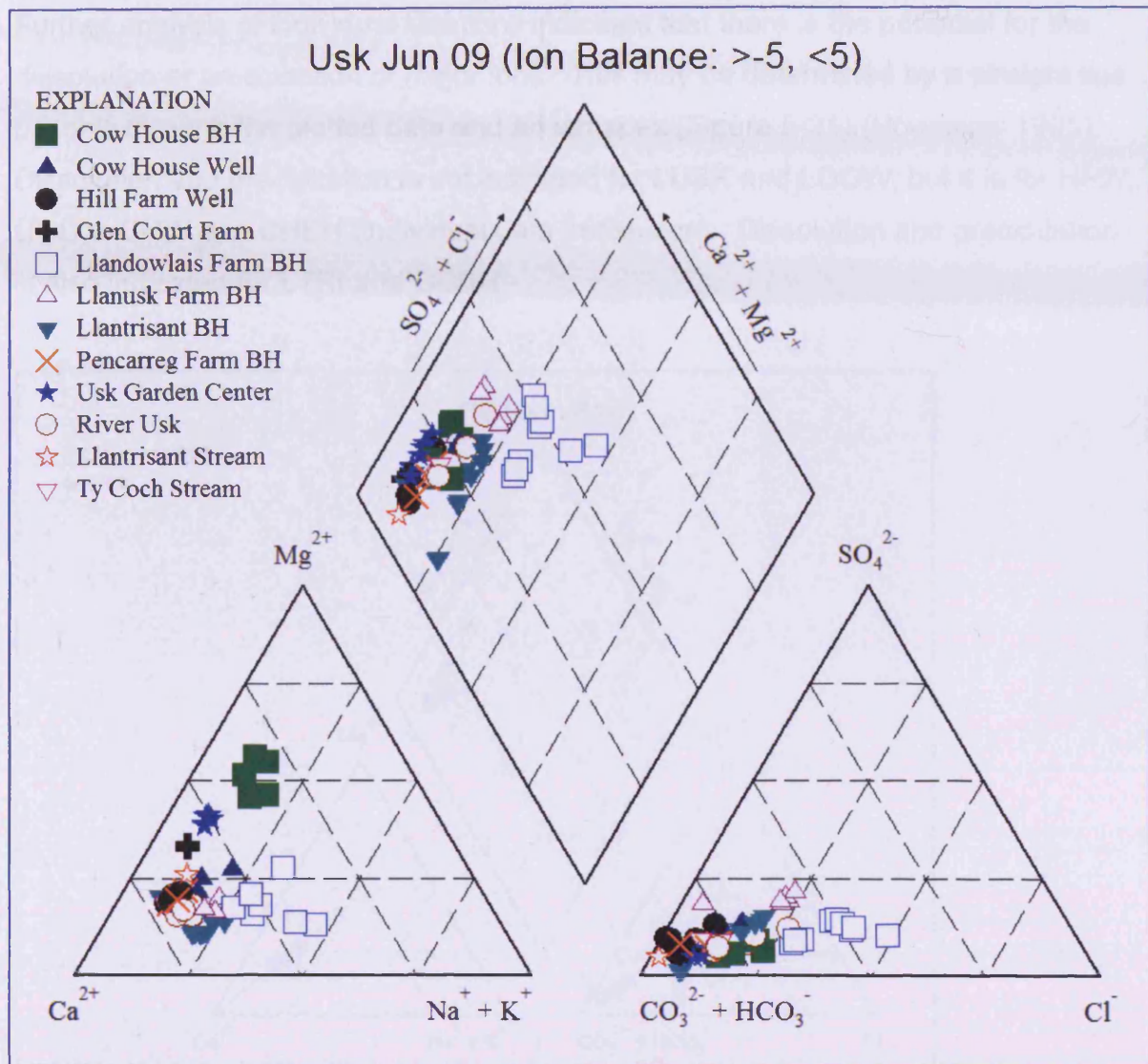


Figure 5-30 Piper diagram of Usk waters. The Piper diagram is shown with ion balance data that achieves the  $\pm 5\%$  criteria. A plot with calculated  $Cl^-$  displays a similar result with the data centre of mass shifted by a few percentage points towards the  $Cl^-$  apex of the diagram. If a 10% criteria is adopted again there is no significant shift in the point centre of mass. The Piper plot is very similar to that presented of the geochemical baseline of the South Wales Devonian aquifer Moreau (2004).

Further analysis of individual locations indicates that there is the potential for the dissolution or precipitation of major ions. This may be determined by a straight line passing through the plotted data and an ion apex (Figure 5-31) (Hounslow 1995). Dissolution and precipitation is not indicated for LUSK and LDOW, but it is for HFW, UGDN, CHW and CHBH (individual data not shown). Dissolution and precipitation is also indicated for LTRI and GCBH.

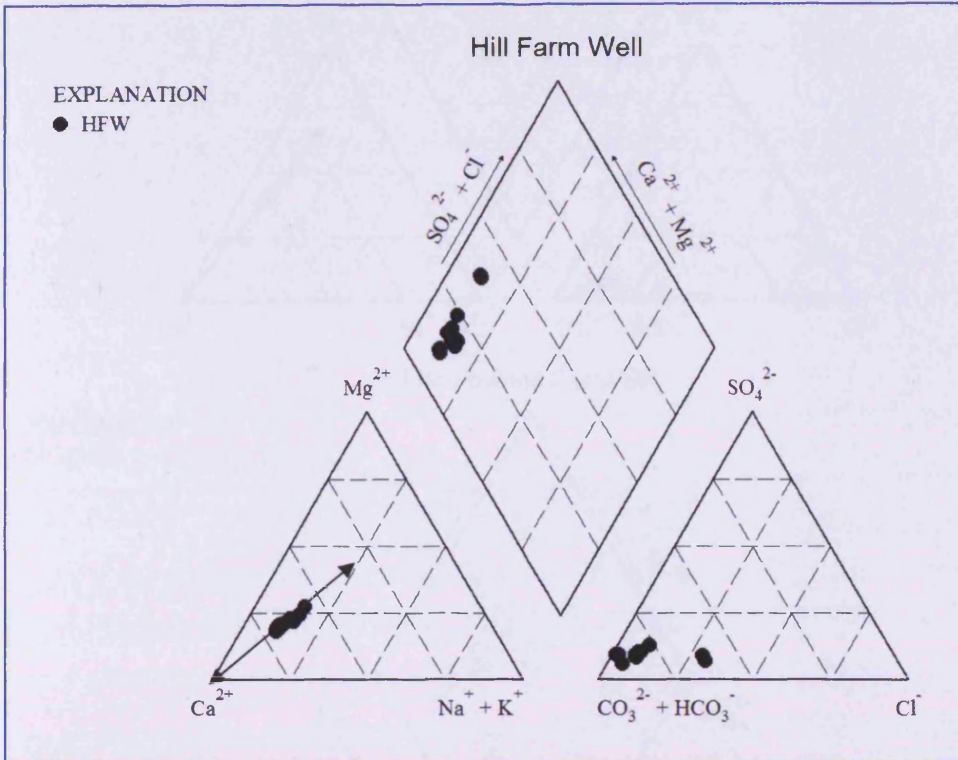


Figure 5-31 Individual locations Usk Valley, showing straight line solution/precipitation relationship with calcium for HFW.

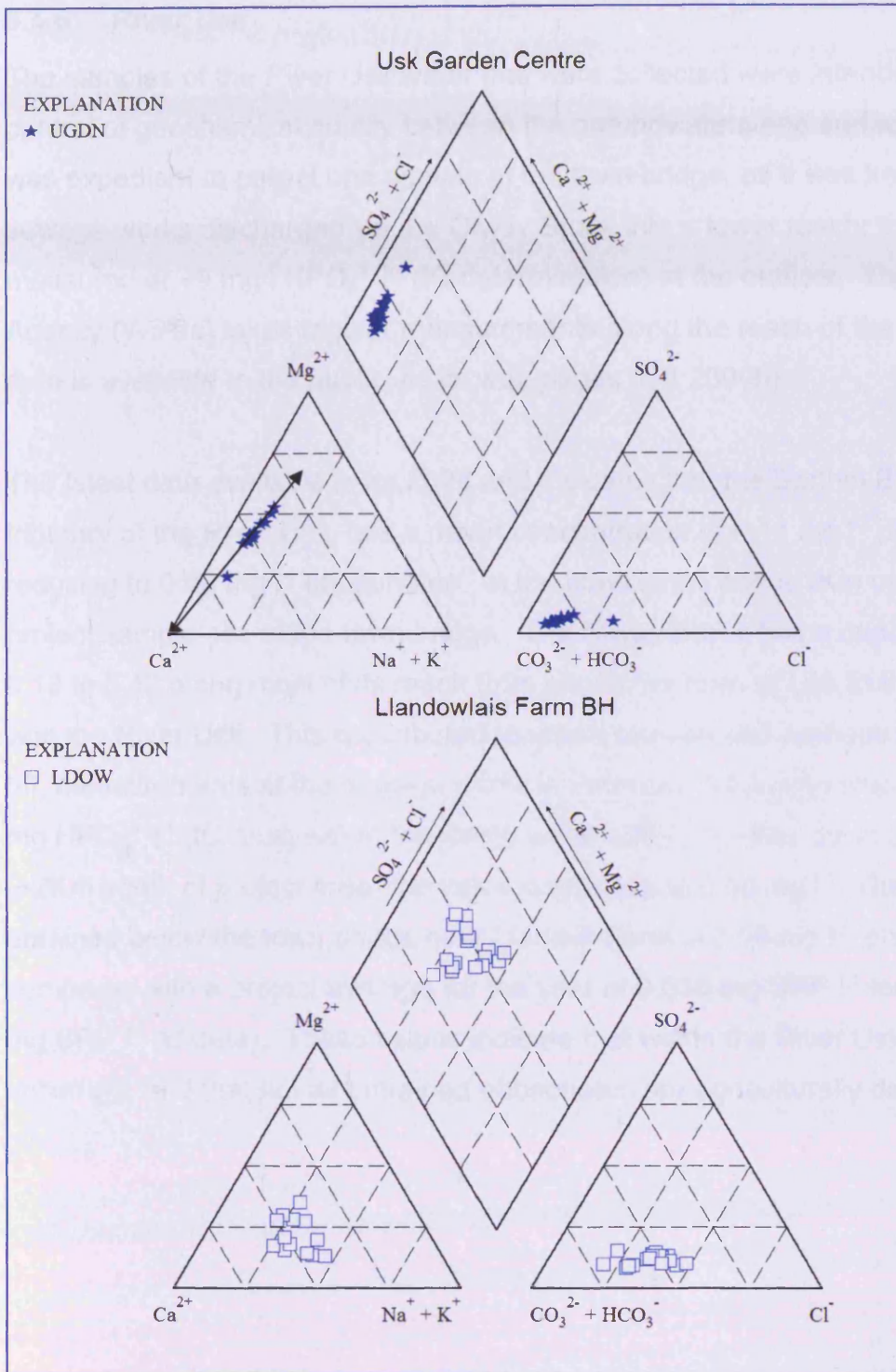


Figure 5-32 Individual locations Usk Valley, showing straight line solution/precipitation relationship with calcium for UGDN. Llandowlais Farm also shown for comparison which indicates no precipitation/ solution relationship.

#### 5.4.6 *River Usk*

The samples of the River Usk water that were collected were intended to act as a control of geochemical quality between the groundwaters and surface waters. It was expedient to collect one sample at the town bridge, as it was known that a sewage works discharged via the Olway Brook into a lower reach; this was measured at  $\sim 9 \text{ mg l HPO}_4^{2-} \text{ l}^{-1}$  (IC determination) at the outflow. The Environment Agency (Wales) takes regular measurements along the reach of the Usk and the data is available to the public via its web pages (EA 2009b).

The latest data available is for 2008 and indicates that the Berthin Brook, a tributary of the River Usk, has a mean concentration of  $0.11 \text{ mg l}^{-1}$  'phosphates' reducing to  $0.08 \text{ mg l}^{-1}$  'phosphates' at the confluence about 1Km upstream of the project sample site at the town bridge. The Olway Brook has a concentration of 0.13 to 0.12 along most of its reach from above the town of Usk to the confluence with the River Usk. This is attributed to urban sewage and perhaps agricultural run-off, measurements at the sewage works in February 2008 produced a value of  $\sim 9 \text{ mg HPO}_4^{2-} \text{ l}^{-1}$  (IC analysis) at the waste water outlet. Further down the reach ( $\sim 2\text{Km}$  south of project area) the value is reduced to  $0.08 \text{ mg l}^{-1}$ . The EA value obtained below the town bridge near Llanusk Farm is  $0.05 \text{ mg l}^{-1}$  'phosphates'; this compares with a project average for the year of  $0.036 \text{ mg SRP l}^{-1}$  for 2008 ( $0.039 \text{ mg SRP l}^{-1}$  all data). These values indicate that within the River Usk dilution is occurring, and that not all entrained phosphates are agriculturally derived.

## 5.5 Geochemical correlations

The geochemistry undertaken in the Usk Valley comprised nine anion species and twenty six cation species. Of these nine anions, bromide, nitrite and fluoride are not considered further. Full correlation tables can be found at Enclosure 1 CD.

### 5.5.1 Occurrence of phosphorus

Phosphorus has been determined by three methodologies, spectrophotometrically (SRP), by IC ( $\text{HPO}_4^{2-}$ ) and ICP-MS (TDP). To calculate the SUP fraction (unhydrolysed organic, polyphosphates and possibly colloidal) a simple difference of  $\text{TP} - \text{SRP} = \text{SUP}$  was calculated. In general the results show that there is within the groundwater an amount of 'not readily available' phosphorus which will contribute to the overall flux at the discharge point. The aquifer correlation between phosphorus species is shown in Table 5-7 and Table 5-8, and suggests that within the aquifer zone there is correlation at different scales. In addition a further check on SRP correlation between locations was done; the results are in Table 5-9. These results suggest that the correlation in Table 5-7 is not ubiquitous throughout the aquifer zone. An aquifer zone correlation between phosphorus species and anions is at Table 5-10. The correlation between phosphorus species and anions at a location is given at Table 5-11. Full results are presented in Enclosure-1.

*Table 5-7 Spearman's aquifer correlation between the phosphorus species for the Usk Valley.*

		TDP	$\text{HPO}_4^{2-}$
SRP	Correlation	.826**	.820**
	Sig.	.000	.000
	N	141	27
TDP	Correlation		.837**
	Sig.		.000
	N		27

\*\*Correlation is significant at the 0.01 level (2-tailed).

Table 5-8 Correlation of SRP and TDP by location

ID			SRP	ID			SRP
CHBH	SRP	r	1	LTRI	SRP	r	1
		Sig.	.			Sig.	.
		N	13			N	16
	P	r	-0.098		P	r	.897**
		Sig.	0.75			Sig.	0
		N	13			N	16
LTRIST	SRP	r	1	LUSK	SRP	r	1
		Sig.	.			Sig.	.
		N	6			N	10
	P	r	0.638		P	r	-0.006
		Sig.	0.173			Sig.	0.986
		N	6			N	10
CHW	SRP	r	1	RUSK	SRP	r	1
		Sig.	.			Sig.	.
		N	16			N	15
	P	r	0.2		P	r	0.175
		Sig.	0.459			Sig.	0.532
		N	16			N	15
HFW	SRP	r	1	PENC	SRP	r	1
		Sig.	.			Sig.	.
		N	16			N	6
	P	r	0.352		P	r	0.232
		Sig.	0.181			Sig.	0.658
		N	16			N	6
LDOW	SRP	r	1				
		Sig.	.				
		N	15				
	P	r	.818**				
		Sig.	0				
		N	15				

\*Correlation is significant at the 0.05 level (2-tailed).

\*\*Correlation is significant at the 0.01 level (2-tailed).

Correlation of SRP between locations was also analysed in order to estimate a degree of heterogeneity or homogeneity within the aquifer (Table 5-9). Spatial analysis of these locations may indicate some proximal relationships. CHBH and LUSK are adjacent to each other; however there may be another factor, iron, (see association with iron section below) influencing their correlation. HFW is up-flow from UGDN; and LTRIST and RUSK are surface waters which have no relationship with groundwater SRP, unless it is a function of baseflow and run-off. However LTRI and LTRIST (the borehole and adjacent stream) have no relationship indicating isolation, and there is no relationship between LTRIST and TYST both local streams. The only negative correlation is that of TYST (a stream) with LDOW which may indicate a runoff/ delay mechanism as TYST is proximal to LDOW.

*Table 5-9 SRP correlations between locations in Usk Valley.*

			LUSK SRP
CHBH	SRP	Correlation	.553*
		Sig.	0.032
		N	15
			UGDN SRP
HFW	SRP	Correlation	.534*
		Sig.	0.033
		N	16
			LTRI SRP
LDOW	SRP	Correlation	.600*
		Sig.	0.018
		N	15
			TYST SRP
LDOW	SRP	Correlation	-.786*
		Sig.	0.036
		N	7
			RUSK SRP
LTRIST	SRP	Correlation	.986**
		Sig.	0
		N	6

\*Correlation is significant at the 0.05 level (2-tailed). \*\*Correlation is significant at the 0.01 level (2-tailed).

The results of the correlation reveal a linear directionality association between the species. A Kruskal-Wallis test was performed; the data are best interpreted as a box plot which also indicates the total measured range in values (Figure 5-33). Box plots of TDP from ICP-MS analysis are also shown in Figure 5-34.

The results show that there is a significant difference in the concentration values at LTRI and LDOW with respect to all the other locations; these two locations are also statistically different from each other. The location at LTRI has not had fertiliser application for a number of years (Pers. comm., land owner) although cattle do graze the field. This location also has the highest water table so perhaps it may be a leaching effect on legacy nutrients within the upper soil. The insert in Figure 5-33 shows that the stream TYST (Dowlais Brook) is also significantly different; this is possibly caused by another input source. A large cattle farm and slurry tank is located upstream at Cwm Dowlais, it may also have preferential inputs from artificial drainage from the potato (POTA) and adjacent fields.

It is possibly significant that within the purple circled group the remaining surface water bodies are included, as is CHW. GCBH is more problematic as it is a deep borehole; however it is located down-slope of a field used for silage that has had poultry litter amendments. The association of LUSK and PENC may be a result of iron sorption as is that of CHBH. The remaining locations HFW and UGDN are linked by a down gradient proximity and lack of inputs.

The concentration of soluble phosphate is controlled by pH and is greatest in near neutral and oxidising conditions (Buss et al. 2005). Examination of the Eh-pH diagrams (Figure 5-20) shows that CHW, UGDN and LTRI could be considered the 'most neutral' locations and that LDOW is slightly more acidic. Given the differences in average concentrations (Figure 5-33) this also suggests a variation in sources and that the phosphate leaching potential is not homogeneous throughout the aquifer zone.

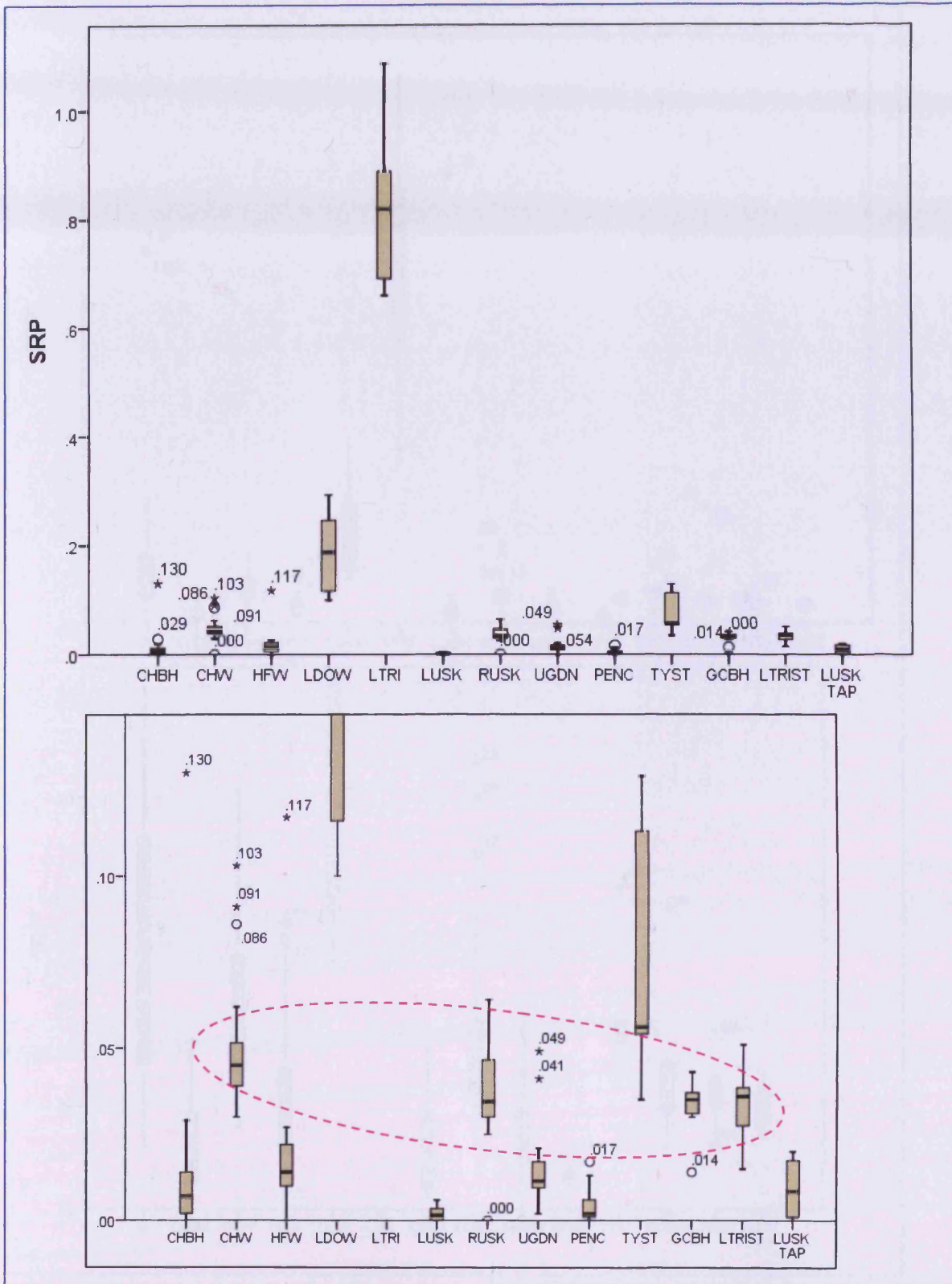


Figure 5-33 Box plot of SRP concentration by location. Inset is enlargement of lower concentration locations. See text for purple ellipse explanation Box whiskers indicate data range. Star represents 'outlier data' beyond 3 box lengths, circles 1.5 box lengths. Units in  $\text{mg l}^{-1}$ .

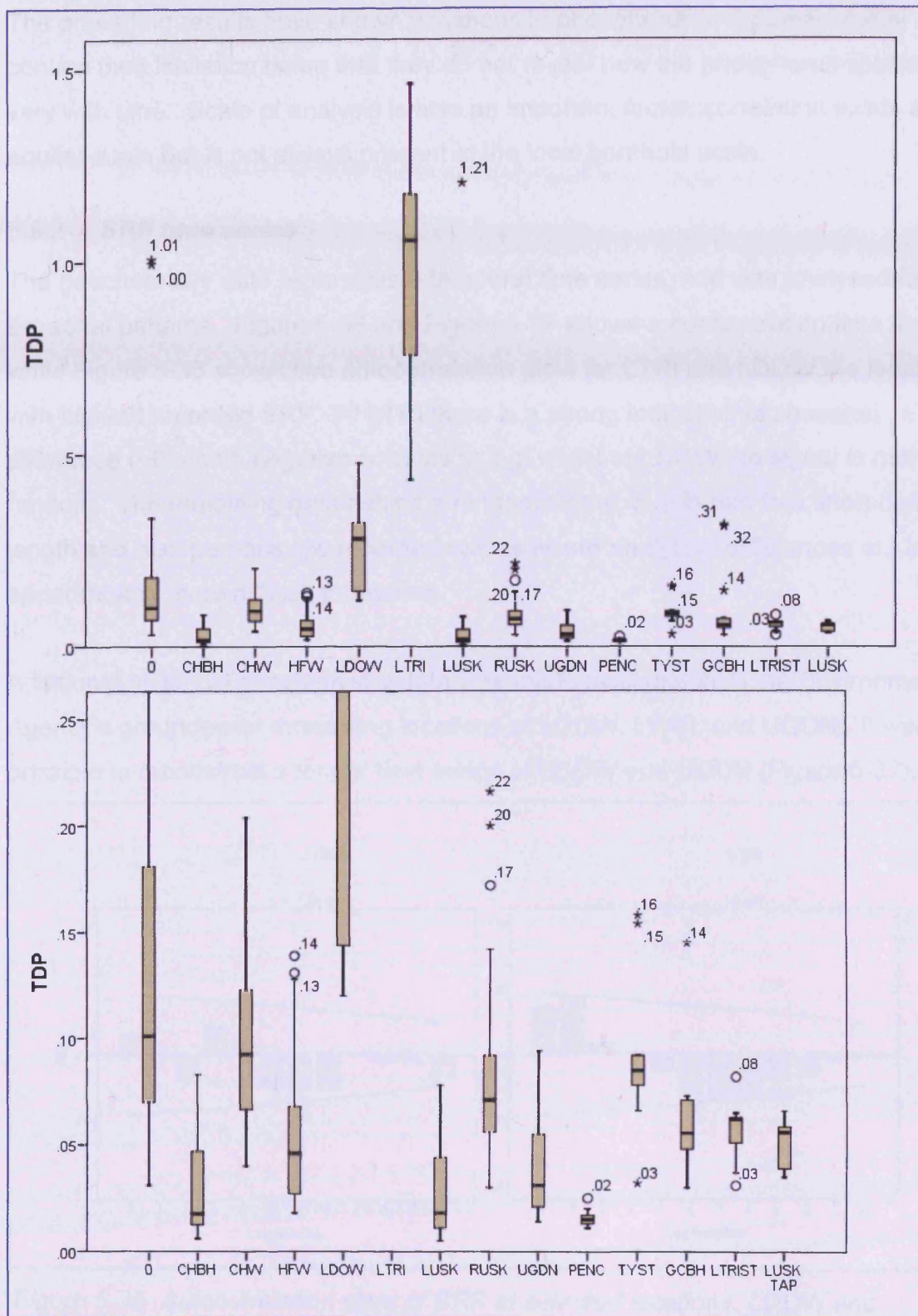


Figure 5-34 Usk Valley total dissolved phosphorus (ICP-MS analysis) ID 0 represents all other locations brigaded together for analysis. Star represents 'outlier data' beyond 3 box lengths, circles 1.5 box lengths. These may represent potential analysis errors or a pulse in concentration. Inset is enlargement of data with LTRI not shown. C.f. Figure 5-33. Units in mg l<sup>-1</sup>.

The preceding results have shown variations in phosphorus in a purely spatial context their limitation being that they do not reveal how the phosphorus species vary with time. Scale of analysis is also an important factor: correlation exists at the aquifer scale but is not always present at the local borehole scale.

### 5.5.2 SRP time series

The geochemistry data represents a temporal time series, and was analysed for seasonal patterns. Figure 5-36 and Figure 5-37 shows a concentration time line while Figure 5-35 shows two autocorrelation plots for LTRI and LDOW the locations with highest recorded SRP. At LTRI there is a strong indication of seasonal difference (~6 month negative correlation lag) whilst at LDOW the signal is more random. The remaining data exhibit a random signal, due in part to a short data length and also perhaps low recorded values where analytical differences are less apparent and more difficult to resolve.

Additional historical geochemistry data was made available from the Environment Agency's groundwater monitoring locations at LDOW, LWEL and UGDN. It was possible to reconstruct a longer time series at LDOW and UGDN (Figure 5-37).

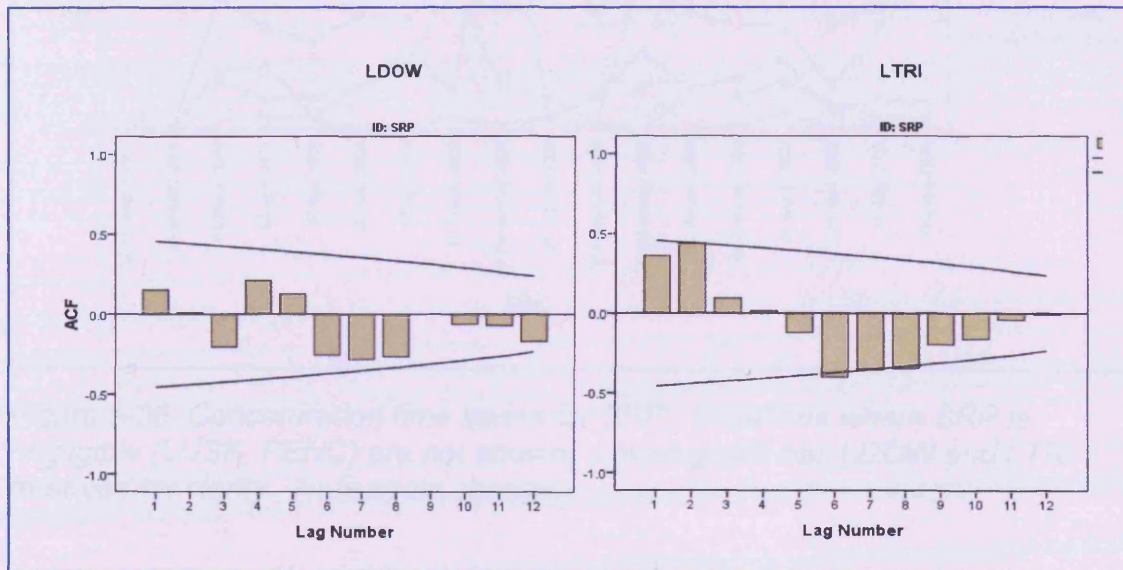


Figure 5-35 Autocorrelation plots of SRP at selected locations. LDOW and LTRI (highest SRP concentrations). Lag interval 1 month.

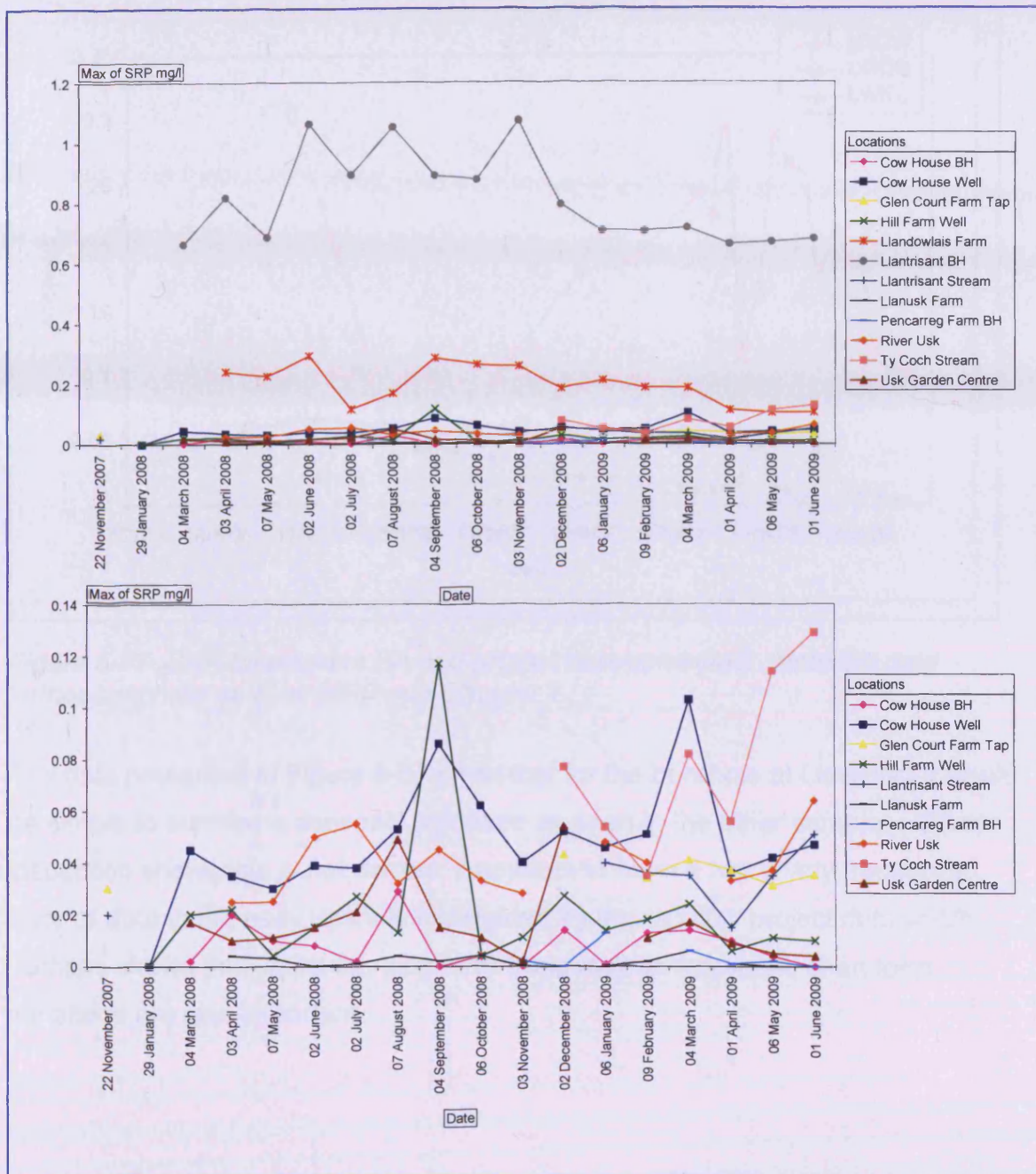


Figure 5-36 Concentration time series for SRP. Locations where SRP is negligible (LUSK, PENC) are not shown. Lower graph has LDOW and LTRI removed for clarity. Note scale change.

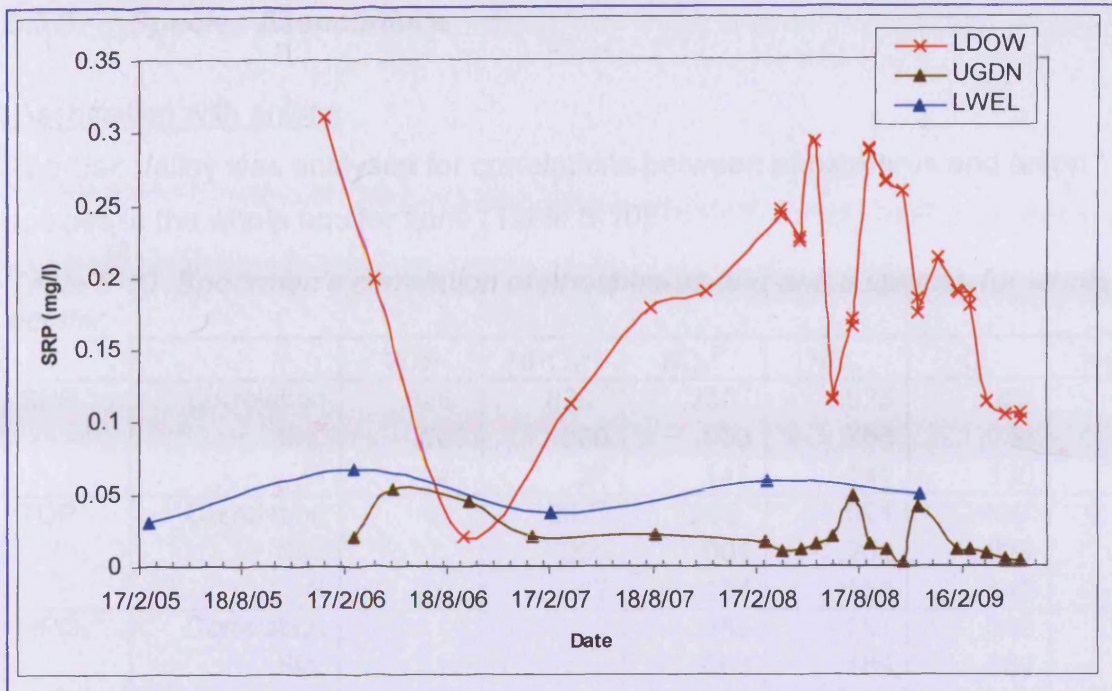


Figure 5-37 SRP time series EA and project data combined. Note EA data 'orthophosphate as P' or MRP see Chapter 2.

The data presented in Figure 5-37 show that for the borehole at Llewellyn it would be simple to surmise a seasonal signature as seen in the other samples. Closer inspection shows this is not correct; it appears to have a two yearly frequency. Lack of data in the early years is highlighted by the monthly project data which perhaps shows that whilst the long term trend may be seasonal, short term variations are also important.

### 5.5.3 Species Associations

#### Association with anions

The Usk Valley was analysed for correlations between phosphorus and anion species in the whole aquifer zone (Table 5-10).

*Table 5-10 Spearman's correlation of phosphorus and anion species for whole aquifer.*

		TDP	HPO <sub>4</sub> <sup>2-</sup>	SO <sub>4</sub> <sup>2-</sup>	NO <sub>3</sub> <sup>-</sup>	Cl <sup>-</sup>	HCO <sub>3</sub> <sup>-</sup>
SRP	Correlation	.826**	.820**	.250**	-.025	.183*	.035
	Sig.	.000	.000	.003	.768	.038	.687
	N	141	27	141	141	130	139
TDP	Correlation		.837**	.255**	-.091	.190*	.077
	Sig.		.000	.001	.263	.024	.346
	N		27	154	154	140	152
HPO <sub>4</sub> <sup>2-</sup>	Correlation			.359	-.261	.340	.440*
	Sig.			.066	.189	.082	.022
	N			27	27	27	27
SO <sub>4</sub> <sup>2-</sup>	Correlation				.731**	.562**	.078
	Sig.				.000	.000	.338
	N				154	140	152
NO <sub>3</sub> <sup>-</sup>	Correlation					.551**	-.052
	Sig.					.000	.521
	N					140	152
Cl <sup>-</sup>	Correlation						.357**
	Sig.						.000
	N						138

\*Correlation is significant at the 0.05 level (2-tailed).

\*\*Correlation is significant at the 0.01 level (2-tailed).

Table 5-10 indicates that within the Usk aquifer area there is no significant correlation with nitrates; however correlation does exist with sulphates and chloride. Further examination of the results by location (Table 5-11) shows that SRP does correlate with nitrate at two locations LDOW and LTRI, but the correlation is in different directions. These two locations had the highest SRP concentrations throughout the study (see Figure 5-33). This difference in correlation direction is also maintained for sulphate and chloride, but in a similar direction for bicarbonate.

Given the general non-sorbing characteristics of chloride, sulphate and nitrate (Krauskopff and Bird 1995; Stumm and Morgan 1996; Fitts 2002; Fetter 2004; Appelo and Postma 2005), this could indicate that different geochemical or physical processes are affecting these two locations. It also reconfirms the issue of scale during analysis and conclusions.

The results for correlation of phosphorus species (SRP, TDP) by location (Table 5-11) show that with the exceptions of LDOW, LTRI and TYST there is no correlation. This suggests that there is no simple mechanism which is converting organic phosphorus to SRP, or that the source zones for both have different inputs.

Table 5-11 Correlation of anions with phosphorus species, by location.

ID			SRP	TDP	HPO <sub>4</sub> <sup>2-</sup>	SO <sub>4</sub> <sup>2-</sup>	NO <sub>3</sub> <sup>-</sup>	Cl <sup>-</sup>	HCO <sub>3</sub> <sup>-</sup>
TYST	SRP	Correlation	1.000	1.000**	.	.571	.393	-1.000**	.450
		Sig.	.	.	.	.180	.383	.	.310
		N	7	7	7	7	7	4	7
	TDP	Correlation		1.000	.	.571	.393	-1.000**	.450
		Sig.		.	.	.180	.383	.	.310
		N		7	7	7	7	4	7
LDOW	SRP	Correlation	1.000	.818**	.750*	.543*	.793**	.614*	-.066
		Sig.	.	.000	.020	.037	.000	.015	.815
		N	15	15	9	15	15	15	15
	TDP	Correlation		1.000	.667*	.714**	.857**	.718**	.263
		Sig.		.	.050	.003	.000	.003	.344
		N		15	9	15	15	15	15
	HPO4	Correlation			1.000	.667*	.633	.667*	-.201
		Sig.			.	.050	.067	.050	.604
		N			9	9	9	9	9
LTRI	SRP	Correlation	1.000	.897**	.762**	-.750**	-.685**	-.676**	-.545*
		Sig.	.	.000	.002	.001	.003	.004	.029
		N	16	16	13	16	16	16	16
	TDP	Correlation		1.000	.724**	-.656**	-.609*	-.524*	-.627**
		Sig.		.	.005	.006	.012	.037	.009
		N		16	13	16	16	16	16
	HPO4	Correlation			1.000	-.289	-.116	-.215	-.496
		Sig.			.	.338	.707	.481	.085
		N			13	13	13	13	13

\*Correlation is significant at the 0.05 level (2-tailed).

\*\*Correlation is significant at the 0.01 level (2-tailed).

Box plots to show the variation in concentration which may be an indicator of sources or sinks for the anions were also produced (Figure 5-38 and Figure 5-39).

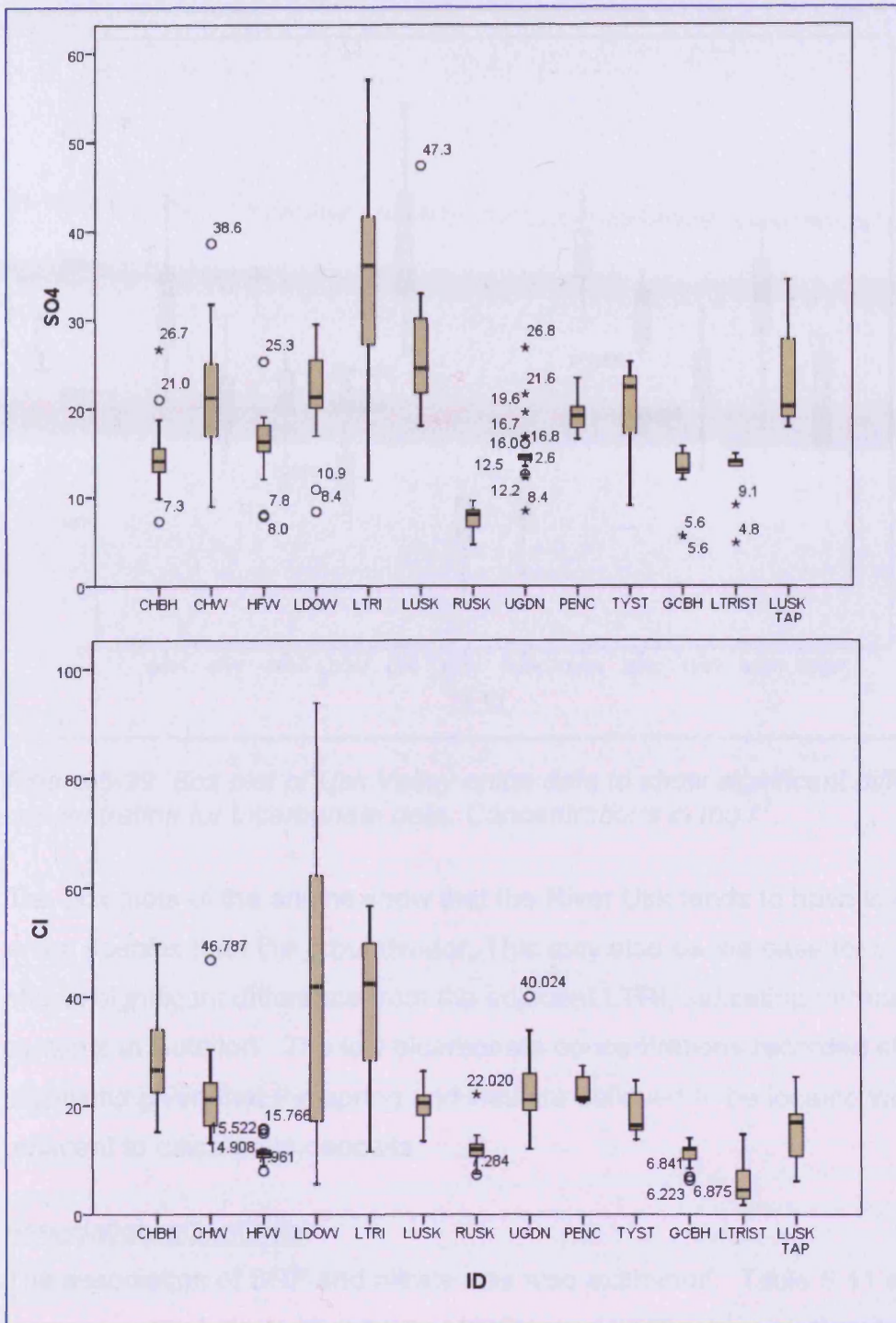


Figure 5-38 Box plot of Usk Valley anion data to show significant difference in concentration for sulphate and chloride, concentrations in mg l<sup>-1</sup>. Outliers are indicated by numeric value. Nitrate box plot is shown in association with nitrate section.

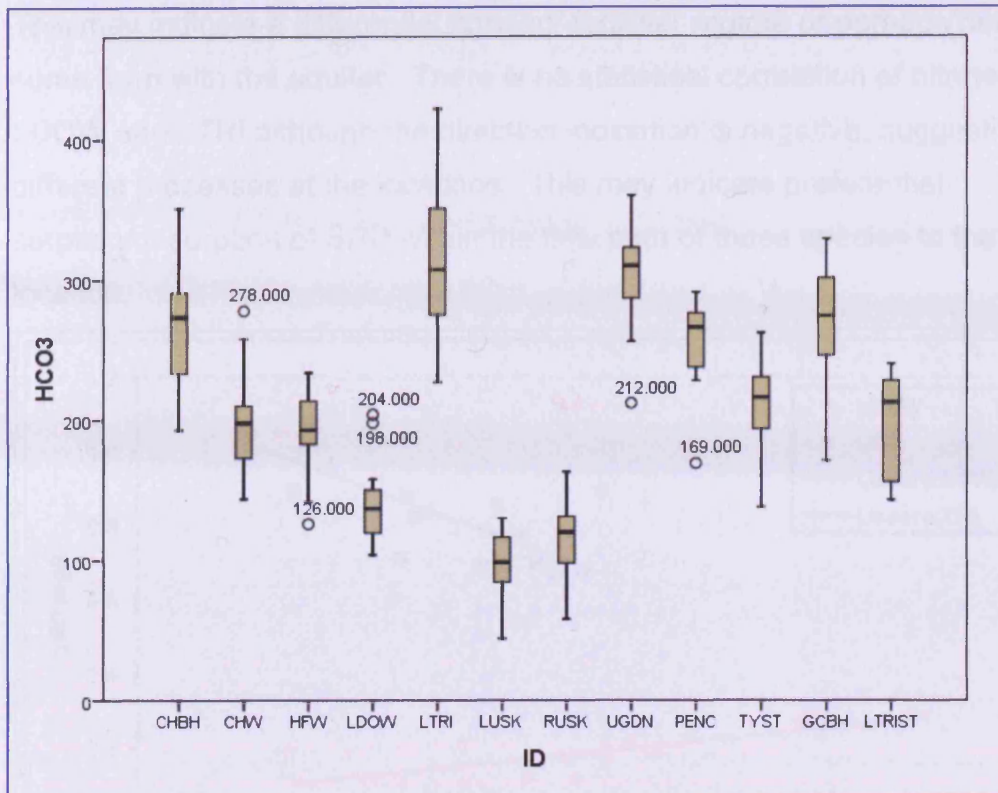


Figure 5-39 Box plot of Usk Valley anion data to show significant difference in concentration for bicarbonate data. Concentrations in  $\text{mg l}^{-1}$ .

The box plots of the anions show that the River Usk tends to have lower levels of anion species than the groundwater. This may also be the case for LTRIST that shows significant difference from the adjacent LTRI, indicating perhaps two systems in isolation. The low bicarbonate concentrations recorded at HFW are surprising given that the spring and well are believed to be located within or adjacent to calcareous deposits.

#### Association with nitrate

The association of SRP and nitrate was also examined. Table 5-11 shows that there is a correlation with nitrate at LDOW and LTRI, although the slope of the correlation is opposite (Figure 5-40). Table 5-10 suggests that overall correlation between SRP and nitrate does not exist in the area. This is also confirmed by correlation of nitrate with phosphorus species by location. A similar opposing correlation regime with chloride and SRP exists at both LDOW and LTRI; chloride being considered as a non sorbing tracer.

This may indicate a differential farming/ fertiliser regime or perhaps heterogeneity in some form with the aquifer. There is no statistical correlation of nitrate between LDOW and LTRI although the direction indication is negative, suggestive of different processes at the locations. This may indicate preferential sorption/desorption of SRP within the flow path of these species to the sampling location.

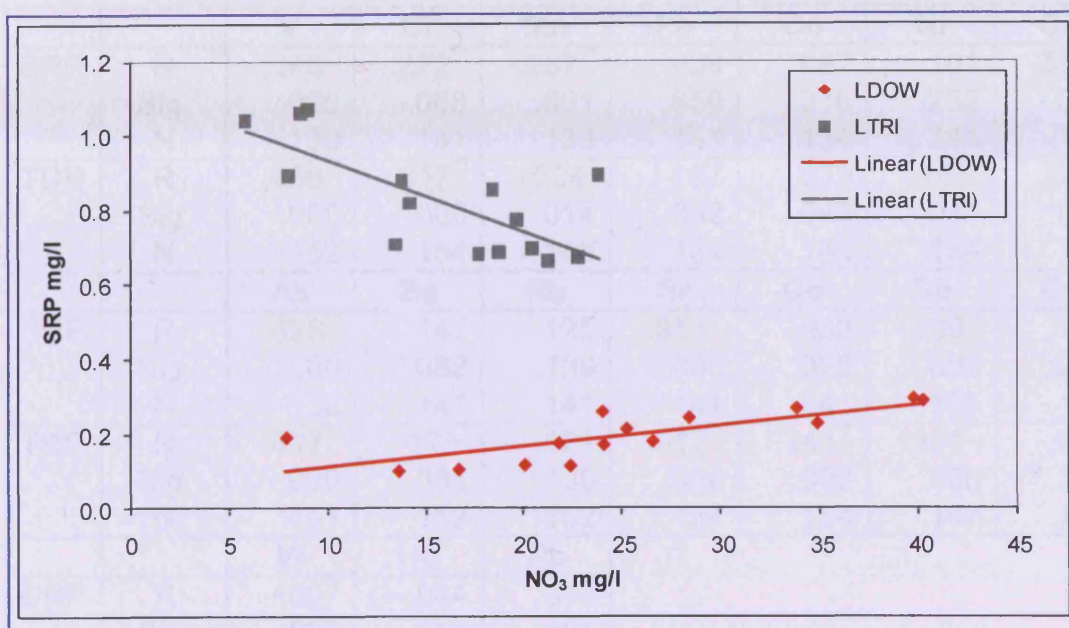


Figure 5-40 Correlation of nitrate and SRP at LDOW and LTRI. Note opposite direction of correlation. A similar observation is made with SRP and chloride. Data is synchronous. Correlation factors  $R^2 = 0.59$  for LDOW and  $R^2 = 0.71$  for LTRI

Examination of the autocorrelation plots for LTRI indicates the seasonal nature of the measured signal at the borehole for both SRP and NO<sub>3</sub> (Figure 5-35, NO<sub>3</sub><sup>-</sup> not shown). There is also a strong negative correlation between the two species at this borehole (Table 5-11). If comparison is made with LDOW more random autocorrelation plots are produced and there is no correlation between the species.

#### Association with cations

An aquifer zone correlation between phosphorus species and cations was undertaken (Table 5-12); the complete correlation table is in Enclosure 1. It is noteworthy that there is a negative correlation with silicon, perhaps a sorption phenomenon. There is also indication (not at statistical significance) of a positive correlation with iron.

Table 5-12 Aquifer zone correlation between phosphorus species and cations.

		SRP	P	Na	Mg	Al	Si	K	Ca
SRP	R		.826**	.445**	-.250**	.164	-.068	.067	.192*
	Sig.		.000	.000	.003	.051	.423	.431	.023
	N		141	141	141	141	141	141	141
TDP	R			.354**	-.233**	.174*	-.337**	.065	.003
	Sig.			.000	.004	.031	.000	.422	.970
	N			154	154	154	152	154	154
		V	Cr	Mn	Fe	Co	Ni	Cu	Zn
SRP	R	.546**	.222**	-.297**	.039	-.087	.101	.346**	-.154
	Sig.	.000	.008	.001	.650	.316	.232	.000	.068
	N	139	141	133	141	134	141	141	141
TDP	R	.466**	.317**	-.204*	.157	.039	.163*	.325**	.048
	Sig.	.000	.000	.014	.052	.643	.044	.000	.556
	N	152	154	146	154	145	154	154	154
		As	Se	Rb	Sr	Cd	Sb	Cs	Ba
SRP	R	.628**	.147	.125	-.353**	.083	.239**	.110	-.105
	Sig.	.000	.082	.139	.000	.328	.005	.209	.214
	N	138	141	141	141	141	136	133	141
TDP	R	.627**	.175*	.121	-.517**	.243**	.301**	.085	-.277**
	Sig.	.000	.031	.139	.000	.002	.000	.313	.001
	N	151	152	152	154	154	147	144	154
		W	Hg	Pb					
SRP	R	-.007	-.044	.074					
	Sig.	.937	.612	.381					
	N	126	138	141					
TDP	R	-.018	.024	.142					
	Sig.	.837	.775	.078					
	N	134	148	154					

\*Correlation is significant at the 0.05 level (2-tailed).

\*\*Correlation is significant at the 0.01 level (2-tailed).

The results of Table 5-12 indicate a mixture of potential aquifer correlations, some of which may be purely artefacts, such as chromium and barium. Phosphate is known to sorb to iron hydroxides although there is not a statistical significance correlation with iron.

Some of the correlations with major cations and accessory nutrients for example calcium, sodium and magnesium may be due to their presence in fertilisers. It is also known that previous feedstock's and pesticides did contain copper and mercury (Warren et al. 2003), and the results may indicate a legacy association.

A further examination of phosphorus species and major cations by location was undertaken, the results of which are at Enclosure 1. Analysis of these results suggests that at each location the correlation with major cations and iron is not always present indicating a potential skew of interpretation of the whole aquifer. A similar correlation was undertaken to assess linear relationships with minor cations, see Enclosure 1.

The results of the correlation by location of the major and minor cations again show a mixed set of results without a discernable pattern. At GCBH, the correlation of phosphate with copper is believed to be an artefact from copper piping from the sampling tap. In a similar fashion, nickel may also be associated through metal parts in boreholes. The correlation with silicon tends to be negative, perhaps indicative of a preferential sorption (if in the form  $\text{SiO}_2$ ); however a positive correlation with silicon is observed at LTRIST a stream which is believed to be runoff. A significant phosphate negative correlation with manganese (data not shown) is observed at LDOW and LTRI, however the remainder of the locations have a mixture of positive and negative associations (not at a statistical significant level); this may account for the whole aquifer correlation in Table 5-12.

#### Association with iron

Phosphate is known to sorb onto ferric hydroxides and reduction of these (together with reduced DO%) has been shown to increase the concentration of SRP or phosphorus (Carlyle and Hill 2001; Skelton 2003). Examination of the DO data and ORP indicate that the waters are all generally oxidising and thus reduction of ferric iron is perhaps not a major influence. The observed multiprobe data indicate a dissolved oxygen content average of  $0.3 \text{ mmol DO l}^{-1}$  (range:  $0.03$  to  $0.85 \text{ mmol DO l}^{-1}$  [ $0.5$  to  $13.5 \text{ ppm}$ ]). These values would indicate an oxic/suboxic environment; DO at normal atmospheric conditions in water is  $0.3 \text{ mmol l}^{-1}$  at  $25^\circ\text{C}$  and  $0.4 \text{ mmol l}^{-1}$  at  $5^\circ\text{C}$ .

Oxidising zones can be further classified as having a DO concentration  $>0.1 \text{ mg l}^{-1}$  ( $0.006 \text{ mmol l}^{-1}$ ) and Eh values  $>200\text{mV}$ , (Robertson et al. 1998). The stability of each species is a function the redox conditions and is different for each (see Figure 5-46). The iron results obtained by ICP-MS analysis are presented in Figure 5-41 are for total iron and not by speciation.

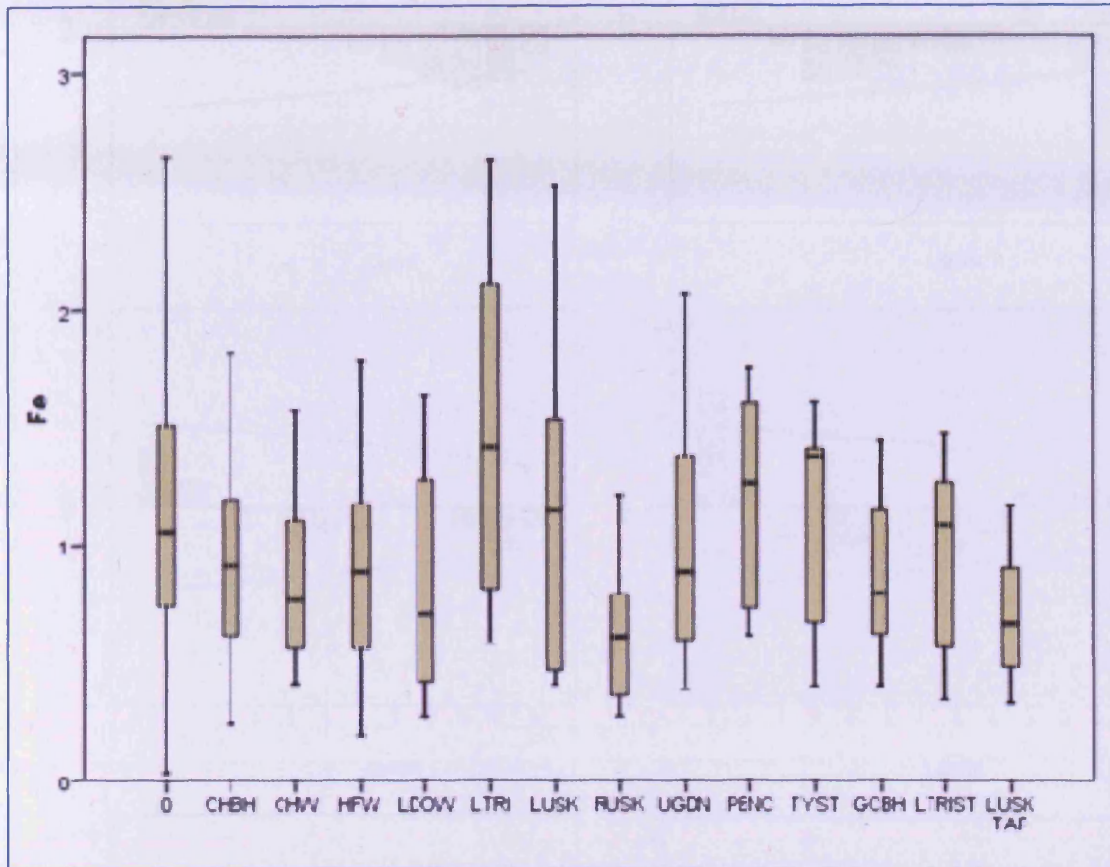


Figure 5-41 Box plot of Fe data for Usk Valley. Values in  $\text{mg l}^{-1}$ .

An association with  $\text{Ni}^{2+}$  loaded iron hydroxides has also been shown to exist (Mustafa et al. 2008), the reaction being pH dependent with sorption decreasing with decreasing pH (more acidic and away from PZC). In time series data (not shown; see Enclosure 1) at the majority of the locations there would appear to be a strong visual negative (or phase shift) correlation of TDP with iron and nickel, although some excursions are apparent. The iron tends to have a cyclic appearance, high in the May/June period, lower in the summer, with a secondary peak in December/January, followed by a slight increase to May. Autocorrelation of the iron data does indicate that with the exception of LUSK there is a seasonal signature and at CHBH the suggestion is that of a longer cycle (Figure 5-42).

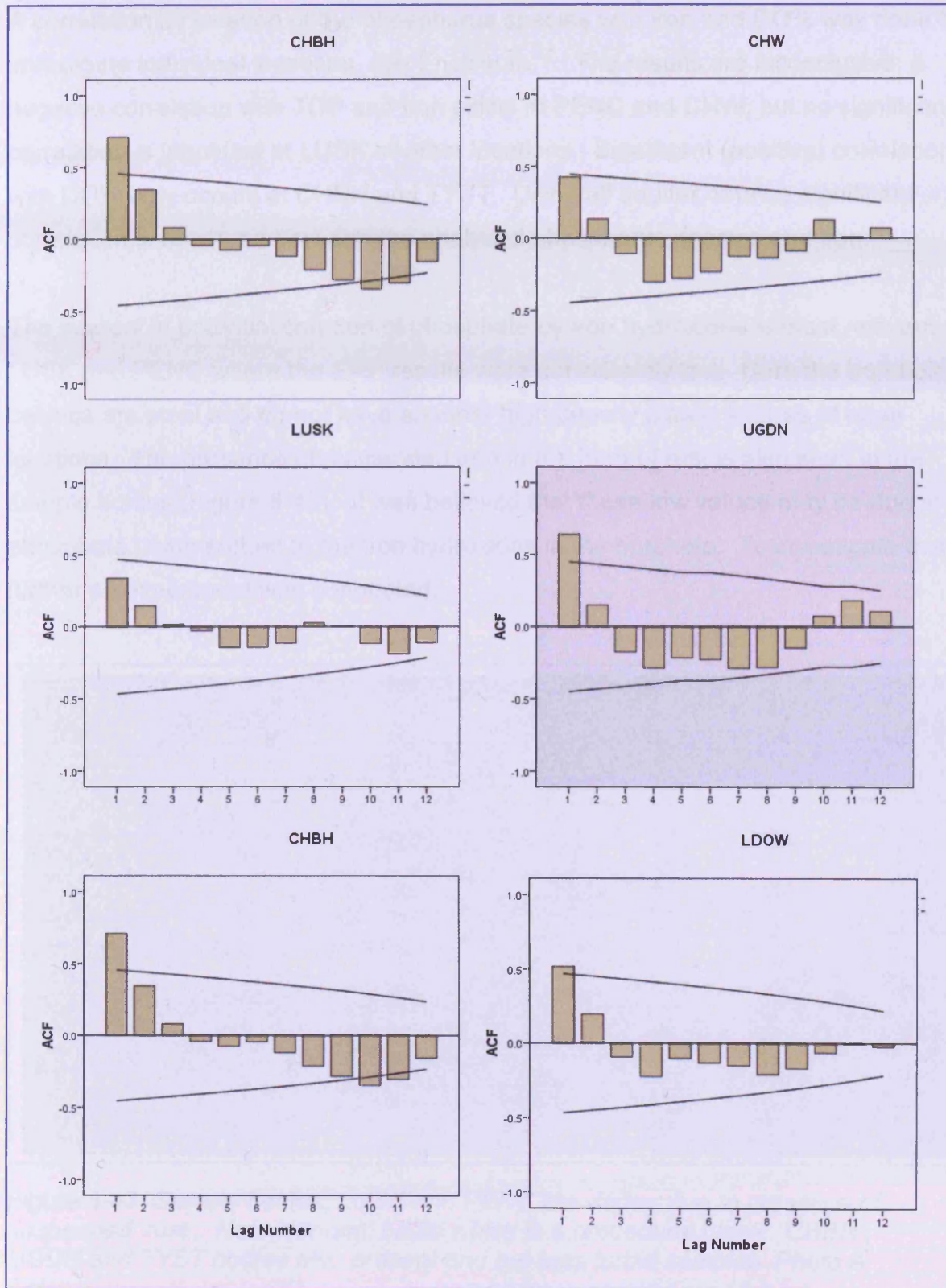


Figure 5-42 Autocorrelation of iron by location. Lag interval 1 month.

A correlation by location of the phosphorus species with iron and DO% was done to investigate individual locations, see Enclosure 1. The results are inconclusive; a negative correlation with TDP and iron exists at PENC and CHW, but no significant correlation is identified at LUSK or other locations. Significant (positive) correlation with DO% only occurs at CHBH and TYST. Using all aquifer data no significant correlation is observed between the analysed phosphorus species and iron.

The interest in potential sorption of phosphate by iron hydroxides is most relevant at LUSK and PENC where the SRP results were consistently low. Here the borehole casings are steel and do not have an inner high density plastic liner as at other locations. The presence of suspended iron in the form of rust is also seen in the sample bottles (Figure 5-43). It was believed that these low values may be due to phosphate being sorbed to the iron hydroxides in the borehole. To investigate this further an experiment was conducted.



Figure 5-43 Sample bottles, LUSK and PENC are darker due to presence of suspended 'rust'. Note 'contam' bottle which is a procedural blank. CHBH, UGDN and TYST bottles also present and are less turbid samples. Photo A Gray.

### *Steel bolt experiment*

Carlye and Hill (2001) demonstrated a phosphate correlation with iron, in that phosphate will sorb onto iron hydroxides. Examination of the SRP and TDP concentrations of UGDN and CHBH show that there is SRP and TDP in measurable quantities in the groundwater. As these locations and a sizeable arable crop field are up-flow from LUSK it may be reasonable to assume that the SRP concentrations would be higher. The SRP soil leaching potential at LUSK was established and there would be a reasonable expectation of SRP in the relatively shallow groundwater; results shown in Chapter 6. A similar situation exists at PENC which is down gradient from LDOW and which may sample from a potentially larger expanse of cultivated land.

A steel bolt was acid washed and cleaned and then placed in a beaker with a  $1\text{ mg P l}^{-1}$  solution (Figure 5-44). The solution concentration was chosen to reflect the Usk location and also so that any differences could be discerned; higher concentration solutions may not have the same resolution using the IC methodology. Samples were taken and analysed by spectrophotometric techniques, the results of which are in Figure 5-45.



*Figure 5-44 Steel bolt sorption experiment, note formation of rust on bolt and precipitate in beaker bottom. Cling film used to seal top. Initial concentration made up from stock dihydrogen potassium phosphate ( $\text{KH}_2\text{PO}_4$ ). Photo A Gray.*

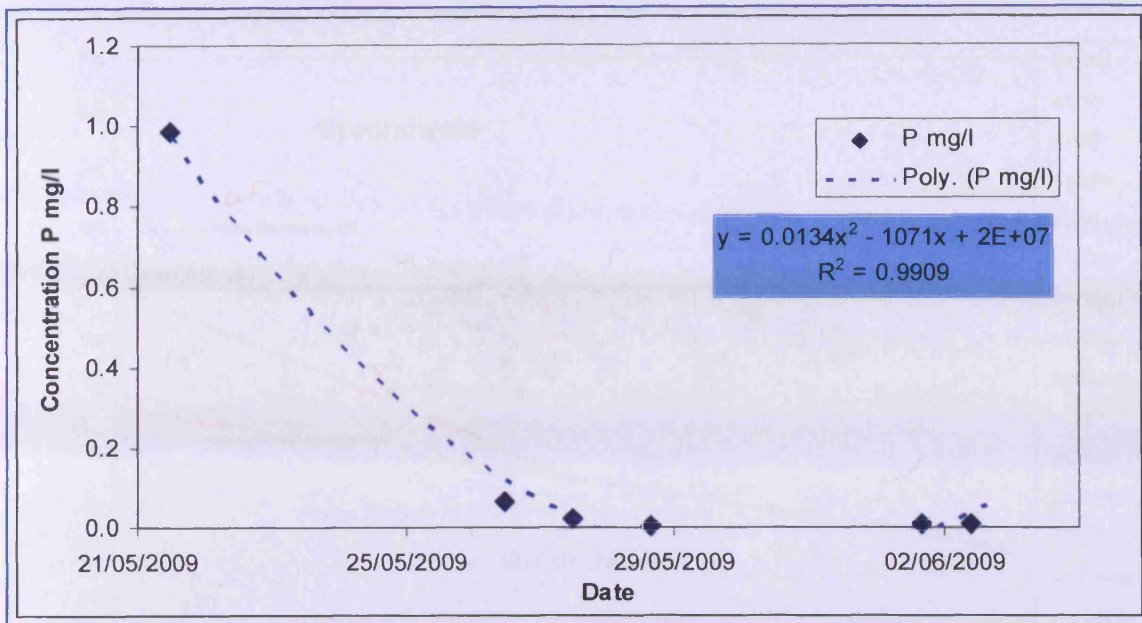


Figure 5-45 Results of steel bolt sorption experiment.

The results of the experiment show that there is a removal of the phosphate from solution with sorption believed to be the mechanism; although a rust coloured precipitate did form (see Figure 5-44). This process is quite rapid, although the beaker was subject to laboratory ambient temperatures that are higher than the groundwater temperatures. Within the time frames of the experiment all the phosphate was effectively removed from solution. This experiment may provide some evidence as to the low SRP concentrations at PENC, LUSK and potentially at CHBH.

In order to assess the type of iron present in these boreholes use of the Nernst Equation and Eh-pH diagrams can be made. The Eh-pH diagram plots the reducing potential, and if a phase stability diagram is superimposed upon the data the dominant species can be qualitatively determined (Figure 5-46).

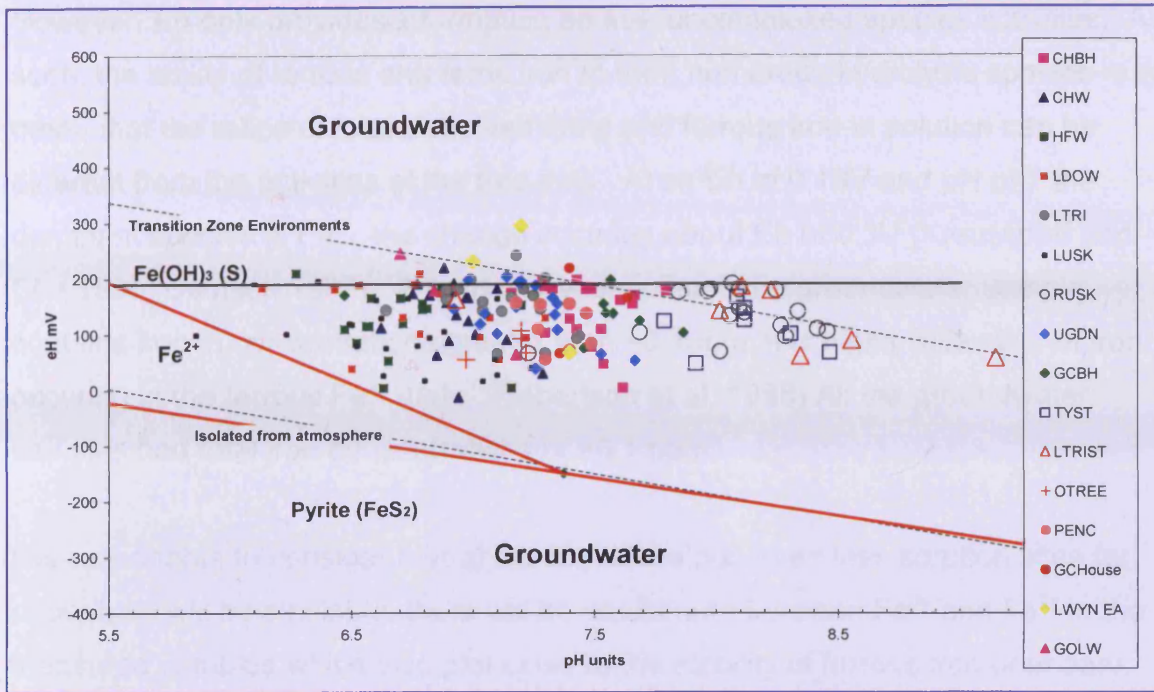


Figure 5-46 Eh-pH diagram of Usk Waters with stability field of iron (red lines at 25 °C) superimposed (Krauskopff and Bird 1995; Deutsch 1997). Black dashed lines are water environment boundaries. Line at +200mV above which is suggestive of oxidising conditions Robertson et al (1998) which would suggest a dominance of ferrous iron and solution of phosphorus species.

Figure 5-46 shows that with the exception of one data point for LUSK all the sampled waters fall within the iron hydroxide stability field at a ferrous activity of  $\sim 10^{-4} \text{ mol l}^{-1}$  (Krauskopff and Bird 1995; Stumm and Morgan 1996; Appelo and Postma 2005). However, as the data plot close to the line it suggests that any iron hydroxides will become more soluble and be in equilibrium with increasing ferrous iron ( $\text{Fe}^{2+}$ ) concentrations (Deutsch 1997). Eh gives relative proportions of species. When the field measured Eh is the same as the standard value for the half reaction (+0.77v) the species activities are equal. If the measured Eh is greater than standard then activity of oxidised species will be greater than reduced, and vice versa for lower Eh measured values.

However, Eh only provides information on free uncomplexed species activities. As such, the ability of ferrous and ferric iron to form numerous hydrolysis species may mean that the ratios of total dissolved ferric and ferrous iron in solution can be different from the activities of the free ions. At an Eh of 0.18V and pH of 7 the dominant species is  $\text{Fe}^{2+}$ , the change occurring about Eh of 0.3V (Krauskopff and Bird 1995; Deutsch 1997). A further caveat is that if the groundwater sample contains iron in concentrations greater than  $\sim 0.1$  ppm it is highly indicative of iron occurring in the ferrous  $\text{Fe}^{2+}$  state (Robertson et al. 1998) All the groundwater samples had total iron concentrations of  $>0.1$  ppm.

It is reasonable to consider that at the Eh values observed less sorption sites for phosphate will be available; there will be equilibrium between  $\text{Fe}^{3+}$  and  $\text{Fe}^{2+}$  in the measured samples which also plot close to the stability of ferrous iron boundary. As Eh reduces at a given pH the iron hydroxide becomes more soluble and becomes in equilibrium with higher concentrations of more soluble ferric iron, thus releasing any sorbed phosphate into solution. In the case of LUSK and PENC there may still be a sufficiency of iron hydroxides (due to the presence of the steel casing) to provide ample sorption sites and further reduce the SRP concentration within the borehole. The precipitation of insoluble iron hydroxides is known to exist with the aquifer (Figure 5-47) which may provide phosphate sorption sites.



*Figure 5-47 Deposition of iron hydroxide in feeder pipe to storage butt at Oaktree Farm spring, (OTREE) The head waters of Llantrisant Brook. Photo A Gray.*

The precipitate that formed in the beaker was also analysed by the SEM (Figure 5-48 and Figure 5-49). The spectrum analysis for these sites of interest is in Table 5-13 and Table 5-14 respectively. The tables show that there is a strong association of phosphorus with parts of the precipitates, which is believed to be a sorption mechanism. It was not possible to assay the bolt for phosphorus content. The phosphorus values obtained were not observed in the same amounts when analysing soils with the same technique (Chapter 6).

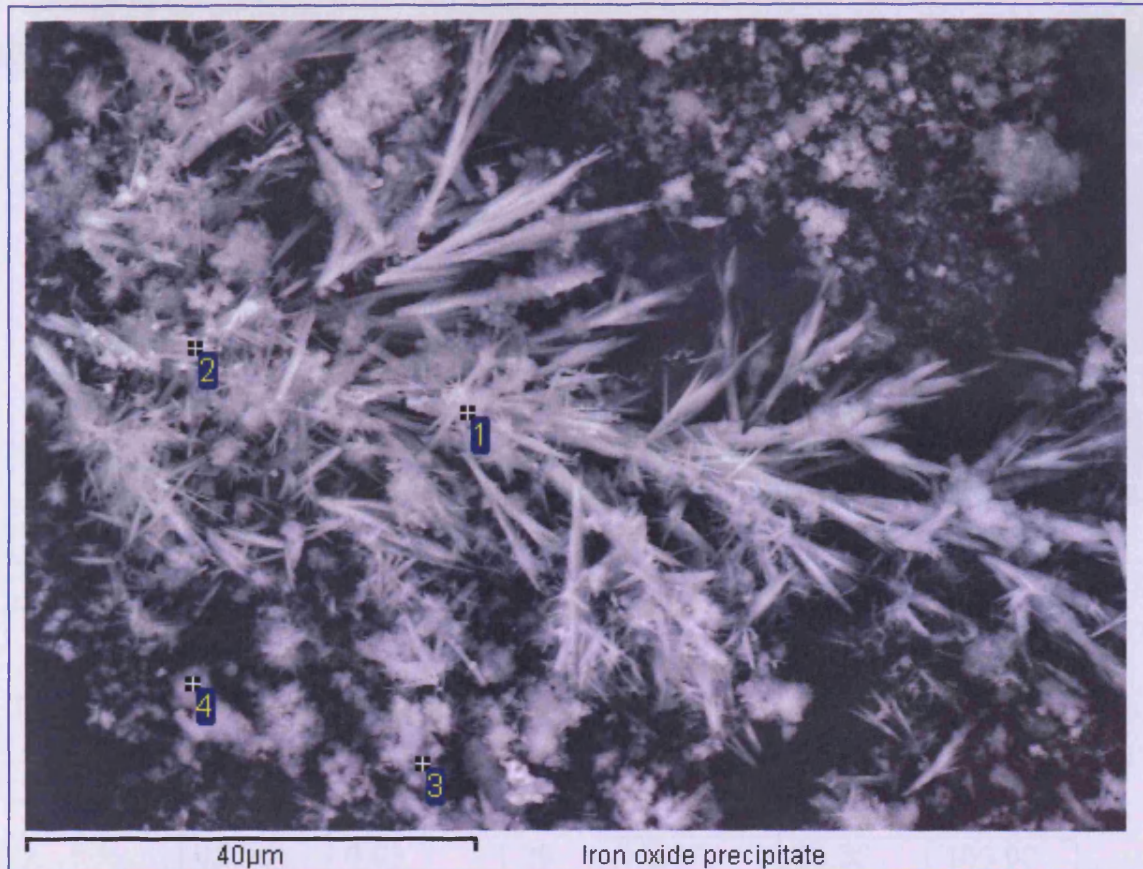


Figure 5-48 SEM image #1 of iron oxide precipitate formed during iron bolt sorption experiment, see Figure 5-44.

Table 5-13 Spectrum analysis for Figure 5-48.

Spectrum	O	Na	Si	P	S	Fe	Total
1	37.92		0.53	0.49		61.06	100.00
2	33.06		0.46			66.48	100.00
3	33.95	1.63		1.88	0.70	61.83	100.00
4	39.29	2.05		1.49	0.65	56.51	100.00

All results in weight%

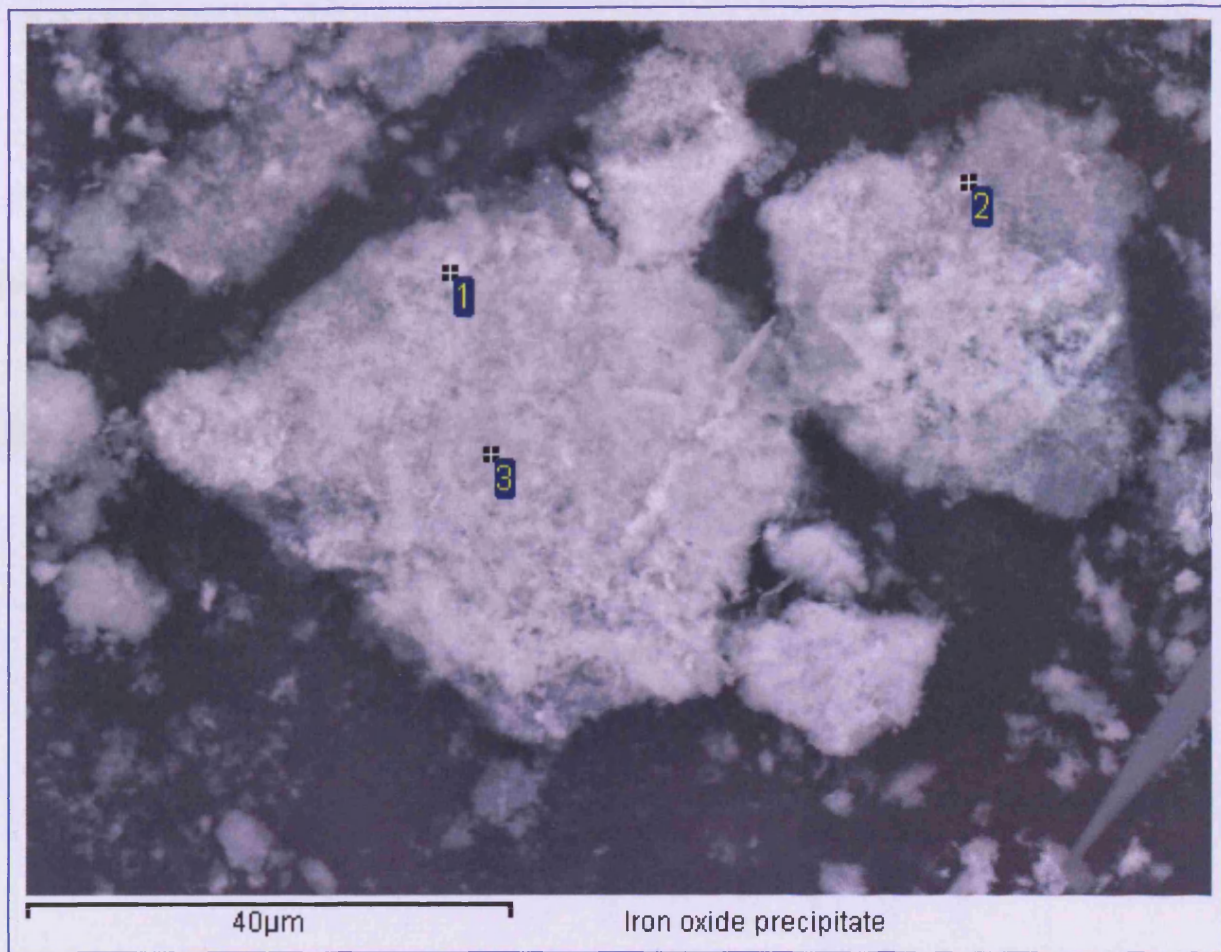


Figure 5-49 SEM image #2 of iron bolt precipitate.

Table 5-14 SEM spectrum analysis for Figure 5-49.

Spectrum	O	Si	P	Cl	Fe	Total
1	36.47	0.52	1.78		61.23	100.00
2	42.05	0.93	1.29	0.37	55.36	100.00
3	30.74	0.52	1.16		67.58	100.00

All results in weight%

### Soluble unreactive phosphorus

Soluble unreactive phosphorus was also detected within the groundwater compartment (TDP-SRP=SUP). Figure 5-50 shows the average SUP and SRP concentrations for the project waters.

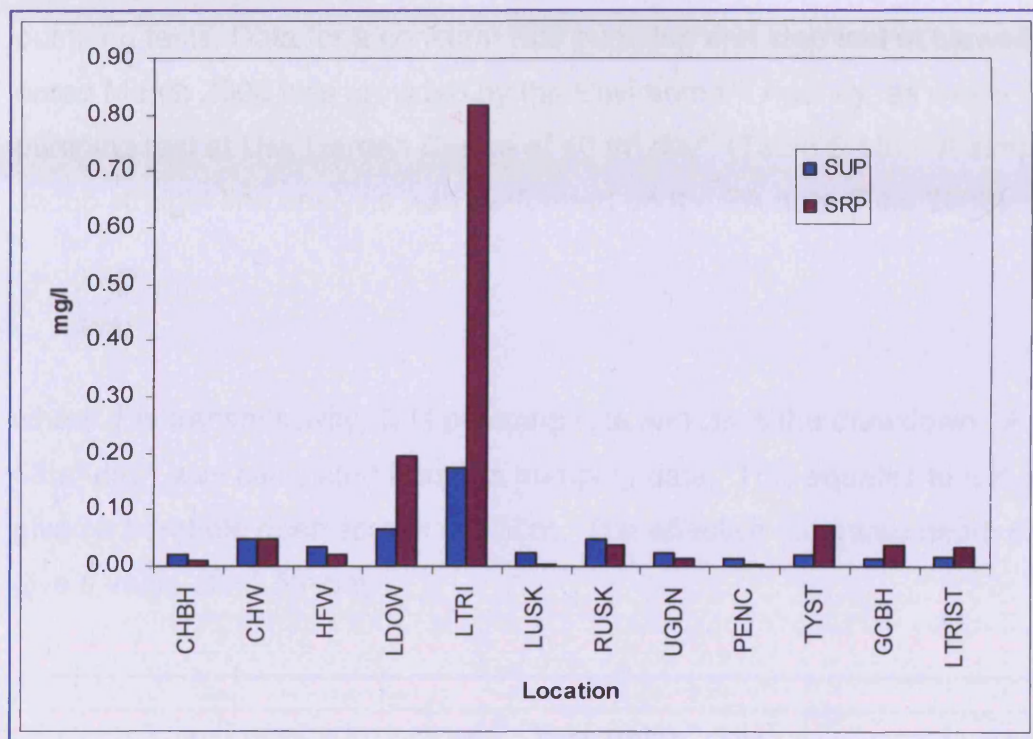


Figure 5-50 SUP and SRP average values for Usk ground and surface waters.

## 5.6 Field testing

### 5.6.1 Hydraulic conductivity determinations

#### Pumping tests

Calculation of aquifer hydraulic conductivity ( $K$ ) is most readily achieved by pumping tests. Data for a constant rate pumping and step test at Llewellyn borehole dated March 2005 was provided by the Environment Agency, as was a value for a pumping test at Usk Garden Centre of  $40 \text{ m}^2 \text{ day}^{-1}$  (Table 5-15). A simple Cooper-Jacob straight line analysis was performed on the EA data (Fitts 2002):

$$T = \frac{2.3Q}{4\pi\Delta s} \quad \text{Eqn 5-2}$$

where  $T$  is transmissivity,  $Q$  is pumping rate and  $\Delta s$  is the drawdown. A value of  $58 \text{ m}^2 \text{ day}^{-1}$  was calculated from the pumping data. This equates to a  $K$  of  $\sim 2 \text{ m day}^{-1}$  given a borehole open screen of  $\sim 30 \text{ m}$ . The effective saturated depth of  $\sim 40 \text{ m}$  will give a value of  $\sim 1.5 \text{ m day}^{-1}$ .

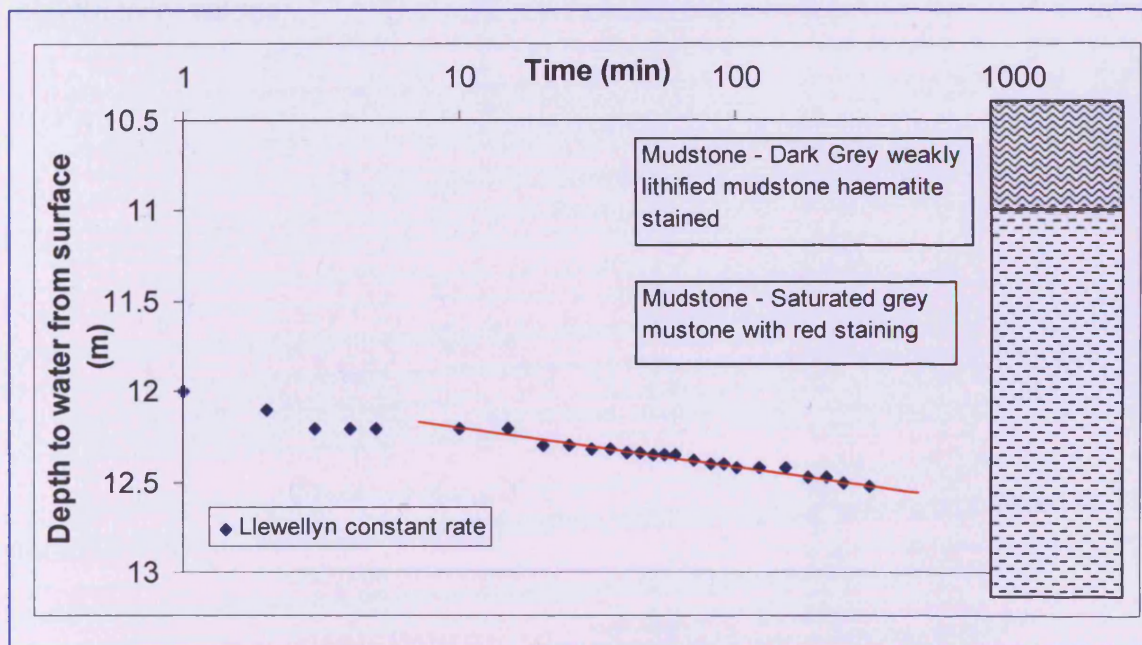


Figure 5-51 Constant rate pumping test at Llewellyn borehole, lithology abstracted from log at same vertical scale to aid interpretation.

A small-scale second constant rate pumping test was also undertaken at CHBH. Jacob and Theis modified analysis was carried out on the data, the results are shown in Figure 5-52. The calculated transmissivity value is  $\sim 25 \text{ m}^2 \text{ day}^{-1}$  or hydraulic conductivity of  $\sim 1 \text{ m day}^{-1}$  given a borehole depth of  $\sim 30 \text{ m}$ .

*Table 5-15 Synopsis of available pumping test data for Usk Valley.*

Location	T $\text{m}^2 \text{ day}^{-1}$	T Recovery $\text{m}^2 \text{ day}^{-1}$	Remarks
Llewellyn EA	58	-	LWEL EA test
Usk Garden Centre	37	40	UGDN (Morris' of Usk)
Cow House BH	25	28	CHBH

The rapid drawdown observed in the CHBH pumping test (Figure 5-52) and borehole logging data (Figure 5-2) may indicate some well and lithology effects. This rapid initial drawdown is not seen in the EA data at Llewellyn borehole (Figure 5-51). The hydraulic conductivity values calculated assume lithology homogeneity throughout the sampled portion of the aquifer. In reality the flow is likely to originate from preferential paths (indicated in borehole logs) with greater individual conductivity values.

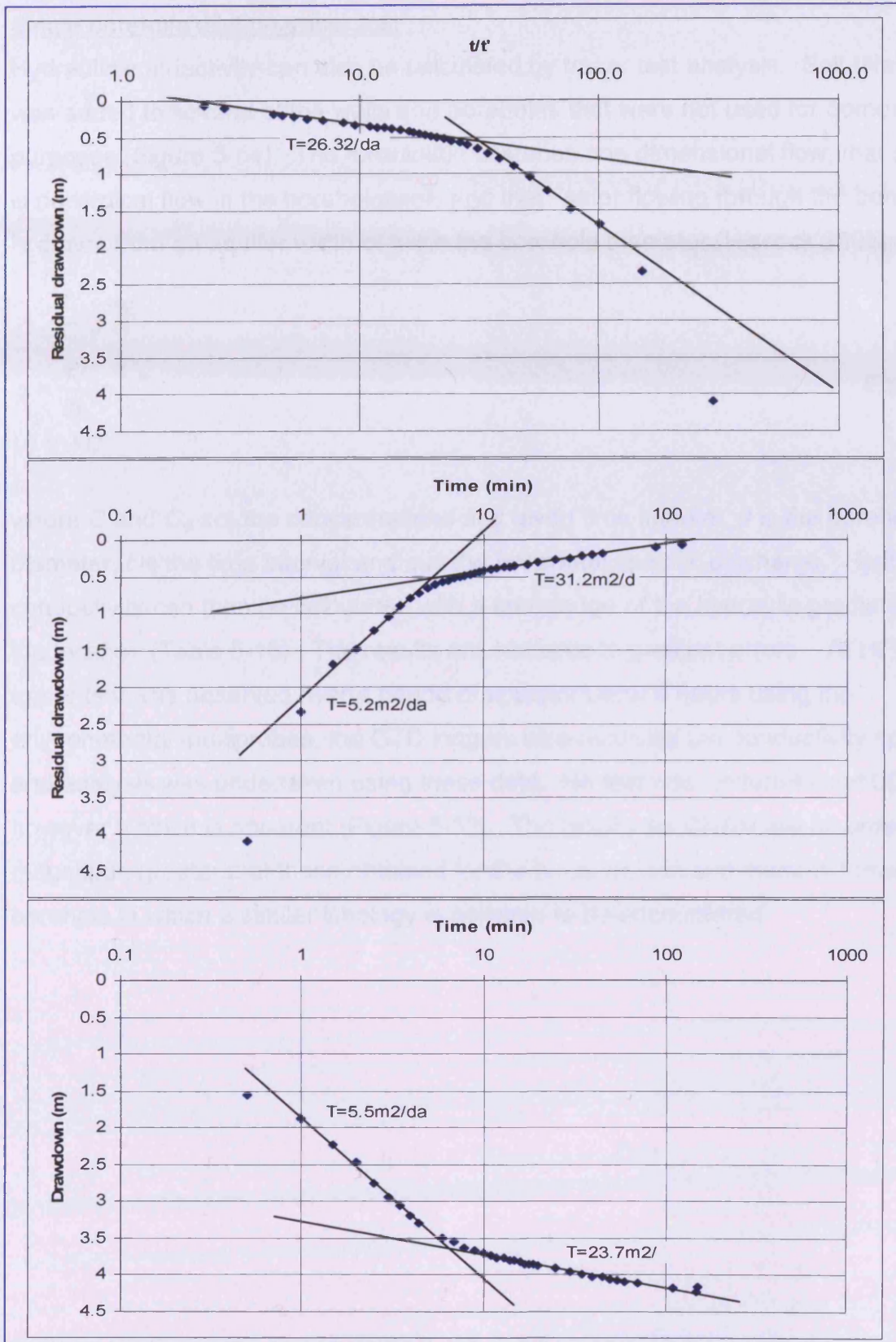


Figure 5-52 Pumping test results and analysis for test undertaken at Cow House BH (CHBH). Upper graph This Modified method, lower Cooper-Jacob Straight Line method.

**Single borehole dilution tracer test**

Hydraulic conductivity can also be calculated by tracer test analysis. Salt (NaCl) was added to several of the wells and boreholes that were not used for domestic purposes (Figure 5-54). The calculation assumes one dimensional flow, that there is no vertical flow in the borehole/well, and that water flowing through the borehole is drawn from an aquifer width of twice the borehole diameter (Hiscock 2005):

$$C = C_0 e^{-\frac{8qt}{\pi d}}$$
$$q = \frac{\pi d}{8t} \ln \frac{C_0}{C} \quad \text{Eqn 5-3}$$

( $q = Ki$ )

where  $C$  and  $C_0$  are the concentrations at a given time interval,  $d$  is the borehole diameter,  $t$  is the time interval and  $q$  is the horizontal specific discharge. Hydraulic conductivity can then be calculated with a knowledge of the hydraulic gradient  $i$  at the location (Table 5-16). The results are sensitive to gradient errors. At HFW, the tracer test was observed over a period of approximately 4 hours using the environmental multiprobes, the CTD loggers also recorded the conductivity spike and analysis was undertaken using these data. No test was undertaken at LDOW, however a spike is apparent (Figure 5-53). The results for CHBH are an order of magnitude greater than those obtained for the pumping test and those of Llewellyn borehole in which a similar lithology is believed to be encountered.

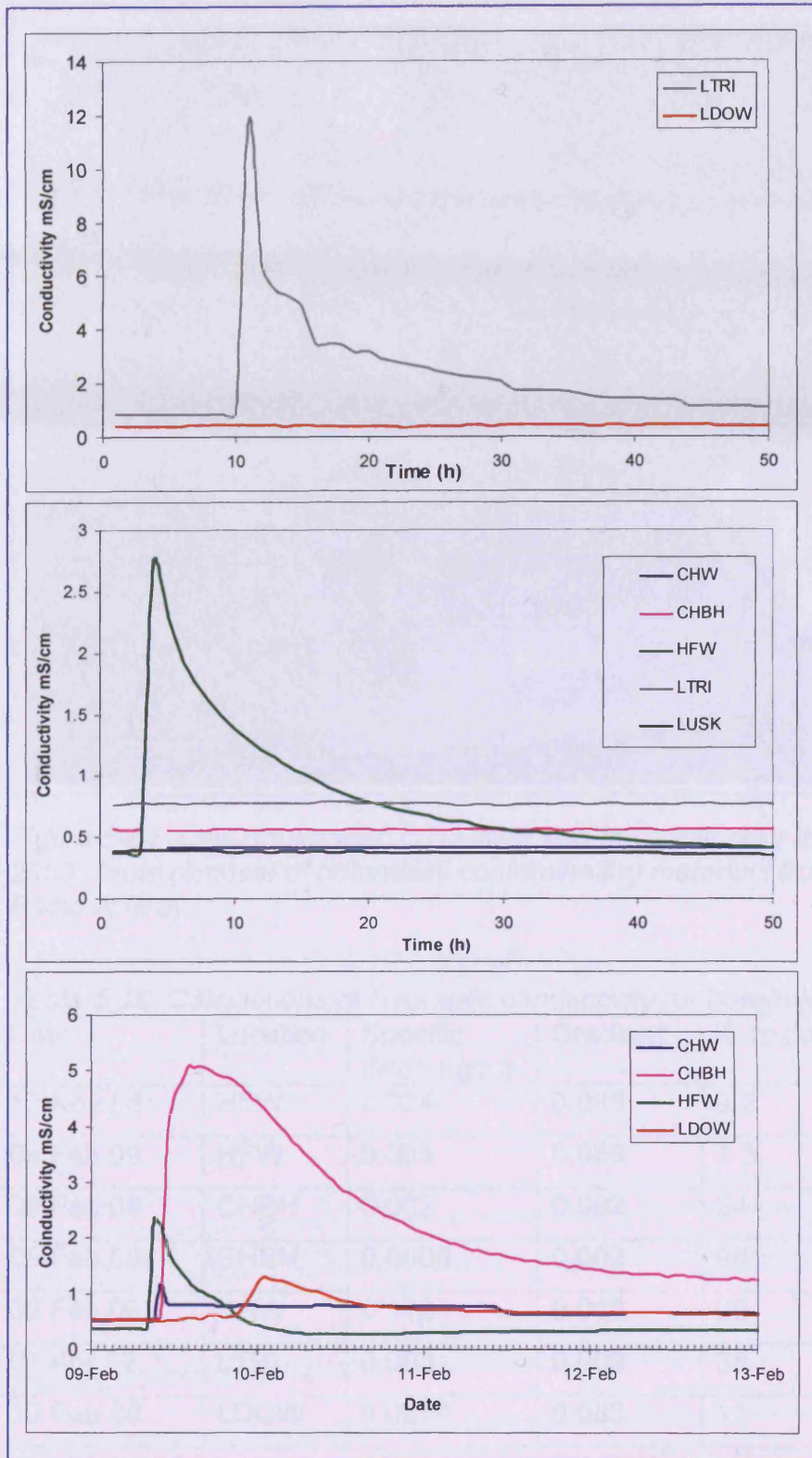


Figure 5-53 Single borehole dilution tracer test for Usk boreholes. Note the spike at LDOW which is unaccounted for and may be the result of road salt / external contamination. A car crash occurred near LDOW at about this period and may be related to this spike. Other locations shown for comparison.

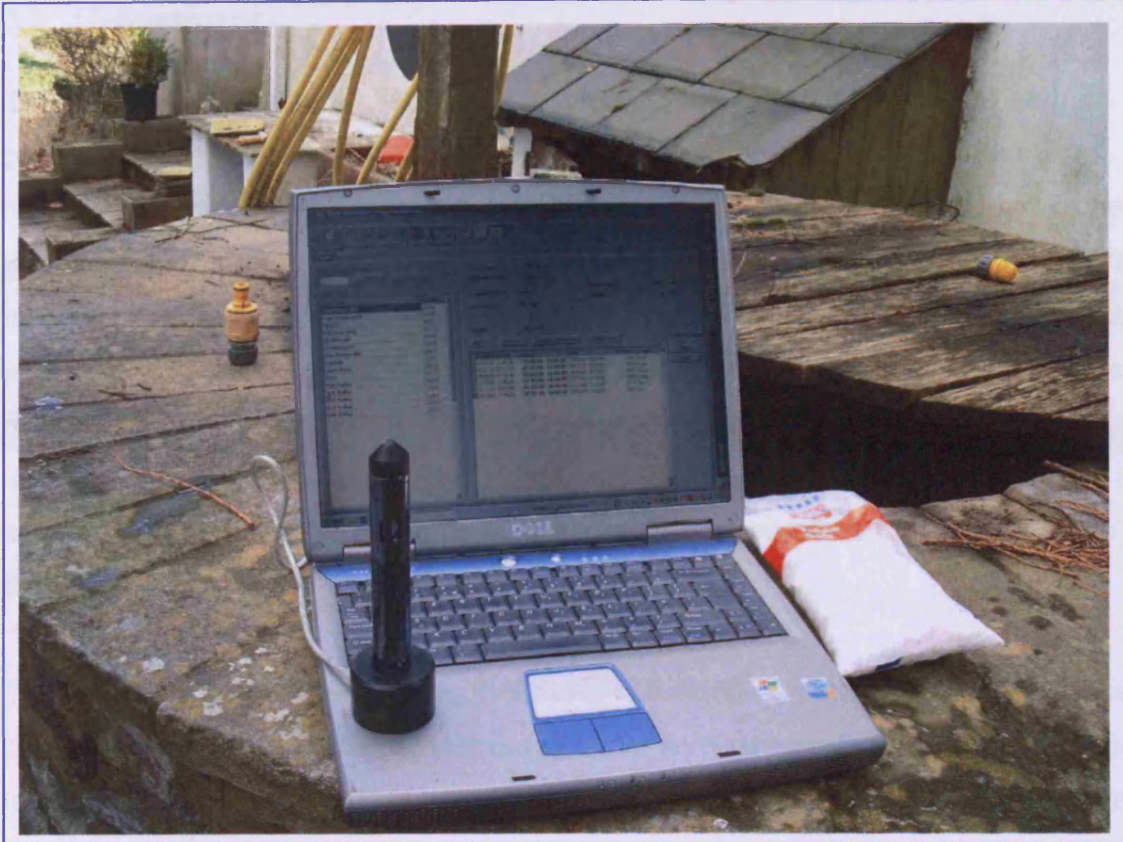


Figure 5-54 Cow house well; CTD diver and table salt prior to tracer test, Feb 2009. Note removal of potentially contaminating materials from earlier periods. Photo A Gray.

Table 5-16 Calculations of Hydraulic conductivity for borehole dilution tests.

Date	Location	Specific discharge $q$	Gradient	$K \text{ m day}^{-1}$	Remarks
12 Nov 08	HFW	0.034	0.088	9.2	
09 Feb 09	HFW	0.005	0.088	1.3	
09 Feb 09	CHBH	0.002	0.002	24	
09 Feb 09	CHBH	0.0008	0.002	96	Late data
09 Feb 09	CHW	0.172	0.002	20	
01 Apr 09	LTRI	0.003	0.002	38	
10 Feb 09	LDOW	0.0014	0.003	11	Unknown source

## 5.7 Summary

The investigation of the Lower Usk Valley groundwaters has been done on both physical and chemical data. The physical measurements show that there is significant positive correlation between boreholes in response to groundwater head variations and temperature. This indicates that at the measured scale the aquifer is acting in a homogeneous fashion. It has not been possible to isolate individual water bearing horizons that are indicated in the borehole logs. The lag response to recharge events is also short, in the order of 1 day although secondary longer duration mechanisms are also indicated. Autocorrelation of the groundwater heads indicates that they are responding to seasonal influences, and they do not exhibit a flashy signature.

The geochemical analysis shows that there is a significant partitioning of the local pH and DO of the borehole waters between valley sides and within the west bank locations. pH is a driver for anion sorption mechanics; DO will affect redox states. Associations have also been investigated which are again scale dependent. Positive correlations with SRP and other species are shown to exist at the aquifer scale, but do not exist at the local borehole scale. This indicates a degree of geochemical heterogeneity within the aquifer zone, caused either by inputs (land use) or geology. This variation in correlation between phosphorus species is also shown to exist. Laboratory experimentation and field observations have shown the importance of iron hydroxides to the availability of SRP.

Physical testing of the aquifer furnished results that are able to be carried forward into later modelling stages where groundwater flow will be assessed.

## Chapter 6 Usk Valley soil

### 6.1 Introduction

Soils from the Usk Valley were collected and a variety of analyses were undertaken. These included soil leaching with 2M nitric acid and deionised water (an adaption of a British Standard's methodology), and analysing the resulting leachate by ICP-MS and IC. X-Ray diffraction and ESEM were used to determine soil mineralogy and the presence or absence of phosphate minerals. The purpose of the soil investigation is to derive values for chemical species that are relevant to the behaviour of phosphate in the soil and subsequently the groundwater. This is important as the soil is the usual first contact zone of phosphate addition and groundwater recharge. A map (Figure 6-1) shows the soil sample locations. The complete soil analysis data results are presented in the CD in Enclosure

The data are presented by location, time and stratigraphic position. Sample depths were top soil, middle or lower depth ~15-20cm, and bottom soils >30cm. Several soil sample locations are coincident with groundwater observation boreholes and were taken within several metres of the boreholes (Figure 6-1). The location POTA was chosen to represent a cultivated field, with fertiliser inputs; the SCRUB location had no recent fertiliser application (within last 5 years); the manure pile MANU to represent hot spots (Figure 6-3). The manure pile is separated from POTA by one field and the stream water sampling location TYST.

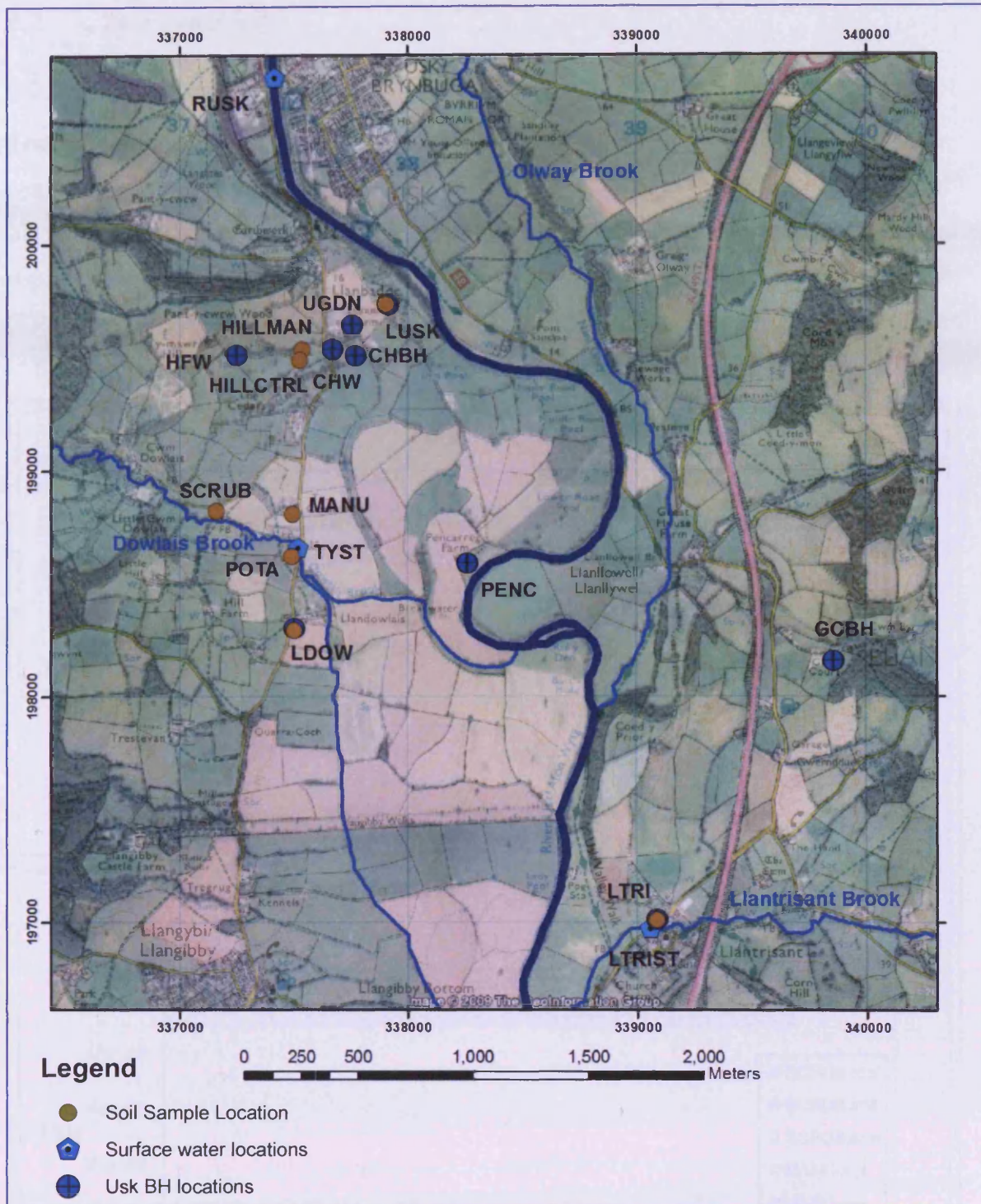


Figure 6-1 Map of soil sample locations for Usk Valley superimposed on imagery photo showing cultivation features. Soil sample locations in brown. (Source Google Earth image dated June 2004).

## 6.2 Soil Leaching

### 6.2.1 Acid leaching results

The leaching in 2M nitric acid is a straightforward procedure, and analysis of the resulting leachate provides a reliable estimate of the maximum concentrations of phosphorus species in the soil. The results of the acid leaching are best represented as a graph (Figure 6-2). The results are quoted as total phosphorus (TP); there may be some resistant organic phosphorus not wholly acid hydrolysed in the sample.

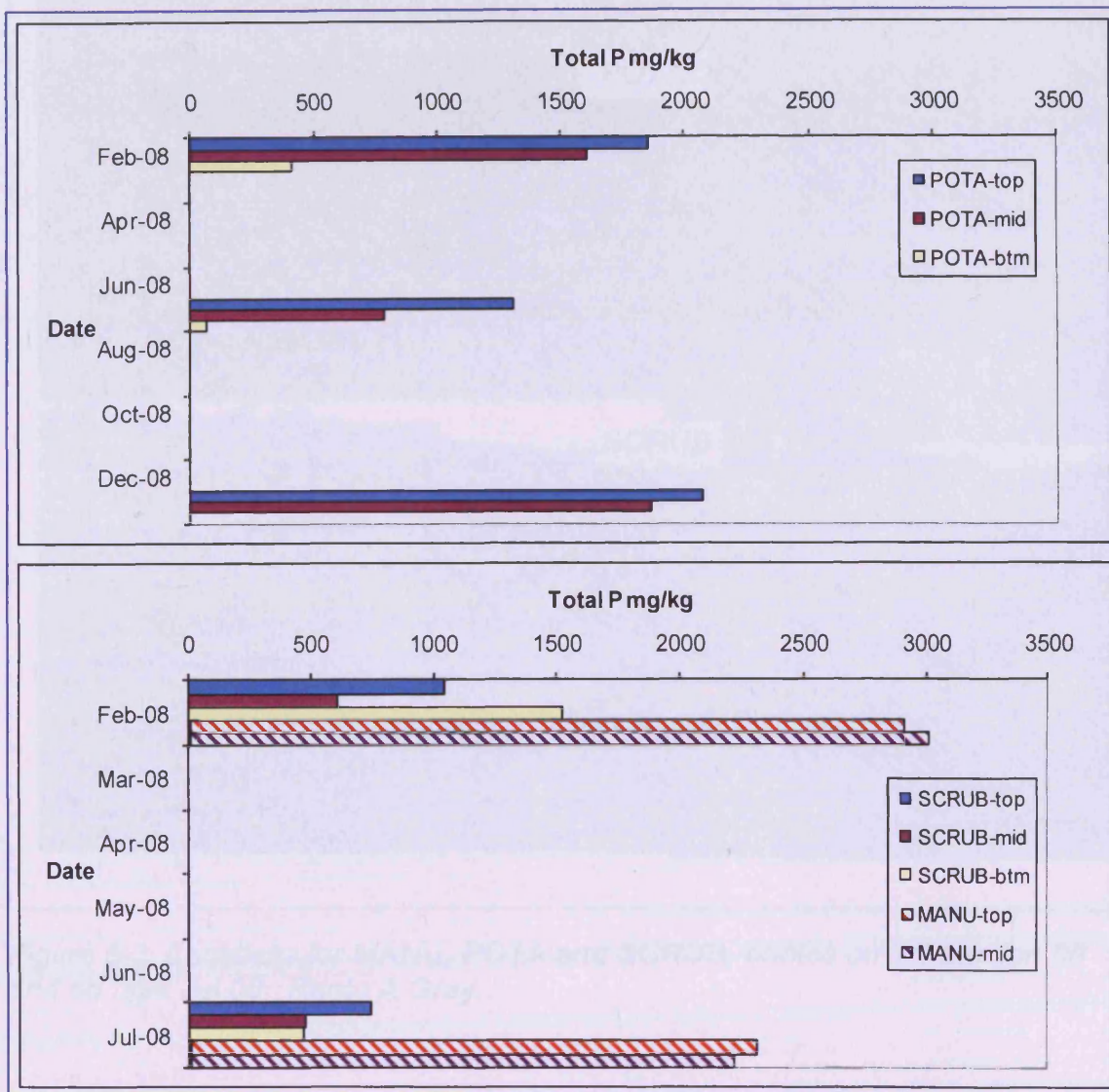


Figure 6-2 Total phosphorus for selected locations, note horizontal scale is same, date scale varies.

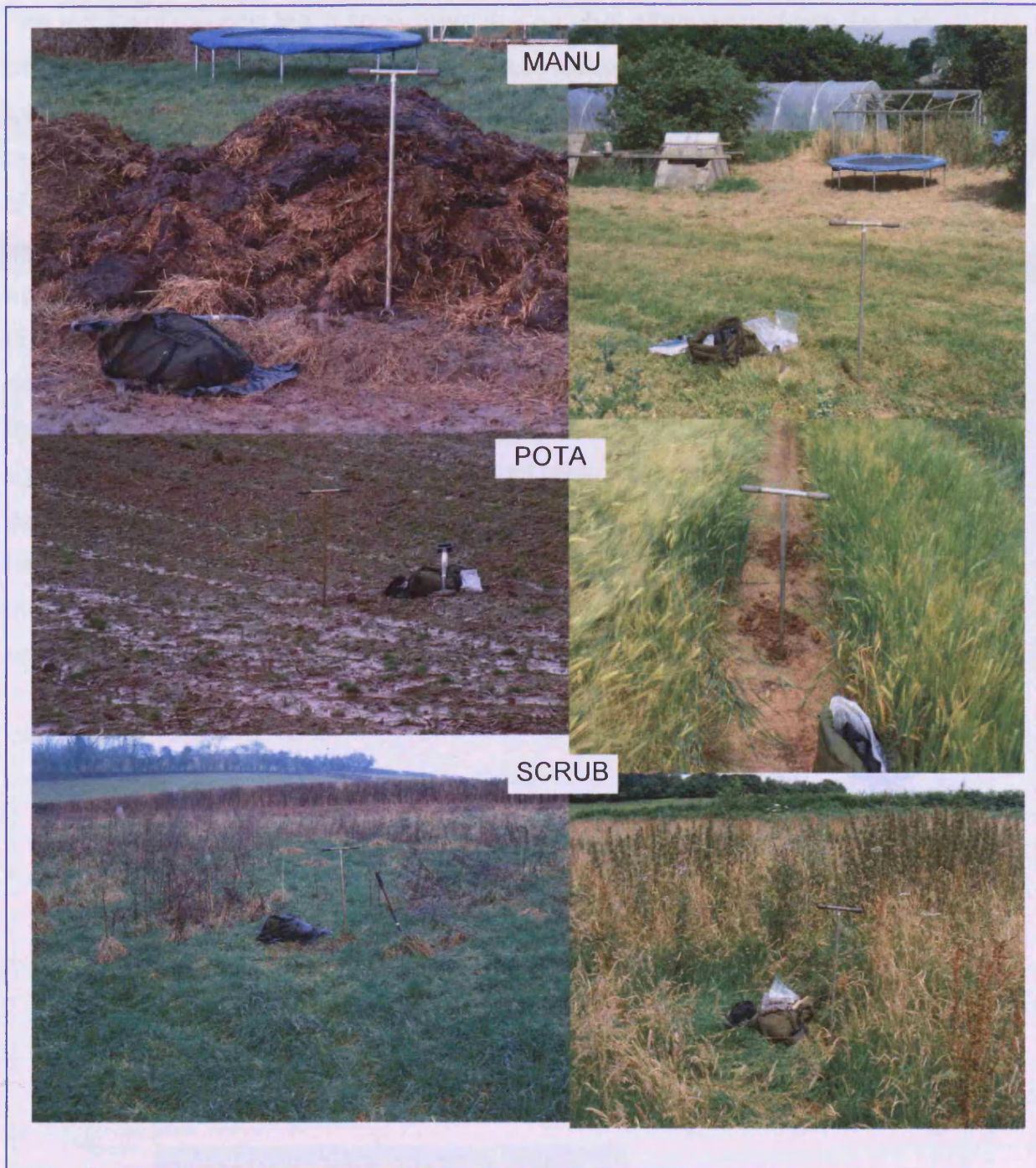


Figure 6-3 Locations for MANU, POTA and SCRUB, photos on left are Jan 08 and on right Jul 08. Photo A Gray.

The results of the acid leach show there is a general attenuation down the soil column, and for POTA there is an apparent seasonal variation. At the manure pile location MANU, the values are much higher than the cultivated field due, it is believed, to seepage of leachate from the manure pile into the local soil. Analysis of a separate manure effluent (Pencarreg manure) has a high concentration of  $\sim 85 \text{ mg l}^{-1} \text{ HPO}_4$ . The other two locations LUSK and LTRI where acid digestion was also done are groundwater analysis boreholes and are shown for completeness (Figure 6-4). It is noted that the concentration at these two locations are almost double that of the MANU location. At LUSK and LTRI there was no cultivation of the land during the project; sheep were kept on the land at LUSK and cattle at LTRI. At LTRI fertiliser amendments had not been made for numerous years (Pers. comm., Landowner). This lack of fertiliser application is slightly perplexing as LTRI had the highest groundwater concentration of SRP, whereas none was recorded in the LUSK borehole, despite it having the largest reported nitrate concentrations; see steel bolt experiment in Chapter 5.

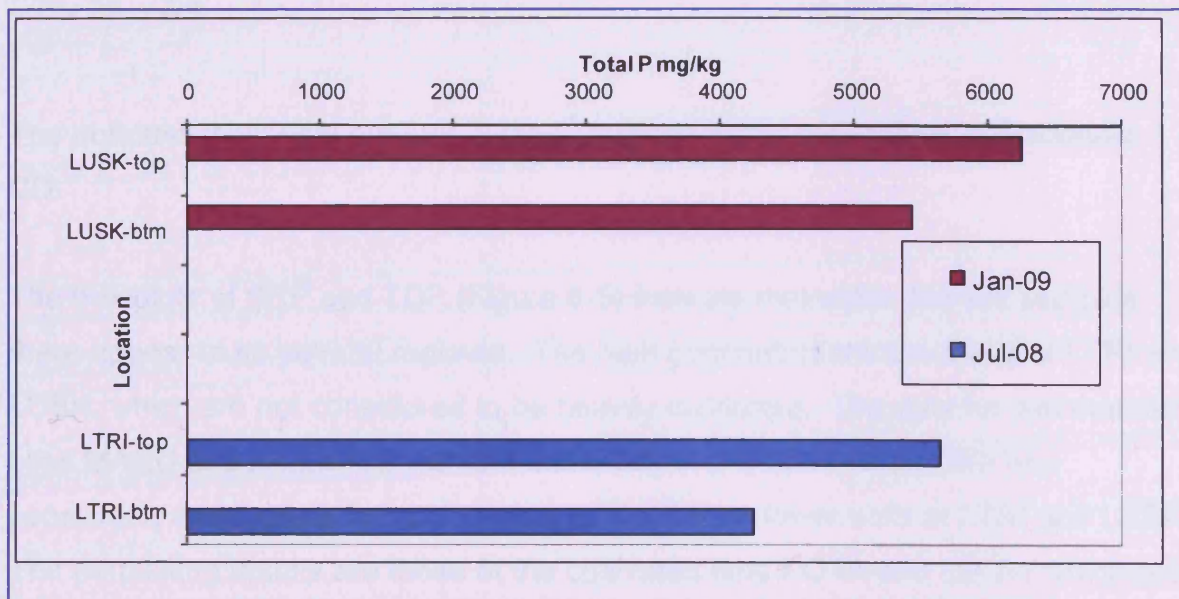


Figure 6-4 Acid leaching results at LUSK and LTRI.

### 6.2.2 Dried soil results

In total 92 analyses of eight different locations were made in order to investigate the soil phosphorus content and desorption potential. At three of the locations temporal data was obtained, at the remaining locations the results are single readings of that particular time. At each location samples were taken from the surface and at a shallow depth. The results are for dried soil powders <0.63µm, and do not include larger soil particles that have a lower reaction (leachable) surface volume.

The results are initially presented as box plots to show the range in analysis values, with concentrations reported as mg/kg soil. These values were obtained by conversion of the concentration results in mg l<sup>-1</sup>; the results can then be converted to a leachable concentration using the soil water factor (Eqn 6-1).

$$\frac{mg}{kg} = \frac{mg}{l} \times \frac{l}{g_{soil\ sample}}$$

Eqn 6-1

$$\frac{mg}{kg} \times \frac{kg}{l} = \frac{mg}{l}$$

The potential leachable amount in mg l<sup>-1</sup> is given in the data tables at Enclosure 1 CD.

The box plots of SRP and TDP (Figure 6-5) indicate that within the soil samples there appear to be several regimes. The high concentrations are those of LTRI and LUSK, which are not considered to be heavily cultivated. The data for two manure piles MANU and HILLMAN, with the exception of the SRP values, are also consistent, and there is indication of overlap with the lower soils at LTRI and LUSK. The perplexing results are those of the cultivated field POTA and LDOW which are known to have fertiliser amendments, and have soil phosphorus values less than LTRI and LUSK which were used for stock rearing, as was HILLCTRL a control sample for HILLMAN. These phosphorus observations are also reflected in the IC (HPO<sub>4</sub><sup>-</sup>) data (Figure 6-7).

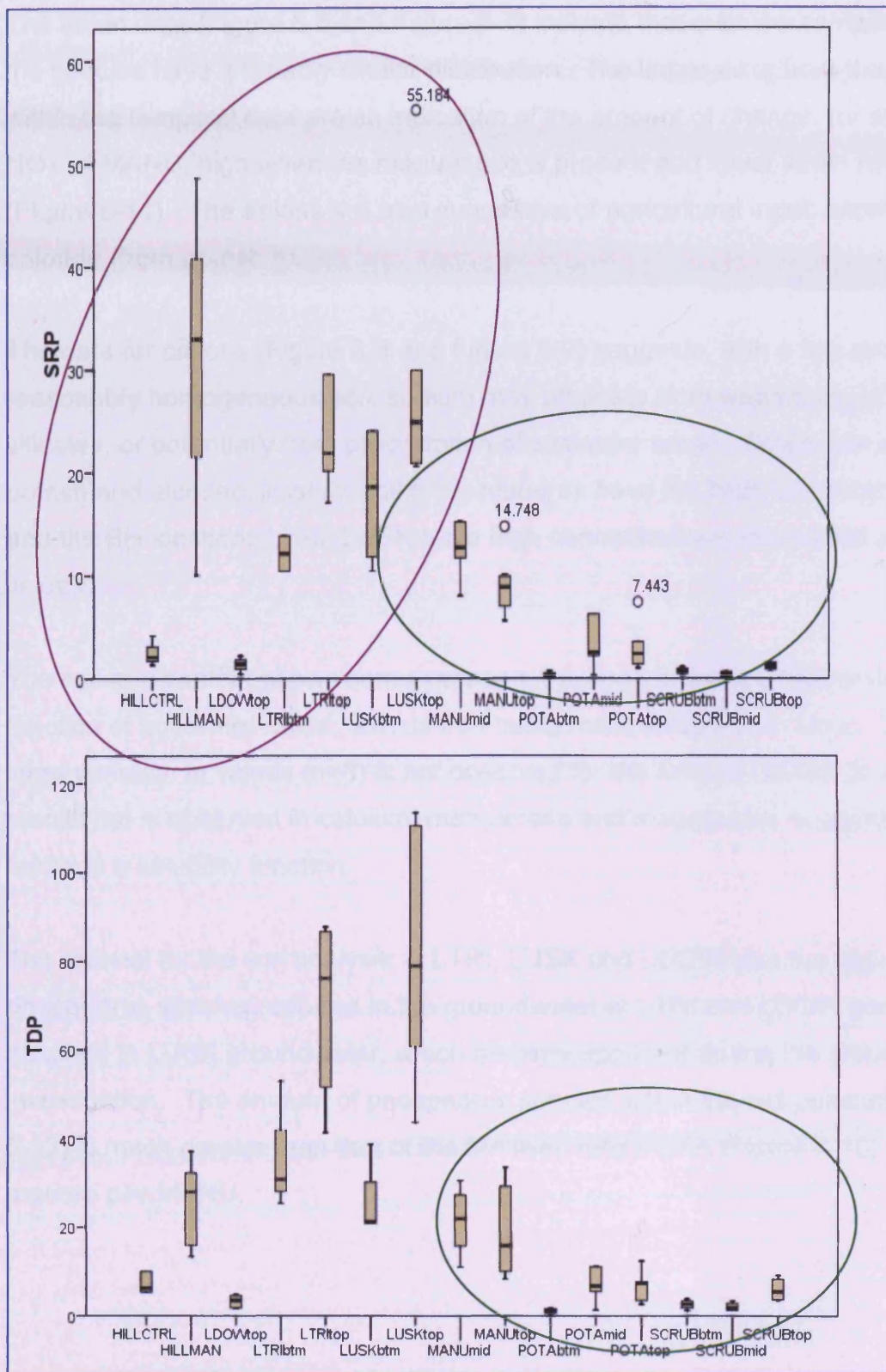


Figure 6-5 Box plots for SRP and TDP (mg/kg) for all locations and epochs. Note change in vertical scale between images. All values corrected for l/g factor. Single epoch data purple ellipse, temporal data green ellipse. Circle represents 'outlier data' beyond 1.5 box lengths.

The anion data (Figure 6-6 and Figure 6-7) indicate that over the sample locations the species have a broadly similar distribution. The larger error bars that occur within the temporal data are an indication of the amount of change; for example  $\text{NO}_3^-$  at MANU, high when the manure pile is present and lower when removed (Figure 6-11). The anions are also suggestive of agricultural input: nitrate and chloride (from potash KCl).

The data for cations (Figure 6-8 and Figure 6-9) suggests, with a few exceptions, a reasonably homogeneous soil; sodium may originate from weathering of sodic silicates, or potentially from precipitation of seawater spray. Potassium sources are potash and aluminosilicates; again the manures have the highest concentrations and the BH locations LTRI, LUSK have high concentrations interpreted as legacy values.

The soil iron content shows some variation; the large box at LUSK-top may be a function of soil water ratios; ferrous iron being more soluble than ferric. The very large variation in values ( $n=6$ ) is not observed for the sodium, silicon or aluminium results but is observed in calcium, manganese and magnesium, suggesting perhaps a solubility function.

The rationale for the soil analysis at LTRI, LUSK and LDOW was the high levels of phosphorus species reported in the groundwater at LTRI and LDOW and the near absence in LUSK groundwater, which became apparent during the groundwater investigation. The amount of phosphorus species within the soil columns (Figure 6-12) is much greater than that of the fertilised field POTA (Figure 6-10) and for the manure pile MANU.

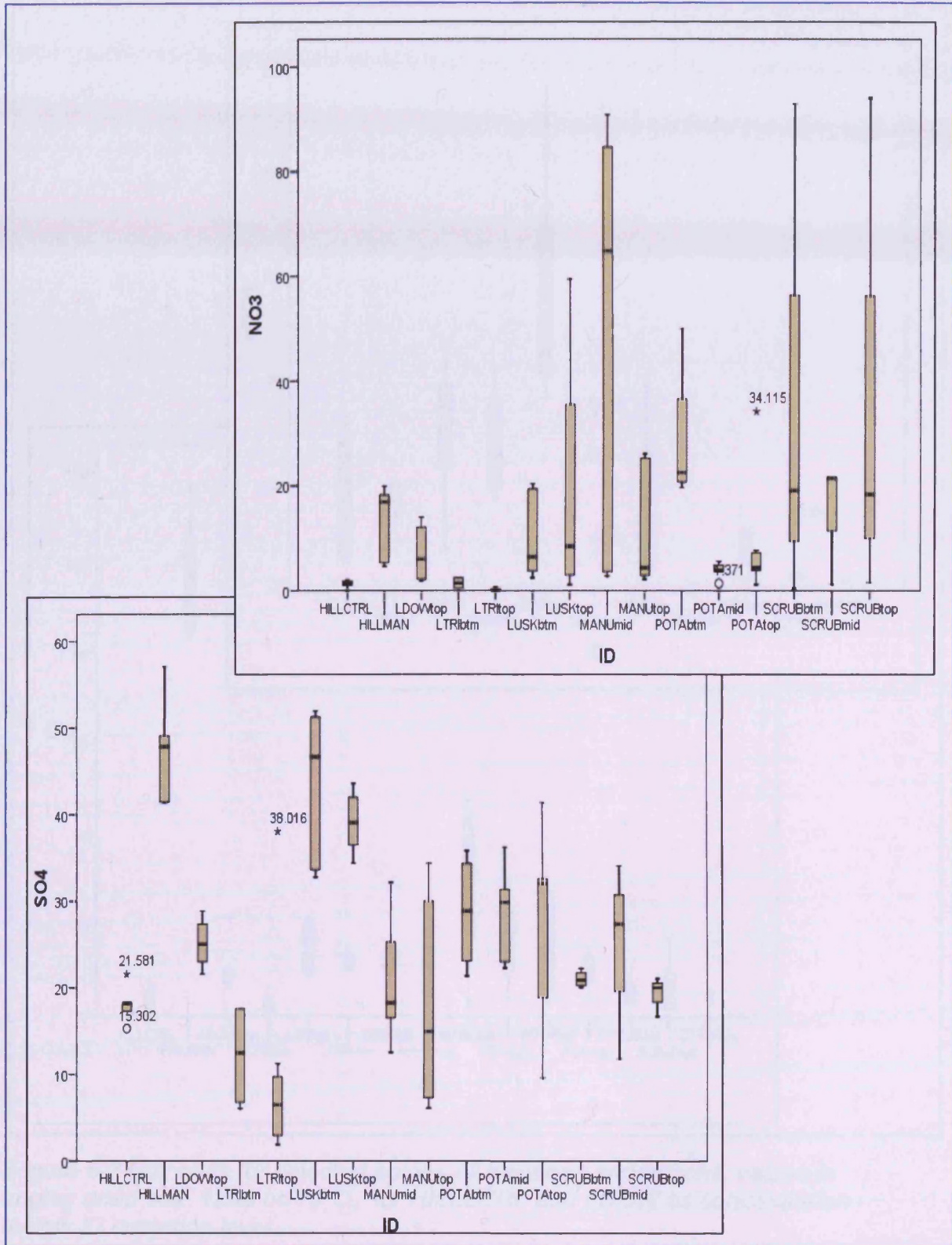


Figure 6-6 Box plots for selected anions all locations and epochs, values in mg/kg dried soil.

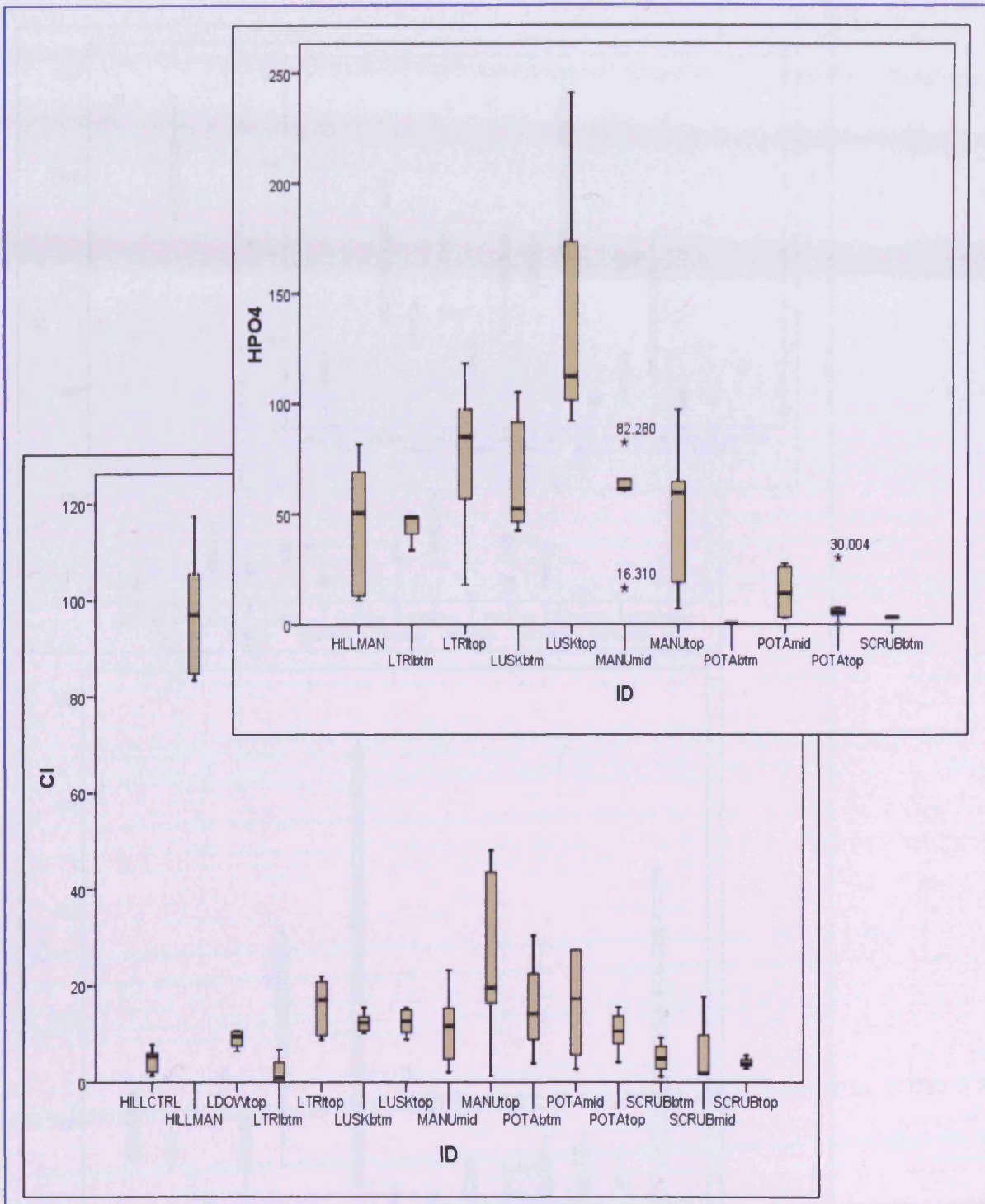


Figure 6-7 Box plots for selected anions all locations and epochs, values in mg/kg dried soil. Note no  $\text{HPO}_4^-$  for HILLCTRL and LDOW as concentration below IC detection level.

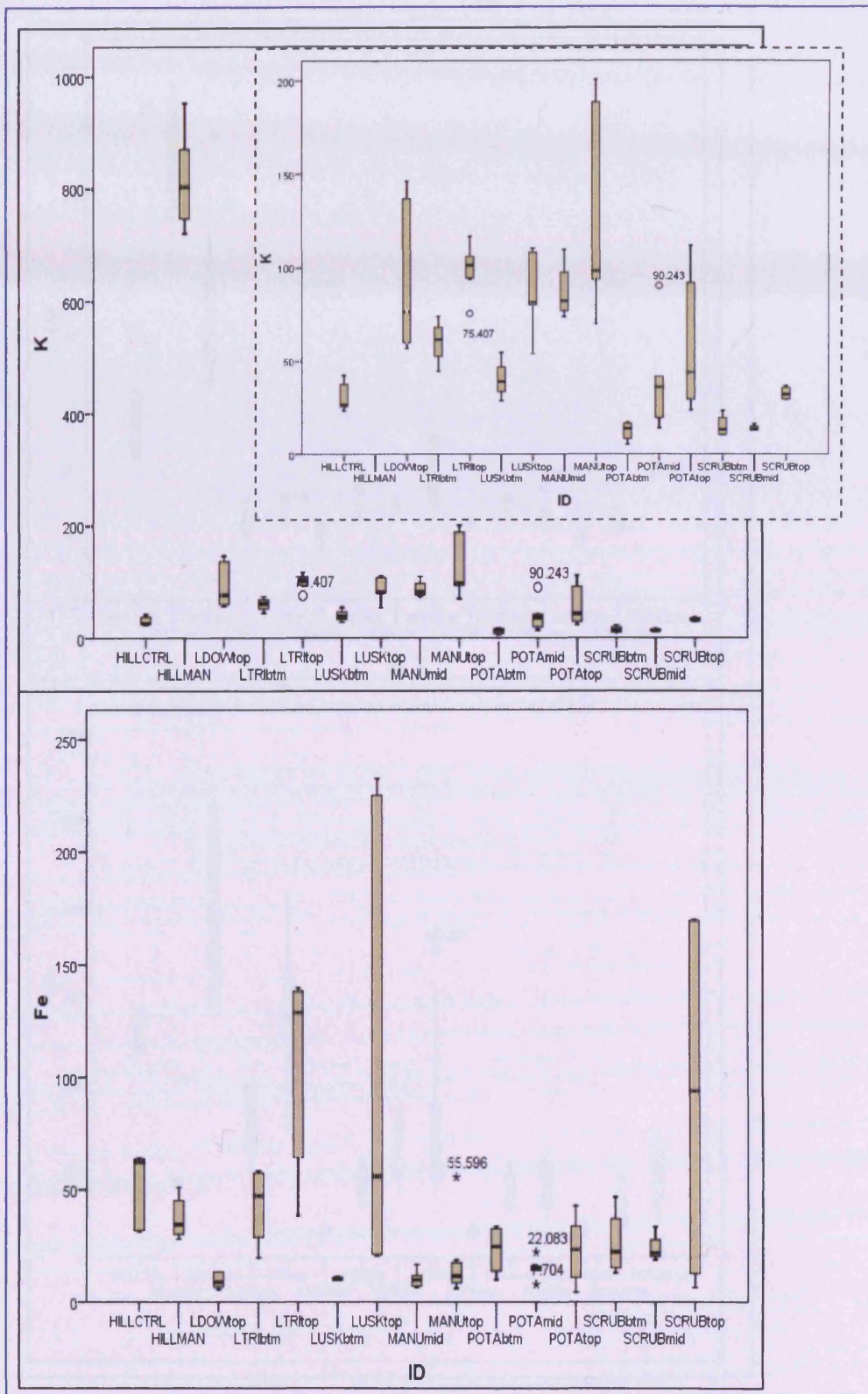


Figure 6-8 Box plots for selected cations: Fe and K all locations and epochs (mg/kg). Note inset for K with HILLMANU removed.

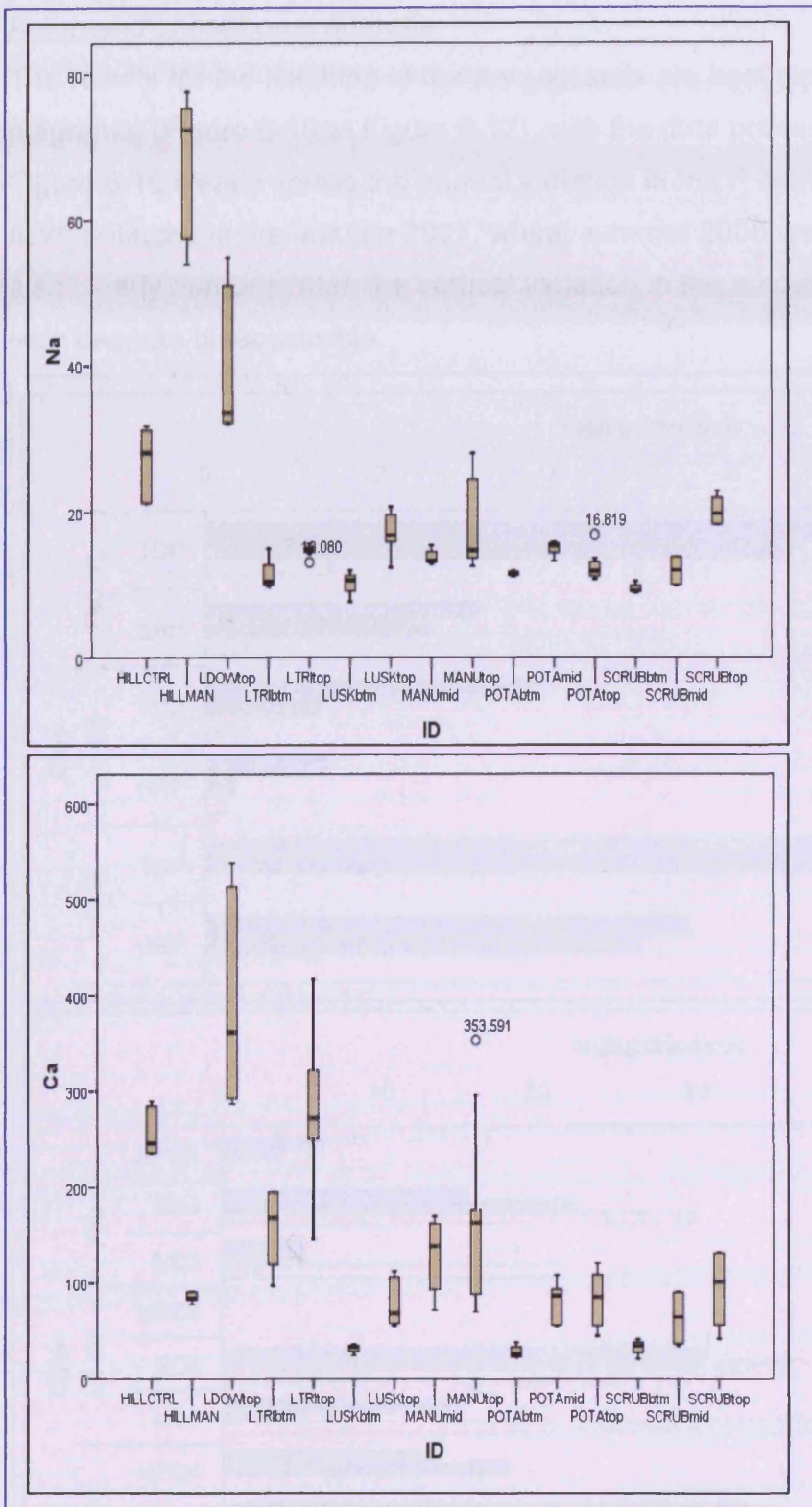


Figure 6-9 Box plots for selected cations: Ca and Na all locations and epochs (mg/kg).

Anion and phosphorus analysis

The results for the leaching of the dry Usk soils are best represented by bar diagrams, (Figure 6-10 to Figure 6-12), with the data presented as averages.

Figure 6-10 clearly shows the annual variation in the P composition for a cultivated field; potatoes in the autumn 2007, wheat summer 2008 and corn summer 2009. It also clearly demonstrates the vertical variation in the amount of phosphorus that may become bioaccessible.

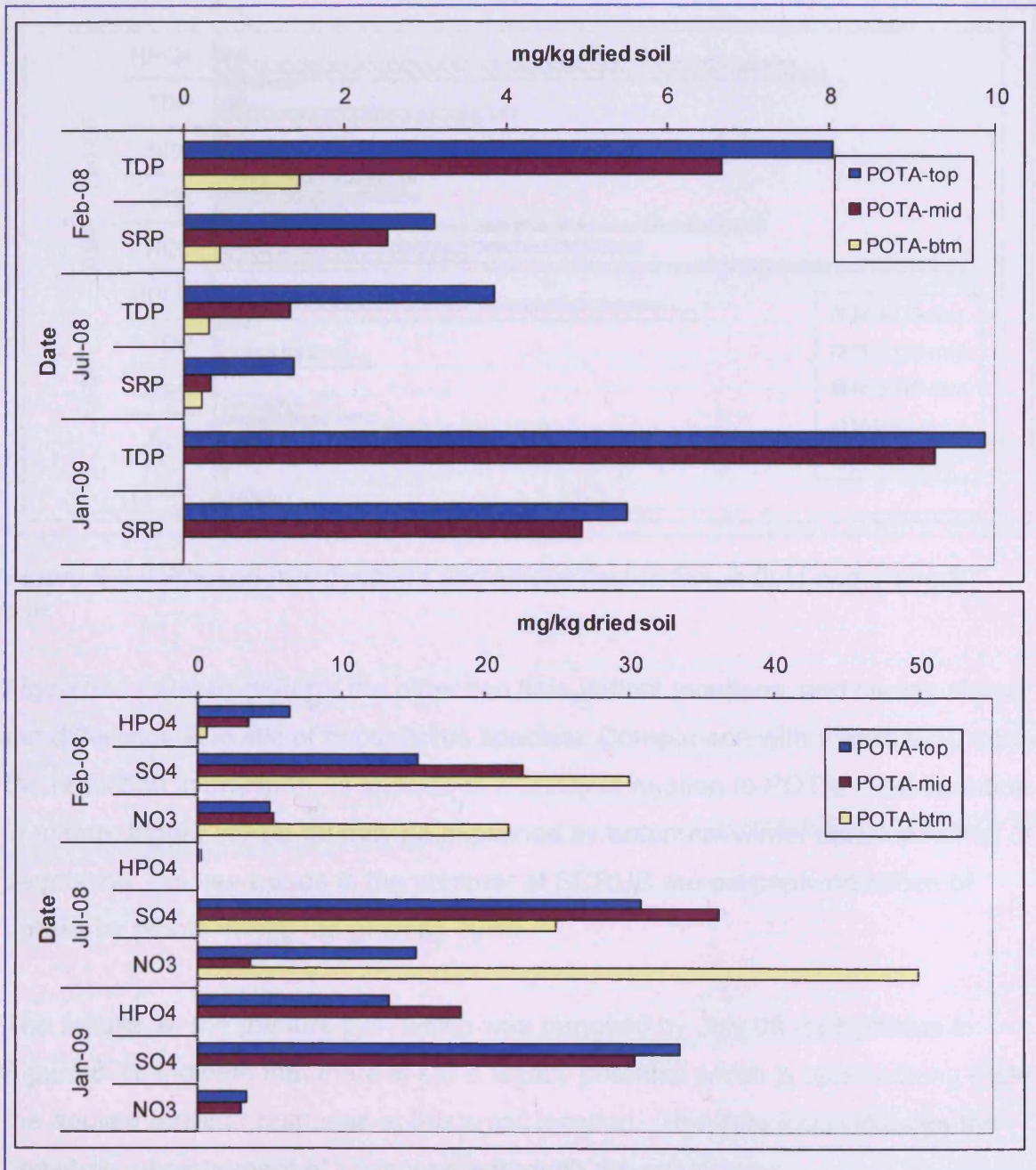


Figure 6-10 Phosphorus fraction for potato field location and selected anions. IC derived HPO<sub>4</sub> shown for completeness.

Figure 6-10 also indicates the movement of nitrate and sulphate through the soil column at this location. The marginally higher values indicated in Jan-09 is believed to be due to a recent application of fertilisers; manure detritus was evident at time of sample collection.

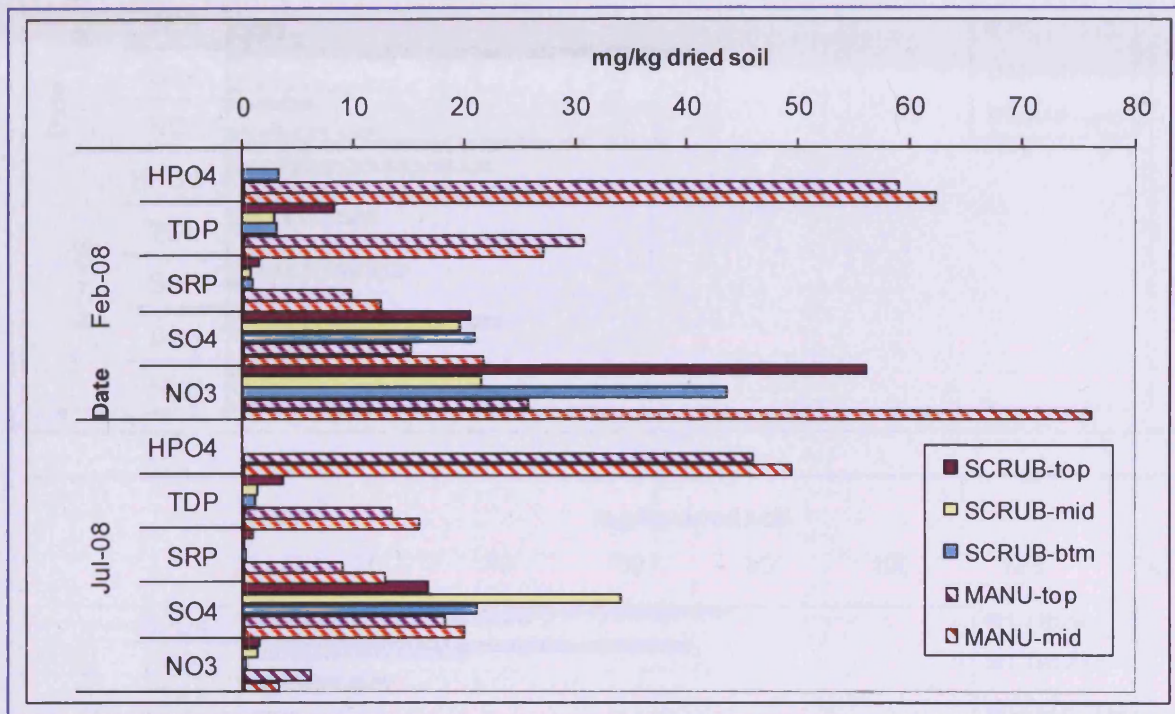


Figure 6-11 Phosphorus fractions and anions for the Scrub field and manure pile.

Figure 6-11 shows data for the other two time variant locations, and clearly shows the difference in levels of phosphorus species. Comparison with Figure 6-10 shows the reduction in phosphorus species at SCRUB in relation to POTA. The variation in nitrate; higher in Feb-08 may be explained by autumnal/winter decomposition of vegetation, the low values in the summer at SCRUB are perhaps indication of uptake by plants during the growing cycle.

The results for the manure pile, which was removed by July 08 (see photos in Figure 6-3), indicate that there is still a legacy potential which is approaching triple the applied fertiliser response at this small location. The data also indicates the possibility of movement of phosphorus through the soil column.

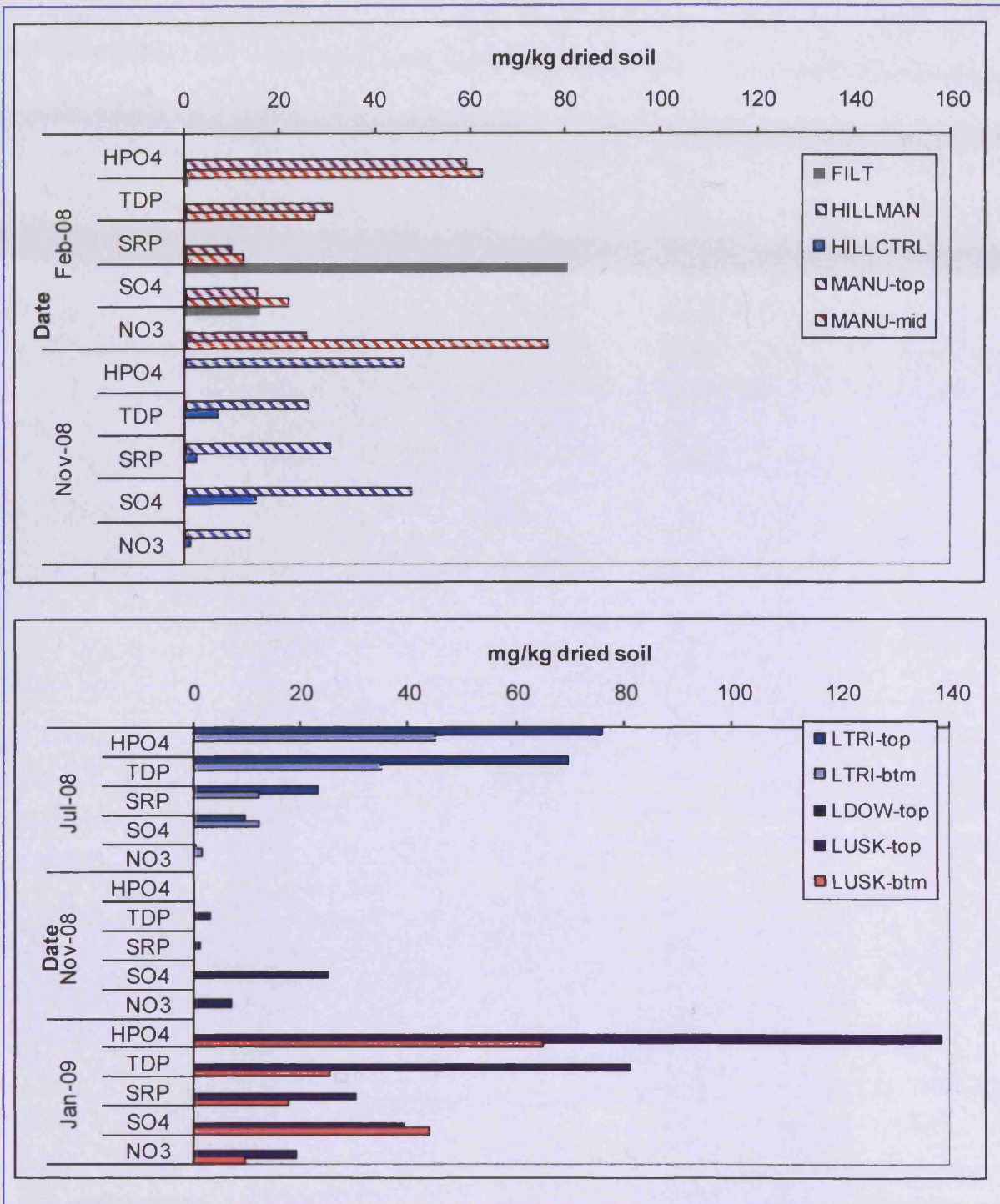


Figure 6-12 Phosphorus fractions and anions for BH locations. MANU included for comparison with manure pile at HILLMAN. Note FILT is a residue from a local water treatment works used as a soil amendment.

### Cation and phosphorus analysis

To complement the anion analysis, selected cations were also considered (Figure 6-13 to Figure 6-15). Iron (total) was chosen for its potential to form under the correct conditions non-apatite phosphorus compounds, and potassium for its inclusion with mineral fertilisers. Potassium salts are generally soluble and have strong sorption potential in clay soils and will move slowly through those soils. Sodium was also considered as it can be considered fairly mobile in soils and waters; its monovalent state ( $\text{Na}^+$ ) means that it will sorb with clay minerals but is likely to be displaced by divalent ions. The concentration of potassium in waters is normally much lower than that of sodium (van der Perk 2006).

Figure 6-13 shows that the amount of potassium varies over the analysis in a similar fashion to TDP and SRP (Figure 6-10 and Figure 6-11), and is indicative of a fertiliser regime. The concentrations of iron and sodium remain fairly constant over the same period, and as such may be considered to have an indigenous origin. The large iron value for SCRUB-top (Jul-08) may be anomalous given the similarities between values for the lower locations. For the manure pile the variation of potassium serves as a good indication that its presence may be indicative of fertiliser application; the slight increase in Jul 08 for MANU-mid perhaps indication of downward migration, given the previous values in Feb-08 when the pile was present.

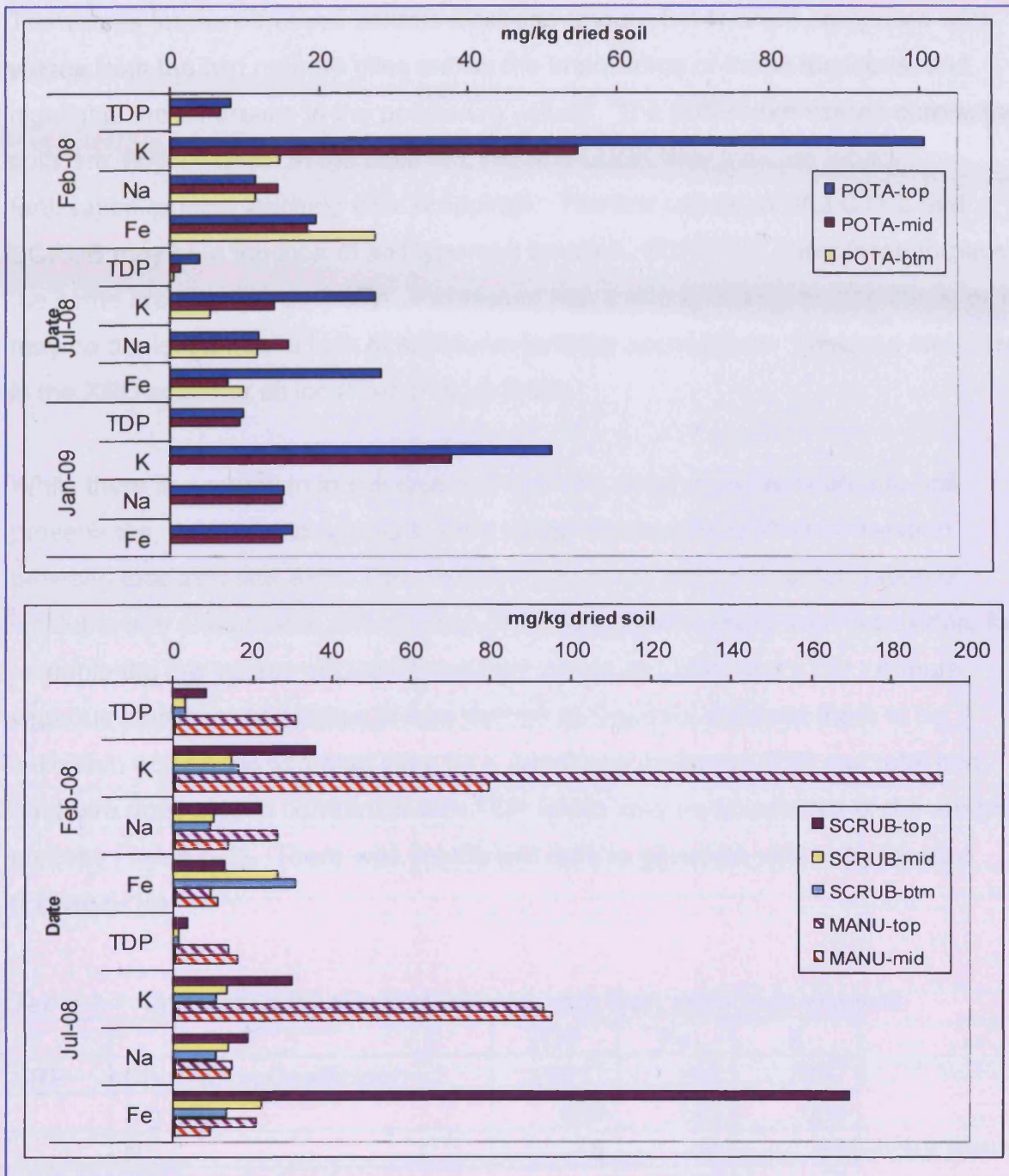


Figure 6-13 Cation analysis for POTA, SCRUB and MANU, TDP data included as comparison for species concentrations.

The values for the other soil sample locations (Figure 6-14) when compared with values from the two manure piles shows the importance of these locations, and highlights the difference in the potassium values. The potassium values across the soils are similar, which in the case of LTRI and LUSK may indicate legacy fertilisation or local leaching from droppings. The low values at HILLCTRL and SCRUB may be a function of soil type and sorption; SCRUB is considered to have the same provenance as POTA. Potassium has a strong affinity to illitic clays, or it may be depletion due to lack of additional fertilizer applications. Illite was identified in the XRD scans at all locations (Figure 6-28).

While there is a variation in soil total iron content, which may be related to soil provenance, there would appear to be a visual but counterintuitive correlation between total iron and SRP. This could be due to the potential for formation of insoluble iron phosphates and sorption of soluble phosphate to iron hydroxides, for example the low values at LDOW and high values at LUSK and LTRI. A more vigorous statistical correlation shows that for all the data obtained there is no indication across the sampled sites for a correlation between SRP and total iron, but there does exist a correlation with TDP which may be an artefact of the analysis process (Table 6-1). There was insufficient data to generate values by location (Figure 6-15).

*Table 6-1 Correlation for selected species, data from dried soils analysis.*

		TDP	Fe	K
SRP	Correlation Coefficient	.961**	.198	.729**
	Sig.	.000	.133	.000
	N	59	59	59
TDP	Correlation Coefficient		.308**	.696**
	Sig.		.003	.000
	N		90	90
Fe	Correlation Coefficient			.012
	Sig.			.911
	N			90

\*\*Correlation is significant at the 0.01 level (2-tailed).

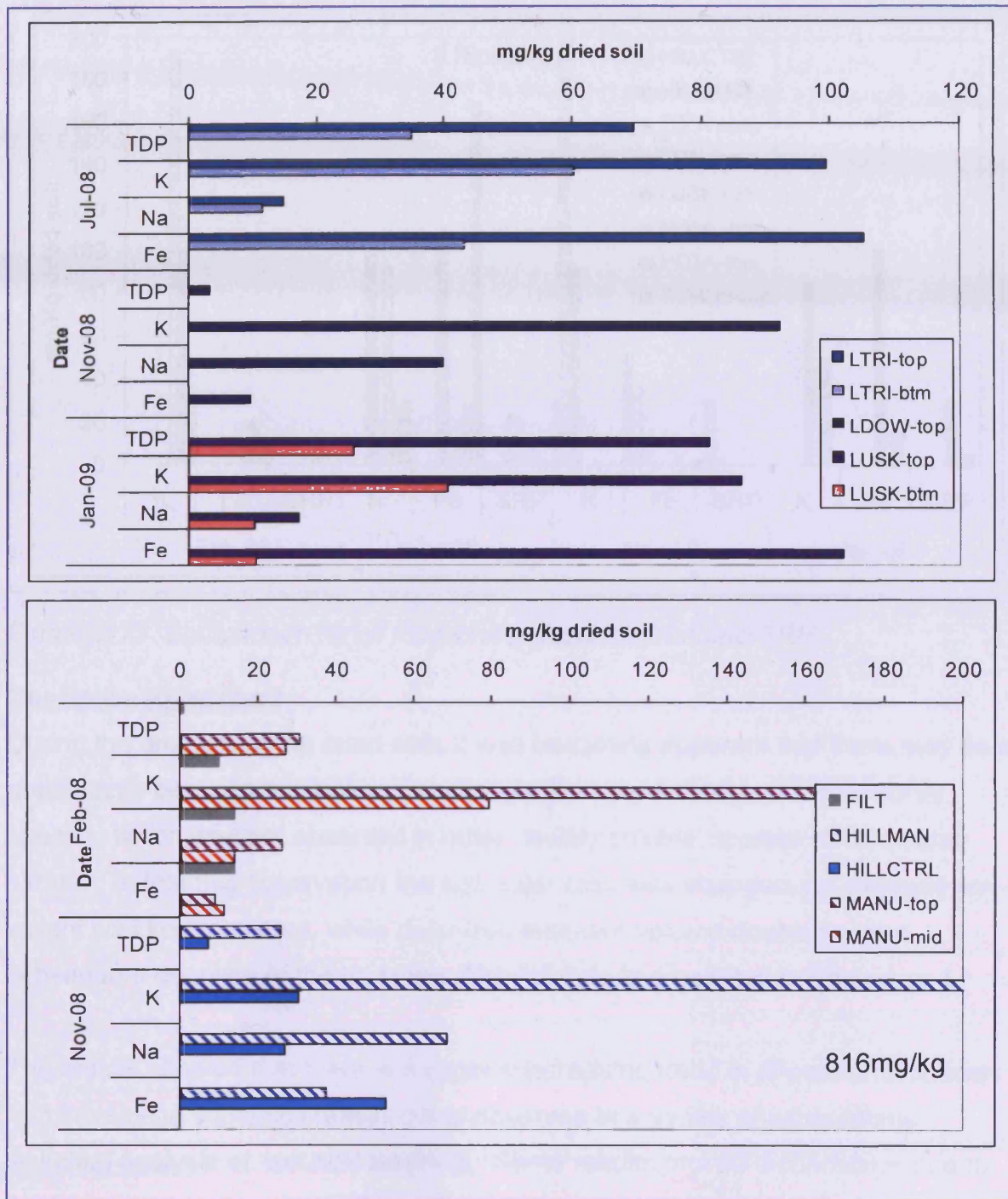


Figure 6-14 Cation analysis for remaining soil sample locations, MANU included for comparison with HILLMAN.

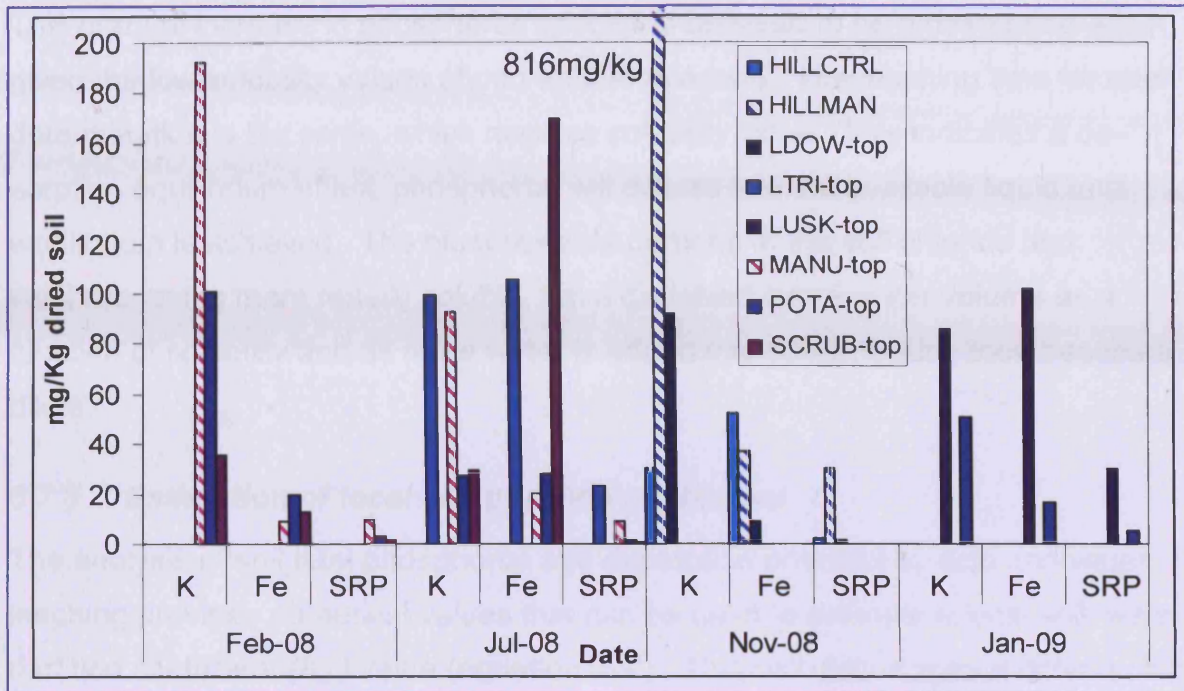


Figure 6-15 Comparison for all locations potassium, iron and SRP.

#### Desorption experiment

During the analysis of the dried soils it was becoming apparent that there may be a relationship between the soil water ratio and the concentration of phosphorus species, which was not observed in other 'readily soluble' species chloride and nitrate. To test this observation the soil water ratio was changed, for example soil weight was kept constant, while deionised leachant volume doubled with a subsequent doubling of the l/g factor. The full data is presented in Enclosure 1.

The results showed that there is a general increasing trend in phosphorus species with increasing liquid/soil ratios; this is observed in a variety of experiments including analysis of 'wet soil' leaching. Some results proved inconclusive due to the low concentrations encountered and an inability to resolve these because of procedural precision. This is evident in the relationship between TDP and SRP in the data where SRP is slightly greater than the TDP value (Enclosure 1).

This suggests analysis imprecision but more importantly it indicates that in the cases presented the SRP fraction is believed to be equal to or just less than the TDP; thus suggesting an upper limit of phosphorus bioaccessibility.

This gradual increase in phosphorus species is believed to be a desorption effect given the low solubility values of non-apatite minerals. The leaching time for each determination is the same, which negates solubility rates. This indicates a desorption equilibrium effect, phosphorus will desorb into the available liquid until equilibrium is achieved. The bioaccessible portions of the soil chloride and sulphate, being more readily soluble, have dissolved into a water volume as a function of solubility and as more water is added this concentration then becomes dilute.

### 6.2.3 *Estimation of local soil partition coefficient*

The analysis of soil total phosphorus and desorption potential by acid and water leaching provides numerical values that can be used to estimate a local soil/ water partition coefficient ( $K_d$ ) value (equation 6-2). This calculation uses a differencing methodology, subtraction of the desorbed concentration of TDP or SRP from the initial soil phosphorus concentration (TP) results in a value of phosphorus still attached to the soil (Table 6-2). The results use the full range of analysis and include potential uncertainty indicated in the desorption experiment. The values serve to indicate an upper or working limit, as the analysis process used powdered (0.63 $\mu$ m) soil which may include particulate phosphate that would otherwise be excluded in natural environments. The retardation factor is calculated in this instance with porosity at 25%, a reduction will increase the factor value (Eqn 6-2).

$$R = 1 + \frac{\rho_b K_d}{n}$$

and Eqn 6-2

$$K_d = \frac{\text{Mass of adsorbate (species) sorbed}}{\text{Mass of species in solution}}$$

**Table 6-2 Mean values of soil phosphorus fractions and calculated  $K_d$  and retardation factors for Usk Valley Soils**

Location	TP mg/kg	TDP mg/kg	SRP mg/kg	$K_d$ TDP	$K_d$ SRP	R for SRP	TDP-SRP mg/kg	Ratio TDP/SRP
LTRI-btm	4252	17.5	4.1	242	1041	4166	13.403	4.3
LTRI-top	5641	34.9	10.0	161	562	2247	24.830	3.5
LUSK-btm	5427	12.8	9.0	424	603	2411	3.767	1.4
LUSK-top	6260	40.5	13.8	154	452	1809	26.685	2.9
MANU-mid	2780	10.7	5.4	258	512	2049	5.305	2.0
MANU-top	2610	9.6	4.0	272	657	2630	5.601	2.4
POTA-btm	329	0.6	0.2	571	1615	6458	0.372	2.8
POTA-mid	1513	3.5	1.6	426	927	3707	1.916	2.2
POTA-top	1732	3.3	1.2	524	1398	5593	2.061	2.7
SCRUB-btm	1308	1.3	0.3	1025	3962	15849	0.945	3.9
SCRUB-mid	561	1.0	0.2	536	3442	13767	0.882	6.4
SCRUB-top	945	3.0	0.4	317	2102	8409	2.523	6.6
HILLCTRL		3.6	0.9				2.7	4.2
HILLMAN		12.9	10.2				2.7	1.3
LDOW-top		1.6	0.5				1.2	3.4
FILT		0.3	0.01				0.3	35.1

Note: FILT is the residue from a local water treatment works applied by the local farmer as a soil amendment.

The value for the calculated  $K_d$  indicates the high local sorption ability of the phosphorus fractions, and is presented as a non-dimensional value as both solute and sorbent are reported in mg/kg and obtained from the same soil sample. The initial concentrations calculated in  $\text{mg l}^{-1}$  being normalised by the soil sample and leachant volume factor. Bulk density and porosity factors are differenced for both. Conversion of the non-dimensional  $K_d$  value to  $\text{l kg}^{-1}$  is achieved by dividing by  $1/\text{density}$ .

Using Equation 6–2 and previously calculated bulk densities and soil moisture contents obtained when drying soil samples, it is possible to estimate a potential retardation factor (R) for TDP and SRP in the local groundwater of the Usk valley. Bulk densities were calculated between 1.5 to 2.0 g cm<sup>-3</sup> (average 1.7 g cm<sup>-3</sup>), an upper and lower soil moisture content of 35% and 11% was obtained depending upon the time of soil collection. An average of 25% was deemed representative although low when compared to literature values. The value for  $K_d$  has already been corrected for by the normalising  $l/g$  factor. The derived retardation factor for the local SRP is in Table 6-2.

The retardation factors appear large, however (Robertson et al. 1998) indicate factors up to 100 with migration at  $\sim 1\text{m year}^{-1}$ , in sandy calcareous soils due to the affinity of phosphates to metal hydroxides with a positive surface charge at normal pH ranges. Given the large amount of iron oxides (red soils) believed to be in the predominantly clayey soils the project values may be justified.

The results are also believed to be sensitive to equilibrium processes and recent fertiliser application. A recent application will have the effect of increasing total soil phosphorus, some of which may not be (at the time of sampling) readily available as SRP, thus altering their local ratio and  $K_d$  value. If the soil phosphorus carrying capacity is not achieved then the ratio between the fractions will also not be in equilibrium.

The values are laboratory derived from prepared powders and scale issues are considered relevant for modelling and deriving values in a more natural environment. The experiments assume equilibrium between adsorption and desorption. The desorption process may in fact be slower (hysteresis) and thus numerical values are low, increasing the size of the calculated local  $K_d$  value (EPA 1999).

### Remedial targets worksheet (Hydrogeological Risk Assessment P20)

The Environment Agency commissioned a report and simple spreadsheet (P20) in order to calculate remedial targets for contaminated land based upon a receptor or compliance point. The procedure works on a series of tiers or levels. The basic is level 1 which considers whether concentrations in the pore water of soils will impact the receptor (ignoring dilution, dispersion and attenuation). More advanced levels deal directly with groundwater: groundwater below the source term, or at a compliance point (Carey et al. 2006a). The calculations require site specific parameters including a soil/ water partition coefficient ( $K_d$ ).

The P20 was used to investigate various conceptual scenarios, the most basic was a level 1 soil remediation target given a target concentration in the soil water of 0.153 mg SRP l<sup>-1</sup> the accepted EQS for groundwater. A graph with a range of  $K_d$  values was produced to reflect the observed ranges calculated for the different soils. The remedial target values should be compared to the observed values in the soil (Table 6-2) of which the TP are in excess of the remedial target value.

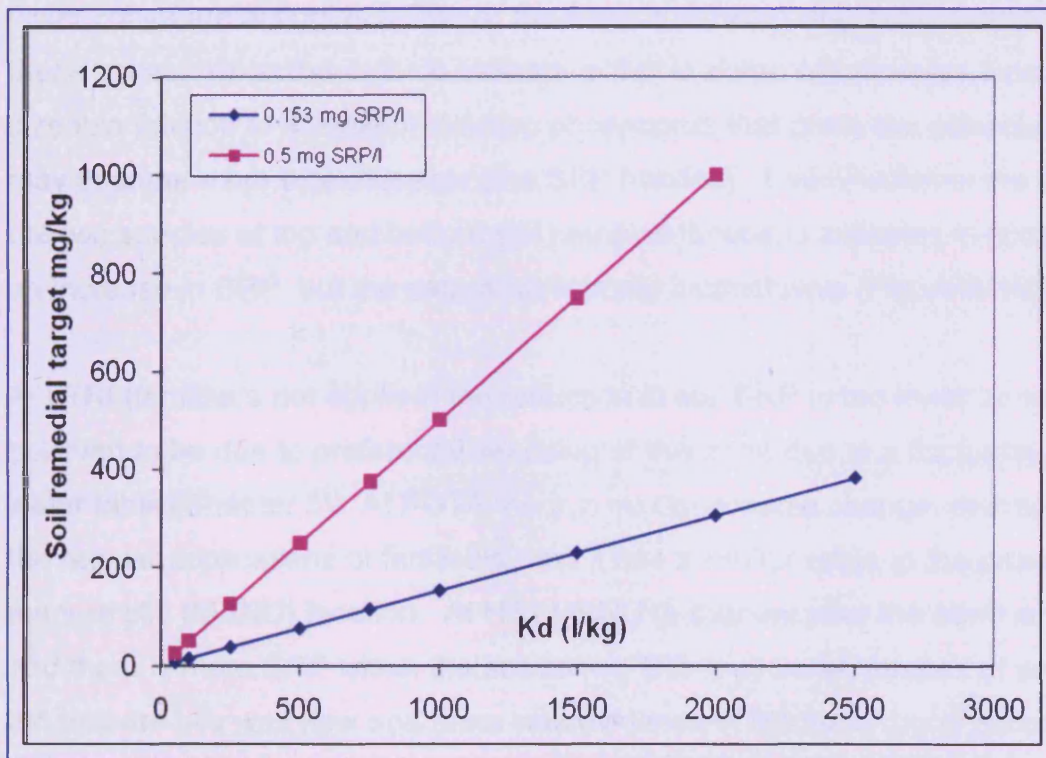


Figure 6-16 Soil remedial targets for comparison with analysed soil total phosphorus concentration (Table 6-2) Two soil water SRP concentration targets curves shown.

An additional level 3 soils investigation, with a 1 hectare conceptual (potato) field 1000m from a receptor (the River Usk) was undertaken. The values used were a representative 1500 mg TP kg<sup>-1</sup> and a lower limit  $K_d$  of 300 l kg<sup>-1</sup>. This calculation indicates a relative dilution factor of 0.7 and soil remedial target of ~140 mg kg<sup>-1</sup>. It is to be noted that the calculation assumes a first order decay rate which is effectively overcome by setting the half-life to an extremely large value 9.9<sup>99</sup>. The P20 calculations for groundwater are in Chapter 7.

#### 6.2.4 **Soluble unreactive phosphorus (SUP)**

This is the fraction that passes through the filtration stage of analysis and consists of unhydrolysed organic and inorganic polyphosphates, and which is not molybdate reactive. This is calculated by the differencing of the TDP and SRP (Table 6-2) and may contain some colloidal but unreactive adhered phosphorus.

The range of values (Figure 6-17 and Table 6-2) indicates that the largest differences are to be found in the uppermost soil zone. This may indicate that the lower zones are acting as a filter or the fraction is being degraded and sorbed in these zones. What the data do indicate is that in some soil samples there is a sizeable fraction of soluble unreactive phosphorus that given the correct conditions may become more bioaccessible (the SRP fraction). Examination of the ratios of the two species at top and bottom soil sampled locations indicates in some cases an increase in SRP, but the data is statistically inconclusive (Figure 6-18).

At LTRI (fertilisers not applied) the reduction in soil SRP in the lower zone is believed to be due to preferential leaching of this zone due to a fluctuating high water table (Chapter 5). At POTA there is no discernable change, perhaps due to the regular applications of fertilisers, and it has a similar value to the proximal manure pile (MANU) location. At HILLMANU (a manure pile) the trend is reversed and there is more SRP within the soil zone. This may be an artefact of sampling as the manure pile was new and there was evidence of leachate runoff puddles from the manure. It does however indicate the greater potential of the manure piles to act as localised hot spots.

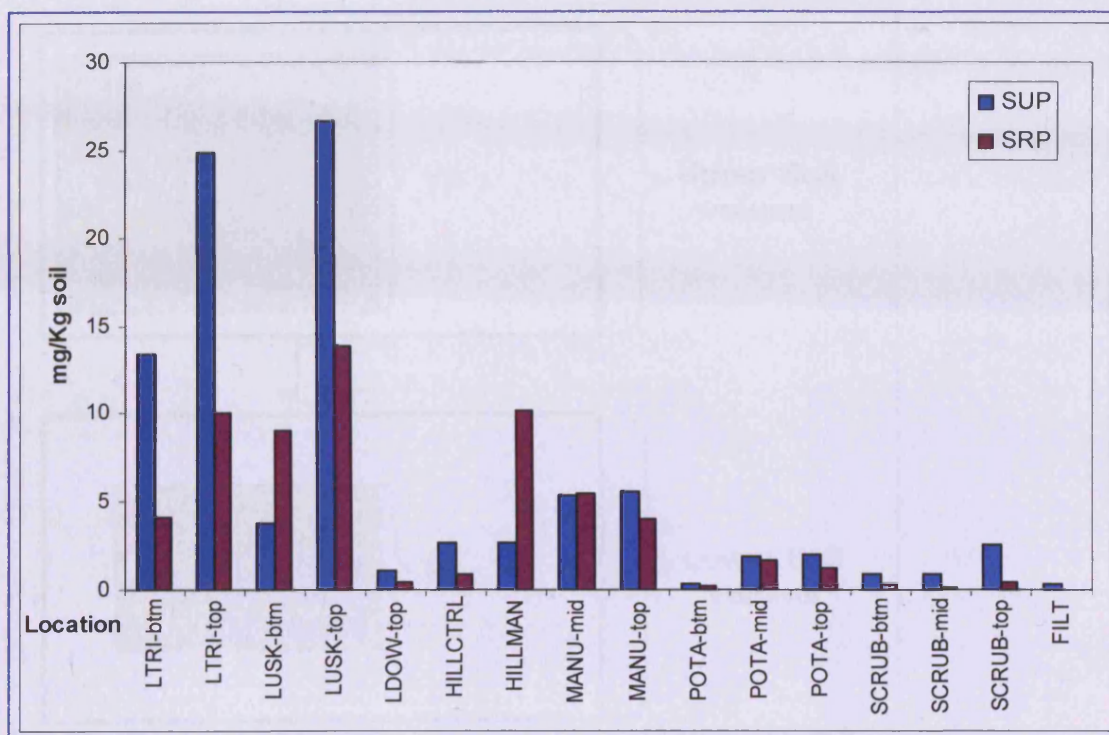


Figure 6-17 Comparison of SUP and SRP for Usk Valley Soils.

A comparison with data shown in Figure 5-54 shows that the relative abundances of SUP and SRP in the soil and groundwater compartments are reversed. This may be further evidence of chemical changes in the SUP fraction during its transit to the water table. This suggests that the individual fractions observed in the soil zone cannot be considered in isolation as the soil SUP may have the potential to provide an additional flux. Data obtained from a manure leachate at Pencarreg Farm indicates SRP at  $82\text{mg l}^{-1}$  with an associated SUP of  $67\text{mg l}^{-1}$

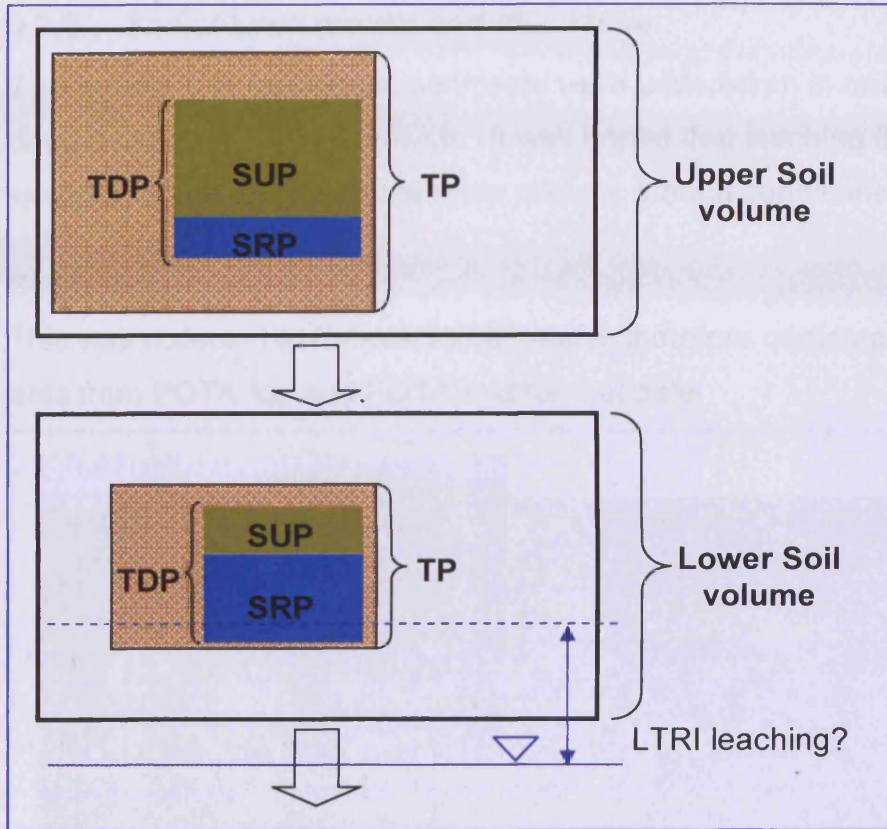


Figure 6-18 Possible movement of phosphorus fraction through the soil zone showing the conceptual relative sizes of the data in Table 6-2.

### 6.2.5 Soil column results and discussion

Two soil column leaching experiments were undertaken in order to augment the dried powders leachate analysis. It was hoped that leaching through a soil column would, in some part, replicate more realistic ground conditions.

#### Soil Column 1

This was collected in February 2008 and is therefore contemporaneous with the data from POTA-top and POTA-mid for that date.



Figure 6-19 Collection of soil column 2 Jan 09. Inset panoramic view of POTA location. Photo A Gray.

The first investigations involved water:soil contact time by re-passing the deionised water 'leachate' three times (experiments 1-3) through the column. The fourth pass (experiment 4) used fresh deionised water. The results show that for the readily leachable species, for example chloride and nitrate, the concentration increases with contact (leaching) duration, and that SRP concentration do not noticeably increase. The flush duration was approximately eight minutes for individual runs, with each experiment lasting around 25 minutes. The column was allowed to 'dry' between experiment 2 and 3 to mimic ground conditions.

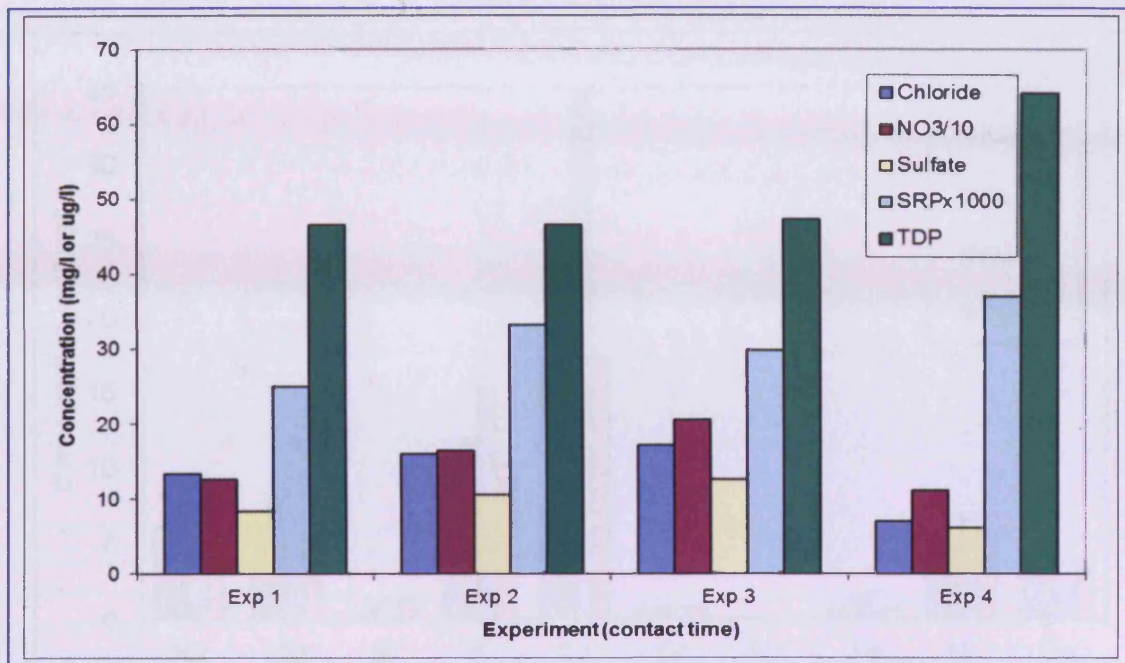


Figure 6-20 Anion data for soil column experiment. Note that to visualize the data, nitrate values have a scalar division of 10, whilst SRP multiplied by 1000. TDP values in  $\mu\text{g l}^{-1}$ .

The results clearly show that for the fresh deionised water (Exp 4) the anions have not been stripped from the column, and continue to dissolve into the leachate albeit in smaller concentrations. The increase in SRP and TDP in experiment 4 may be an indication of desorption equilibrium in experiments 2 and 3. The concentrations as  $\text{mg/kg}$  soil are given in Table 6-3 and should be compared to the long (24hr contact) dried soil leaching values.

Table 6-3 Results of Exp 1 as concentration equivalents. Note change in units for TDP.

	Chloride	Nitrate	Sulfate	SRP	TDP
Exp 1 $\text{mg kg}^{-1}$	2.220	21.003	1.379	0.004	7.9
$\mu\text{g kg}^{-1}$					
Exp 1 $\text{mg l}^{-1}$ ( $\mu\text{g l}^{-1}$ )	13.395	126.730	8.321	0.025	46.5

The major cation leaching results are presented in Figure 6-21 and show the pattern of increased concentration with contact (residence) time and continued dissolution with 'fresh leachant' in experiments four and five.

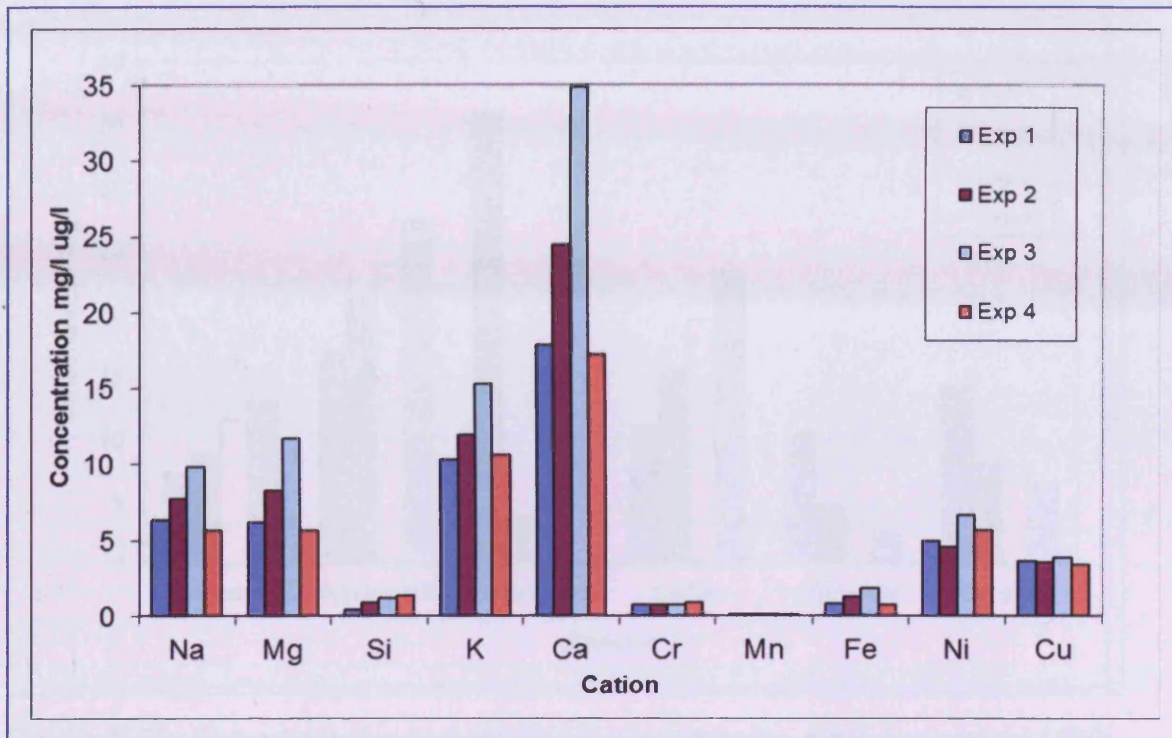


Figure 6-21 Cation data for soil column leaching experiment. Concentration in  $\text{mg l}^{-1}$  for all except chromium, nickel & copper  $\mu\text{g l}^{-1}$ . Note copper is found in pig manures from the pig's diet supplements.

The quantity of iron that is leached is quite small, perhaps an indication of its insolubility and presence as ferric iron. The pH of the leachant was 5.85 at the end of experiment four; and also an indication that calcium phosphate minerals are unlikely to form in the soil zone.

#### Spiked soil column 1 experiment

The soil column experimentation continued with the passing of a spiked  $1 \text{ mg P l}^{-1}$  solution through the column. This experiment was devised to investigate phosphorus sorption and also the continuing leaching of the column. A common ion effect was considered to be minimal, and cations and anions could still leach. The column was allowed to 'dry' between the experiments. The experiment consisted of passing the spike through the column twice and then removing a subsample for analysis. The experiment was done four times with the same concentration spike.

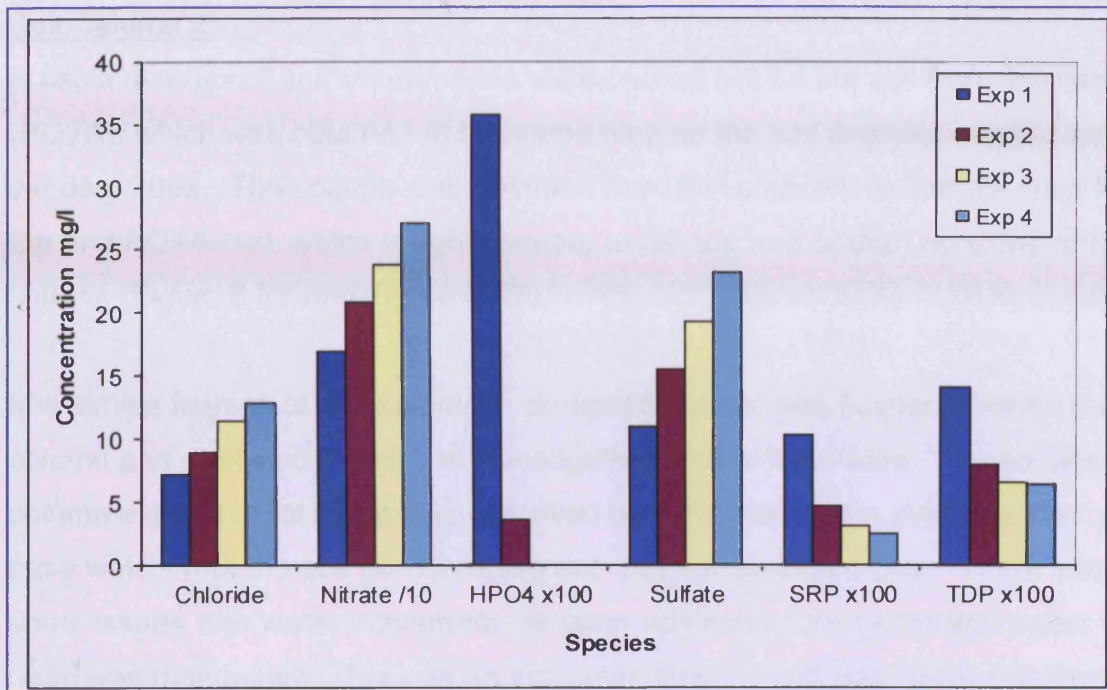


Figure 6-22 Spiked column results for all experiments. Note scalars on  $\text{HPO}_4$ ,  $\text{NO}_3^-$ , SRP and TDP to aid visualisation. Original stock values for  $\text{HPO}_4$  775.1, SRP 102.0 and TDP 94.0 at scalar values.

The results for the anions and TDP clearly show that chloride, nitrate and sulphate continue to leach from the soil column and that contact time is important. The most important result is that the phosphorus species values are all decreasing, which is interpreted as sorption within the column; precipitation would have to be rapid under these experimental conditions. These results should be compared to the initial leaching experiment where overall the amount of SRP and TDP leached did not increase significantly over the course of the experiments.

### Soil Column 2

A second series of soil column tests were carried out on the soil from the same site (POTA), which was obtained at the same time as the soil analysis sample for January 2009. The column was obtained from soil adjacent to sample sites POTA-top and POTA-mid, which roughly equate to the top and bottom horizons of the column (Figure 6-23 and Figure 6-27).

In a similar fashion to soil column 1, de-ionised water was flushed through the column and analysed in order to investigate potential leachates. The second column experimental setup was improved by the addition of a cellulose filter at the base which kept the soil from 'eroding out' into the porcelain filter. There were also some issues with water movement, as upon addition of the de-ionised water the head was maintained. This was an indication that the soil was 'sealed' to the tube edges preventing by-pass flow, and this is attributed to swelling clays. There is further evidence for these swelling clays in surface water and also desiccation cracks at the location (Figure 6-23).



*Figure 6-23 Ty-Coch Farm Potato Field (POTA), standing water and desiccation cracks, which is evidence for swelling clays. Photo A Gray.*

This second investigation passed the same volume of deionised water through the column during each experiment; this was done five times. It was deemed not necessary to re-pass the leachant through more than once as the retention times were longer than that of the first column experiment. The results are presented in Figure 6-24.

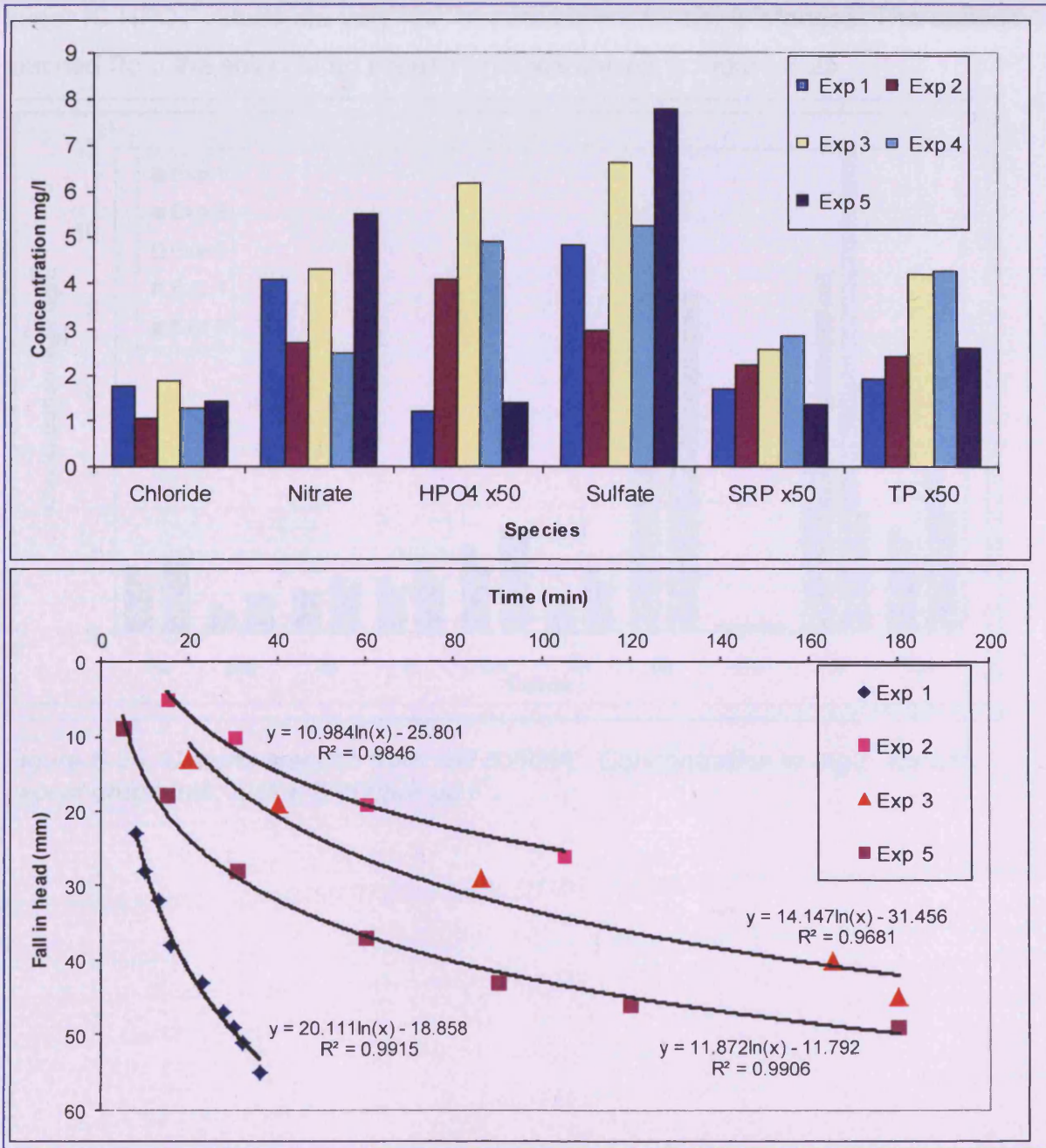


Figure 6-24 Anion leachate results for 2<sup>nd</sup> soil column experiment. Note scalar on phosphorus species to aid interpretation. Falling head data (lower graph) for leachate experiments to show differences in contact times. Exp 4 not shown to aid clarity as time values are large: 240 to 1380 minutes.

The data require considered interpretation as the leachant contact time is not the same in all experiments. It is also noted that the range in concentrations (same soil and leachant volume) are quite similar, which suggests that in this instance residence time is not a major factor in the leachate anion and phosphorus species quality. It is also seen that the SRP and TDP species are of similar magnitude. The larger IC  $\text{HPO}_4^-$  values are very low, but are shown for completeness. The cations leached from the soil column experiments are shown in Figure 6-25.

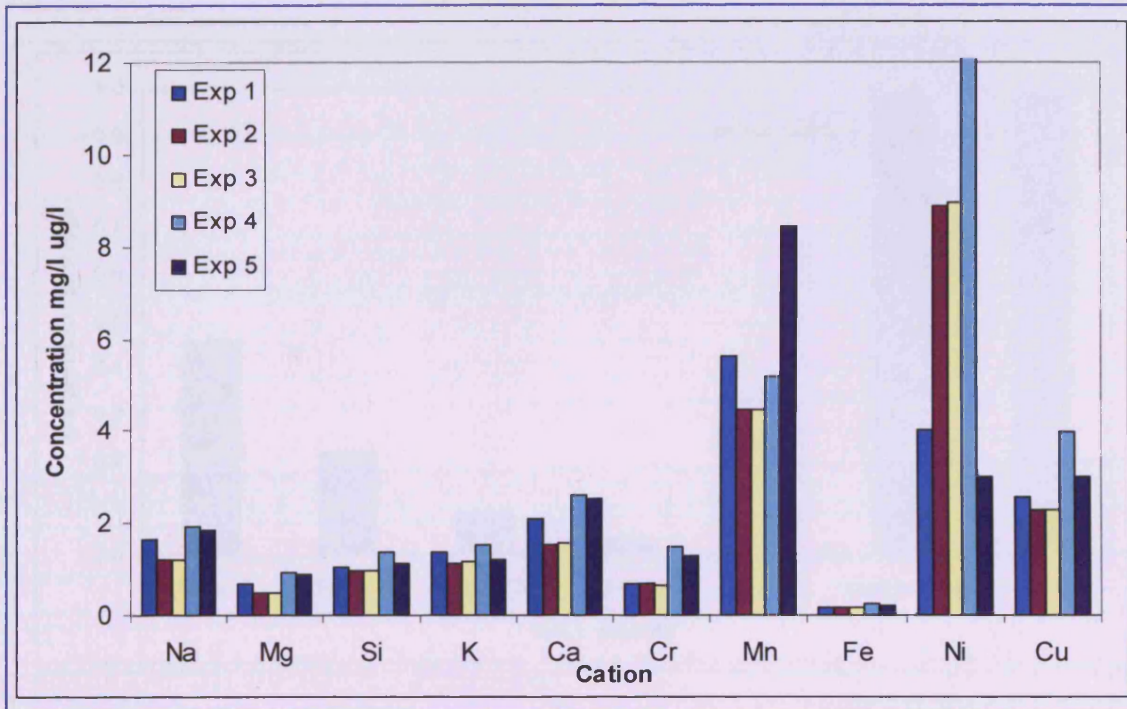


Figure 6-25 Cations leached from soil column. Concentration in  $\text{mg l}^{-1}$  for all except chromium, nickel & copper  $\mu\text{g l}^{-1}$ .

### Spiked soil column 2 experiment

A spiked sample of the same concentration,  $1 \text{ mg P l}^{-1}$  solution, was also passed through the second soil column as it has been shown in soil column one that phosphorus species do dissolve or desorb into the leachant and have the capacity to re-sorb (Figure 6-22)

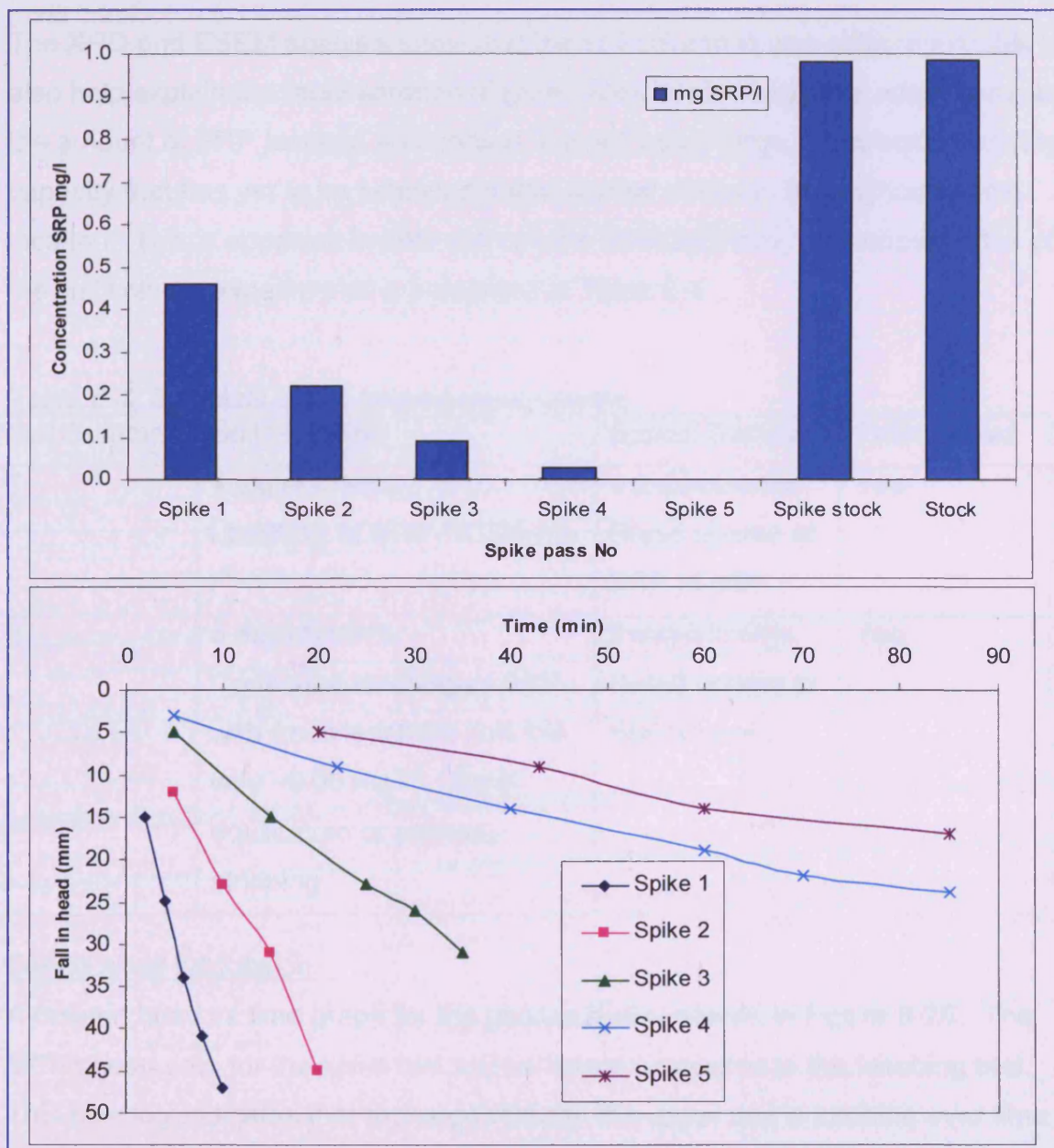


Figure 6-26 Results of spiked sample passed through soil column. Note standard stock solution and original spike shown for completeness. Lower graph is falling head measurements for indication of contact time.

The results of the spiked sample analysis are shown in Figure 6-26 and clearly demonstrate the removal of SRP from solution into the soil column. It is noted that the retention time of the spikes is again different between the passes. Robertson (1998) concludes that attenuation of phosphate is almost 'complete' in non-calcareous terrains under acid conditions, whereas only minor attenuation is achieved in calcareous settings.

The XRD and ESEM analysis show that the soil column is non-calcareous; this may also help explain the rapid sorption (Figure 6-26). It also suggests when comparing the amount of SRP leached and sorbed, the soil has a large phosphorus carrying capacity that has yet to be achieved under normal usage in this particular field location. This is apparent in both soil column investigations. A synopsis table of the soil column experiments is presented at Table 6-4.

*Table 6-4 Synopsis of soil column experiments.*

Soil Column	Soil Leaching	Spiked Sample	Falling head
1	4 experiments. Leaching of SRP $\sim 0.035 \text{ mg l}^{-1}$	4 experiments. Rapid uptake of SRP to soil	Yes
2	5 experiments. Continued leaching of SRP with fresh leachant until fall-way $\sim 0.05 \text{ mg l}^{-1}$ . Semi-equilibrium or pathway stripping	5 experiments. Rapid uptake of SRP to soil	Yes

#### Falling head calculation

A column head vs time graph for the passes is also shown in Figure 6-26. The falling head data for the spike test appear linear compared to the leaching test. This possibly indicates that recharge through the upper soil is variable over time as swelling clays impart an effect. The falling head data for the spike test clearly show a reduction in velocity (hydraulic conductivity) as the column is exposed to increasing amounts of water (Figure 6-27).

The falling head test data can be used to calculate an estimate for the hydraulic conductivity of the soil column, and flow data (from the first soil column testing) can also be used to provide an estimate of  $K$ :

The falling head permeameter equation is given by (Todd and Mays 2005):

$$K = \frac{AL}{at} \times \ln \frac{h_1}{h_2} \quad \text{Eqn 6-3}$$

where  $A$  and  $a$  are the areas of the water filled tube (in this case the same),  $L$  is the length of the sample which the water passes through and  $h_1$  and  $h_2$  are the heads at time  $t$ . A total of 8 determinations were made from both soil column investigations. The results are in Table 6-5.

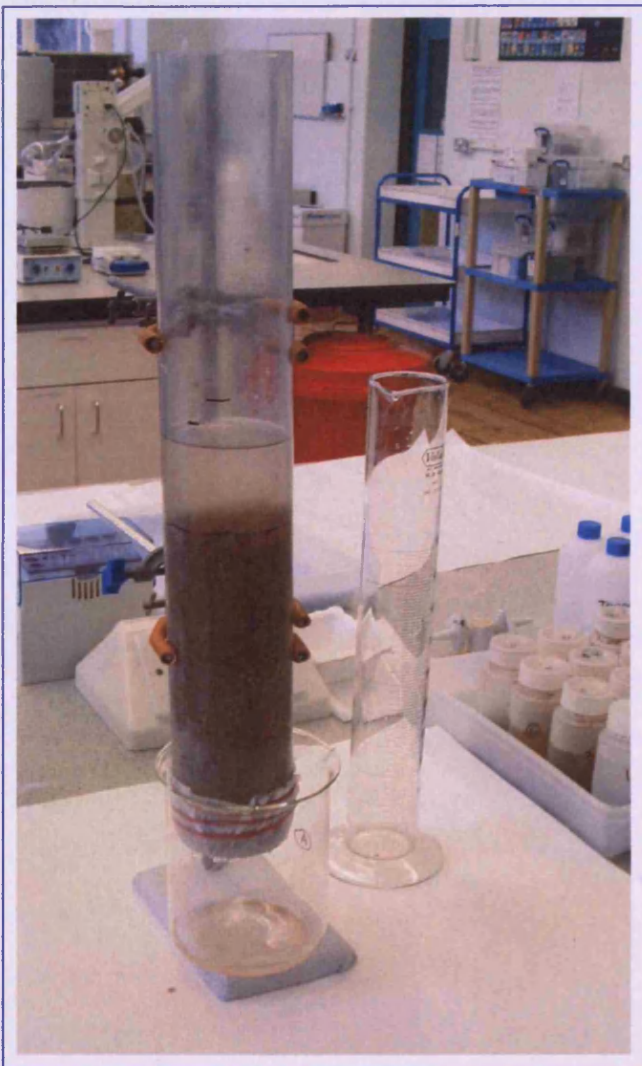


*Figure 6-27 Soil column 2 experimental setup and falling head measurements. Note head of water above soil see also Figure 6-23. Photo A Gray.*

**Table 6-5 Hydraulic conductivity values obtained from soil column experiments.**

Date	K m day <sup>-1</sup>	Method	Remarks
20 May 08	1.4 to 1.0	Darcy	Leachant test
17 Sep 08	1.7 & 1.1	Darcy	Spike
18 Sep 08	153 & 74	Falling head	Spike
11 Feb 09	13 to 3.7	Falling head	Leachant test
18 Feb 09	3.6 to 1.0	Falling head	Leachant test
17 Mar 09	4.2 to 0.1	Falling head	Leachant test
18 Mar 09	14.6 to 1.1	Falling head	Leachant test
26 May 09	44.8 to 1.0	Falling head	Spike

## 6.3 Geochemistry and mineralogy

### 6.3.1 XRD results and discussion

A total of 22 analyses were undertaken; including bulk soil analysis, and targeted searches for common phosphate minerals. The semi-quantitative bulk mineralogy is a function of the area under the specific mineral peaks, as those minerals have variable strength diffractions: quartz, for example, has a strong refractive signal. The results show that quartz dominates all the samples, and that there is a variety of clay minerals such as kaolinite, clinoclore, illite, montmorillonite; albite is also present. However; if a particular mineral is present, but its bulk is less than 5%, it is likely to be masked within the noise of the analysis; or in the case of goethite it may be masked by quartz peaks.

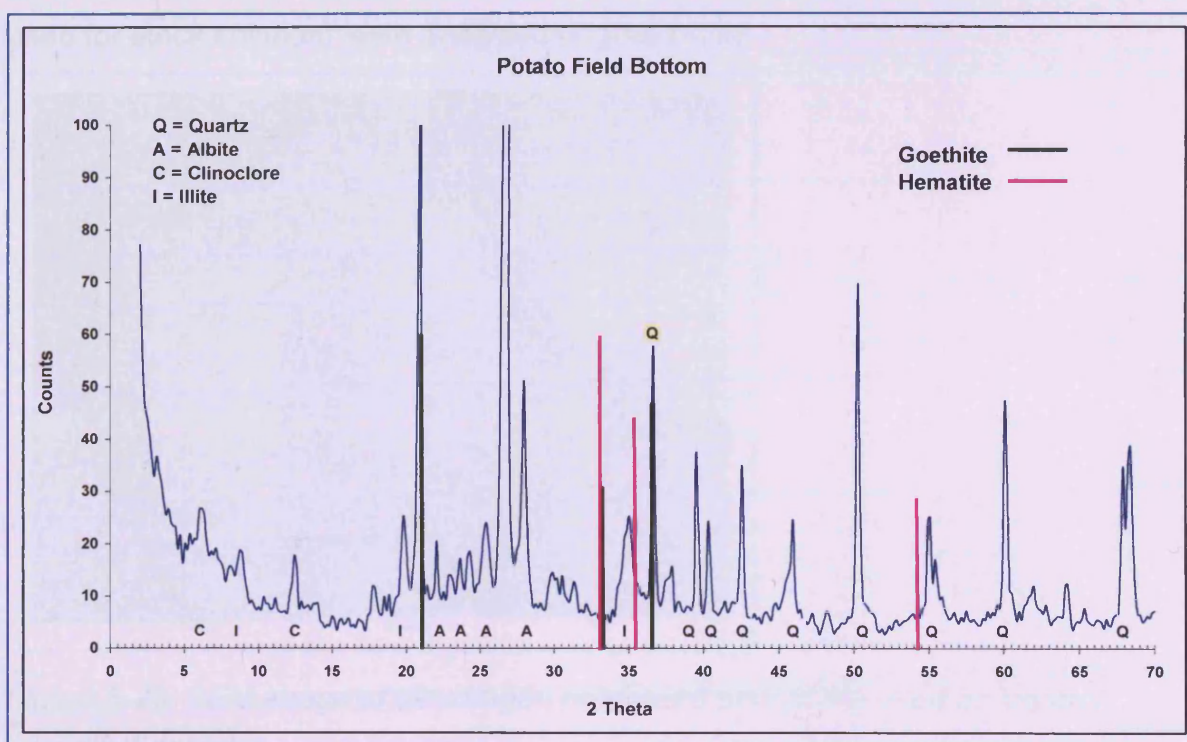


Figure 6-28 Diffractogram for Potato Field Bottom (POTA-btm) soil with locations for Goethite and Hematite indicated, note potential for goethite to be masked by quartz. Y-axis shortened to aid visualisation.

Iron hydroxide minerals, for example hematite, were believed to be present although their spikes were masked by other mineral peaks. However the general 'red' colour of the soil samples and green reduction spots observed in the soil profiles at Glen Court Farm suggest the presence of iron within the soil column.

Particular emphasis was placed on the identification of phosphate minerals that may precipitate: vivianite and strengite which have been previously identified by XRD methodology (Cornforth 2008). They have also been found in proximity to septic systems (Robertson 1989) but these were not apparent in the local samples. The similarity of the composition of the diffractograms indicates homogeneity of bulk composition; however accessory elements/minerals may differ. In conclusion, the XRD analysis was not able to positively identify iron or aluminium phosphate minerals within the soil bulk composition.

### 6.3.2 Scanning electron microscope results and discussion

The soil was analysed under ESEM, specifically looking for phosphorus 'hotspots' and attached phosphorus. All 22 soil samples and a 'phosphorus' control ( $\text{KH}_2\text{PO}_4$  used for stock solution) were analysed (Figure 6-29).

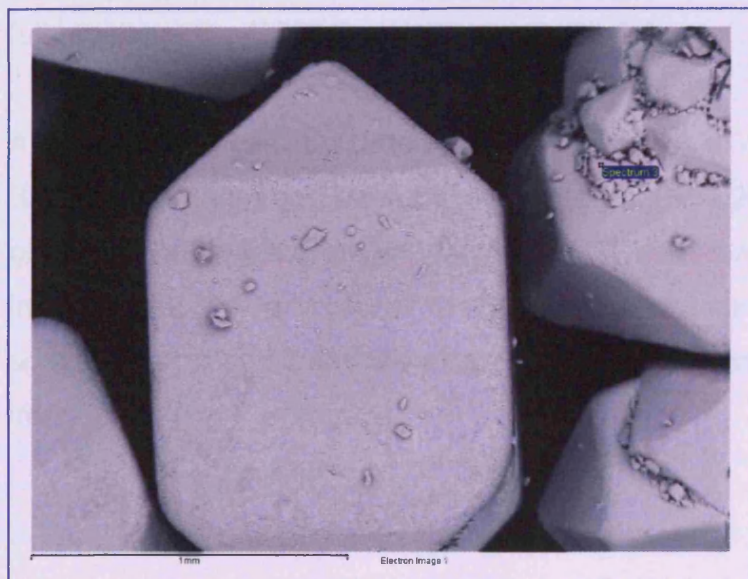


Figure 6-29 SEM image of dihydrogen potassium phosphate used as 'control' for soils analysis.

Table 6-6 SEM spectrum analysis of dihydrogen potassium phosphate.

Element	Weight%	Atomic%
O	46.01	65.72
P	24.73	18.25
K	26.79	15.65
Cr	0.25	0.11
Nd	0.44	0.07
Au	1.44	0.17
Po M	0.34	0.04
Totals	100.00	

The results of the spectrum analysis (Table 6-6) show that the weight % calculations are consistent to within ~1% with the assay ( $\text{KH}_2\text{PO}_4$  atomic weights 39, 31, 64 total 134; H not analysed). Some monazites, an original phosphate mineral obtained from the weathering of granites and found as placers were identified in the samples.

The soils from the Usk Valley occasionally contained phosphorus in the analyses, but this was inconsistent throughout the investigation. For example, phosphorus was found in LUSK soils, but not in the soils at Hill Farm manure pile (HILLMAN) (Figure 6-30, Figure 6-31 and Figure 6-32). This may be a result of trying to find small targets under SEM. However SEM-EDX spectral mapping of an area was also used, but again proved inconclusive (Figure 6-33). The SEM was also used to investigate the residue on the  $0.45\mu\text{m}$  filters from the groundwater analysis. The full results of the ESEM are in Enclosure 1 CD.

Anion adsorption is known to occur on the edges of clay minerals (Krauskopff and Bird 1995; Stumm and Morgan 1996; van der Perk 2006), and what appear to be platy mineral edges are seen in Figure 6-31, with the spectrum analysis presented in Table 6-8. The analysis of the edges does not indicate phosphorus, however spectrum locations 3 and 6 do show that phosphorus is present associated with iron.

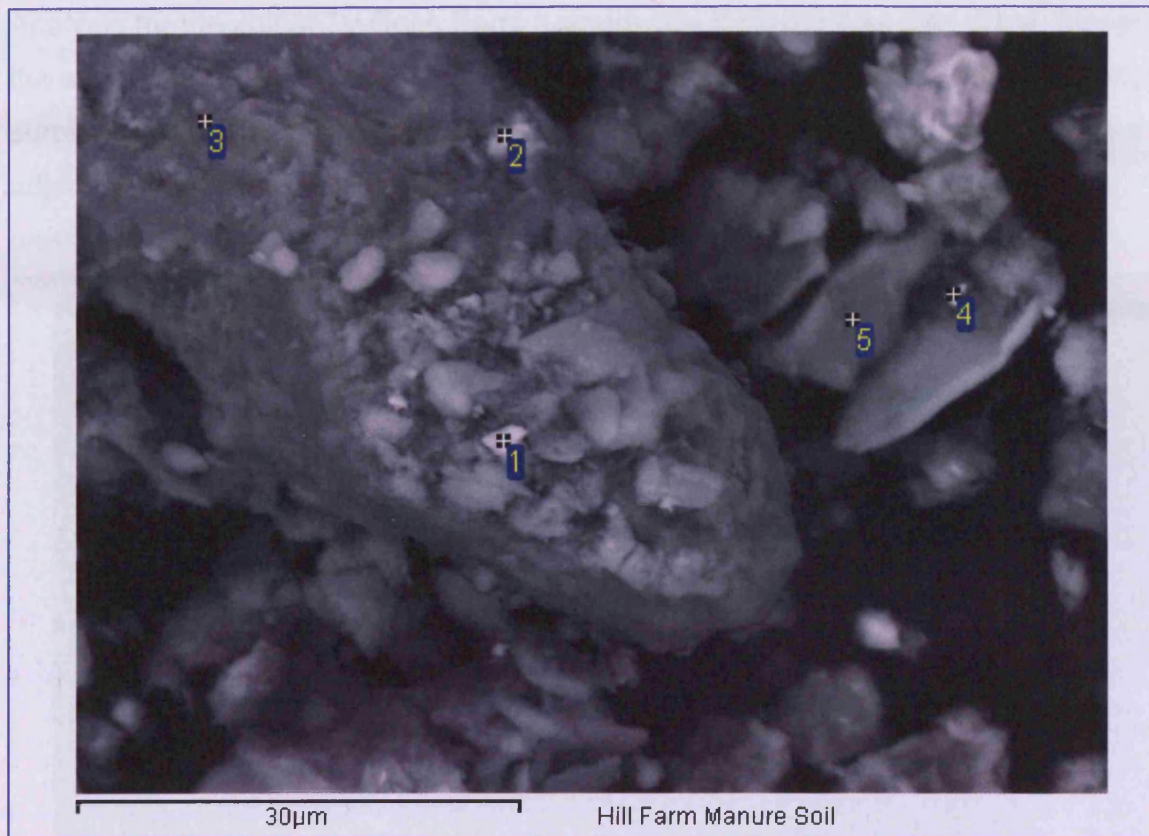


Figure 6-30 SEM image of soil from Hill Farm manure pile (SOI1) (HILLMAN).

Table 6-7 Spectrum analysis for soil at Hill Farm manure pile (HILLMAN) at SOI1.

Spectrum	O	Mg	Al	Si	K	Ca	Ti	Mn	Fe	Zr	W
1	50.86	0.63	3.04	4.91	0.58		16.96	3.21	19.81		
2	56.09	0.55	3.76	24.08	1.06	0.34			1.71	10.25	2.16
3	47.00	0.49	1.81	49.87					0.84		
4	28.76	2.72	8.55	15.47	1.04				43.45		
5	54.26	0.39	1.18	42.55					1.62		

All results in weight%

The results for Hill Farm manure soil indicate a lack of phosphorus, despite known manure leachates penetrating the soil and being subsequently leached from the same soil powders.

Analysis for the soil at Ty-Coch Farm manure pile (MANU) was also done, however the spectrum analysis did not reveal the presence of phosphorus. This is a surprising result, similar to HILLMAN, given the runoff from the manure pile. The adjacent locations POTA (potato field) and SCRUB did also not indicate the presence of phosphorus.

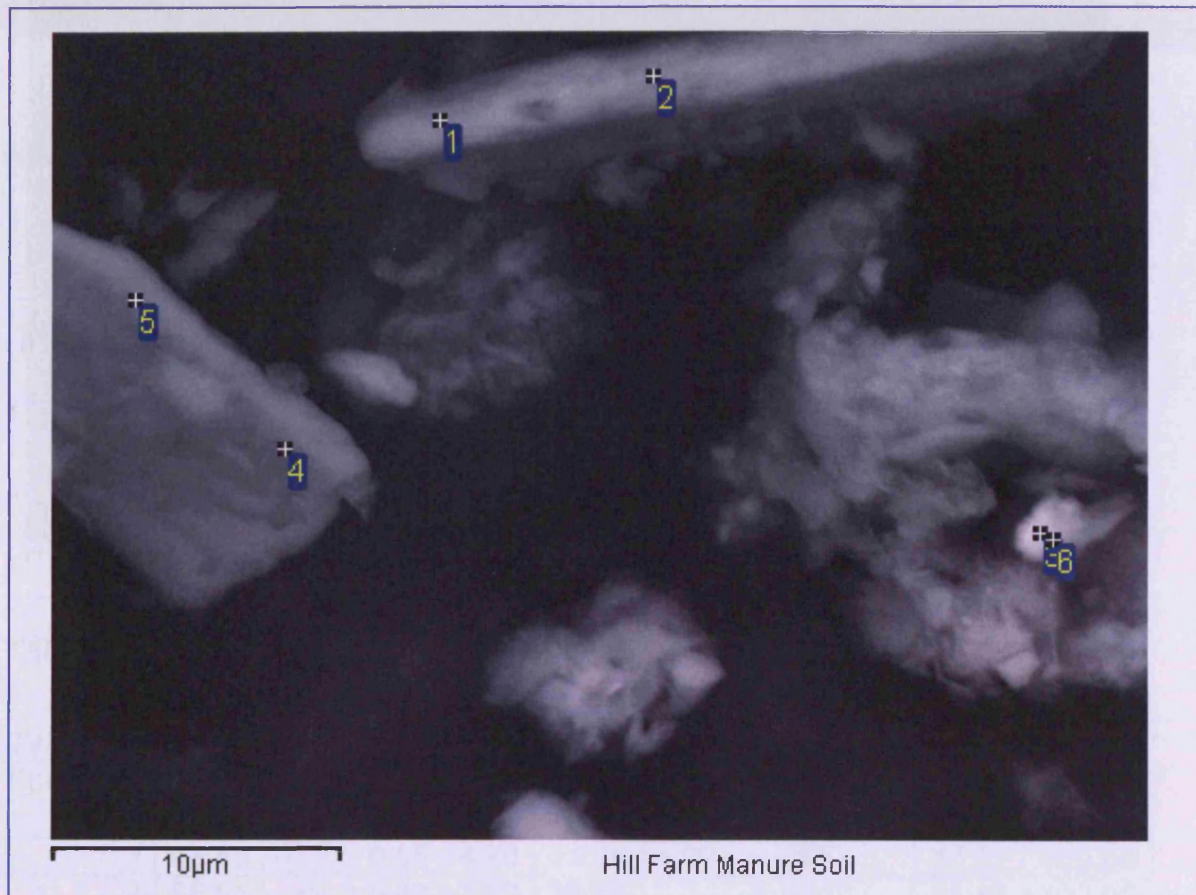


Figure 6-31 SEM image of soil from Hill Farm manure pile (SOI2) Spectrum analysis undertaken on what are believed to be clay mineral edges.

Table 6-8 Spectrum analysis for Hill Farm manure pile at SOI2.

Spectrum	O	Na	Mg	Al	Si	P	K	Ca	Ti	Fe
1	52.04	0.57	1.44	15.10	20.95		6.83		0.59	2.48
2	53.30		1.17	15.38	20.61		6.75		0.61	2.18
3	27.34		1.60	8.70	13.68	0.71	1.72	0.49		45.76
4	51.57	0.71	0.98	16.56	20.81		6.90			2.47
5	55.13	0.83	0.79	15.74	19.86		6.00			1.66
6	35.77		1.73	11.00	18.67	0.66	2.38	0.43	0.55	28.81

All results in weight% Note association of P with Fe, spectrum 3 and 6.

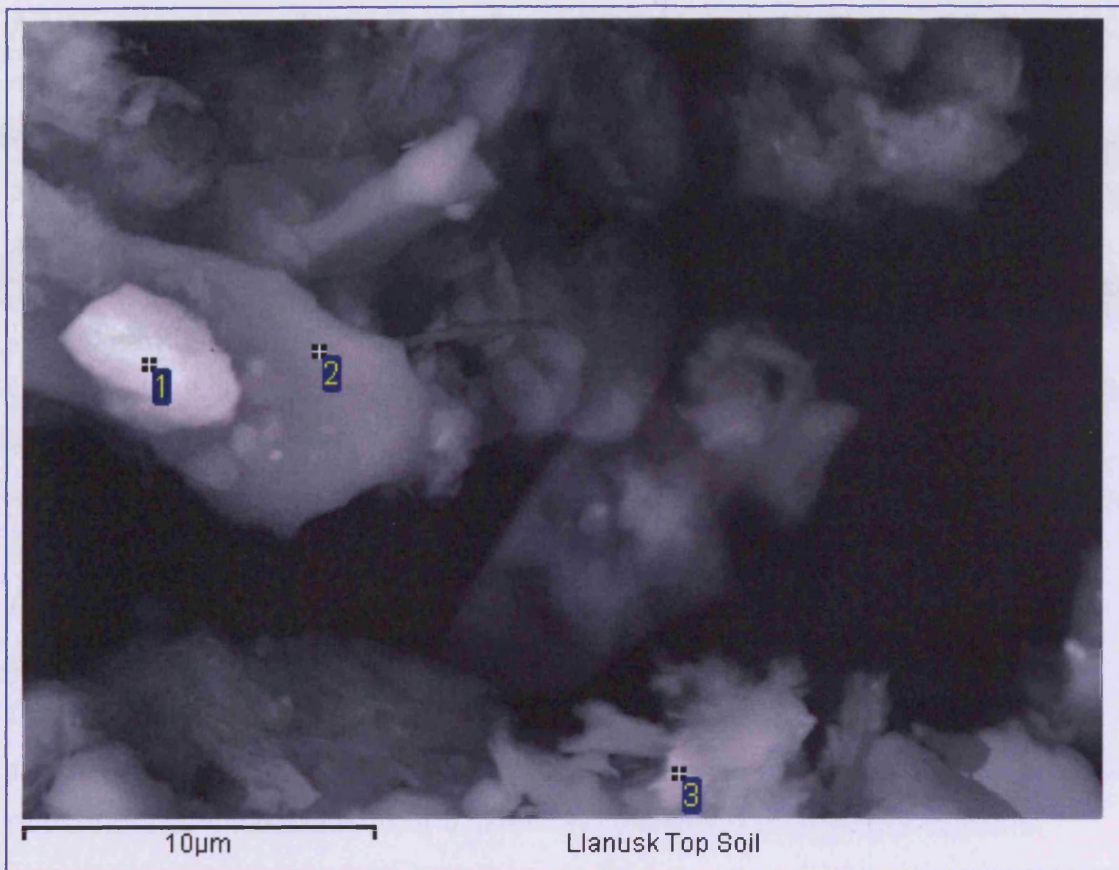


Figure 6-32 SEM image for soil (SOI1) at Llanusk Farm BH (LUSK).

Table 6-9 Spectrum results for LUSK soil (SOI1).

Spectrum	O	Na	Mg	Al	Si	P	K	Ti	Fe	Total
1	43.55		0.55	4.70	11.68	1.02	0.58		37.91	100.00
2	58.01		0.42	1.82	38.00		0.35		1.40	100.00
3	53.54	0.65	1.86	9.71	19.90	0.68	2.04	0.98	10.64	100.00

All results in weight%

The results for the soil analysis at LUSK show that there is an association with phosphorus and iron, at the spectrum locations 1 and 3. This suggests that phosphorus mineral(s) are found within the soil zone at this location. Since the weight% values do not match 'standard' phosphate mineralogy (Ralph and Ralph 2009), this suggests sorption rather than precipitation.

Additional analysis of Llandowlais Farm (LDOW) and LUSK soils (SOI2 and SOI3 data not shown) also show that the presence of phosphorus does not always occur with iron in 'high' quantities. Robertson (1998) found the precipitation of phosphate as grain coatings and overgrowths when investigating septic tank sewage plumes, and suggested that precipitation is actively occurring in association with iron.

#### SEM filter analysis

Used filters were analysed (0.45µm Millipore) to investigate if phosphate may be adhering to colloids (100–0.001µm). It was observed that at some locations a significant residue was produced, such as LTRI where dark particles were common and believed to be detrital peat material (Pers. comm., local landowner).

Additionally at LUSK and PENC where a reddish-brown residue believed to be iron oxide was seen. The results (Figure 6-36) show that there was no phosphorus on the filters. Any phosphorus found within the filters would equate to particulate phosphorus, the fraction that passes through the filters equating to total dissolved phosphorus, which will consist of SRP and dissolved organic phosphorus.

The 'hotspot' mapping feature shows the presence of iron at spectrum location 2; yellow circle (Figure 6-33, see also Table 6-10). Although the mapping indicates the presence of phosphorus throughout the image some clustering is recorded at the spectrum points. This perhaps explains why phosphorus is elusive during point source investigations and is not present in sufficient concentration to be readily detected. It also suggests that there is perhaps a sufficiency of manganese and iron oxides sorption sites to accommodate phosphorus and provide a carrier on small detached particles in groundwater transport.

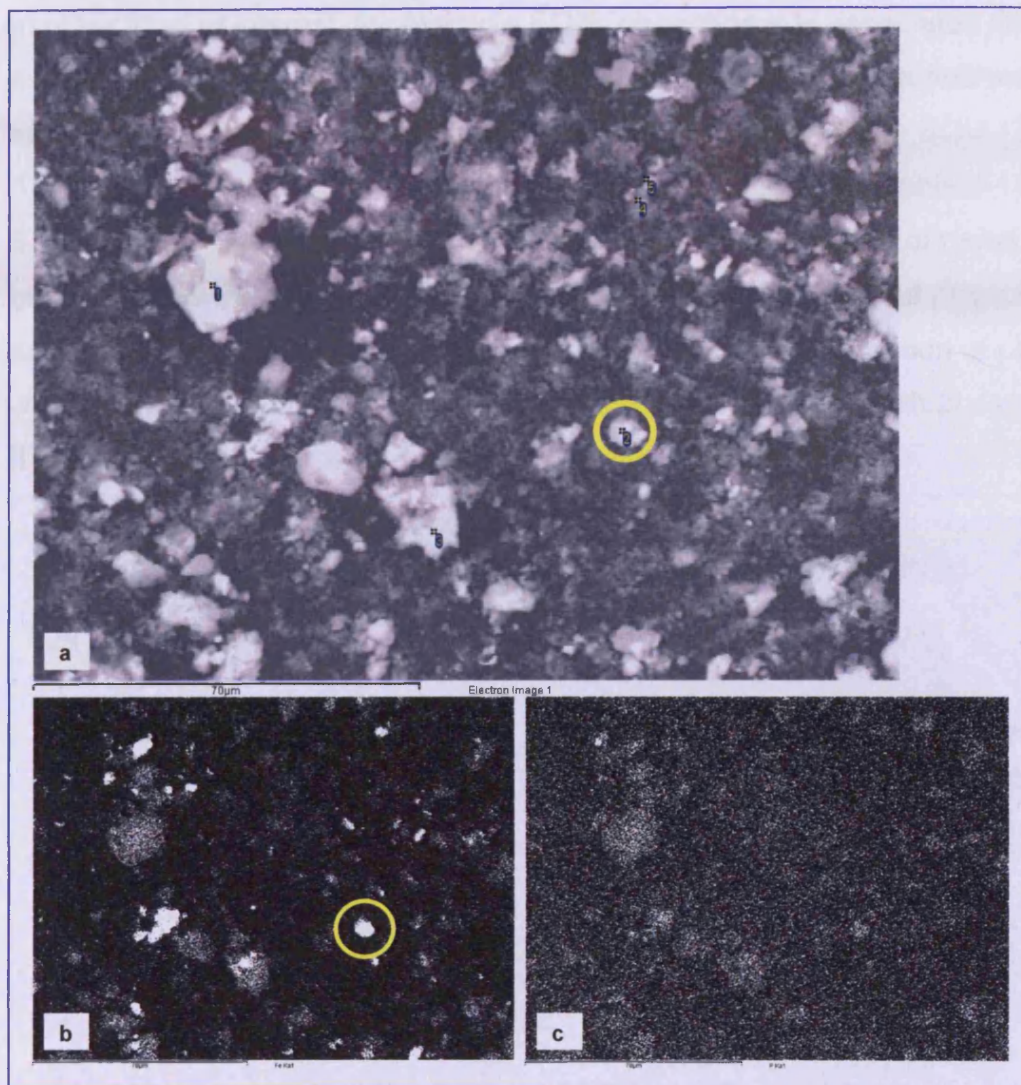


Figure 6-33a-c SEM image of filter residue at LTRI BH; (SOI2). (a) filter residue, (b) Iron hotspot mapping for area in image (a). (c) Phosphorus hotspot mapping for area in image (a).

Table 6-10 Spectrum SEM data for LTRI filter (SOI2).

	Na	Mg	Al	Si	P	S	K	Ca	Mn	Fe	Cu	Zn	O
1	0	0.87	1.39	1.96	0.81	0	0.79	5.35	58.84	2.32		1.24	25.87
2				4.64	0.82			1.25	1.67	65.53			26.1
3			1.23	2.47	0.73		0.85	4.92	57.34	1.94	1.11	1.71	25.23
4	0	0	2.88	6.54	1.24	0.93		5.09	52.88				30.44
5	3.68	0	2.09	2.72	0	0	0.74	5.29	57.32	2.31			25.85

All results in weight% (Total column and some minor elements not shown)

The results for the filter analysis at LTRI show that phosphorus is present in the filter detritus, and that the particles are dominantly composed of iron or manganese oxides to which substantial phosphorus is adhered.

In other sites of interest, for example SOI5, phosphorus is associated with manganese. However this is not a ubiquitous relationship as iron and manganese are observed without accompanying phosphorus, for example in SOI4 (Table 6-12). A similar analysis was undertaken for the filters at LUSK BH, (Table 6-11, Table 6-12, Figure 6-34, Figure 6-35 and Figure 6-36). The presence of metal iron oxides believed to be from the steel casing (Figure 6-37) and associated phosphorus was apparent. Most importantly the LUSK filters indicate no association of phosphorus with calcium detritus, and that not all of the iron is associated with phosphorus (Figure 6-36).

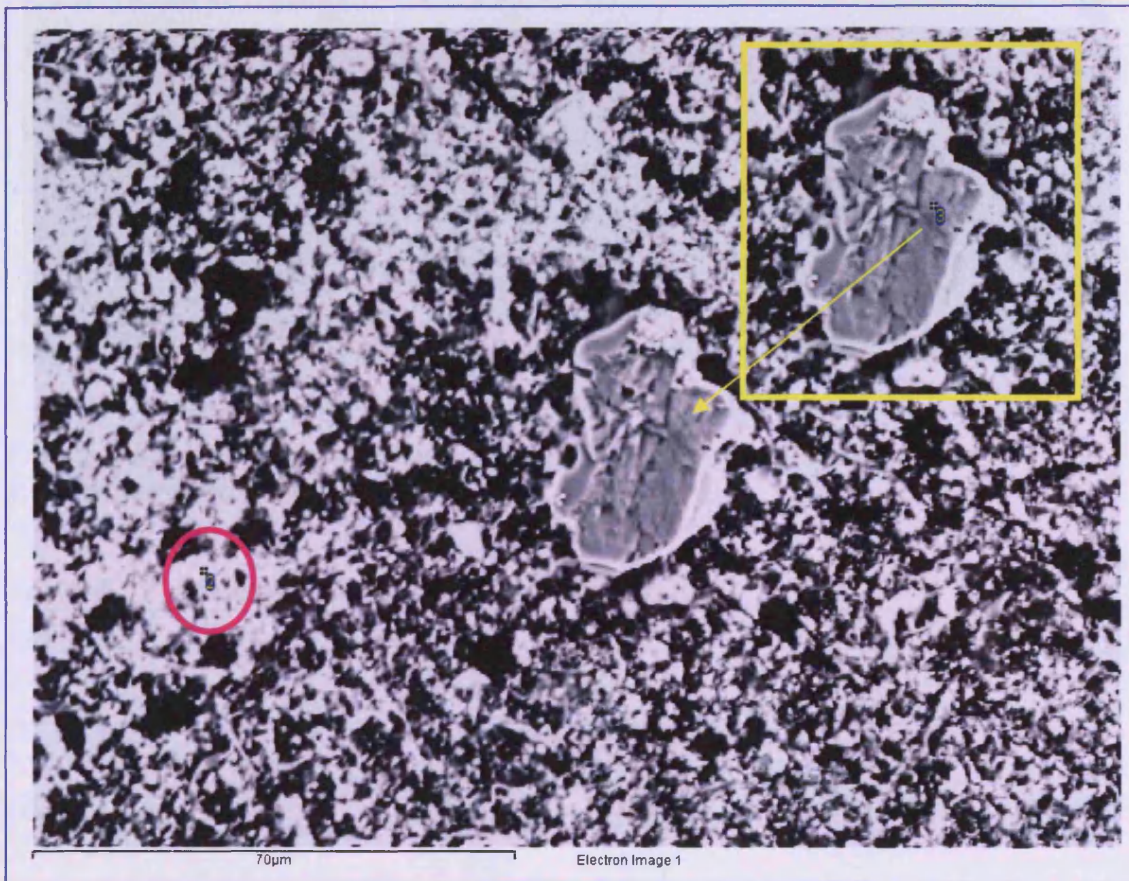


Figure 6-34 SEM image of filter detritus at LUSK BH, inset is location of spectrum #3 and #1 (not shown) Note bright areas in image are due to presence of metals (Image SOI3) Spectrum #2 purple circle.

Table 6-11 SEM spectrum results for LUSK filter.

Spectrum	Na	Mg	Al	Si	P	Ca	Fe	Te	O	Total
1	0	0	0	0	0	71.47			28.53	100
2	0	1.22	1.01	4.05	0.62	1.47	65.21		26.4	100
3	0	0	0		0	62.24		10.32	27.43	100

All results in weight%

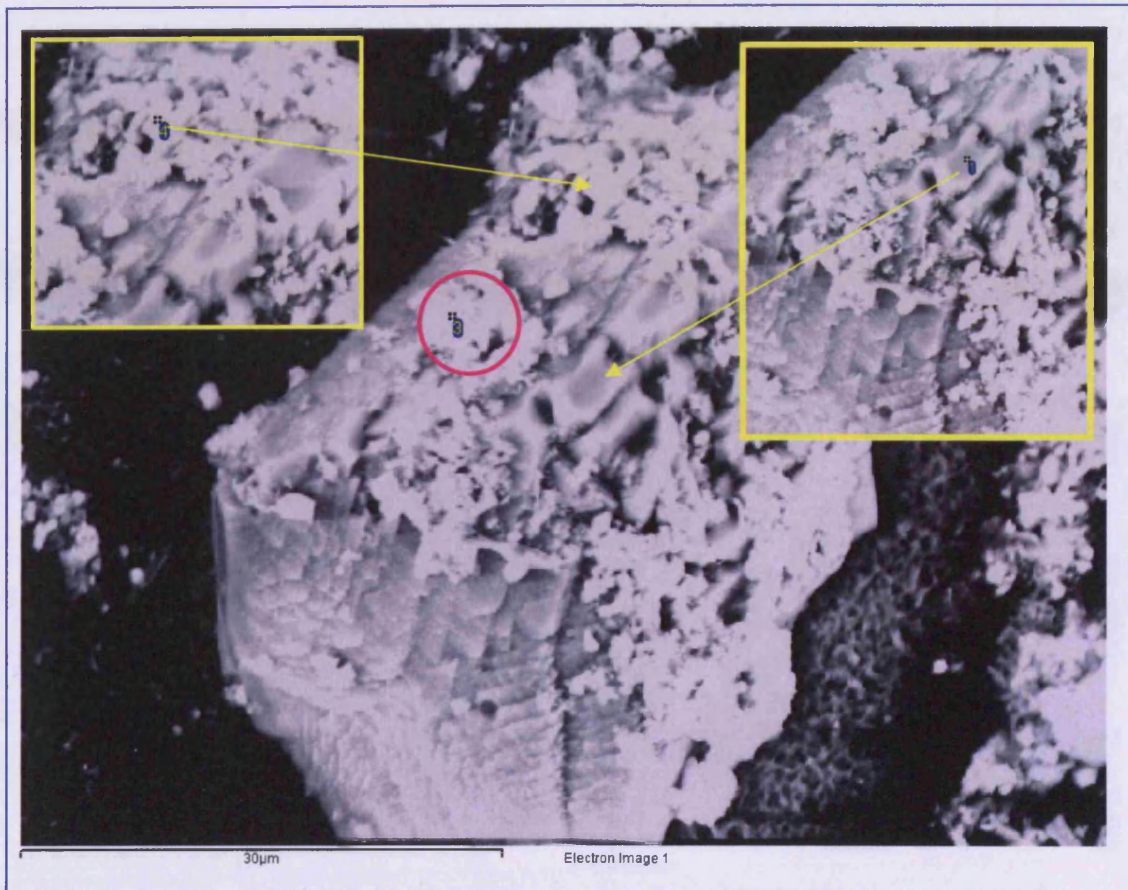


Figure 6-35 SEM image of filter detritus from LUSK BH (SOI4). Insets is location for spectrum #1 and ~#4.

Table 6-12 Spectrum results for LUSK filter (SOI4).

Spectrum	Mg	Al	Si	P	Ca	Fe	O	Total
1	1.13	0	0	0	70.14		28.74	100
2	0	0	0	0	71.47		28.53	100
3		1.28	3.64	0.63	16.72	50.5	27.23	100
4		1.79	4.72		12.79	53.34	27.36	100

All results in weight%

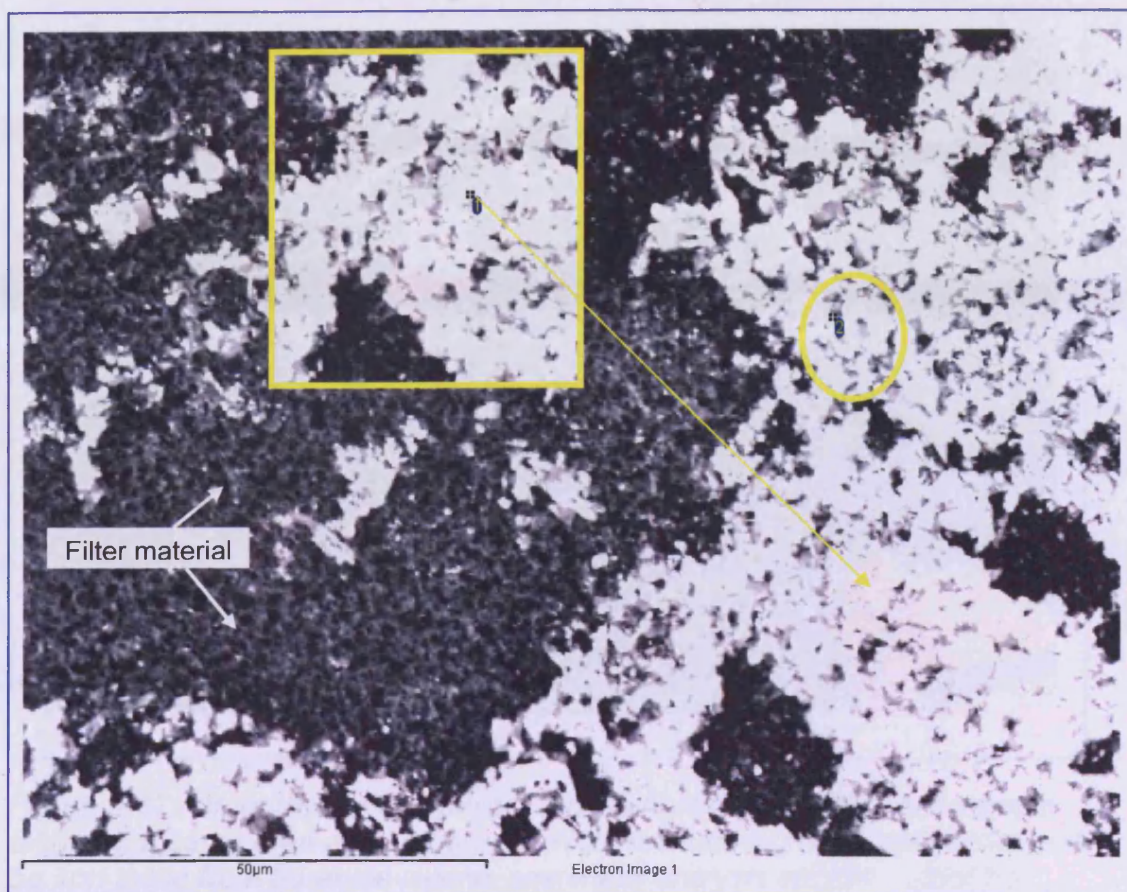
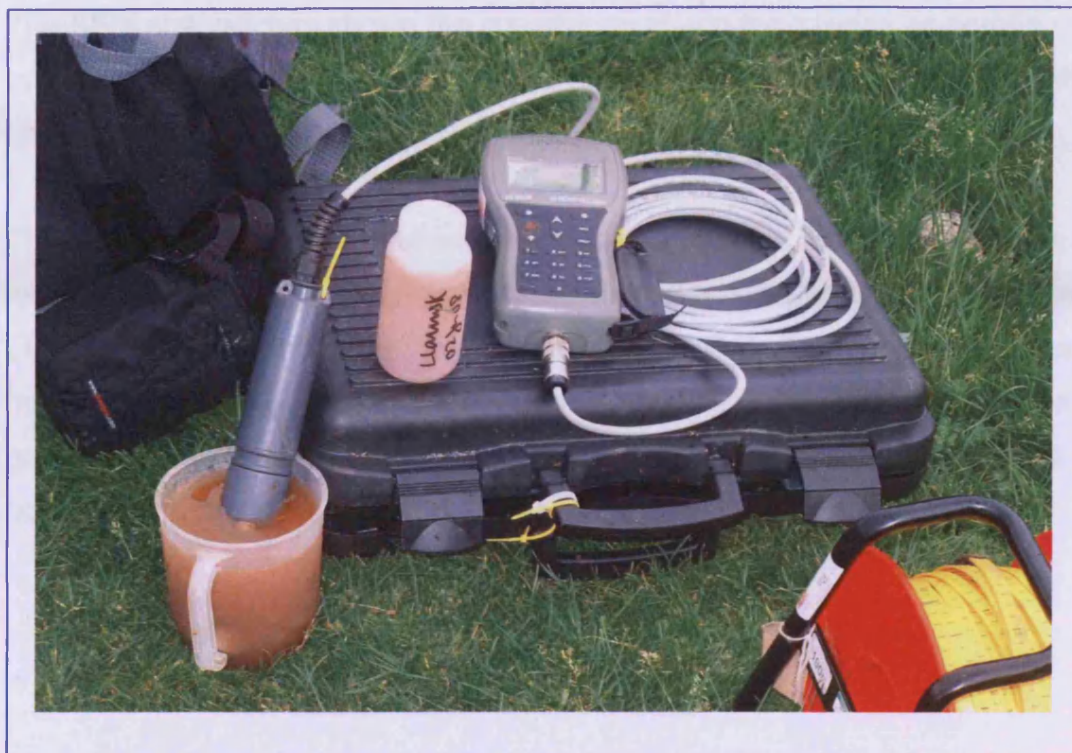


Figure 6-36 SEM image for LUSK filter, spectrum # 2 yellow circle, note dark membrane filter material 'behind' residue. Inset spectrum #1 which returned a zero P analysis despite a high 71.8 weight% – 91.5 compound%.

Table 6-13 Spectrum analysis #2 for LUSK filter (SOI1).

Element	Weight%	Atomic%	Compd%	Formula
Al	1.56	1.85	2.94	Al <sub>2</sub> O <sub>3</sub>
Si	4.59	5.23	9.82	SiO <sub>2</sub>
P	1.21	1.25	2.78	P <sub>2</sub> O <sub>5</sub>
Ca	2.13	1.70	2.98	CaO
Fe	61.67	35.34	79.34	FeO
In	1.78	0.49	2.15	In <sub>2</sub> O <sub>3</sub>
O	27.07	54.14		
Totals	100.00			



*Figure 6-37 Groundwater sample at Llanusk Farm BH (LUSK), soil sample taken from same area as photograph. Note red staining of sample believed to be iron oxide from borehole casing, see water analysis section - steel bolt experiment. Photo A Gray.*

#### 6.4 Summary

The analysis of the Usk Valley soils has shown that there is phosphorus within this compartment that is readily bioaccessible through the action of water recharge and leaching. There is evidence to suggest the migration of leached phosphorus down the soil column. The presence of accessory fertiliser minerals, especially potassium, suggests that the phosphorus has an agricultural fertiliser derived provenance and is not in-situ. There is also evidence to suggest that the amount of bioaccessible phosphorus (SRP) is a function of water contact time and volume. This phosphorus results from desorption processes, as mineral phosphorus was not found in the XRD and ESEM analysis. Spiked sample analysis also suggests that the local soil has an ability to readily sorb mobile SRP from agricultural inputs.

The soluble unreactive phosphorus fraction is also evident within the soil compartment, and may be acting as another pool of phosphorus which can be converted to SRP given the correct local environmental conditions.

The SEM analysis has shown the importance of iron hydroxides as sorption sites and these particles may act as colloidal vehicles for phosphorus transport within groundwater.

The soil analysis also has shown the importance of local hot spots in the form of local manure piles and feeding station locations. It has also shown that in the case of LUSK, which has recorded low groundwater SRP throughout the investigation, that the local soil contains abundant phosphorus. This reaffirms the sorption of groundwater SRP to the iron hydroxides produced by the steel casing of the borehole and the local soil minerals.

## Chapter 7 Lower Usk Valley groundwater modelling

### 7.1 Introduction

In this chapter, to better understand groundwater and contaminant transport, the Lower Usk Valley groundwater is modelled. The models use information detailed in the preceding chapters, including the location desk study that defines the model domain and initial parameters. Modelling and interpretation was made using FlowNet a 2D finite difference flownet program (Wang 2005), MODFLOW V3.0 (MacDonald and Harbaugh 1988) a 3D industry approved program, and the EA P20 Risk Assessment model (Carey et al. 2006b). The 2D modelling was done in order to screen literature, calculated or observed parameters in order to carry them forward to the more robust 3D modelling stage. A 3D regional model was then constructed and calibrated in order to generate parameters to carry forward into a more localised model. Two different boundary condition scenarios were run in order to assess the contribution and uncertainty that their inclusion or exclusion will have on the modelled results. The models were vigorously tested by sensitivity analyses.

The models underwent a series of evolutions throughout the project. The initial flownet models were produced early on in the project to assess the groundwater flow based on the first observed heads. Toth type models were also constructed to assess local flow patterns (Toth 1962; Fitts 2002; Fetter 2004). As a greater understanding of the aquifer was developed throughout the project, it was possible to revise the Lower Usk Valley initial conceptual model and produce an improved hydrological and geochemical version, which was tested using the more robust modelling techniques.

## **7.2 Hydrological conceptual model**

### **7.2.1 Topography**

The modelling requires an understanding of the topographic surface as this defines interfluvies and catchment zones, but not necessarily the groundwater 'catchment' (Peach 2006), although 'the water table is often a subdued reflection of the surface topography' (Fetter 2004). Moreau (2004) states that the South Wales Devonian aquifer is believed to be topographically controlled. A topographic surface digital terrain model (DTM) was created from Ordnance Survey digital data available through the Edina web portal (EDINA 2006) (Figure 7-1 and Figure 7-5).

The DTM model clearly shows the Lower Usk Valley running north to south and the broad floodplain between the valley flanks. The Olway Brook Valley is also indicated. The town of Usk is situated at the confluence of valleys. The line of the A449 is also shown running along the base of the east flank.

### **7.2.2 Water table**

Groundwater flow direction can be inferred from the observed dip data. In order to reconcile dip data to the national datum a GPS survey was undertaken to provide accurate positions and elevations; height accuracy is deemed as between 1 and 2cm. A schematic of the available logs was produced at a vertical and horizontal scale to indicate relative spatial distribution (Figure 7-2). It also serves to show the discrete water strikes, general direction of groundwater flow and the variability in lithology. The borehole at GOLW is situated on a small hill, which explains the higher water strike elevations; this may produce a local driver for cascade and doming in the groundwater flow. The project boreholes, from which samples and measurements were taken, are not shown in this diagram as logs for these locations were not available.

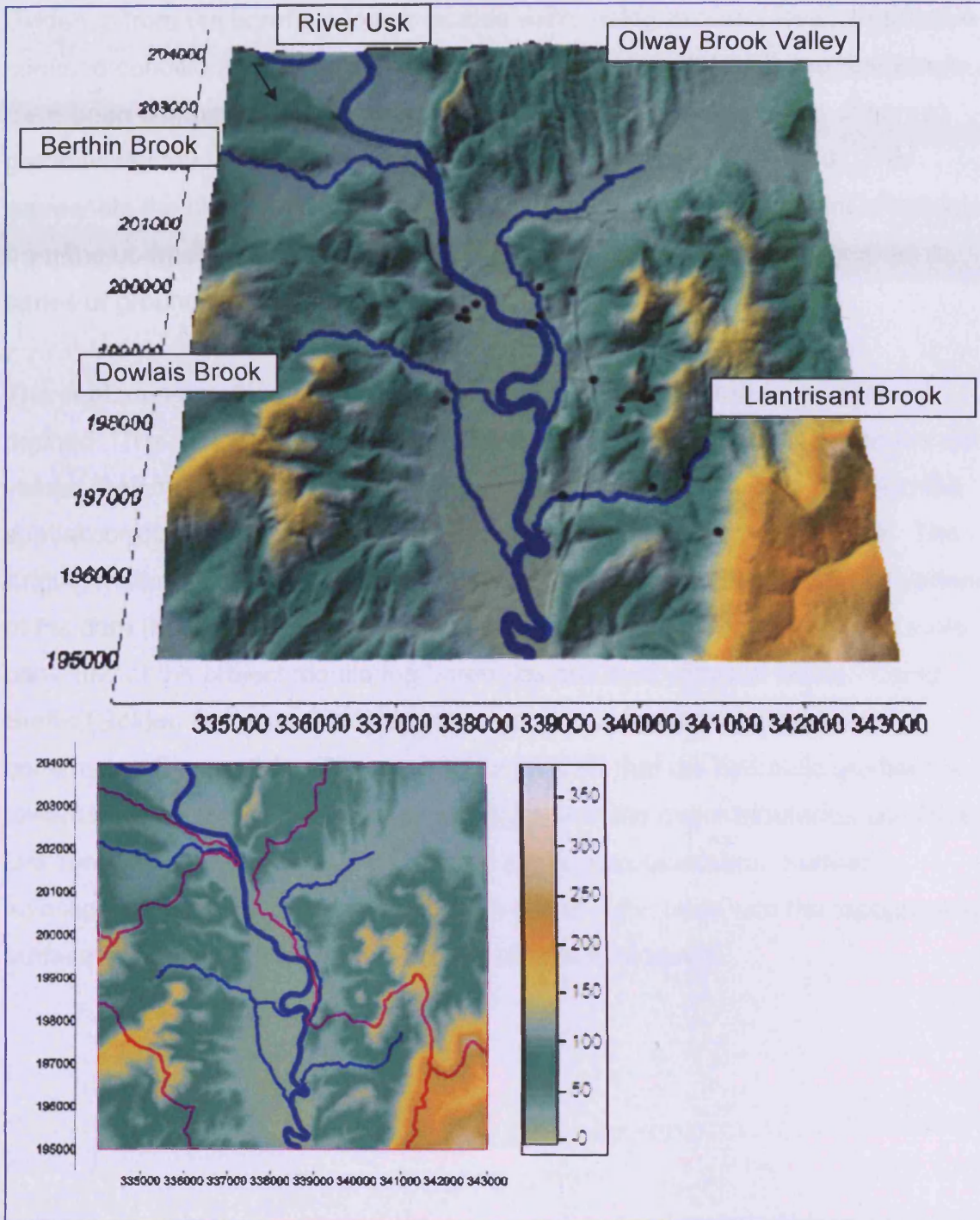


Figure 7-1 DTM of the Usk Valley and environs, black dots are sample locations; note slight vertical exaggeration. Vertical scale bar in m AOD. Inset map is orthographic view of DTM, purple lines are EA catchment delineations. See also endpaper maps.

Evidence from the borehole logs indicates water rising to a rest level, suggestive of confined conditions and vertical gradients. Due to limited data these rest levels have been combined and contoured as one element. Where project observed groundwater levels are included, the January 2008 values were used. This represents the highest level AOD as seasonality in the water rest level is indicated from the borehole hydrographs. These water levels are best represented as a series of groundwater contour maps.

The contouring method used was Kriging, which is considered to be a robust method. The method assumes that there is a spatial correlation between the data values (height). It has been suggested that hydrogeological parameters exhibit spatial correlation, for example hydraulic conductivity or effective porosity. The Kriging method takes into account the spatial density, location and spatial variance of the data (Kresic 2007). The first line data available to construct a water table consisted of the project monitoring boreholes and their reduced levels. Using Surfer (Golden Software 2003) an initial set of groundwater contours was constructed (Figure 7-3). These contours indicate that the hydraulic gradient is towards the River Usk, and they also suggest that the major tributaries and River Usk are gaining systems as the contours are convex upstream. Further investigation shows a poor harmonisation of the water table with the topographic surface, indicating that a greater density of data is required.

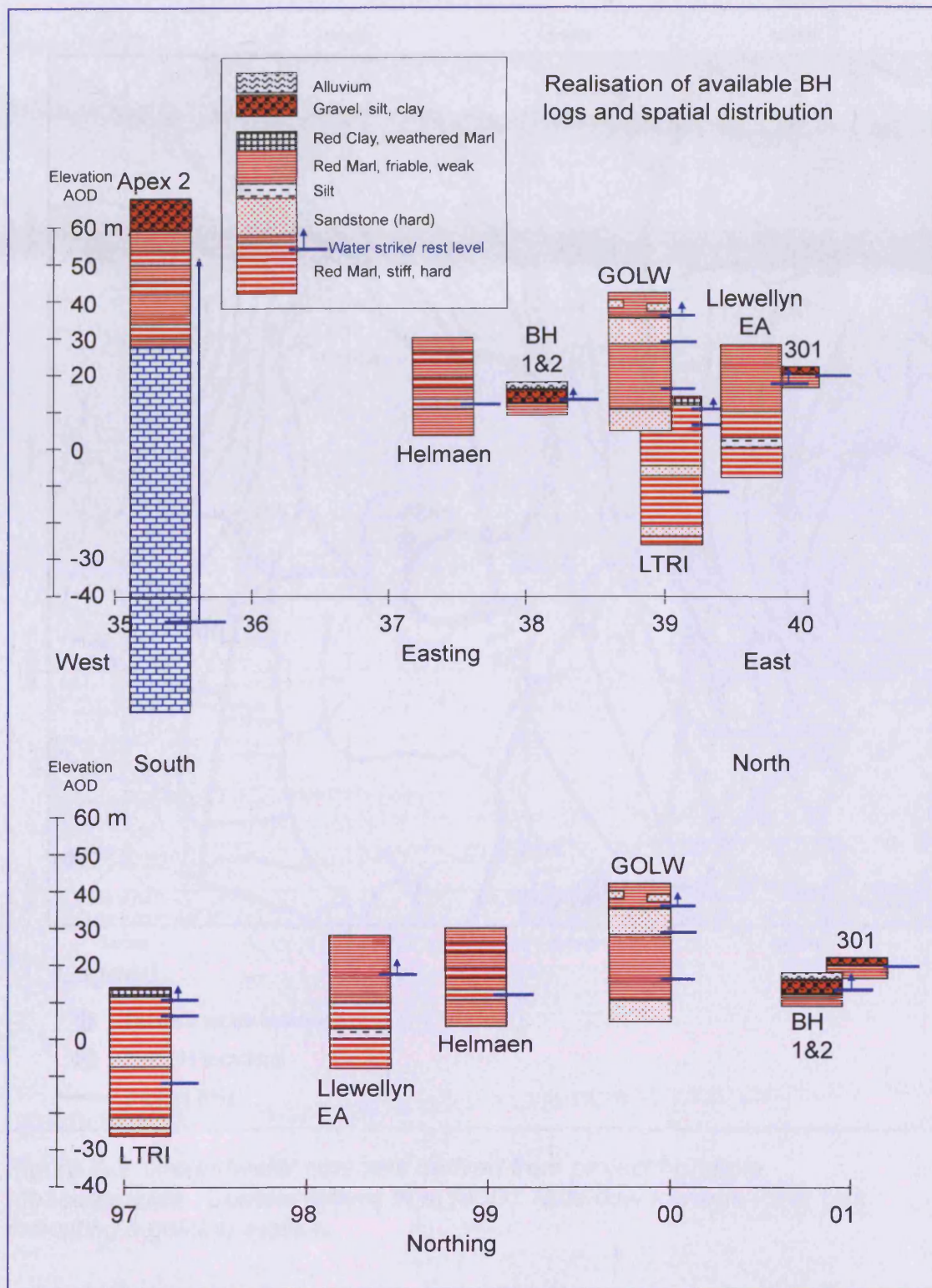


Figure 7-2 Schematic realisation of the borehole logs and lithology for the Usk Valley. Lithology descriptions from logs. Borehole log synopsis is at Enclosure 1 (CD) data from BGS archive. Note Borehole logs span ~50 years.

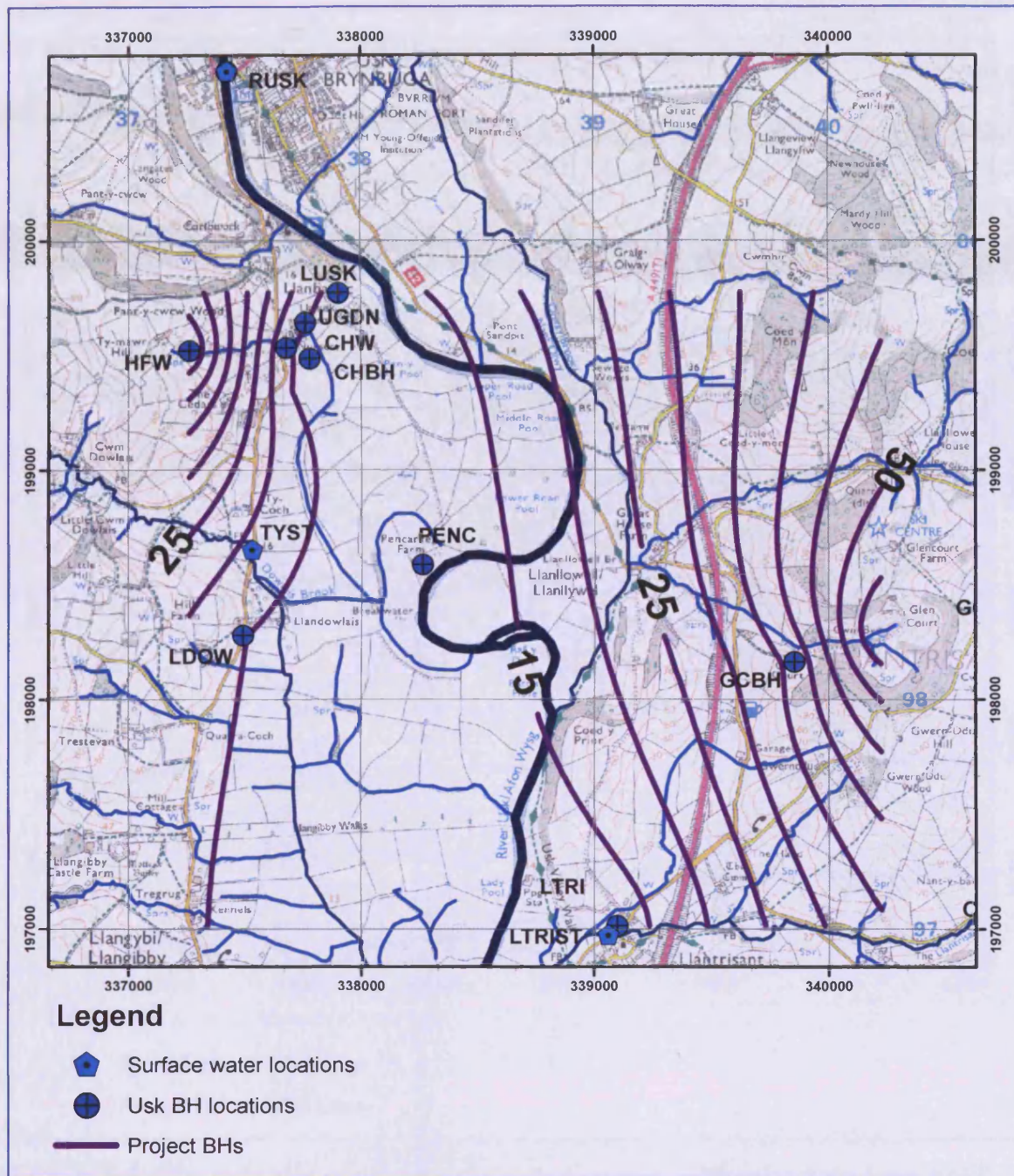


Figure 7-3 Groundwater contours derived from project borehole measurements. Contour values in m AOD. Note flow towards River Usk indicating a gaining system.

Using water rest levels from borehole logs supplied by the BGS and APEX Drilling further refinement was made. It is noted at this point that the values are not synchronous: one log is dated 1948 (Figure 7-4). The ‘sharpness’ of the intersection of the groundwater contours and the River Usk also indicate that the base flow or exchange between the groundwater and the river is ‘low’

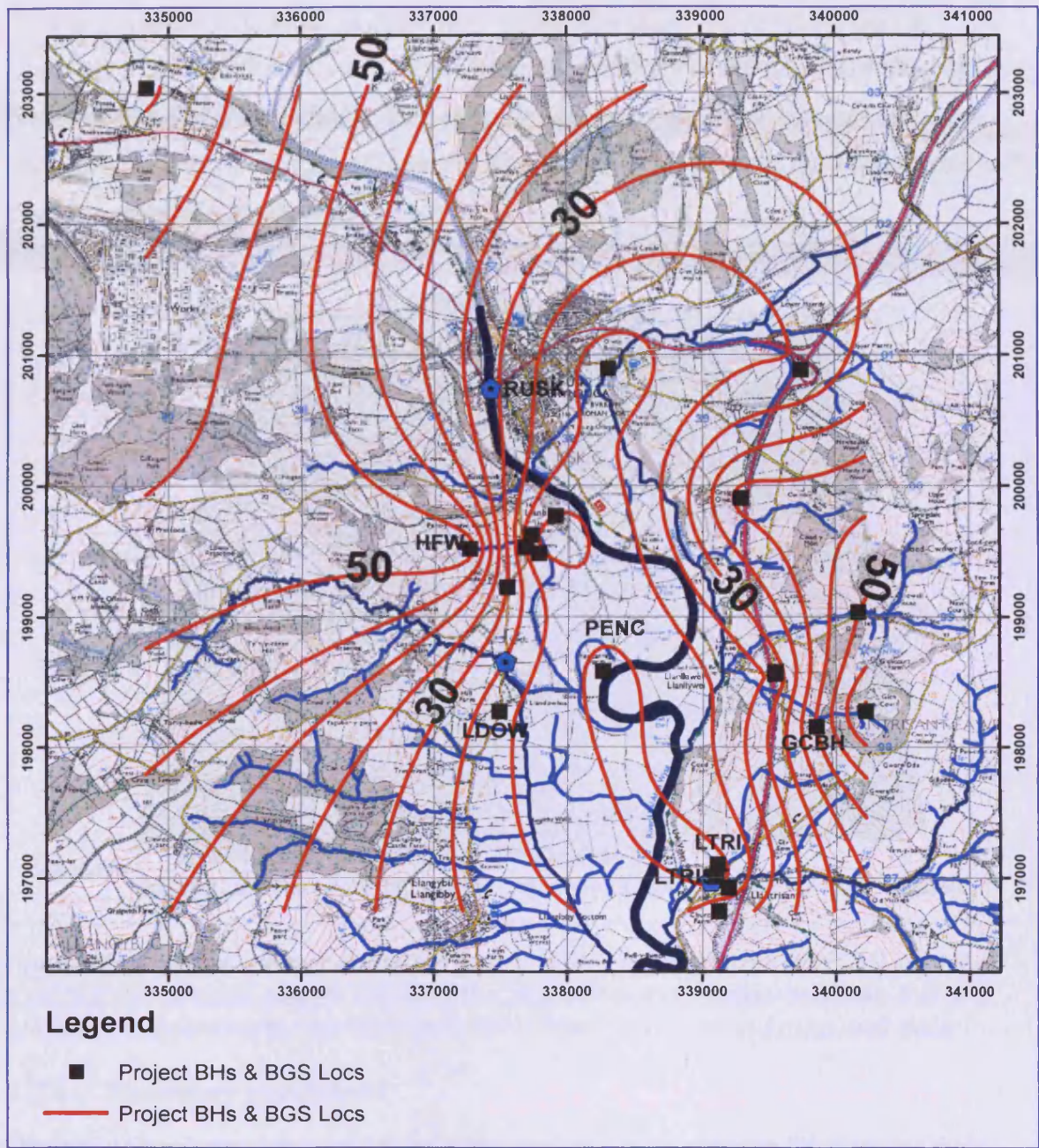


Figure 7-4 Groundwater contours using additional groundwater data from BGS and Apex Drilling borehole logs. Contour values in m AOD. Note loss of data spatial density in northwest.

Further refinement was still required as the contour data loses integrity in the northwest, and recourse was made to available mapping. The Ordnance Survey mapping (OS 2005c, 2007) and historical maps show the presence of wells which can be considered to be indication of the presence of groundwater at 'shallow' depths. This water at a topographic elevation may be the driver for flow through underlying fractured lithologies (Moreau et al. 2004).

This well spatial data was digitised and water elevations were estimated by applying a 3m 'depth to water'. This value is based on observations at the two project wells CHW and HFW. This refinement improves the visualisation of the contours but still does not address the lack of harmonisation of the water table with the topographic surface (Figure 7-5).

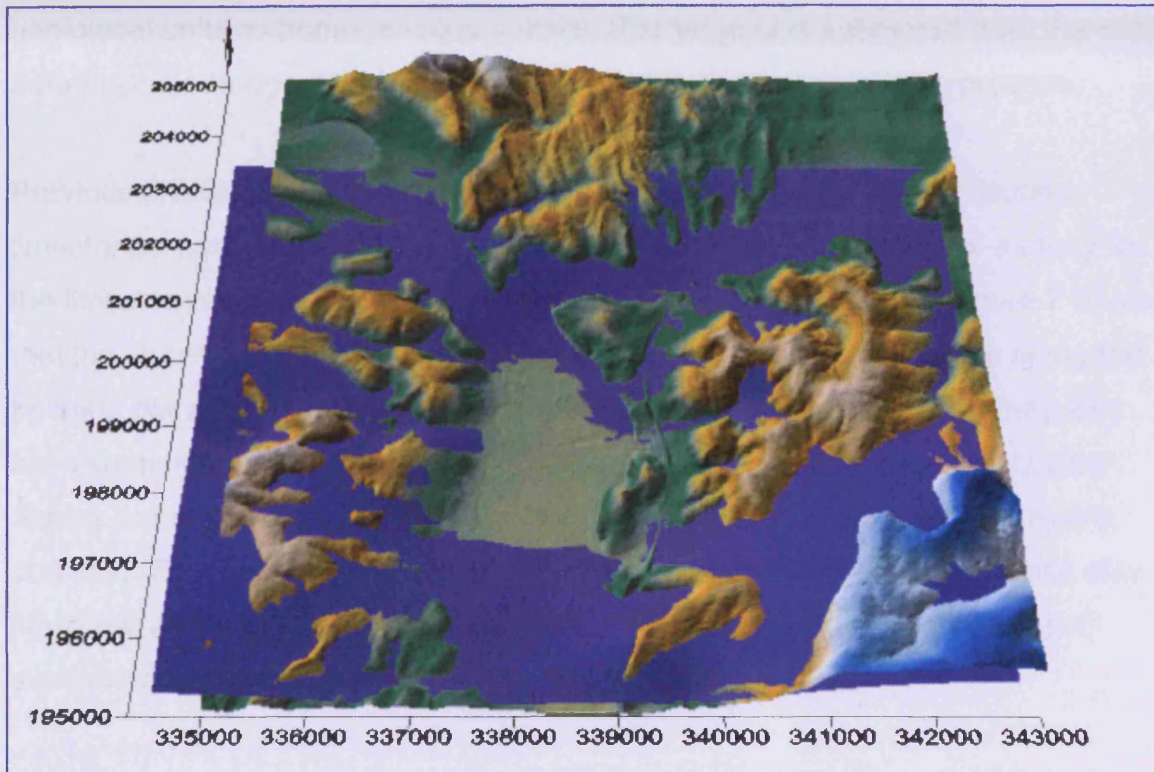


Figure 7-5 Intersection of modelled groundwater table (purple surface) and the topographic surface clearly showing the lack of harmonisation between the two surfaces. Groundwater surface generated from borehole and map well data.

### 7.2.3 Boundary conditions

Distinct natural groundwater boundaries such as impermeable lithology or river systems are scarce in the immediate project area. The River Usk provides a discharge zone and is likely to influence groundwater flow from both valley flanks. It has been suggested by Moreau (2004) that the groundwater flow is topographical controlled; the higher ground to the east, west and north would therefore provide potential boundary (interfluvial) zones for regional modelling (USCAE 1999; Kresic 2007). These interfluvial zones were used as a regional boundary during the MODFLOW analysis. In addition at the southern boundary the conceptual flow is believed to easterly and westerly from both valley flanks (Figure 7-4), this would provide a no-flow boundary condition in this part of the model domain.

#### 7.2.4 **Hydraulic parameters**

There is a scarcity of local hydraulic parameters in the literature. Transmissivity from two pumping tests was calculated and served as an initial model parameter as did the falling head tests from the soil column and borehole dilution tests. Due to the lack of lithological profiles it was deemed necessary to consider the individual geological units as homogeneous entities. Recharge was estimated from the rainfall data at Chain Bridge (CEH 2005), and refined during the modelling process.

Previous investigations by Gray (2004) in the Abberley Hills area of Silurian limestones, contemporaneous with the Usk Inlier, have been used as a proxy for the limestones on the west flank (Welch et al. 1961). The photos (Figure 7-6) show that the Upper Ludlow Shales are massive and have distinct pathways along the bedding planes that are orientated sub-vertical as in the Usk region. They also have some smaller fractures perpendicular to the bedding. The Lower Ludlow Shales are in the same orientation and show a fractured nature and low matrix porosity. The Aymestry Limestone has several thick inter-bedded bentonite clay horizons (ash fall deposits) in the Abberley Hills area, although these are not mentioned in Welch (1961).

There are two modelling options for the Downton Castle Sandstone. Firstly, as the name suggests, as sandstone that is likely to have a greater hydraulic conductivity. However, examination of geological mapping shows the sandstone to be a thin lithology stratigraphically above Upper Ludlow Shales and the Aymestry Limestone (BGS 1971). Previous work on these lithologies indicates that they are likely to have a low permeability (Gray 2004); the combined conductivity for these two different lithologies might therefore be reduced. The near vertical orientation of the beds is also expected to impede horizontal flow thus providing a conduit for vertical (bedding fracture) flows.

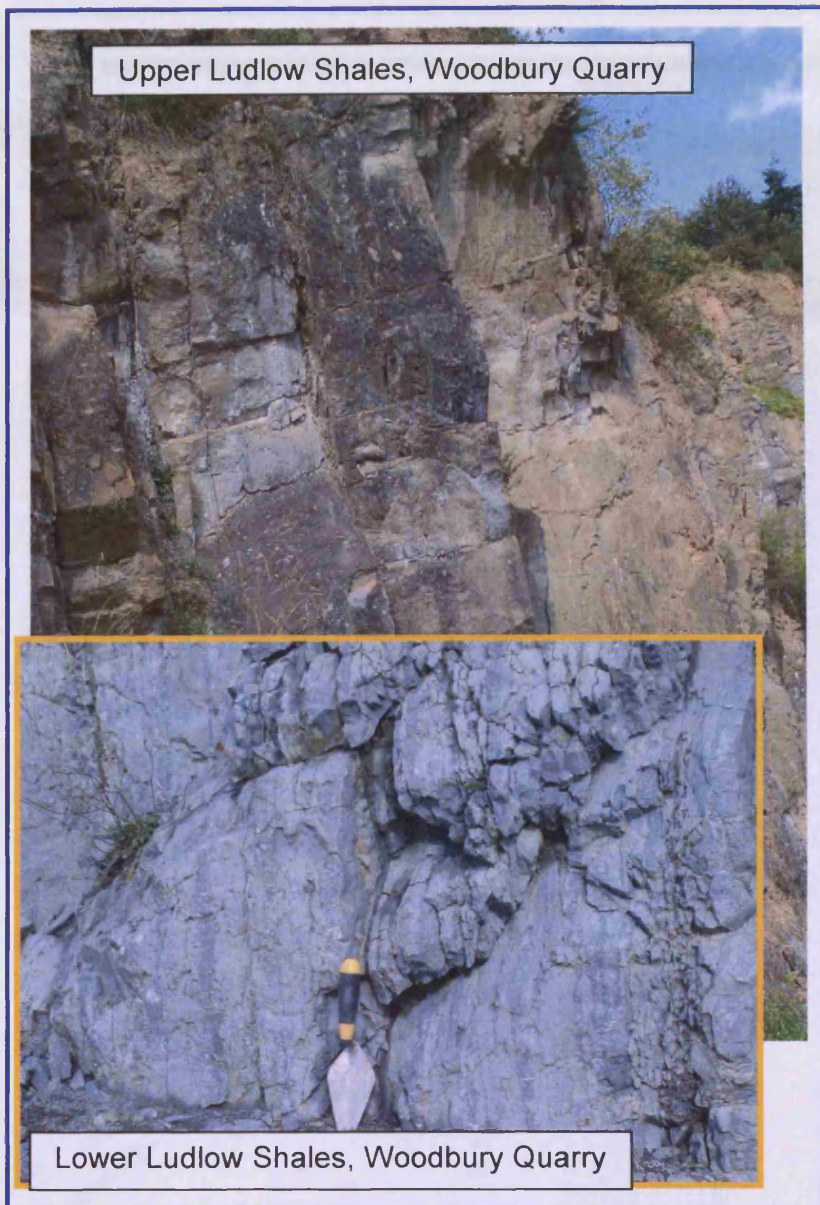


*Figure 7-6 Ludlow Shales at Woodbury Quarry from Gray (2004). Proxy location used to assess hydraulic conductivity of the west flank limestones.*

### 7.2.5 **Conceptual model**

The refined hydrogeological Usk Valley conceptual model (Figure 7-7) differs from the initial conceptual model in that there are less lithological zones and distinct geochemical processes have been identified. Borehole log evidence indicates discrete lithological horizons; however pumping test analysis is for the combined strata. The resolution of the individual lithologies in the borehole logs is insufficient to construct definitive horizons.

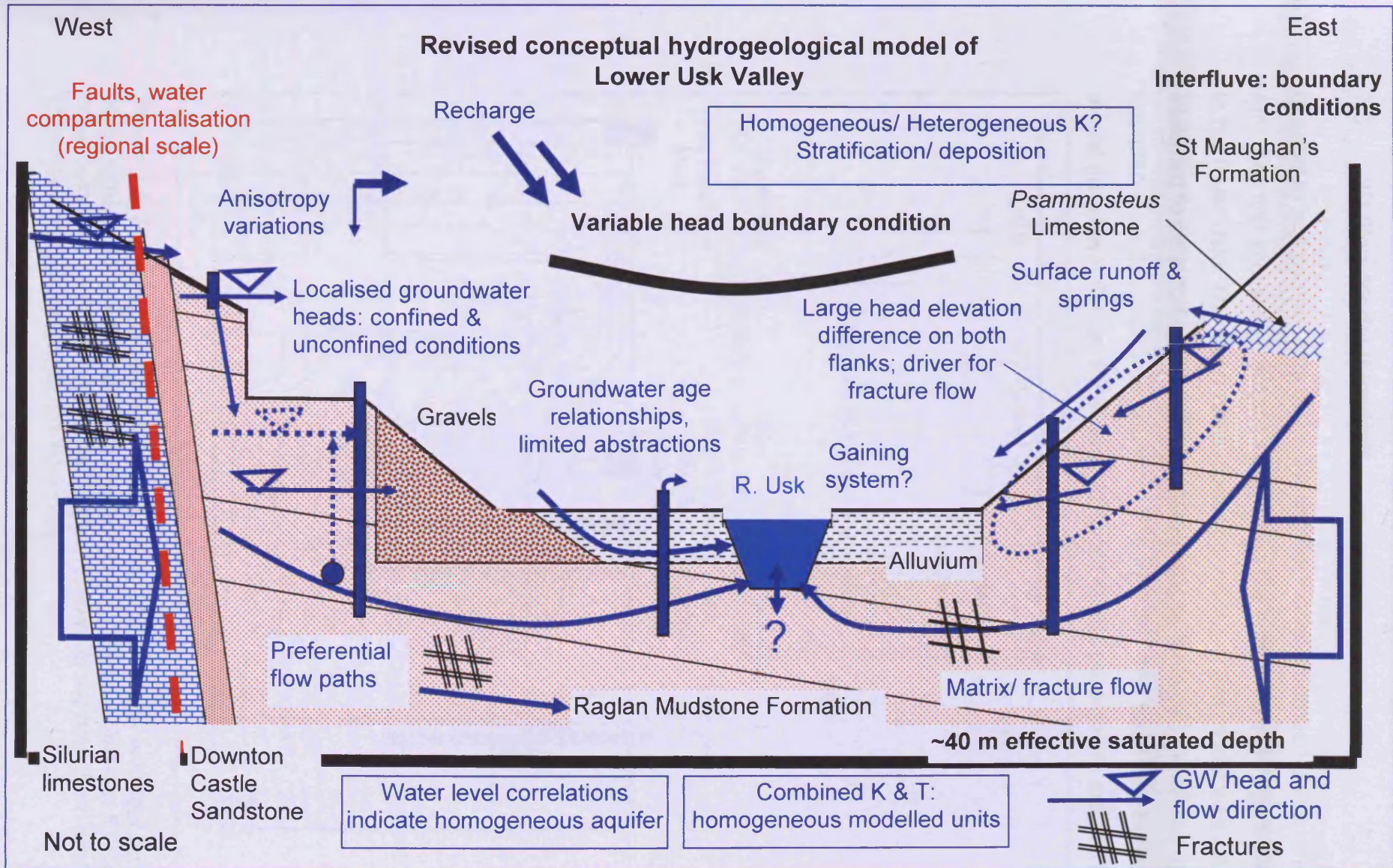


Figure 7-7 Revised conceptual model of the Usk Valley hydrogeology processes

### 7.3 2D Flow Model (FlowNet)

In order to test components of the conceptual model a number of scenarios were run. The first involved a model incorporating the profile from Hill Farm Well (HFW) to the River Usk. The water table (upper boundary) in this model was initially assumed to be a no flow boundary, subsequent variants can model the upper boundary as a flux/ recharge boundary (Figure 7-8). The head distributions for the model are shown in Figure 7-9, and accepted model parameters are at Table 7-1

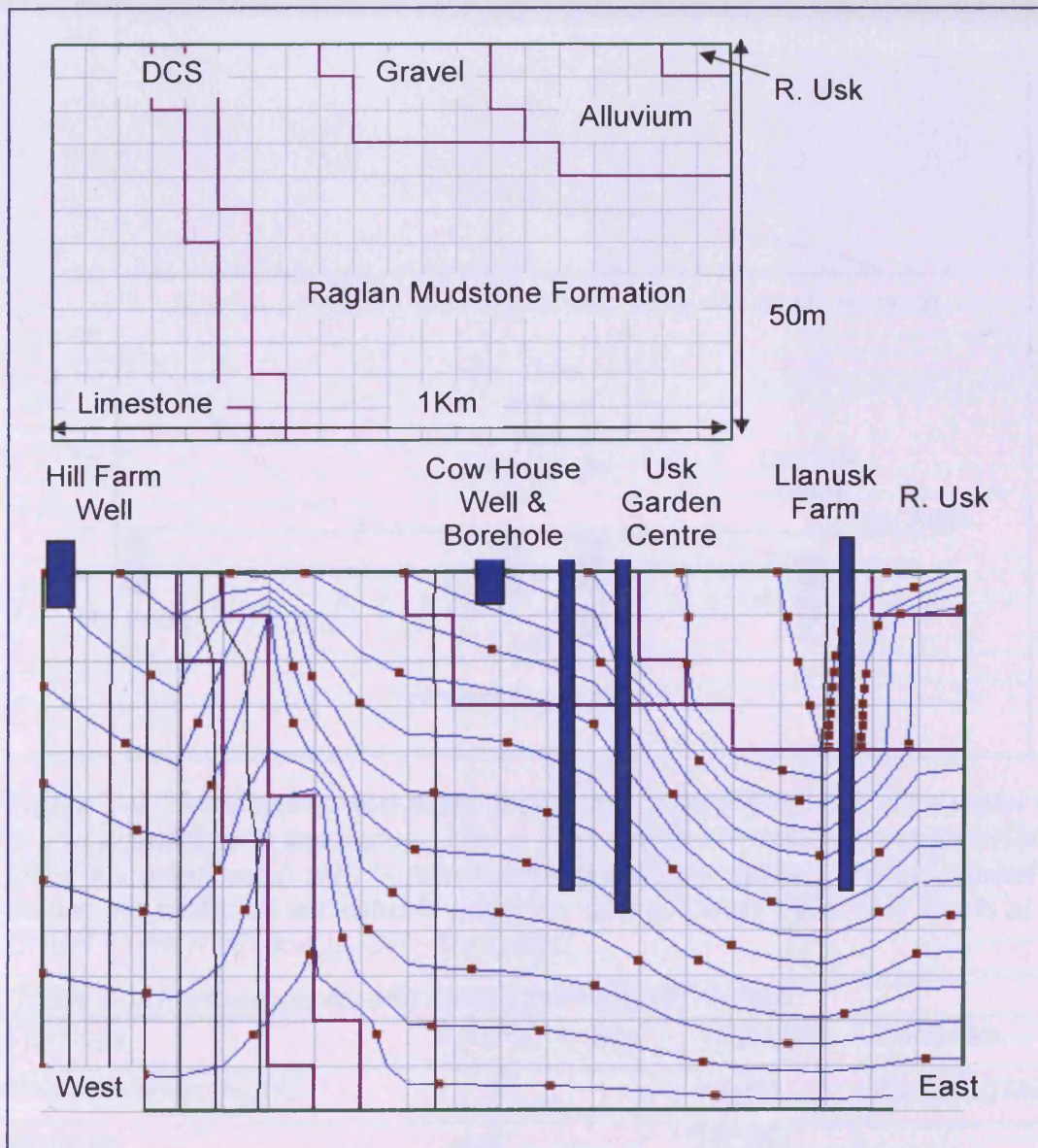


Figure 7-8 Flownet model HFW to River Usk. Upper image is model domain. Stream tubes 15, particle markers 5 years, head difference interval 5. Column scale 50m, row scale 5m. Note Usk Garden Centre is set back from profile line. Upper boundary is recharge flux boundary.

The water rest level at HFW was obtained from the borehole loggers and the stage of the River Usk was estimated from knowledge of the elevation at Pencarreg Farm. Various combinations of hydraulic properties were investigated, with the Downton Castle Sandstone being slightly problematic. The problem was the level of influence on flow from the limestones to the Raglan Mudstone Formation, and this determining whether it should be modelled as a separate entity or an extension of the bounding lithologies.

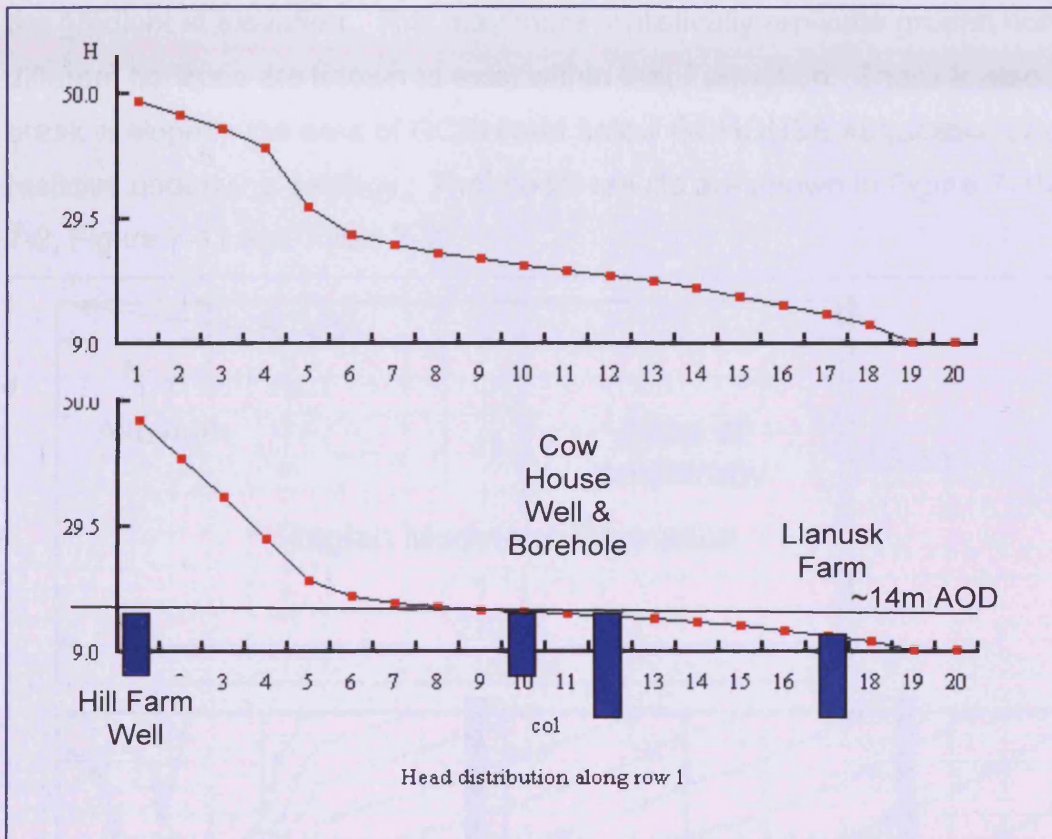


Figure 7-9 Head distribution along model row 1 for Figure 7-8. The water table is presented for two scenarios. Upper with a larger K value for the limestones, lower accepted value with borehole locations along profile. The calculated head values are within an acceptable accuracy of the known water rest levels at CHBH ~14m AOD and LUSK ~10m AOD.

Table 7-1 Parameters for Hill Farm Well Flownet model.

Lithology	Kx/Ky m day <sup>-1</sup>	Porosity	Remarks
Raglan Mudstone Fm	1 & 2	0.25	Pumping test
Alluvium	0.1	0.35	
Gravels	3	0.3	
Limestones	0.08	0.15	Fractures
Downton Castle Sandstone	0.5	0.1	High?

To complement the west bank model a similar model was constructed for the east flank (Figure 7-10). The hydraulic gradient in this area is believed to be steeper, with values at Glen Court House ~60m AOD and Glen Court Farm ~35m AOD. The topography also suggests a steeper gradient. The borehole locations on this flank do not align as well as on the west flank, therefore comparison with computed and observed head values are more subjective. This model also required the addition of a lower conductivity zone in the Raglan Mudstone Formation in order to increase the gradient at elevation. This may more realistically replicate ground conditions as different horizons are known to exist within that Formation. There is also a distinct break in slope in the area of GCBH and below GCHOUSE suggestive of a more resistive underlying geology. The model results are shown in Figure 7-10, Figure 7-2, Figure 7-11 and Table 7-2.

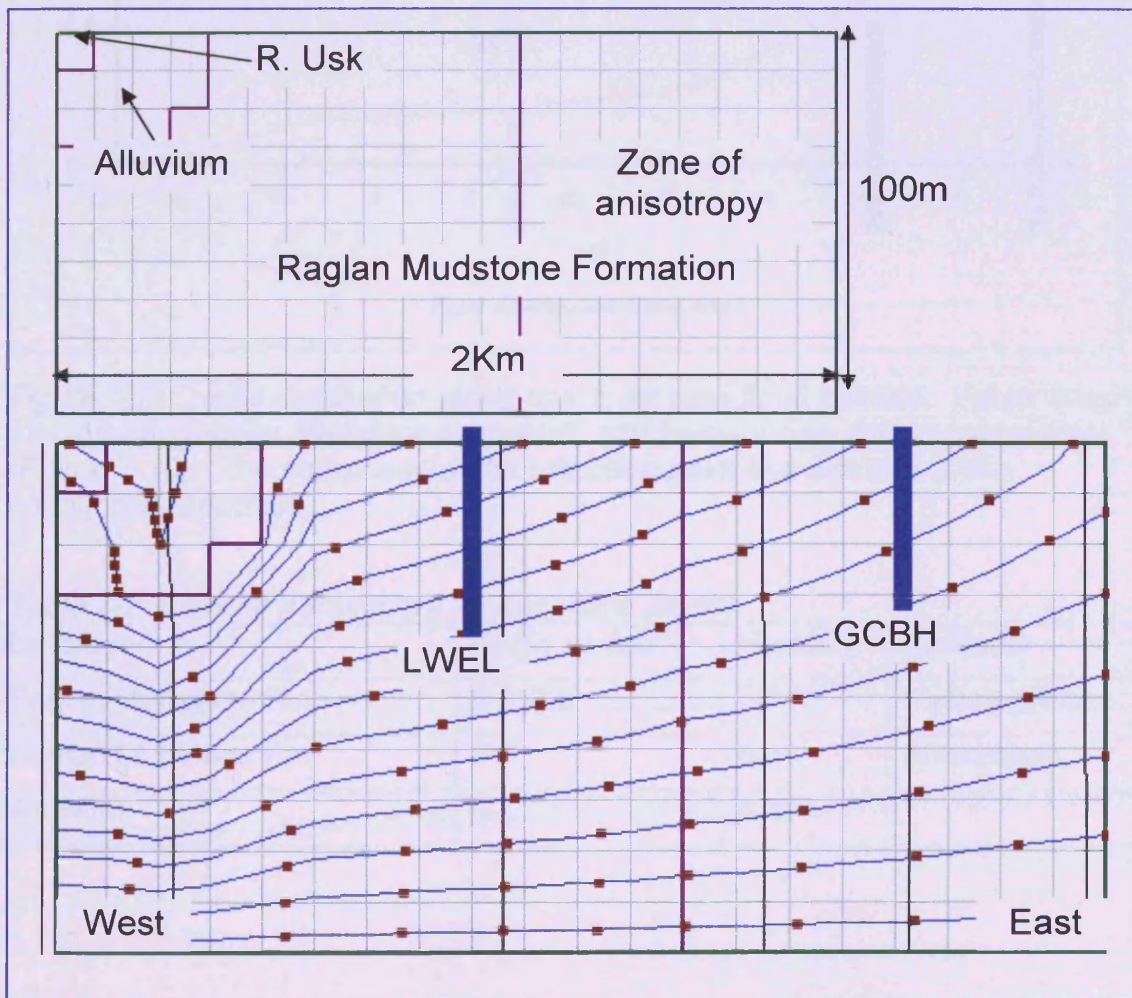


Figure 7-10 East flank model, Glen Court House to the River Usk. Upper boundary modelled as flux/recharge boundary. Stream tubes 15, head difference 10m, particles 5 years. Column scale 100m, row scale 10m. Note schematic positioning of LWEL and GCBH location.

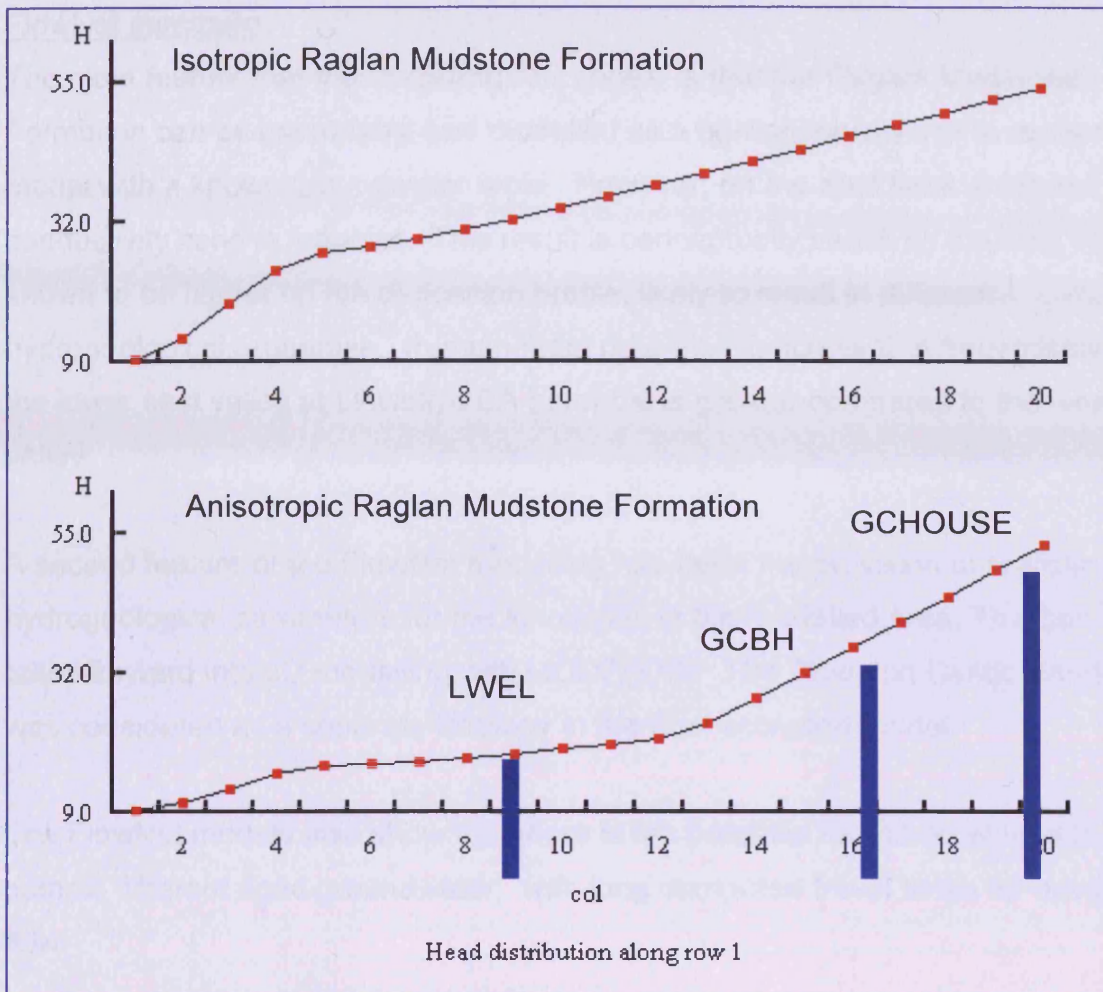


Figure 7-11 Head distribution along row 1; for east flank models. Upper image for isotropic Raglan Mudstone formation, and lower image anisotropic system (Figure 7-10). The sharpness of the inflection point is a function of the conductivity contrast.

Table 7-2 Flownet parameters for east flank model.

Lithology	$K_x/K_y \text{ m day}^{-1}$	Porosity	Remarks
Raglan Mudstone Fm	2 & 0.5	0.25	Pumping test
Raglan Mudstone Fm	0.5	0.25	Anisotropic
Alluvium	0.1	0.35	

### FlowNet summary

The main feature that the modelling has shown is that the Raglan Mudstone Formation can be reasonably well modelled as a homogeneous unit to realise the model with a known groundwater table. However, on the east flank a second lower conductivity zone is required. This result is conceptually viable as the east flank is known to be higher up the deposition profile; likely to result in different hydrogeological properties. Pumping test data also indicates that transmissivity in the lower east valley at Llewellyn EA borehole is greater compared to the western valley.

A second feature of the FlowNet modelling has been the provision of realistic hydrogeological parameters for the lithologies in the modelled area. This can be taken forward into 3D modelling with MODFLOW. The Downton Castle Sandstone was considered as a separate lithology in the final accepted model.

The FlowNet models also show that there is the potential for the boreholes to sample different aged groundwater, with long computed travel times for advection flow.

## 7.4 3D regional modelling with MODFLOW

### 7.4.1 Regional model

#### Model domain

In order to realistically assess the groundwater regime in the project area it is necessary to extend the model zone to account for any external influences. This extension is normally done to known boundaries, such as sources, sinks or significant geological changes. Once this regional model is acceptable, it is possible to transfer the modelled heads to a more localised model with the new boundary conditions. The regional model extent was 9 km x 9 km (334000 195000 to 343000 204000) and encompassed the high ground of the valley flanks and the northern reach of the River Usk and Olway Brook. It is recommended (Kresic 2007) that the model be orientated along the predominant direction of anisotropy, however as this was not known it was aligned with the National Grid.

The model comprised four layers with the base elevation representing -30m below sea level, which is designed to represent the ~40m of saturated flow thickness of the Upper and Lower Old Red Sandstones beneath the valley floor (Jones et al. 2000). The cell resolution was 450 m x 450 m.

The top (topographic) surface was obtained through Edina from Ordnance Survey DTM data. The lower surfaces were derived by application of a dip value taken from the geological mapping. This was deemed a suitable method as definite horizon data from borehole logs was not of sufficient resolution to indicate individual beds over the model extent. Therefore, the model considers the bedrock lithologies as a single unit in line with the hydrogeological conceptual model (*Figure 7-7*, *Figure 7-12* and *Figure 7-15*).

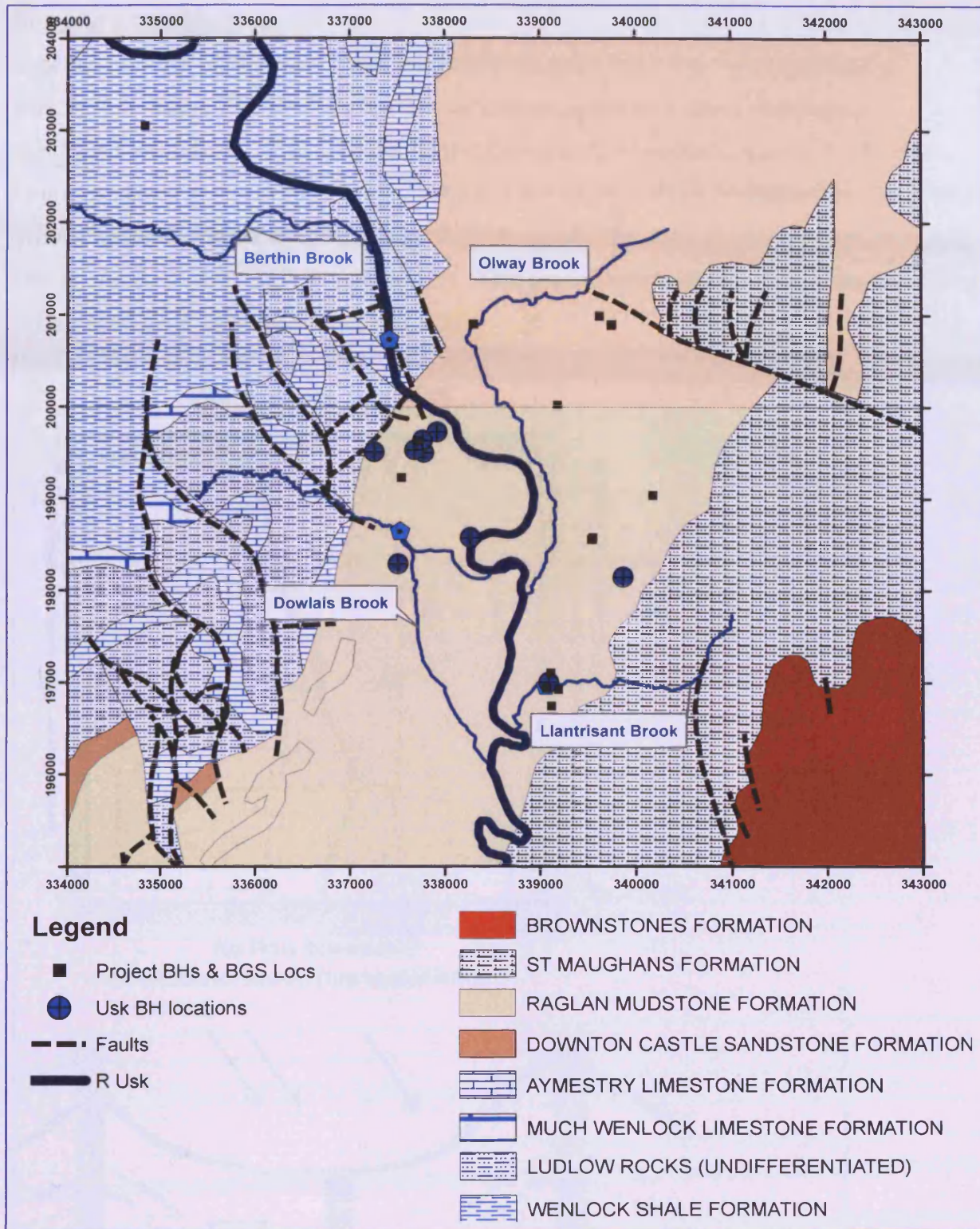


Figure 7-12 Geological setting for MODFLOW Regional model domain. Note Psammosteus limestone (between Raglan and St Maughan's Formation not shown).

### Boundary conditions

In order to more easily determine the model domain from the hydrogeological conceptual model (Figure 7-7) further conceptualisation of model boundary conditions was done. Two options were considered; specified head and no-flow boundary conditions (Figure 7-13). Whilst it is permissible to consider the groundwater divide as a no flow boundary its spatial context may vary with time and conditions (USCAE 1999; Kresic 2007). The groundwater divide may also be considered as a specified head boundary.

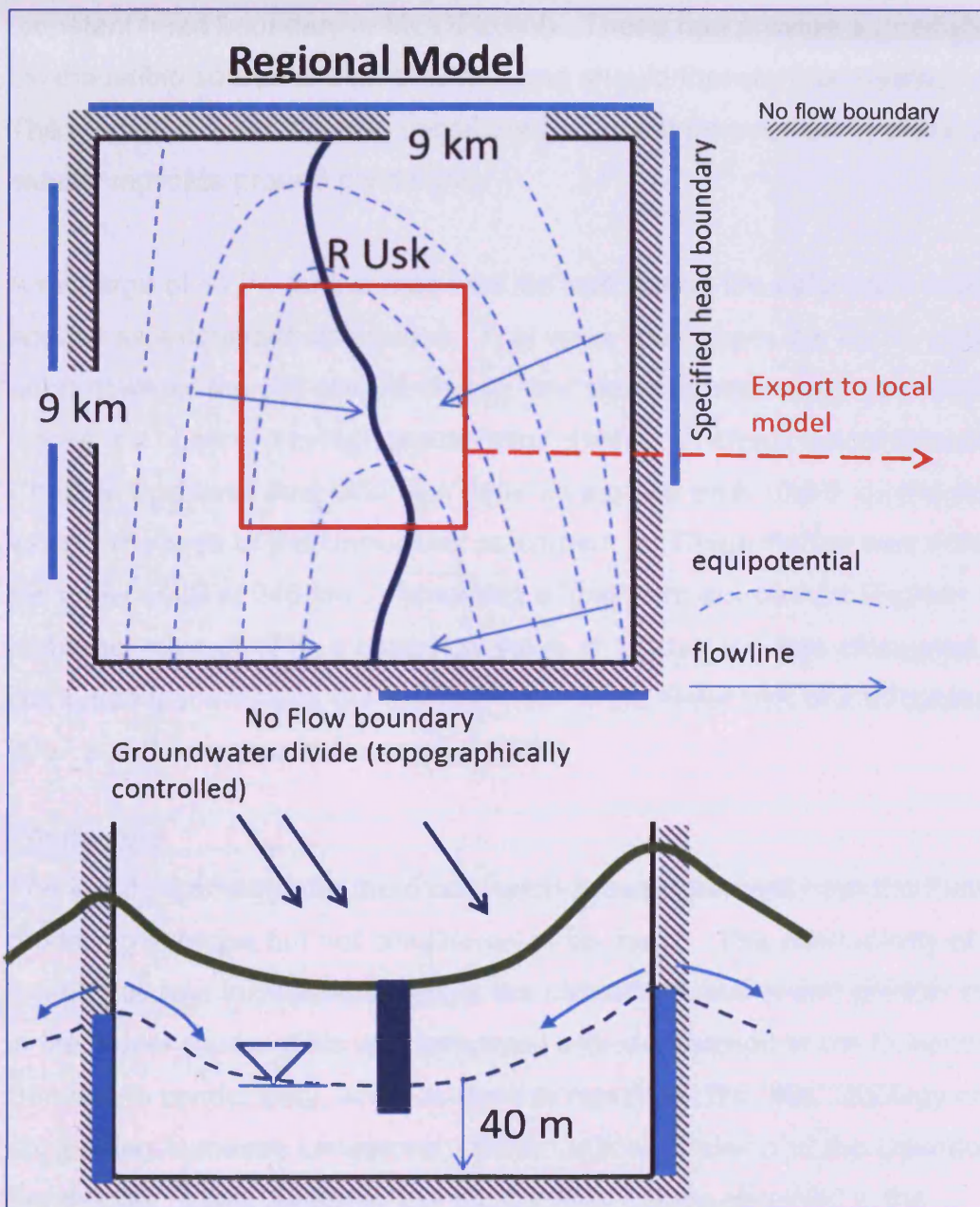


Figure 7-13 Conceptual boundary conditions in plan and profile for Regional model. Placement of specified head boundary are diagrammatic.

The no flow boundary conceptualisation (Figure 7-13) also treats the domain as a self-contained unit akin to an isolated basin. In this condition, equilibrium would become established between groundwater heads, recharge and discharge through the River Usk. This dictates that while the model edges have a high degree of uncertainty, given the correct parameter estimation, the central region is likely to reach a degree of harmonisation with ground truth. In order to reduce uncertainty in the model due to the no-flow boundary condition it was deemed appropriate to also model the east and west flank domain with specified head boundaries (constant head boundary in MODFLOW). These can provide a (modelled) inexhaustible source or sink of water, and should therefore be treated with caution. The modelled rivers are also considered as constant sources or sinks and may not exactly replicate ground conditions.

A recharge of ~17% for the area was derived during the calibration process and applied as a constant distribution. This value may seem low for an agricultural area, however the soil zone is clayey, and standing water and overland flow down slopes are observed in high precipitation events. A check calculation using the Chain Bridge base flow data was done as a gross error check on the recharge value. The area of the Upper Usk catchment for Chain Bridge was obtained from the project GIS at 248 km<sup>2</sup>. Assuming a long term equilibrium (Ingram 1978) and a recharge value of 17%, a base flow value of 1.8cumeecs was calculated. This compares favourably to the low flow data of the River Usk of 2.07cumeecs in July 2007 and 3.5cumeecs in September 2007.

### Parameters

The initial parameters for the model were brought forward from the Flownet modelling exercise but not considered to be 'fixed'. The conductivity of the limestones was increased to reflect their fractured nature and greater sampled zone in the model space. This was tempered with a reduction in the Downton Castle Sandstone conductivity, which is used to represent the 'thin' lithology change comprising Aymestry Limestone; Upper Ludlow Shales and the Downton Castle Sandstone. It was assigned low conductivity values obtained in the conceptualisation model and consistent with field observations (Figure 7-6).



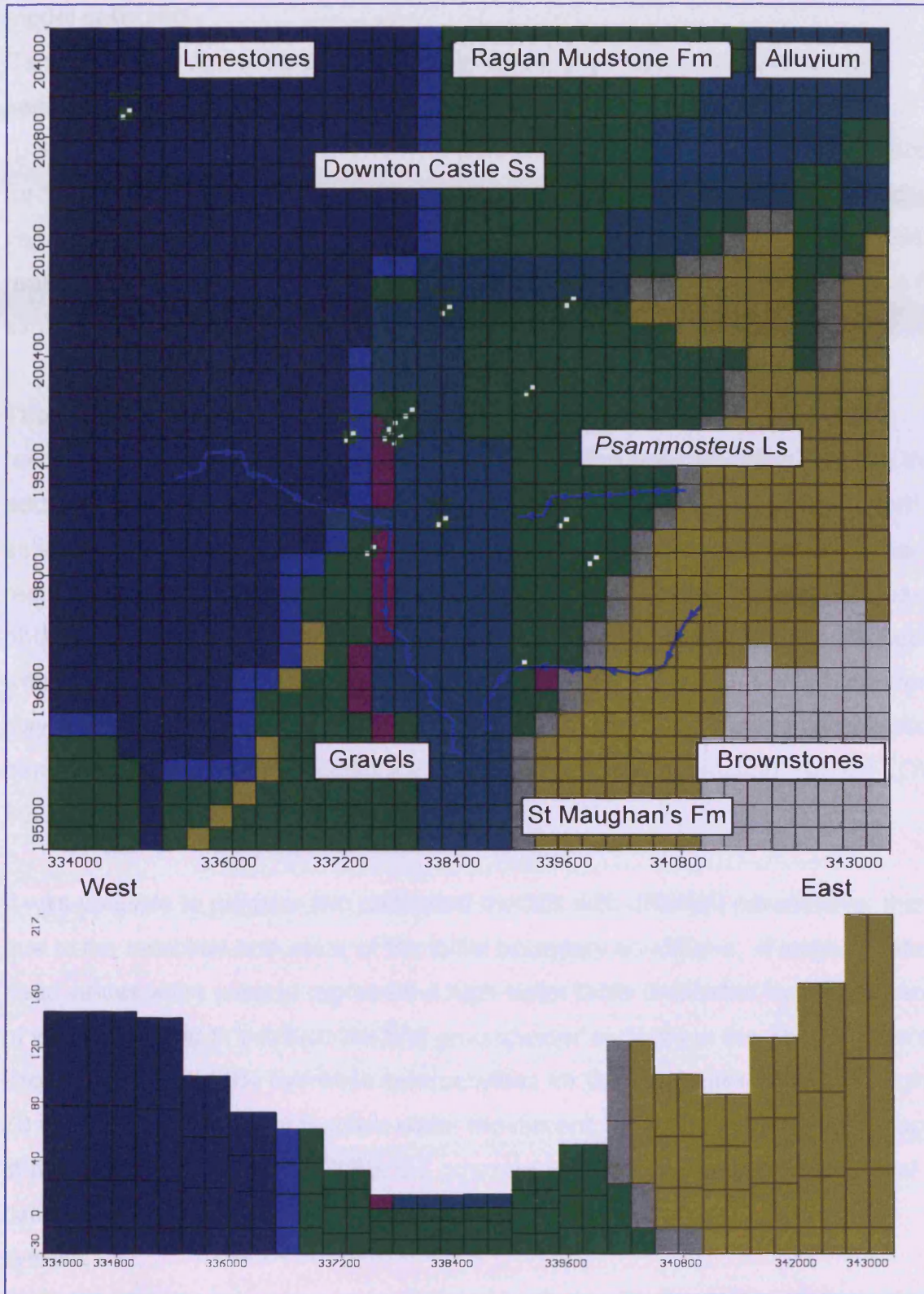


Figure 7-15 Realisation of the ground to the Regional model surface, lower image typical row profile. Head calibration points (BH locations) also shown.

### Model calibration

Calibration was achieved by a trial and estimate process, in conjunction with sensitivity analysis, using the previously derived Flownet parameter values (USCAE 1999; Kresic 2007). The hydraulic conductivity of  $\sim 1$  to  $2 \text{ m day}^{-1}$  obtained for the Raglan Mudstone Formation was considered to be the only 'semi-fixed value'. The adjacent lithology parameters were refined during this process and reality checks on literature values were made. Both steady state and transient flow simulations were undertaken using two boundary condition scenarios.

The observed borehole heads can be considered to have a good temporal resolution, but poor model spatial distribution. During the calibration process the addition data from the BGS and Apex Drilling borehole logs was used as a further estimator of convergence towards a realistic representation of the groundwater regime. The inbuilt inverse parameter estimation (PEST) function was also used to obtain optimisation of a calibrated solution, however the results must be accepted with caution as "PEST does not differentiate between a sand and gravel aquifer or a clay confining unit; it simply uses the information it has to estimate a combination of parameter values that minimized the objective [calibration] function" (MODFLOW 2002).

It was possible to produce two calibrated models with different parameters; this was due to the selection and value of the initial boundary conditions. If large constant head values were used to represent a high water table (indicated by the presence of wells and used to produce the first groundwater surface) in the St Maughan's and Brownstones, then the hydraulic conductivities for the lithologies were also high  $\sim 70$  to  $130 \text{ m day}^{-1}$  in order to allow water movement. A similar situation developed in the limestones. This highlights the potential for 'non-uniqueness' in a model calibration, the results of which must be tempered with understanding of the system.

#### 7.4.2 ***Specified head boundary condition***

The specified head boundary modelling was done in order to test the potential of elevated groundwater on the valley flanks providing the driver for fracture flow within the aquifer zone (Moreau et al. 2004). Using this boundary to simulate the groundwater flow on the domain edges was problematic as addition of specified heads and an increase in lithology conductivity can result in the same calibration agreement. This inverse calibration was also undertaken in conjunction with various recharge and streambed conductance estimates. During the calibration process it became apparent that the River Usk was acting as a partition between the calibration boreholes on either side of the river, which is also indicated in the Flownet modelling and geochemistry results. This calibration also highlighted the fact that the lithologies are unlikely to be homogeneous at the model scale. This was apparent in the lack of calibration harmonisation most notably at LDOW, LWEL and GCBH.

The final accepted calibration for the Regional model was in general within 1m of the measured value. The exceptions were Llandowlais Farm (LDOW), the calculated value being too high by ~4.5m indicating too much water in the system and Glen Court Farm (GCBH) where the modelled level was below observed values by ~15m. This confirms the Flownet modelling that a local heterogeneity may influence the local groundwater flow within this area.

Table 7-3 MODFLOW accepted hydraulic parameters  $K$  for Regional specified head boundary condition.

Lithology	$K_{xy}$ m day <sup>-1</sup>	$K_z$ m day <sup>-1</sup>	Remarks
Limestones	5	10	Axial fractures
Raglan Mudstone Formation	3	2	Pumping test. Homogeneous unit
St Maughan's Formation	25	10	Channel sandstones
Brownstones	30	25	Flaggy
Alluvium	$5 \times 10^{-3}$	$5 \times 10^{-4}$	
<i>Psammosteus</i> Limestone	0.1	0.1	(Jones et al. 2000)
Downton Castle Sandstone	0.01	1	Sub-vertical orientation
Terrace gravels	6	4	

#### Sensitivity analysis

As part of the calibration process a sensitivity analysis was also undertaken; a selection for the Raglan Mudstone Formation is presented in Table 7-4. These data are best presented in tabular format.

Table 7-4 Sensitivity analysis results for Raglan Mudstone Formation, constant  $K_z$  and accepted boundary condition. All values in m AMSL.

$K_{xyz}$ m day <sup>-1</sup>	LTRI	LUSK	PENC	CHBH	CHW	GCBH	HFW	LDOW	LWEL
Observed	11.66	12.09	11.35	12.68	15.76	35.43	50.19	12.55	17.94
1,1,2	20.8	12.95	9.66	16.69	17.65	25.97	43.41	26.34	24.36
2,2,2	17.93	11.92	9.69	14.58	14.95	23.16	42.48	25	21.32
3,3,2	16.3	11.53	9.71	13.68	13.85	21.61	42.07	22.72	19.7
4,4,2	15.08	11.25	9.71	12.84	12.94	20.6	41.47	19.42	18.84

Additional lithology data not shown

### Model characteristics

The model has some distinctive characteristics. There is apparent groundwater flow from both valley flanks towards the River Usk, indicative of a gaining system. The model also indicates that topography and the faults are factors in the groundwater flow. The flow is from higher topography to lower zones, although the unexpected result is that of a northerly flow direction from the area west of the observation boreholes; HFW and CHW towards the Berthin Brook and River Usk (Figure 7-16). This is partially explained by the resolution of the model and the fractured nature of the modelled aquifer. Large variations in altitude will induce a strong potential hydraulic gradient forcing the movement of groundwater through the (sandstone) aquifer (Moreau et al. 2004); this will also affect the limestones. The Berthin Brook may be a local gaining system which will induce these northerly flows. The model processes the upper two layers as dry cells, which may be indication of the fracture flow, it is also considered to be a more accurate interpretation of 'water table aquifers' (Kresic 2007).

The contrast in groundwater behaviour in the different modelled lithologies is also apparent. The main contrast zones are between the *Psammosteus* Limestone and the Downton Castle Sandstone. These lower conductivity zones are acting as a semi-barrier, as evidenced by the location of spring lines at their base. It is believed that these modelled zones are important controls within the groundwater regime. During calibration it was evident that changes in their properties altered the calibration quality of fit by allowing 'more water' into the lower valley zone.

The zone of the Dowlais Brook may be imperfectly modelled; this brook incises a narrow west to east draining valley on the west flank. It is expected that some groundwater movement occurs southwards due to topography controls (in a similar fashion to the Berthin Brook) as the valley is expected to act as a surface water sub-catchment (Figure 7-16 and Figure 7-19).

## Flowlines

The groundwater 'velocity vectors' option is a tool for indicating the model groundwater flow direction (Figure 7-16).

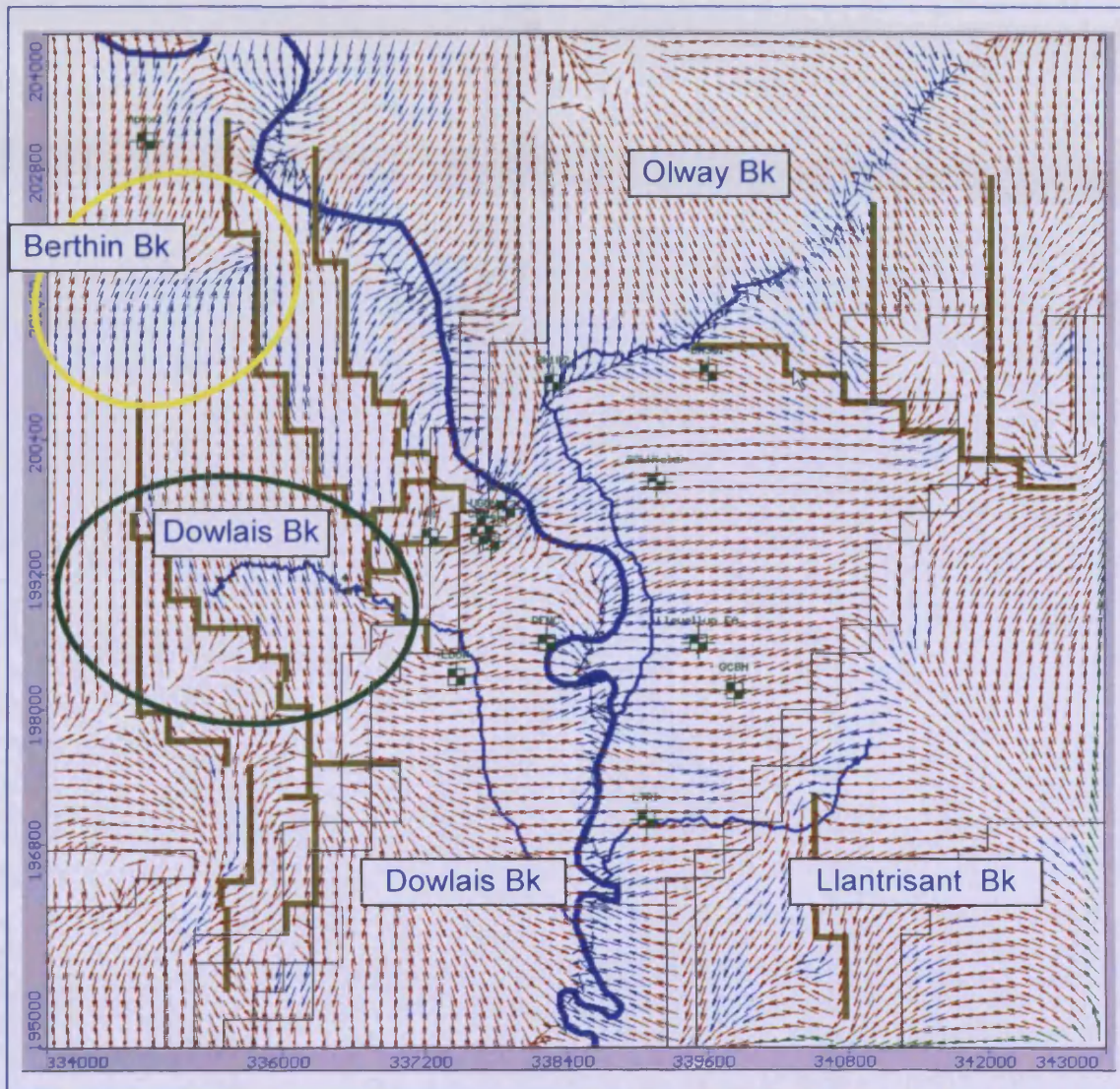


Figure 7-16 MODFLOW Layer 3 groundwater direction vectors for whole model domain. Vector colours indicate; Blue out of plane of view, Red into plane; Green in plane. Berthin Brook zone yellow ellipse, Dowlais Brook zone green ellipse.

### 7.4.3 No-flow boundary condition

This was undertaken to consider the concept of the groundwater divides acting as no flow zones and with a state of equilibrium within the centre of the model.

The model was run with the same recharge and river conditions as in the specified head model. Again during the calibration process it became apparent that the lithologies were heterogeneous at the model scale. In a similar result to the specified head modelling the locations LDOW, LWEL and GCBH proved difficult to calibrate. The final accepted conductivity values for the model are in Table 7-5.

*Table 7-5 MODFLOW accepted parameters K for the Regional no-flow boundary condition.*

Lithology	$K_{xy}$ m day <sup>-1</sup>	$K_z$ m day <sup>-1</sup>	Remarks
Limestones	0.5	1	Axial fractures
Raglan Mudstone Formation	3	2	Pumping test. Homogeneous unit
St Maughan's Formation	25	10	Channel sandstones
Brownstones	30	25	Flaggy
Alluvium	$5 \times 10^{-3}$	$5 \times 10^{-4}$	
<i>Psammosteus</i> Limestone	0.1	0.1	(Jones et al. 2000)
Downton Castle Sandstone	0.01	1	Sub-vertical orientation
Terrace gravels	6	4	

#### Sensitivity analysis

Again a sensitivity analysis was performed as part of the calibration process, and the results are presented in graphical and tabular formats (Table 7-6 and Figure 7-17). The investigation shows that there is a lack of response at some locations, such as PENC and HFW. This believed to be due to HFW sampling the limestones and Downton Castle Sandstone, and the proximity of PENC to the River Usk (~70m), which is influencing the modelled head values; a 1.4m range was observed during the manual dip investigations. Additional sensitivity analysis for the other lithologies and rainfall is in Enclosure 1 CD.

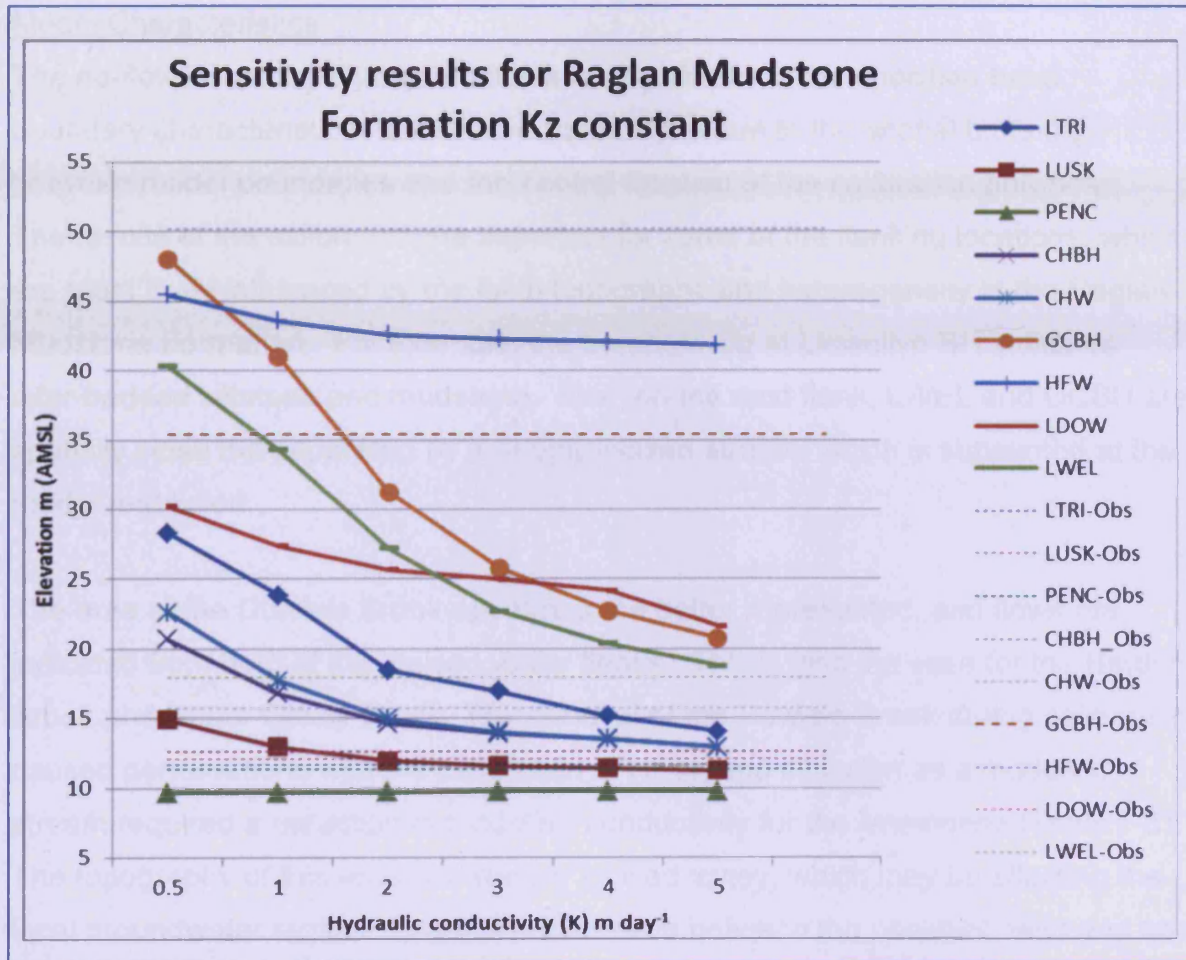


Figure 7-17 Sensitivity analysis graph in Raglan Mudstone Formation for no-flow boundary condition. Note lack of impact at some boreholes.

Table 7-6 Sensitivity analysis results for Raglan Mudstone Formation, constant  $K_z$  and no-flow boundary condition. All values in m AMSL.

$K_{xyz}$ m day <sup>-1</sup>	LTRI	LUSK	PENC	CHBH	CHW	GCBH	HFW	LDOW	LWEL
Observed	11.66	12.09	11.35	12.68	15.76	35.43	50.19	12.55	17.94
0.5, 0.5,2	28.29	14.9	9.65	20.68	22.59	48.02	45.44	30.22	40.32
1,1,2	23.82	12.97	9.66	16.77	17.71	41.03	43.6	27.36	34.3
2,2,2	18.45	11.94	9.69	14.64	15	31.25	42.62	25.66	27.19
3,3,2	16.96	11.59	9.72	13.88	14.03	25.79	42.26	24.99	22.69
4,4,2	15.17	11.41	9.74	13.47	13.51	22.69	42.06	24.17	20.37
5,5,5	14.06	11.24	9.75	12.91	12.92	20.72	41.84	21.65	18.78

Additional lithology data not shown

### Model Characteristics

The no-flow boundary characteristics are very similar to the specified head boundary characteristics. It is believed that this is due to the spatial buffering between model boundaries and the central location of the calibration boreholes. The results of the calibration are imperfect for some of the flanking locations, which are most likely influenced by the local topography and heterogeneity in the Raglan Mudstone Formation. For example, the borehole log at Llewellyn BH indicates inter-bedded siltstone and mudstone. Also, on the east flank, LWEL and GCBH are spatially close but separated by a deeply incised stream, which is subsumed at the model resolution.

The area of the Dowlais Brook appears to be better represented, and flows are indicated from both of the incised valley flanks. This is also the case for the Berthin Brook and Upper Olway Brook. The removal of the Dowlais Brook during calibration caused perturbations with the calibration of HFW, and inclusion as a modelled stream required a reduction in modelled conductivity for the limestones (Table 7-5). The topography of this area is a steeply incised valley, which may be affecting the local groundwater regime. There is a difference between the constant head and no-flow models in the *Psammosteus* Limestone area which may be influencing the poor calibration at GCBH and LWEL.

The model flowlines also appear to follow the potential and conceptual groundwater divide, if existing within the regional area, better than the specified head boundary condition (Figure 7-19).

### Flowlines

Figure 7-18 shows the modelled flowlines for the no-flow boundary condition. In addition the flowlines have also been superimposed on the DTM (Figure 7-19) in order to graphically assess the model groundwater divides as imposed by the topography and recharge.

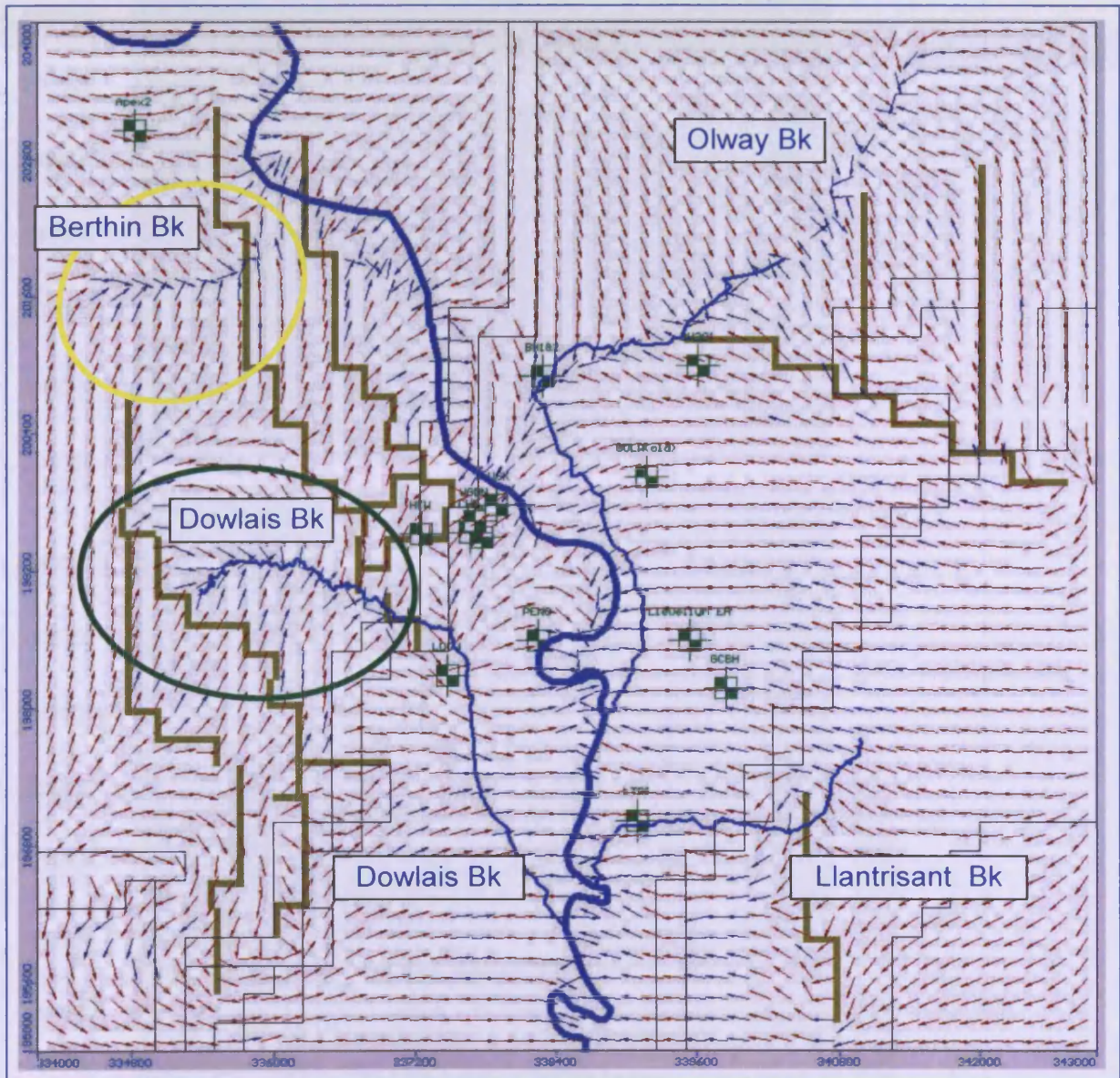


Figure 7-18 MODFLOW Layer 3 groundwater direction vectors for whole no-flow boundary model domain. Vector colours indicate; Blue out of plane of view, Red into plane; Green in plane. Berthin Brook zone yellow ellipse, Dowlais Brook zone green ellipse. This figure should be compared with Figure 7-16 and Figure 7-19.

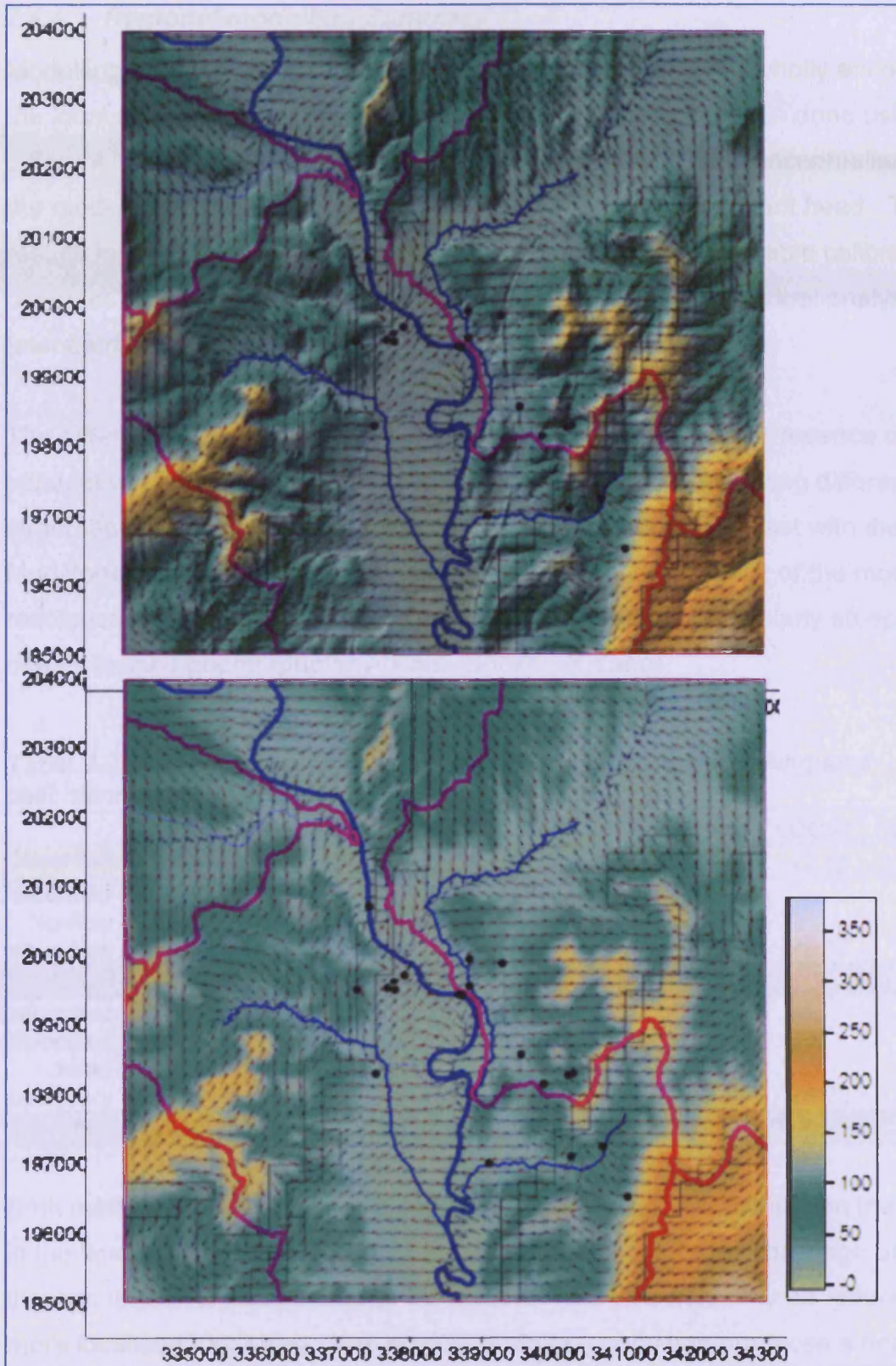


Figure 7-19 MODFLOW Flowlines for no-flow boundary condition superimposed on DTM. Purple lines are EA catchment delineations. Velocity vectors as direction and not scaled. Elevation scale in m AMSL

#### 7.4.4 Regional modelling Summary

Modelling has been carried out on a regional scale in order to wholly encompass the local area with the groundwater observations. This has been done using two different conceptual methodologies, the distinction being the conceptualisation of the model domain boundary conditions; either no-flow or constant head. The results for both models are similar, and both achieve an acceptable calibration with observed data. The results of the accepted calibration and residual analysis (standard deviation) are in Table 7-7.

The differences between the two models indicate the probable presence of local conductivity heterogeneity, possibly due to the boreholes sampling different stratigraphic horizons and exacerbated by the local dip to the east with the Raglan Mudstone Formation. They may also be caused by the inability of the model resolution to adequately harmonise with the topography, particularly steep and deeply incised geomorphology (Pers. Comm., Y Yang).

Table 7-7 Final accepted calibration results for Regional modelling and calibration residual analysis

	LTRI	LUSK	PENC	CHBH	CHW	GCBH	HFW	LDOW	LWEL	SDev
Observed	11.66	12.09	11.35	12.68	15.76	35.43	50.19	12.55	17.94	
Calculated No-flow boundary	16.97	11.63	9.72	13.95	14.16	25.79	47.09	25.17	22.7	
Residual	-5.31	0.46	1.63	-1.27	1.6	9.64	3.1	-12.62	-4.76	5.9
Calculated Specified head boundary	16.3	11.53	9.71	13.68	13.85	21.61	42.07	22.72	19.7	
Residual	-4.64	0.56	1.64	-1	1.91	13.82	8.12	-10.17	-1.76	6.3

Both methods produce a similar result, although due to its distribution the variation in the limestone conductivity may be problematic for HFW and passage of water through to the Raglan Mudstone Formation. This influence may be reduced in the more localised modelling. The no-flow boundary condition produces a better residual and visually the flow lines appear to better follow the topography. In addition the model is not unduly influenced by excessive water supplied from the specified head boundaries.

## **7.5 3D local modelling with MODFLOW**

### **7.5.1 Local Model**

#### **Model domain**

The regional area model provided insights into possible boundary conditions and initial hydraulic parameters for a localised project area model. This local model has an areal extent of 5km x 6km (195300 336000 to 341000 201300), and the grid resolution was 100m x 100m cells with 50 x 60 rows/columns (Figure 7-20). This model still has a buffer of ~1200m from the east west model edge to the calibration boreholes.

#### **Boundary conditions**

Boundary conditions were taken from the regional modelling exercise, with the east west boundary chosen to coincide, where possible, with a topographic ridge. Initial specified head values were taken from the Regional model and applied (Figure 7-21). The use of specified head boundaries can provide infinite water to the model therefore their use must be carefully considered. To monitor this potential water flux the system was also modelled as no-flow boundaries to investigate the sensitivity of the calibration to changes in these parameters.

#### **Parameters**

Initial parameters, including recharge, were carried forward from the Regional model and served as a basis for local model calibration. The Dowlais and Llantrisant Brooks were also included.

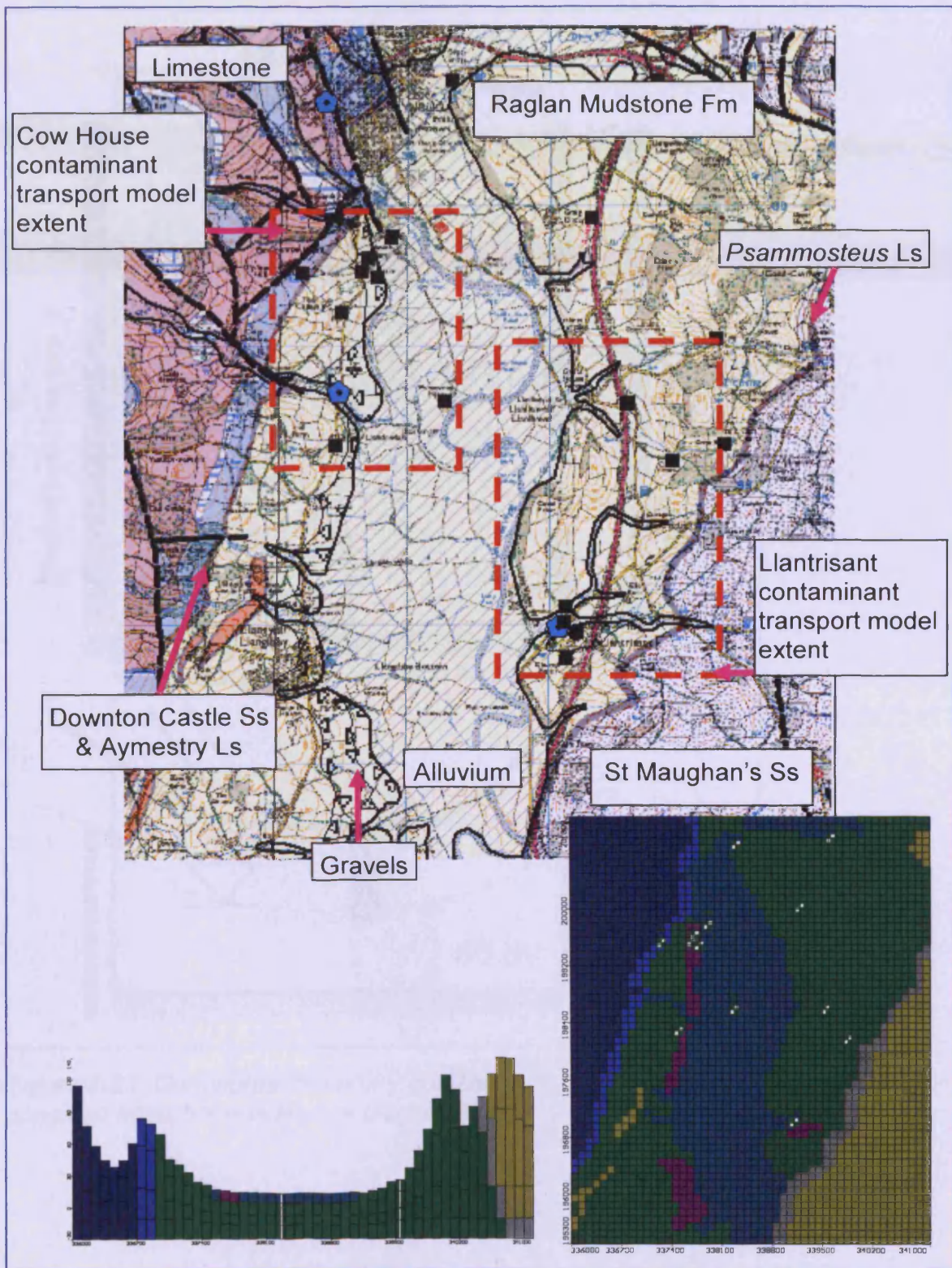


Figure 7-20 MODFLOW realisation of the local area with the Local model domain. Colours and lithology are the same as the conceptual and Regional models. Red dashed boxes are extents of refined contaminant transport models.

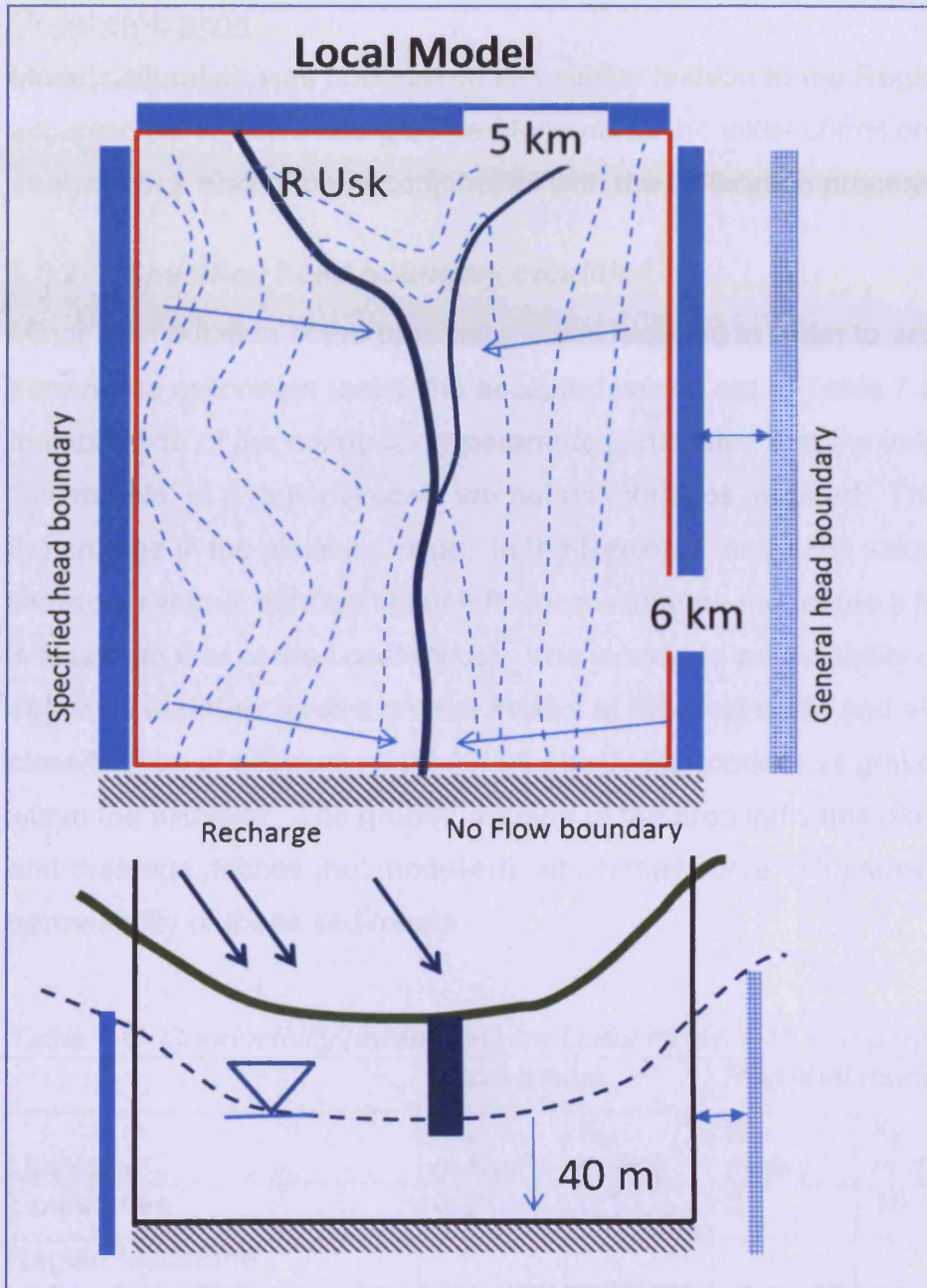


Figure 7-21 Conceptual boundary conditions for local model. Placement of specified head boundaries are diagrammatic.

### Model calibration

Model calibration was undertaken in a similar fashion to the Regional model, the accepted parameters being carried forward as the initial condition. Sensitivity analysis was also done in conjunction with the calibration process.

#### 7.5.2 *Specified head boundary condition*

Minor manipulation of the parameters was required in order to achieve an acceptable calibration result; the accepted values are in Table 7-8. The manipulation of the conductivity parameters indicates that the initial values while 'acceptable' at a regional scale are not as robust as required. This is indicated by the change in the alluvium value. In the Regional model the values are within literature ranges, although their influence within the model (as a function of volume) is less than that of the Local model. The increased permeability of these sediments suggests that they have a greater impact at the local scale and also that the classification of alluvium might not be strictly appropriate as gravel is reported within the alluvium. The ground-truthing of the area indicates old cut-off meanders and drainage ditches (not modelled), which may serve to increase the overall permeability of these sediments.

*Table 7-8 Conductivity parameters for Local model with comparison data.*

	Local model		Regional model	
	$K_{xy}$ m day <sup>-1</sup>	$K_z$ m day <sup>-1</sup>	$K_{xy}$ m day <sup>-1</sup>	$K_z$ m day <sup>-1</sup>
Limestones	0.08	0.1	5	10
Raglan Mudstone Formation	3.5	2.5	3	2
St Maughan's Formation	20	10	25	10
Brownstones	-	-	30	25
Alluvium	0.9	0.5	$5 \times 10^{-3}$	$5 \times 10^{-4}$
<i>Psammosteus</i> Limestone	0.05	0.05	0.1	0.1
Downton Castle Sandstone	0.008	0.5	0.01	1
Terrace gravels	12	8	6	4

### Sensitivity analysis

The sensitivity analysis for the Local model calibration is shown in Table 7-9. This clearly shows that HFW is isolated, in model terms, from the Raglan Mudstone Formation, and that the Formation is heterogeneous requiring different conductivities to harmonise individual calibration boreholes. There is a much better congruence at LDOW and LWEL, at the expense of HFW and GCBH.

*Table 7-9 Sensitivity analysis results for Raglan Mudstone Formation and limestones for specified head boundary condition. All values in m AMSL*

$K_{xyz}$ m day <sup>-1</sup>	LTRI	LUSK	PENC	CHBH	CHW	GCBH	HFW	LDOW	LWEL
Observed	11.66	12.09	11.35	12.68	15.76	35.43	50.19	12.55	17.94
1,1,2	No convergence								
2,2,2	13.44	11.24	9.8	12.67	12.67	22.01	19.07	14.5	18.27
3,3,2	12.66	11.05	9.81	12.1	12.12	20.73	18.89	13.39	17.48
3.5,3.5,2	12.38	10.99	9.81	11.9	11.93	20.27	18.83	13.03	17.21
4,4,2	12.18	10.96	9.82	11.77	11.8	19.92	18.79	12.75	17.01
5,5,2	11.86	10.89	9.82	11.55	11.58	19.34	18.73	12.32	16.66
Limestone sensitivity using accepted Raglan Mudstone Formation values									
5,5,10	12.38	10.99	9.81	11.9	11.93	20.27	18.83	13.03	17.21
0.5,0.5,	12.38	11.22	9.86	12.78	12.79	20.28	25.12	14.88	17.21
0.1	12.38	11.22	9.86	12.77	12.78	20.28	25.35	14.86	17.21
0.08,0.08,0.1	12.38	11.28	9.87	13.0	13.62	20.28	32.26	15.26	17.21
Downton Castle Sandstone using accepted values									
0.008,0.008,,0.5	12.36	11.58	9.93	14.08	14.1	20.24	47.07	17.57	17.12

Accepted values in grey cells.

In general the model results were within 1m of the mean measured value and are approaching a more robust solution (Figure 7-22). At CHW the difference was ~2m, however at the adjacent CHBH the mean difference was within ~0.5 to 0.75m. This lack of harmonisation is due to model scale and well type, the well is believed to be locally perched within the gravels, whereas the CHBH penetrates to the underlying Raglan Mudstones.

At Hill Farm Well (HFW) the addition of a constant head in this area to simulate the higher heads (see conceptualisation and flownet models) resulted in a less well-adjusted calibration for the other boreholes. The well is in the low permeability zone of the Downton Castle Sandstone and down slope of a spring; further evidence of low permeability. However, a change in horizontal hydraulic properties of the Downton Castle Sandstone (Table 7-9) is shown to produce a better harmonisation; this confirms the conceptual model representation of this lithology with the near vertical bedding impeding horizontal flow.

#### *Model Characteristics*

The main difference between the Local model and that of the Regional model is the change in the conductivity values for the limestones, terrace gravels and Downton Castle Sandstone. These changes have been shown to affect only the boreholes which sample those particular lithologies; for example changes in the limestone conductivity have a minimal effect at CHBH or LUSK (Table 7-9). The model is still unable to fully calibrate the locations at HFW and GCBH, and LDOW is marginal. This again suggests that local heterogeneities must exist with the aquifer zone that are not replicated in the model.

#### *Flowlines*

The model flowlines are shown in Figure 7-22, superimposed on the local DTM. They clearly show the effect of the topography which is believed to be the driver for flows (Moreau et al. 2004). The Dowlais Brook zone is believed to be better represented and is very similar to the no-flow boundary condition Regional model. The flowlines also indicate the influence that the model DTM has on flows, which is believed to be replicated on the ground.

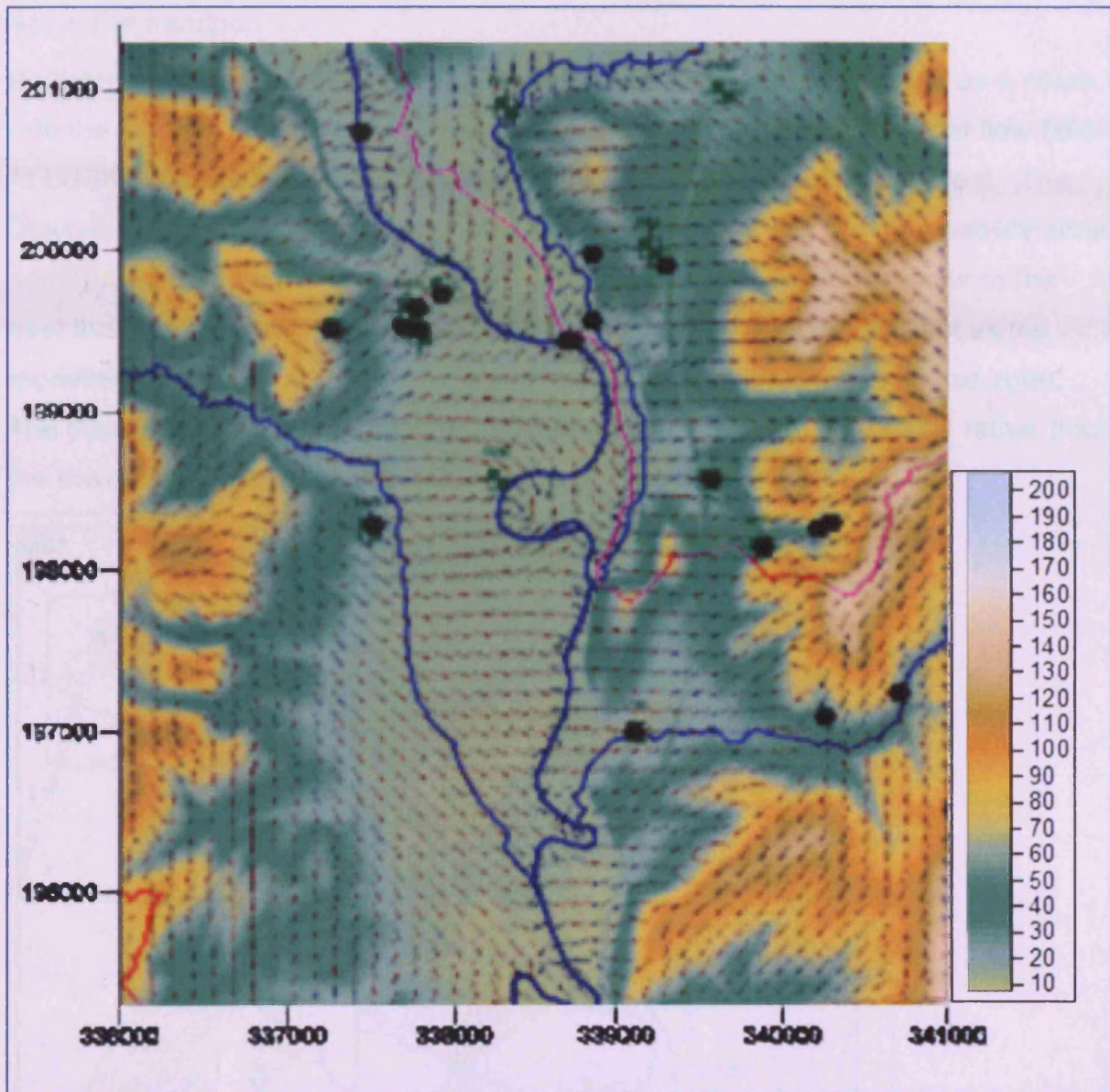


Figure 7-22 MODFLOW Flowlines for local specified head condition boundary superimposed on DTM. Note change in vertical scale from Figure 7-19. Purple line is sub-catchment boundary; elevation scale in m AMSL.

### Advective transport

Particles were released in the Local model to investigate flow paths and as a check with the Regional model. In general the trend is the same as the regional flow field. At LUSK the influence of the Downton Castle Sandstone is not as apparent. The Dowlais Brook valley zone still appears to flow northward; the low permeability zone perhaps acting as a barrier. There is evidence that some flow does occur to the east through the zone of the valley mouth. This may be a model artefact as the modelled stream is indicated as a losing system (above limestones) in this zone. The steady state tracking option terminates a particle at a source or sink rather than the travel time option which terminates the particle a set epoch.

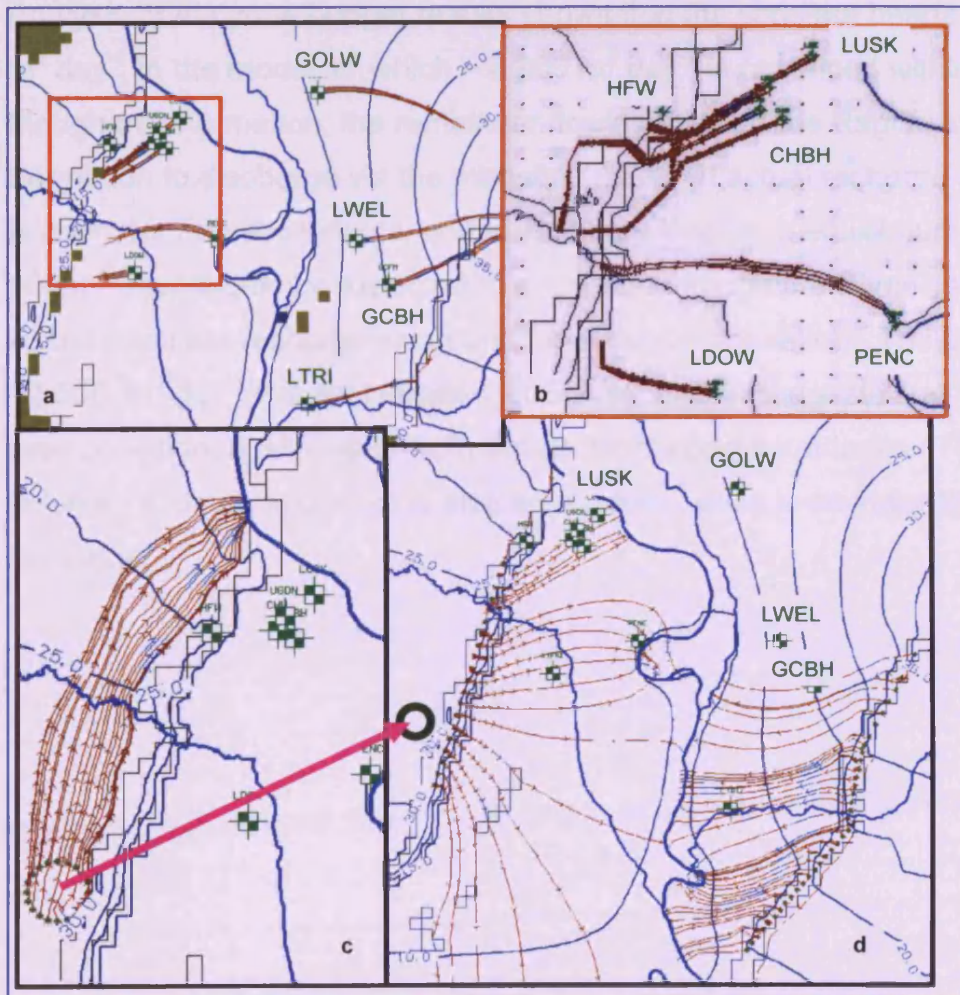


Figure 7-23 MODFLOW particle tracking. (a) Steady state backward tracking from boreholes. (b), layer 4 steady state enlargement of zone around Cow House orange outline in (a); (c), enlargement of particles released up gradient of Downton Castle Sandstone showing model flow towards north; possibly with lithology acting as a barrier (d), particles released from low conductivity zones in layer 4. Path line ticks every 10 years.

### Water balance

The zone budget function in MODFLOW calculates water flow and mass balance between designated model zones. It is stated that if the mass balance error for a well calibrated model is more than 2%, there is likely to be some inconsistencies in the results (MODFLOW 2002). The function was run in both transient and steady state modes and the mass balance error was checked. Zone budgets for the model were assigned to the different lithologies in order to consider the contributions that each lithology may make to the groundwater system.

The water budgets (Table 7-10) are from the transient flow simulation for day 1064. Analysis of the zone budget results shows that the constant heads provide ~ 18 000 m<sup>3</sup> day<sup>-1</sup> to the model, of which ~ 8 000 m<sup>3</sup> day<sup>-1</sup> is contained within the St Maughan's Formation; the remainder flowing through the Raglan Mudstone Formation to discharge via the modelled rivers. If actual recharge alone was to account for modelled inputs, and assuming a long term equilibrium, then about 19 000 m<sup>3</sup> day<sup>-1</sup> would be expected to discharge through the River Usk. This value is based upon the recharge value and model area calculation. The difference of ~2 500 m<sup>3</sup> day<sup>-1</sup> (model indicates 21 564 m<sup>3</sup> day<sup>-1</sup>) suggests that the model is not over conditioned with water from the constant head boundaries. The mass balance between sources and sinks is also acceptable, which is an indication of stability in the model.

Table 7-10 MODFLOW zone budget values for Local Mode; specified head boundary condition. Values in  $m^3$  day<sup>-1</sup>. Gravels values not tabulated. Values are rounded and if less than 100  $m^3$  day<sup>-1</sup> not presented. Source and sinks highlighted in grey.

From Zone	To Zone								
	Limestones	Raglan Mudstone Fm	Alluvium	St Maughan's Fm	<i>Psammosteus</i> Limestone	Downton Castle Ss	Rivers	Constant Head	Totals
Recharge	2580	7254	4035	2093	533	481			16976
Limestones						543	631	560	1734
Raglan Mudstone Fm			15314	964		143	6191	3718	26330
Alluvium		4863					14582		19445
St Maughans Fm					1684			9047	10731
<i>Psammosteus</i> Limestone									0
Downton Castle Ss		473					160		633
Rivers			151						151
Constant Head		10482		7893					18375
Totals	2580	23072	19500	10950	2217	1167	21564	13325	

### **7.5.3 No-flow boundary condition**

The Local model was assessed for sensitivity to the specified head boundary condition by processing using a no-flow boundary condition (similar to the Regional modelling). The accepted parameters for this model are the same as those for the specified head boundary model. This indicates that the model is insensitive to the boundary condition type.

#### **Sensitivity analysis**

The sensitivity analysis results are in Table 7-11, and again show that certain boreholes are insensitive to large changes in adjacent lithology's flow parameters. The accepted results are generally within an acceptable agreement of the observed values. There is a marked improvement in the result at HFW, with a slight deterioration at LDOW, suggesting that the area of the Dowlais Brook, and connection between the limestones, Downton Castle Sandstone and Raglan Mudstone Formation is imperfectly modelled; several faults are reported in the BGS mapping in this area (BGS 1971). Furthermore LDOW's position at the break in slope of a rounded spur is probably imperfectly modelled given the resolution of the cell size and DTM.

#### **Model Characteristics**

The model is essentially the same as that of the specified head boundary condition model. Some variation is observed in the flowlines at the edges of the model, this is to be expected

#### **Flowlines**

A map of the flowlines for the no-flow boundary condition is in Figure 7-24.

**Table 7-11 Sensitivity analysis results for Raglan Mudstone Formation and limestones with no-flow boundary condition. All values in m AMSL**

$K_{xyz}$ m day <sup>-1</sup>	LTRI	LUSK	PENC	CHBH	CHW	GCBH	HFW	LDOW	LWEL
Observed	11.66	12.09	11.35	12.68	15.76	35.43	50.19	12.55	17.94
0.5,0.5,2	25.01	13.6	9.79	18.89	18.67	41.69	32.76	24.97	31.78
1,1,2	18.98	12.75	9.85	17.31	17.11	28.77	31.96	23.58	22.41
2,2,2	14.43	12.21	9.95	16.17	16.01	20.64	31.45	22.65	16.9
3,3,2	12.74	11.79	9.96	14.86	14.8	17.51	30.9	19.66	14.82
4,4,2	11.86	11.49	9.96	13.8	13.8	15.82	30.4	17.67	13.7
5,5,2	11.33	11.32	9.96	13.15	13.17	14.76	30.1	16.23	13.01
6,6,2	10.99	11.2	9.95	12.7	12.74	14.01	29.89	15.23	12.53
7,7,2	10.67	11.12	9.95	12.38	12.42	13.46	29.74	14.49	12.17
10,10,2	10.34	10.97	9.94	11.79	11.84	12.38	29.46	13.12	11.47
3,3,0.5	No convergence								
3,3,0.75	No convergence								
3,3,1	12.82	11.87	10.04	14.94	14.88	17.6	30.93	19.71	14.91
3,3,2.5	12.7	11.78	9.95	14.84	14.79	17.49	30.9	19.65	14.8
3,3,3	12.68	11.77	9.94	14.83	14.77	17.48	30.9	19.64	14.78
3.5,3.5,2.5	12.2	11.6	9.95	14.24	14.21	16.54	30.61	18.58	14.17
Limestone sensitivity using accepted Raglan Mudstone Formation values									
0.1,0.1,1	12.2	11.7	9.96	14.56	14.57	16.54	45.08	19.03	14.17
0.1,0.1,0.5	12.2	11.7	9.96	14.57	14.57	16.54	45.85	19.03	14.17
0.1,0.1,0.1	12.2	11.71	9.96	14.57	14.58	16.54	46.17	19.03	14.17
0.05,0.05,0.1	12.2	11.74	9.96	14.66	14.68	16.54	55.47	9.09	14.17
0.08,0.08,0.1	12.2	11.72	9.96	14.69	14.61	16.54	49.02	19.05	14.17
Recharge of 20% using accepted values									
	12.71	11.93	10	15.29	15.29	17.56	55.3	20.18	14.88
Downton Castle Sandstone									
0.008, 0.05	12.19	11.71	9.96	14.6	14.61	6.54	53.01	19.06	14.17
0.08, 0.5	12.2	11.8	9.96	14.8	14.89	16.54	27.56	18.99	14.17
0.08,0.1	12.2	11.72	9.96	14.6	14.61	16.54	52.98	19.06	14.17

Accepted values in grey cells.

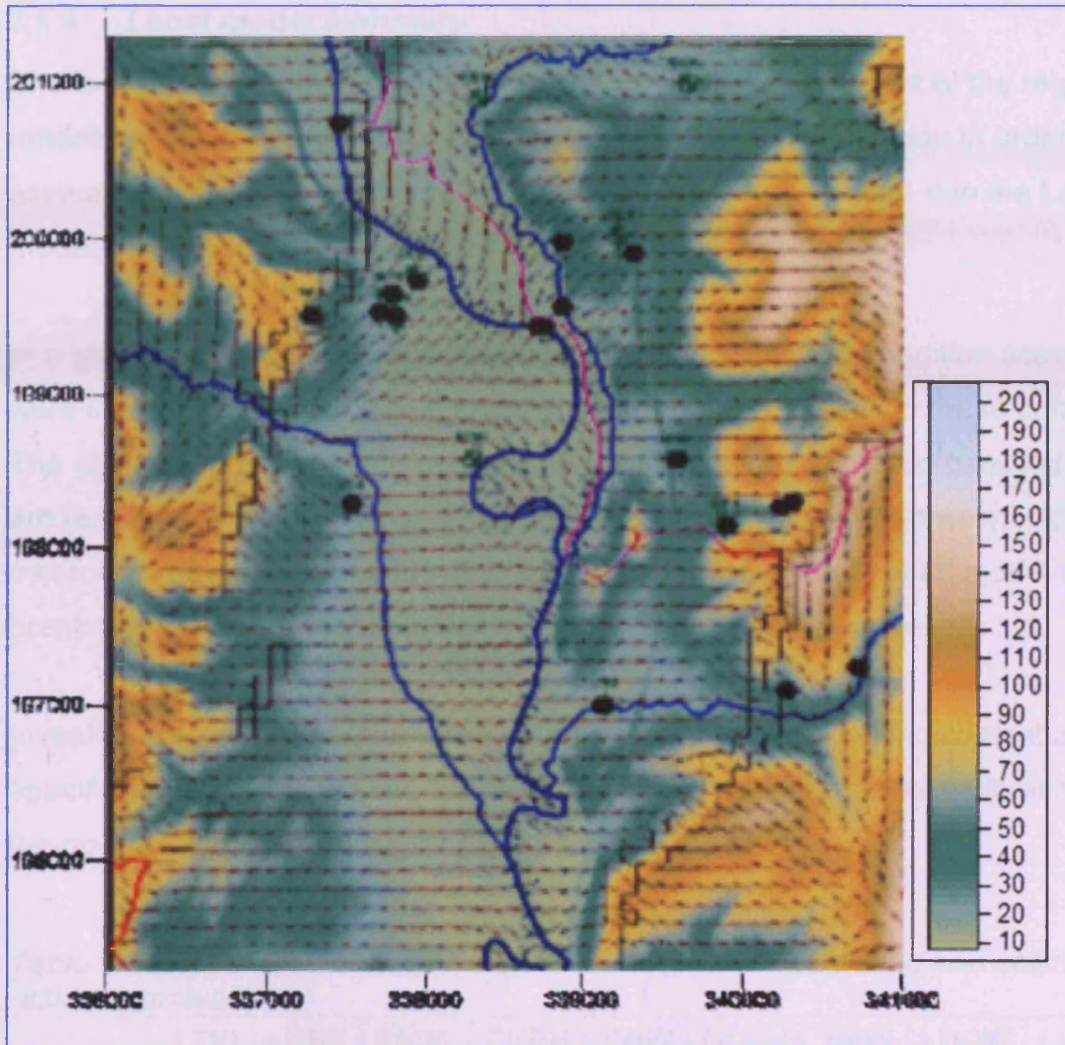


Figure 7-24 MODFLOW Flowlines for no-flow boundary head condition boundary superimposed on DTM. Note change in vertical scale from Figure 7-19. Purple line is sub-catchment boundary; elevation scale in m AMSL.

### Zone budget

The zone budget results (data not shown; see Enclosure 1 CD) are essentially very similar to the specified head boundary results with the exception of discharge to the rivers. The mass balance indicates base flow of  $\sim 16\,600\text{ m}^3\text{ day}^{-1}$ . The potential expected flow is in the order of  $19\,000\text{ m}^3\text{ day}^{-1}$ . Together with the sensitivity analysis this suggests that this model is slightly conservative with respect to water flow.

#### 7.5.4 Local model summary

The local modelling is by nature of its methodology independent of the regional modelling. The Regional model served as a first line investigation in order to assess and provide hydraulic parameters to be brought forward into the Local model.

In a similar fashion to the regional modelling, two boundary condition scenarios were investigated in order to test the sensitivity of the models to these conditions. The close alignment of both methods suggests that the accepted parameter values are reasonable and that non-unique model convergence is not present, and the method is robust. The models indicate, in line with the conceptual model and borehole logs, that heterogeneity exists, but is imperfectly modelled.

Investigation of the sensitivity analysis residuals (Table 7-12) indicates that the specified head boundary condition (SDev = 5.2) result in a better calibration than the no-flow boundary condition (SDev = 6.7).

*Table 7-12 Final accepted calibration results for local modelling and calibration residual analysis.*

	LTRI	LUSK	PENC	CHBH	CHW	GCBH	HFW	LDOW	LWEL	SDev
<b>Observed</b>	<b>11.66</b>	<b>12.09</b>	<b>11.35</b>	<b>12.68</b>	<b>15.76</b>	<b>35.43</b>	<b>50.19</b>	<b>12.55</b>	<b>17.94</b>	
Calculated no-flow boundary	12.2	11.72	9.96	14.6	14.61	16.54	52.98	19.06	14.17	
<i>Residual</i>	<i>-0.54</i>	<i>0.37</i>	<i>1.39</i>	<i>-1.92</i>	<i>1.15</i>	<i>18.89</i>	<i>-2.79</i>	<i>-6.51</i>	<i>3.77</i>	<b>6.7</b>
Calculated specified head boundary	12.36	11.58	9.93	14.08	14.1	20.28	47.07	17.57	17.12	
<i>Residual</i>	<i>-0.7</i>	<i>0.51</i>	<i>1.42</i>	<i>-1.4</i>	<i>1.66</i>	<i>15.15</i>	<i>3.12</i>	<i>-5.02</i>	<i>0.82</i>	<b>5.2</b>

The results from both modelling scenarios indicate that the modelling methodology is robust and that the accepted parameters are insensitive to fluxes from a specified head boundary condition. The zone budget results for baseflow suggest that the most probable solution lies between the two methods, most likely achieved by a spatial reduction in specified head boundaries and magnitude.

## 7.6 Contaminant transport

Using a calibrated local model it is possible to simulate the transport of contaminants of interest to investigate their potential provenance and fate. A selection of models was considered, for example sorbing or advective transport, as were the contaminants of interest: specifically soluble reactive phosphate (SRP). Initial considerations show that with the calibrated model particle (advection) transport has large time durations (particle ticks are 10 years (Figure 7-23), similar to the FlowNet results). This long duration transport must be considered in light of the available project geochemical data and calculated large local  $K_d$  and retardation values. It is therefore not efficient to model SRP in the calibrated model, however conceptually its transport properties will be similar to a non-sorbing species but highly retarded.

The SRP concentration results obtained in 2008/09 are most probably derived from a variety of fertiliser applications and groundwater mixing. It is therefore deemed implausible to introduce with confidence a source term of known concentration and duration given the different fertiliser regimes employed for crop rotations. It is also not permissible to recalibrate the conductivity parameters in order to provide a convergence with geochemical data as the former are now considered to be a robust representation of the groundwater regime. Thus the contamination transport results are a function of model calibration with ground conceptualisation.

### 7.6.1 *Geochemical conceptual model*

A refined geochemical conceptual model (Figure 7-25) has been derived based on the investigations in Chapters 5 and 6. It can be interpreted as a single document, but should also be read in conjunction with the refined hydrological conceptual model for a holistic understanding.

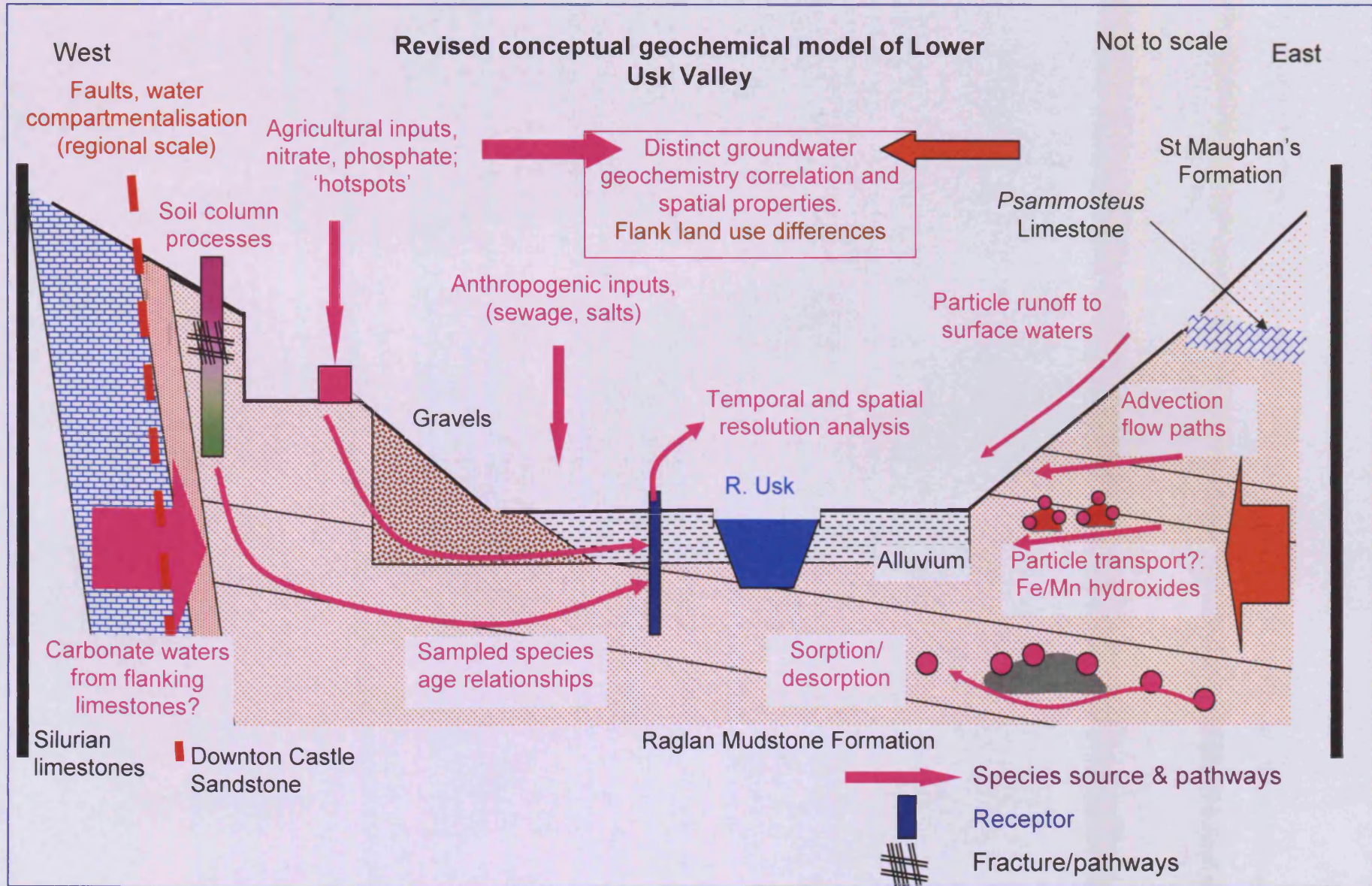


Figure 7-25 Refined geochemical conceptual model of the Usk Valley.

### Basic transport model

The basic Transport model (a replica of the Local model) contains modelled rivers and stream segments. The contaminant transport solver MT3DMS cannot process both river and stream segments. Recourse was therefore made to process the 'streams' as 'small rivers', however, the new rivers provided an infinite source of water and degrade the quality of the accepted hydrological calibration. The models were run without the stream package, the results show that the accepted calibrations are not changed significantly (if at all) suggesting that their inclusion is superfluous at the model scale.

In order to conceptually assess the potential migration of species plumes, initial concentrations (background values) were set at zero despite known soil conditions. Sorption models were not run due to the large local calculated  $K_d$  values for SRP and limit of reasonable temporal prediction. A non-sorbing species nitrate was used as this may also offer some insight into the previous correlations observed in the groundwater geochemical data. The number of dry cells in layer 1 also proved problematic especially on the flanks of the model and required emplacing potential source terms within layer 2. This basic Transport model proved unsatisfactory due to scale issues; domain size and grid resolution. To overcome this, two sub-models were produced to more readily represent local conditions (Figure 7-20).

### Cow House Model

The first model, centred on Cow House, was made by modifying and reducing the domain size by use of the inactive flow facility to 2km x 1.5km. A further refinement of grid and layer resolution to 50 x 50m cells and 7 layers was also made. The model size excluded the east flank locations, the River Usk effectively being the eastern boundary (Figure 7-20). The addition of higher conductivity faster layers  $K_{xy}$  and  $K_z$  10 and 6m day<sup>-1</sup> was also introduced to simulate layering, but did not improve the quality of the calibration to any significant level other than at LDOW (observed 12.76m, modelled 11.33m).

Increased conductivity is required for calibration at LDOW see Table 7-9 and Table 7-11. The only other significant change was the reduction in hydraulic conductivity value of the Raglan Mudstone Fm;  $K_{xy}$  and  $K_z$  to 2 and 1m day<sup>-1</sup>, c.f. values of 3.5 and 2.5m day<sup>-1</sup>. The addition of a constant head boundary to the west of HFW in conjunction with an increase in limestone conductivity provided an acceptable calibration with this location without a detrimental effect on the calibration of the valley borehole locations. This fits with the conceptualisation, however, it also suggests that the limestones are fully saturated to this head level, which may not be ground truth given the fractured nature of the lithologies. The borehole log for Apex 2 indicates a rest level ~8m bgl and a water strike of 43m bgl in the limestones (Figure 7-2) and data tables in Enclosure 1 (CD). Results and synopsis of the second Llantrisant – Llewellyn model are also contained in Enclosure 1.

The use of path lines was made in order to investigate flow paths, these deviate somewhat from the Local model in that the source zone for the northern boreholes: CHW, LUSK have moved north due to the presence of the modelled constant head boundary near HFW( Figure 7-26).

Simulations were run with species constant concentrations and recharge concentrations in a non-sorbing advection transport model. The recharge concentration is designed to model species being introduced with the recharge, such as fertilizer application to soils. The constant concentration models a source term of constant concentration for a known duration, for example a temporary manure pile (Figure 7-27 and Figure 7-28).

The species recharge concentration was set at 50mg l<sup>-1</sup>; the drinking water standard for nitrate. This value is supported as being reasonable by the soil concentration values obtained during the leaching experiments (average 14mg l<sup>-1</sup>, max at manure pile 90mg l<sup>-1</sup>). A constant recharge source term was also modelled; this was placed within the limestones to the north of HFW and has a reducing vertical concentration to simulate possible lower concentrations within the fracture zone with depth (after Goody et al 1998). The model path line ticks also indicate that advection transport does travel far across the model, which will have similar implications for a non-sorbing solute within the aquifer zone.

Dispersivity was set at 10 the default value, as was the individual layer options of 0.1 for the ratio of horizontal to longitudinal and 0.01 ratio of vertical to longitudinal dispersion. These values are also used by Fitts (2002). The model dispersion is a factor which is applied in order to aid simulation of the 'ground truth' mechanical dispersion of a solute plume. The value of the dispersion parameter for the model is a function of modelled transport size; aquifer heterogeneity and transient flow. The modelled results, depending upon the dispersive ratios, will tend to present plumes as regular or smooth distributions when in reality a solute plume will be more irregular in shape (Fitts 2002; Fetter 2004; van der Perk 2006).

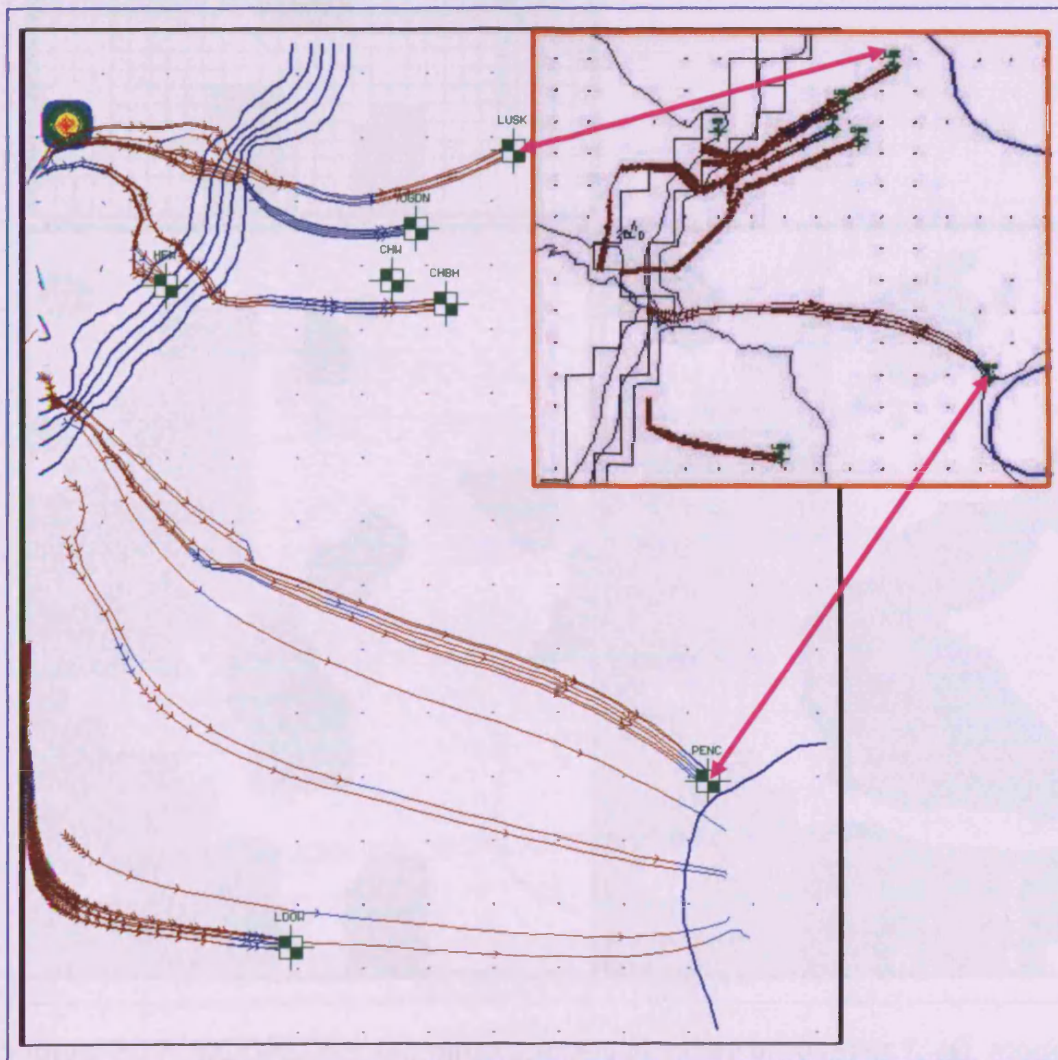


Figure 7-26 MODFLOW, larger scale model of western locations. Forward and reverse particle tracing in layer 3. Note the provenance of the northern boreholes which has switched to the north of HFW and originates within the limestones due to the presence of constant head boundary. Inset copy of Figure 7-23b for comparison of model flow paths. Path line ticks 10 years.

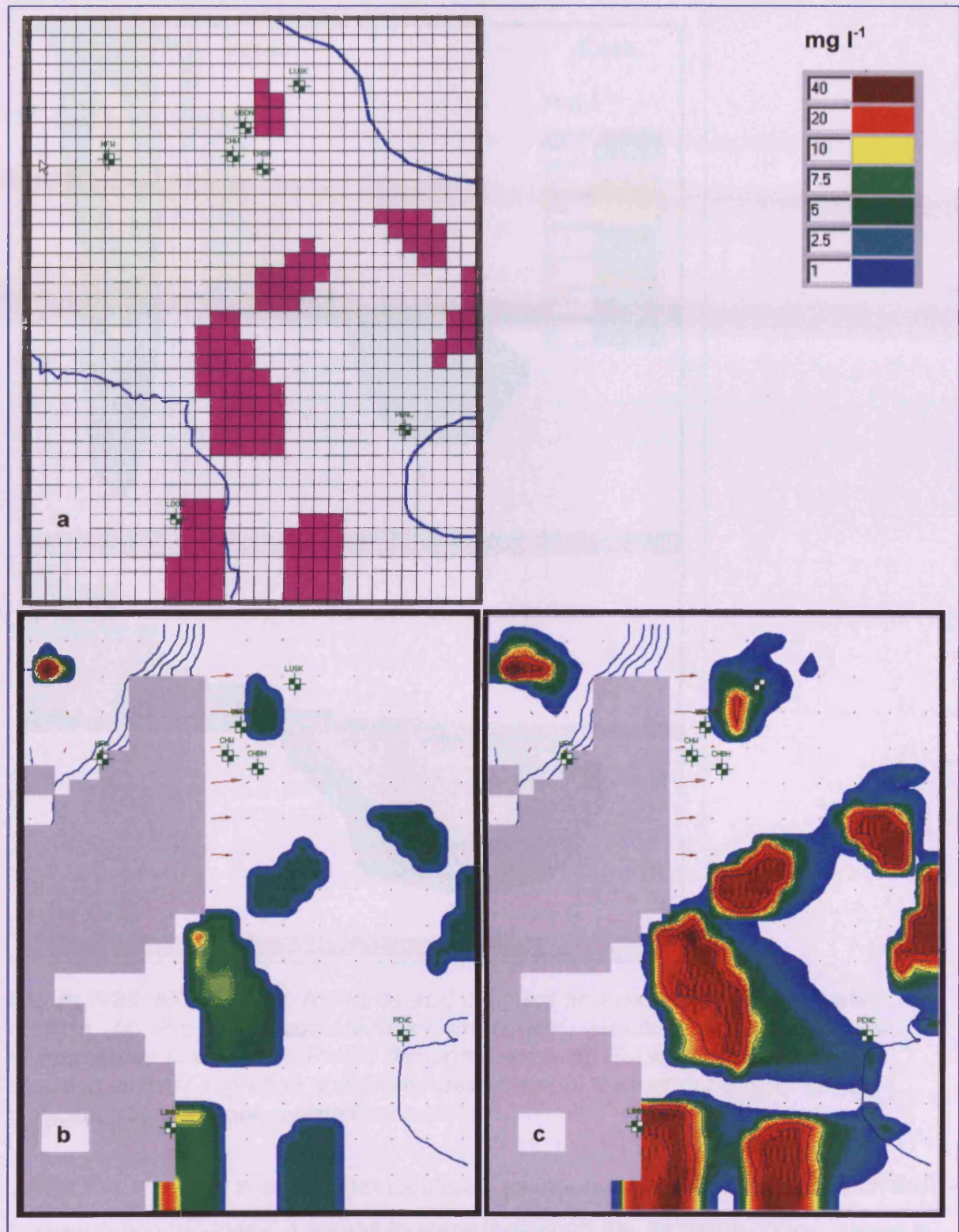


Figure 7-27 MODFLOW, recharge species in valley area layer 1; (a), model domain with allocated zones coincident with mapped fields; (b), species distribution after 365 days; (c), species distribution after 20 years. Grey cells are modelled as dry. Note species in NW corner is vertical constant concentration source term location. Colour contour in  $\text{mg l}^{-1}$ .

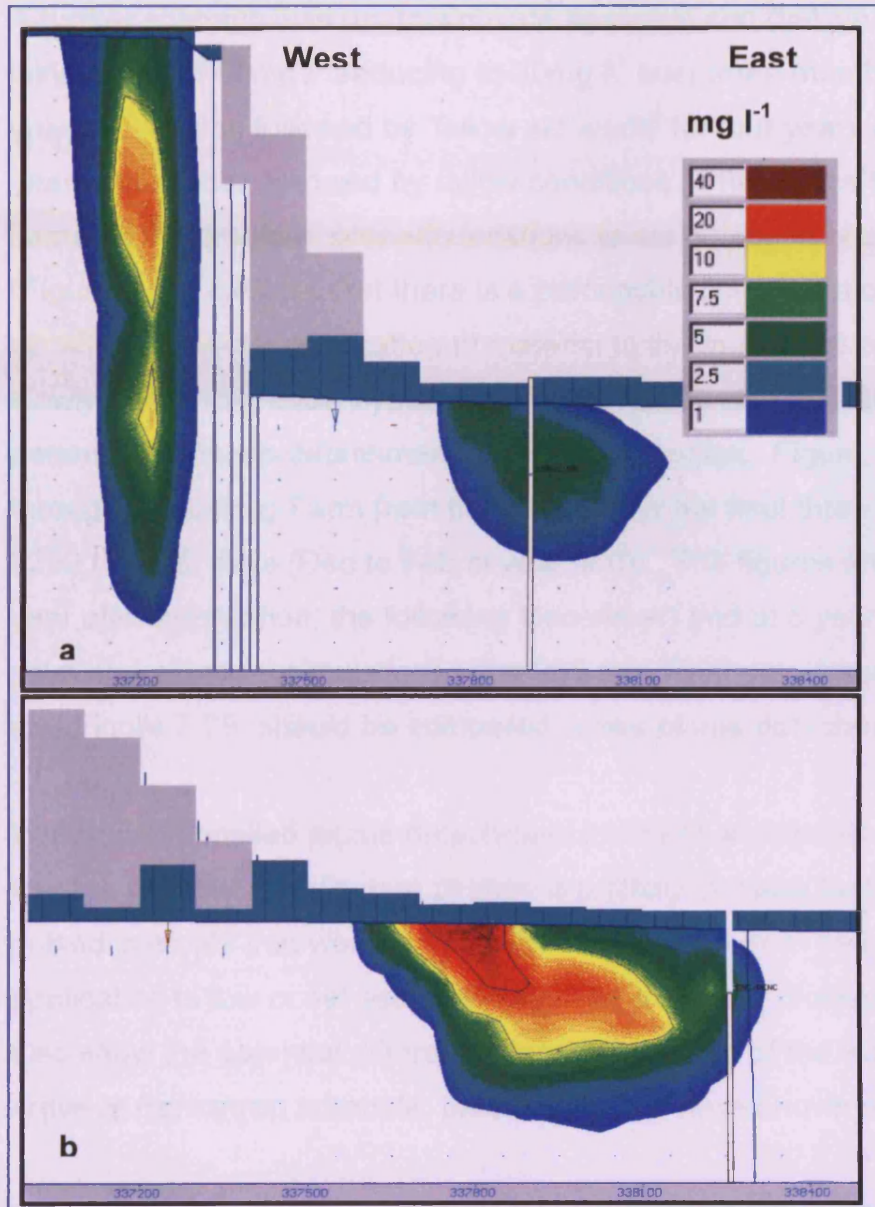


Figure 7-28 MODFLOW, recharge and constant source term species plume profiles. (a), Profile through Llanusk Farm (LUSK) with constant term modelled in limestones to west; (b), Profile through Pencarreg Farm Borehole (PENC) showing vertical migration and plume development throughout aquifer zone. Concentration contours in  $\text{mg l}^{-1}$ .

Whilst this scenario is somewhat idealised, as inputs are likely to be seasonal with concentration fall-away, it serves to show that when the recharge concentration is of sufficient magnitude there is a gradual build-up of species concentration within the modelled Raglan Mudstone that is not being diluted by the groundwater flow. The model also indicates that with the constant recharge such as a semi-permanent manure pile, species concentration at a sample point will elevate over time.

A further scenario was run to simulate seasonal and (fallow) set-aside inputs; an initial value of  $50\text{mg l}^{-1}$  reducing to  $30\text{mg l}^{-1}$  over three months was applied for three years. This was followed by 'fallow set-aside' for four years and then a further two years application followed by fallow conditions. The source term locations were the same as the previous scenario locations to aid detection of changes. The results, (Figure 7-29) indicate that there is a perceptible concentration increase which builds up with the regular application of material to the model soil zone. This dissipates slowly during the fallow cycle. The model results also indicate that there is the potential for plume detachment during fallow cycles. Figure 7-30 shows a profile through Pencarreg Farm from the period after the final three months application at 3299 to 3392 days (Dec to Feb in year 9/10). The figures are timed at 4015 days (1 year after application; the following December) and at 5 years and 10 years (7300 days end of model simulation). The 365 and 7300 day images from Figure 7-28 and Figure 7-29 should be compared to see plume detachment.

Whilst this modelled plume detachment indicates a potential scenario it is believed that the existence of discrete plumes is unlikely. A more likely scenario is a series of pulsed intervals that would represent the transition from periods of higher fertiliser application to low or set aside periods. The modelled profiled results (Figure 7-30) also show the potential difference in origin and age of the water which is likely to arrive at Pencarreg borehole, previous figures have shown path lines in plan view.

The graphic results of Figure 7-29 and Figure 7-30 may be hard to reconcile with the data shown in Figure 5-40, which clearly shows opposing correlations of nitrate (non-sorbing) with SRP at two locations. The pulsed interval effect could conceptually explain this as a 'non-sorbing plume' detaches resulting in a negative correlation within a zone. Conversely, another 'plume' may move into a zone of net SRP increase resulting in a positive correlation.

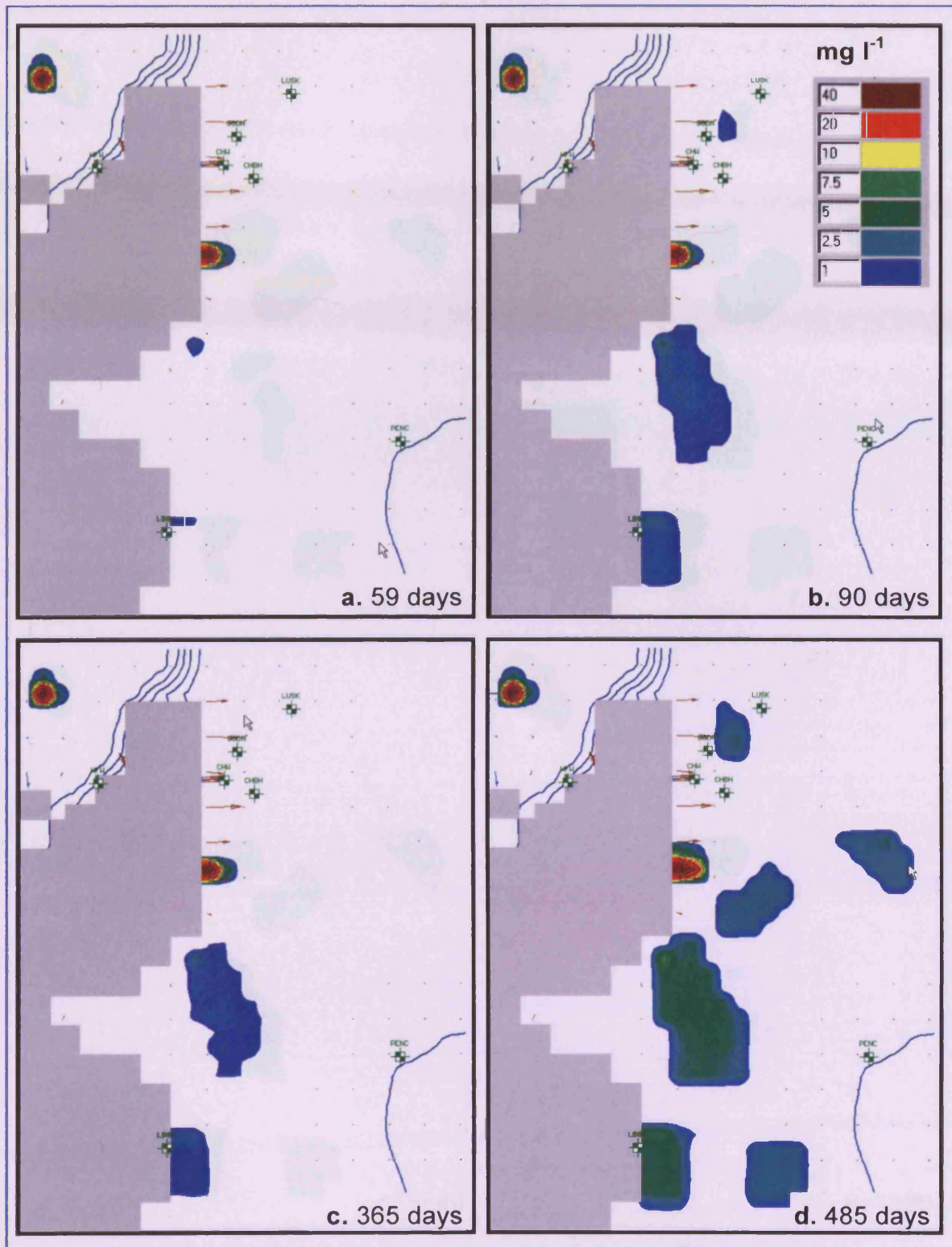


Figure 7-29 MODFLOW, seasonal recharge source term simulations. (a-d), first two years of application showing a slight waning after 365 days. Values in model days and  $\text{mg l}^{-1}$ .

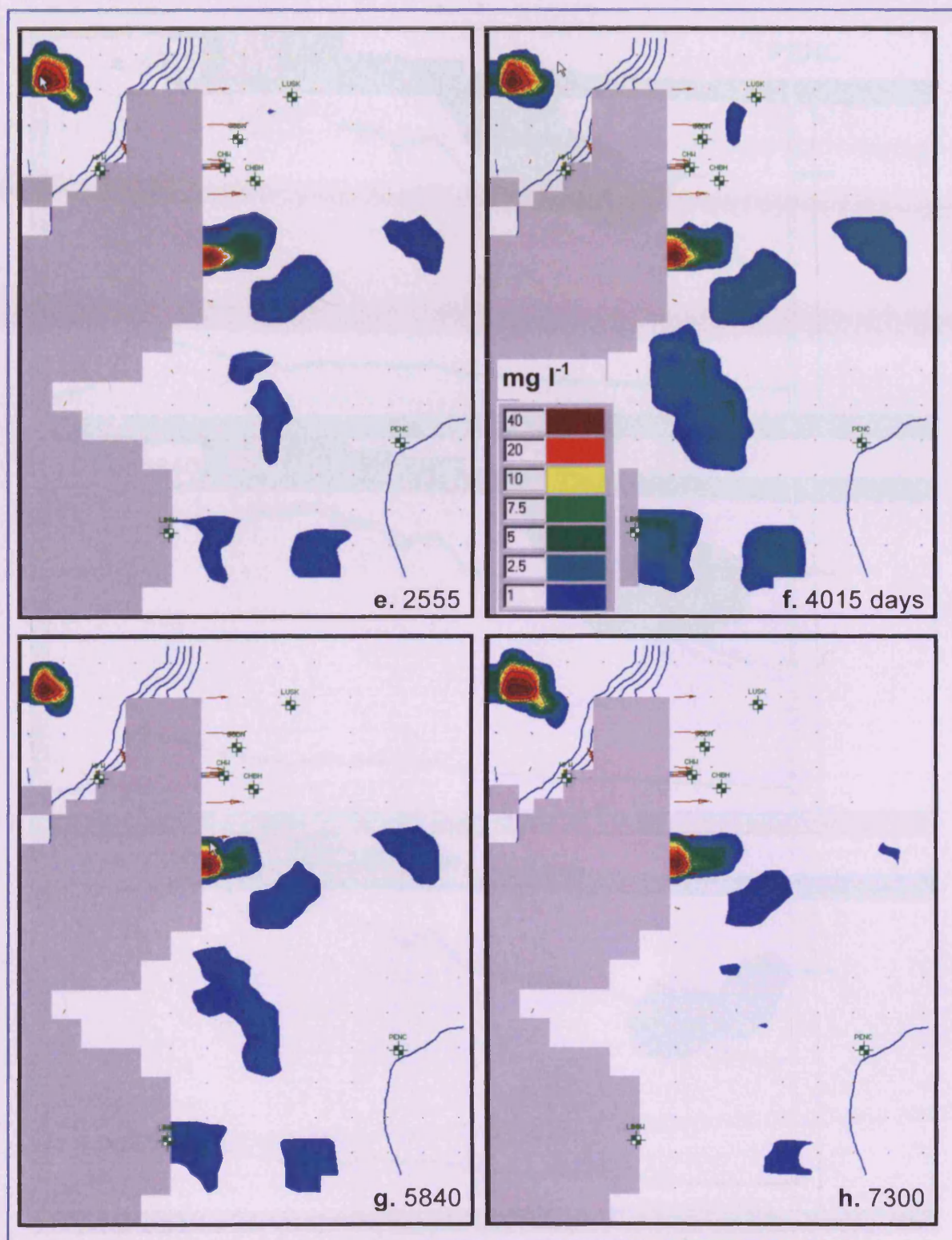


Figure 7-29 cont. (e), 2555 days; waning after a 4 year fallow cycle. (f-h), waxing and waning after final application at 3020 and 3392 days. Concentration values in  $\text{mg l}^{-1}$ . Note constant source term included for comparison of plume development. All figures from Layer 1.

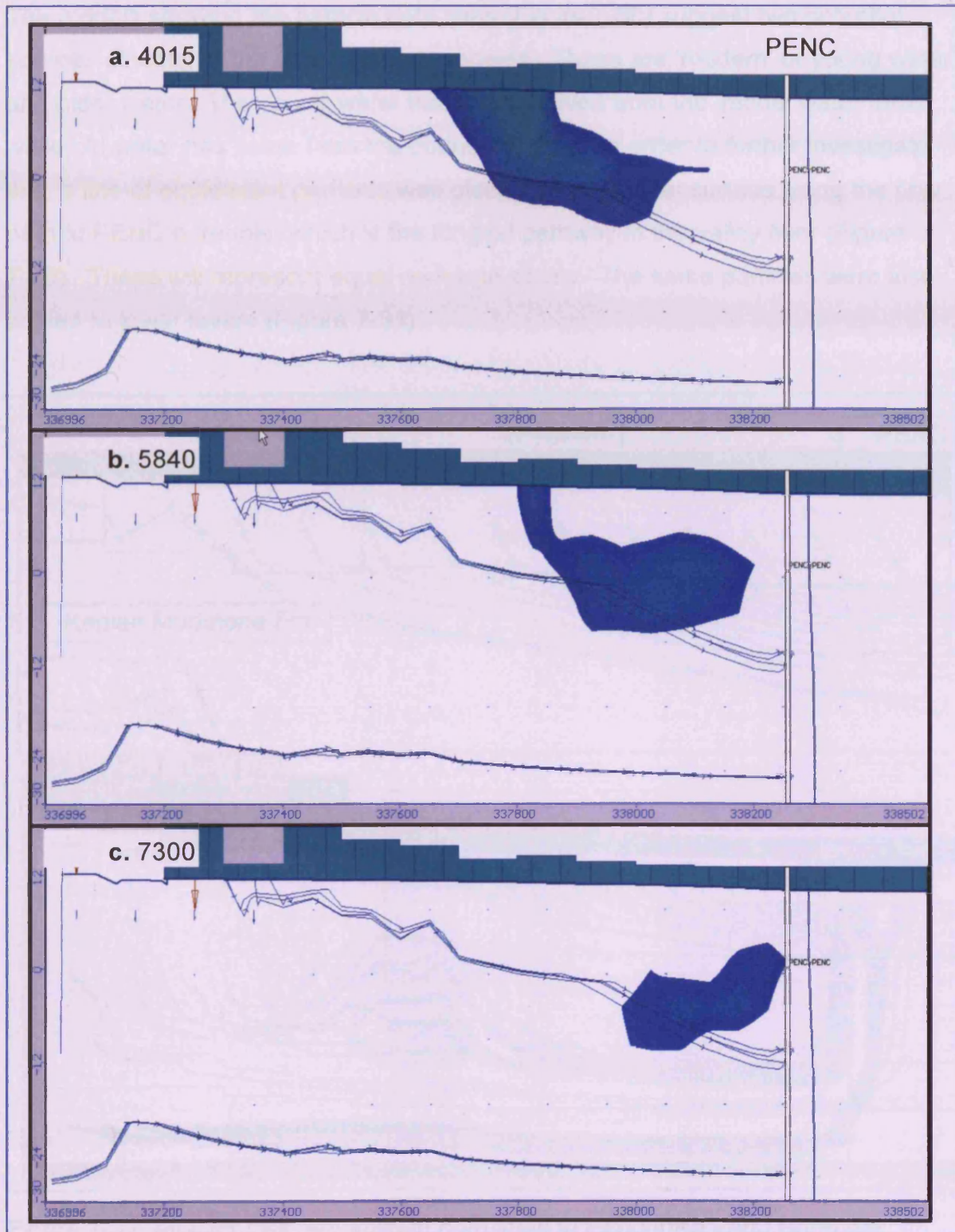


Figure 7-30 MODFLOW seasonal recharge source term simulation profile views through Pencarreg Farm Borehole. (a-c), show plume development and detachment during fallow cycle, values in model days. Compare time line with Figure 7-29. Note position of particle path lines in saturated zone and low concentration values.

The models showing the particle path lines (Figure 7-30) suggest two potential sources of water in the observation boreholes. These are 'modern' or young water and older water. The young water has been derived from the 'model water table' while old water has come from the boundary zone. In order to further investigate this, a line of equidistant particles was placed on the model surface along the flow path to PENC borehole, which is the longest pathway in the valley floor (Figure 7-26). These will represent equal recharge zones. The same particles were also copied to lower layers (Figure 7-31).

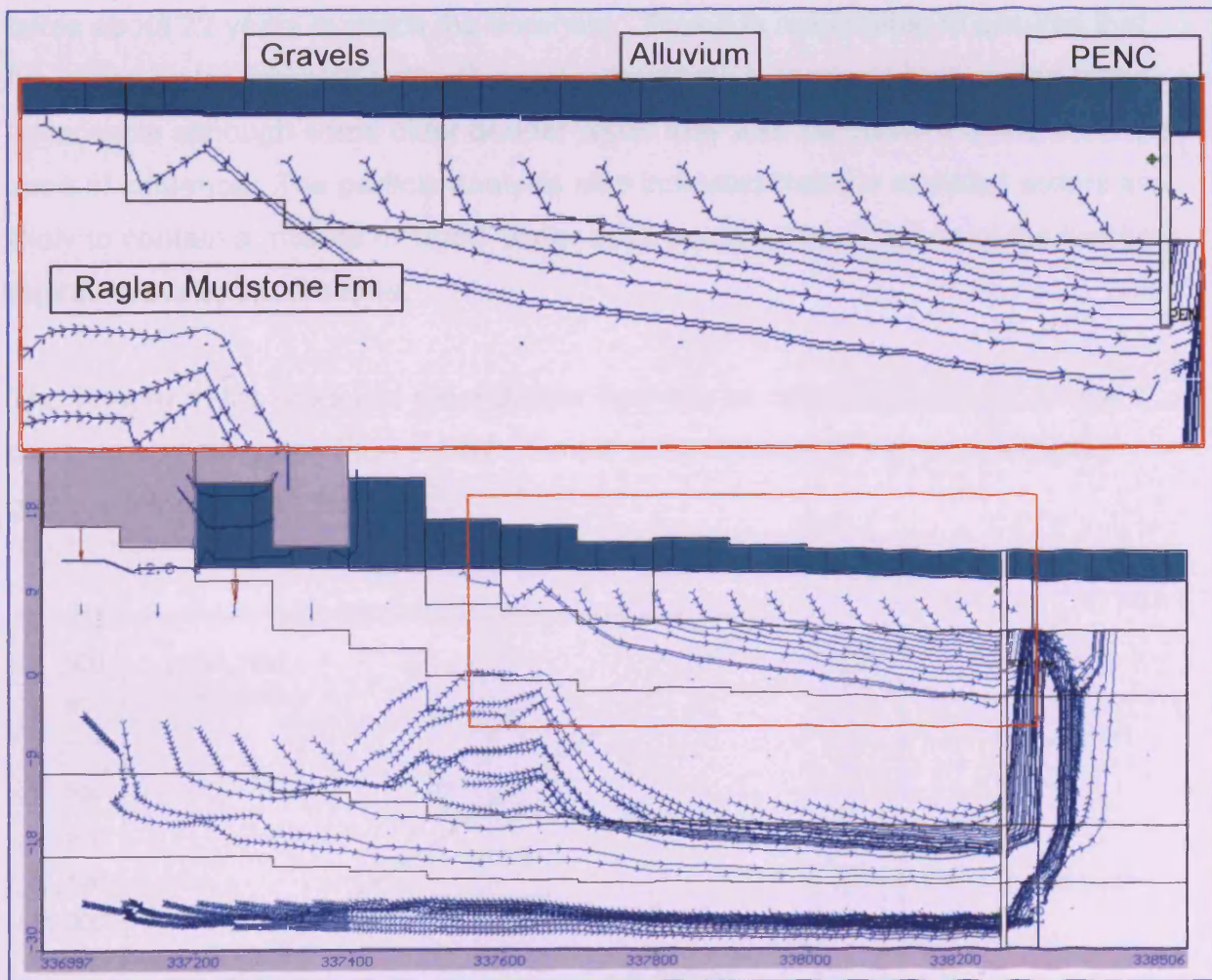


Figure 7-31 MODFLOW, equidistant path lines to Pencarreg Farm Borehole, upper image enlargement of model flow path profile orange box. Path line ticks are 1 year intervals. Note this model has 'faster layers' see conductivity boundary lines. Particle line No.14 not shown.

A total of 15 particles from the surface reached the PENC borehole; the remainder were positioned under dry cells and thus were not processed. The particles reached the borehole at a depth of about 12m (the actual borehole is deeper). In order to assess travel times and quantities of water in the borehole it is necessary to establish a definition of modern water. This has previously been described as recharge arriving at the water table after pumping (or beginning of model time) is initiated (Butcher et al. 2003). The borehole at Pencarreg Farm is used for domestic purposes only, approximately  $0.25$  to  $0.5\text{m}^3 \text{day}^{-1}$ , and thus a pumping regime is not considered as a dominant factor in the simulation. Particle No.15 takes about 22 years to reach the borehole. Thus it is reasonable to assume that the actual water sampled in the Pencarreg borehole is modern: it originates at the water table although some older deeper water may also be drawn into the borehole zone of influence. The particle analysis also indicates that the sampled waters are likely to contain a mixture of 'aged' water each bearing the signature of the leaching regime prevalent at the time.

The velocity of the modelled groundwater flow can be calculated using a simple distance vs time graph Figure 7-32. Simple differentiation of the linear equation gives a velocity of  $44.7\text{m year}^{-1}$ .

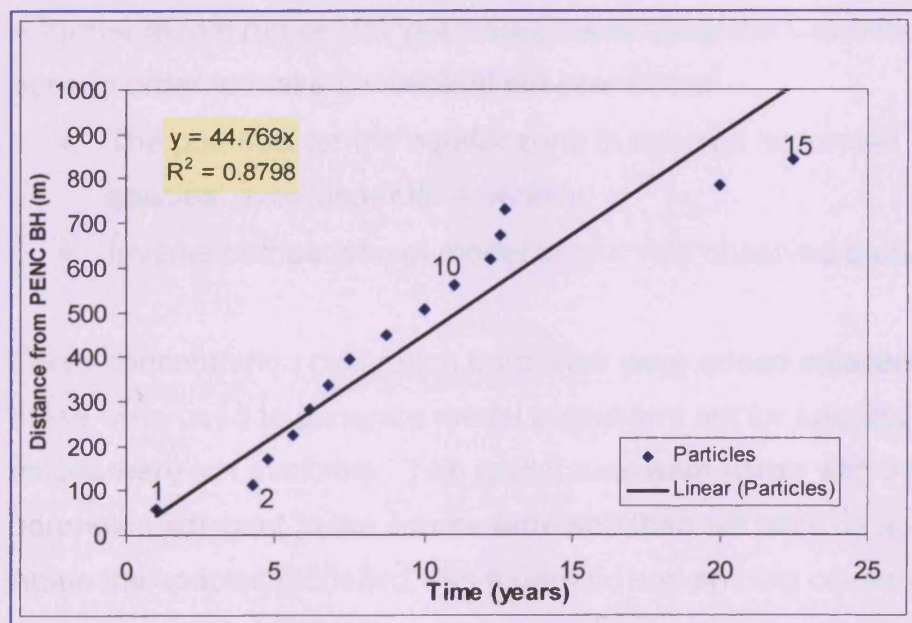


Figure 7-32 Distance v Time graph for particles released at surface to travel to PENC borehole. Note particle numbers. Polynomial curves provide better coefficient of determination ( $R^2$  value) which suggests a potentially nonlinear function.

It is possible to consider the validity of the calculated water velocity of  $44.7\text{m year}^{-1}$ . The average linear velocity of water through a porous medium is derived from the Darcy equation and:

$$Q = -KAi$$

$$Q = 2\text{m day}^{-1} \times 1\text{m}^2 \times 0.002$$

$$Q = 0.004\text{m}^3 \text{ day}^{-1}$$

but

$$\bar{v} = \frac{Q}{An_e}$$

Eqn 7-1

$$0.12\text{m day}^{-1} = \frac{0.004\text{m}^3 \text{ day}^{-1}}{1\text{m}^2 \times n_e}$$

$$n_e = 0.03$$

Equation 7-1 indicates that the effective porosity of the total system that the particles are travelling through is 0.03, this is considered very small; but is an aggregate value of the alluvium and Raglan Mudstone Formation from which the original value was obtained.

#### 100 year model – pseudo species observations

A further model run of 100 years was made using the Cow House model; this was done in order to make conceptual assessment of:

- The potential for the aquifer zone to become 'saturated in agricultural species' over longer time periods.
- Inverse comparison of model output with observed data.

Three concentration calibration boreholes were added adjacent to source zones; these were used to generate model output and not for species calibration as input values were not available. Two model runs were made with the observation boreholes adjacent to the source term and then set back by about 100m down flow. Again the species modelled was a generic non-sorbing conservative species.

The rationale behind this investigation was to consider the present aquifer in terms of long term conditions and consider the potential for discrete plumes or pulsed intervals. Recharge and boundary conditions were set based upon the existing model, and results must be considered as idealised given the changed nature of land use, fertiliser application and recharge. A background concentration value was not used in order to more fully assess the impact of the recharge source term. This source term was reduced to an annual flux of  $70 \text{ mg l}^{-1}$  over the spring months, with a monthly model time period for the first 20 years and annually thereafter. Set aside periods were included in this flux.

The model breakthrough curves (Figure 7-33) show that an increase in groundwater species concentration is apparent until a dynamic equilibrium is reached with discharge to the River Usk. The proximity of the observation well also has a bearing on the model breakthrough curve. Well 3 was left adjacent to the source term and has a more sensitive response to the inputs while at wells 1 and 2 set back by  $\sim 100\text{m}$  the curves are smoother. This suggests that the predicted pulse intervals are potentially present but their observation will be a function of spatial and temporal sampling resolution. Dispersivity values were not altered during these simulations.

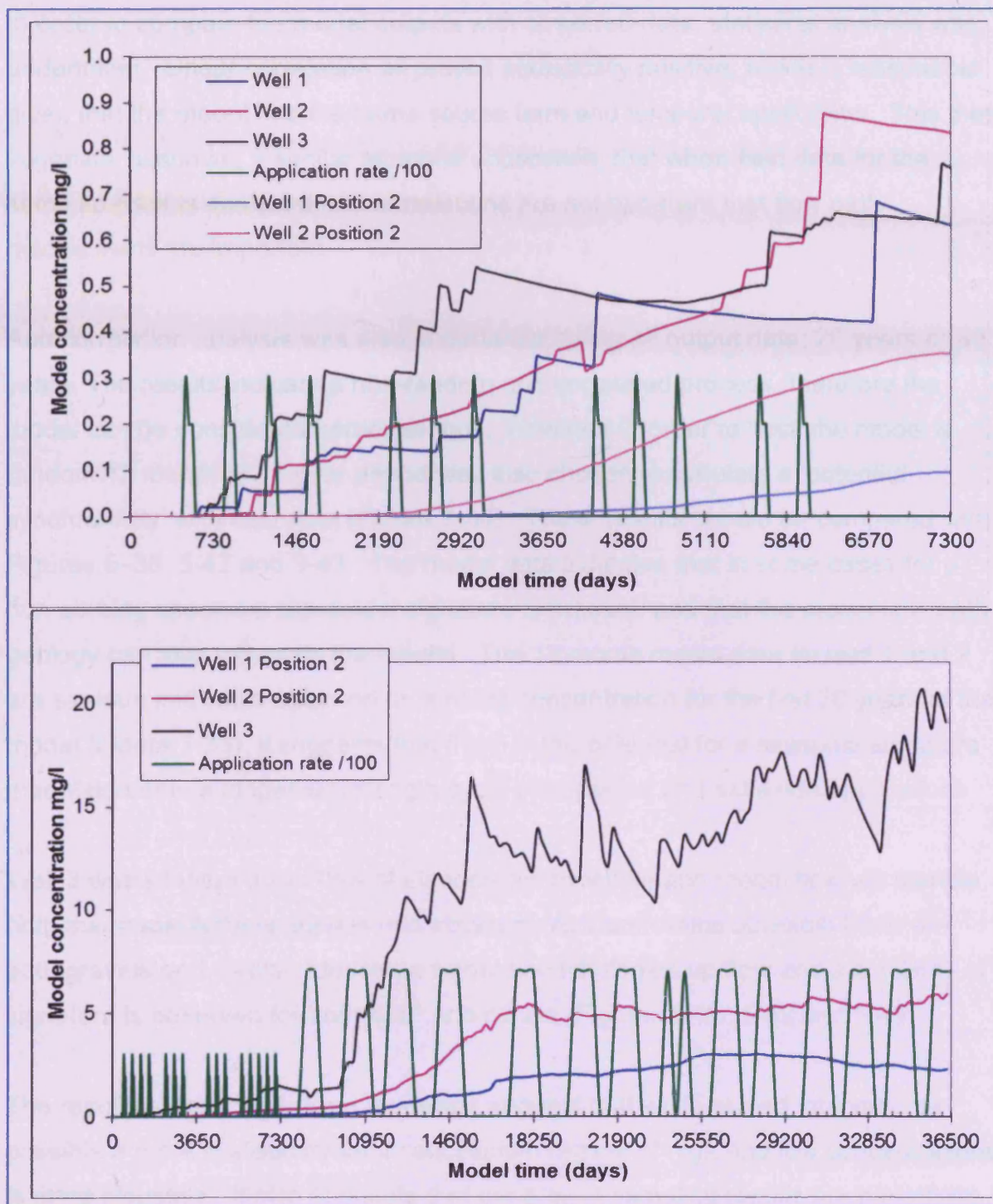


Figure 7-33 Pseudo breakthrough curves for non-sorbing conservative species at three different observation Boreholes. The upper graph shows breakthrough for the 20 year model (monthly time period), and the potential for dilution and pulses. The lower graph shows the breakthrough for the 100 year model. Note Well 3 was adjacent to the source term in both simulations to act as a control, whilst wells 1 & 2 were moved. Differences in curves due in part to lithology: Llandowlais Farm has cultivated fields in both the gravels and alluvium. Note also that the upper graph coincides with first 7300 days in lower graph. Green line to indicate periods of simulated species application, (flux divided by 100).

In order to compare the model outputs with observed data, statistical analysis was undertaken. Linear correlation all proved statistically positive, which is reasonable given that the model had the same source term and temporal application. This then suggests, assuming a similar temporal application, that when field data for the same species is analysed and correlations are not apparent that flow path mechanisms are important.

Autocorrelation analysis was also undertaken, using all output data; 20 years or 80 years. The results indicate a non-random and correlated process, therefore the model can be considered homogeneous. However in order to 'test' the model a random 18 month or 18 year period was also chosen to simulate a 'potential synchronicity' with field data (Figure 7-34). These results should be compared with Figures 5-35, 5-42 and 5-43. The model data indicates that in some cases for a non-sorbing species a sinusoidal signature is present, and that the model flow path geology can also influence the results. The 18 month model data for well 1 and 2 are sinuous and while obtained on a rising concentration for the first 20 years of the model (Figure 7-33), it suggests that there is the potential for a seasonal signature modulated onto a longer wavelength cycle of seasonal and set aside applications.

Well 3 was situated down flow of Llandowlais borehole and model flow will sample both the model terrace gravels and alluvium. At Llandowlais borehole there are both gravels and Raglan Mudstone Formation lithologies up flow and a similarity of signature is observed for both SRP and nitrate (Figures 5-35, 5-42 and 5-43).

The results of the longer term modelling suggest that while pulsed intervals are possible a more realistic dynamic equilibrium regime of high and low concentrations is more plausible. It also suggests that the project sampling results are part of this regime, with their placement on the possible temporal scale indicated on the breakthrough curves of Figure 7-33.

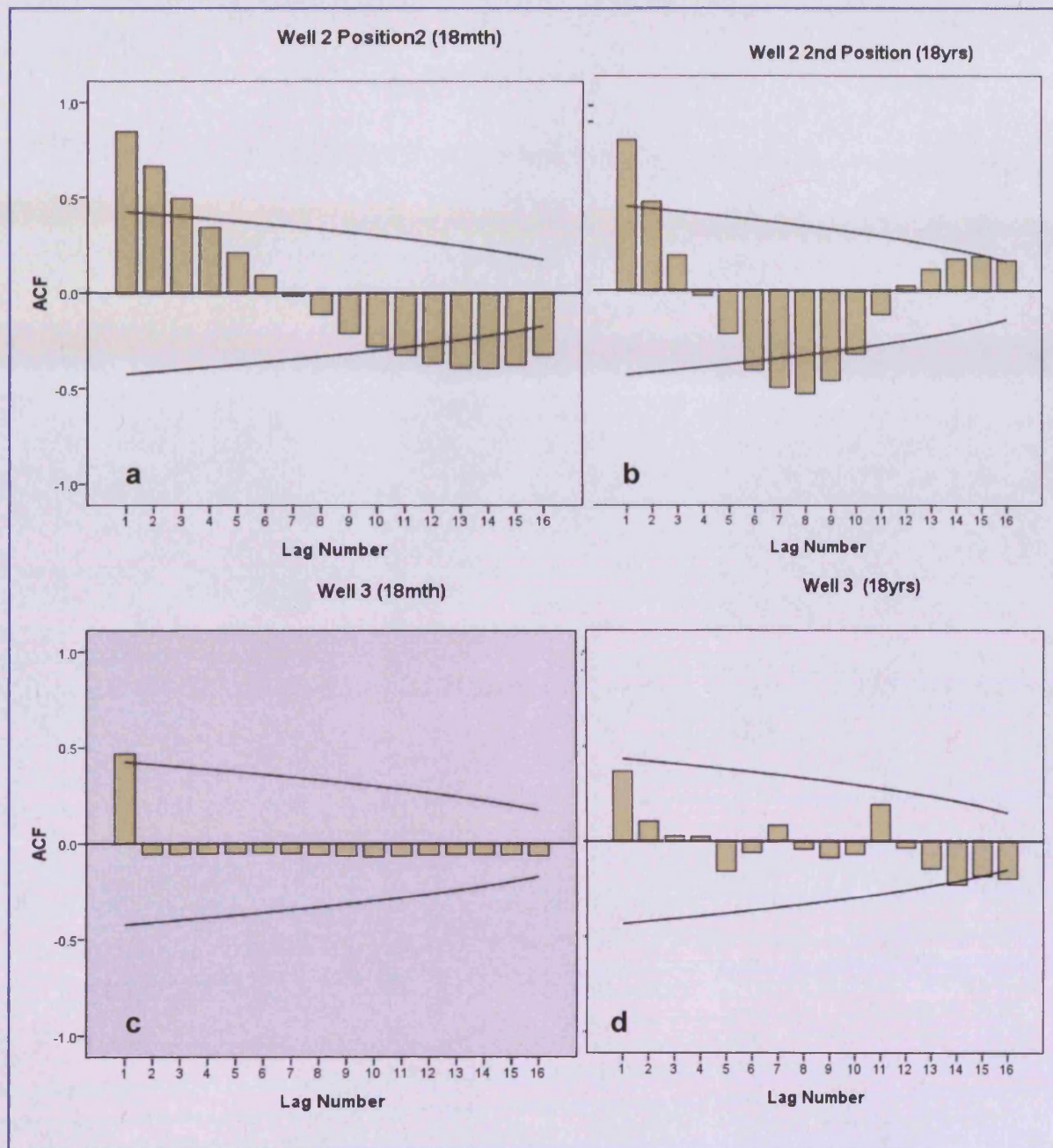


Figure 7-34 Autocorrelation of model species concentration output. (a) and (b) are outputs for well 2 in 20 year monthly time period (rising concentrations) and 100 year annual time periods (dynamic equilibrium). These correlograms indicate a sinusoidal system not necessarily seasonal. In (c) and (d) no correlation between successive time periods is indicated, this may be a function of flow path model geology as a similar sinusoidal correlogram is indicated for well 1 and 2 when adjacent to and down flow of the source term. Note the lag intervals are not truly monthly and annual;  $\sim 37$  and 205 days respectively.

## 7.7 Risk assessment modelling with P20 ver 3.1

These calculations were used to investigate the sensitivity of the measured parameters such as groundwater concentrations and hotspots. The soil analysis (Chapter 5) has already shown that the local soils have a large concentration of total phosphorus, some of which is leachable to the water table as SRP and SUP. There may be some re-sorption down the soil profile. The level 3 groundwater calculation calculates an attenuation factor to be applied the source term. The half life is set at a large value ( $10^{99}$ ) in order to simulate no degradation within the groundwater.

The effect of plume size on field source terms and different hotspot concentrations was investigated. For the field source term a fixed plume thickness of 10m within a saturated zone of 40m was chosen; the plume (or field) width was varied. A constant 10m x10m area representing a hotspot with different SRP concentration was also modelled. It has already been shown that agricultural effluents have high SRP concentrations: Pencarreg Farm manure pile  $\sim 80 \text{ mg SRP l}^{-1}$ , some of which is likely to be sorbed within the soil column. The previously calculated  $K_d$  values were used in the calculation. The results are presented as breakthrough curves to a receptor 1000m away (Figure 7-35).

The results show that the effect of large fields is to maintain the source term concentration down flow. The results assume a homogeneous leaching and recharge profile; this has been verified at the aquifer scale with the cross correlation analysis of rainfall and water rest levels. For the hotspot investigation the effect of attenuation is clearly seen down gradient, although the high values calculated were not observed in the field results obtained from the Usk Valley boreholes.

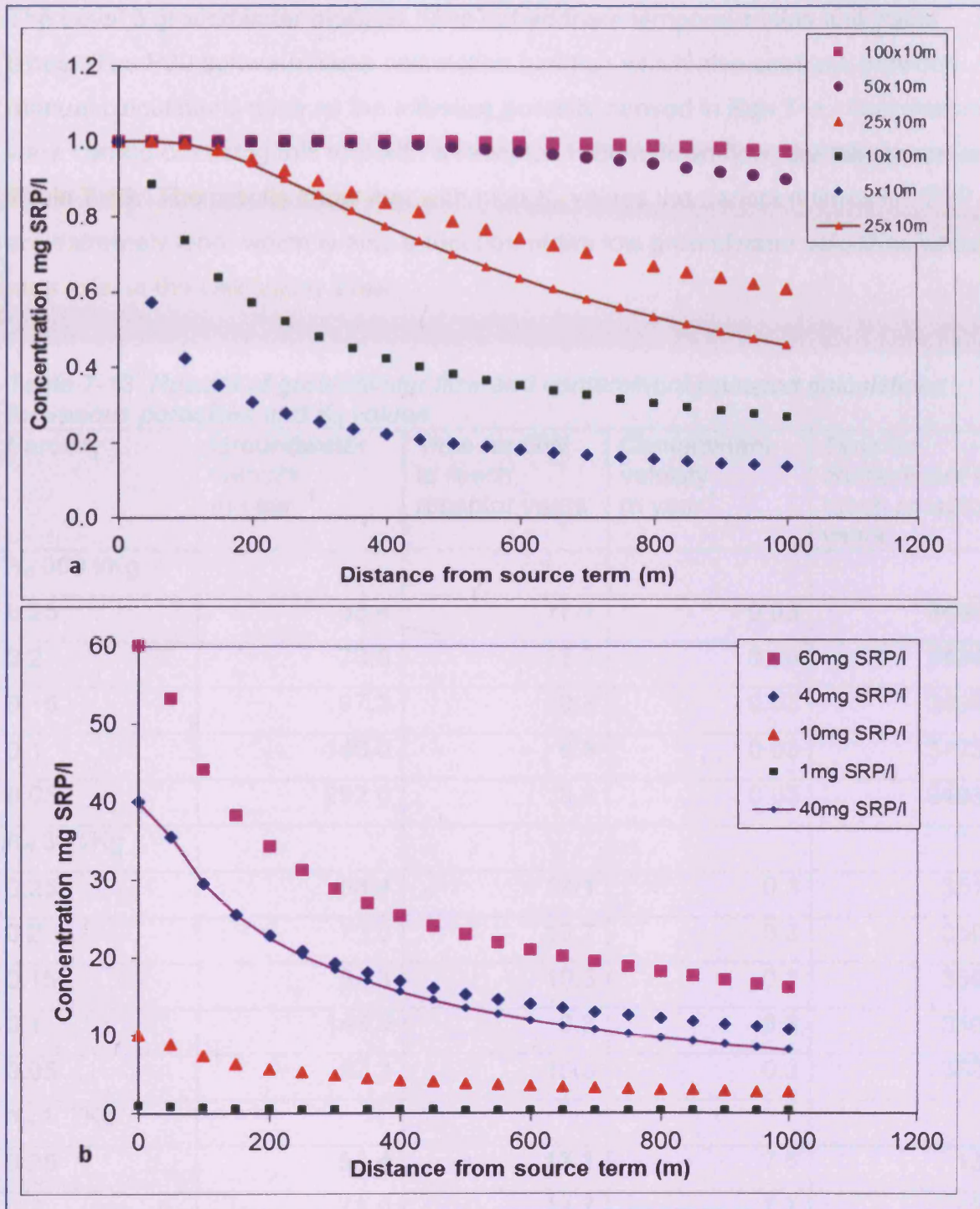


Figure 7-35 Breakthrough curves for groundwater SRP as a function of areal extent and concentration. (a) Effect of fixed 1 mg SRP l<sup>-1</sup> source term with varying width to simulate field source term size relationships. Values in m; note fixed plume thickness at source of 10m. (b) Effect of source term concentration at a fixed size of 10m x 10m to represent a large manure pile. For comparison the 1 mg SRP l<sup>-1</sup> in (b) is the same as the 10x10 curve in (a) In both graphs the solid line symbol denotes a plume in the centre of the aquifer with vertical dispersion in two directions.

The Level 3 groundwater analysis does not address temporal scales and travel times. The P20 software has a calculation function which also confirms previous manual calculations such as the effective porosity derived in Eqn 7-1. Calculations were carried out using this tool with a receptor 1000m down flow; the results are in Table 7-13. The results show that with high  $K_d$  values the transport times for SRP are extremely long, which is also a function of the low groundwater velocities which may exist in the Usk Valley area.

**Table 7-13 Results of groundwater flow and contaminant transport calculations for various porosities and  $K_d$  values**

Porosity	Groundwater velocity m year <sup>-1</sup>	Time for GW to reach receptor years	Contaminant velocity m year <sup>-1</sup>	Time for contaminant to reach receptor years
<b><math>K_d</math> 300 l/Kg</b>				
0.25	58.4	17.1	0.03	34948
0.2	73.0	13.7	0.03	34945
0.15	97.3	10.3	0.03	34941
0.1	146.0	6.8	0.03	34938
0.05	292.0	3.4	0.03	34934
<b><math>K_d</math> 30 l/Kg</b>				
0.25	58.4	17.1	0.3	3510
0.2	73.0	13.7	0.3	3506
0.15	97.3	10.3	0.3	3503
0.1	146.0	6.8	0.3	3500
0.05	97.3	10.3	0.3	3503
<b><math>K_d</math> 1 l/Kg</b>				
0.25	58.4	17.1	7.5	133
0.2	73.0	13.7	7.7	130
0.15	97.3	10.3	7.9	126
0.1	146.0	6.8	8.1	123
0.05	292.0	3.4	8.3	119

The Level 3 groundwater calculations indicate that the groundwater transport of soluble phosphate is very slow as is the relative value of an advecting solute with potential seasonal and application variations (Figure 7-29). The calculations use a local lower limit SRP  $K_d$  of  $300 \text{ l Kg}^{-1}$  which is higher than the value for TDP, see Chapter 5. Given the distribution of SRP throughout the project area and known soil values, a system of local diffuse soluble phosphate recharge is affecting the area. This is likely to be augmented by temporal and spatially distributed hot spots. The groundwater velocity calculations, which are independent of  $K_d$ , indicate the potential of mixed aged water in the sample boreholes.

## 7.8 Modelling summary

The refined conceptual modelling was based on the empirical data detailed in the preceding chapters. The building of the different models and interpretation of the model results has improved understanding of the groundwater flow and chemistry in the Usk Valley.

An important result was an understanding of the role of scale; the MODFLOW modelling shows that at a regional small scale the lithological units can be modelled as a homogeneous entity, whereas larger scale local models require a refinement as was shown in the Flownet, local and contaminant transport model. This scaling issue is also important when considering the potential of different physical and geochemical processes that were identified in Chapter 6 that also act at different scales. The models, as yet, do not have a sufficient resolution to account for this.

The modelling has undergone, at every stage, an analysis of sensitivity to model parameters and inputs. This has shown that the methodology is robust, and only requires further field observations with which to carry out a more rigorous calibration. The 3D MODFLOW was designed in such a way that errors in conceptualisation at the boundaries would have a minimal effect in the centre of the model, where the investigation and observations have taken place.

The application of agricultural fertilizer is fairly ubiquitous throughout the project area. The models show that, given enough time, the 'mobile' chemical species found in the fertilizer have the capacity to permeate through the aquifer zone, and the rate of their advance is a function of physical and chemical aquifer properties. The risk assessment modelling shows the sensitivity of SRP transport times to these aquifer properties. The results elucidate the diffuse nature of SRP ingress into the water table, and that this ingress is strongly influenced by the chemical concentrations and scale of the source zones.

## **Chapter 8 Eden Valley case study**

### **8.1 Introduction**

#### **8.1.1 General**

The Eden Valley is located in Cumbria, northwest England. It is orientated northwest-southeast and is approximately 65 km long. It is 10 km wide in the southeast, this increases to about 23 km in the northwest (Figure 8-1). The River Eden runs along the central valley and drains the high ground on both flanks. It supports mainly agriculture in the form of dairying and some cereal production. The main town is Penrith, and there are several smaller towns and villages located throughout the valley.

The Eden Valley has been chosen as a comparative case study for the following reasons:

- Previous work has been undertaken by the author on the Penrith Sandstone aquifer; (Butcher et al. 2003; Gray 2006), and a conceptual understanding of this major aquifer is established.
- There is long term monitoring data, which was made available by the Environment Agency NW.
- The Eden Valley contrasts with the Usk valley in aspects of scale and lithology.

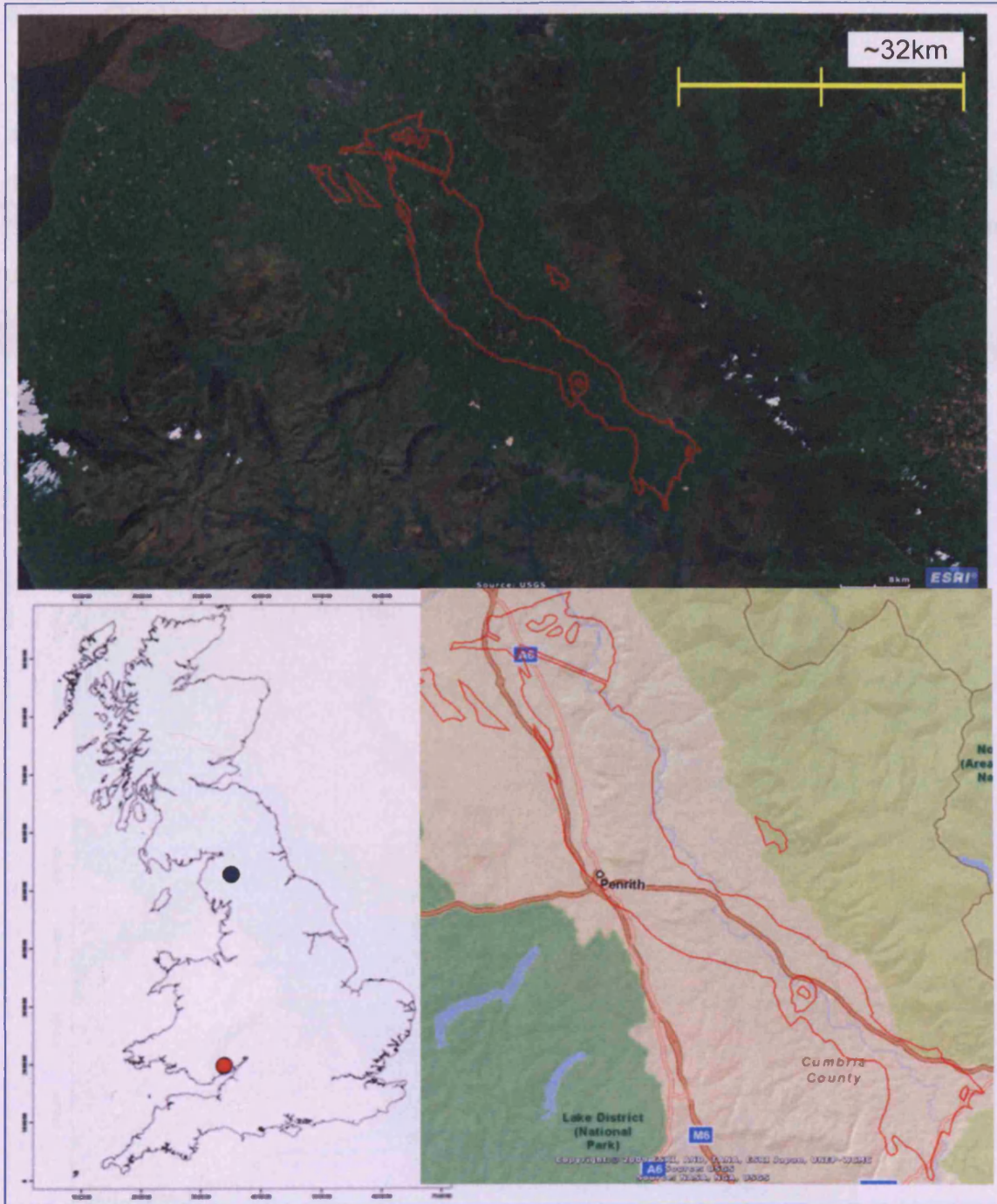


Figure 8-1 Eden Valley location maps. Base mapping from ESRI and Edina, red circle is Usk valley location for comparison. The extent of the Penrith Sandstone is outlined in red.

## 8.2 Geological setting

The geology of the valley comprises Upper Palaeozoic and Lower Mesozoic sediments, with Recent and Pleistocene drift deposits. The lower units are conformable and there is evidence for transgression and regression episodes within the central valley sequences. The older Formations form a wide downward facing asymmetrical synform. Figure 8-2 and Figure 8-3 show the main Formations.

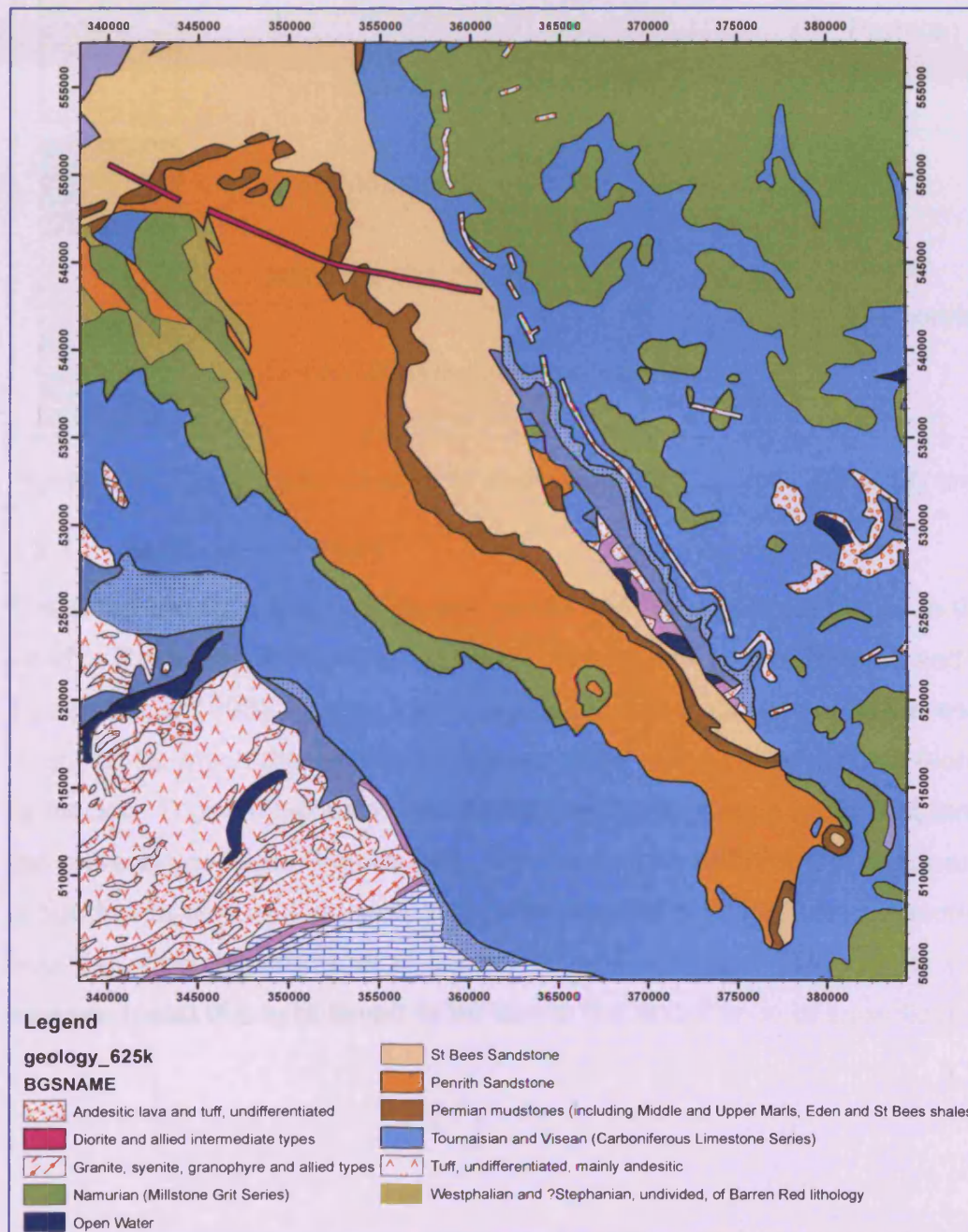


Figure 8-2 Geological map, of the Vale of Eden and surrounding stratigraphy, Drift not included. Based on BGS 1:625 000 nomenclatures. Some minor lithologies not included. Legend based upon BGS nomenclature.

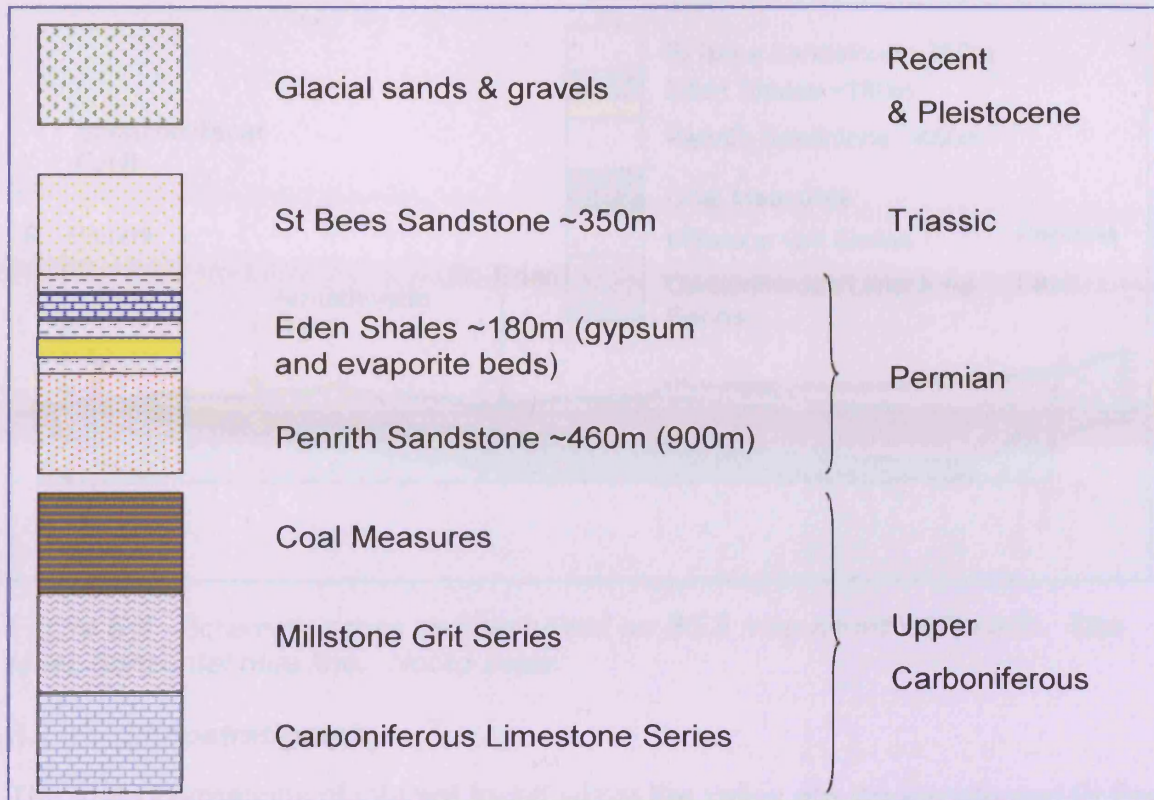


Figure 8-3 Stratigraphic column of main geological units in the study area.

### 8.2.1 Regional structure

The Eden Valley is bounded by the Alston and Askrigg horst blocks to the east and south. The valley is downthrown from these blocks by the Pennine and Dent Faults, (BGS 1996). Geological mapping indicates a series of northwest/southeast major faults which dissect the northern portion of the valley forming elongate units or blocks. These blocks are also partitioned by conjugate faults that terminate on the more major faults (Figure 8-8). The faults may partition the regional groundwater regime into compartments with restricted but interconnected cross-boundary flow, (Seymour et al. 2006). In the south of the valley faults are not indicated, and this is believed to be due to the abundance of superficial cover.

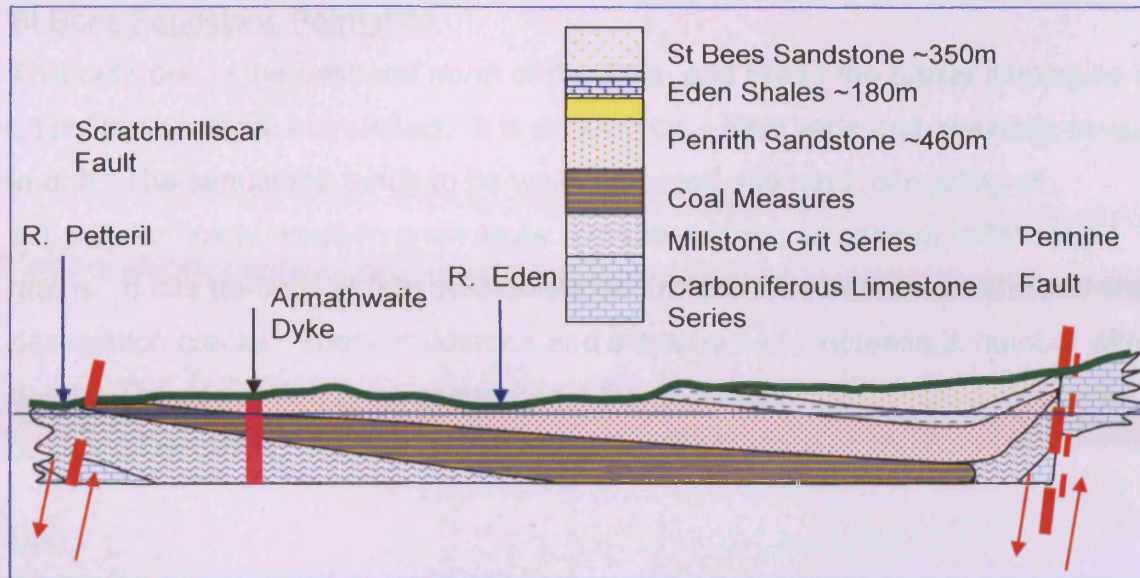


Figure 8-4 Schematic cross section based on BGS map sheet 24 Penrith. Sea level, horizontal blue line. Not to scale.

### 8.2.2 Lithostratigraphy

The main Formations of interest found within the valley are the Penrith and St Bees Sandstones. For a detailed lithostratigraphy of the flanking lithologies see Milne (1994) and Arthurton (1981). As the Penrith Sandstone is the main unit of interest in this study it is discussed at greater length in a following section.

#### Eden Shales Formation

The Eden Shales are exposed on the eastern flank of the Penrith Sandstone. They consist of interdigitated mudstones and siltstones with interspersed gypsum and anhydrite evaporite beds and lenses; four of which have been correlated across the unit. The Belah Dolomite is evidence of their marginal marine and marine facies. The evaporites occur in economic quantities and have been mined at Kirkby Thore (NY) 364000 525800 and Glassonby (NY) 357700 538900 (Ingram 1978; Arthurton 1981). There is evidence that the Eden Shales are conformable with the Penrith Sandstone, although deposition of the Penrith Sandstone may have ceased and the Shales were deposited in deflation (erosion) hollows (Arthurton et al 1978; Arthurton et al 1981). The 1974 BGS map shows that in the north of the Vale the Eden Shales are in juxtaposition with the Carboniferous Limestone Series, due to the presence of the Pennine Fault. The Eden Shales tend to be covered by Drift.

### St Bees Sandstone Formation

This outcrops in the east and north of the Vale, and flanks the earlier lithologies in all but the southern extremities. It is about 5Km – 6Km wide and generally covered in drift. The sandstone tends to be well-cemented and hard, consisting of subangular fine to medium grain sizes with the occasional coarser millet seed grains. It has partings of thin mudstones and micaceous siltstones with sand filled desiccation cracks. These mudstone and siltstone beds increase in number with depth. The deposition is interpreted as a fluvial, braided river system, with over-bank mud deposits. (Ingram 1978; Arthurton 1981; Milward 2003).

### Drift

Except in the high fells areas, the majority of the Vale of Eden is covered by superficial deposits comprising a mixture of till, glacial sand and gravel, glacial lake deposits, river terrace deposits and alluvium (Figure 8-5). Peat tends to be confined to the upland Pennine area, although some small pockets are recorded in the valley proper such as Cliburn Moss SSSI, (BGS 1974b, 2004). The thickness of the drift is believed to be between 10m to 20m with a maximum of 30m (Butcher et al. 2003). Drift is used throughout as a generic term, when required individual lithology descriptions are used to differentiate the surface cover, (see also Figure 8-8). Within the drift at least one palaeo-structure was observed at Bonniemount Quarry (NY 354800 531400, here a channel type deposit was observed. The contacts between the drift deposits were also seen to be sharp (Figure 8-5).



*Figure 8-5 Till over Glacial sands and gravels at Bonniemount Quarry. Note trees for scale. Photo A Gray.*

A drift thickness of at least 5m is considered to be the minimum critical thickness required to protect an underlying aquifer, although the lithological composition is also crucial, (Robins 1998). The complexity of the drift cover is believed to give rise to perched water tables, ponds and shallow wells, (Butcher *et al* 2003). Ingram (1978) quotes an 80% drift cover across the Penrith Sandstone (250Km<sup>2</sup> over of an outcrop size of 310Km<sup>2</sup>), and over the St Bees Sandstone 65% (92Km<sup>2</sup> over 140Km<sup>2</sup>).

### Soils

Two main soil types dominate the valley: well-drained permeable or loamy soils in the immediate area of the River Eden, and sand and gravel type soils in the adjacent areas. On the high fells a surface of solid rock lithologies is indicated (Anon 2005).

### **8.2.3 Penrith Sandstone**

#### General description

The Penrith Sandstone is classed as a major aquifer (Allen et al. 1997). It forms the central lithology of the Eden Valley lying along the valley axis. As such, it is the bedrock geology that forms the high plateaux which becomes dominant in the northern half of the valley. The topographic and field evidence suggest that the plateaux are formed by a series of very well cemented hard bands or silcretes. The plateaux tend to be drift free with only a very thin soil covering, and in places the bedrock is exposed (Figure 8-8). The plateaux include Lazonby Fell, Wan Fell and Blaze Fell (NY) 349500 543500. In the south and west the Penrith Sandstone is covered in drift of varying depth. Along the banks of the River Eden it outcrops in a steep gorge extending about 8km downstream from Armathwaite (NY) 350500 546000. Massive dune cross bedding is visible at this location.

The Formation (Figure 8-6) is interpreted as barchan type aeolian dunes, (Pers observation; Ingram 1978; Shotton 1956; Arthurton et al 1981). Red hematite staining is prominent on the coarse to medium sized grains. Three facies types have been ascribed to the sandstone; (1) well sorted "millet seed" type, (2) less well sorted and very (3) well cemented grains (Lovelock 1972). Evidence for playa type lakes has also been described, thin mudstone intercalations, and wadi type deposits are also present.

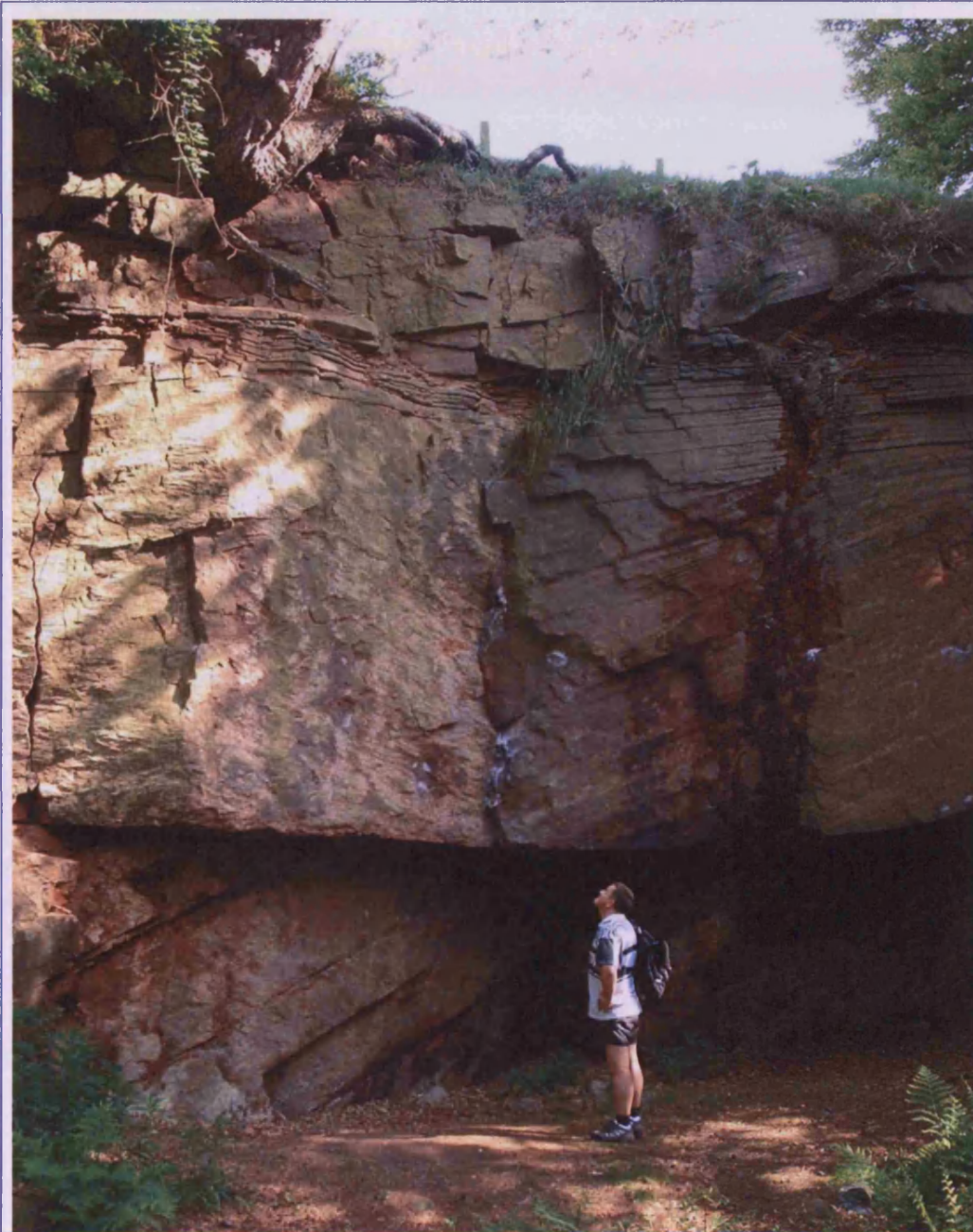


*Figure 8-6 Massive dune bedding at Cowraik Quarry. Note thin soils on top of bedrock. Photo A Gray.*

### Grain size

Outcrop and core sample analysis show a variability in grain size. Examination of the BGS EV2 Langwathby core and outcrops show that there is a variability of grain size between successive beds, from fine through medium to coarse with variability in sorting (Figure 8-7). Lovelock (1979) suggests that the Formation is “subject to a good deal of facies variation”.



*Figure 8-7 Penrith Sandstone core plugs. Note difference in grain size, and potential porosity/hydraulic conductivity. Samples show the difference between facies type, well graded “millet seed” coarse grains on right, finer grained on left. Photo A .Gray.*

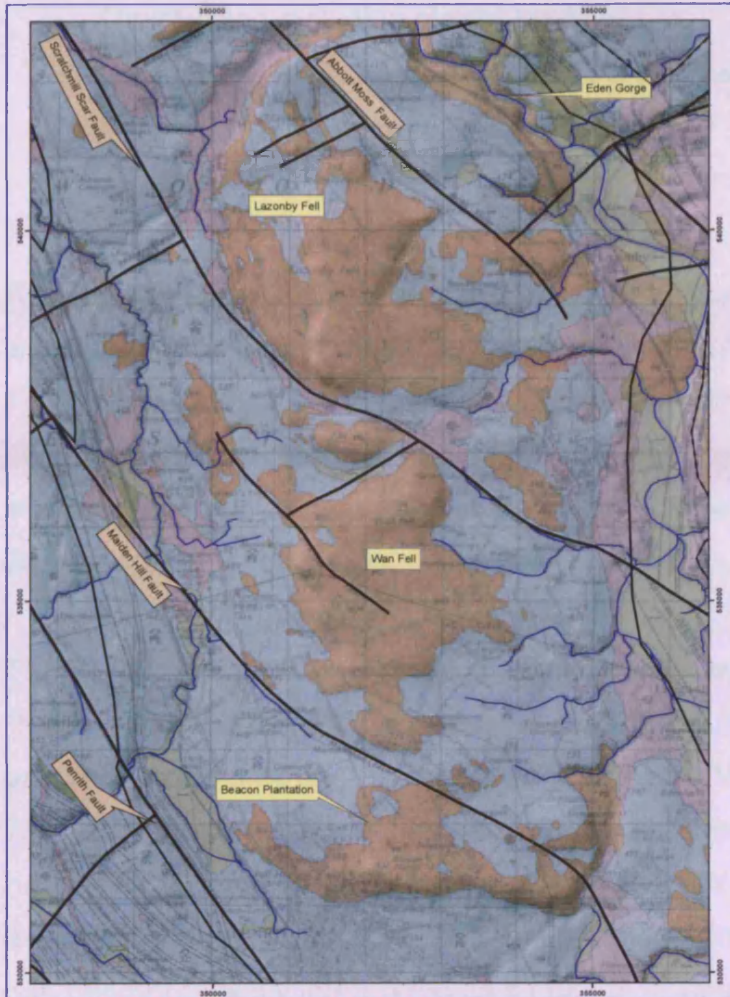


Figure 8-8 Major faults and locations of the high fells area north of Penrith. Base map BGS map sheet 24 Penrith solid & drift. Orange areas are drift fee Penrith Sandstone: Wan Fell.

### Fractures and veining

Field observations show that there is variation in the fracture patterns of the upper more competent beds, these are:

- Bedding conformal fractures, which tend to form flaggy horizons.
- Vertical, cross bedding fractures.
- Steeply dipping diagonal cross bedding fractures.

Core logging and downhole camera (BGS borehole EV2, Langwathby) reveal a variety of fracture features. There are high angle  $\sim 70^\circ$  fractures, which have been confirmed in several borehole records, along with less steep fractures. Some of these fractures have been re-cemented. The origin of these fractures is unknown and may be potentially due to:

- Overburden including glacial loading.
- Post glacial rebound (Pers. comm., A Butcher).
- Re-activation features of deeper faults.
- Hydro-fracturing.

A variation in fracture pattern, showing all three types can be observed laterally within the same exposure horizon at Cowraik Quarry (NY) 354100 531000.

Fracture density also varies with location and within exposures; this is also confirmed by Allen et al (1997) where an anisotropy effect is attributed to “the lack of permeable vertical fracturing in the area”. Figure 8-9 shows fracture patterns at various scales.

The observed infill of fractures or veining is believed to be silica-rich fluid that has “fused” the fractures, (field observation A Butcher), it does not react with dilute HCl, and the surrounding zones can appear ‘leached’. Veining size varies from ~2mm to 2cm, and density is also variable although as a general observation they seem to be associated with larger fractures or faults. South of Armathwaite there is evidence of more competent cementation and bedding conformal “veining”. This has been previously interpreted as a change in water table; possibly a function of capillary forces and different palaeo-groundwater levels (Gray 2005).

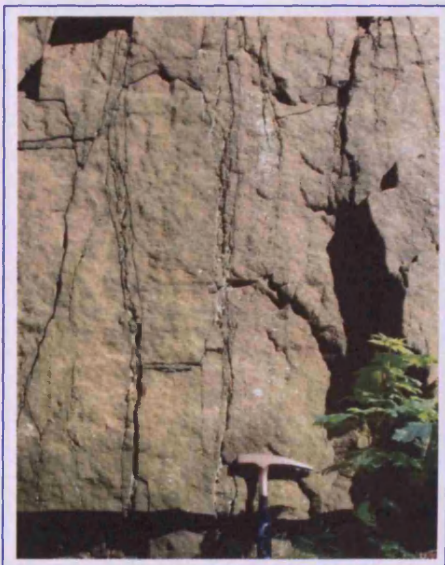


*Figure 8-9 Fracture patterns in well-cemented competent Penrith Sandstone at Cowraik Quarry. Note vertical cross bedding fractures and massive bedding. Photo taken at top of sequence shown in Figure 8-6. Photo A Gray.*

### Hard bands

Hard bands are present throughout the plateaux exposures and borehole records. They have been described as palaeo-silcretes, common under semi-arid weathering. The hard bands are associated with the plateaux, and are therefore not prevalent in the more southern area of the valley. Field observations and borehole logs indicate that the hard bands exist as distinct horizons, and they can be massive, up to 10m thick. They are bounded by less well cemented friable sandstone. The logs suggest that they extend no more than about 150m depth, from the upper levels (although boreholes do not tend to extend below this level). Lovelock (1972) suggests that these very well cemented bands are a result of their higher palaeo-permeability.

The hard band boundaries are not always sharp and well defined; although at one location the bands appear to be bedding conformal (Figure 8-10). The silification is not uniform throughout the lateral extent of a bed form and the presence or absence is variable (Hughes 2003) large amounts of poorly silicified sandstone was extracted from a pit (NY) 352170 534690 as fill for the M6 motorway construction, this was from an area of generally well silicified sandstone (Arthurton et al 1981).

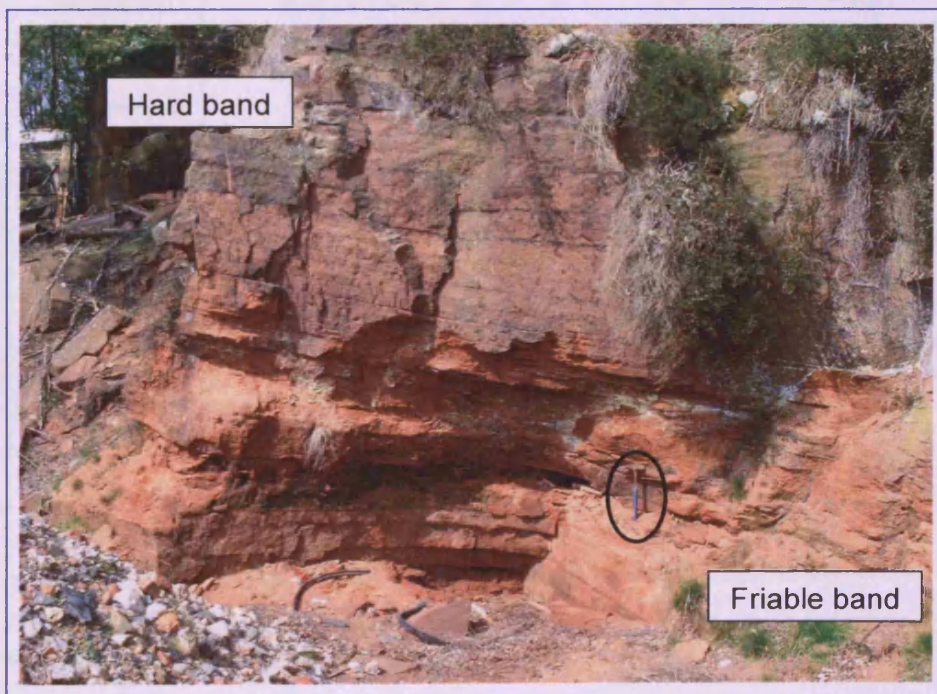


*Figure 8-10 Friable sands below hard bands at Bowman's Quarry, note hammer (circled) for scale. Photo A Gray.*

### 8.2.4 General sequence

The general sequence of the lithology consists of the following: (Figure 8-11)

- Regolith of various thicknesses.
- Weathered blocky zone, evidence of root fracturing in places (Figure 8-12).
- Hard; silicified; massive beds; tend to be lighter in colour.
- Locally, friable poorly cemented/ uncemented beds, possibly not latterly extensive (Figure 8-10).
- Massive well cemented beds (evident at Eden Gorge).
- Large, moderately cemented well preserved dune bedded sequences with distinct veining.

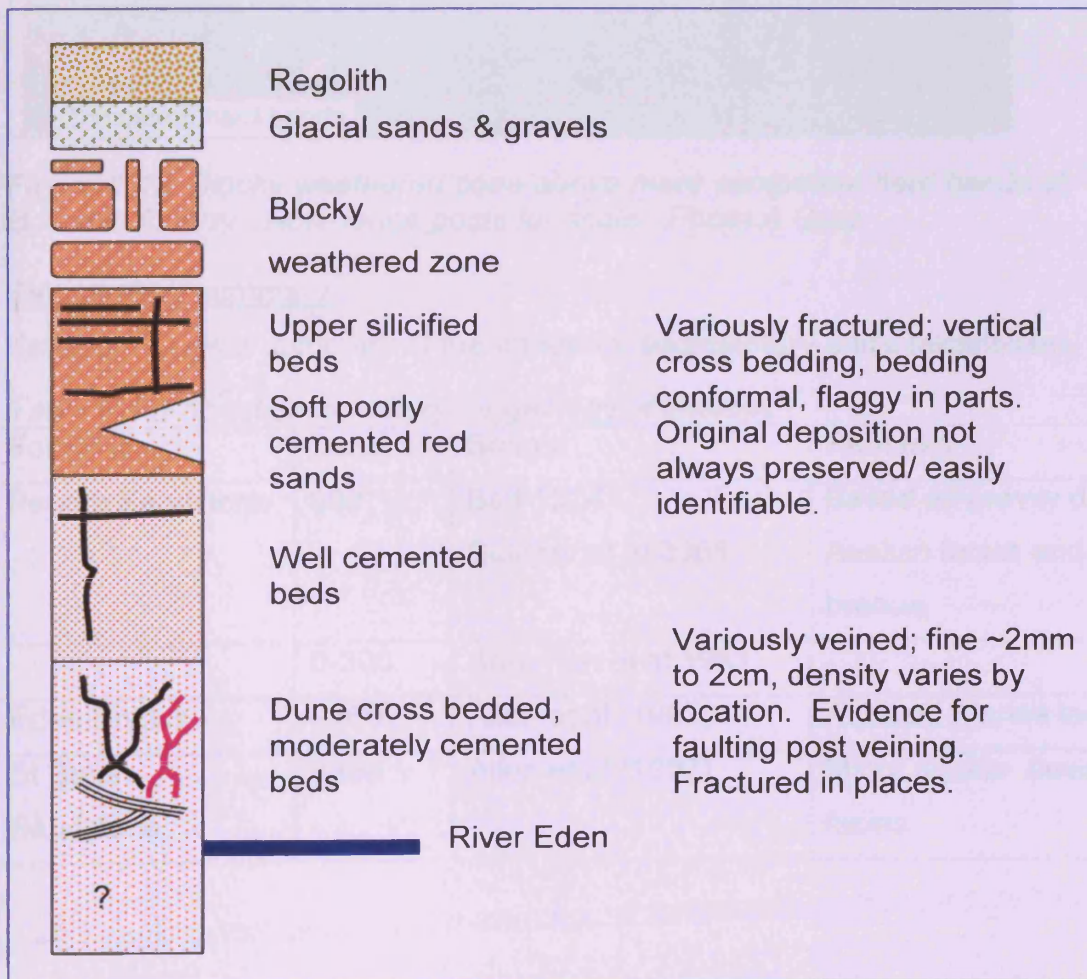


Figure 8-11 General lithological sequence in northern and plateau zones of Penrith Sandstone. Not to scale.

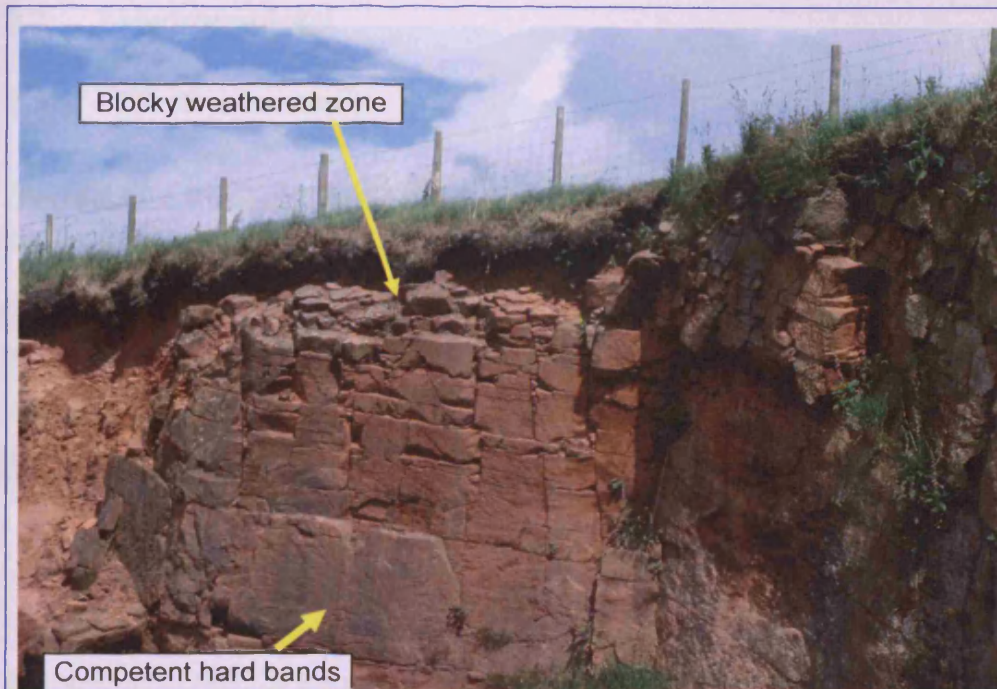


Figure 8-12 Blocky weathered zone above more competent hard bands at Bowscar Quarry. Note fence posts for scale. Photo A Gray.

### Sedimentary summary

Table 8-1 gives a summary of the important sedimentary unit's thicknesses.

Table 8-1 Formation summary for geology of interest.

Formation	Depth m	Source	Remarks
Penrith Sandstone	900	Bott 1974 Butcher et al 2003	Based on gravity data Aeolian facies and basal breccia
	0-300	Arthurton et al 1981	
Eden Shales	<180	Allen et al (1997)	Aquitard marine facies
St Bees Sandstone	<350	Allen et al (1997)	Minor aquifer fluvial facies

## 8.3 Hydrogeology

### 8.3.1 *Water sources*

#### Rainfall and evapotranspiration

Rainfall for the region was obtained from the Meteorological Office rainfall and evaporation calculation system (MORECS). The Eden Valley is located within grid squares #78 and #84, the division occurring at Appleby. The following rainfall data was obtained from Butcher et al (2003):

- Square 78 1 148mm/year
- Square 84 2 328mm/year
- Mean 1 738mm/year

Butcher et al (2003) suggest that the rainfall for the centre of the Vale is more typically 850-900mm/year, this difference being due to a positive skewing of MORECS data towards the elevated more wetter bounding regions. Ingram (1978) uses a value of 900mm/year over the Penrith Sandstone and 950mm/year for the St Bees Sandstone. Monkhouse and Reeves (1977) give a mean value based on sub-catchment details of 1 110mm/year. Additional data from the Centre for Ecology and Hydrology (CEH) based on Meteorological Office data for sub-catchment rainfall at gauging stations was also obtained (CEH 2008). These values are more localised for stations within the valley and do show a rainfall gradient along the axis. The mean value for rainfall in the valley is 1513mm based on the 1961-90 average rainfall data (Table 8-2).

Table 8-2 CEH river gauging station rainfall data.

Station	Easting	Northing	Elevation m	Rainfall mm/y	CEH Stn	River
Kirkby Stephen	377300	509700	158.1	1 483	76014	Eden
Temple Sowerby	360500	528300	92.4	1 146	76005	Eden
Warwick Bridge	347000	556700	17.5	1 272	76002	Eden
Udford	357800	530600	90.9	1 777	76003	Eamont
Pooley Bridge	347200	524900	144.2	2 154	76015	Eamont
Eamont Bridge	352700	528700	113.3	1 814	76004	Lowther
Hurraby Green	341200	554500	20.1	9 45	76010	Petteril
			mean	1 513		

The potential and actual evapotranspiration data for the MORECS squares are similar; approximately 480mm/year, Butcher et al (2003) and Milne (1994) quote 425mm/year in the valley and 350mm in the Pennines. Ingram (1978) suggests 450mm/year, while Monkhouse and Reeves (1977) quote 428mm/year (Table 8-3).

Table 8-3 Summary of rainfall and evapotranspiration for Eden Valley and environs.

Source	Rainfall mm/year	Evapotranspiration mm/year
MORECS	1 738	480
Butcher <i>et al</i> (2003)	850-900	480 (MORECS)
Ingram (1978)	900-950	450
Milne (1974)	1 000	425 350
CEH	1 513	No data
Monkhouse & Reeves (1977)	1 110	428

### Surface water

The River Eden is the main water course running south to north along the valley axis, its major tributaries are; The Belah, Scandal Beck, Lyvennet, Leith, Lowther, Eamont and Croglin Water. The River Petteril drains the northwest shoulder of the Penrith Sandstone, resulting in a sub-catchment interfluvium. Numerous smaller becks, gills, sikes and waters tend to drain the eastern slopes of the St Bees Sandstone and Carboniferous strata. The major tributaries tend, with the exceptions of Croglin Water and River Belah, to drain the western slopes, which are the Carboniferous Limestone Series and younger strata (Figure 8-13).

The River Eden can be considered to be a gaining system for the majority of its reach, except between Temple Sowerby (NY) 361100 527100 and Langwathby. Here it is isolated from the Penrith Sandstone by the Eden Shales (Allen et al. 1997). Observation of the river bed below Armathwaite (NY) 350500 546000 show bedding planes that are contemporaneous with moderately cemented dune bedded sandstones on the east bank. The mean flows at Warwick Bridge are  $34 \text{ m s}^{-1}$  and at Temple Sowerby  $14.6 \text{ m s}^{-1}$ , (CEH 2008).

There are several large surface water bodies or ponds located within the central valley (Figure 8-14). There are also a number of moss' or mires in the area, which are located on the upper east flanks of the fells. The mires and moss' are probably located on low permeability, un-fractured or sealed silicified sandstone. The area is generally well-drained due in part to the lack of bogs, with the exception of the Edenhall area (NY) 356500 532500 (Figure 8-14). Several areas of possible seepage were observed by their distinct vegetation change and proximity to slope breaks.

### Springs

Numerous springs are recorded on the Ordnance Survey mapping. It is possible that these indicate the outcrop between permeable sands and impermeable hard bands on slopes. These may also be seepages from draining fissures in outcropping hard bands.

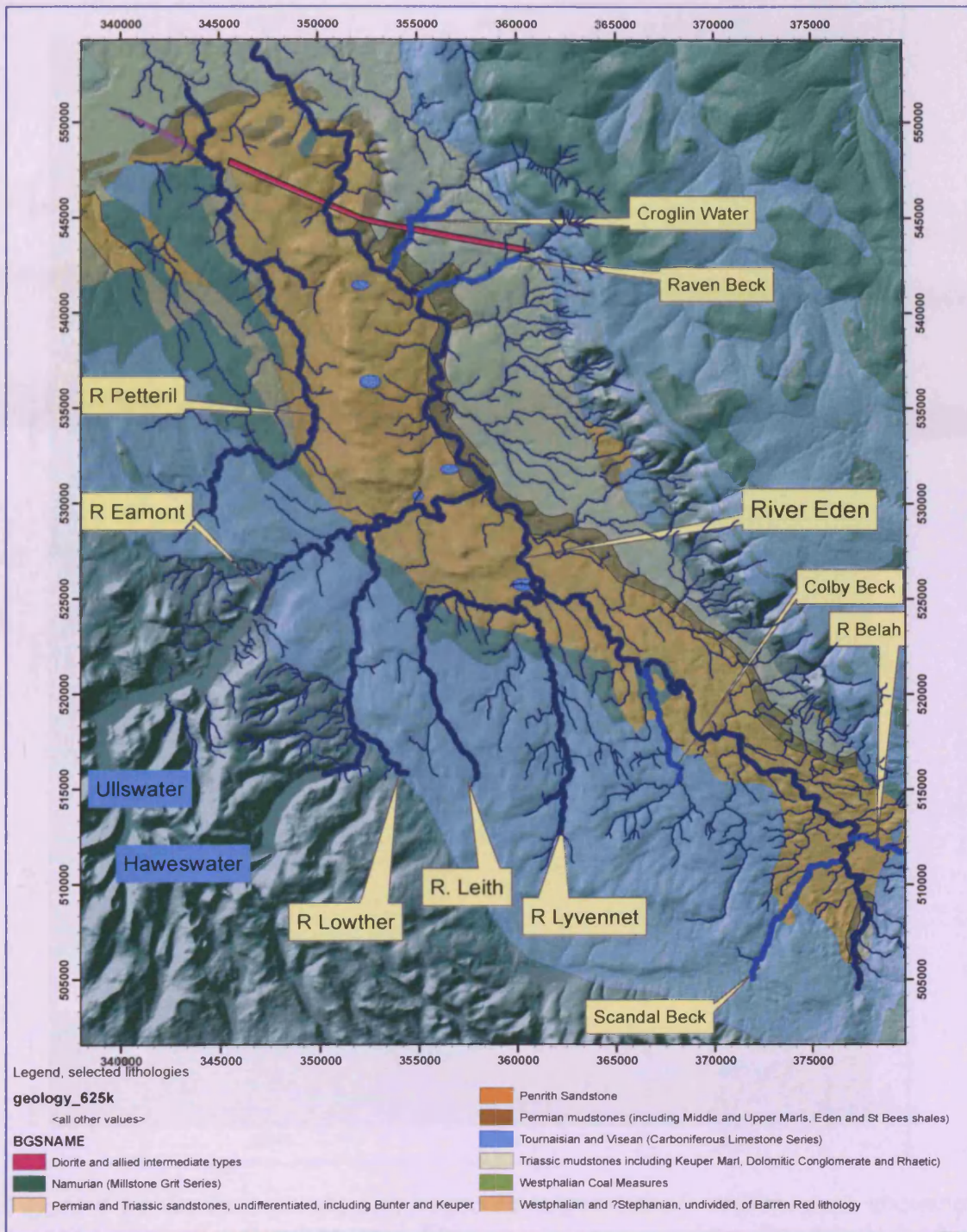


Figure 8-13 Surface water features: Major tributaries of the River Eden with selected sedimentary lithologies. Smaller drainage features also marked. Small blue ellipses are mires or bogs.

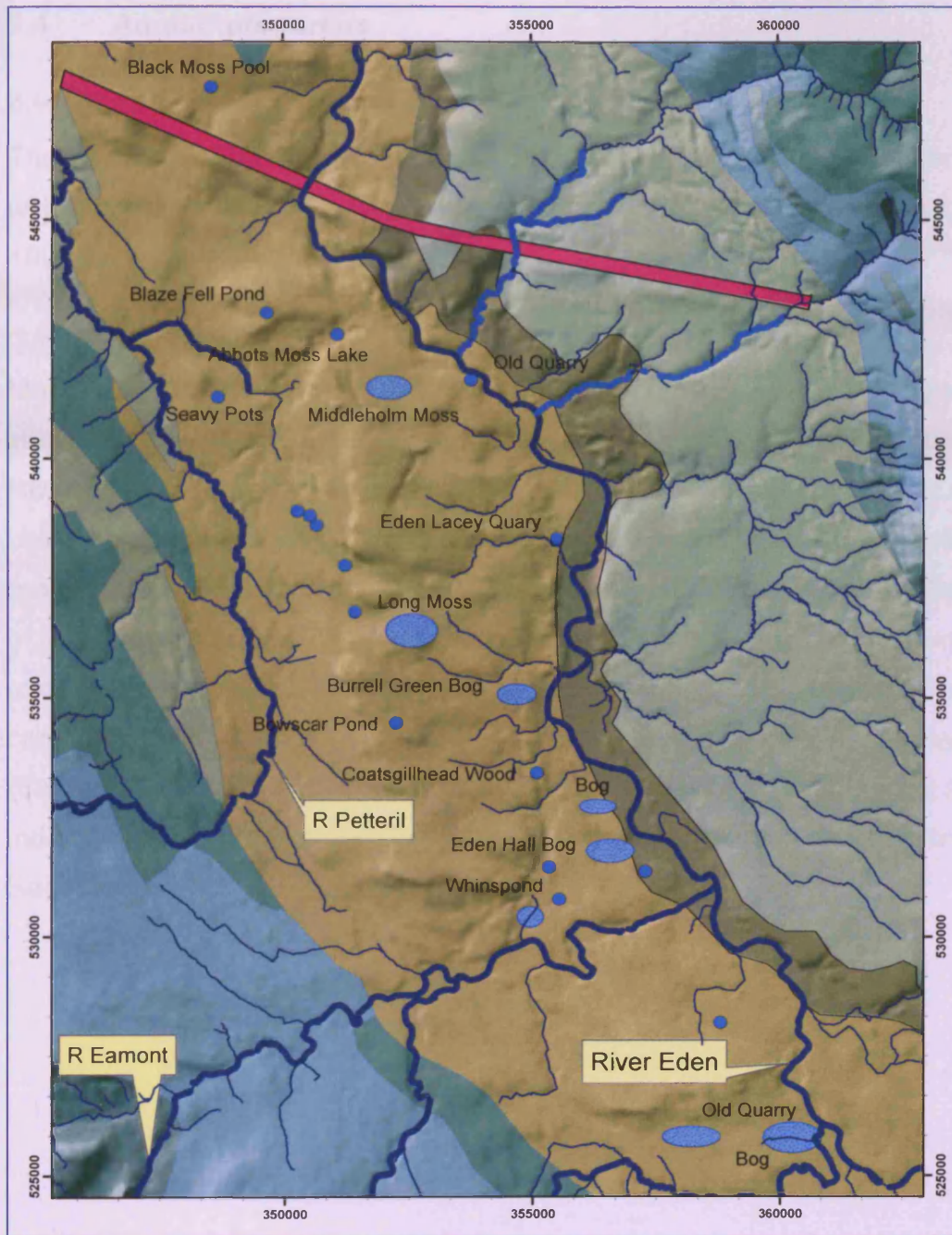


Figure 8-14 Surface ponds and bogs. Enlargement of northern area showing location of small water features. Ellipses are bogs or mires. See key in 8.13.

## **8.4 Aquifer properties**

### **8.4.1 Penrith Sandstone Formation**

The Permo-Triassic sandstones form the second most important aquifer in the UK with properties affected by both depositional and diagenetic processes (Allen et al. 1997).

#### **Groundwater flow**

Maps commissioned by the Environment Agency (Streetly and Chillingworth 2001) show that the River Eden is a gaining system, with groundwater flow towards the River Eden. Groundwater contours for this project were derived independently using all available data. The results (Figure 8-15), correspond with earlier mapping projects undertaken by Ingram (1978) and the Environment Agency. Examination of the contours seems to reflect the more general asymmetrical synform of the underlying geology, which is steeper on the east limb. The potential presence of compartmentalisation is not represented at the regional scale in this mapping (Seymour et al. 2006). The steeper hydraulic gradient evident from the mapping are indicative of lower hydraulic conductivity, due to low permeability silicified St Bees Sandstones.

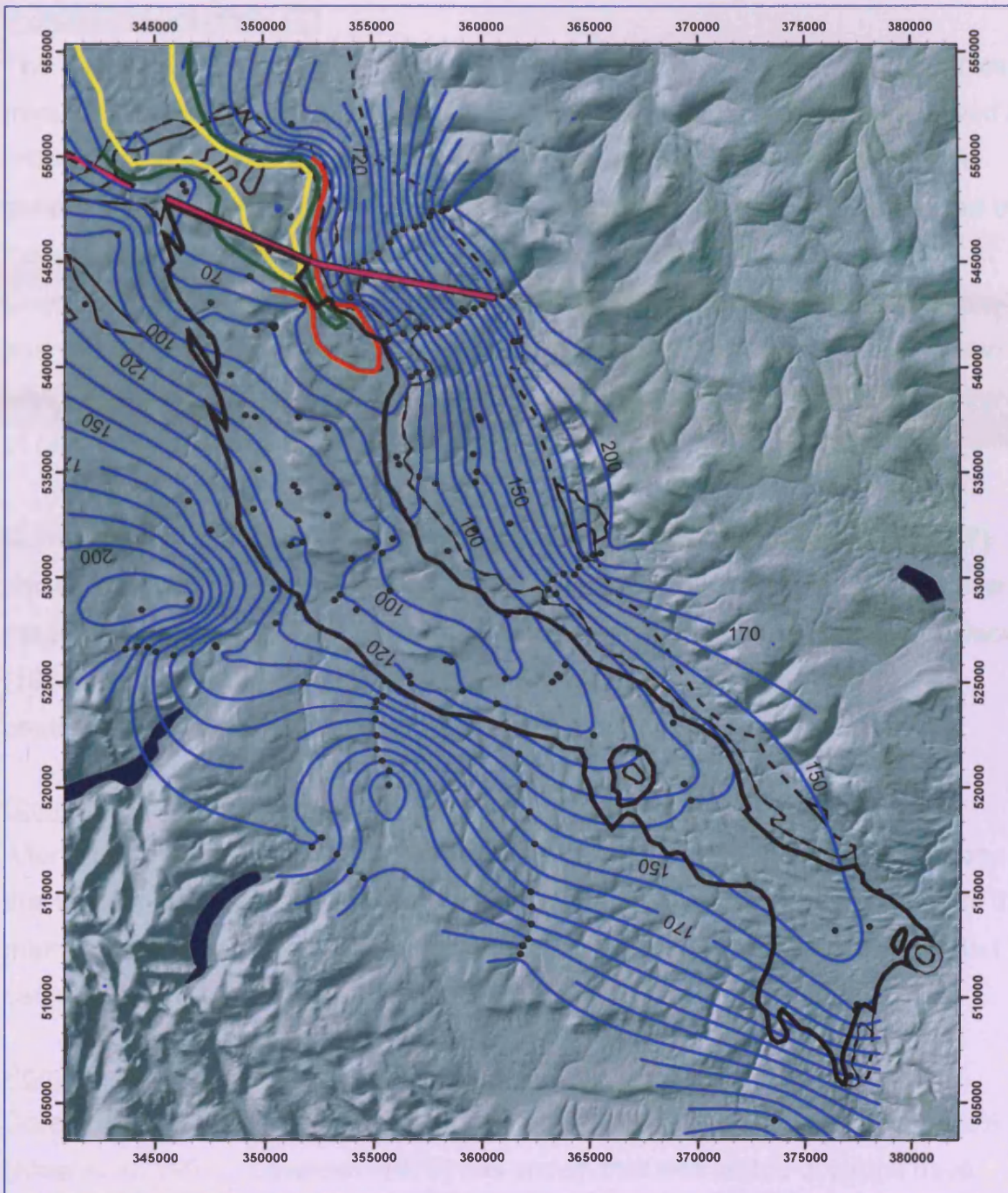


Figure 8-15 Groundwater contours. Contours based on borehole water rest levels and intersection of rivers with topographic surface. Very high degree of uncertainty on extremes of data limits. Coloured contours added by hand to compensate for process artefacts in the contouring package. Dots represent data points consisting of boreholes and rivers.

### Hydraulic conductivity (K)

The results that Allen et al (1997) quote are based upon over 2000 core samples from the Cliburn boreholes. The range of  $3.5\text{m day}^{-1}$  to  $26.2\text{m day}^{-1}$  are believed to reflect the variability in cementation. The horizontal hydraulic conductivity is in general about 10 times that of the vertical hydraulic conductivity, and is caused by the interbedding of well sorted and less well sorted grains (Lovelock 1972).

Lovelock (1979) states that the silicified beds have conductivities of  $3 \times 10^{-4}\text{m day}^{-1}$  and well sorted sediments have a hydraulic conductivity of  $7.5\text{m day}^{-1}$  compared to less well sorted beds of  $0.28$  to  $1.3\text{m day}^{-1}$ . There is no indication as to the degree of cementation of these un-silicified units.

Comparison of pumping test data with calculated results from Allen et al (1997) shows that in all but one or two boreholes the transmissivity are at least an order of magnitude greater than the well sorted millet seed facies. This supports Lovelock's (1972) statement that "aquifer transmissivity is dominated by fissure flow, contributing 93% of flow but only less than 1% of the porosity".

### Storage (S)

Allen et al (1997) quote a geometric mean of  $1.1 \times 10^{-4}$  for the Penrith Sandstone, this value indicative of a confined aquifer; due in part to a lack of dewatering of the matrix on the time scale of the pumping tests. Ingram (1978) also suggests that the cemented hard bands near the water table will effectively confine the aquifer.

### Porosity

Core porosities, believed to be from the Cliburn boreholes, vary from 5% to 36% (Allen et al. 1997). Lovelock (1979) has shown that well sorted outcrops have porosities of about 30%, reducing to between 25% and 30% for less well sorted samples, while the hardened silicified bands have reduced porosities of 5% to 8%.

### Transmissivity (T)

Published transmissivity values (Allen et al 1997) for 15 different pumping test sites in the Penrith Sandstone have results varying from 10's m<sup>2</sup> day<sup>-1</sup> to 1900m<sup>2</sup> day<sup>-1</sup> at Cliburn. This is interpreted as a variation of cementation properties in the Formation with a geometric mean of 390m<sup>2</sup> day<sup>-1</sup>. The large transmissivity at Cliburn is attributed to more permeable horizons or sub-horizontal bedding plane fractures. The Cliburn values exceed the matrix transmissivity of 128m<sup>2</sup> day<sup>-1</sup> obtained from core data (Ingram 1978). The transmissivity of the aquifer is controlled by the flow in the small 1-3mm wide fissures that are prevalent; this contributes 93% of total flow but less than 1% of the aquifer porosity (Lovelock et al. 1975).

Packer testing at the Cliburn borehole suggests that in general the smaller fractures in the borehole wall are not permeable and that the majority of flow, 85%, came from two (presumably larger) horizontal fractures (Gray 2006). The data show that water is entering the well at the upper level, and exiting via a 39m lower fracture. A distinct lack of vertical fracturing is also reported at this location (Allen et al. 1997). An analysis of available pump test data was undertaken, which indicates a wide range of values and indicates both leaky and dewatering features throughout the aquifer.

### Drift cover

It is believed that preferential recharge windows may exist (Butcher et al. 2003), a view which is supported by field and report observations:

- Mires and bogs, over non-fractured silicified zones.
- Sandy soils over fractured silicified zones for example above Cowraik Quarry (Figure 8-6 and Figure 8-12).
- Possible glacial sand and gravel incised channel fill.
- Clay rich loamy soils over fractured silicified zones, observed during a walkover survey.
- Soft sands in silicified zones observed in an M6 construction quarry.

These recharge windows may be additionally augmented by surface runoff from areas of more clay rich till, which will focus recharge at the till edge (Butcher et al. 2003). Interflow may also be enhanced along preferential conduits, such as pebble beds in the glacial sands and gravels; thus providing more rapid lateral movement.

### Regolith

The soil survey map for the area shows four distinct soil types (Figure 8-16); these are characterised in Table 8-4.

**Table 8-4 Soil characteristics. Information from Soils map legend handbook (SSLRC 1983a).**

Soil Name	Map Symbol	Geology	Characteristics	Land use	Catchment location
Wick 1	541r	Glaciofluvial or river terrace drift	Deep well drained coarse loamy and sandy soils, locally over gravel.	Dairying in Cumbria	Northern part of Penrith SS outcrop less elevated fells. Thin band on east flank of Eden between Kirkby Thore and Warcop
Crannymoor	631f	Glaciofluvial drift	Well drained sandy soils, mostly under woodland and very acid. Associated with sandy soils affected by groundwater.	Dry lowland heath habitats	Elevated fells regions, including Cliburn
Clifton	771n	Reddish Till	Slowly permeable seasonally waterlogged reddish fine and coarse loamy soils. Some deep coarse loamy soils seasonally affected by groundwater.	Grassland in northern areas.	Southern portion of catchment and west of River Petteril.
Newport 1	551d & a	Glaciofluvial drift	Deep well drained sandy and coarse loamy soils some sandy soils affected by groundwater.		Eamont Valley and Cliburn area, east flank of catchment and R Eden.

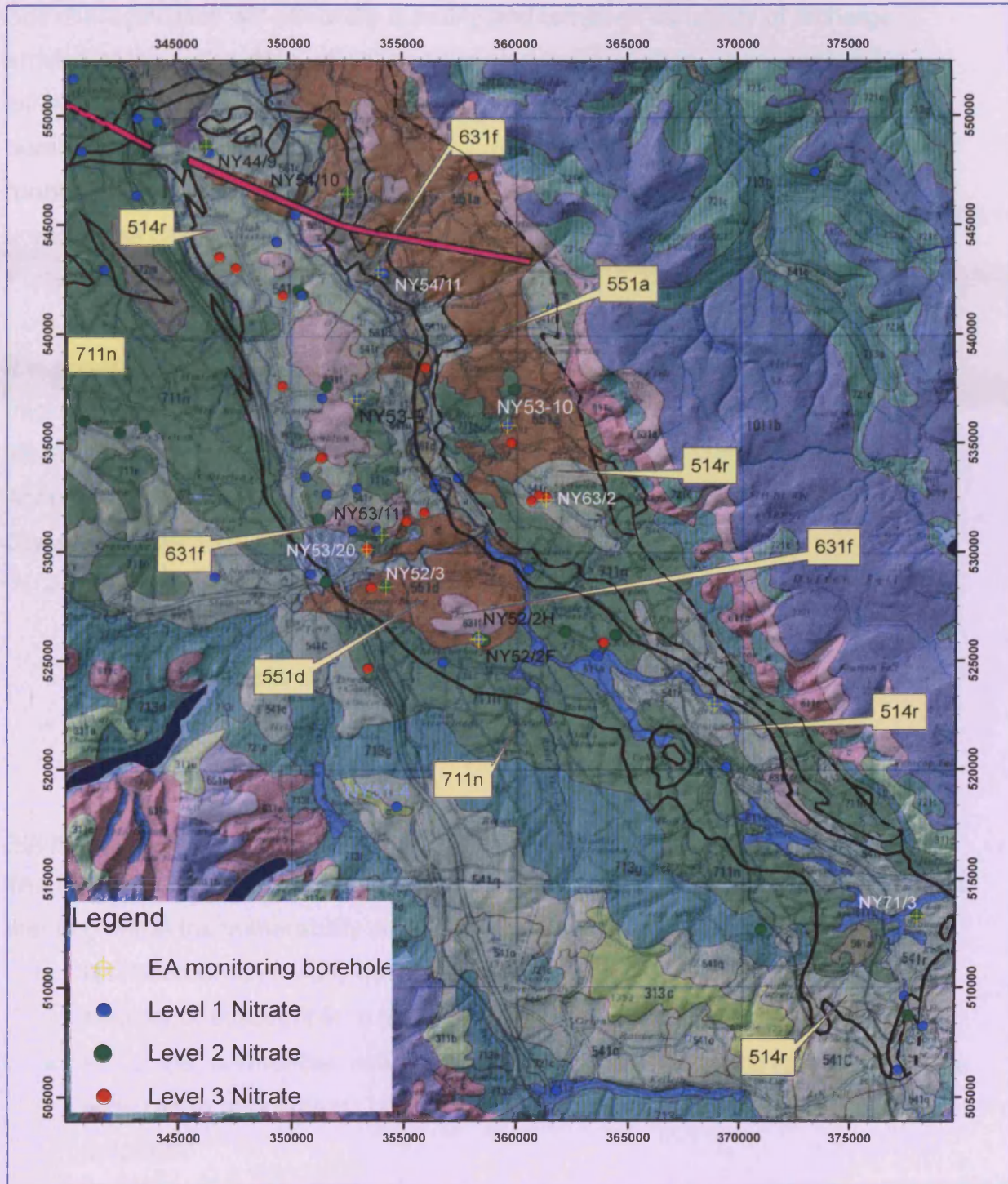


Figure 8-16 Soils map of Eden Valley. See also Table 8-5 for soils explanation (SSLRC 1983b).

Soil characteristics will affect the quantity and temporal variability of recharge arriving at the water table. It will also act as a first line attenuation medium for infiltration contaminants. These effects are likely to be local to the soil type and borehole catchment zone. A clay rich till, type 771n may impede or influence local runoff to water courses. These are more common in the southern and west flank areas of the catchment. On the west flank, surface water may drain to the River Petheril and be removed from the system.

It is generally accepted that a covering of about 5m of drift deposits is the minimal thickness required to protect an underlying aquifer, however local conditions and lithological components are also important, (Robins 1998). The Winter Rain Acceptance Potential map (WRAP) indicates that the valley is designated as Class 1 (SSEW 1977):

- Well drained permeable sandy or loamy soils and shallower analogues over highly permeable (limestone, chalk) sandstone or related drifts.
- Earthy peaty soils drained by dykes or pumps.
- Less permeable loamy over clayey soils on plateaux adjacent to very permeable soils in valleys.

#### Aquifer vulnerability

The Environment Agency aquifer vulnerability mapping of the Eden Valley indicates that in general the vulnerability class is High, H1, 2 & 3, (SSLRC 1997a, b, c, d)

- H1: Soils which readily transmit liquid discharges because they are either shallow or susceptible to rapid flow directly to rock, gravel or groundwater.
- H2: Deep, permeable, coarse-grained textured soils, which readily transmit a wide range of pollutants because of their rapid drainage and low attenuation potential.
- H3: Coarse-textured or moderately shallow soils, which readily transmit non-adsorbed pollutants and liquid discharges, but which have some ability to attenuate adsorbed pollutants because of their organic matter contents.

Along the course of the River Eden, the class is again High, but for a minor aquifer designation. The Eden Valley is further classified in its ability to attenuate pollution in the form of fraction of organic carbon (*foc*), total inorganic carbon (TIC) and cation exchange capacity (CEC); in all classes the Penrith Sandstone is classed as low (Smith and Lerner 2007).

#### 8.4.2 ***Conceptual hydrogeology Eden Valley***

Figure 8-17 shows a conceptual model diagram of the Eden Valley hydrogeology and agricultural inputs. This indicates the influence that the hard bands may be having on the groundwater regime in that they may cause stratification of flow and also cause perching in the unsaturated zone. The potential for recharge windows through the drift are also shown, as is the possible attenuation potential within the soil zone.

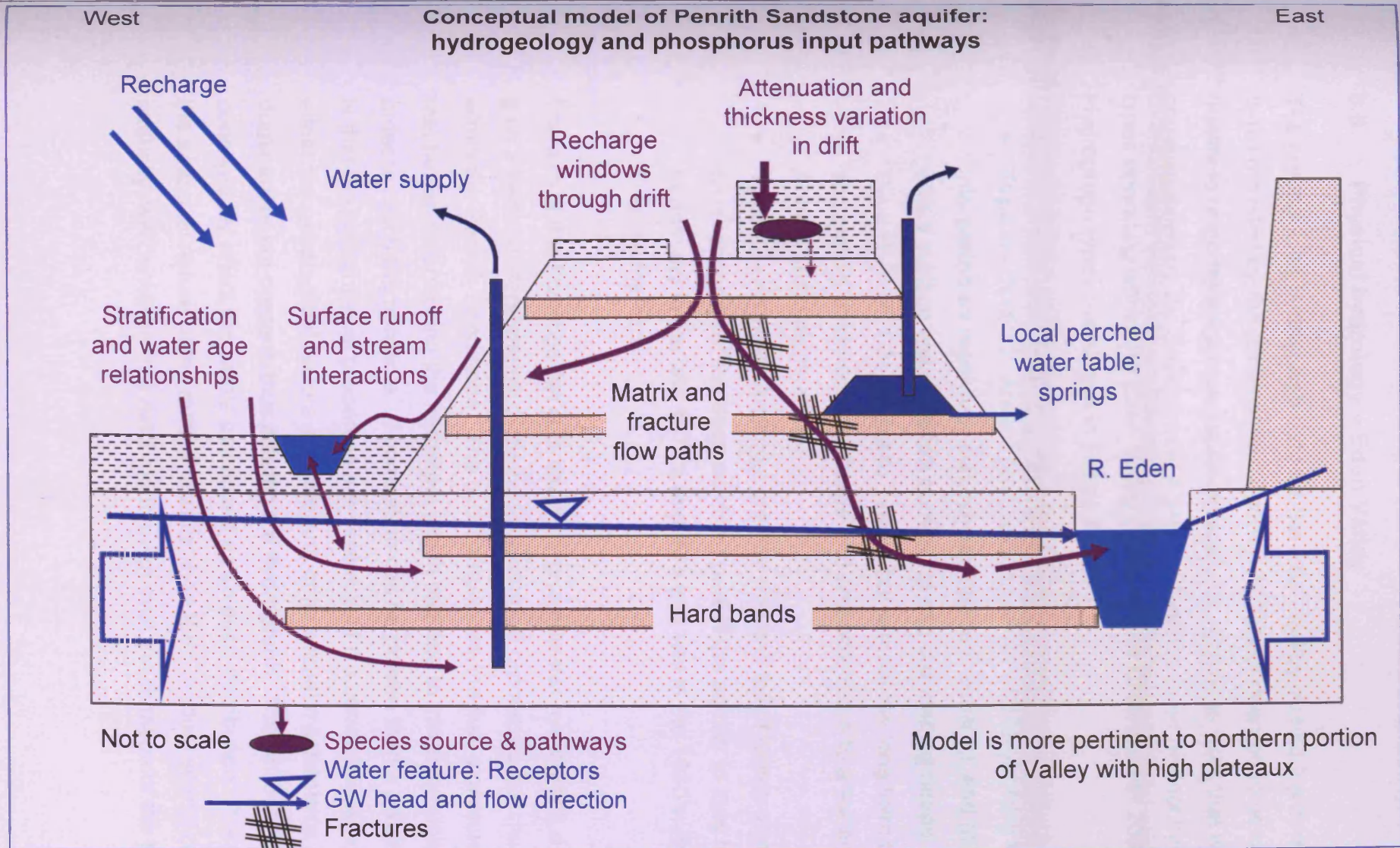


Figure 8-17 Conceptual diagram of Eden Valley Hydrogeology and agricultural inputs.

## 8.5 Physical hydrology – Eden Valley

The groundwater hydrograph data for the Eden Valley monitoring boreholes (Figure 8-18) provided by the Environment Agency (NW) was deemed to be of sufficient quality to undertake rigorous statistical analysis. Previous work that was commissioned by the Environment Agency, identifies three distinct hydrograph types operating within the Eden Valley (Streetly and Chillingworth 2001).

Hydrograph types are shown in Figure 8-19.

- **Type A** – NY63/2; Annual fluctuations of ~1m with larger long term trends. Interpreted as receiving relatively unimpeded recharge, and not in contact with a surface water feature controlling and dampening heads.
- **Type B** – NY71/3; Similar to Type A but without the long term trends, suggesting unimpeded recharge and probably close to a surface water body. Annual fluctuations >1m.
- **Type C** – NY44/9; A distinct gradual rise and fall of heads and is believed to be a response of the deep confined part of the aquifer to long term recharge trends; dry in the late 1970's and 90's and wet in the 1980's. Annual fluctuations <1m.

The aim of this investigation is to examine groundwater hydrograph data in order to gain a better understanding of the hydrogeological processes that may be occurring within the Penrith Sandstone. The hydrographs are the final signature of the mechanisms controlling the recharge, which has had to travel through the aquifer in order to reach the borehole. If correlation can be proven then a pivotal assumption is that the geo-physical properties are similar, and if a correlation is not proven then either the geophysical factors are different, or individual mechanisms are either dominant or not present, thus altering the hydrograph. Rainfall data is assumed to conceptually effect the whole catchment as an even distribution. It is believed that the seasonal nature of the rainfall, and its short term random spatial occurrence and intensity, will converge to a catchment mean over the duration of the study.

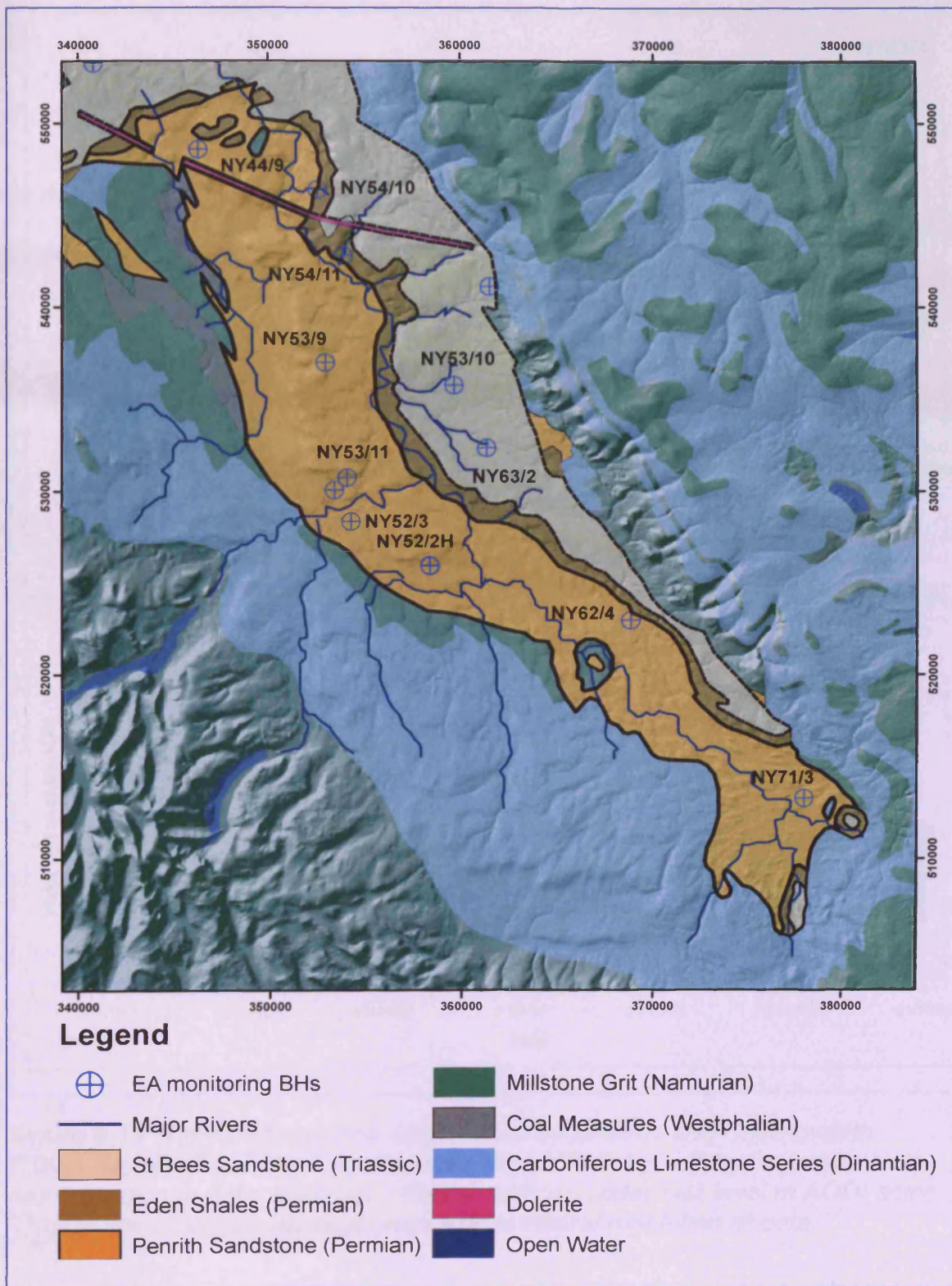


Figure 8-18 EA monitoring borehole location and geology map. Data rendered onto DTM and showing higher plateaux in northern portion of valley. An endpaper map is enclosed for aid of location identification.

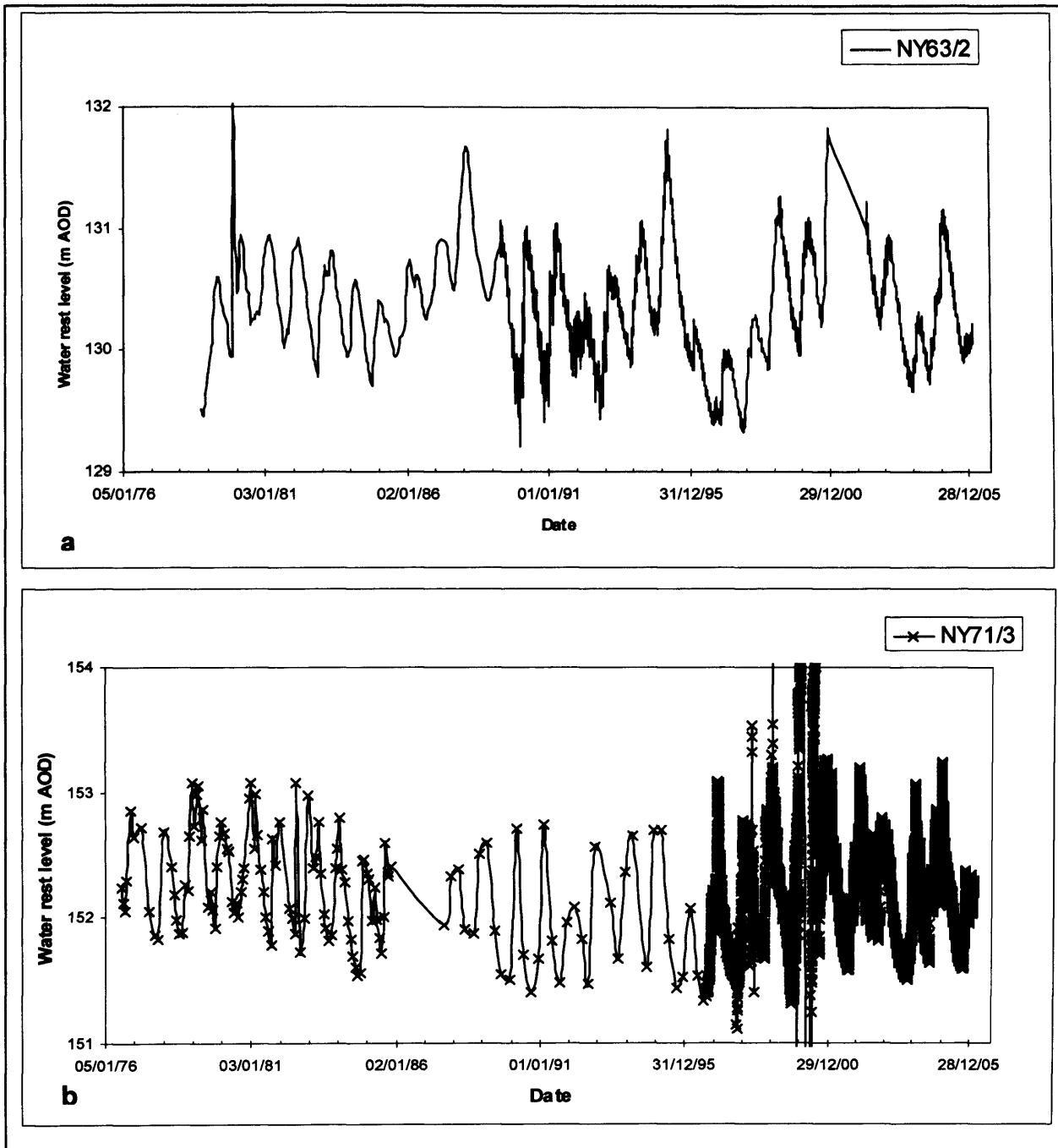


Figure 8-19 Type hydrographs as identified by Streetly and Chillingworth (2001). (a) NY63/2 Type A hydrograph. (b) NY71/3 Type B hydrograph. Note same horizontal date scale but different vertical (water rest level m AOD) scale. Thicker lines/markers indicate change in temporal resolution of data.

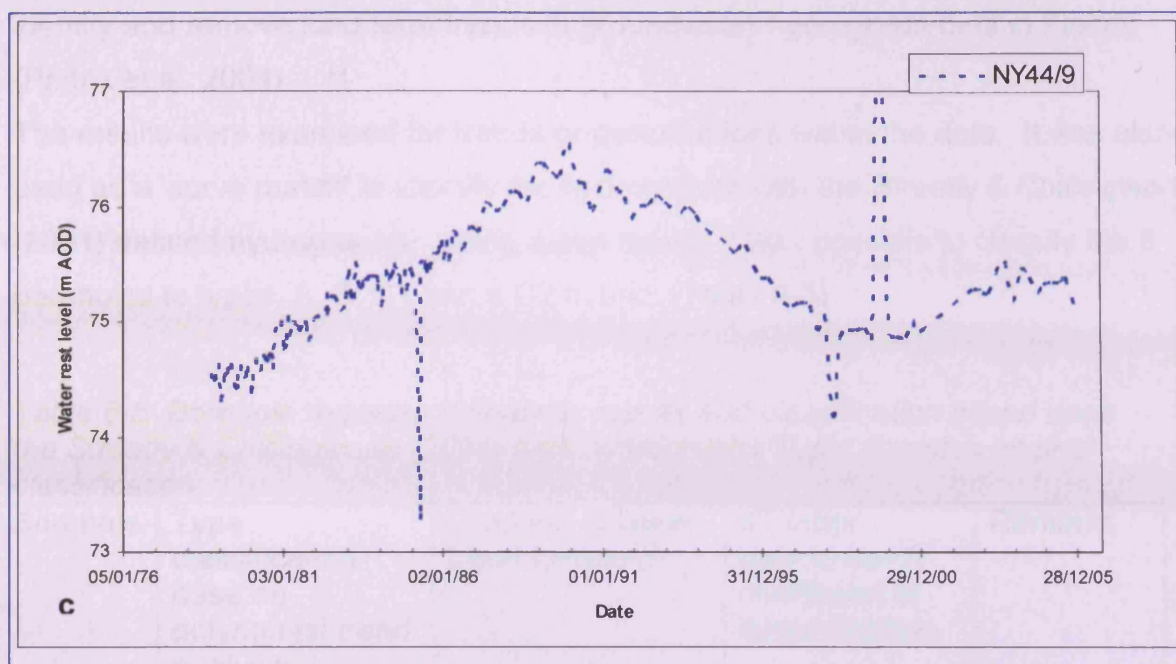


Figure 8-19 cont. (c) NY44/9 Type C hydrograph. Note same horizontal date scale but different vertical (water rest level m AOD) scale. Thicker lines/markers indicate change in temporal resolution of data.

The following investigative techniques were used:

- Analysis of hydrograph data to examine temporal trends and determine type hydrographs, (Streetly and Chillingworth 2001)
- Autocorrelation of the hydrograph data.
- Correlation of the hydrograph data to establish relationships between hydrographs.
- Investigate borehole geo-physical and spatial patterns.

### 8.5.1 Results and discussion

#### Analysis of hydrograph data

##### *Hydrograph polynomial trend analysis.*

The hydrographs were initially normalised by their mean value. Curve fitting using 6th order polynomial trend analysis (embedded within Excel 2002) was undertaken to establish a best fit regression curve. The analysis is a method of obtaining high order terms for non-linear relationships between the two variables present; rest water level and time. Polynomial and linear regression analysis has been used to

identify and remove long term trends in groundwater hydrograph data in Florida (Prinos et al. 2004).

The results were examined for trends or perturbations within the data. It was also used as a 'curve match' to identify the hydrographs with the Streetly & Chillingworth (2001) defined hydrographs. Using these results it was possible to classify the 8 boreholes to types, A, B, C1 and a C2 hybrid, (Table 8-5).

*Table 8-5 Borehole regression analysis results and classification based upon the Streetly & Chillingworth (2001) type hydrographs Type' demotes original classification.*

Borehole	Type classification base on polynomial trend analysis	Gradient of linear trend ( $y=mx+c$ )	6 <sup>th</sup> order polynomial $R^2$ coefficient of determination	Remarks
NY44/9	C1	Positive ( $6e-5$ )	0.673	Type curve
NY53/9	C1	Negative ( $-7e-5$ )	0.822	
NY53/11	C1	Negative ( $-8e-5$ )	0.812	
NY52/2H	Hybrid C2	Positive ( $3e-5$ )	0.500	
NY54/10	Hybrid C2	Positive ( $3e-4$ )	0.546	
NY52/3	A	Negative ( $-4e-5$ )	0.167	
NY53/10	A	Positive ( $4e-5$ )	0.117	
NY62/4	A	Negative ( $-5e-5$ )	0.334	
NY63/2	A	Positive ( $5e-6$ )	0.019	Type curve
NY54/11	B	Negative ( $-2e-7$ )	0.116	
NY71/3	B	Positive ( $2e-6$ )	0.001	Type curve

### Hydrograph visual analysis

Visual inspection of the hydrographs show other distinctions between the C1 and C2 groups. There is not a long term rising and regressing limb in NY52/2H (C2) and NY53/11 (C1) compare this with NY 53/9 and NY44/9 (see Figure 8-19).

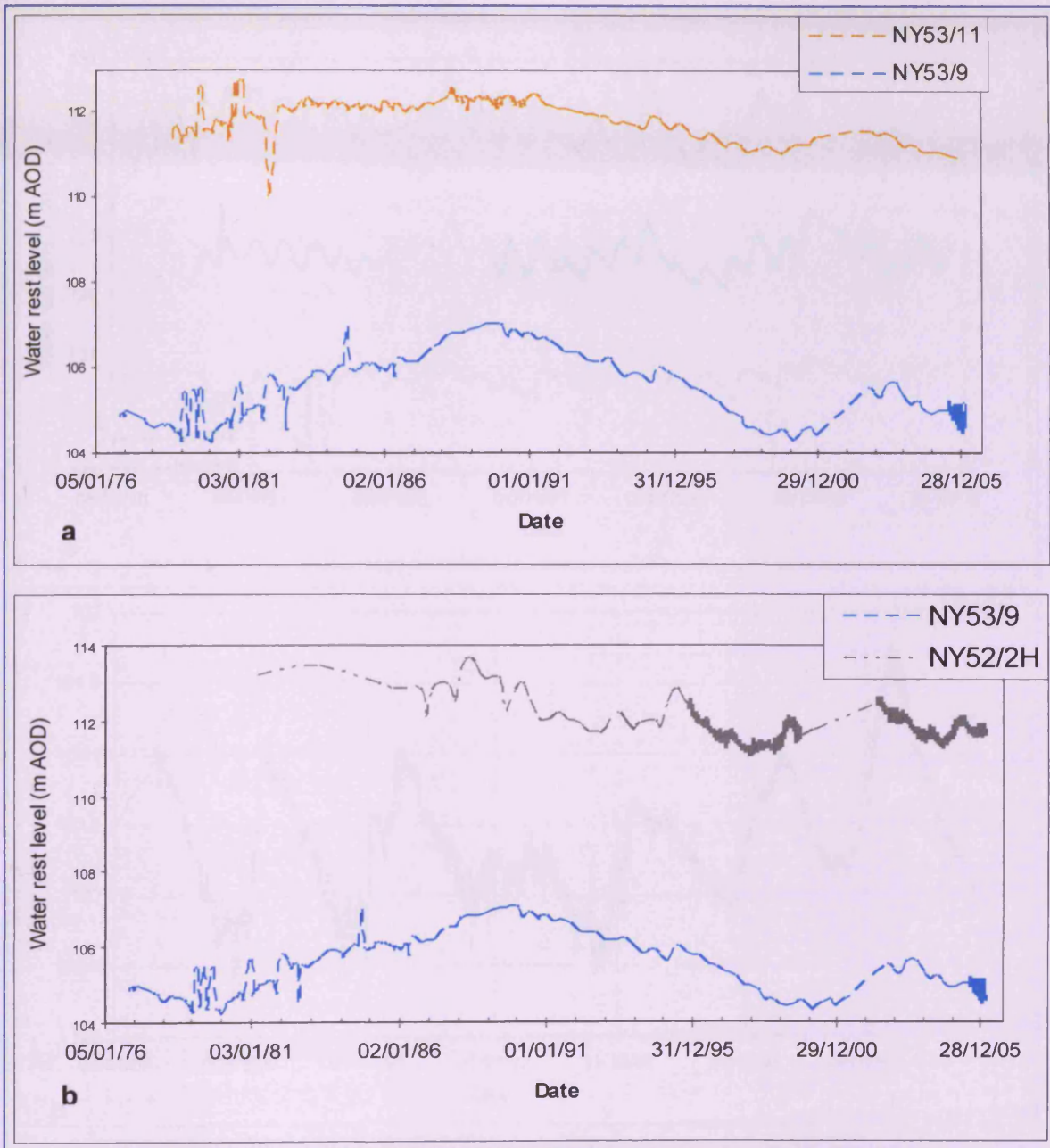


Figure 8-20 C type hydrographs for Eden Valley.

For the A and B type hydrographs, the visual distinction is more apparent (Figure 8-21). Where the data is of sufficient resolution these borehole types experience peak levels normally by the end of the year's first quarter, a gradual but steep fall then occurs until the onset of the autumnal rains.

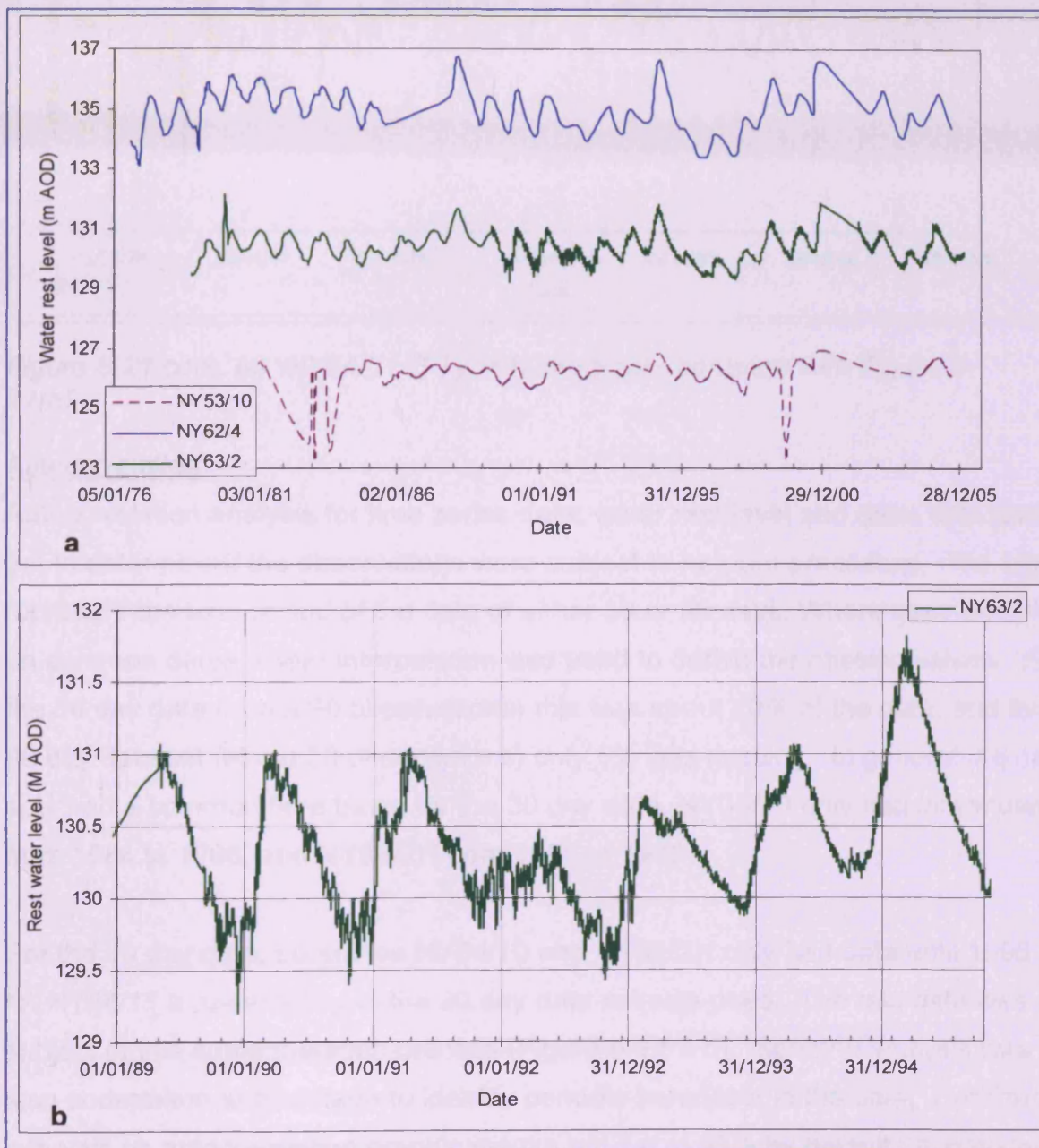


Figure 8-21 A and B Type hydrographs. (a). A Type (NY62/4 and NY63/2) and B Type (NY53/10) hydrographs. (b). Snap shot of NY63/2 to show steep rise and fall over a yearly cycle. Note low level during 1992-93, which corresponds with low rainfall during this period, see Fig 5b. Note scale change on axis.

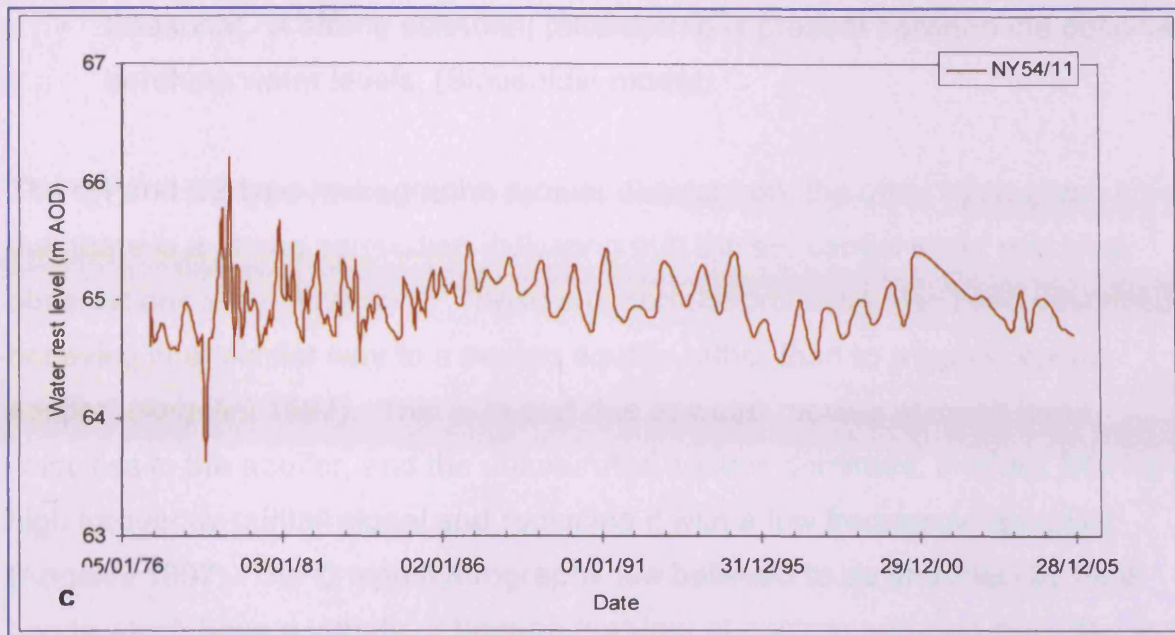


Figure 8-21 cont. (c) NY54/11 B Type hydrograph, compare with Figure 8-21(a).

### Autocorrelation

Autocorrelation analysis for time series data; water rest level and date, was carried out to determine if the observations were subject to random processes. The lags represent the time period of the data of either 30 or 90 days. Where gaps occurred on common dates, linear interpolation was used to derive the missing values. For the 30 day data (about 90 observations) this was about 10% of the data, and for the 90 day data set (about 50 observations) only 5% was missing. In general the data sets had a common time base, for the 30 day data, NY53/10 only had information from 1984 to 1986, and NY52/2H from 1995 to 1999.

For the 90 day data, boreholes NY54/10 and NY52/2H only had data until 1996 and for NY54/11 a re-sampling of the 30 day data set was used. The rain data was also subject to this autocorrelation process (Figure 8-22 a-n). Spectral analysis was also undertaken at this stage to identify periodic behaviour in the data. Confidence intervals on autocorrelation graphic results are set at 95% by default. A synopsis of results is in Enclosure 1 (CD). Three standard type curves could be obtained and can be interpreted as:

- Autocorrelated. There is a statistical relationship between observed borehole water levels extending for a number of months.

- Random. There is no statistical relationship between borehole water levels.
- Seasonal. A strong seasonal relationship is present between the observed borehole water levels, (Sinusoidal model).

The C1 and C2 type hydrographs remain distinct from the other hydrograph types in that there is a strong correlation indicating that the sequential water rest level observations are not random. These autocorrelations have also been described as behaving in a “similar way to a porous aquifer rather than to a typical karstic aquifer” (Angelini 1997). This is in part due to water moving at much lower velocities in the aquifer, and the unsaturated zone is dominant, in effect filtering any high frequency rainfall signal and replacing it with a low frequency signature (Angelini 1997). The C type hydrographs are believed to be underlain by hard bands which have a variety of fracture features at outcrop and also recorded in the logs. The A and B type hydrographs show a seasonal signal which is also shown by the annual spectral periodicity (Figure 8-22 and Figure 8-23). The rainfall data for both the 30 day and 90 day data shows seasonal signatures and yearly periodicity (Figure 8-21).

In order to ascertain if the autocorrelation lag is significant, partial autocorrelations (PACF) were also run (Figure 8-22). If significance is indicated this partial autocorrelation will again be non-zero or above a quality line (Box and Jenkins 1976).

The PACF measures the correlation of the lag, independent of the internal correlation of the data. For example lag number 5 is calculated with the effects of the previous lags removed. The results of the PACF indicate that the autocorrelations are not just explained by the propagation of the lag-1 autocorrelation, through the data and that seasonality and monthly relationships are present in the A & B type hydrographs. However they are on the border line of statistical significance.

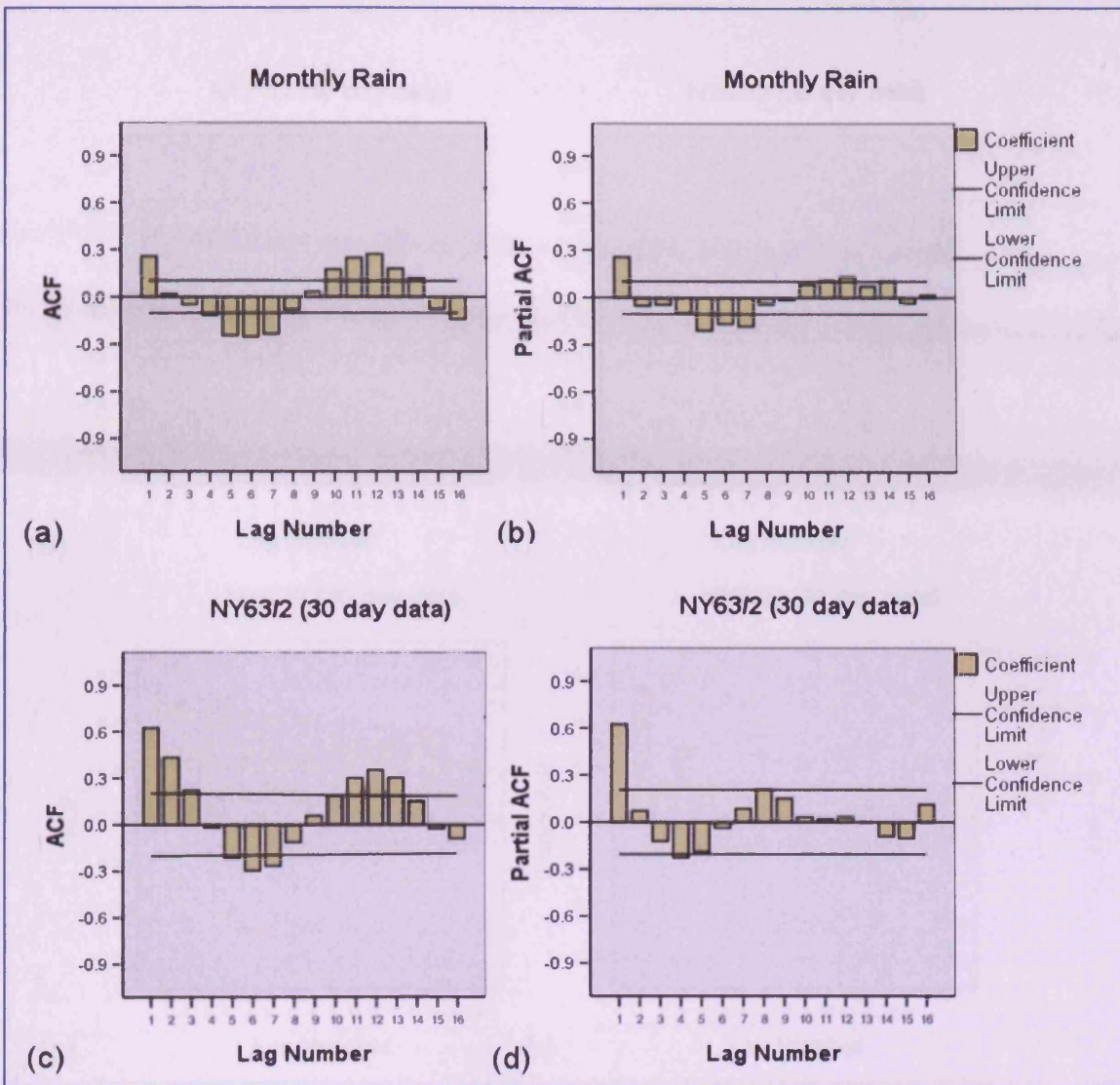


Figure 8-22 a-d Selection of autocorrelation and partial autocorrelation (PACF) plots for the Type hydrographs. (a) Average monthly rainfall indicating a seasonal nature. (b) PACF of monthly rainfall showing that there is statistical significance in the data and that the autocorrelation results are not just a function of the lag 1 value propagating through the data. (c & d) NY63/2 A type hydrograph, showing seasonal signature and PACF confirming statistical significance out to 9 months.

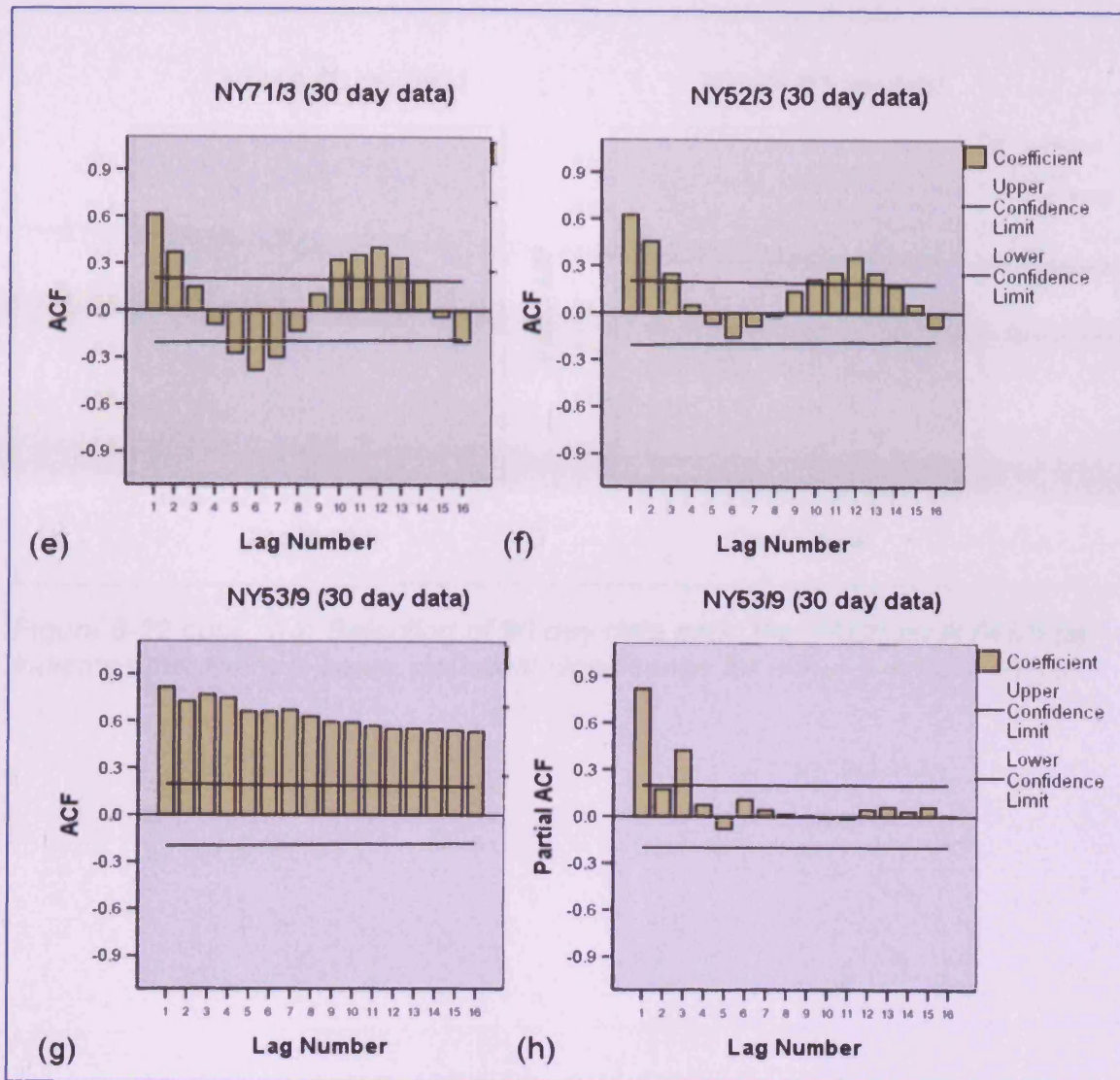


Figure 8-22 cont. (e & f) NY71/3 B Type and NY52/3 showing seasonal nature of the rest water level values. (g & h) NY53/9 C Type, indicating that sequential monthly water rest levels are related, PACF (h) indicates that this has statistical significance for about 3 months, compare PACF with (b) and (d) PACF plots for rainfall and A Type hydrograph.

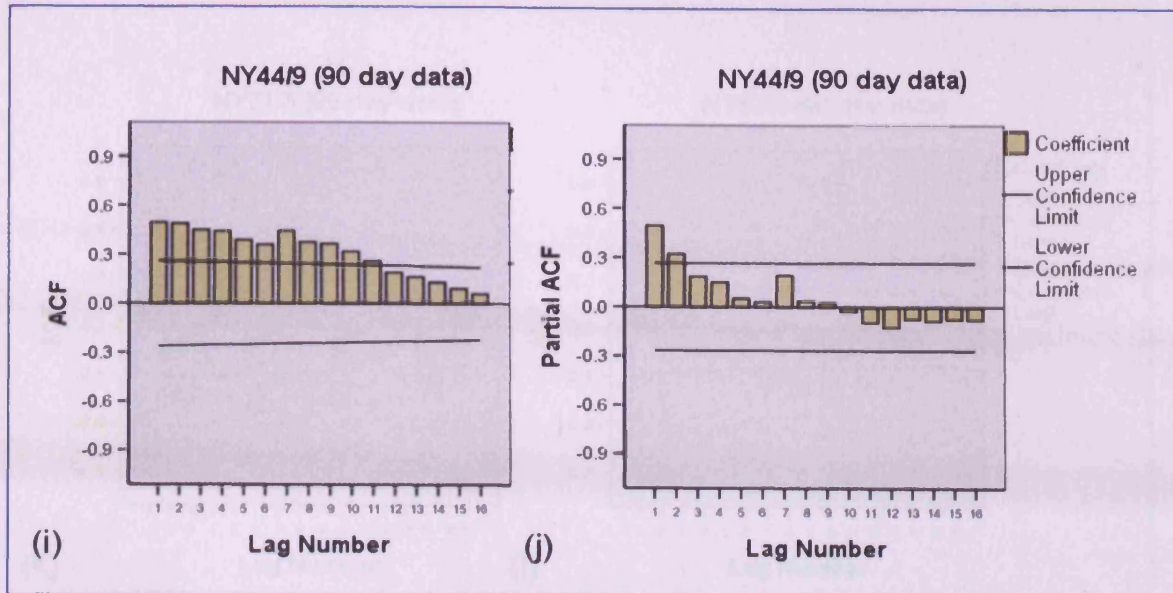


Figure 8-22 cont. (i-j) Selection of 90 day data sets, the PACF for NY44/9 (8j) indicates that there is some statistical significance for about 3 months (lag2).

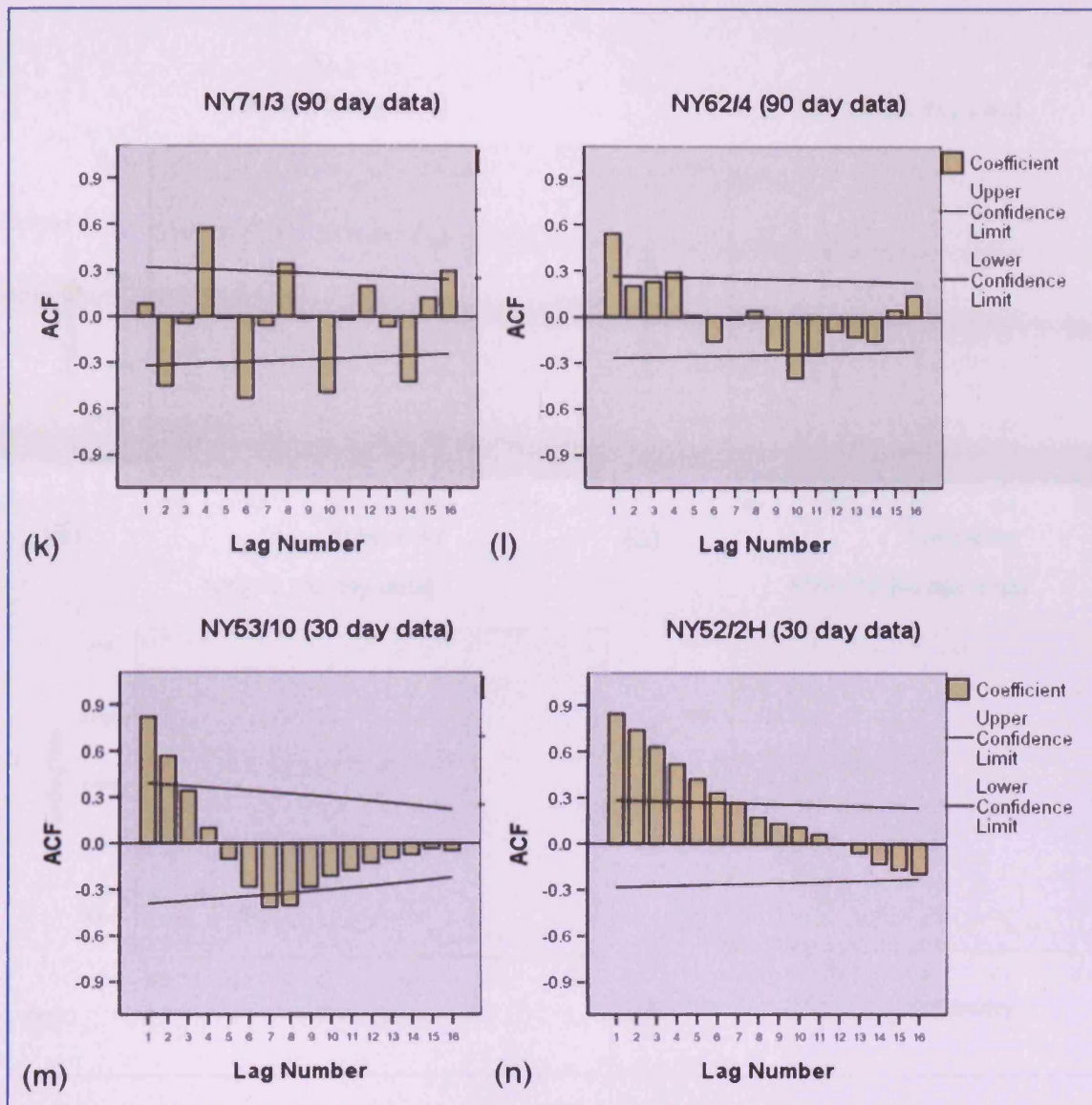


Figure 8-22 cont. (k) NY71/3 is interpreted as a strong seasonal signature, showing opposing correlation every 6 months. (l) Shows decay of the signal, potentially a weak seasonal signature but not statistically significant. (m & n) Hybrid NY52/2H and A Type NY53/10 displaying a similar auto correlation signature, both PACF (not shown) indicate that there is no statistical evidence of results and most probably due to propagation of the lag 1 data in the data set.

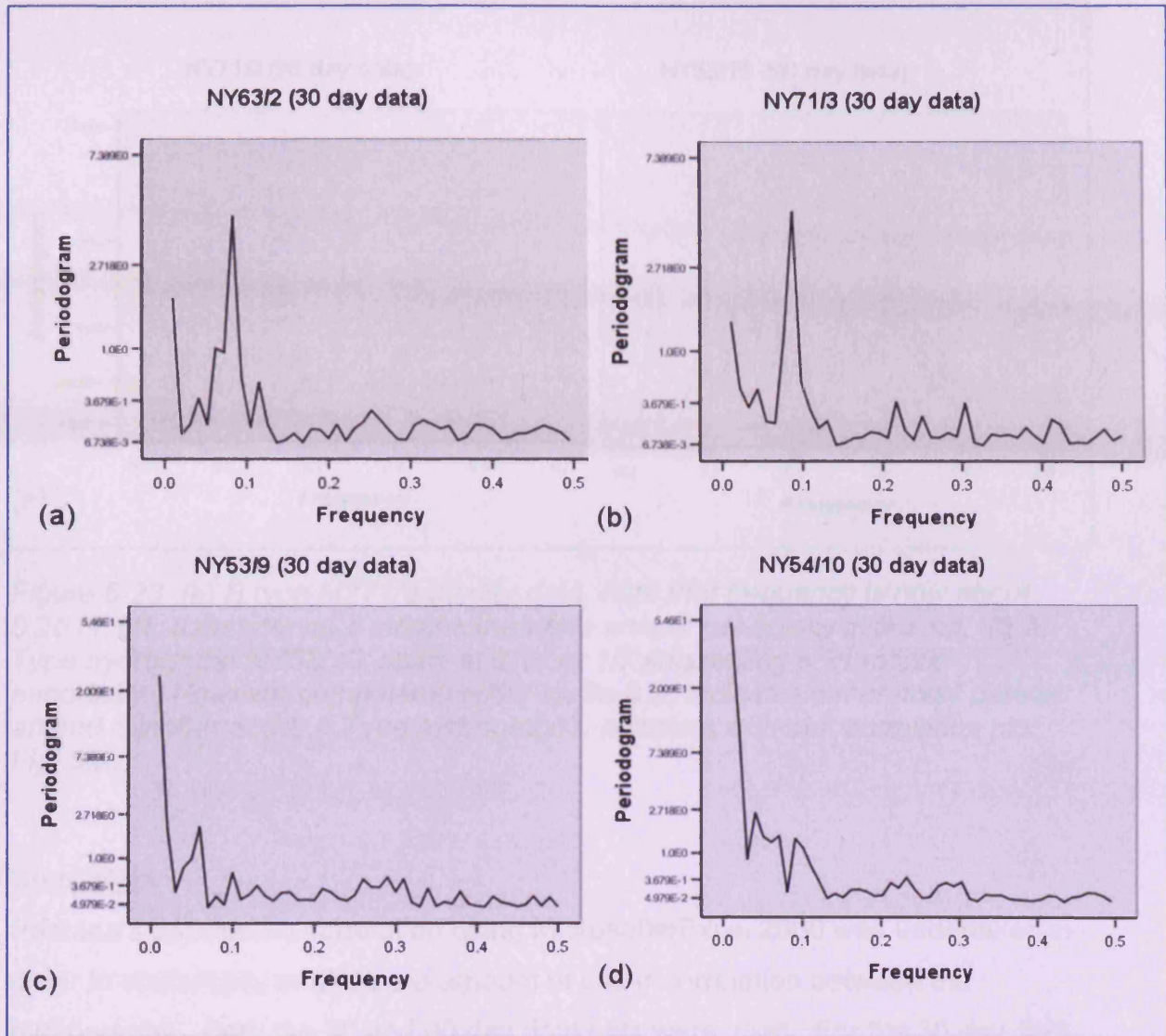


Figure 8-23 Selected spectral analysis plots for Type Hydrographs. (a-d) Type hydrographs, (a) NY63/2 A Type, frequency spike at approximately 0.083 or 1/12 indicating a period of 12 months as data interval is monthly (30 days). (b) NY71/3 B Type indicating an annual periodicity, compare with 90 day data set (Fig. 9e.). (c) NY53/9 C type hydrograph, rapid decay, and no periodicity spike. (d) NY54/10 C2 hybrid type, similar to NY53/9 C type.

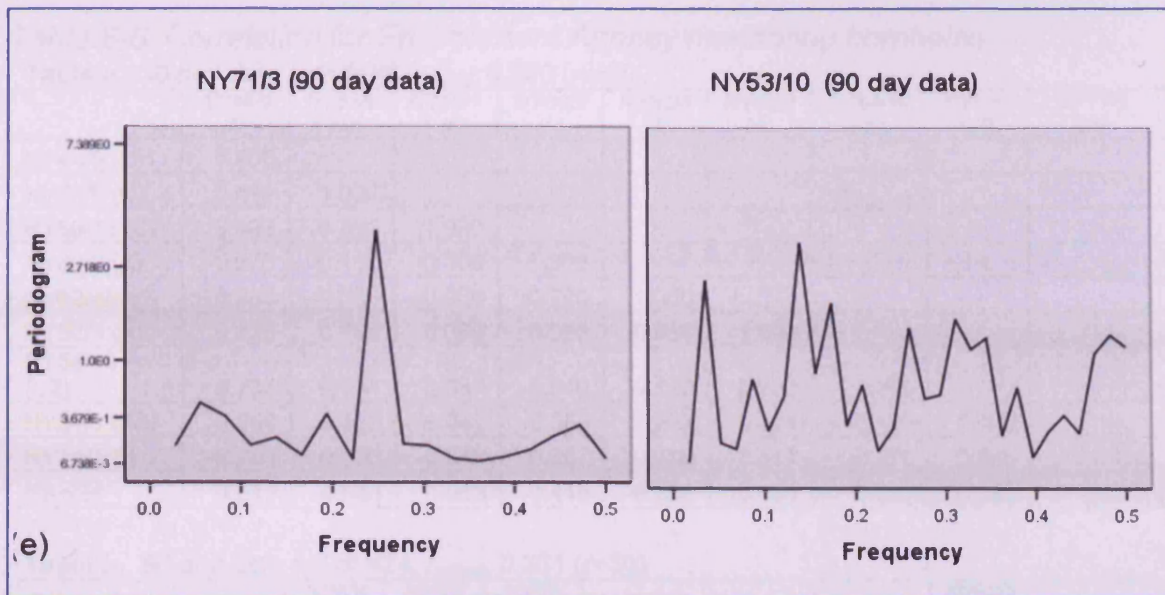


Figure 8-23 (e) B type NY71/3 90 day data, note that frequency is now about 0.25 or 1/4, data interval 3 months therefore annual periodicity indicated. (f) A Type hydrograph NY53/10, spike at 0.14 or 1/7 suggesting a 21 month periodicity. However comparison with Fig. 9a & b, indicates either noisy data or an end member of the A Type hydrographs, compare with autocorrelation plot Fig. 8m.

### Correlation

Pearson's parametric correlation using Microsoft®Excel 2000 was undertaken in order to statistically analyse the amount of linear correlation between the hydrographs. Both the 30 and 90 day data sets were used. For the 30 day data set, 87 common observations (85 degrees of freedom (df=85)) were available; for the 90 day data, two sub-sets were also available with 52 and 36 (df=50 & 34) common observations. Boreholes NY54/10, NY52/2H and NY71/3 have less common data. The results of the correlation and critical values are in Table 8-6.

Table 8-6 Correlation for Environment Agency monitoring boreholes.

Table a. 30 day data set  $df=85$   $r_{critical}: 0.220$  ( $r=80$ )

	NY44/9 (C)	NY53/9 (C)	NY53/11 (C)	NY63/2 (A)	NY62/4 (A)	NY52/3 (A)	NY54/10 (C2)	NY54/11 (B)	NY71/3 (B)	Rainfall
NY44/9 (C)	1.000									
NY53/9 (C)	0.679	1.000								
NY53/11 (C)	0.402	0.396	1.000							
NY63/2 (A)	-0.075	-0.168	-0.106	1.000						
NY62/4(A)	-0.208	-0.256	-0.060	0.786	1.000					
NY52/3 (A)	0.225	0.186	0.060	0.696	0.588	1.000				
NY54/10 (C2)	0.734	0.741	0.387	-0.049	-0.122	0.298	1.000			
NY54/11 (B)	-0.066	0.122	-0.041	0.358	0.268	0.494	-0.123	1.000		
NY71/3(B)	-0.263	-0.390	-0.279	0.267	0.199	0.411	-0.370	0.550	1.000	
Rainfall	0.013	-0.063	0.003	-0.410	-0.386	-0.488	0.007	-0.342	-0.277	1.000

Table b. 90 day data set  $df=34$ ,  $r_{critical}: 0.361$  ( $r=30$ )

	NY44/9 (C90)	NY53/9 (C90)	NY53/11 (C90)	NY62/4 (A90)	NY53/10 (A90)	NY52/3 (A90)	NY54/10 (C290)	NY52/2 H (C290)	NY71/3 (B90)	Rainfall
NY44/9 (C90)	1.000									
NY53/9 (C90)	0.902	1.000								
NY53/11 (C90)	0.884	0.939	1.000							
NY62/4 (A90)	0.259	0.256	0.410	1.000						
NY53/10 (A90)	-0.100	-0.253	-0.038	0.612	1.000					
NY52/3 (A90)	0.298	0.203	0.343	0.695	0.521	1.000				
NY54/10 (C290)	0.562	0.735	0.698	0.475	0.062	0.307	1.000			
NY52/2H (C290)	0.385	0.540	0.505	0.673	0.235	0.472	0.857	1.000		
NY71/3 (B90)	0.216	-0.029	0.117	0.465	0.538	0.786	0.081	0.135	1.000	
Rainfall	0.160	-0.026	-0.015	-0.058	0.062	0.074	0.008	-0.198	0.456	1.000

Table c. 90 day data set  $df=50$   $r_{critical}: 0.279$ 

	NY44/9 (C90)	NY53/9 (C90)	NY53/11 (C90)	NY62/4 (A90)	NY53/10 (A90)	NY52/3 (A90)	Rainfall
NY44/9 (C90)	1.000						
NY53/9 (C90)	0.693	1.000					
NY53/11 (C90)	0.673	0.973	1.000				
NY62/4 (A90)	0.153	0.015	0.232	1.000			
NY53/10 (A90)	-0.428	0.010	0.153	0.331	1.000		
NY52/3 (A90)	0.276	0.309	0.402	0.294	0.139	1.000	
Rainfall	-0.015	-0.179	-0.126	0.017	0.020	-0.011	1.000

Analysis of correlations for the 30 day data sets shows good correlation between the C1 hydrographs and the hybrid C2 NY54/10. NY54/10 is located on the edge of the Penrith Sandstone, which may explain the close correlation and hybridisation. The nearest borehole to NY54/10 is NY54/11 (B type), which is located within the Eden Shales and has no statistical correlation with the C types. The hybrid (NY54/10) indicates a positive correlation with NY52/3 (A type) both of which are located on the periphery of hard band areas. The negative correlation with NY71/3 (B type) may also contain an element of distance (Figure 8-18). No positive statistical correlation at the 95<sup>th</sup> percentile is indicated between the C type hydrographs and the A and B type hydrographs other than NY52/3 (A type), negative correlation is however indicated between the C types and NY71/3 a B type.

A positive correlation exists between the A and B type hydrographs, and correlation with rainfall is also negative. There is no statistically significant correlation indicated with the C type.

For the 90 day data,  $df=36$  (Table 8-6b), there is positive internal correlation between the hydrograph types. A positive correlation between NY53/11 (C type) and NY62/4 (A type) is indicated in this data set, but not in the 30 day data. Positive correlation between the hybrid NY52/2H and NY52/3 (A type) is shown, but not with NY53/11 (C type), all three boreholes are located within the central zone of the Penrith Sandstone, (Figure 8-18). The negative correlation between the A and B type hydrographs and the rainfall is no longer present, however a positive correlation is indicated with NY71/3 (B type).

The longer 90 day data set (Table 8-6c) indicates the internal correlation between the C and A type hydrographs, although no correlation is indicated between NY52/3 and NY53/10 (A types). Positive correlation is indicated between NY52/3 and C types NY53/9 and NY53/11. This may be a function of proximity in the case of NY53/11, and similar topography for NY53/9, where both are located between plateaux. No statistical correlation is indicated with any hydrograph type and the rainfall.

### Borehole geophysical and spatial patterns

The C1 and C2 hydrographs all occur within the northern portion of the Penrith Sandstone. This area is known to be underlain by intermittent hard bands of very well cemented sandstone, intercalated with more porous and friable sands (Lovelock 1972; Lovelock 1979). Type A hydrographs occur both in the St Bees Sandstone and Penrith Sandstone located within the central portion of the valley. The C2 hybrid type hydrographs are located on the southern and northwest periphery of the hard band plateaux (Fig 1) and NY54/11 penetrates the Eden Shales. All have broadly similar structures; steeply dipping fissures, hard bands and more friable sands. The B type hydrographs have one interesting feature in common; poorly cemented/ uncemented sandstone facies at the base of the borehole and cavities are reported within the logs. The spacing of joints (although not measured) in a bed is proportional to the thickness of the layer, (Bloomfield 1996), which may affect flow across or through well cemented bands.

The A type hydrographs all have a superficial deposit thickness of 10m or less, the B type have about 20m or more, and the C1 types have an intermediate thickness 10m to 16m; C2 range from 4m to 18m. Borehole logs suggest that the C type superficial deposits are more clay-rich than the A and B types. The logs indicate sandy till for NY62/4 and NY63/2; for the other two boreholes in this group (A Type) NY53/10 is weathered St Bees Sandstone and boulders; NY52/3 is again a silty till with large clasts. The B type hydrographs also have sandy till with clasts cover.

Soil type investigations from Soil Survey Mapping 1: 250 000 scale indicates that the boreholes are located in soil types Wick1 (541r) and Newport1 (551a & d); described as “deep well drained coarse loamy and sandy soils” both glaciofluvial in origin (SSLRC 1983b). Only the soil thickness would appear to vary.

Streetly & Chillingworth (2001) suggest that the B type hydrographs are control by proximal water bodies, and from map inspection this would appear to be the case. For the A type hydrographs there are no major water bodies close to the boreholes, except that NY53/10 is artesian with four springs located nearby. The C2 hybrids are also close to water features, NY52/2H is about 300m NW of Cliburn Moss and NY54/10 is located above a large stream.

At the regional scale (Figure 8-18), the confining sandstone in the deep part of the aquifer is believed to be restricted to the northern elevated region of the Penrith Sandstone. To the east of the plateaux there is an open arable area that may be acting as a recharge zone, drift thickness from the BGS BSTM model suggest a thin covering in the region of 1m to 5m (Morris and Flavin 1994). The River Petteril runs from south to north and is a losing stream in the upper reaches near the west flanks of the plateaux. Groundwater flow across the Carboniferous Permo-Triassic boundary south of Penrith is likely to be significant, (Ingram 1978). North of Penrith, it may be reduced due to the presence of numerous major NW/SE and subsidiary perpendicular trending faults producing a series of blocks. It has been shown that in other Permo-Triassic sandstones these blocks restrict groundwater flow especially perpendicular to the flow although parallel flow may be enhanced (Seymour et al. 2006).

### Interpretations

The hydrograph is the response to a variety of geo-physical properties, these include,

- Recharge; which is subject to temporal and spatial factors, overlying regolith lithology and heterogeneity and unsaturated flow properties. Butcher et al., (2006) states that “the travel time for water to move from the ground surface to ... boreholes are very variable”.
- Saturated zone; porosity (matrix and fissure), hydraulic conductivity and gradient.
- Data resolution; the data representing a true hydrograph or a temporal snapshot. It has been shown that without continuous monitoring there is a real danger of missing meaningful data which can alter interpretations (Ling 2007)

The curve matching using polynomial trend analysis has identified four hydrograph types, with an additional hybrid to the work of Streetly and Chillingworth (2001). Examination of these curves may also highlight variations in the mechanisms controlling the hydrographs.

## Eden Valley interpretation models

### Seasonal model

A seasonal system model has to satisfy several criteria; rapid rise and falls in response to a seasonal recharge character, and satisfy the known geological log. The logs for the A and B type boreholes indicate the presence of fissuring and a mixture of fine grained sands, mud and siltstones (St Bees Sandstone). The finer sediments may give rise to reduced storativity, and the fractures a mechanism for the flashy nature, delivering recharge to the borehole area.

Figure 8-24 proposes a model that shows rapid fissure flow through a mixture of well cemented hard bands and less well cemented but fine / medium grained competent sands. Modelling undertaken by Butcher, et al (2006) indicates that fracture zones transport water more rapidly to boreholes. The modelling also indicates that higher recharge rates through exposed sandstones near to the boreholes allows a larger proportion of modern water to reach the boreholes more rapidly. Slope aspect and run-off coefficients may also impart an as yet un-quantified influence.

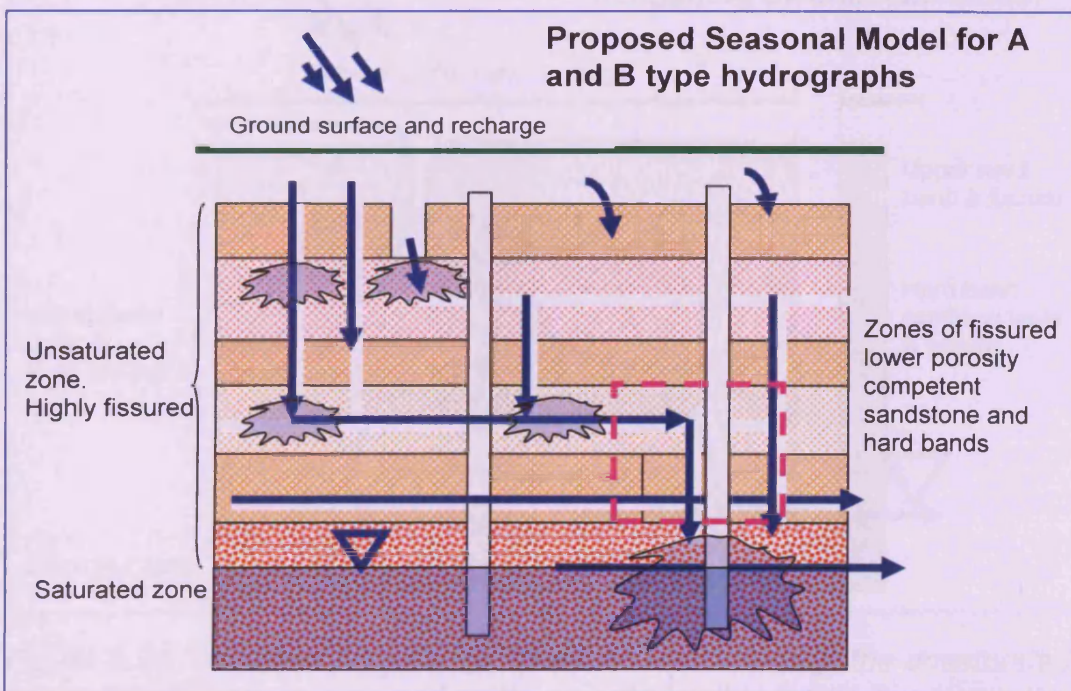


Figure 8-24 Seasonal conceptual model to illustrate rapid movement of recharge to the water table.

Where they are above the water table the more friable and porous sands would cause a recharge delay. This may also help explain the lower heads in the B hydrographs which have a thicker superficial cover. At the water table a local doming is observed due to seasonal pulses which accounts for the rapid hydrograph rise, this would then recede after the end of the recharge pulse. This model may help explain the seasonal nature of the A & B type hydrographs.

*Dampening (positive autocorrelation) mechanism*

A cascading effect is proposed where recharge is potentially delayed within porous unsaturated zones, which are interspersed between hard bands. This stratification is present with the C1 and C2 borehole logs and the adjacent areas. Perched aquifers are also believed to exist on top of the hard bands; there is some evidence to associate the hard bands with water strikes, (Table 8-7). Hard bands are not believed to extend to the south of the Penrith Sandstone although the basal breccia is reported as 'much fractured' in some logs (NY70/15), which may also account for the C1 and C2 hybrid boreholes only being located in the northern hard band regions.

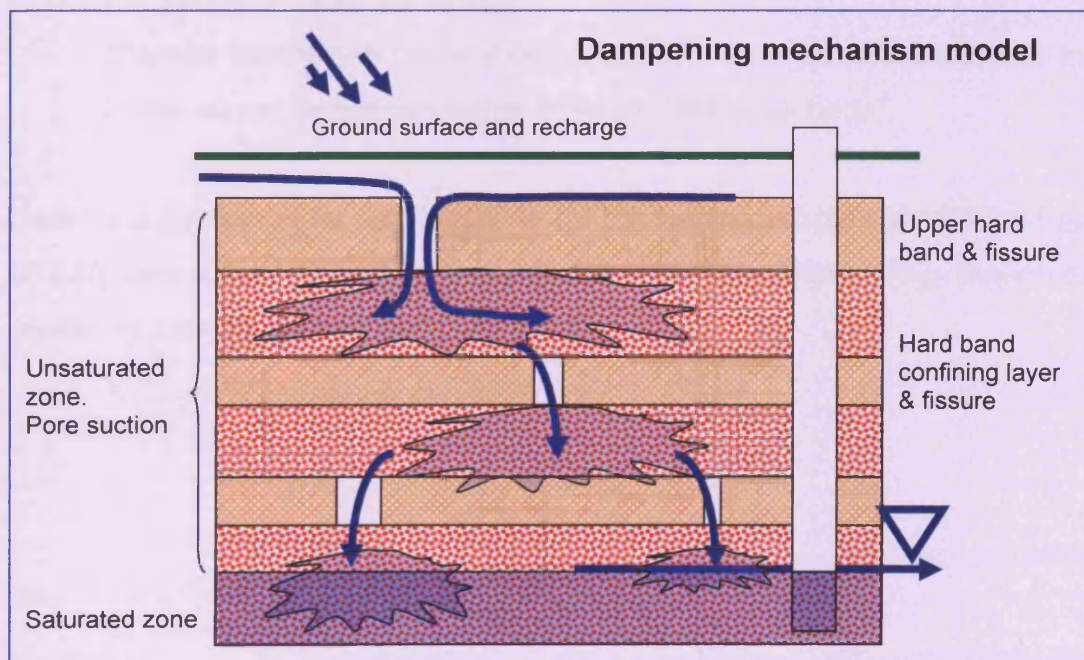


Figure 8-25 Schematic of potential cascade effect through the unsaturated zone. Due to pore suction and moisture deficit within the porous layers the recharge is dampened at every layer and can only proceed when the local moisture deficit is satisfied. Note vertical fissure flow in top hard band near to surface in thin or Drift absent areas.

The general rainfall pattern observed (Fig 5b), wetter in the 70's and 80's would account for the rising limb on the C type hydrographs and drier in the 90's for the observed receding limb. The following has been extracted from the borehole logs and provides evidence of the geology in support of the dampening model:

- NY53/9 (C1) (well dip in the region of 54m)  
“Penrith Sandstone. Distinct hard band at depth. Friable in places and beds of unconsolidated sand between 40m and 71m”.

This model will also allow for a steady increase in water levels as the saturated zone moves upwards in response to more wet periods. A step as observed in NY54/10 could be induced as the saturated zone crosses hard bands. Extracts from the C2 hybrid logs show that at:

- NY52/2F (a proxy for NY52/2H  $\approx$ 50m distant; well dip  $\approx$ 20m)  
“Penrith Sandstone. Soft red sandstone at top to about 21m then hard bands followed by soft and hard sandstone bands 10cm intervals. Some interleaved cement”.
- For NY54/10 (well dip  $\approx$ 25m)  
“Penrith Sandstone. Poorly cemented and uncemented sandstone in upper levels  $\approx$ 34m; better cemented beneath. Massive beds”.

Data for a pumping test was available for adjacent boreholes, at NY53/11 and NY53/9 they are described as leaky and at NY44/9 as dewatering, though this may be due to local faults and an igneous dyke.

**Table 8-7 Hard band and water strike data for Eden Valley borehole logs.**

Borehole	Hard band 1 Top m AoD	Hard band 2 Top m AoD	Water Strike 1 m AoD	Water Strike 2 m AoD	Water Strike 3 m AoD	Remarks
NY52/10	93				92	Fractured at 43 & 65m.
NY52/11	112			111		
NY52/2A	114		112			
NY53/33	114		112			Level 3 nitrate. St Bees Sandstone
NY53/9	150		152			
NY54/41		-28	-34			
NY62/2	89		85			Artesian
NY62/31	110	104	107	105		

*Fissure density*

This may impart a storativity signal on proximal boreholes; increased fissure density in more competent sandstone will increase the storativity coefficient, and reduce the rise in head (Figure 8-26). The presence of hard bands may be acting as confining and low permeability layers, (Streetly and Chillingworth 2001). Fissure density has been observed to be spatial variable, and is also believed to be the controlling mechanism for aquifer transmissivity (Lovelock 1972; Allen et al. 1997). The density variation may act locally but affect a larger area; fissures are believed to be controlled by major faulting in the area. NY 54/11 (B type ) and NY53/9 (C1 type) are both adjacent to mapped faults (BGS 1974b, 2004).

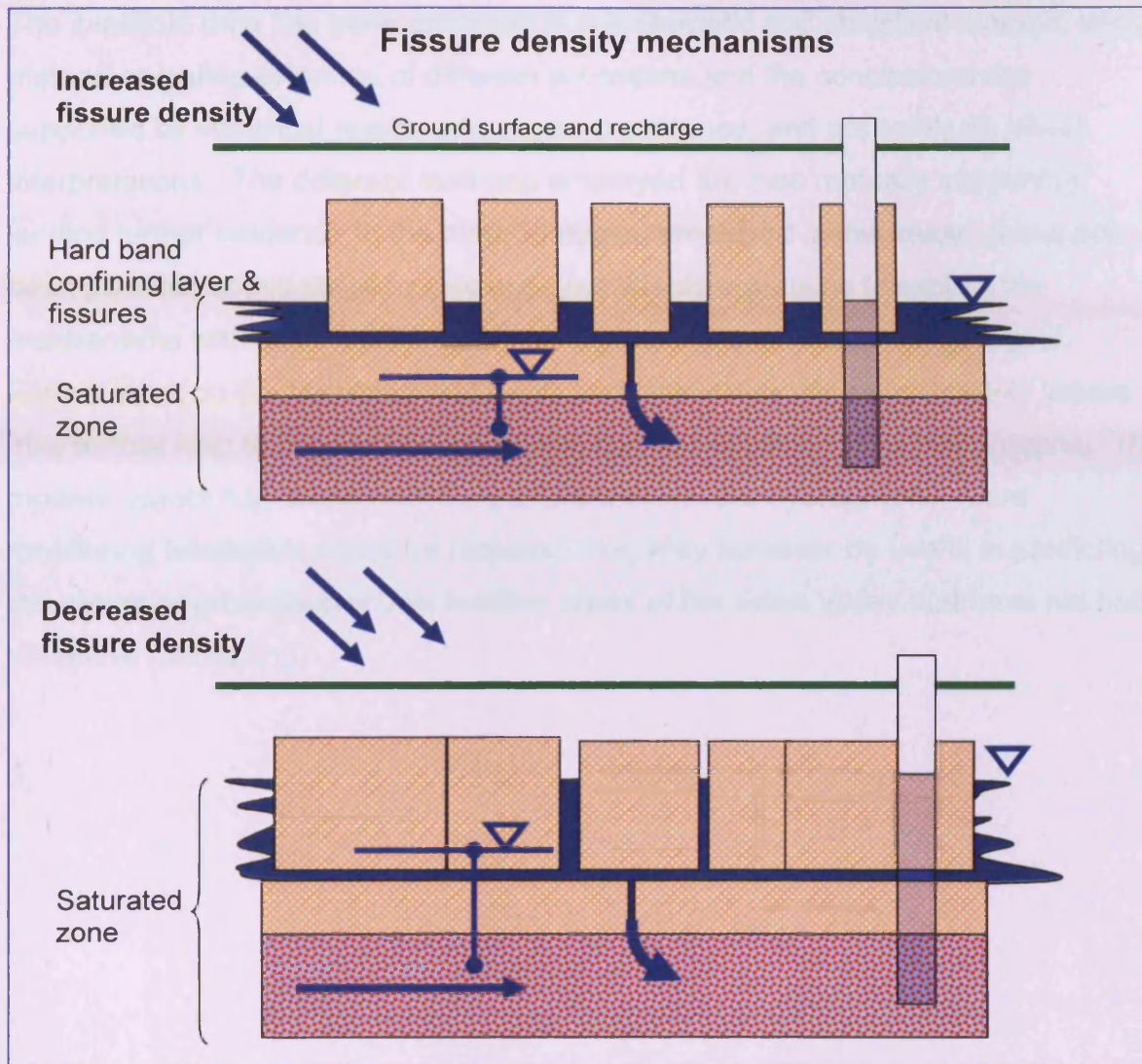


Figure 8-26 The effect of fissure density and storativity on a local area. Upper image shows increased fissure density, resulting in a lower head in the fissure zone. Lower image shows reduced fissure density for the same amount of rainfall. Both are on top of a low permeability hard band.

### 8.5.2 Eden Valley physical hydrology conclusion

The models proposed attempt to explain in a conceptual fashion the various processes that may be occurring within the Penrith Sandstone aquifer and adjacent lithologies. The conclusions are based upon the very different and spatially distinct hydrographs that are present with the Eden Valley. In the natural environment, end member extremes are rare; two processes which occur in distinct geological settings have been identified within the Eden Valley. A degree of convergence towards the middle ground has also been shown with the B type and C2 hybrids.

The available data has been analysed in a systematic and statistical manner, each method revealing evidence of different processes and the conclusions are supported by statistical results and physical evidence, and not solely on visual interpretations. The different methods employed are also mutually supporting, lending further credence to the methodologies employed in this study. It has not been possible at this stage to produce quantifiable equations to explain the mechanisms within the aquifer that may be impacting on the recharge signal. Further work on the impact of faults and local transmissivity and storativity values may further help to explain the processes that are controlling the hydrographs. The models cannot fully explain all the perturbations in the hydrographs, more monitoring boreholes would be required; they may however be useful in predicting the nature of groundwater flow in other areas of the Eden Valley that have not had extensive monitoring.

## 8.6 Groundwater geochemistry

### 8.6.1 Introduction

Geochemistry data for the Eden Valley was provided by the EA (NW). The data while extensive is limited in both temporal and species resolution. The better data sets were those of the public water supply boreholes at Bowscar and Nord Vue. The data was filtered to reject locations and epochs that did not have an associated phosphorus analysis. The complete data set is in Enclosure 1 (CD).

A reconnaissance visit to the Eden Valley was made in the summer 2007, and samples were collected in conjunction with the Environment Agency's routine monitoring campaign. Additional investigation of effluent locations at several farms was also undertaken.

### 8.6.2 Eh-pH diagram

Unfortunately the data supplied by the Environment Agency (NW) does not contain ORP (Eh) data and cannot therefore be plotted. Data obtained during a reconnaissance visit in June 2007 is however shown (Figure 8-27).

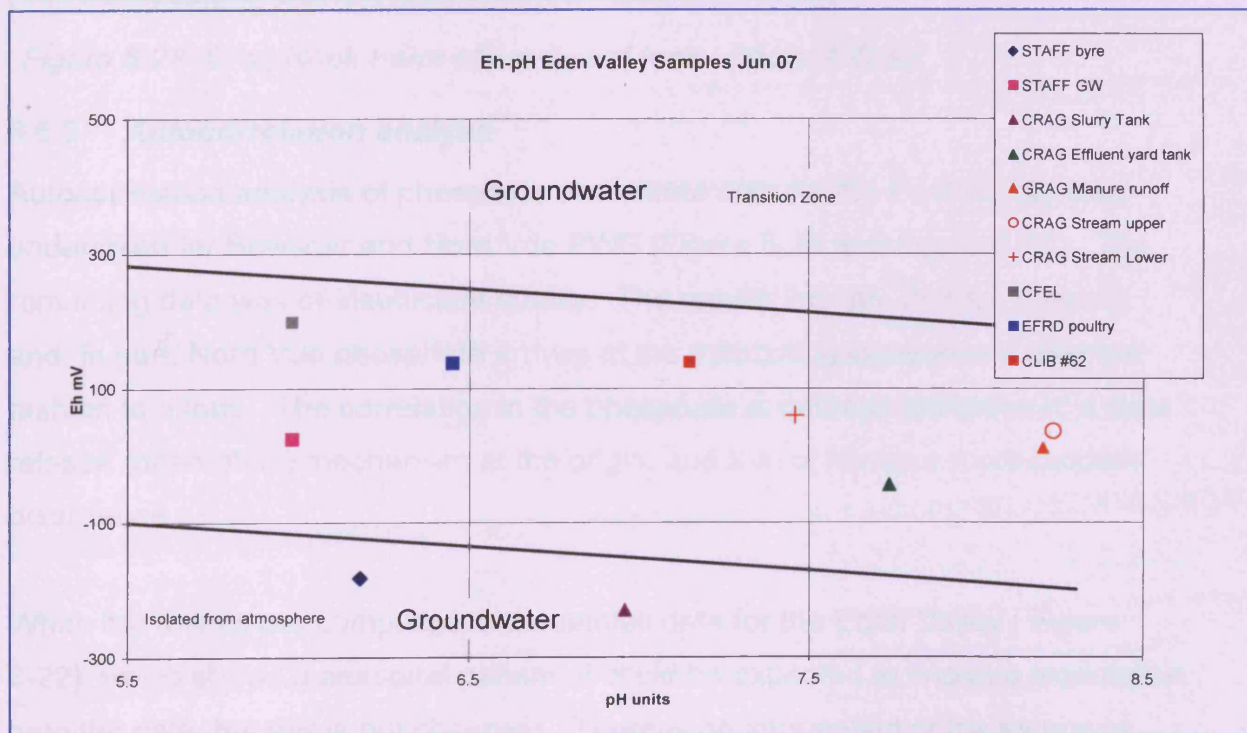


Figure 8-27 Eh-pH data for Eden Valley samples. Black lines are environment boundaries.

It is of interest to note that the data for CRAG manure and effluent tank plot is in the groundwater isolated from the atmosphere zone. This is considered to be an artefact of biological processes as the yard tank and manure runoff are believed to be derived from meteoric waters. The effluent from Crag Nook Farm yard tank, (Figure 8-28) contains in the order of  $85\text{mg HPO}_4^{2-} \text{ l}^{-1}$  (IC analysis), which is disposed of '...not over a very wide area...' (Pers. comm., local farmer); this could be considered to be a localised ephemeral hot spot.



Figure 8-28 Crag Nook Farm effluent yard tank. Photo A Gray.

### 8.6.3 Autocorrelation analysis

Autocorrelation analysis of phosphate and nitrate data for the Eden Valley was undertaken for Bowscar and Nord Vue PWS (Figure 8-29 and Figure 8-30). The remaining data was of insufficient quality. The results indicate that for Bowscar and, in part, Nord Vue phosphate arrives at the monitoring location in a different fashion to nitrate. The correlation in the phosphate is perhaps indicative of a slow release (desorption) mechanism at the origin, and that of nitrate a more random occurrence.

When the results are compared to the rainfall data for the Eden Valley (Figure 8-22), which shows a seasonal pattern, it could be expected to impart a modulation onto the data, but this is not observed. There is no information of the source or application rates of the nitrate and phosphate, however a semi-seasonal function may be expected.

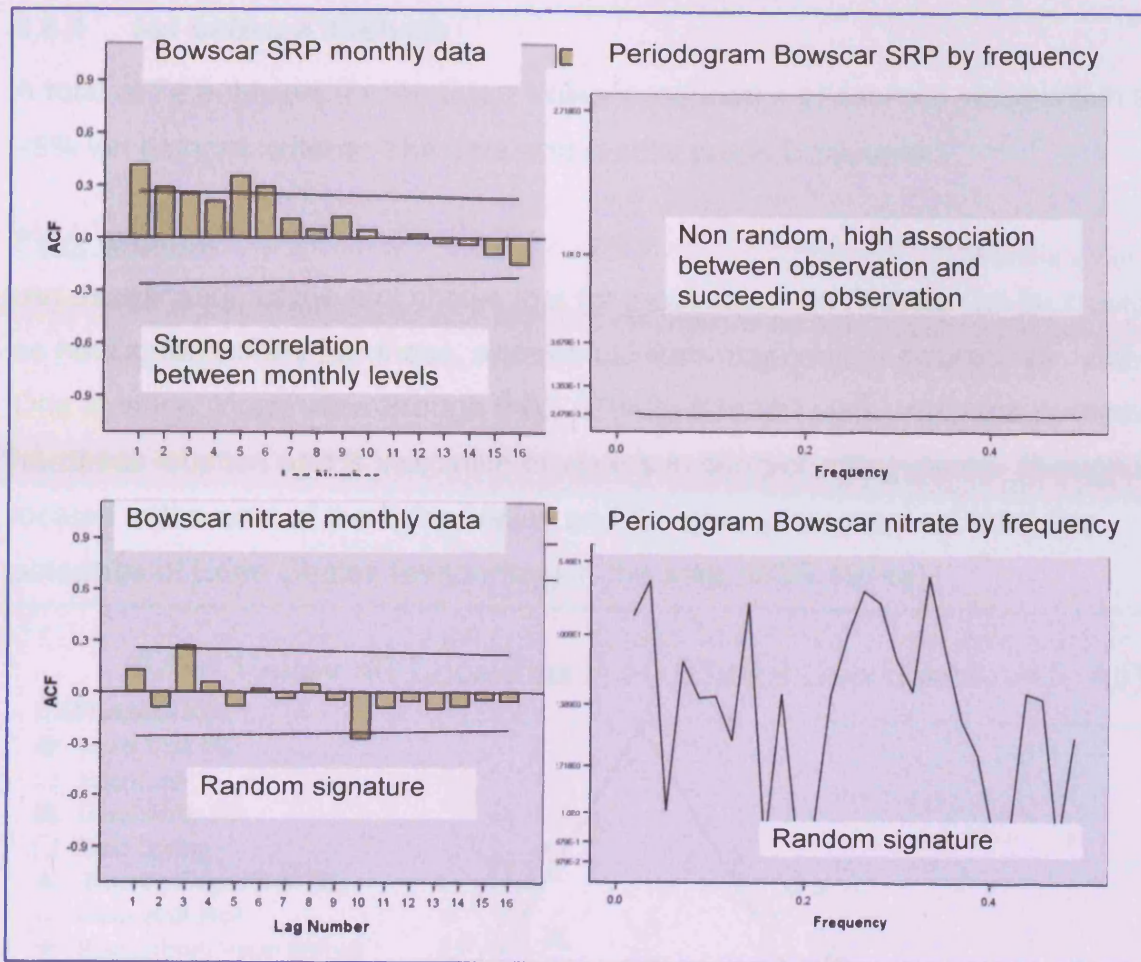


Figure 8-29 Autocorrelation and spectral analysis plots for phosphate and nitrate levels at Bowscar raw water borehole. Data interval ~1 month, length 53 months.

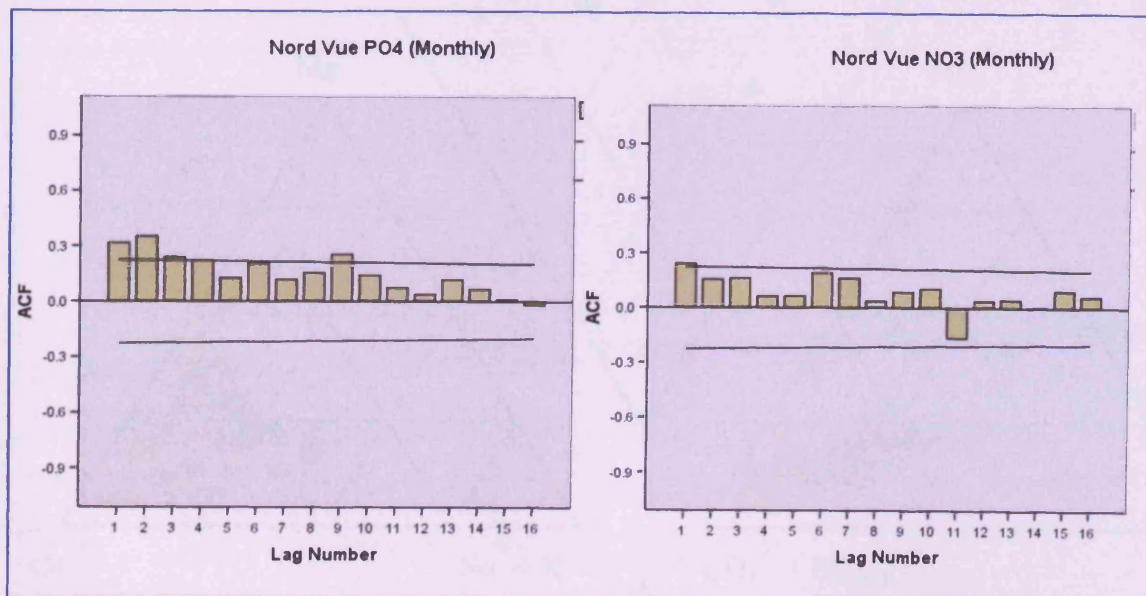


Figure 8-30 Autocorrelation plots for phosphate and nitrate levels at Nord Vue raw water borehole. Data interval ~1 month, length 76 months.

### 8.6.4 Ion balance analysis

A total of 74 analyses for the Eden Valley produced a phosphate value within the  $\pm 5\%$  ion balance criteria. The data and results are in Enclosure 1.

#### Piper diagram

An examination of the plot shows that for most cases the waters can be classified as having temporary hardness, and are calcium-magnesium-bicarbonate waters. One location, West View Brough (NY) 378460 514990 plots within the permanent hardness location and is indicative of waters in contact with gypsum. Brough is located in the east of the Eden Valley and the geological map indicates the presence of Eden Shales (evaporites) in the area (BGS 1974a).

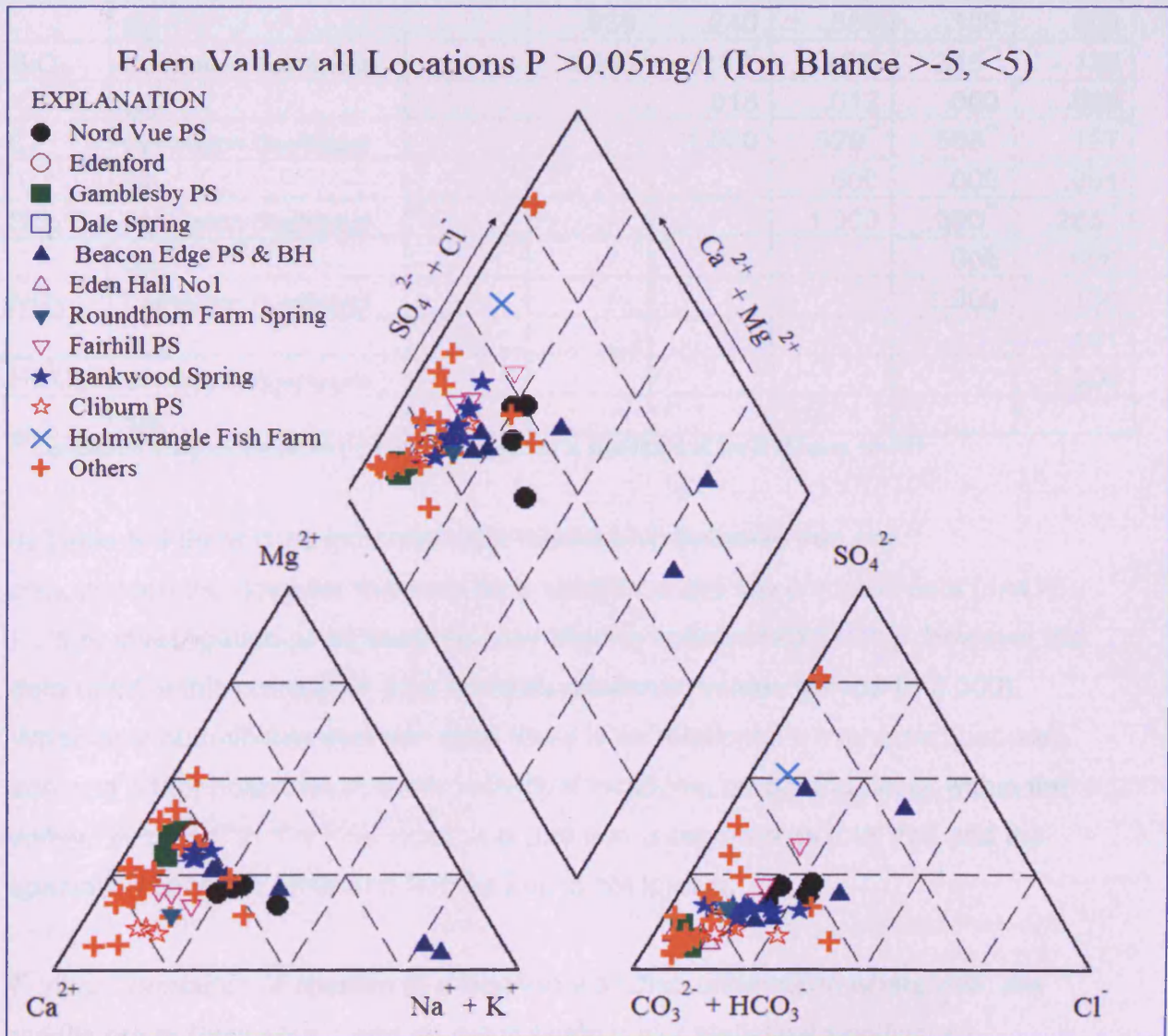


Figure 8-31 Piper diagram of the Eden Valley data meeting the ion balance criteria of  $\pm 5\%$ .

### 8.6.5 Geochemical correlation

Spearman's correlation was undertaken on the ion balance data. Spearman's correlation is deemed correct in this instance as it is not known how the data was collected and if there are temporal discontinuities between locations. The data are presented as correlation with anions and cations in two tables (Table 8-8 and Table 8-9). Silica is included in the analysis as this can interfere with spectrophotometric determinations,

*Table 8-8 Spearman's correlation of orthophosphate and anions, Eden Valley.*

		SRP <sup>-</sup>	SiO <sub>2</sub>	Cl <sup>-</sup>	SO <sub>4</sub> <sup>2-</sup>	NO <sub>3</sub> <sup>-</sup>	HCO <sub>3</sub> <sup>-</sup>
SRP	Correlation Coefficient	1.000	-.006	-.093	-.014	-.128	-.291**
	Sig		.938	.240	.865	.106	.000
SiO <sub>2</sub>	Correlation Coefficient		1.000	.187*	.198*	.315**	-.130
	Sig.			.018	.012	.000	.099
Cl <sup>-</sup>	Correlation Coefficient			1.000	.529**	.568**	.137
	Sig.				.000	.000	.084
SO <sub>4</sub> <sup>2-</sup>	Correlation Coefficient				1.000	.360**	.285**
	Sig.					.000	.000
NO <sub>3</sub> <sup>-</sup>	Correlation Coefficient					1.000	.130
	Sig.						.101
HCO <sub>3</sub> <sup>-</sup>	Correlation Coefficient						1.000
	Sig.						

\*\* Correlation is significant at the 0.01 level.\*Correlation is significant at the 0.05 level. N=161

In Table 8-9 there is no indication of a relationship between iron and orthophosphate, however this may be a function of the low common data (n=41). Further investigation of all locations may show a species relationship, however the data used in this correlation also contains maximum values (n=169 P<0.000). When only quantifiable data are used there is no relationship expressed between iron and orthophosphate at either individual locations, n= 68 and 34, or within the valley. A caveat to this investigation is that iron is reported as total iron and the speciation between ferric and ferrous iron is not known.

Further correlation of species at a location was also undertaken where n≥5, the results are in Enclosure 1 and do not indicate major statistical significance.

Table 8-9 Spearman's correlation of orthophosphate and cations, Eden Valley.

		SRP <sup>-</sup>	Ca	K	Mg	Na	Fe	EC
SRP <sup>-</sup>	Correlation Coefficient	1.000	-.272**	-.131	-.112	-.104	-.214	-.204
	Sig.		.000	.098	.157	.191	.178	.143
Ca	Correlation Coefficient		1.000	.393**	.511**	.220**	.287	.780**
	Sig.			.000	.000	.005	.069	.000
K	Correlation Coefficient			1.000	.063	.493**	.009	.530**
	Sig.				.427	.000	.956	.000
Mg	Correlation Coefficient				1.000	.081	.064	.560**
	Sig.					.306	.693	.000
Na	Correlation Coefficient					1.000	.023	.247
	Sig.						.888	.074
Fe	Correlation Coefficient						1.000	.191
	Sig.							.574

\*\* Correlation is significant at the 0.01 level.

N is 11 for EC & Fe, 53 for EC and 41 for Fe, 161 for remainder.

### Association with nitrate

Previous work undertaken in conjunction with the EA and BGS investigated the presence of rising and anomalous nitrate concentrations within the Eden Valley (Butcher et al. 2003; Daily et al. 2006). Table 8-8 shows that for the Eden Valley there is no relationship at monitoring locations. However if individual locations are considered there may be correlations. Despite a low coefficient of correlation the graphs in Figure 8-32, suggest a trend. Statistical analysis (Table 8-10) shows that there is correlation at Nord Vue PWS and not at Bowscar PWS; this may be an indication of heterogeneity within the aquifer. In Table 8-10 chloride is included as this species can be considered to be a non-sorbing tracer; its provenance with fertilisers cannot be proven, despite potash (KCl - sylvite) being amended to soils and high concentrations ( $\sim 150 \text{ mg l}^{-1}$ ) being observed in farm yard effluents (Figure 8-28).

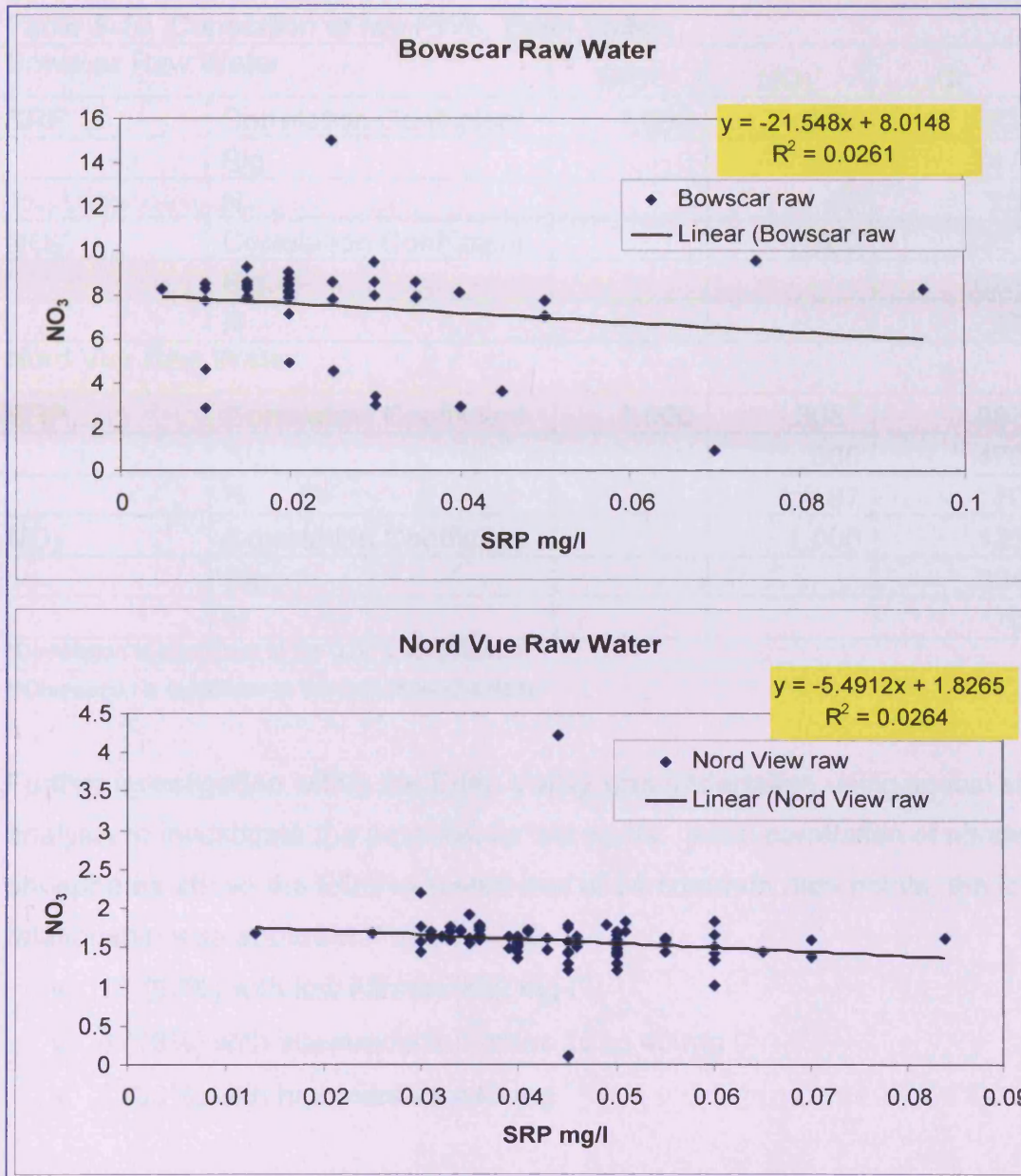


Figure 8-32 Correlations of SRP and NO<sub>3</sub> at Bowskar and Nord View PWS boreholes.

Table 8-10 Correlation of two PWS, Eden Valley.

Bowscar Raw Water		SRP	NO <sub>3</sub> <sup>-</sup>	Cl <sup>-</sup>
SRP	Correlation Coefficient	1.000	-.134	.063
	Sig.	.	.399	.747
	N		42	29
NO <sub>3</sub> <sup>-</sup>	Correlation Coefficient		1.000	.423*
	Sig.			.028
	N			27
Nord Vue Raw Water				
SRP	Correlation Coefficient	1.000	-.368**	-.087
	Sig.		.000	.473
	N		87	70
NO <sub>3</sub> <sup>-</sup>	Correlation Coefficient		1.000	.125
	Sig.			.304
	N			70

\*Correlation is significant at the 0.05 level (2-tailed).

\*\*Correlation is significant at the 0.01 level (2-tailed).

Further investigation within the Eden Valley was undertaken using spatial statistical analysis to investigate the potential for hot spots. Initial correlation of nitrates and phosphates above the EQS indicated that of 24 common data points, the following relationship was apparent (Figure 8-33):

- 12 (50%) with low nitrates <20 mg l<sup>-1</sup>;
- 4 (16%) with intermediate nitrates 20 to 40 mg l<sup>-1</sup>
- 8 (33%) with high nitrates >40 mg l<sup>-1</sup>

The spatial statistic returns a Z score value, and the results indicate that for a 95% level of confidence the spatial distribution of the nitrates may be the result of a random chance; there are no apparent hotspots. Analysis of the available phosphate data indicated that there was statistical confidence that two phosphate hot spots exist, these are at Roundthorn Farm and Carleton Farm (Figure 8-33), adjacent to each other and to the east of Penrith. These two locations also record low average nitrates.

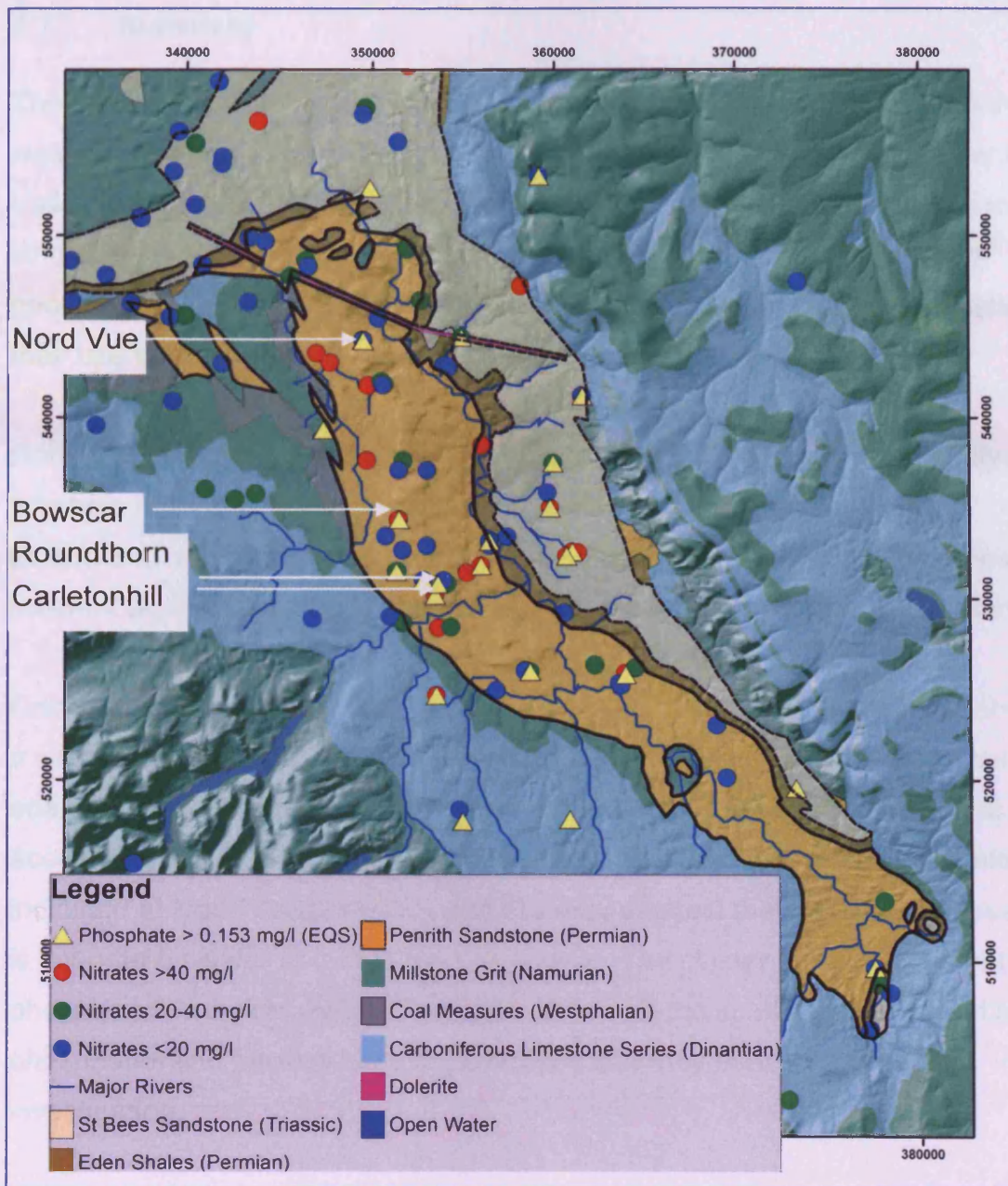


Figure 8-33 Occurrence of groundwater phosphates above EQS and distribution of nitrates in the Eden Valley.

## 8.7 Summary

The Penrith Sandstone of the Eden Valley is an important aquifer in the provision of water for domestic, agricultural and industrial use. It differs from the Lower Usk Valley in scale, lithology and importance. The Penrith Sandstone and adjacent lithologies have been well studied; there exists abundant hydrological and geological data. Hydro-geochemical data sets are however less well furnished and their use in temporal and statistical analysis is limited.

Robust statistical analysis of the hydrograph data has been used to identify different borehole response types which also have a spatial and hence geological correlation. Interpretative models have also been produced which hypothesise the different aquifer mechanics that are responsible for the hydrograph signature.

Geochemical analysis of the data has also been undertaken, the water plots within a similar location on a Piper diagram as the Usk Valley data. The statistical analysis does not indicate correlations with the major cations and anions at an acceptable significance level at the aquifer scale. Some correlation with nitrate is indicated at Nord Vue borehole, and this may suggest that the scale of observation is important; similar to that of the Usk Valley. The cluster analysis does not indicate phosphorus hotspots within the aquifer, although the spatial distribution of high phosphates and nitrates hints at processes that may be worthy of further investigation.

## Chapter 9 Conclusions

### 9.1 Synopsis

It has been shown that phosphorus is a ubiquitous element within the global environment, and that it has a capacity for bringing both benefits and problems to mankind. It helps increase agricultural outputs, but excess can cause eutrophication of still water bodies with the associated water quality issues. It is not found in the environment in its elemental state, but in a variety of forms both organic and inorganic; this leads to measurement issues and definitions of what form or fraction is actually being measured. Good analytical methodologies and procedures can achieve reliable precision over a range of different analysis.

The two study sites that were chosen for this project are different in scale, geology, importance and available data. The Eden Valley has had numerous studies undertaken within its environs whilst that of the lower Usk Valley site has had very few. Both have agriculture as their dominant activities and thus could be considered to have broadly common inputs, scale being a factor. The two study sites can therefore be compared and contrasted to better understand the processes within each location.

Despite the volume of available geochemical data from the Environment Agency (NW) for the Eden Valley, it was not of a sufficient temporal and spatial resolution with which to undertake rigorous statistical analysis. There was however an indication of some possible correlations which could be investigated with a better resolved data set. The groundwater level data was of excellent quality and this enabled a methodical differencing approach to analysing the data in order to investigate the potential for variations in aquifer mechanisms. This methodology was also used on the Usk Valley data. The requirement for robust statistical analysis being that if a significance level can be attributed to any relationship it is then possible to consider the process as major or minor, and perhaps worthy of further investigation.

It was hoped to bring all the observations together in a groundwater model of the respective areas, this proved problematic due to the lack of data from the two study areas.

### 9.1.1 *Aquifer mechanics*

The analysis of the borehole water level data provides an overall picture of the aquifer mechanisms; it does not indicate the presence of individual horizons which may have their own characteristics. The simplest conceptual analysis works on the assumption that the geology is homogeneous. If the specific yield of an area is the same and an equal recharge is applied, then it is reasonable to expect the same hydrograph response between spatially distinct boreholes (homogeneous aquifer). If however the aquifer mechanics are different between different boreholes then the hydrograph will vary by the relative influence of all these factors. By curve matching with regression trend analysis this smoothes out the perturbations in the hydrograph and makes a visual analysis easier. The variations in the hydrographs are likely to represent individual mechanisms, and understanding those relationships may result in a better understanding of their individual importance within the aquifer regime. By consideration of hydrograph trends it has been possible to identify differences that relate to the autocorrelation results, and ultimately what is believed to be heterogeneity in the aquifer mechanics.

The autocorrelation analysis of the Eden and Usk Valley data clearly show that there is a degree of homogeneity within the Usk and heterogeneity in the Eden Valley. This analysis begins to clarify the mechanisms of the aquifer and can distinguish between a flashy (quick response) and a more dampened system. Together with the cross correlation analysis of borehole response and rainfall this begins to allow basic interpretations to be made.

In the case of the Eden Valley it was not possible to cross correlate the borehole data due to its temporal resolution. The data does however, in conjunction with borehole logs, allow the development of models, the 'Seasonal' model for A and B type hydrographs and the 'Dampened' model for the C type hydrographs in Chapter 8.

Using these models, together with an understanding of the geochemistry of phosphorus and nitrate, it may be possible to deduce relationships. The borehole at Bowscar in the Eden Valley, due to its position, would be predicted to be a C type borehole; here the 'Dampening' model would be appropriate as the borehole log indicates firm sandstone over hard bands. The autocorrelation of the available phosphate data reflects a non-random process which would fit with entrained SRP or retardation in the soil zone. The autocorrelation of the nitrate values however reveal a different mechanism and suggest a random pattern of arrival. Furthermore there is no correlation between phosphate and nitrate. There is however a correlation between nitrate and phosphate in the borehole at Nord-Vue PWS. This borehole (Nord-Vue) would be predicted by virtue of its position (and therefore geology) to again be a C type due to proximity of high plateaux; however hard bands are not recorded in the borehole log. The auto correlation suggests a non-random response for both phosphate and nitrate although the statistical significance is low. At Nord Vue there is a significant negative correlation between phosphate and nitrate, which suggests that the controlling factor is in the soil zone, given that they are both entrained species. This assumes that a phosphate sorption-desorption equilibrium is established within the saturated zone.

The methodology developed to examine the Eden Valley data clarified the type of data required for a similar investigation of the Usk Valley. Despite the data covering a shorter time duration it is still possible to undertake a reasonably vigorous statistical analysis.

The initial analysis of groundwater level trends using polynomials indicated that for the Usk the groundwater trend at all boreholes was consistent. Some slight lags are observed between Hill Farm Well and Llanusk Farm, which may be a function of geology as Hill Farm Well is located on the Limestone boundary. The proximity of the boreholes to each other also precludes the possibility that the variations are caused by different rainfall patterns. This observation is also borne out by the positive correlation values observed ( $p < 0.01$ ) suggestive of a homogeneous system. The autocorrelation performed on both monthly and fortnightly filtered data also indicates that the boreholes can be considered to have a non-random or seasonal pattern which is consistent with the recharge pattern.

Daily autocorrelation indicates a dampening or non-flashy system for recharge. Although some locations do not give a 'classic' seasonal signature this may be due to individual or local heterogeneities within an overarching homogeneous system. Again a lag is suggested between Hill Farm Well and Llanusk Farm. This lag of one day is also observed in the cross correlation response to rainfall between these two locations. This lag may be a 'piston type' response as Hill Farm Well is topographically higher than Llanusk Farm

These season signatures would predict that any entrained conservative species (or natural tracer) would also present this signature at the sampling location. This is observed with nitrate in the Usk Valley.

It was hoped that groundwater temperature could provide information on aquifer properties, perhaps the presence of warmer, preferential flow paths. This it did not do, however the trend analysis did show that the water may have a varying degree of insolation/insulation, which could be attributed to deeper sampling zones. The observed temperature spikes were also shown to be related to rainfall events, cooling and warming occurring as a result of seasonal rainfall perturbing the borehole temperature. There is also evidence that with the rise in groundwater in response to rainfall the electrical conductivity is seen to vary, a dilution and flushing effect. This suggests that when flushing occurs, ionic species (including organic) are transported from the surface zone to the water table, this occurs in the higher water table locations, at LUSK and CHW.

The positive correlation at LDOW between rainfall and borehole level is believed to be flushing caused by proximity to the road or farming activities in the adjacent fields including ploughing breaking up the soil. The negative or dilution factor may be due to lower water tables with larger recharge zones causing dilution; or possibly land use. At LTRI, HFW and CHBH, there is not much additional impact on the land in by fertiliser addition or farming activities.

The examination of the groundwater data obtained from the logger data would upon first impressions suggest that the aquifer zone of interest is homogeneous. More in-depth investigations reveal that small and subtle heterogeneities exist. These are revealed by an investigation utilising all the data and their interdependencies. It is not possible to quantify or qualify the aquifer properties using only one set of observations.

### 9.1.2 *Soil analysis*

The initial primary objective of the soils analysis was to generate values that would be carried forward into the modelling component of the project. It evolved into a larger investigation as preliminary work indicated a complex leaching and precipitation system. The understanding of the behaviour of phosphorus and its compounds in groundwater must start within the soil zone. This could be considered to be a major source, notwithstanding pollution incidents or poor management practices within agricultural areas. It can also, in the context of groundwater, be considered as a phosphorus reservoir, ready to provide mobile phosphorus throughout the year if desorption, dissolution and recharge conditions are favourable. An important function of the soil analysis was the determination of local partition coefficients for SRP and TDP. These values were used as a working figure and in reality are believed to represent an upper limit. Sensitivity analysis on their magnitude was undertaken in the modelling section.

The soil analysis has shown that in the locations where no phosphorus was detected in the groundwater, such as Llanusk Farm and Pencarreg Farm, that there is actually significant phosphorus present. Geochemical interactions with the borehole steel casing cause the lack of phosphorus detection. The values of soil leachable SRP and TDP at Llanusk Farm are in the order of 20 mg kg<sup>-1</sup> and above, whilst at Llandowlais which has the second highest SRP values recorded has lower soil SRP and TDP values of about 2 mg kg<sup>-1</sup>. The potato field (POTA) is potentially groundwater up-flow from Llandowlais and Pencarreg Farm and has leachable soil SRP in the order of ~3 mg kg<sup>-1</sup>, which suggests that the low values of groundwater SRP at Llanusk and Pencarreg Farms are a local anomaly. This also highlights the potential for retardation of SRP in an aquifer with sufficient iron hydroxide content to provide sorption sites.

The leachable values of SRP from the soil are, as would be expected, larger than those obtained from immediately adjacent borehole groundwater. Llantrisant soil has a calculated value of 20 to 50 mg SRP l<sup>-1</sup> (all values) but a groundwater concentration of only ~0.8 mg SRP l<sup>-1</sup>. This indicates a 20 to 50 times dilution factor for leached SRP within the groundwater. A similar situation exists with the dilution of Ty-Coch stream (TYST). The soil leachable potential is from ~1 to 10 mg SRP l<sup>-1</sup> from POTA and SCRUB; that of the manure piles (MANU and HILLMAN) is ~ 20 mg SRP l<sup>-1</sup>. The stream concentration at TYST is ~0.08 mg SRP l<sup>-1</sup>, again indicating an appropriate amount of dilution. At TYST it is noted that the SRP concentration increased in the summer months, perhaps suggestive of either direct inputs or a seasonal fluctuation.

The larger difference between TDP and SRP for the soils suggest that there is more organic phosphorus, as expected, within the soil zone than in the water. The smaller amount of dissolved organic phosphorus (DOP) within the groundwater is believed to be due to the leaching effect of the recharge. Only a small fraction of the soil organic phosphorus will be hydrolysed and leach to the water table.

The soil column results have shown that the soil has a good capacity for releasing SRP through leaching or de-sorption processes; there was no general decline in the amount of TDP or SRP in the leachates suggesting that the soil still had a 'good store' of phosphorus. The spiked column results did show a marked decline in the concentration of the spike with contact time, indicating that there was still a sufficiency of sorption sites for phosphorus and that the column had not reached the phosphorus carrying capacity limit. It is not possible to state whether equilibrium is established between retention and release within the soil; by-pass flow has also not been quantified. Due to the short contact time between the soil columns and spike it was thought that precipitation reactions would not be a major component in the removal of phosphate from solution. This is also borne out by the lack of precipitated phosphate minerals found in either XRD or ESEM analysis. The ESEM analysis also clearly indicates the association of phosphorus with iron within the soil zone.

### 9.1.3 **Groundwater analysis**

The groundwater investigation looked at a series of temporal snapshots of the groundwater quality from which it was possible to determine 'whole aquifer' and individual location groundwater relationships. The physical and geochemical measurements have been instrumental in identifying variations within the 'whole' aquifer system, not so much as isolated zones, but more as a transition effect over the complete aquifer. Robust analysis indicates that there are seasonal signatures in the physical parameters such as temperature, and also in the geochemical parameters such as pH and ORP. There are indications of seasonal and non seasonal signatures in the variations in the levels of various chemical species for both the Eden and Usk Valleys.

The Piper plots generated from the time series geochemical data also shows that there is the potential for precipitation and dissolution reactions within the Usk Valley. This may be occurring with calcium at HFW and UGDN, but does not confirm if the reactions involve calcium phosphate minerals. These are only considered to be viable in more alkaline soil conditions, which were not observed in the valley. Calcium phosphate minerals were also not observed in the XRD or ESEM analysis, so if they do exist they may be considered to be a minor component within this environmental setting. Overall the correlation analysis indicates that significant correlation does not exist between SRP and nitrate, a finding that could influence future analysis. However a more detailed analysis at a smaller more focussed scale shows that at two locations significant correlation does exist between SRP and nitrate, and in opposite directions. The correlation of species is also seen for iron and manganese, and phosphorus has been shown to be associated with these two elements. It is thus concluded that within the aquifer system there may be heterogeneity in the flow paths, geochemistry or surface phosphate in-puts.

The geochemistry data lack two important parameters that would enhance the analysis; these are groundwater age and profile depth sampling. However as the monitoring locations were all working wells with varying degrees of pumping activity it is most likely that age relationships and discrete horizon sampling would be negated due to mixing. Modelling might provide some insights into age relationships.

An important result from the geochemical analysis was the association of iron and SRP. The steel bolt experiment and data from LUSK and PENC clearly shows that SRP will sorb to iron hydroxides if they are contained within the aquifer in sufficient quantities. The correlation of SRP with iron has the potential to provide a simple proxy by association to phosphorus availability or presence, however in the Usk valley this was not observed to a significant level in the ion species and physical parameters analysis.

#### 9.1.4 **Modelling**

The Usk Valley has been modelled, accepting the limitations of data availability and uncertainty about some parameters, to produce a basic conceptualisation of the system. Initial modelling was undertaken by both 2D flow net and fully 3D MODFLOW models. Whilst there was a reasonable resolution of temporal data, the models would have benefited from more data on the important parameters of conductivity and storativity values. The pumping tests that were undertaken all reported a similar transmissivity value, suggesting conceptually homogeneous lithology; accepting the constraints due to the pump size and pumping time duration.

The initial modelling was based upon the theory of elevated valley flank groundwater heads driving flow through the aquifer, (Moreau et al. 2004), and the initial hydrogeological conceptual model. The flow net models show a realistic interpretation with groundwater discharging to the River Usk and older water being encountered at depth. This has implications for geochemical characteristics: lower older nitrates tend to be found in older deeper waters in the Eden Valley (Pers. comm., A Butcher).

Using the results from the flow nets it was possible to undertake a conceptualisation using a more robust MODFLOW model. This was useful as a quality check on model parameters, as a single model may have more than one unique solution. An important result of the modelling in terms of calibration was that the model did not support the original conceptualisation of a fully saturated zone and elevated groundwater on the flanks. It was not possible to calibrate the models with a boundary condition at these elevations. This indicates that the conceptualisation could be improved. The water is known to be at these elevations (presence of wells), however the wells may be more associated with spring lines and perhaps the water is supported above a low permeability layer over more fractured bedrock.

Further model iterations supported this conclusion. It was possible to model these elevated groundwater flanks at a very local scale, and not within a more regional context. This may, in part, be due to the lack of sound knowledge of the lithology heterogeneities. The model calibration also highlights differences in ground truth and outputs. The calibration data show a 'saw-tooth response' over the range and duration, which is known to produce a seasonal auto correlated model, whereas the model outputs are more subdued.

The potential recharge rate may also be slow; given a horizontal conductivity of  $\sim 1 \text{ m day}^{-1}$ , vertical conductivity could be estimated as  $0.1 \times$  the horizontal rate, which would give a recharge penetration of only  $3 \text{ m year}^{-1}$ . This is in broad agreement to the  $1 \text{ m year}^{-1}$  in chalk based upon tritium analysis (Darling 2009). This also suggests that once entrained geochemical species do not travel far in a year. This was supported by basic groundwater transport calculations.

The results of the contaminant modelling show that given a constant source term over a wide area the aquifer will eventually become 'fully contaminated'. This is however an unrealistic scenario as agricultural applications have seasonality and layover periods. The geochemical investigation of the soil column indicates that there is the potential for phosphate to be both retained and leached from the soil during agricultural activity.

Once entrained the modelling suggests that pulse fronts may reflect this activity and that within the Usk Valley it is likely to be fairly ubiquitous; albeit in quantities that are in general below the environmental quality standard  $0.05 \text{ mg SRP l}^{-1}$  ( $0.153 \text{ mg phosphate l}^{-1}$ ) (UKTAG 2006). However the association with iron and the elevated soil values at Llanusk Farm suggest that the actual groundwater phosphate concentrations in the lower more cultivated valley bottom may be higher than actually recorded. This may lead to false environmental conclusions.

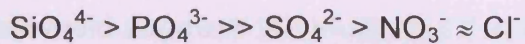
The local models did not have the ability to better replicate and allow predictions of future phosphate concentrations. The modelling showed that with a locally calibrated system the groundwater reaching a sampling borehole is likely to contain a percentage of both modern water and older water. Each portion will have its own geochemical characteristics obtained at the time of its last contact with the surface zone and the en-route aquifer processes.

#### 9.1.5 *Interpretation*

The results of the investigation at both the Eden and Usk Valley have shown that different groundwater flow characteristic will impart a signal at the point of measurement. This may be unaltered in form from the original input signal although subject to a temporal lag, scale change or a new signal form may be generated. These signals have themselves a temporal dependency. It is reasonable to infer that an entrained conservative species would also follow the advection groundwater flow. Variations in values will therefore reflect source term functions and other characteristics subsumed in the measured borehole signal.

Phosphate has been shown to have two characteristics signals in groundwater. A non-random or dampened function in the Eden Valley is observed, which is suggestive of the advection flow mechanism that is believed to operate. A seasonal signature is observed within the Usk Valley, which also mirrors the hydrograph signal. This is perhaps not unexpected as the measured quantity is dissolved or soluble, and is entrained. Sorption desorption equilibrium is likely to have been established along the flow path. Although for long flow paths concentrations may not yet reached equilibrium.

Strong opposing correlations between conservative species are also observed at some locations, which are interpreted as different flow paths mechanisms. The order of sorption potential of these species is:



It is possible that these correlations are a function of delay within the soil zone and that there may even be age relationships between the measured species at a borehole, inasmuch that the arrival times may be different Figure 9-1.

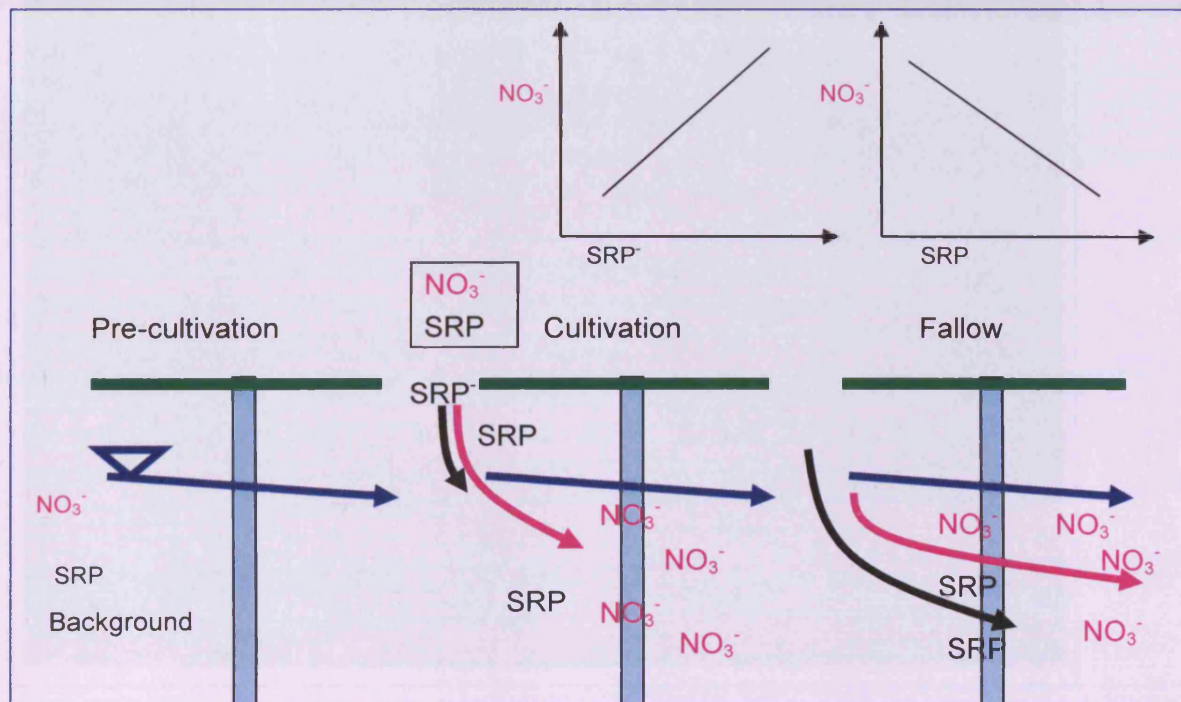


Figure 9-1 A schematic to show retention of phosphorus in soil zone. During fertilizer amendments phosphorus is preferentially retained in soil zone and nitrate is preferentially leached to water table and transported at the advecting groundwater flow velocity. The correlation between the two species will be positive for a period. During 'set aside' the remaining nitrate is leached in reducing quantities whilst retained phosphorus becomes more dominant in the sample analysis. The entrained nitrate is also transported away from the borehole zone at a faster advecting rate. This model would also work on shorter temporal spans.

The application of fertilisers is a pseudo seasonal process, as they are not applied during the autumnal winter rains in order to minimise leaching and run-off. They are applied to match the crop and soil condition requirements, which may be several times during the cereal and grass season. The matching of these inputs to outputs would augment the study, but this would also require water age data Figure 9-2.



*Figure 9-2 Eden Valley manure application on grassland (June 2006). This location is up gradient of the Bowscar public water supply BH. Photo A Butcher.*

## 9.2 Revised conceptual model

The analysis that has been undertaken of the geology, hydrogeology and physical drivers of the Eden and Usk Valley now enables a more robust conceptual model of the fate and transport of phosphorus and its compounds in groundwater. This has been derived by an 'inverse' approach in the investigation, where if the answer is the measured parameter, then the question is 'what influenced this result'? The main components can be split into two major categories:

- Physical drivers; lithology and recharge patterns
- Chemical processes; application and aquifer geochemical properties

Two conceptual models of processes and outputs are presented in Figure 9-3 and Figure 9-4. They are of necessity conceptual and highlight the main drivers identified in the original conceptualisation of the aquifer systems. They must be considered in terms of both individual and holistic processes interconnected at every stage. They do not provide quantitative result but serve as a basis for further investigations.

### 9.2.1 *Physical drivers*

The flow path geology has been shown to impart a signal on the groundwater flow, within the Eden Valley, where certain rock types are modulating the 'seasonal signal' to a dampened or smoothed variant. When there is no obvious change to the recharge signal it is reasonable to consider that the advection flow through the geology occurs in a 'piston' type manner, and flow paths are probably well connected. The dampened or non-random signal suggests that any pulse or piston flow is subsumed within a more dominant process. Large water bodies may have some influence on the signal, but in contrast to Streetly and Chillingworth (2001) are not believed to be directly correlated, which indicates a more internal geological function.

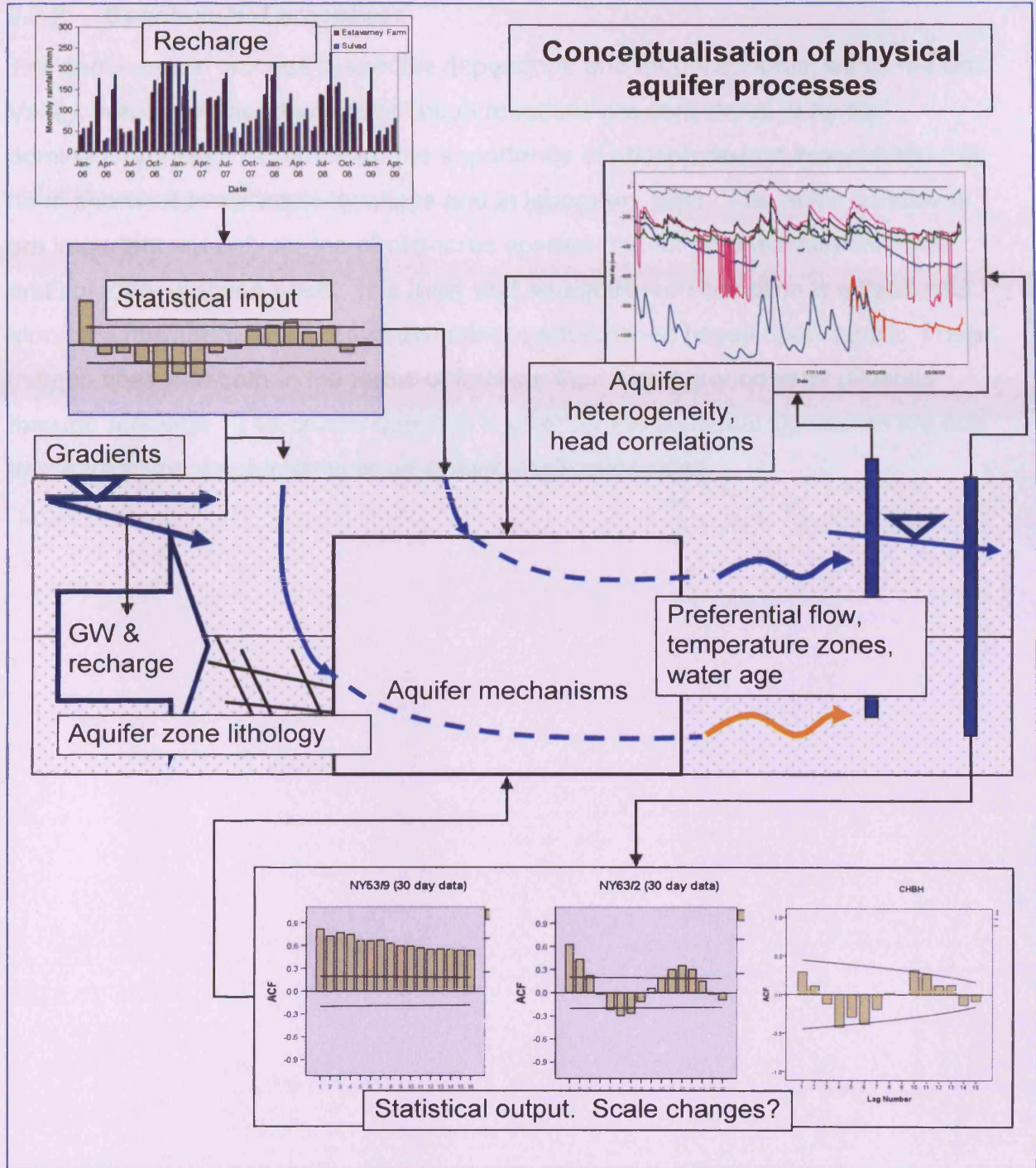


Figure 9-3 Revised conceptualisation of physical process active in the Eden and Usk Valley aquifers.

### 9.2.2 **Geochemical processes**

The geochemical process is species dependent, and for phosphorus, within the Usk Valley, sorption rather than precipitation reactions are considered to be the dominant process. Evidence for the importance of phosphate-iron associations has been shown at two sample locations and in laboratory tests. The redox conditions are important not only for the phosphorus species, but for potential sorption sites and solubility of these hosts. It is likely that an equilibrium condition is established along the flow path, which may have minor perturbations based upon inputs. These may be seasonal both in the terms of fertiliser inputs and groundwater dilutions through recharge. The crucial question is whether the seasonal signatures are due to the transport mechanisms or up-stream application rates.

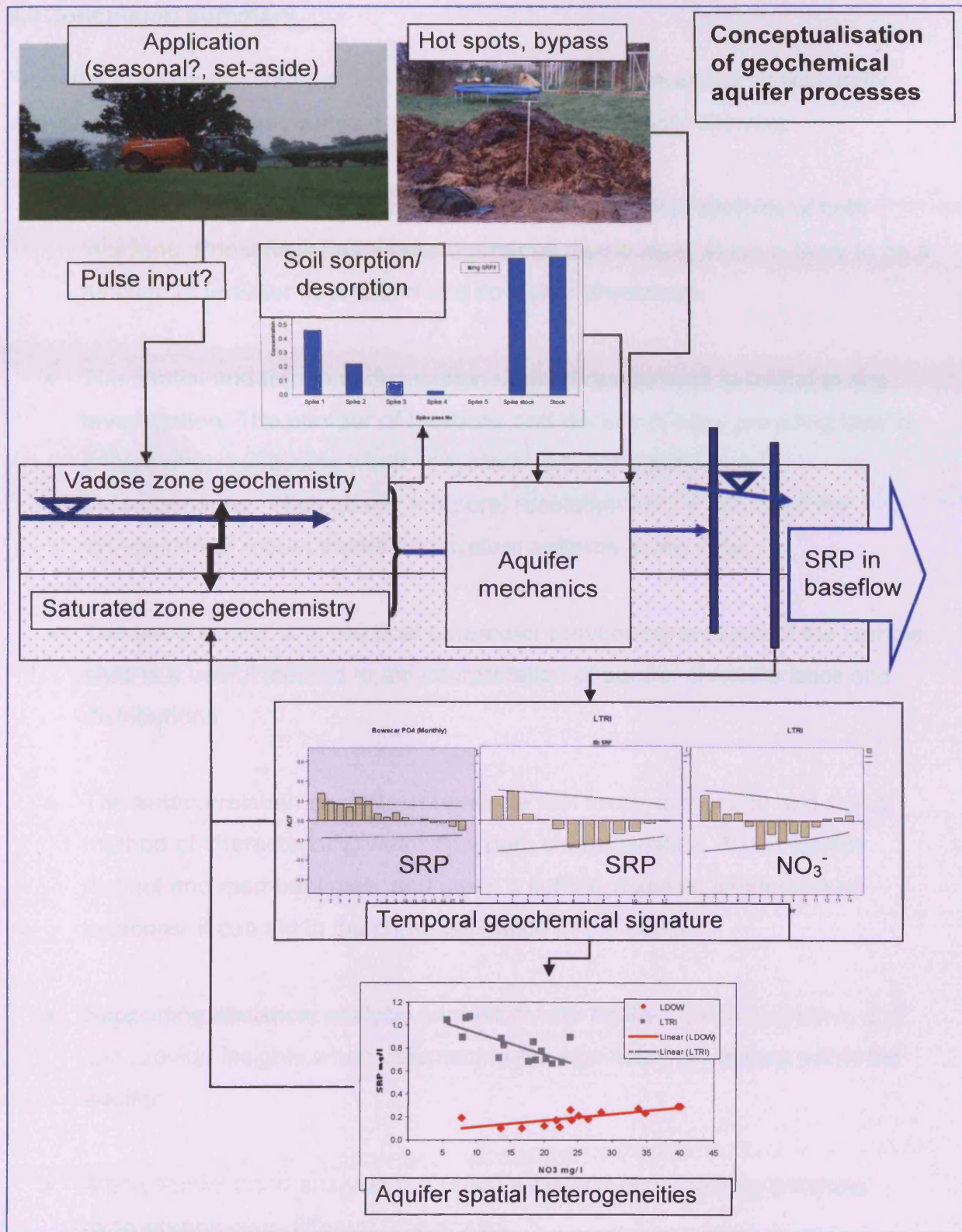


Figure 9-4 Revised conceptualisation of geochemical process active in the Eden and Usk Valley aquifers.

### 9.3 Conclusion summary

From the investigation into the fate and transport in groundwater of agriculturally derived phosphorus compounds it is possible to conclude the following:

- Phosphate is a ubiquitous compound within the aquifer systems of both locations. Phosphate has a heterogeneous distribution, which is likely to be a function of fertilizer application and flow path processes.
- The spatial and temporal distribution of good quality data is critical to any investigation. The number of locations and density of sites providing data is critical when assessing whether systems are homogenous or heterogeneous. High quality temporal resolution and length allow the recognition of robust trends and system patterns in the data.
- The geochemical and physical parameter partitioning analysis of the sample sites is a useful method to aid interpretation of aquifer characteristics and distributions.
- The autocorrelation analysis of borehole rest levels is a sound and robust method of characterising water flow path characteristics. It can identify distinct end member types, and given a sufficient spatial distribution of locations, it can aid in the characterisation of the aquifer.
- Supporting statistical analysis can assist with aquifer characterisation, and can provide insights when determining the significant processes within the aquifer.
- A polynomial trend analysis is a reliable method of comparing borehole hydrographs over different time scales.

- The soil zone is acting as a buffer to phosphate migration to the groundwater table, however within the soils studied there is a good sorption and desorption leaching potential. Local  $K_d$  values were calculated which serve as a benchmark value for further investigations.
- Within the Usk Valley, the soil leachate tests suggest that groundwater phosphate concentrations are not controlled by precipitation/ dissolution reactions of phosphate minerals. This may be due to soil type and concentration source terms.
- Soil phosphate hot spots do exist. Farmyard effluents, leaching manure piles and feeding stations will contribute a significant, if locally temporal, phosphate flux to the surrounding soil zone. This will then have a future potential to migrate to the water table.
- There are some strong geochemical associations with other groundwater species, which could have potential as indicator species given a sound knowledge of local redox conditions. However, these species associations must be treated with caution as they have both a macro and meso distribution, further supporting the need for good spatial distribution of data.
- It is most likely that the groundwater samples obtained are a mixture of different aged water; each of which has its own geochemical signature. It is likely that there are concentration pulses within the flow paths caused by a function of phosphate application and augmentation.
- Not all the phosphate in the River Usk is of agricultural origin; some may be derived from existing lithologies, such as the possible peat horizon at Llantrisant BH. However the potential for a continuous agriculturally derived low level flux through base flow will exist for a number of years.
- There is significant potential for phosphate sorption to iron and manganese hydroxides given the correct geochemical conditions. Groundwater samples

from the Usk Valley, where boreholes were unlined and the water was in direct contact with the soil, showed an extremely low concentration (at the limits of detection) of phosphate, whilst the local soils were shown to have very high (local) values. These unlined boreholes may not be uncommon, so it is important to factor the borehole construction into groundwater phosphate interpretations.

- The MODFLOW software models the aquifer as a system of 3D cells which represent ground parameters such as hydraulic conductivity or storage. These are a mixture of observed, calculated or literature values. Over the model domain, which is scale dependent, it is necessary to group these parameters. This causes an element of homogeneity which may not reflect ground truth.. It is not possible to accurately model heterogeneity or fracture flow. Profiles at Glen Court Farm and the Llewellyn borehole log shows that the Raglan Mudstone may be approaching an interim between matrix and fracture flow properties.

#### **9.4 Recommendations**

The following recommendations are made for future study within the Usk Valley, the main focus of this investigation:

- Establishing a data base that records the historical land use, as well as local and regional fertiliser applications. This will aid the interpretations of physical and modelling results.
- More robust soil mesocosm investigations of phosphorus species sorption characteristics to evaluate local  $K_d$  values.
- Laboratory investigation and verification of the potential precipitation of phosphorus species in agricultural hot spot localities.
- A deeper soil profile is obtained to investigate the movement of phosphorus species through the deeper soil zone.

- Several small pilot boreholes be constructed to investigate groundwater species away from the influence of working boreholes. In addition, undertake small scale tracer testing.
- Extend the borehole monitoring network with the deployment of more automated loggers.
- Groundwater age data to be acquired to resolve temporal transport scales.
- Increased groundwater sampling temporal resolution to include weather perturbations.
- Obtain, if possible, more robust aquifer properties for local scale modelling.
- Geophysical investigations be undertaken to obtain data to be incorporated into both conceptual and groundwater models.

### Acknowledgment

I would like to thank first and foremost my project supervisors Drs Tim Jones and Yuesuo Yang and Prof. Charles Harris. They have given me immeasurable support and help throughout this project. I would also like to thank Tony Oldroyd and Dr Iain MacDonald for their help and assistance with sample analysis and chemistry questions. I also thank Drs Peter Brabham and Emma Paris together with all the permanent staff at the University of Cardiff from their help, encouragement and friendship during my time there. I also wish at this time to acknowledge all of my scientific tutors and peers and especially Dr Hazel McGoff for giving me the opportunity to return to education. I also wish to thank my friends, old comrades in arms, family and fellow PhD researches for their encouragement and perseverance. Final thanks to Tim Jones for the friendship he has shown me whilst at Cardiff University.

## References:

Allen D, Brewerton L, Coleby L, Gibbs B, Lewis M, MacDonald A, Wagstaff S and Williams T 1997. *The Physical properties of major aquifers in England and Wales*. Nottingham: British Geological Survey. p. 312.

Andrews J E, Brimblecombe P, Jickells T, Liss P and Reid B 2004. *An Introduction to Environmental Chemistry*. 2 ed. Oxford: Blackwell, p. 296.

Angelini P 1997. Correlation and spectral analysis of two hydrogeological systems in Central Italy. *Hydrological Sciences Journal/Journal des Sciences Hydrologi [HYDROL. SCI. J./J. SCI. HYDROL.]*. Vol. 42(3), pp. 425-438.

Anon. 2005. *Eden Catchment Flood Management Plan – Scoping Report*. Environment Agency. . Available at: <URL: [www.environment-agency.gov.uk/regions/northwest](http://www.environment-agency.gov.uk/regions/northwest) > [Accessed: May 2006].

APHA. 1999. *Standard Methods for the Examination of Water and Wastewater*. American Public Health Association. Available at: <URL: <http://www.umass.edu/tei/mwwp/acrobat/sm4500P-E.PDF>> [Accessed: February 2007].

Appelo C and Postma D 2005. *Geochemistry, groundwater and pollution*. 2nd ed. Lieden: A.A. Balkema (Taylor & Francis), p. 672.

Arthurton R S 1981. *Geology of the Country around Penrith. Memoir for 1:50 000 geological sheet 12*. British Geological Survey, p. 192.

Bernard S and Delay F 2008. Determination of porosity and storage capacity of a calcareous aquifer (France) by correlation and spectral analyses of time series. *Hydrogeology Journal* 16(7), pp. 1299-1309.

BGS 1969. Newport. *Geological Survey of England & Wales*. Keyworth, Nottingham: British Geological Survey.

BGS 1971. Usk-Cwmbran (Special Sheet). *Geological Survey of Great Britain (England & Wales)*. Keyworth, Nottinghamshire: British Geological Survey.

BGS 1974a. Brough-under-Stainmore. *Geological Survey of England & Wales*. Keyworth, Nottingham: British Geological Survey.

BGS 1974b. Penrith *Geological Survey of England & Wales*. Keyworth, Nottingham: British Geological Survey.

BGS 1981. Chepstow. *Geological Survey of England & Wales*. Keyworth, Nottingham: British Geological Survey.

BGS 1986. Hydrogeological Map of South Wales. *Hydrogeology Maps*. Keyworth: NERC.

BGS 1996. Tectonic Map of Great Britain, Ireland and Adjacent Areas. Sheet 1, 1: 1 500 000 Series NERC.

BGS 2004. Appleby. *Geological Survey of England and Wales*. Keyworth Nottingham: British Geological Survey.

Bloomfield J 1996. Characterisation of hydrogeologically significant fracture distributions in the Chalk: an example from the Upper Chalk of southern England. *Journal of Hydrology* 184(3-4), pp. 355-379.

Boorman D, Hollos J M and Lilly A 1995. *Report No 126. Hydrology of soil types: a hydrologically based classification of the soils of the United Kingdom*. Wallingford, Oxfordshire: Institute of Hydrology. p. 146.

Box G E P and Jenkins G 1976. *Time Series Analysis: Forecasting and Control*. 3 ed. Prentice Hall, p. 592.

Boxall A B A, Fogg L A, Blackwell P, Pemberton E J and Kay P 2002. *Review of veterinary medicines in the environment*. Environment Agency. p. 251.

BSI 2002. *Characterisation of waste. Leaching. Compliance test for leaching of granular waste materials and sludges. One stage batch test at a liquid to solid ratio of 10 l/kg for materials with particle size below 10 mm (without or with size reduction)*. British Standards. p. 30.

BSI 2006. *Soil quality — Pretreatment of samples for physico-chemical analysis*. British Standards. p. 18.

BSI 2007. *Water quality — Sampling — Part 11: Guidance on sampling of groundwaters (Draft)*. British Standards. p. 45.

BSI 2008. *Soil quality. Guidance on leaching procedures for subsequent chemical and ecotoxicological testing of soils and soil materials*. British Standards. p. 46.

Buss R, Rivett M O, Morgan P and Bemment C D 2005. *Attenuation of nitrate in the sub-surface environment*. Environment Agency. p. 97.

Butcher A, Lawrence A, Jackson C, Cunningham J, Cullins E, Hasan K and Ingram. J A 2003. *Investigation of rising nitrate concentration in groundwater in the Eden Valley, Cumbria. Scoping Study*. NERC. p. 80.

Carey M, Marsland P and Smith J 2006a. *Remedial Targets Methodology: Hydrogeological Risk Assessment for Land Contamination*. Bristol: Environment Agency. p. 129.

Carey M, Marsland P and Smith J 2006b. *Remedial Targets Methodology: Hydrogeological Risk Assessment for Land Contamination (P20)* Bristol: Environment Agency. .

Carlson R E and Simpson J. 1996. A Coordinator's Guide to Volunteer Lake Monitoring Methods. . *North American Lake Management Society* [online]. Available at: <URL: <http://dipin.kent.edu/Phosphorus.htm>> [Accessed: January 2007].

Carlyle G C and Hill A R 2001. Groundwater phosphate dynamics in a river riparian zone: effects of hydrologic flowpaths, lithology and redox chemistry. *Journal of Hydrology* 247(3-4), pp. 151-168.

CEH. 2005. *Catchment Spatial Information*. Available at: <URL: [http://www.ceh.ac.uk/data/nrfa/catchment\\_spatial\\_information.htm](http://www.ceh.ac.uk/data/nrfa/catchment_spatial_information.htm)> [Accessed: June 2005].

CEH. 2008. *National Rivers Flow Archive*. NERC. Available at: <URL: <http://www.ceh.ac.uk/data/nrfa/index.html>> [Accessed: February 2006].

Clarke S and Wharton G 2001. *Using Macrophytes for the Environmental Assessment of Rivers: The Role of Sediment Nutrients*. Bristol: Environment Agency. p. 97.

Cornforth I, S. 2008. *The fate of phosphate fertilisers in soil*. New Zealand Institute of Chemistry. Available at: <URL: <http://nzic.org.nz/ChemProcesses/soils/index.html>> [Accessed: May 2009].

Daily P, Ingram J A and Johnson R 2006. *Groundwater quality review: The Permo-Triassic Sandstone aquifers of the Eden and Carlisle Basin groundwater quality monitoring unit*. Environment Agency. p. 37.

Daly K, Jeffery D and Tunney H 2001. The effect of soil type on phosphorous sorption capacity and desorption dynamics in Irish grassland. *Soil use and Management* 17, pp. 12-20.

Darling G 2009. Chalk catchment transit time: unresolved issues. In: *Darcy Lecture: Groundwater tracers and quantitative hydrogeology*. Burlington House, Geological Society of London: Hydrogeological Special Interest Group.

DEFRA. 2002. *The Government's Strategic Review of diffuse water pollution from agriculture in England Paper 1: Agriculture and water: a diffuse pollution review*. Available at: <URL: <http://www.defra.gov.uk/environment/water/quality/diffuse/agri/reports/dwpa01a.htm>> [Accessed: June 2008].

DEFRA. 2007. *Farming: Codes of Good Agricultural Practice*. Available at: <URL: <http://www.defra.gov.uk/farm/environment/cogap/index.htm>> [Accessed: June 2008].

Deutsch W, J. 1997. *Groundwater Geochemistry: Fundamentals and Applications to Contamination*. CRC Press, p. 232.

EA. 2009a. *Information about your groundwater quality analysis results*. Environment Agency. Available at: <URL: <http://publications.environment-agency.gov.uk/pdf/GEHO0807BNAO-E-E.pdf>> [Accessed: GEHO0807BNAO-E-E].

EA. 2009b. *River Quality*. Environment Agency. Available at: <URL: <http://maps.environment-agency.gov.uk/wiyby/wiybyController?topic=riverquality&layerGroups=default&lang=e&ep=map&scale=4&x=346893&y=1>> [Accessed: Various 2007].

EDINA 2006. Digital Mapping, JISC National Data Centre. Edinburgh.

EEC 1975. Drinking Water Abstraction Directive (consolidated): Council Directive 75/440/EEC of 16 June 1975 concerning the quality required of surface water intended for the abstraction of drinking water in the Member States as amended by Council Directive 79/869/EEC (further amended by Council Directive 81/855/EEC and Council Regulation 807/2003/EC) and both amended by Council Directive 91/692/EEC (further amended by Regulation 1882/2003/EC) 75/440/EEC. Eionet Reporting Obligations Database (ROD)

EPA 1999. *Understanding Variation in Partition Coefficient, K<sub>d</sub>, Values*. Washington DC: United States Environmental Protection Agency. p.

EU 1980. Groundwater Directive dangerous substances (consolidated): Council Directive 80/68/EEC of 17 December 1979 on the protection of groundwater against pollution caused by certain dangerous substances as amended by Council Directive 91/692/EEC (further amended by Council Regulation 1882/2003/EC).80/68/EEC. Eionet Reporting Obligations Database (ROD)

EU 2007. Directive 2006/118/EC of the European Parliament and of the Council of 12 December 2006 on the protection of groundwater against pollution and deterioration (Daughter to 2000/60/EC).2006/118/EC. Eionet Reporting Obligations Database (ROD)

Ferdowsian R and Pannell D 2009. Explaining long term trends in groundwater hydrographs. In: *World IMACS/MODSIM*. Cairns, Australia.

Fetter C W 2004. *Applied Hydrogeology*. 4th ed. New Jersey: Prentice-Hall, p. 598.

Fetter C W 2008. *Contaminant Hydrogeology*. 2nd ed. Long Grove, Illinois: Waveland Press Inc, p. 500.

Fitts C R 2002. *Groundwater Science*. London: Academic Press, p. 450.

Gill R ed. 1997. *Modern Analytical Geochemistry*. Longman, p. 282.

Golden Software 2003. Surfer; Surface Mapping System. Golden, Colorado: Golden Software.

Goody D C, Withers P J A, McDonald H G and Chilton P J 1998. Behaviour and impact of cow slurry beneath a storage lagoon: 2. Chemical composition of Chalk porewater after 18 years. *Water, Air, & Soil Pollution*. 107, pp. 1-4.

Gray 2004. Report On: GO3MP6 Mapping Project Abberley Hill Area. Reading University. p. 38.

Gray 2005. Field Notebook; Majorca Reading University.

Gray A 2006. *Evaluating structural controls within the Penrith Sandstone Aquifer and their influence on the frequent anomalous nitrate levels observed at spatially distinct boreholes*. MSc Thesis (Unpublished),

Griffioen J 2006. Extent of immobilisation of phosphate during aeration of nutrient-rich, anoxic groundwater. *Journal of Hydrology* 320(3-4), pp. 359-369.

Hansard L. 2002. *Diffuse pollution of water by Agriculture*. House of Lords. Available at: <URL: <http://www.parliament.the-stationery-office.com/pa/ld200102/ldhansrd/vo020627/text/20627w03.htm>> [Accessed: January 2006].

Haygarth P M and Jarvis S C 1997. Soil derived phosphorus in surface runoff from grazed grassland lysimeters. *Water Research* 31(1), pp. 140-148.

Haygarth P M, Warwick M S and House W A 1997. Size distribution of colloidal molybdate reactive phosphorus in river waters and soil solution. *Water Research* 31(3), pp. 439-448.

Heathwaite A L, Dils R M, Liu S, Carvalho L, Brazier R E, Pope L, Hughes M, Phillips G and May L 2005a. A tiered risk-based approach for predicting diffuse and point source phosphorus losses in agricultural areas. *Science of The Total Environment* 344(1-3), pp. 225-239.

Heathwaite L, Haygarth P, Matthews R, Preedy N and Butler P 2005b. Evaluating Colloidal Phosphorus Delivery to Surface Waters from Diffuse Agricultural Sources. 34(1), pp. 287-298.

Heredia O S and Fernandez Cirelli A 2007. Environmental risks of increasing phosphorus addition in relation to soil sorption capacity. *Geoderma* 137(3-4), pp. 426-431.

Hill T and Lewicki P. 2007. *STATISTICS Methods and Applications*. . StatSoft Inc. Available at: <URL: <http://www.statsoft.com/TEXTBOOK/sttimser.html#analysis>> [Accessed: June 2008].

Hiscock K 2005. *Hydrogeology: Principles and Practice*. Oxford: Blackwell Sciences Ltd, p. 389.

Holman I, Howden N and Whelan M. 2008. *An Improved Understanding Of Phosphorus Fate And Transport Within Groundwater And The Significance For Associated Receptors*. Secure Archive For Environmental Research Data (SAFER) managed by Environmental Protection Agency Ireland. Available at: <URL: <http://erc.epa.ie/safer/iso19115/displayISO19115.jsp?isoID=102>> [Accessed: September 2008].

Hounslow A 1995. *Water Quality Data: Analysis and Interpretation*. London: CRC Press, p. 397.

Howard A 1994. Problem Cyanobacterial blooms: explanation and simulation modelling. *Transactions of the Institute of British Geographers*, 19(2), pp. 213-224.

Hughes A 2003. *Permian and Triassic rocks of the Appleby district (part of Sheet 30, England and Wales)*. Research Report RR/02/01 BGS, NERC. Keyworth: BGS, p. 21.

Ingram J A 1978. The Permo-Triassic sandstone aquifers of North Cumbria. North West Water. p. 29.

JAGDAG. *Joint Agency Groundwater Directive Advisory Group: Determination of substances for the Purposes of the EC Groundwater Directive (80/68/EEC)*. Environment Agency. Available at: <URL: <http://www.environment-agency.gov.uk/commondata/acrobat/109645>> [Accessed: March 2006].

Jarvie H P, Withers J A and Neal C 2002. Review of robust measurement of phosphorus in river water: sampling, storage, fractionation and sensitivity. *Hydrology and Earth System Sciences* 6(1), pp. 113-131.

Jeffers E. *Method for Computing Alkalinity Based On Total Inorganic Carbon (TIC) and Related Data*. Star Instruments Inc. Available at: <URL: <http://www.starinstruments.com/products/alk/docs/alk%20tech%20note.pdf>> [Accessed: March 2008].

Jones H K, Morris B, Cheny. CS, Brewerton. LJ, Merrin. PD, Lewis. MA, MacDonald. AM, Coleby. LM, McKenzie. AA, Bird. MJ, Cunningham. J, Robinson. VK and Talbot. JC 2000. *The physical properties of minor aquifers in England and Wales*. NERC p. 234.

Krauskopff K B and Bird D K 1995. *Introduction to Geochemistry*. 3rd ed. Singapore: McGraw-Hill, p. 647.

Kresic N 2007. *Hydrogeology and Groundwater Modeling*. 2 ed. Boca Raton, Fl: CRC Press, p. 807.

Lawton G 2006. *Pee-cycling*. New Scientist. 23/30 December 2006. pp. 45-47.

Leeson J, Edwards A, Smith J W N and Potter H A B 2003. *Hydrogeological Risk Assessments for Landfills and Derivation of Groundwater Control Trigger Levels*. Bristol: Environment Agency p. 104.

Ling S 2007. *Assessing the effectiveness of landfill restoration and remediation at a closed landfill site (unpublished PhD Thesis)*. Cardiff.

Lovelock P E R 1972. *Aquifer properties of the Permo-Triassic Sandstones of the United Kingdom*. University College, London.

Lovelock P E R 1979. Aquifer properties of the Permo-Triassic Sandstones of the United Kingdom. *Bulletin of the Geological Survey of Great Britain* 56(50).

Lovelock P E R, Price M and Tate T K 1975. Groundwater Conditions in the Penrith Sandstone at Cliburn, Westmorland.

MacDonald M and Harbaugh A 1988. *A modular three-dimensional finite-difference ground-water flow model* U.S. Geological Survey. p. 586.

Manahan S 2005. *Environmental Chemistry*. 8th ed. London: CRC Press, p. 783.

McKelvie I D ed. 2005. *Separation, preconcentration and speciation of organic phosphorus in environmental samples* *Organic Phosphorus in the Environment*. CABI Publishing, p. 432.

Met. Office. 2007. *Historic station Data*. Available at: <URL: <http://www.metoffice.gov.uk/climate/uk/stationdata/index.html>> [Accessed: March 2007].

Military Survey 1988. *Manual of Military Map Reading*. Army Code 70947(R1988). HMSO, Crown Copyright. p. 325.

Milward 2003. *Geology of the Appleby District: a brief explanation of the geological map Sheet 30 Appleby*. NERC, p. 30.

MODFLOW 2002. *Visual MODFLOW*. Waterloo: Waterloo Hydrogeologic Inc.

Moreau M, Shand P, Wilton N, Brown S and Allen D 2004. *Baseline Report Series: 12. The Devonian aquifer of South Wales and Herefordshire*. Keyworth: BGS & EA. p. 55.

Morris D G and Flavin R W 1994. Sub-set of UK 50 m by 50 m hydrological digital terrain model grids. NERC. Institute of Hydrology, Wallingford.

Mustafa S, Zaman M I, Gul R and Khan S 2008. Effect of Ni<sup>2+</sup> loading on the mechanism of phosphate anion sorption by iron hydroxide. *Separation and Purification Technology* 59(1), pp. 108-114.

NHM. 1998. Phosphate Recovery Phosphorus availability in the 21st century: Management of a non-renewable resource. *Phosphorus & Potassium* [online], (217). Available at: <URL: <http://www.nhm.ac.uk/research-curation/research/projects/phosphate-recovery/p&k217/steen.htm>> [Accessed: May 2007].

Nielson D R and Wendroth O 2003. *Spatial and Temporal Statistics*. Catena Verlag GMBH, p. 398.

Nurnberg G 1984. Iron and hydrogen sulfide interference in the analysis of soluble reactive phosphorus in anoxic waters. *Water Research* 18(3), pp. 369-377.

O' Dell J 1993. *Method 365.1 Determination of Phosphorus by Semi-Automated Colorimetry* US Environmental Protection Agency. p. 17.

OS 2005a. The English Lakes, North Eastern Area. *Explorer Series*. Southampton: Ordnance Survey.

OS 2005b. Howgill Fells & Upper Eden Valley. *Explorer Series*. Southampton: Ordnance Survey.

OS 2005c. Newport & Pontypool *Explorer Series*. Southampton: Ordnance Survey.

OS 2007. Cardiff & Newport, *Landranger Series*. Southampton: Ordnance Survey.

Peach D 2006. Introduction talk. In: *Catchment Scale Hydrogeology*. Burlington House, London: Hydrogeological Group, Geological Society.

Perzynski G M ed. 2000. *Methods of phosphorous analysis for soils, sediments, residuals and waters*. Kansas State University, p. 110.

Pickering R. 1980. *Quality Water Technical Memorandum No. 80.27; WATER QUALITY -- New Parameter Codes for pH, Alkalinity, Specific Conductance, and Carbonate/Bicarbonate*. USGS. Available at: <URL: <http://water.usgs.gov/admin/memo/QW/qw80.27.html>> [Accessed: March 2008].

Prinos S T, Lietz A C and Irvin R B 2004. *Design of a Real-Time Ground-Water Level Monitoring Network and Portrayal of Hydrologic Data in Southern Florida*. USGS. p. 115.

Ralph J and Ralph I. 2009. *MINDAT.org*. Available at: <URL: <http://www.mindat.org/>> [Accessed: Various 2008-2009].

Reynolds C S and Davies P S 2001. Sources and bioavailability of phosphorus fractions in freshwaters: a British perspective. *Biological Reviews* 76(01), pp. 27-64.

Robards K, McKelvie I D, Benson R L, Worsfold P J, Blundell N J and Casey H 1994. Determination of carbon, phosphorus, nitrogen and silicon species in waters. *Analytica Chimica Acta* 287(3), pp. 147-190.

Robertson W, Schiff S and Ptacek C 1998. Review of Phosphate Mobility and Persistence in 10 septic system plumes. *Groundwater* 36(6).

Robins ed. 1998. *Recharge: the key to groundwater pollution and aquifer vulnerability*. London: Geological Society, Special Publications, p. 224.

Rounds S 2006. *National Field Manual V3. Chapter 6.6 Alkalinity and Acid Neutralizing Capacity*. USGS. p. 53.

Schachtman D P, Reid R J and Ayling S M 1998. Phosphorus Uptake by Plants: From Soil to Cell. *Plant Physiology* 116, pp. 447-453.

Schibler J, Moore D and De Borba B. 2007. Setting meaningful detection and quantitation limits for chromatography methods. [online]. Available at: <URL: [http://www.dionex.com/en-us/webdocs/52823\\_LPN-1926-Chromeleon.pdf](http://www.dionex.com/en-us/webdocs/52823_LPN-1926-Chromeleon.pdf)> [Accessed: December 2009].

Seymour K J, Ingram J A and Gebbett S J 2006. *Structural controls on groundwater flow in the Permo-Triassic sandstones of NW England*. London: Geological Society, p. 346.

Sheils A K. 1993. *Hydrogeology and European legislation*. Available at: <URL: <http://qjieggh.lyellcollection.org/cgi/content/abstract/26/3/227> > [Accessed: 3 26].

Shuman L M 2003. Fertilizer source effects on phosphate and nitrate leaching through simulated golf greens. *Environmental Pollution* 125(3), pp. 413-421.

Skelton P ed. 2003. *The Cretaceous World*. Cambridge University Press, p. 360.

Smith J, W, N. and Lerner D, N. 2007. A framework for rapidly assessing the pollutant retardation capacity of aquifers and sediments. *Quarterly Journal of Engineering Geology and Hydrogeology* 40(Part 2), pp. 137-146.

SNIFFER 2008. *An Improved Understanding of Phosphorus Origin, Fate and Transport within Groundwater and the Significance for Associated Receptors*. Edinburgh: SNIFFER. p. 139.

Squirrell H, C., Downing R, A. and Kelk B 1969. *Geology of the South Wales Coalfield Part I. The Country around Newport (Monmouthshire)*. 3 ed. London: HMSO, p. 333.

SSEW 1977. Soil Survey of England & Wales. Southampton: Ordnance Survey.

SSLRC 1983a. *Legend for the 1:250 000 soil map of England and Wales (A brief explanation of the constituent soil associations)*. MAFF. p.

SSLRC 1983b. Soils of North West England, Sheet 1, 1:250 000. *Soil survey of England and Wales* Southampton: Ordnance Survey.

SSLRC 1983c. Soils of South West England, Sheet 5, 1:250 000. *Soil Survey of England and Wales*. Southampton: Ordnance Survey.

SSLRC 1996. Groundwater Vulnerability of Gwent, South & Mid Glamorgan, *.Groundwater Vulnerability Maps Sheet 36 1:100 000*. Environment Agency.

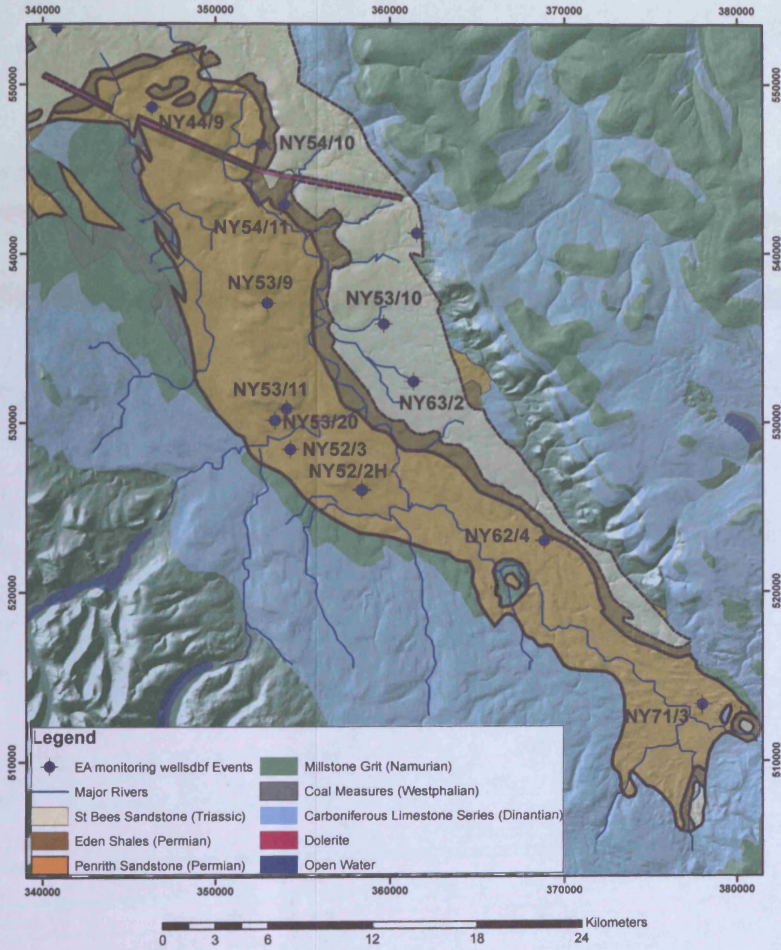
- SSLRC 1997a. Groundwater Vulnerability of North-West Cumbria. *Groundwater Vulnerability Maps Sheet 3 1:100 000*. Environment Agency.
- SSLRC 1997b. Groundwater Vulnerability of Northern Pennines. *Groundwater Vulnerability Maps*. Environment Agency.
- SSLRC 1997c. Groundwater Vulnerability of South-West Cumbria. *Groundwater Vulnerability Maps Sheet 6 1:100 000*. Environment Agency.
- SSLRC 1997d. Groundwater Vulnerability of Yorkshire Dales. *Groundwater Vulnerability Maps Sheet 7 1:100 000*. Environment Agency.
- Streetly M J and Chillingworth G 2001. Groundwater levels in the North West Region. (*Unpublished*). ESI.
- Stumm W and Morgan J 1996. *Aquatic Geochemistry*. 3rd ed. Wiley, p. 1022.
- Todd D K and Mays L W 2005. *Groundwater Hydrology*. 3 ed. Wiley, p. 636.
- Toth J 1962. A theory of ground-water motion in small drainage basins in central Alberta, Canada. *Journal of Geophysical Research* 67(11), pp. 4375-4387.
- UKTAG 2006. *UK Environmental Standards and Conditions (Phase 1)*. UK Technical Advisory Group on the Water Framework Directive. p. 73.
- USCAE 1999. *Engineering and Design Groundwater Hydrology*. Washington DC: United States Corps of Army Engineers, p. 122.
- van der Perk M 2006. *Soil and groundwater contamination; from molecular to catchment scale*. London: VV Balkema (Taylor Francis), p. 389.
- Wang H 2005. *Flownet: FDM Modelling of Groundwater*. Tsinghua University, Beijing.
- Warren N, Allan I J, Carter J E, House W A and Parker A 2003. Pesticides and other micro-organic contaminants in freshwater sedimentary environments--a review. *Applied Geochemistry* 18(2), pp. 159-194.
- Weiner E 2008. *Applications of Environmental Aquatic Chemistry: A Practical Guide*. 2 ed. CRC Press, p. 456.
- Welch F, B.A., Trotter F, M., Lawrie T, Smith J and Elliot R 1961. *Geology of the Country around Monmouth and Chepstow*. London: HMSO, p. 163.
- Westgard J, O. 2008. Basic Method Validation. *Method Validation - The Detection Limit Experiment*. ISBN13: 978-1886958-258.  
<http://www.westgard.com/lesson29.htm>

WHO. 2002. *Eutrophication and Health*. European Commission, Luxembourg.  
Available at: <URL: <http://ec.europa.eu/environment/water/water-nitrates/eutrophication.pdf>> [Accessed: January 2006].

Wisconsin 1996. *Analytical detection limit guidance & laboratory guide for determining method detection limits*. Wisconsin Department of Natural Resources Laboratory Certification Program. p. 33.

Worsfold P J, Gimbert L J, Mankasingh U, Omaka O N, Hanrahan G, Gardolinski P C F C, Haygarth P M, Turner B L, Keith-Roach M J and McKelvie I D 2005. Sampling, sample treatment and quality assurance issues for the determination of phosphorus species in natural waters and soils. *Talanta* 66(2), pp. 273-293.

Eden Valley Location Map – EA monitoring boreholes Base map BGS Geology

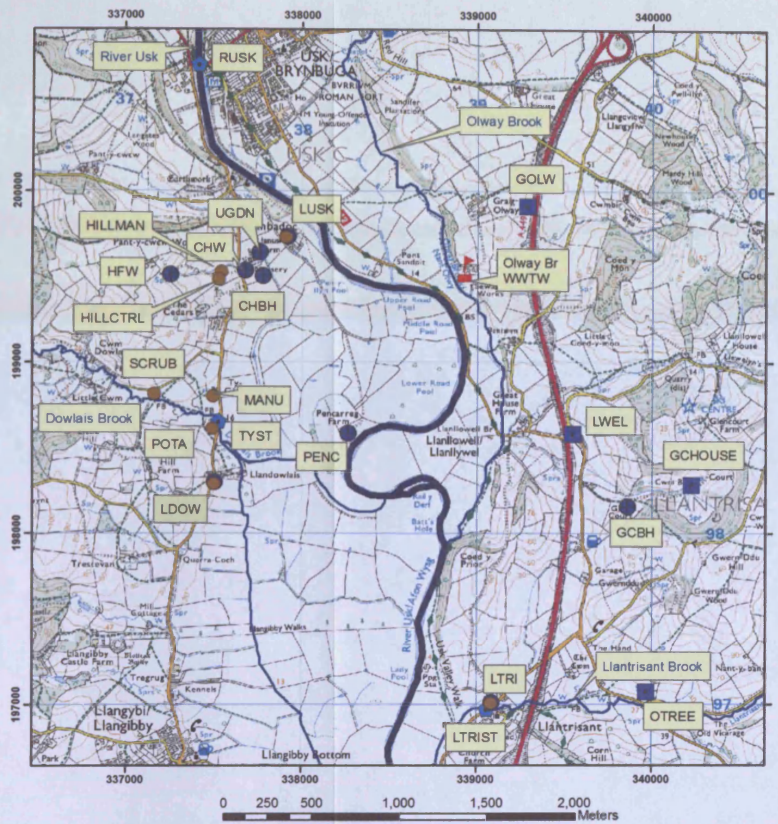


Usk Valley Location Map – Base map Google Earth image



- Legend**
- Soil Sample Locations
  - Usk BH Locations
  - Additional Locations
  - ◆ Surface Water Locations
  - 🚧 Sewage work
  - Streams

Usk Valley Location Map – Base map OS 1:25 000 mapping



**Legend**

- Soil Sample Locations
- Usk BH Locations
- Additional Locations
- ▲ Surface Water Locations
- Sewage work
- Streams

